PROGRESS IN RHEOLOGY OF BIOLOGICAL AND SYNTHETIC POLYMER SYSTEMS

Edited by
A. C. Diogo, N. B. Alvarenga, J. Canada, S. Ferro Palma and J. Dias

INSTITUTO BEJA POLITÉCNICO

GER

SPR

PROGRESS IN RHEOLOGY OF BIOLOGICAL AND SYNTHETIC POLYMER SYSTEMS

Edited by
A.C. Diogo, N. B. Alvarenga,
J. Canada, S. Ferro Palma
and J. Dias

Progress in Rheology of Biological and Synthetic Polymer Systems

Edited by

António Correia Diogo
Sociedade Portuguesa de Reologia, Portugal

Nuno Bartolomeu Alvarenga
Área Depart. de Ciência e Tecnol. dos Alimentos, Escola Superior Agrária de Beja, Portugal

João Boavida Canada
Área Depart. de Ciência e Tecnol. dos Alimentos, Escola Superior Agrária de Beja, Portugal

Silvina Ferro Palma
Área Depart. de Ciência e Tecnol. dos Alimentos, Escola Superior Agrária de Beja, Portugal

João Mestre Dias
Área Depart. de Ciência e Tecnol. dos Alimentos, Escola Superior Agrária de Beja, Portugal

TECHNICAL FILE

Published by
Instituto Politécnico de Beja
R. Santo António, n.º 1 – A
7800 – 906 Beja, PORTUGAL
Tel. 284 314 400 Fax. 284 314 401
Email: ipbeja@ipbeja.pt
http://www.ipbeja.pt

Design by
Departamento GRÁFICO do IPB

Printed by
GTO 2000, Soc. de Artes Gráficas, Lda. - Bombarral
http://www.gto2000.pt

ISBN: 972-99301-0-4
Legal Deposit: 214819/04

Year 2004
Prints: 500

Preface

IBERHEO'04 is a Joint Meeting involving the national Rheology Societies of Spain and Portugal: Grupo Español de Reologia and Sociedade Portuguesa de Reologia. It will be held in Beja (Portugal), from 9 to 11 September 2004, on the main subject: "*Progress in Rheology of Biological and Synthetic Polymer Systems".*

This Meeting is actually the fourth one where both societies were involved in the organisation. The first one, held in Estoril (Portugal) in 1989 (November 23-25), was a joint British-Spanish-Portuguese Rheology Meeting entitled "*Molecular Structure and Rheology of Polymers (both Synthetical and Biological)*". Ten years later, both societies, together with the Italian, Greek and Slovenian Societies of Rheology, were involved in the organization of the Southern European Conference of Rheology held in Falerna Lido (Calabria, Italy), in 1999 (September 7-11). In 2002, a Joint Meeting of the British, Italian, Portuguese and Spanish Rheologists entitled "*Progress in Rheology: Theory and Applications*" took place in Torremolinos (Malaga, Spain) from 24 to 26 April. All these Meetings involved about 70 to 130 participants, which looks very good as compared to other similar european meetings.

IBERHEO'04 involves about 70 communications and more than 80 participants, mainly from Spain and Portugal. Most of the work presented covered the following topics:

- Gels and Emulsions
- Colloids and Suspensions
- Biopolymers and Biological Materials
- Food Rheology and Processing
- Greases and Bituminous Mixtures
- Polymer Melts and Blends

The above list is roughly representative of the balance among the different activities performed by rheologists in Spain and Portugal and may be useful to identify a few main streams in research. First, there is a noticeable tendency for people to orient themselves to outside, to the borders between rheology and other sciences. For instance, there is a strong increase in matters related to Biology *lato sensu*: biopolymers, biological materials, food rheology. Complex fluids (involving in general multiphase systems) is also a hot topic both for theory and applications: gels and emulsions, foams and froths, colloids and suspensions, greases and bituminous mixtures, polymer blends. Polymer rheology and simulation of complex flows with improved constitutive equations is another component.

Finally it is a pleasure to acknowledge the support of all sponsors as well as the enthusiastic work and dedication of the team of the Food Science and Technology Department of Escola Superior Agrária de Beja on the preparation of this Joint Meeting.

A. Correia Diogo

Scientific Committee

Anabela Raymundo (I. Piaget, Almada)

António Correia Diogo (IST, Lisboa)

Antonio Guerrero (Un. Sevilla)

Antxon Santamaria (UPV, S. Sebastian)

Críspulo Gallegos (Un. Huelva)

Elvira Costell (Un. Valencia)

Fernando Tavares de Pinho (Un. Minho)

Isabel de Sousa (ISA, Lisboa)

João Canada (ESAB, Beja)

João Maia (U. Minho)

José Covas (U. Minho)

Jose Muñoz (Un. Sevilla)

Maria Eugenia Muñoz (UPV, S. Sebastian)

Maria Fernanda Bahia (FFUP, Porto)

Maria Pilar Gonçalves (FEUP, Porto)

Nuno Bartolomeu Alvarenga (ESAB, Beja)

Pedro Partal (Un. Huelva)

Table of contents

5. FOOD RHEOLOGY & PROCESSING 197

1. INVITED COMMUNICATIONS

FT-RHEOLOGY: A VERY SENSITIVE EXPERIMENTAL TECHNIQUE TO CHARACTERIZE THE NON-LINEAR REGIME IN MATERIALS

M. Wilhelm

wilhelm@mpip-mainz.mpg.de
Max-Planck-Institut für Polymerforschung, P.O.-Box 3148, 55021 Mainz, Germany

Rheology allows the characterization of different mechanical properties, of simple and complex topological structures, in melts or solution, both in the linear and non-linear regime. In general, processing and utilize conditions include high strain or high shear rates consequently lead to non-linear material response. This will effect dynamics, orientation and fatigue of the polymer materials and dispersions. Experiments in the non-linear regime are expected to be crucial with respect to the characterization and formation of interfaces, morphologies, different topologies and failure. Additionally quality control will also benefit from simple non-linear characterization techniques that allow a non-linear quantification..
In this lecture I would like to give first an overview with respect towards a very sensitive, but still simple, mechanical technique where large amplitude oscillatory shear (LAOS) using a frequency $\omega_1/2\pi$ is applied and the torque response is analyzed in frequency space. The non-linear response generates mechanical higher harmonics at $3\omega_1$, $5\omega_1$, $7\omega_1$ and so forth. A Fourier transformation can unravel the intensities and phases in a spectrum $I(\omega)$; consequently we use the term "FT-Rheology" for this technique. The experimental set-up is shown in Fig.1.

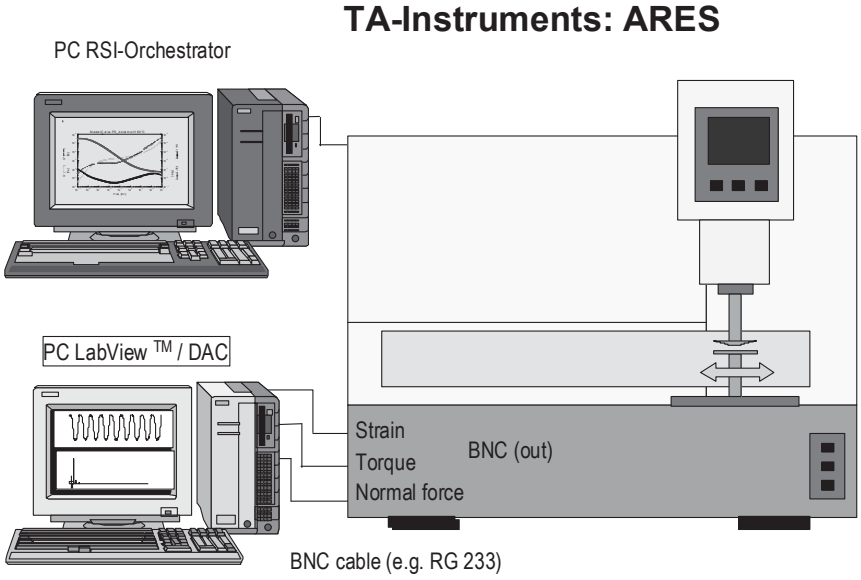

Figure 1: Experimental set up for FT-Rheology experiments. The strain, torque and normal forces are digitized via a ADC in a stand alone PC where the Fourier transform of e.g. the torque is conducted.

The rheometer is controlled via the usual PC that allows to measure linear mechanical properties via the commercial software.

A typical FT-rheology spectrum is shown in Fig. 2, where a signal to noise ratio of 100,000 : 1 can be achieved.

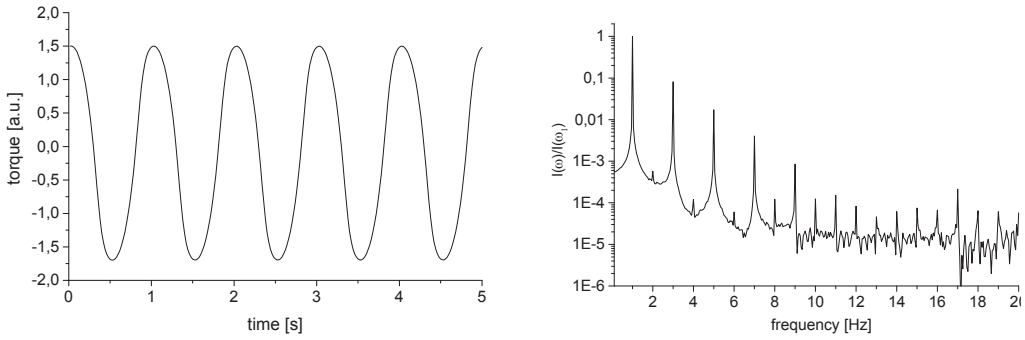

Figure 2: Time, respective frequency data set for polyvinylalcohol solution, at T = 278°K, $\gamma_0 = 20$, $\omega_1/2\pi = 1$ Hz for a single measurement. The S/N of the spectrum is in the range of 100,000 : 1.

Several application of FT-Rheology with respect to rubbers, dispersions and resins are presented. One emphasis in this talk is the correlation between topology and non-linear mechanical response in polymer systems. These systems are made of polystyrene: linear, 3 and 4 arm stars and serve as models for more complex systems like H, combs, and long chain branched structures. The result show a strong correlation between the phase of the third harmonic and the topology. Further more the correlation between the non-linear mechanical response and finite element simulations using the Polyflow package are presented. A second emphasis of this presentation is towards the influence of shear on the complex macroscopic morphology in a diblock copolymer system. The block copolymer was macroscopically first oriented and afterwards the shear conditions where changed so that the orientation tilted by 90 degrees. Using 2D-SAXS and FT-Rheology the kinetics of the reorientation was followed in detail.

Lit.:

[1] M. Wilhelm, P. Reinheimer, M. Ortseifer; High Sensitivity Fourier-Transform Rheology; *Rheol. Acta* **38** (1999) 349

[2] M. Langela, M. Wilhelm, U. Wiesner, H.W. Spiess; Microphase reorientation in block copolymer melts as detected via FT-Rheology and 2D-SAXS; *Macromolecules* **35** (2002) 3198

[3] M. Wilhelm; FT-Rheology (feature article); *Macromol. Mater. Eng.* **287** (2002) 83

[4] T. Neidhöfer, M. Wilhelm, B. Debbaut; Fourier-Transform rheology experiments and finite-element simulations on linear polystyrene solutions; *J. Rheol.* **47** (2003) 1351

USING MACROMOLECULAR ARCHITECTURE FOR EXPLORING COMPLEX DYNAMICS

Dimitris Vlassopoulos

Foundation for Research and Technology-Hellas (FO.R.T.H.),
Institute of Electronic Structure and Laser, and
University of Crete, Department of Materials Science and Technology
71110 Heraklion, Crete, Greece.

Recently, the elucidation of the relaxation mechanisms of branched and hyperbranched macromolecules has emerged as a field of great significance, both from the scientific and the technological viewpoints. We present a systematic approach to analyze the response of model polymers with progressive complexation in architecture, both in the melt and in solution.

We show dynamic data on series of well-defined nearly monodisperse branched polymer melts (polystyrenes, polybutadienes and polyisoprenes) of the Cayley-tree, comb and star-comb types. We discuss quantitatively the complex relaxation of these systems in terms of hierarchical motions. We demonstrate the possibilities of altering the rheology of polymeric systems in a controlled way by introducing branches. Based on these results we also show that it is possible to analyze the viscoelastic response of telechelic polymers forming dendritic supramolecular structures in the melt.

In solution, dendritic structures can be viewed as colloidal particles exhibiting ultrasoft interactions, which can be tailored on the molecular level, and their dynamic response spans the range from polymeric to colloidal behavior. Such soft suspensions can exhibit complex dynamics which is interpreted in terms of colloidal glass transition. This suggests possibilities for obtaining a unified description of the response of suspensions of varying interactions and thus controlling their flow behavior.

2. GELS & EMULSIONS

VISCOELASTIC CHARACTERIZATION OF CARRAGEENAN SOLUTIONS AND GELS OBTAINED FROM PORTUGUESE SEAWEEDS

L.. Hilliou[1,*], *P. Abreu*[2], *AM. Ramos*[2], *A. Sereno*[1] *and M.P. Gonçalves*[1]

[1]REQUIMTE, Departamento de Engenharia Química, Faculdade de Engenharia da Universidade do Porto, Rua Dr. Roberto Frias, s/n, 4200-465 Porto, Portugal.
[2] REQUIMTE, Centro de Química Fina e Biotecnologia., Faculdade de Ciência e Tecnologia, Universidade Nova de Lisboa, Quinta da Torre, 574, 4900 Viana do Castelo, Portugal
* email: hilliou@fe.up.pt

Keywords: Mastocarpus stellatus; carrageenan; viscosity; DRIFT

Abstract

In the frame of a project aiming at engineering new *green* edible films for food coatings and packaging, the potential use of seaweeds collected on the Portuguese coast as a source of natural thickening and gelling agents has been screened. DRIFT spectra were recorded for the chemical identification of carrageenans obtained by alkali extraction from *Gigartina Pistillata* and *Mastocarpus Stellatus*. The viscoelastic properties of carragenan solutions at different concentrations in water were determined by steady stress sweep tests

Chemical analysis showed that *Mastocarpus stellatus* is essentially a κ-ι hybrid carrageenan, whereas *Gigartina Pistillata* is from the λ type.

Preliminary rheological studies indicate that *Mastocarpus stellatus* solution viscosity is very similar to the one exhibited by a standard κ-carrageenan of food grade as far as concentrations below the macromolecular overlap are concerned. Above the overlap concentration, flow curves show similarities, the concentration dependence of the zero shear viscosity being different, as a result of possible different macromolecular interactions due to different carrageenan compositions.

1. INTRODUCTION

Carrageenans are natural polysaccharides extracted from certain families of red seaweeds. Their ability to form salt or cold setting reversible gels at low concentration in water, explains the extensive use of these polyelectrolytes in the formulation of food products or pharmaceuticals. During the last few years, the total carrageenan market showed a grow rate of 3% per year reaching an estimated world wide sales of US$ 310 millions in 2000. Therefore, there is an increasing industrial interest in finding new seaweed sources of carrageenan in order to supply the natural texturing agent market with a constant product quality.

In the frame of a project aiming at engineering new *green* edible films for food coatings and packaging, the potential use of seaweeds collected on the Portuguese coast as a source of natural thickening and gelling agents has been screened. After an estimation of the availability on the northern Portuguese coast of specific seaweed families known for their polysaccharide content, two specific algae retained our attention, namely the *Mastocarpus stellatus* and the *Gigartina pistillata*. These algae can be chemically treated for the extraction of κ and ι carrageenan mixtures of industrial quality, that is to say, with good enough gelling and solution thickening properties. This report will therefore present the preliminary results of a chemical and rheological study of the polysaccharides extracted from *Mastocarpus stellatus* and *Gigartina pistillata* specimen.

2. EXPERIMENTAL

Seaweed sampling and extraction

Mastocarpus stellatus and *Gigartina pistillata* specimen were collected in February and May 2004 at Vila Praia de Ancora. (see figure 1). Right after sampling, seaweeds were washed several times with tap water and dried at 60ºC for 48 hours in a ventilated oven. An alkali pre-treatment (200g dried algae in 0.1M Na_2CO_3 at room temperature) was performed during 48 hours in order to likely convert the biological precursor μ-carrageenan into κ-carrageenan. Extraction (40g dried alga in 4 litres tap water) was performed at 95ºC during 2 hours at pH 8.5. The extract was then filtered with metallic screens followed by cotton clothes, prior to water evaporation performed at 60ºC. The resulting concentrated extract was then precipitated in ethanol (95%). The recovered polysaccharide was then filtered and washed with further ethanol, and cleaned by a freezing (-22ºC) and thawing process. Finally, the product was dried at 60ºC and under vacuum until constant weight was reached.

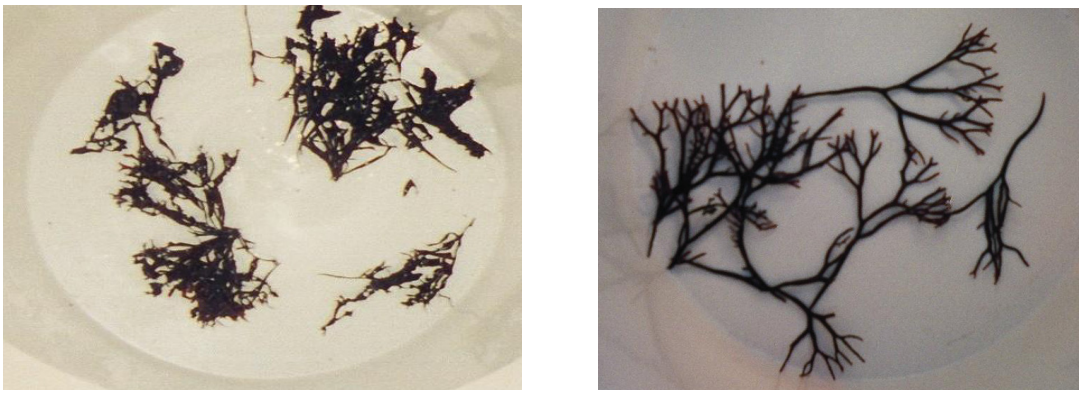

Figure 1. Snapshots of collected Mastocarpus stellatus (left) and Gigartina pistillata (right).

Diffuse Reflectance Infrared Fourier Transform spectroscopy (DRIFT).

Powders obtained as described above were directly inserted in a DRIFT spectrometer (Nicolet 510P) under nitrogen environment, and spectra were recorded between 400 and 1400 cm-1.

Rheological measurements

Rheological measurements were performed at 25ºC with a controlled stress rheometer AR2000 (TA Instruments, Delaware, USA) fitted with a 40 mm diameter cone and plate geometry (angle 4º). Before performing the experiments, powders were diluted in distilled water and strongly agitated for 2 hours at 60ºC. Then, the non water soluble material was separated from the soluble polysaccharide by centrifugation (20ºC, 20 000g for 25 minutes). Finally, the water-polysaccharide mixtures were gently evaporated under vacuum to reach the desired solution concentration.

Intrinsic viscosity was measured at 25ºC in 0.1M NaCl with a capillary Ubbelhode rheometer. NaCl solutions were prepared by direct mixing of the extracts powders and solvent at 60ºC for 2 hours, followed by centrifugation (20ºC, 20000g for 25 minutes).

3. RESULTS AND DISCUSSIONS

Chemical composition of polysaccharides.

Figure 2 shows the infrared spectrum of the polysaccharide extracted from *Gigartina pistillata*, together with model commercial carrageenan (Sigma-Aldrich) samples. The latter are called model carrageenans, since these products are virtually made of one single type of

polysaccharide. As such they can serve as standards, which will help in assigning the absorption bands to one specific carrageenan type. Focusing on the 700 to 800 cm-1 range, it can be seen that the spectrum from *Gigartina pistillata* is rather similar to the one from a λ-carrageenan. It is worth mentioning that no peak in resolved in this spectral range, which is opposite to the spectral pattern displayed by both ι- and κ-carrageenan samples. From Figure 2 we can therefore conclude that the polysaccharide extracted from *Gigartina pistillata* is essentially a λ-carrageenan. This result is in agreement with earlier reports [1] on similar seaweed collected on the northern Portuguese cost during the winter time, the latter season corresponding to the tetrasporic stage of the seaweed.

Figure 3 displays the DRIFT spectra of 2 *Mastocarpus stellatus* powders extracted from seaweeds collected in the early spring (top) and in winter (second from top), together with the model carrageenans. In the 700 to 800 cm-1 range, no broad absorption is seen. Instead, 3 peaks are resolved, together with 2 absorption bands at 850 and 932 cm-1. These bands indicate that the polysaccharide extracted from *Mastocarpus stellatus* is a mixture of *k*- and *i*-carrageenan units. Literature is now well documented with clear evidence that carrageenophyte seaweeds produce polysaccharides possessing sequences of *k*-type carrageenan alternating with sequences of *i*-type carrageenan [2], rather than mixtures of *k*-carrageenan polymers with *i*-carrageenan polymers. A DSC study performed on hydrated powder extracts and is currently conducted in our laboratory, in order to confirm this issue. No seasonal effect on the carrageenan type obtained from Mastocarpus stellatus can clearly be evidenced from the spectra of figure 3. Earlier studies [1] suggested that the degree of κ-ι hybridisation was in fact sensitive to season. In our case, ^{13}C NMR spectra are required to confirm this issue, as well as further seasonal sampling.

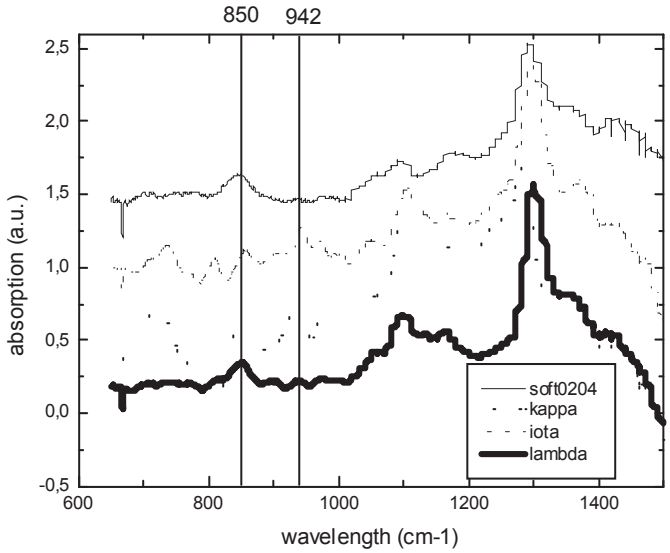

Figure 2. From top to bottom: infrared spectra of the polysaccharide extracted from Gigartina pistillata, a model k-carrageenan, a model i-carrageenan and a model l-carrageenan.

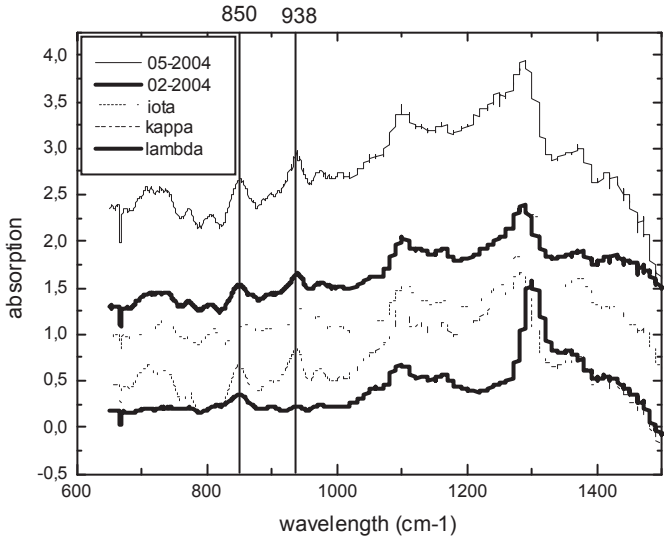

Figure 3. From top to bottom: infrared spectra of Mastocarpus stellatus polysaccharides obtained in May and February, of i-carrageenan, k-carrageenan and l-carrageenan

Rheological behavior.

Figure 4 presents the concentration dependence of the scaled specific viscosity η_{sp} of the polysaccharide extracted from *Mastocarpus Stellatus* sample collected in February 2004, and measured in 0.1 M NaCl solutions at 25ºC. The intrinsic viscosity of this polysaccharide can be estimated from the extrapolation to zero concentration of η_{sp}., thus giving $[\eta]$ = 1.91 ± 0.3 g/dl.

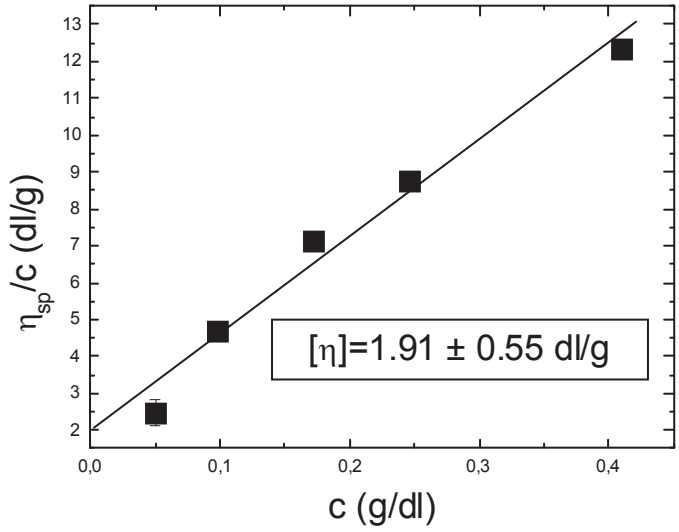

Figure 4. Concentration dependece of the specific viscosity measured at 25ºC in 0.1M NaCl solutions of carrageenan extracted from *Mastocarpus stellatus*.

Inserting $[\eta]$ in the Mark-Houwink equation and using the constants usually reported in the literature [3] for κ-carrageenan polymers in 0.1M NaCl at 25ºC (which basically means that this polysaccharide adopts a coil conformation in this solvent), we end up with a viscosity

average molecular weight of roughly $1x10^4$ g/mol. The latter is two orders of magnitude smaller than the molecular weight of molecules used in the industry.

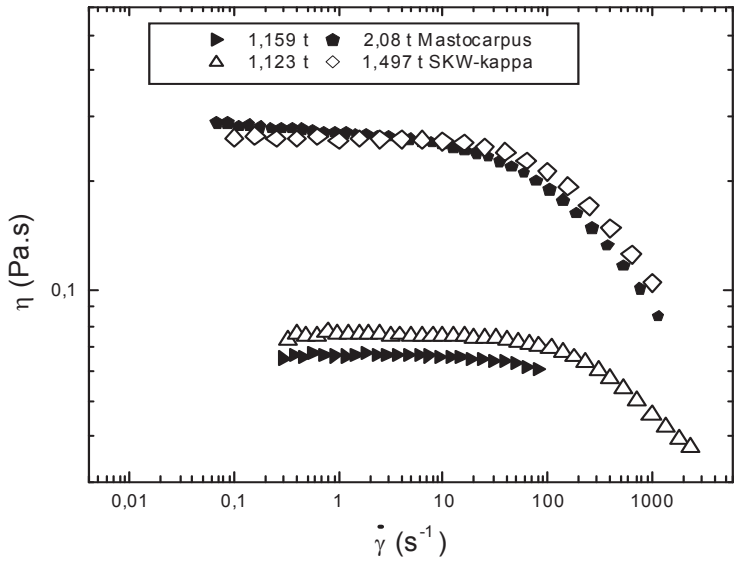

Figure 5. Shear rate dependence of the steady state viscosity for water solutions of food grade κ-carrageenan (open symbols) and carrageenan ectracted from *Mastocarpus stellatus* (solid symbols).

The determination of $[\eta]$ also allows for an estimation of the overlap concentration in water, which separates the dilute regime from the semi-dilute regime. For that estimation, The Einstein relationship $c^* = (2.5/[\eta])x100$ (in % w/v) is to be used, together with the further assumption that carrageenan polymers adopt a coil conformation in water. Doing that, we end up with c^*=1.3 % wt.

Figure 5 displays the flow curves obtained with stepped stress sweeps performed on water solutions of carrageenan extracted from *Mastocarpus stellatus* and κ-carrageenan of food grade. Each step stress was applied during 15 sec before the record of the corresponding viscosity. It has been checked that this duration is long enough to insure steady state flow. Increasing the stress or decreasing the stress resulted in identical flow curves, which indicates that the solutions did not show any thixotropic behaviour, even at the highest concentration measured (3.3 %wt, data not shown). The flow curves show a Newtonian behaviour at low shear rates, followed by a shear thinning characterised at higher shear rates by a power low behaviour which depends on the concentration. Results indicate that beside the different concentration dependence of the zero shear viscosity (see figure 6), both carrageenan samples show fairly similar flow curves. The flow curves of the two food grade k-carrageenan solutions do not superimpose, which suggests that these concentrations belong to two different concentration regimes. The carrageenan extracted from *Mastocarpus stellatus* mainly differs from an industrial κ-carrageenan in the concentration dependence of the zero viscosity.

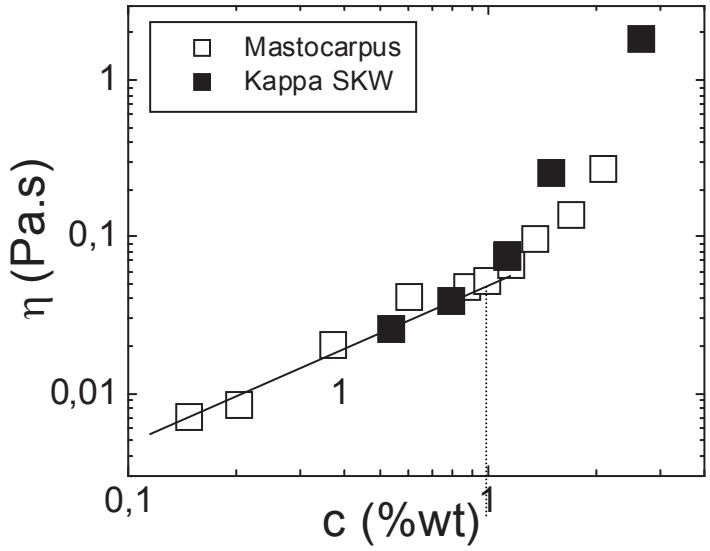

Figure 6. Concentration dependence of the zero shear viscosity obtained at 25ºC from stress sweeps similar to the ones shown in figure 5. Open symbols: food grade κ-carrageenan; solid symbols: carrageenan *from Mastocarpus stellatus*.

Figure 6 illustrates this point. First we note that in the low concentration regime (materialised by a slope 1 in order to indicate a dilute regime), both carrageenans show similar viscosity values. However, the high concentration regime underlines the difference between the 2 types of macromolecules, which are now overlapping. The food grade κ-carrageenan shows a steeper concentration dependence of the viscosity, thus justifying its use for industrial applications as a thickener. On the other hand, the carrageenan extracted from *Mastocarpus stellatus* shows a smoother concentration dependence, which can be partially explained by the rather small molecular weight of the macromolecules, when compared to industrial ones. Finally, we note that the 3 last data points for *Mastocarpus stellatus* sample are off the line with slope 1, and do not seem to follow a power law. These data therefore suggest that a) a polydispersity in the molecular weight of these macromolecules could be at the origin of a non power law behaviour, and b) the dilute regime ends at a concentration that can be materialised by the vertical dashed line, the latter hitting the x axis at roughly c=1.3 %wt. This results nicely matches the overlap concentration c^* extrapolated from the intrinsic viscosity measurements.

3. Results and discussion

The preliminary results presented here should be augmented by light scattering molecular weight determination, NMR spectroscopy measurements, further seasonal sampling and viscoelastic characterisation of the extracted polysaccharides, in order to screen the potential industrial applications of the carrageenans extracted from Portuguese seaweed. The extraction process will be optimised, mainly with a better alkaline pre-treatment and a softer extraction process to allow for the production of carrageenan mixtures with higher molecular weights. This is the condition for obtaining products with better thickening properties.

ACKNOWLEDGEMENTS

This work received financial support from Fundação para a Ciência e a Tecnologia (Project POCTI/2002/EQU/45595).

REFERENCES

[1]. Pereira, L. and Mesquita, J.F. (2003). Carrageenophytes from occidental Poertuguese coast: 1-spectroscopic analysis in eight carrageenophytes from Buarcos bay. *Biomolecular Engineering*, 20, 217-222.

[2]. Van de Velde, F., Peppelman, H.A., Rollema, H.S. and Tromp, R.H. (2001).On the structure of k/i-hybrid carrageenans. *Carbohydrate research*, 331, 271-283.

[3]. Andrade, C.T., Azero, E.G., Luciano, L., Gonçalves, M.P. (2000). Rheological properties of mixtures of k-carrageenan from Hypnea musciformis and galactomanan from Cassia javanica. *International Journal of Biological Macromolecules,* 27, 359-353.

RHEOLOGICAL CHARACTERIZATION OF OIL-IN-WATER PEA PROTEIN-STABILIZED EMULSIONS WITH ADDED LUTEIN AND PHYCOCYANIN

Ana Paula Batista[1]; Isabel Sousa[2]; José Empis[3], José Maria Franco[4], Anabela Raymundo[1].

[1]Centro de Investigação de Eng.ª Alimentar e Biotecnologia. Instituto Piaget – ISEIT de Almada. Quinta da Arreinela de Cima, 2800-305 Almada, Portugal. Tel: +351 21 294 62 69; Fax: +351 21 294 15 84. pbatista@almada.ipiaget.org; araymundo@almada.ipiaget.org.
[2]Secção de Ciência e Tecnologia dos Alimentos / DAIAT – Instituto Superior de Agronomia. Tapada da Ajuda, 1349-017 Lisboa, Portugal. isabelsousa@isa.utl.pt.
[3]Centro de Engª Biológica e Química – Instituto Superior Técnico. Av. Rovisco Pais, 1049-001 Lisboa, Portugal. jempis@iniap.min-agricultura.pt.
[4]Universidad de Huelva, Faculdad de Ciências Experimentales, Departamento Ingeniería Química. Campus del Carmen, 21071 Huelva, Spain. franco@uhu.es.

Keywords: Emulsions, pea-protein, lutein, phycocyanin, microstructure

1. Introduction

Animal proteins from eggs and milk can be replaced in several food products by using vegetable proteins from leguminous seeds, which present some additional advantages, such as: (i) no cholesterol, (ii) positive agricultural impact and (iii) expectable superior microbiological quality. Several vegetable proteins from soy [1-2], lupin [3-4], pea [5-6], sunflower [7] or tomato seed [8] have been tested successfully to stabilize oil-in-water (o/w) emulsions, due to their capacity to reduce the interfacial tension between hydrophobic and hydrophilic components.

Lutein is an orange xantophyll found in green leaf vegetables. Besides its colouring action, there has been growing evidence that the consumption of lutein can reduce the incidence of eye related diseases like age-related macular degeneration (AMD) and cataracts [9], and certain types of cancer. These effects result from the previously reported anti-oxidant effect of lutein.

Phycocyanin is a blue photosynthetic pigment extracted from cianobacteria. It is an hydrophilic phycobiliprotein composed by an apoprotein linked to coloured prosthetic groups (tetrapyrrolic chromofores). This pigment is widely used as a fluorescence marker in clinical diagnosis, and also as colouring in the pharmaceutical and cosmetics industry. The application of phycocyanin in food products has been studied [10] and antioxidant action has been detected [11] in vitro.

The addition of lutein and phycocyanin to the oil and aqueous phases, respectively, of oil-in-water pea protein stabilized-emulsions was studied. The emulsions were characterised in terms of linear viscoelastic behaviour and flow behaviour. These rheological measurements were monitored with the microscope (optical analysis system) coupled to the Rheometer equipment (RheoScope, Haake, Germany), in order to access the structural modifications that occur under different shear stresses. Droplet size distribution measurements were also performed. Evolution of colour parameters (L*a*b*) over time was previously reported [12]. The phycocyanin emulsions presented blue tonalities, while lutein promoted orange colours and using mixtures of both pigments resulted in a range of green hues.

2. Materials and Methods

Oil-in-water emulsions were prepared with 65% (w/w) vegetable oil, 32% (w/w) deionised water and 3% (w/w) pea protein isolate (Pisane HD, Cosucra, Belgium). The protein isolate was dispersed in the water under magnetic stirring (30 min, at room temperature) and emulsification was carried out using an Ultra Turrax homogenizer (T-25, IKA, Germany), at 13000 rpm, 5 min [3]. Phycocianin protein, obtained from *Arthrospira maxima* (INETI-DER, Portugal) and lutein (FloraGlo, Kemin Foods, USA) were dissolved in the aqueous and oil phases respectively. Emulsions containing different concentrations of lutein and phycocianin

(0,25-1,25% w/w) were prepared, as well as emulsions with mixtures of both pigments, in different proportions (0,50% w/w total pigment).
The rheological measurements were performed in a Rheoscope rheometer coupled with an optical microscope and a digital video camera integrated under the temperature controlled base plate (Thermohaake, Germany). Samples were covered with a layer of paraffin oil, to prevent moisture loss.
Oscillatory tests were performed using a cone and plate system (C35/2) in a frequency range of 0.001 – 100 Hz, using stress values comprised in the linear viscoelastic region for each emulsion (4-20 Pa). The Plateau modulus (G^0_N) estimated as the value of G' for the minimum value of the loss tangent ($\tan\delta = G''/G'$) was the parameter used to compare emulsions. For steady-state flow measurements, a serrated parallel plate system was used (pp20), in order to overcome the slip effect [13]. Viscosity *versus* shear stress curves were performed using a logarithmic ramp of stresses increasing in 30 min from 0.1 to 2000 Pa. The comparison of the flow curves resulted from the adjustment of the Carreau model:

$$\eta = \eta_0 / [1 + (\dot{\gamma}/\dot{\gamma}_c)^2]^s \quad (1)$$

Where η_0 is the limiting viscosity for the first newtonian region, $\dot{\gamma}_c$ is the critical shear rate for the onset of the shear-thinning behavior and s is a parameter related to the slope of this region.
Droplet size distribution measurements were carried out in LASER light scattering equipment (Mastersizer-X, Malvern, UK). Values of the Sauter mean diameter [14], which is inversely proportional to the specific surface area of droplets, were obtained as follows:

$$d_{sv} = \sum n_i d_i^3 / \sum n_i d_i^2 \quad (2)$$

Where n_i is the number of droplets with a diameter d_i.
The results were analysed in terms of ANOVA – *Post Hoc Comparisons*, Sheffé contrast test $p<0,05$, using the program STATISTICA from StatSoft, version 5.0.

3. Results and Discussion

The use of natural pigments promoted significant modifications on the rheological behaviour of oil-in-water pea protein-stabilized emulsions. The effects were distinct according to the nature of the pigment, particularly the affinity to the aqueous or to the oil phase, and are in agreement with texture parameters determined in previous studies [15].
The addition of lutein to the oil phase of the emulsions resulted in a significant ($p<0.05$) decrease of the rheological parameters as can be observed in table 1. Although, no significant differences were found when varying the lutein content. The effect of adding lutein, on droplet size diameter was less pronounced, being observed small variations on d_{sv} values. Lutein is dispersed within the oil droplets, but due to the presence of 2 terminal hydroxyl groups it could present some interfacial activity. However, at constant emulsionant (pea protein) concentration (3%), only a small variation on d_{sv} was observed, which indicates that the major role at the interface is played by the protein.

Table 1: Results of the rheological parmeters and d_{sv} values of o/w emulsions containing lutein (mean ± standard deviation of 5 determinations)*.

Lutein (% w/w)	G^0_N (Pa)	η_0 (kPa.s)	s ($Pa.s^2$)	γ_c ($s^{-1}*10^{-4}$)	d_{sv} (μm)
0.00	850 ± 17 [a]	197 ± 22 [a]	0.47 ± 0.02 [a]	6.3 ± 1.5 [a]	2.23 ± 0.40 [a]
0.25	329 ± 60 [b]	32 ± 10 [b]	0.39 ± 0.02 [b]	3.6 ± 1.2 [a]	2.42 ± 0.23 [ab]
0.50	331 ± 58 [b]	44 ± 4 [b]	0.40 ± 0.01 [b]	3.0 ± 1.0 [a]	3.18 ± 0.03 [c]
0.75	393 ± 95 [b]	15 ± 4 [b]	0.38 ± 0.01 [b]	6.3 ± 2.7 [a]	2.90 ± 0.09 [bc]
1.00	294 ± 19 [b]	25 ± 9 [b]	0.39 ± 0.01 [b]	4.4 ± 1.2 [a]	3.21 ± 0.52 [c]
1.25	380 ± 101 [b]	20 ± 3 [b]	0.39 ± 0.03 [b]	5.6 ± 2.7 [a]	2.15 ± 0.30 [a]

*Means in the same column with different letters are significantly different ($p<0.05$).

On the other side, emulsions with phycocyanin presented improved rheological characteristics (Table 2). It can be observed that the G^0_N and η_0 values increased linearly and significantly ($p<0.05$) with pigment concentration.

Phycocianin was added to the aqueous phase, but due to its protein nature, presents an amphiphilic character, being able to lower the tension at the oil-water interface [16]. The presence of different types of proteins in oil-in-water emulsions might lead to a synergistic interaction, providing an improvement in the quality of the final product [17] by reinforcing the protein layer or to a decrease in the emulsion stability, due to the formation of weaker and more disordered mixed interfacial layers [18], due to thermodynamic incompatibility or to competitive adsorption.

It was observed, for higher phycocianin concentrations (>0.75%), a steep increase of the d_{sv} values which should be related with interfacial destabilization mechanisms. However, the rheological characteristics continued to improve, which is probably related to an increase on the viscosity of the continuous phase due to the presence of important amounts of unadsorbed proteins and to the formation of supramolecular entanglements among protein molecules, adsorbed and non-adsorbed at the interface [19].

Table 2: Results of rheological parmeters and d_{sv} values of the o/w emulsions containing phycocyanin (mean ± standard deviation of 5 determinations)*.

Phycocyanin (% w/w)	G^0_N (Pa)	η_0 (kPa.s)	s ($Pa.s^2$)	γ_c ($s^{-1}*10^{-4}$)	d_{sv} (μm)
0.00	850 ± 17 [a]	197 ± 22 [a]	0.47 ± 0.02 [a]	6.3 ± 1.5 [a]	2.23 ± 0.40 [a]
0.25	867 ± 236 [a]	230 ± 44 [ab]	0.46 ± 0.02 [a]	3.5 ± 1.1 [a]	3.40 ± 0.05 [b]
0.50	1297 ± 139 [ab]	370 ± 31 [bc]	0.46 ± 0.01 [a]	4.7 ± 1.4 [a]	2.59 ± 0.20 [c]
0.75	1493 ± 146 [ab]	380 ± 71 [cd]	0.45 ± 0.00 [a]	3.2 ± 0.4 [a]	2.18 ± 0.17 [a]
1.00	1833 ± 189 [b]	487 ± 40 [cd]	0.47 ± 0.01 [a]	3.8 ± 0.7 [a]	3.14 ± 0.10 [b]
1.25	1863 ± 248 [b]	504 ± 37 [d]	0.47 ± 0.01 [a]	4.7 ± 0.7 [a]	5.58 ± 0.06 [d]

*Means in the same column with different letters are significantly different ($p<0.05$).

For the emulsions containing both pigments the rheological parameters have increased significantly ($p<0.05$) with phycocyanin proportion (Table 3). A synergistic effect between both pigments can be observed, since the emulsions without lutein presented lower G^0_N, η_0 and s values, than the emulsions with 25 and 40% lutein. In terms of the d_{sv} values, small variations were observed.

Table 3: Results of rheological parmeters and d_{sv} values of the o/w emulsions with 0.5% (w/w) of phycocianin and lutein in different proportions (mean ± standard deviation of 5 determinations)*.

Phycocyanin (P) and lutein (L) proportion	G^0_N (Pa)	η_0 (kPa.s)	s ($Pa.s^2$)	γ_c ($s^{-1}*10^{-4}$)	d_{sv} (μm)
100%P : 0%L	1297 ± 139 ^{ac}	370 ± 31 ^{ab}	0.46 ± 0.01 ^{a}	4.7 ± 1.4 ^{a}	2.59 ± 0.20 ^{ab}
75%P : 25%L	2110 ± 152 ^{b}	499 ± 63 ^{a}	0.48 ± 0.01 ^{a}	5.4 ± 0.2 ^{a}	2.83 ± 0.12 ^{a}
60%P : 40%L	1750 ± 408 ^{ab}	442 ± 71 ^{a}	0.47 ± 0.01 ^{ab}	5.7 ± 1.3 ^{a}	2.74 ± 0.06 ^{a}
50%P : 50%L	972 ± 144 ^{cd}	307 ± 14 ^{bc}	0.45 ± 0.01 ^{bc}	3.3 ± 0.6 ^{a}	2.78 ± 0.12 ^{a}
40%P : 60%L	864 ± 39 ^{cde}	215 ± 18 ^{cd}	0.44 ± 0.01 ^{bc}	2.4 ± 0.2 ^{a}	2.39 ± 0.09 ^{b}
25%P : 75%L	651 ± 36 ^{de}	125 ± 21 ^{de}	0.43 ± 0.01 ^{c}	2.8 ± 0.6 ^{a}	2.63 ± 0.04 ^{ab}
0%P : 100%L	331 ± 58 ^{e}	44 ± 4 ^{e}	0.40 ± 0.01 ^{d}	3.0 ± 1.0 ^{a}	3.18 ± 0.03 ^{c}

*Means in the same column with different letters are significantly different ($p<0.05$).

The use of the Rheoscope equipment, combining both rheological and microscope techniques has revealed to be an interesting tool to access the microstructure modifications undergone by the emulsion systems under shear stress.

In Figures 1 to 4, the steady-state flow curves of selected emulsions (control, 0.75% lutein, 0.75% phycocyanin and 50%P:50%L, respectively) are represented. Microscopic photographs of the emulsions, under different shear rates, were associated with certain points of the curves.

All the emulsions studied presented a shear thinning behaviour with a zero-shear rate limiting-viscosity (η_0) at very low shear rates ($\dot{\gamma}$). The shear thinning region is a consequence of a dramatic shear-induced structural breakdown, related to a mechanism of oil droplet deflocculation, as previously reported for other concentrated food emulsions [3].

From Figures 1 to 4, the differences on the emulsions microstructure can be clearly observed, when within the Newtonian region, at low shear rates, and within the shear thinning region.

For the control and lutein emulsions the photographs are more explicit since they are more fluid and easier to see under the microscope. Besides that, these two emulsions presented a narrow Newtonian region, making it possible to obtain various points within the shear-thinning region, corresponding to different shear rates.

The phycocyanin and mixed pigments emulsions were very consistent and opaque, being difficult to obtain accurate microscopic measurements. Nevertheless, it is also clear the microstructural transition from the Newtonian to the shear-thinning region from the photographs presented on figures 3 and 4. These emulsions presented a large Newtonian plateau, where small microstructure variations are observed. For a certain critical shear rate value, a rupture occurred, leading to an abrupt decrease of the apparent viscosity.

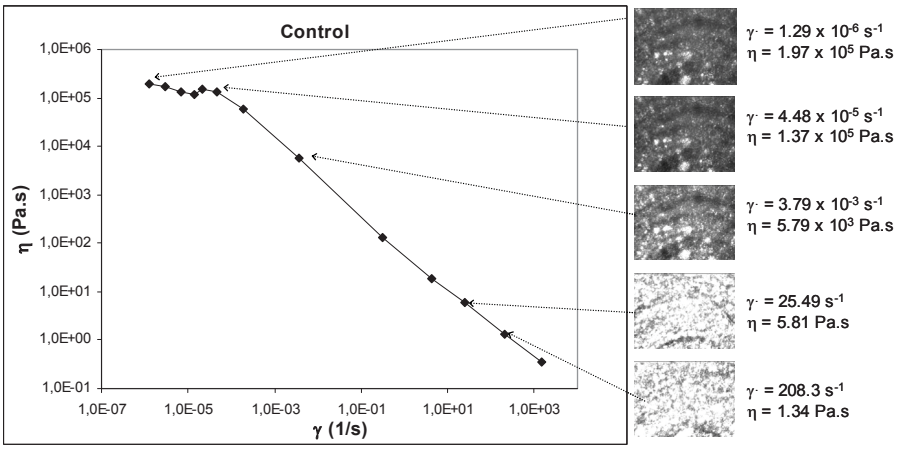

Figure 1. Steady-state flow curve of a o/w emulsion without pigment addition, and microscope photographs taken at different shear rates.

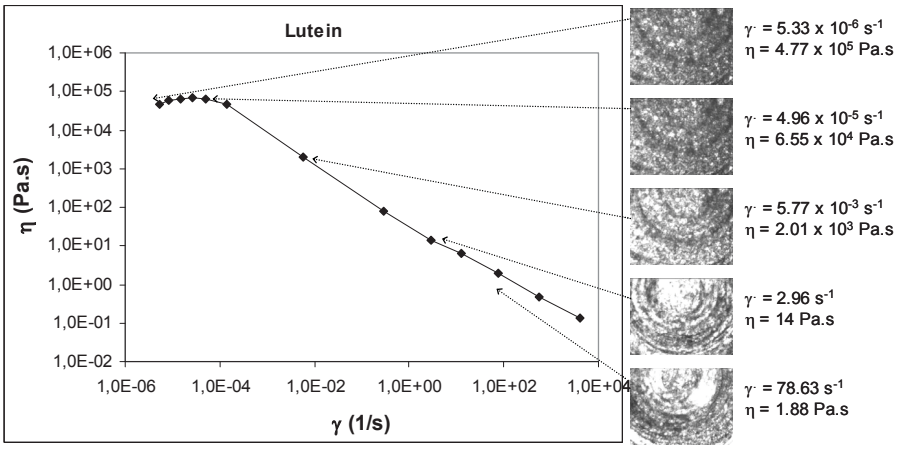

Figure 2. Steady-state flow curve of a o/w emulsion with 0.75% lutein addition, and microscope photographs taken at different shear rates.

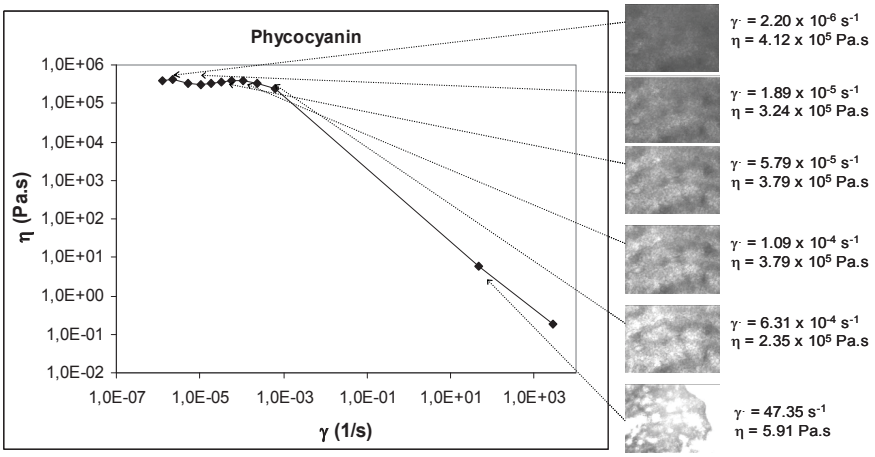

Figure 3. Steady-state flow curve of a o/w emulsion with 0.75% phycocyanin addition, and microscope photographs taken at different shear rates.

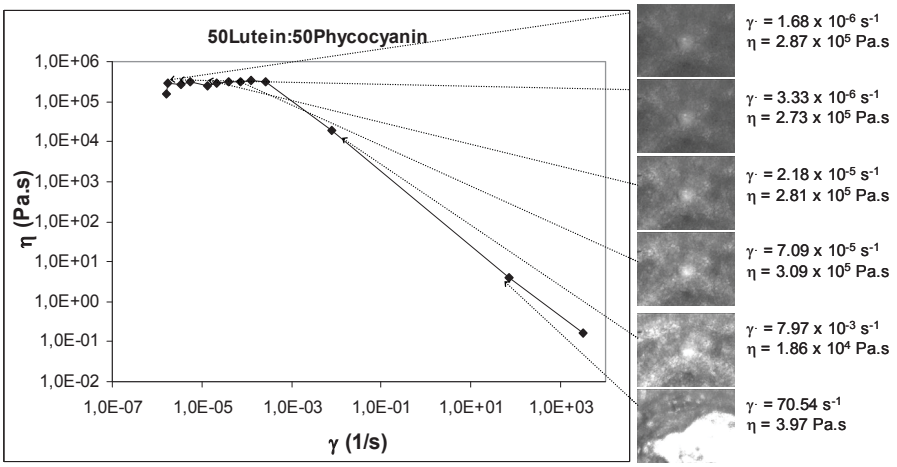

Figure 4. Steady-state flow curve of a o/w emulsion with 0. 50% total pigment (lutein and phycocyanin emulsions in the same proportion), and microscope photographs taken at different shear rates.

In terms of oscillatory dynamic measurements, monitoring the emulsions microscopic images under different frequency values, did not present significant changes, since these tests were performed within the linear viscoelastic region of stresses for each emulsion. In fact, the photographs of the emulsions, along the whole frequency range studied, are similar to the photographs corresponding to the first points of the flow curves (at very low shear rates) (Figures 1-4), and for this reason they are not represented.
Nevertheless, in Figure 5, the mechanical spectra of selected emulsions with phycocyanin (0.75%), lutein (0.75%), both pigments (50:50) and the control are presented. The linear viscoelastic behaviour shown by these emulsions is typical of protein-stabilized emulsions in which an elastic network develops due to the occurrence of an extensive bridging flocculation process [3]. The storage modulus (G') was always higher than the loss modulus (G") in the frequency range studied, and the evolution of G' with frequency shows a tendency to the development of a plateau region, followed by a minimum in G". The emulsion with phycocyanin, and with a mixture of both pigments presented higher values for the viscoelastic functions than the control; while lutein emulsion presented much smaller values.

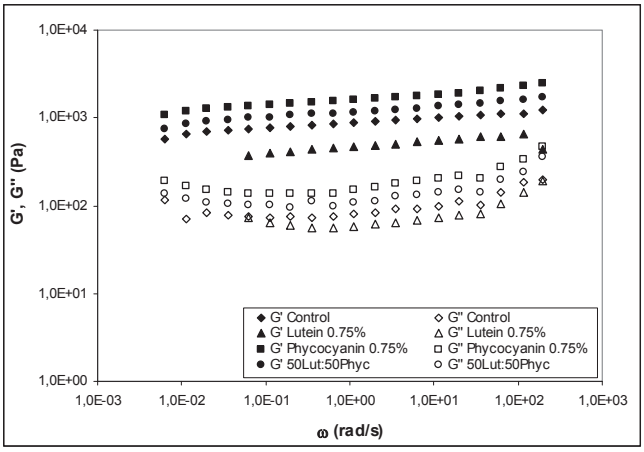

Figure 5. Mechanical spectra of o/w emulsions with phycocyanin, lutein, and a mixture of both pigments (and a control withouth pigment addition).

Aknowledgements

The authors thank PhD Alberto Reis (INETI-DER) for the phycocianin production; Profs. Joana Neiva Correia and Jorge de Carvalho for permitting the use of Malvern Mastersizer equipment (DQ/IST/UTL) and Eng. Remígio Machado for technical support. We also thank Cosucra and Kemin for providing the pea protein and lutein samples, respectively.

References

[1] Eliazalde, B.E.; Bartholomai, G.B.; Pilosof, A.M.R. (1996). *Lebensm. Wiss. Technol*,(29) :334-339.
[2] Roesch, R.R.; Corredig, M. (2002). *Journal of Food Science*, 67(8): 2837-2842.
[3] Franco, J.; Raymundo, A.; Sousa, I.; Gallegos, C. (1998). *Journal of Agric. Food Chem*., (46): 3109-3115.
[4] Raymundo, A.; Franco, J.M.; Empis, J.; Sousa, I. (2002). *J. Am. Oil Chem. Soc*., (79): 783-790.
[5] Bogracheva, T.; Davydova, Y.; Bespalova, N.Y.; Kondrashina, M.G.; Bezrukov, E.E.; Tolstoguzov, V.B. (1994). *Nahrung*, (2): 121-127.
[6] Tomoskozi, S.; Lasztity, R.; Haraszi, R.; Baticz, O. (2001). *Nahrung Food*, 45(6): 399-401.
[7] Rossi, M.; Pagliarini, E.; Pegri, E. (1985). *Ibid*., (18): 293-299.

[8] Velev, D.O.; Nikolov, A.D.; Denkov, N.D.; Doxastakis, G.; Kiosseoglu, V.; Stadilidis, G. (1993). *Food Hydrocolloids*, (1): 55-71.
[9] Richer, S. (2001). *Journal of the American Nutraceutical Asociation*, 4(2): 6-24.
[10] Shoten, K.K.S.; Kogyo, D.I.K. (1981). *Method for food coloring*, Japanese Patent, 56,005,143.
[11] Romay, C.H.; Armesto, J.; Remirez, D.; Gonzalez, R.; Ledon, N.; Garcia, I. (1998). *Inflamm Res*, 47, 36-41.
[12] Raymundo, A.; Osório, N.; Reis, A.; Sousa, I.; Empis, J. (2002). *Functionalities of pigments in food – Conference Proceedings*. Sociedade Portuguesa de Química Publ .Lisbon, Portugal. (ISBN 972-960-65-8-7).
[13] Franco, J.M.; Gallegos, C.; Barnes, H.A. (1998). *J. Food Eng.*, 36, 89-102.
[14] Sprow, F.B. (1967). *Chem. Eng. Sci.*, 22, 435-442.
[15] Batista, A.P.; Raymundo, A.; Sousa, I.; Empis, J. (2004). *Third International Congress on Pigments in Food – more than colours*. Ed. L. Dufossé. Pág.: 118-120. Quimper, França. ISBN: 2-9521516-0-1.
[16] Chronakis, I.S.; Galatanu, A.N.; Nylander, T.; Lindman, B. (2000). *Colloids & Surfaces A*, 173, 181-192.
[17] Clark, D.C.; Wilde, P.J.; Wilson, D.R.; Wustneck, R. (1992). *Food Hydrocolloids*, 6, 173-186.
[18] Imm, J.Y.; Regenstein, J.M. (1997). *J. Food Sci.*, 62, 967-975.
[19] Riscardo, M.A.; Franco, J.M.; Gallegos, C. (2003). *Food Sci. Tech. Int.*, 9(1), 53-63.

PHYSICOCHEMICAL AND MICROBIOLOGICAL CHARACTERISATION OF SHAMPOOS CONTAINING DIFFERENT SURFACTANTS, THICKENING AGENTS AND PRESERVATIVES

*A. Raposo, V. Grilo, M. Lopes, H. M. Ribeiro**

UCTF - Faculdade de Farmácia da Universidade de Lisboa
Av. Forças Armadas, 1600 Lisboa, Portugal
Tel: 00.351.217 946 400; Fax: 00.351.217 937 703
helena.ribeiro@ff.ul.pt

Introduction: A shampoo is a product generally made available as a liquid, gel or cream that is formulated using a surface active agent and displays detergent, wetting, emulsifying, and foaming properties, thereby ensuring cleaning the hair, while leaving it soft, supple, lustrous and easy to manage. The error is often made of thinking that good foaming and detergent properties suffice to formulate a perfectly satisfactory shampoo. However, good shampoos must clean and must have aesthetic appeal combined with safety and mildness in use[1, 2].
Cleansing is a function of the primary surfactant. To be an effective cleansing agent the surfactant system must work quickly at a relatively low temperature. It must be effective in hard and soft water, be able to remove lipids and other soils and residues left after previous hair treatments and it must not leave any residues of its own. It must be non-toxic and reasonably non-irritant to skin and eyes. Foam is also a function of the primary surfactant and few materials. Additional materials may depress the foam or make it creamier and stabilise it. Dialkanolamides were the favourite for three decades.
Viscosity is an important aspect of shampoo formulation. Products must have sufficient viscosity to stay on the palm of the hand prior to application but must not come out of the bottle as a globular lump. Anionic systems may be thickened by the addition of electrolytes or non-ionic compounds or by betaines. Sodium chloride and cocamidopropyl betaine are the materials of common choice but others are worth consideration.

Sodium laureth sulfate is relatively inexpensive, is colourless and odourless, has good cleansing properties, gives good flash foam and forms products that are readily thickened. The foam however is relatively loose and unstable. It is irritant and leaves the hair feeling dry and with flyaway. Sulfosuccinates are a wide group of chemicals exhibiting different application properties. Disodium laureth sulfosuccinate is a typical example. They do not produce stable foams but are relatively mild and find application as secondary surfactants. The cocoamphodiacetate is used to improve mildness of the anionics, improve cleansing and lather performance.
For thirty years cocamide DEA, lauramide DEA were unassailable as the most common secondary surfactants to be used with alkyl sulfates and alkyl ether sulfates. They improve foam heights and foam stability; they are excellent solubilising agents; they assist in viscosity build and they are relatively inexpensive. The monoethanolamides, lauramide MEA and cocamide MEA are very used in hair care[3, 4].

Preservatives should inhibit the growth of mold and prevent fermentation in shampoos. However to preserve the product from microbial contamination, some materials can cause harm to the consumer. The formulators are making great efforts to keep the preservative amount necessary to the minimum [5].

The main goal of this study is to characterise the physicochemical and microbiological properties of shampoos containing different surfactants (alkyl ether sulfates and sulfosuccinates), thickening agents (cocamide MEA and sodium chloride) and preservatives (5-bromo 5-nitro 1,3-dioxane and diazolidinyl urea, methylparaben and propylparaben).

Materials and methods: Three shampoos were prepared using different concentrations of surfactants: 12:0:0 (reference); 7:5:0 (Formulation A); 6:3:3 (Formulation B), sodium laureth sulfate (Texapon N70®, Cognis, Dusseldorf, Germany), disodium cocoamphodiacetate (Rewoteric AM 2C NM ® , Degussa, Goldschmidt Ag, Germany) and disodium laureth sulfosuccinate (Rewopol SB FA 30® , Degussa, Goldschmidt Ag, Germany), as shown on table 1. Cocamide DEA (Comperlam KD®, Cognis, Dusseldorf, Germany) (3%) and sodium chloride (2%) were added as thickening agents.

Table 1: Shampoos formulations

FORMULATION	SURFACTANT sodium laureth sulfate, disodium cocoamphodiacetate and disodium laureth sulfosuccinate (%)	NaCl (%)	Cocamide DEA (%)
Reference	12:0:0	2.5	0.0
A	7:5:0	3,0	2,0
B	6:3:3	3,0	3,0

Some physical and chemical properties of the shampoos were evaluated: *pH:* A potenciometric method (Methrom Herisau, pH meter E 516) was used on shampoos; *Rheology:* A Brookfielfd viscometer (Model DVII, SSA, SPD nº 27 at 25 °C) was used to determine the apparent viscosity and the reograms; *Foam expansion*: the ratio between the volume of foam and the volume of liquid from which the foam is generated; *Percentage of active substance:* according to the NP 1204 [(6)].
Challenge tests were also conducted in several preservatives: 5-bromo 5-nitro 1,3-dioxane (Bronidox L ®, Cognis, Dusseldorf, Germany), and diazolidinyl urea, methylparaben and propylparaben (Germaben II®, ISP, Barcelona, Spain).

Results and Discussion:
All the results are shown on table 2.

Table 2. : Physicochemical characterisation of the shampoos

FORMULATIONS	APPEARANCE OF SHAMPOOS	pH*	FOAM EXPANSION (cm)*	APPARENT VISCOSITY (mPa)	% ACTIVE SUBSTANCE *
Reference	▪ Colourless ▪ Clear ▪ Fluid	3,47 (± 0,01)	2,7 (± 0,20)	2170 (± 52,3)	11 (± 0,58)
A	▪ Pale yellow ▪ Clear ▪ Thick	7,99 (± 0,02)	2,6 (± 0,35)	27400 (± 418,6)	7,0 (± 1,00)
B	▪ Pale yellow ▪ Clear ▪ Fluid	8,02 (± 0,01)	2,0 (± 0,44)	7600 (± 171,0)	8,0 (± 2,08)

*** n = 3**

The pH value for the reference was very low: 3,5. The shampoos must be as neutral as possible, so as not to interfere with ingredients of other hair care preparations. So, this data is not acceptable for shampoos and can also interfere with the preservative. The formulations made with mixed anionic surfactants (formulation A and B) reveal more acceptable values (8). The amount of foam generated by all the surfactants and the foam stabilizers was similar in all preparations while the viscosity and the reograms (figure 1) were very different. All the shampoos provided Newtonian flow curves with good reproducibility.

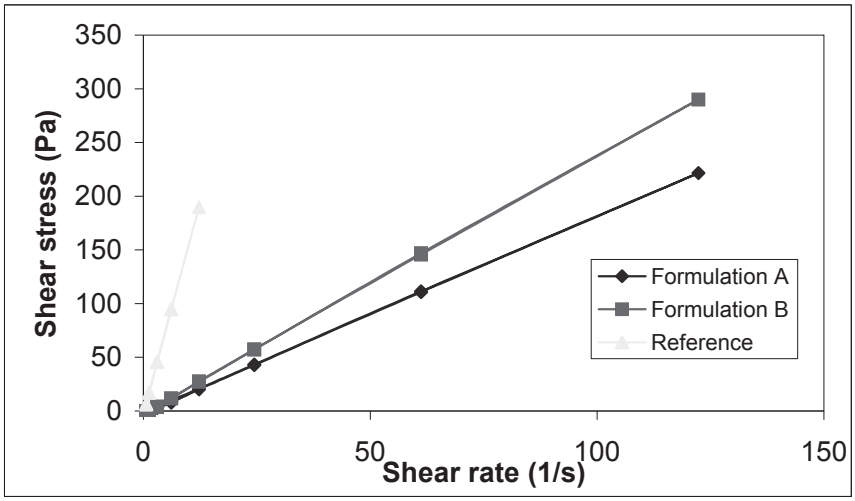

Figure 1: Shampoos' Rheograms

Viscosity is simply achieved through the addition of electrolyte, usually common salt. Salt solutions are not beneficial to hair but they may improve the cleansing power of the surfactants. However, there are other means of achieving viscosity using materials that are obviously more expensive but which confer additional benefits such as solubilising or conditioning properties. Cocamide DEA is good solubilising agent, thickening aid and foam stabiliser. Also, sensory analysis shows that consumers prefer Newtonian flow behaviour, obtained using high molecular weight thickening aids but product stability, particularly at elevated temperatures, is improved using low molecular weight additives. A combination, as it appears in formulation A and B, is therefore necessary [7,8].

The mechanisms of hair cleansing are complex. Undamaged hair has a hydrophobic surface to which lipids are strongly adsorbed. When hair is shampooed anionic surfactants are adsorbed to hair by their hydrophobic tails and the negatively charged heads orientate outwards. The fibre surface is thus wetted and non-polar materials are displaced. Semi-polar materials are solubilised into micelle structures and are removed by rinsing. Surfactants are a wide group of chemicals exhibiting different application properties. The percentage of active substance showed a variation from 8 to 11%. The daily shampoos are based on very mild anionic detergents, such as amphodiacetate and sulfosuccinate. The reference reveal the highest value which can be aggressive to the hair [2].

From the Challenge tests [9] we can conclude that both preservatives possessed the same efficacy against the standard strains. However, we should have in count not alone the preservative efficacy but also the its physical behaviour. This study reveals an elevated efficacy for both the preservatives tested, but does not permit distinguish itself this efficacy of the preservatives added to the formulations.

Table 3: Efficacy of the preservatives in the formulation A concerning the reference: **5- bromo 5-nitro 1,3-dioxane**

	Log reduction				
	0 day	**2 days**	**7 days**	**14 days**	**28 days**
Candida albicans	2	7	7	7	7
S. aureus	7	7	7	7	7
P. aeruginosa	8	8	8	8	8
A. niger	NR	8	8	8	8

diazolidinyl urea and methylparaben and propylparaben

	Log reduction				
	0 day	**2 days**	**7 days**	**14 days**	**28 days**
Candida albicans	2	7	7	7	7
S. aureus	7	7	7	7	7
P. aeruginosa	8	8	8	8	8
A. niger	NR	8	8	8	8

Table 4: Efficacy of the preservatives in the formulation B concerning the reference: 5- bromo 5-nitro 1,3-dioxane

	Log reduction				
	0 day	**2 days**	**7 days**	**14 days**	**28 days**
Candida albicans	2	7	7	7	7
S. aureus	7	7	7	7	7
P. aeruginosa	8	8	8	8	8
A. niger	NR	8	8	8	8

diazolidinyl urea and methylparaben and propylparaben

	Log reduction				
	0 day	**2 days**	**7 days**	**14 days**	**28 days**
Candida albicans	2	7	7	7	7
S. aureus	7	7	7	7	7
P. aeruginosa	8	8	8	8	8
A. niger	NR	8	8	8	8

NR: no recover

Conclusions:

The physicochemical and microbiological characterisation of these shampoos showed that all the products were acceptable. Mixed preparations of anionic surfactants (formulation A and B) were used because of their superior properties in comparison to the properties of individual surfactant (reference). In addition the shampoos A and B improved foaming and rheological properties and presented mild detergency. The efficacy of antimicrobial preservation was also performed for two preservatives.

References:

1. Barata, E., *"Cosméticos – Arte e Ciência"*, Lidel, Lisboa, (2002) 92-95.
2. Polo, K., *"A Short Textbook of Cosmetology"*, 1st ed. Verlag fur Chemische Industrie, H. Ziolkowsky GmbH, 1998, pág. 64-73
3. Mainkar, A. R., Jolly, C. I., *"Formulation of natural shampoos"*, Int.J. of Cosmetic Science, **23**, (2001),59-62
4. N. C. Christov, N. D. Denkov, P. A. Kralchevsky, K. P. Ananthapadmanabhan, A. Lips, *Synergistic Sphere-to-Rod Micelle Transition in Mixed Solutions of Sodium Dodecyl Sulfate and Cocoamidopropyl Betaine*. ,*Langmuir 20 (2004) 565-571.*
5. Baird, R. M., Bllomfielfd, S. F., *"Microbial Quality Assurance in Cosmetic, Toiletries and Non-Sterile Pharmaceuticals"*, 2ª edição, Taylor & Francis, 1996, pág. 3-187
6. Norma Portuguesa 1204, 1976
7. Duarte, A.T., Silva, L.T., Salústio, P., Ribeiro, H.M., *"Abordagem do comportamento reológico de champôs contendo diferentes espessantes"*, Ver. Port. Farm., vol. II, 1, supl 124, 2003.
8.Ribeiro, H. M., Morais, J. A., Eccleston, G. M. Structure and rheology of emulsions o/w containing different polymers, Int. J. of Cosmetic Science, 2004, **26**, 47-59
9. European Pharmacopeia, (1997), 286-287.

EFFECT OF COMPOSITION ON THE RHEOLOGICAL BEHAVIOUR AND MICROSTRUCTURE OF PEA / KAPPA – CARRAGEENAN / STARCH GELS

Nunes, M.C.[1], Raymundo, A.[2], Sousa. I.[3]*

1 – Instituto Piaget. ISEIT de Mirandela. CERTA. Avenida 25 de Abril 5370-202 Mirandela. Portugal. Phone: 351 278 200150; Fax: 351 278 265203; cnunes@mirandela.ipiaget.org
2 - Instituto Piaget. ISEIT de Almada. CIEAB. Quinta da Arreinela de Cima 2800-305 Almada. Portugal. Phone: 351 21 2946269; Fax: 351 21 2941584; araymundo@almada.ipiaget.org

3 - Secção de Ciência e Tecnologia dos Alimentos. Instituto Superior de Agronomia. Universidade Técnica de Lisboa. Tapada da Ajuda, 1349-017 Lisboa. Portugal. Phone: 351 21 3653543; Fax: 351 21 3653200; isabelsousa@isa.utl.pt

*-corresponding author

Keywords: κ-carrageenan; pea protein; rheology; texture; confocal scanning laser microscopy.

Abstract: The objective of this study was to investigate the effect of the composition on the texture properties of a mixed gel system with pea protein, κ-carrageenan and native maize starch. An experimental design based on the response surface methodology (RSM) was used. The independent variables considered were pea isolate (0-4%), κ-carrageenan (0-0.3%) and starch (0-5%). Texture variables were determined from the texture profile analysis using a texturometer. In order to understand the gelation mechanism and rheological characteristics of mixed gels, oscillatory measurements (temperature, time and frequency sweeps) were performed in a controlled stress rheometer. Confocal laser scanning microscopy (CLSM) was used to draw conclusions about the role of the biopolymers on the gel network. The results show that texture properties globally increase with pea protein, κ-carrageenan and starch content. According to rheology and CSLM, an increase in pea protein, κ-carrageenan or starch favours the mechanical gel properties as a result of complexity increase on protein/κ-carrageenan interactions and starch reinforces the structure acting as a filler.

1. INTRODUCTION

Due to recent animal diseases, there is a greater pressure for the consumption of vegetable proteins in food products. The challenge is to develop novel protein foods using plant proteins for imparting texture and appearance to the traditional animal protein based products[1-2].

Our research project aims to develop "dairy desserts"-like products in which egg and milk proteins are fully replaced by vegetable protein isolates. Although these dairy puddings already have in the market some substitutes, produced with soybean protein, their flavour and texture is not always appealing to the consumer.

Moreover, in the last decades gel research focuses more strongly on biopolymer mixtures as a result of industrial demands for new materials with specific textures[3-5].

In a recent paper[6], we have demonstrated that the gelation ability of a mixed system with pea protein, kappa-carrageenan and native maize starch can be an interesting alternative to gelled dairy desserts.

In this study, the influence of composition on the texture properties of the mixed gel with pea protein, κ-carrageenan and starch was investigated. An experimental design based on the response surface methodology (RSM) was used. The independent variables considered were hydrocolloids content: pea isolate, κ-carrageenan and native starch. Multivariate analysis of complex biopolymer systems is a useful tool to quantify the influence of the different

variables as well as interaction effects between the variables, with a reasonable small number of experiments[7-9].
Rheological properties of some gels were studied in a controlled stress rheometer by means of oscillatory measurements. How the structures were formed, was also investigated by studying the kinetics of gel formation and the consequent mechanical behaviour of the mixed gels.
The microstructures formed were described using confocal scanning laser microscopy (CSLM) and analysed in relation to the rheological properties of the mixed gelled systems.
Syneresis behaviour, a measure of water-holding ability, was measured by centrifugation as described by Xu *et al*.[7] and Aguilera & Kessler[10].

2. MATERIALS AND METHODS

Pea protein isolate (Pisane, Cosucra, Belgium), kappa-carrageenan (Satiagel AMP45, Degussa, France) and native maize starch (Vitena A, Copan, Portugal) were kindly provided by the respective manufacturers. Sucrose was commercial grade.
A central composite rotatable experimental design based on the response surface methodology (RSM) was used. The independent variables chosen were pea isolate, κ-carrageenan and starch content, tested at five levels, resulting in 15 formulations. The concentration range studied was 0-4% (w/w) for pea isolate (x_1), 0-0.30% (w/w) for κ–carrageenan (x_2) and 0-5% (w/w) for starch (x_3). Sucrose content was fixed at 15% (w/w). These bounds of variation were chosen according to the composition of commercial desserts[11] and considering practical limitations such as biopolymers solubility and the final cost of the product. Statistical analysis was performed using the software *Statistica* (version 5.1, StatSoft Inc., USA), using texture parameters as the dependent variables.
Mixed solutions (500g) were made by dispersing the dry ingredients in demineralised water, under mechanical stirring (300 r.p.m, 1h) at room temperature. The suspensions were heated to 95ºC in a thermal controlled water bath and treated at this temperature for 5 min.
For texture analysis, samples were, immediately, poured into 6 cm diameter cylindrical containers filled up to 3.5 cm height, and allowed to set at a temperature of 5-7ºC. Texture variables were determined from the texture profile analysis using a TA-XT2i (Stable Micro Systems, UK) texturometer. Penetration tests were performed with a cylindrical probe (25 mm diameter, 10 mm of penetration, 5 s of waiting time and 2 mm/s of crosshead speed). The experiments were carried out 8 days after preparation, in order to allow full maturation of the gels. Before performing any measurements, gels were allowed to equilibrate at 20ºC for approximately 3h in a temperature-controlled room. Results for each gel were determined at least three times. Firmness and adhesiveness were the most representative parameters.
Rheological measurements were performed in a controlled-stress rheometer (RS-300, Haake, Germany), using cone-plate system (35 mm, 2º). After thermal treatment, gelling biopolymer solutions were immediately loaded onto the rheometer-measuring system, which was preheated to 40ºC. Viscoelastic moduli: storage modulus G´ and loss modulus G´´, were continuously recorded as the temperature was decreasing and during maturation. The temperature was varied from 40ºC to 5ºC at 0.5ºC/min. Time sweep tests were conducted at 5ºC, during a reasonable period of time (24 or 35h), at a constant frequency of 1 Hz (6.28 rad/s). After this period, without disturbing the sample, frequency sweeps were conducted at 5ºC, with oscillation frequencies ranging from 0.01 to 115.6 rad/s. A constant shear stress within the linear viscoelastic region of the material was used in all measurements. The samples were covered with a layer of paraffin oil to prevent moisture loss.
Confocal Scanning Laser Microscopy (CSLM) was performed with a Leica Microsystems (SP2, AOBS) microscope, using 20×/0.7NA/dry/HGPL-APO and 40x/UV/1.25

NA/oil/HCXPL-APO CS objective lenses. Fluorescent probe rhodamine B was used for the non-covalent labelling of protein and starch (excitation wavelength at 568 nm and emission maxima at 625 nm). The samples were placed between a concave slide and a coverslip and sealed to prevent evaporation. After gel maturation at 5-7ºC during 48h, samples were examined at room temperature.
Gel syneresis was measured as the percentage of supernatant liquid after centrifugation of the gel. After thermal treatment, samples (around 10 g) were placed into centrifuges tubes, stored in a vertical position at 5º-7ºC for 1, 2, 3 and 4 weeks and centrifuged at 1359 × g (5ºC) using a 12111-H rotor in a *Sigma* (3K3OH, Germany) ultracentrifuge for 20 min.

3. RESULTS AND DISCUSSION

3.1. Texture

Statistical equations obtained for firmness (F) and adhesiveness (A) as function of biopolymers concentration were:

$$F\ (N) = 0.09 - 0.09\ x_1 - 1.39\ x_2 - 0.13\ x_3 + 2.08\ x_1\ x_2 + 0.07\ x_3^2 \quad (R^2 = 0.85,\ MS\ Residual = 0.03370) \qquad (1)$$

$$A\ (-N.s) = -0.22 + 0.05\ x_1 + 0.67\ x_2 + 0.05\ x_3 \quad (R^2 = 0.86,\ MS\ Residual = 0.00143) \qquad (2)$$

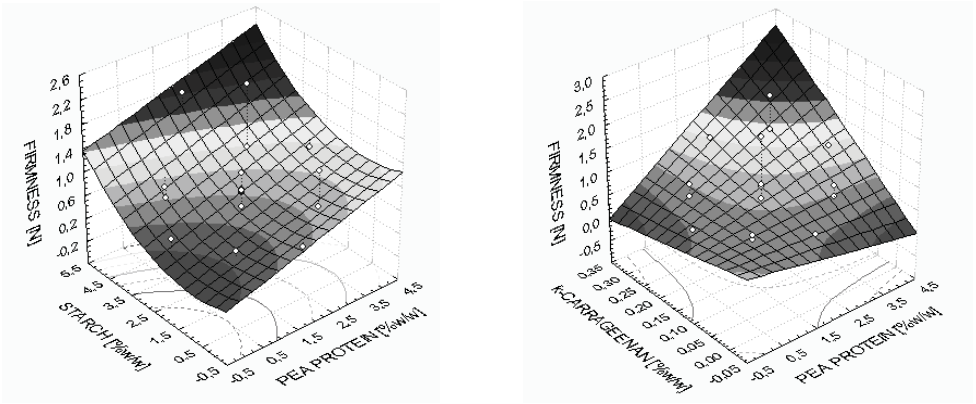

Figure 1: Response surfaces for firmness of pea/κ-carrageenan/starch gels with different composition.

From the above equations and the response surfaces for firmness shown in Figure 1 (response surfaces for adhesiveness are not presented), it can be observed that texture properties globally increase with pea protein, κ-carrageenan and starch content. Firmness shows a negative linear dependence in all the variables, which is overcome by a stronger positive interaction between pea protein and κ-carrageenan and a quadratic effect on starch content. Adhesiveness is linearly dependent on all the three biopolymers being this dependence stronger on κ-carrageenan. An important result is the lower values of texture parameters in the case of formulations without one of the three macromolecules (0.15% κ-car/2.5% S; 2% PP/2,5% S; 2% PP/0.15% κ-car) as these formulations did not produce gels but a viscous suspension. This result, valid in the concentration domain studied, seemed to reflect the importance of conjugation of different interactions between each of the three biopolymers.

3.2. Rheology

In order to clarify the kinetics of gel formation and the consequent mechanical behaviour, rheology of some gels (central and star points of the experimental design) was explored.

Figure 2 shows the cooling curves from 40 down to 5ºC and maturation kinetic curves at 5ºC over 24 or 35h.

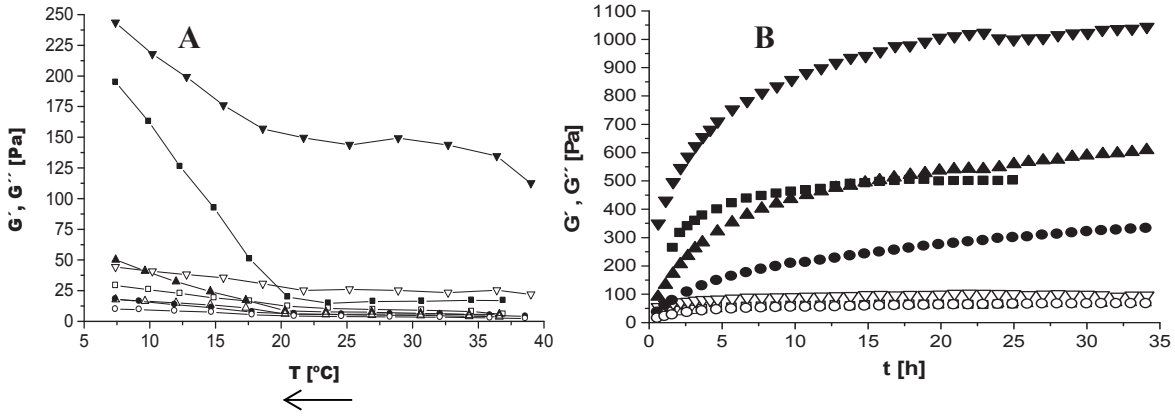

Figure 2: Cooling (A) and maturation kinetic (B) curves of pea/κ-carrageenan/starch gels with different composition. (●): 2% PP, 0.15% κ-car, 2.5% S. (■):4% PP, 0.15% κ-car, 2.5% S. (▼): 2% PP, 0.15% κ-car, 5% S. (▲):2% PP, 0.30% κ-car, 2.5% S. G´ (filled symbol), G´´ (open symbol).

From Figure 2A where G´ is always above G´´ it is possible to conclude that the sol-gel transitions occurred above 40ºC. G´ and G´´ have similar magnitudes from 40ºC down to 20ºC and there is a sudden steep increase in G´ around 20ºC that must be the building up of the carrageenan and protein networks. Although, this effect is less pronounced for the κ-carrageenan enriched gel (2% PP, 0.3% κ-car, 2.5% S) and central point (2% PP, 0.15% κ-car, 2.5% S). In the case of the gel with higher starch concentration (2% PP, 0.15% κ-car, 5% S) the G´ departure value is much higher, due to stronger contribution of starch gelatinisation. Thus, the increase on G´ around 20ºC is not so pronounced when compared with protein enriched gel (4% PP, 0.15% k-car, 2.5% S).

Figure 2B shows that maturation curves failed to get steady, within the long time range considered. To estimate the long-time limiting modulus, i.e. G´ at equilibrium (G'_{equ}), the approach previously described [6] was used (Table 1).

Table 1: *G'_{equ} for the gels with different composition on pea protein, starch and κ-carrageenan.*

System	G'_{equ} (Pa)	G'_t (Pa)	$\frac{G'_{equ} - G'_t}{G'_{equ}}$
2% PP, 0.15% κ-car, 2.5% S	428	335 (35h)	0.217
4% PP, 0.15% κ-car, 2.5% S	533	502 (24h)	0.059
2% PP, 0.30% κ-car, 2.5% S	739	613 (35h)	0.170
2% PP, 0.15% κ-car, 5.0% S	1136	1056 (35h)	0.070

According to these results, the gel made with higher pea protein concentration is characterised by a lower maturation period, as G'_{24h} is only 5.9% less than G'_{equ}. Although κ-carrageenan enriched gel needs more time to develop full structure, it presents higher G'_{equ}. Starch enriched gel is characterised by a higher structuring level (G´ higher values), consistent with texture results.

Figure 3A shows the frequency spectra of these structures at 5ºC. These gels present a typical weak gel-like response, i.e., G´ is always higher than G´´ (at about one decade) with both moduli slightly frequency dependent. The linear viscoelastic data for protein and κ-

carrageenan enriched gels are qualitatively similar, higher than those of the central point and lower than starch enriched gel, in agreement with previous results.

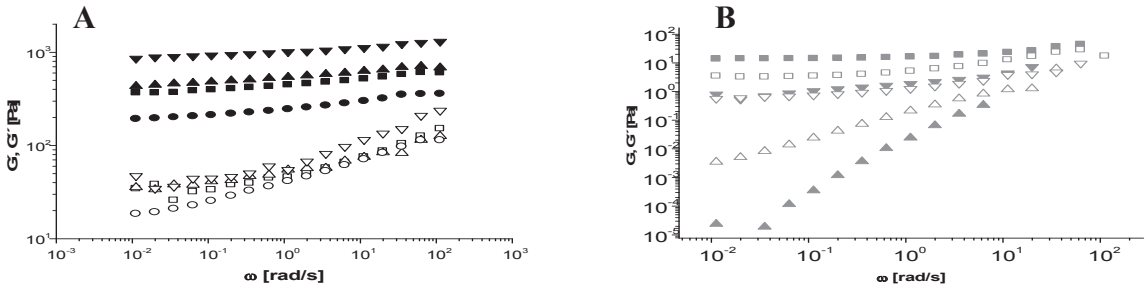

Figure 3: Mechanical spectra of pea/κ-carrageenan/starch systems with different composition at 5ºC. (●): 2% PP, 0.15% κ-car, 2.5% S. (■):4% PP, 0.15% κ-car, 2.5% S. (▼): 2% PP, 0.15% κ-car, 5% S. (▲):2% PP, 0.30% κ-car, 2.5% S. (■): 0.15% κ-car, 2.5% S. (▲):2% PP, 2.5% S. (▼): 2% PP, 0.15% κ-car. G´ (filled symbol), G´´ (open symbol).

Mechanical spectra of the systems, prepared with only two of the three biopolymers studied (Figure 3B), were obtained using samples from the flask containers stored at 5-7ºC during 8 days. These tests were performed to demonstrate the viscous character of the system without κ-carrageenan and poor internal structure of the systems without pea isolate or starch, in agreement with texture results.

3.3. Syneresis

Syneresis is an undesirable parameter of great importance from a practical point of view and increased with time and higher starch concentration (Figure 4). The three gels with only 2.5% starch had stronger water binding characteristics.

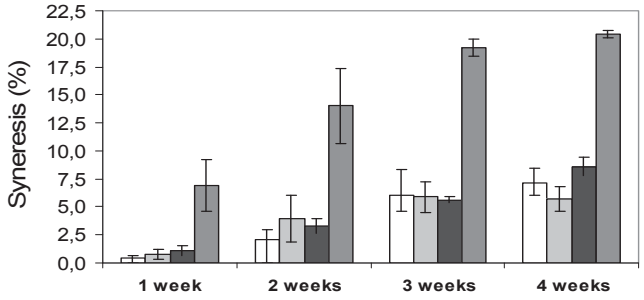

Figure 4: Syneresis of pea/κ-carrageenan/starch gels with different composition. 2% PP, 0.15% κ-car, 2.5% S (white bar). 4% PP, 0.15% κ-car, 2.5% S (light gray bar). 2% PP, 0.30% κ-car, 2.5% S (black bar). 2% PP, 0.15% κ-car, 5% S (dark gray bar).

3.4. CSLM

CSLM pictures (Figure 5) show that phase separation between protein (**white** areas) and κ-carrageenan (**grey** areas) takes place. The formation of κ-carrageenan network and protein aggregates network is observed. **Dark** areas represent swollen starch granules. As expected, from the central point (2% PP, 0.15% κ-car, 2.5% S) to starch enriched gel (2% PP, 0.15% κ-car, 5.0% S) an increase on dark spots is noticeable.

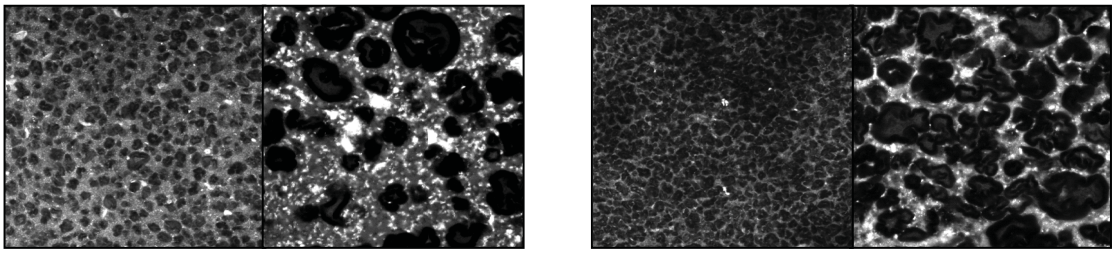

2% PP, 0.15% κ-car, 2.5% S 2% PP, 0.15% κ-car, 5.0% S

Figure 5: CSLM pictures of pea/κ-carrageenan/starch gels with different composition.

4. CONCLUSION

Texture properties globally increase with pea protein, κ-carrageenan and starch content. Systems without one of the three macromolecules did not formed a gelled structure, which reflects the importance of conjugation of different interactions between the three biopolymers. Higher starch concentrations formed firmer and structured gels, but showed higher syneresis.
Rheology and CSLM results allow us to conclude about the role of the biopolymers on the gel network. Interaction between pea protein and κ-carrageenan results in phase separation, probably by depletion–flocculation mechanism, which will increase local polymer concentration. Starch reinforces the gel structure acting as a filler. However, further investigation on single and mixtures of two hydrocolloids is needed to confirm.

5. ACKNOWLEDGEMENTS

This work is part of a research project, sponsored by FCT Portugal (Reference POCTI/AGR/38251/2001) and C.I.E.R.T. of Instituto Piaget.

References

[1] D.E. Pszczola, F. Katz, J. Giese (2000). Research trends in healthful foods. *Food Technology*, 54 (10), 45-52.
[2] H. Bollinger (2001). Consumer expectations and eating behavior over time. *Food Marketing & Technology*, 15, 10-15.
[3] V.B. Tolstoguzov (1991). *Food Hydrocolloids*, 4, 429.
[4] V.B. Tolstoguzov (1998). Functional properties of protein-polysaccharide mixtures. In *Functional Properties of Food Macromolecules*, eds. S.E. Hill, D.A. Ledward, J.R. Mitchell. Aspen Publishers 2nd Ed, Maryland, pp. 252-275.
[5] Morris, E.R. (1998). Mixed polymer gels. In Food Gels, ed. P. Harris. Elsevier Applied Science, London and New York, 291-359.
[6] M.C. Nunes, P. Batista, A. Raymundo, M.M. Alves, I. Sousa (2003). Vegetable proteins and milk puddings. *Colloids and Surfaces B: Biointerfaces*, 31, 21-29.
[7] S.Y. Xu, D.W. Stanley, H.D. Goff, V.J. Davidson, M.Le Maguer (1992). Hydrocolloid/milk gel formation and properties. *Journal of Food Science*, 57 (1), 96-102.
[8] L. Lundin & A.M. Hermansson (1998). Multivariate analysis of the influence of LBG, α-casein, κ-casein on viscoelastic prop. of Na-κ-carrageenan gels. *Food Hydrocolloids*, 1998, 12, 175-187.
[9] I. Sousa, A. Raymundo, J. Empis, J. Franco, C. Gallegos (1998). Rheology and texture of lupin protein-stabilized emulsions: a statistical approach. *Les Cahiers de Rhéologie*, Vol XVI, 1, 112-116.
[10] Aguilera, J.M. & Kessler, H.G. (1989). Properties of mixed and filled-type dairy gels. *Journal of Food Science*, 54 (5), 1213-1221.
[11] P. Batista, M.C. Nunes, I. Sousa (2002). Physical Characterisation of Commercial Dairy Desserts. In *Progress in Rheology: Theory and Applications*, eds. F. Martinez Boza, A. Guerrero, P. Partal, J. Franco, J. Munoz. Publicaciones Digitales, Spain, pp. 449-452.

SUBSTITUTION OF SUCROSE BY ASPARTAME ON GELLAN GUM GELS. EFFECT ON THE VISCOELASTIC PROPERTIES

S. Bayarri, L. Durán and E. Costell*

Laboratory of Physical and Sensory Properties
Instituto de Agroquímica y Tecnología de Alimentos (CSIC)
PO Box 73, 46100 Burjassot, Valencia (Spain)
e-mail: sabator@iata.csic.es
Phone: 96 390 00 22 Fax: 96 363 63 01

Keywords: sucrose, aspartame, gellan gum, viscoelasticity

ABSTRACT
The influence of sucrose at relatively low concentrations (10 and 20% w/w) and of aspartame (0.08 and 0.16% w/w) on the viscoelastic properties of gellan gum gels at two gum concentrations (0.3 and 1.2% w/w) have been studied. Oscillatory measurements were performed in a controlled-stress rheometer. A serrated parallel plates (6 cm in diameter) geometry was used to avoid slippage during oscillation. The measuring gap between the serrated plates was 1 mm and the exposed edges of the sample were covered with paraffin oil to prevent evaporation of water during measurement. The applied strain, 0.5%, was well within the linear viscoelastic region. Dynamic spectra were obtained from measurements within the frequency range 0.01-10 Hz at 22ºC. The mechanical spectra of gels at both concentrations (0.3 and 1.2% w/w) can be considered as typical of tridimensional networks, indicating true gel formation, As it was to be expected, higher hydrocolloid concentration (1.2% w/w) gels showed higher G', G'' and G* values than the ones of lower concentration (0.3% w/w). The effect of addition of sweetener to gellan gels varied depending on the hydrocolloid concentration. While in hard gellan (1.2% w/w) gels, addition of 20% sucrose produced an increase in G' and G'' values, in the soft gellan (0.3 % w/w) gels addition of either sucrose or aspartame produced a decrease. When comparing tan δ values at 0.1 Hz, these values were lower for higher gellan concentration, which indicated that the increase of polymer concentration enhanced the elastic character of the gellan systems.

1. INTRODUCTION

Sugars are commonly used in food gels as sweetening and texturising agents. Sucrose, a major sweetener in dessert and confectionery products, also affects gel structure and texture. In some diets the energetic value of sucrose is considered an undesirable feature. Substitution of sucrose by other sweeteners will affect the system's viscoelasticity (1,2,3).

Gellan gum is a bipolar polysaccharide that in the low acyl form provides firm but brittle gels even at low concentrations and has been used in the last decades as a very effective gelling agent (4,5). Addition of sucrose has been reported to increase the gelling temperatures of gellan solutions, except when both cation and sucrose concentrations were high (6). Papageorgiou *et al*. (7) investigated the changes in mechanical properties of deacylated gellan gels in the presence of sucrose-corn syrup blends by dynamic oscillation tests. The effect of sucrose, at concentrations between 0 and 50% in the mixture, was to raise gradually the gelling temperature and the mechanical strength of the gellan network. Whittaker *et al*. (8) observed that higher amounts of gellan gum or of sucrose up to 30% resulted in an earlier gelation and that the addition of sucrose up to 30% lead to an increase in storage modulus values, but on raising the sucrose content from 40 to 60%, weakening of the gellan network occurred.

Among non-saccharide sweeteners, aspartame (L-aspartyl-L-phenylalanine methyl ester) which is 100 to 150 times sweeter than sucrose (9) is commonly used in low caloric food products. In this type of products, the substitution of aspartame for sucrose may affect their rheological behaviour. In this way, Moritaka and Naito (10) found that the addition of aspartame (0.02% w/w) did not alter the rupture properties of agar and gelatin gels. Wilson and Brown (11) observed differences between the effect of the addition of sucrose (10% w/w) and that of aspartame (0.062% w/w) on the rupture properties of gelatine gels. Such differences were bigger at the higher gelatine concentrations. Recently, Bayarri *et al*. (12), reported that addition of sucrose (10 and 15% w/v) affected the compression resistance in both kappa-carrageenan and gellan gum gels, while addition of aspartame (0.08 and 0.12% w/v) did not have any effect. No information is at present available on the effect of aspartame on the viscoelastic properties of gelled systems.

The objective of this paper is to analyse the effect of the substitution of sucrose by aspartame on the viscoelastic properties of gellan gum gels by oscillatory rheological methods.

2. MATERIALS AND METHODS

2.1. Gel preparation and composition

Dry gellan gum powder (Kelcogel®F, CP Kelco ApS, Chicago, IL, USA) was dispersed, together with a small quantity of sucrose, in deionised water and agitated. The rest of the sucrose was then added and the mixture agitated mechanically for 10 min and heated up to 90ºC, then cooled to 75ºC and 0.088% w/w $CaCl_2 \cdot 2H_2O$ (6mM) added. Gels containing aspartame were prepared the same way except that the aspartame powder, previously dispersed in water, was added just before the calcium chloride, holding the mixture at a temperature of about 80ºC.

Gel samples were prepared at two total polymer concentrations – 0.3 and 1.2% w/w - each without and with two sucrose contents - 10 and 20% w/w - or two aspartame contents - 0.08 and 0.16% w/w -.

2.2. Rheological measurements

Oscillatory measurements were performed in a controlled-stress rheometer (Haake RheoStress 1, Karslruhe, Germany) with temperature controlled by a Haake circulating water bath. A serrated parallel plates (6 cm in diameter) geometry was used to avoid slippage during oscillation. The measuring gap between the serrated plates was 1 mm and the exposed edges of the sample were covered with paraffin oil to prevent evaporation of water during measurement.

Hot (70ºC) solutions were poured directly into the rheometer plate, previously heated to the same temperature. The temperature was lowered from 70 to 10ºC at a fixed rate of 0.5ºC/min, allowing solutions to gel, and then heated to 22 ºC at the same rate.

The gels were first tested over a range of strains to determine appropriate conditions for non-destructive testing. Strain sweeps at 22 ºC and at a frequency of 1 Hz were performed in all the gel systems studied to determine the linear viscoelasticity zone. Frequency sweep tests, at 0.5% strain and at a temperature of 22 ºC, were performed from 0.01 to 10 Hz. Measurements were made in at least two preparations of each composition.

3. RESULTS AND DISCUSSION

The mechanical spectra of the gels could be considered as typical of tridimensional networks, indicating true gel formation, according to Clark and Ross-Murphy (13). Storage modulus (G') values were always higher than those of loss modulus (G'') through the whole range of frequencies applied, corresponding to a solid state, and independent of frequency as characteristic of an elastic network. A slight increase in G'' with frequency was observed in all cases but maintaining the predominantly elastic character (G'>10G''). This type of behaviour has been reported by other authors for gellan gum gels (14, 15). As it was to be expected, higher hydrocolloid concentration (1.2% w/w) gels showed higher G'and G'' values than the ones of lower concentration (0.3% w/w).

3.1. Influence of sweetener type and concentration on both storage and loss moduli of model systems

The effect on both moduli of the addition of the two tested sucrose concentrations not only depended on them but also on the concentration of hydrocolloid added. In soft gellan gum gels, addition of 10% sucrose resulted in a small decrease in the values of G' and G'', measured at 0.1 Hz. The storage modulus values went down from 3045 to 1668 Pa and the loss modulus values from 274 to 124 Pa. Addition of 20% sucrose continued to slightly decrease both moduli, G' going down to 574 Pa and G'' to 53 Pa (Figure 1a). In contrast, in hard gellan gels, 10% sucrose addition did not affect the gel viscoelasticity but on adding 20% sucrose, G' increased from 9827 to 18490 Pa and G'' from 407 to 1471 Pa (Figure 1b).

(a)

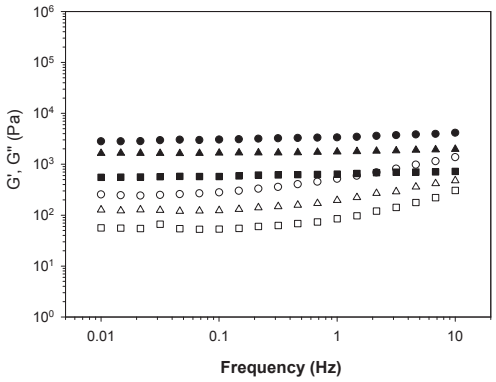

(b)

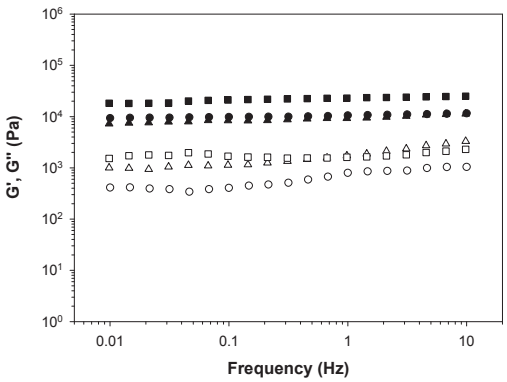

Figure 1. Storage modulus (filled symols) and loss modulus (empty symbols) values of soft (a) and hard (b) gellan gum gels without sweetener (circle) and with sucrose (triangle= 10% w/w, square=20% w/w)

Papageorgiou *et al*. (7) studied the mechanical properties of gellan gels (0.5%) with sucrose additions (0 to 60%), and observed that increasing sucrose produced a corresponding increase in the gel network strength, as shown by G' values. In a similar study, Whittaker *et al.* (8) found that addition of low sucrose concentrations (0 to 30%) to gellan gels (0.5%) resulted in an increase in the storage modulus. This process was discussed on the basis of increasing polymer/polymer interactions supported by hydrogen bonding with water molecules. Addition of higher sucrose concentrations (40 to 60%), however, weakened the gellan gel network. Miyoshi *et al.* (16) studied the effects of glucose and mannose (up to 4.0 M) and konjac glucomannan (up to 4%) on the gel-sol transition in gellan gum (0.5 or 1.0%) aqueous solutions. They found that in the presence of sugar, G' became larger than that without sugar; however they found a slight decrease in the thermal stability, not observed in previous studies. Moritaka, *et al.* (17) have reported that the dynamic Young modulus E' decreased by the addition of sugars, in line with our results for soft gels.

In the case of aspartame addition, slight decreases in G' and G'' values were detected in soft gellan gels at both aspartame concentrations (Figure 2a). In hard gellan gels, no important change in the viscoelastic properties was observed when aspartame was added (Figure 2b).

(a)

(b)

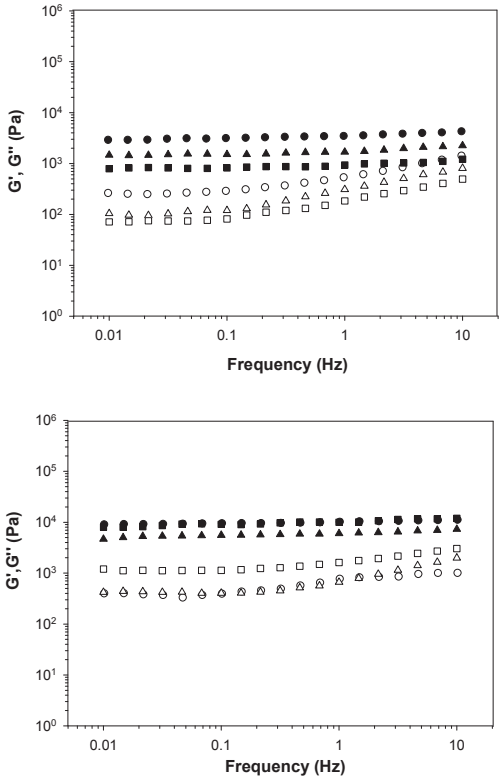

Figure 2. Storage modulus (filled symols) and loss modulus (empty symbols) values of soft (a) and hard (b) gellan gum gels without sweetener (circle) and with aspartame (triangle= 0.08% w/w, square=0.16% w/w).

3.2. Influence of sweeteners on the gel resistance to deformation (G*) and on loss angle (tan δ)

Comparing the studied unsweetened gelled systems, it was observed that G* values at 0.1 Hz were higher for hard gellan gum gels (9835 Pa) than for the soft ones (3057 Pa) (Figures 3a and 3b).

The effect of the addition of sweetener to gellan gels varied depending on the hydrocolloid concentration. In the soft (0.3% w/w) gels, addition of either sucrose or aspartame produced a decrease in G* values (Figure 3a). In hard (1.2% w/w) gels, addition of 20% sucrose produced an increase in G*, which went up to 18490 Pa (Figure 3b).

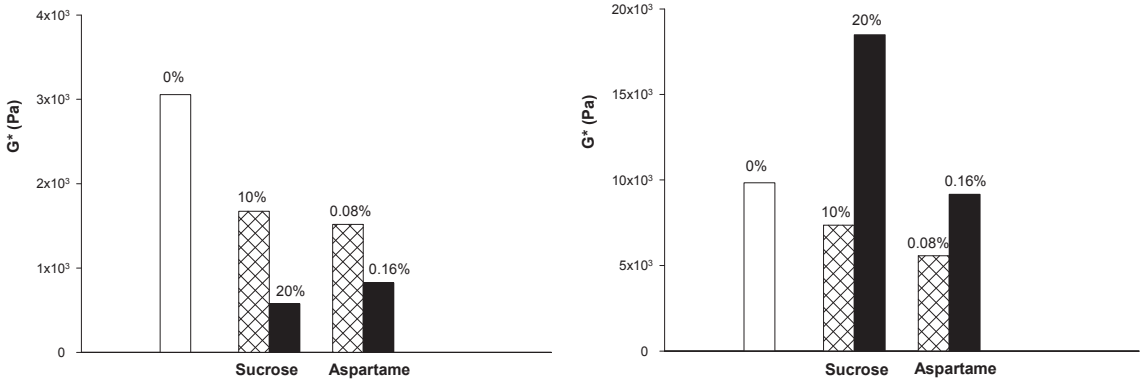

Figure 3. Complex modulus values, at 0.1 Hz, of soft (a) and hard (b) gellan gum gels without and with sucrose or aspartame.

When comparing tan δ values at 0.1 Hz, the increase of polymer concentration enhanced the elastic character of the gellan systems, as also reported by Rodríguez-Hernández *et al*. (15), who found that the loss angles were lower for higher gellan concentration. Our results showed that tan δ values decreased from 0.09 to 0.04 when gellan concentration increased from 0.3 to 1.2% w/w.

Addition of any sweetener did not modify loss angle values in soft gellan gels. In hard gellan gels, addition of sucrose or aspartame slightly increased tan δ values, up to a range between 0.07 and 0.12.

ACKNOWLEDGEMENTS

This work has been carried out under Projects AGL2000-1590 and AGL2003-0052, financed by MCyT (Spain). Authors also thank MEC (Spain) for author Bayarri's fellowship and the Spanish agents of Premium Ingredients, S.L. for providing free samples of gellan gum.

REFERENCES

1. Grosso, C.R.F., & Rao, M.A. (1998). Dynamic rheology of structure development in low-methoxyl+pectin+Ca^{+2}+sugar gels. *Food Hydrocolloids*, 12, 357-363.

2. Evageliou, V., Richardson, R.K., & Morris, E.R. (2000). Effect of PH, sugar type and thermal annealing on high-methoxy pectin gels. *Carbohydrate Polymers*, 42, 245-259.

3. Oakenfull, D., & Scott, A. (1986). Stabilization of gelatin gels by sugars and polyols. *Food Hydrocolloids*, 1 (2), 163-175.
4. Sanderson, G.R.; Bell V.L.; Clark R.C., & Ortega D. (1988). The texture of gellan gum gels. In Phillips, G. O., Williams, P.A., & Wedlock, D.J. (Eds), *Gums and stabilisers for the food industry.*(Vol 4) (pp. 219-229). Oxford: IRL Press Ltd
5. Mao, R., Tang, J., & Swanson, B.G. (1999). Texture properties of gellan gels as affected by temperature. *Journal of Texture Studies*, 30, 409-433.
6. Tang, J., Mao, R., Tung, M.A., & Swanson, B.G. (2001). Gelling temperature, gel clarity and texture of gellan gels containing fructose or sucrose. *Carbohydrate Polymers*, 44, 197-209.
7. Papageorgiou, M., Kasapis, S., & Richardson, R.K. (1994). Glassy-state phenomena in gellan-sucrose-corn syrup mixtures. *Carbohydrate Polymers*, 25, 101-109.
8. Whittaker, L.E., Al-Ruqaie, I.M., Kasapis, S., & Richardson, R.K. (1997). Development of composite structures in the gellan polysaccharide/sugar system. *Carbohydrate Polymers*, 33, 39-46.
9. Kim, S.-H., & Dubois, G.E. (1991). Natural high potency sweeteners. In S. Marie & J.R. Piggott, *Handbook of Sweeteners* (pp.117-185). Glasgow and London: Blackie and Son Ltd.
10. Moritaka, H., & Naito, S. (2002). Agar and gelatin flavour release. *Journal of Texture Studies*, 33, 201-214.
11. Wilson, C.E., & Brown, W.E. (1997). Influence of food matrix structure and oral breakdown during mastication on temporal perception of flavor. *Journal of Sensory Studies*, 21, 69-86.
12. Bayarri, S., Durán, L., & Costell, E. (2003). Compression resistance, sweetener's diffusion and sweetness of hydrocolloids gels. *International Dairy Journal,* 13, 643-653.
13. Clark, A.H., & Ross-Murphy, S.B. (1987). Structural and mechanical properties of biopolymer gels. *Advances in Polymer science*, 83, 57-192.
14. Miyoshi, E., Takaya, T., & Nishinari, K. (1994). Gel-sol transition in gellan gum solutions. I. Rheological studies on the effects of salts. *Food Hydrocolloids*, 8(6), 505-527.
15. Rodríguez-Hernández, A.I., Durand, S., Garnier, C., Tecante, A., & Doublier, J.L. (2003). Rheology-structure properties of gellan systems:evidence of network formation at low gellan concentrations. *Food Hydrocolloids*, 17, 621-628.
16. Miyoshi, E., Takaya, T., & Nishinari, K. (1998). Effects of glucose, mannose and konjac glucomannan on the gel-sol transition in gellan gum aqueous solutions by rheology and DSC. *Polymer Gels and Networks*, 6, 273-290.
17. Moritaka, H., Nishinari, K., Nakahama, N., & Fukuba, H. (1994). Effects of sucrose, glucose, urea and guanidine hydrochloride on the rheological properties of gellan gum gels. *Journal of Japanese Society of Food Science and Technology*, 41(1), 9-16 (in Japanese with English summary).

STUDY OF THE INFLUENCE OF THE GELLING AGENTS CONCENTRATION ON THE TEXTURAL PROPERTIES OF LIPOGEL/HYDROGEL MIXTURES

P. Junghans; A. la Chica; I. P. Neto; M. T. Vasconcelos; T. Vasconcelos; I. F. Almeida; P. Costa; M. F. Bahia*

Pharmaceutical Technology Department, Faculty of Pharmacy, Oporto University
Rua Anibal Cunha, nº164, 4050-047 Porto, Portugal
Phone +351 222078949 Fax +351222003977
*ifalmeida@ff.up.pt

Keywords: texture, response surface methodology, lipogel / hydrogel mixtures

ABSTRACT

Gels can be aqueous systems (hydrogels) or lipophilic formulations (lipogels), which are obtained adding a gelling agent to a liquid phase. Semisolid products can be obtained mixing both type of gels. The aim of this study was to evaluate the influence of the gelling agents concentration on the firmness and adhesiveness of lipogel/hydrogel semisolid mixtures (bigels). This study was based on the response surface methodology with a central composite design. Twelve experiments were performed based on an experimental matrix. The twelve different bigels systems were obtained by mixing with a mechanical stirrer and at room temperature, 10% of a Sorbitan monostearate and sweet almond oil lipogel with 90% of a Carbopol® 934 hydrogel. The gelling agents concentration ranged from 17 to 20 wt % of sorbitan monostearate in the lipogel and from 0.5 to 1.0 wt % of Carbopol® 934 in the hydrogel. It was carried out the characterization of the textural properties of the different mixtures. The texture profiles of the different mixtures were qualitatively similar but quantitatively different. The analysis of the results showed that the concentration of gelling agent of the hydrogel was the only factor that significantly ($p < 0.05$) influenced the textural parameters of the lipogel/hydrogel mixtures.

1. INTRODUCTION

Gels have received considerable attention over the past two decades as platforms for drug delivery applications, mainly as a result of the wide range of physicochemical properties offered by such systems[1]. Depending on the nature of the liquid medium, gels can be classified as hydrogels (aqueous systems) or lipogels (gels obtained with lipophilic liquids). Hydrogels have been extensively studied while lipogels only recently have captured the attention of the scientific community. Interest in this field has increased due to the strikingly rise of the discovery of substances that are able to gel organic solvents [2]. There are few reports of the application of lipogels in the pharmaceutical/cosmetic area [3,4,5] and many of their potentialities are still unexploited. In previous studies, systems were developed based on the mixture of both type of gels. Based on short-term stability and organoleptic features, a semisolid mixture obtained with a hydrogel of polyacrylic acid and an lipogel of sorbitan monostearate and sweet almond oil (90:10) was considered to be the most promising. In this work, it was studied the influence of the concentration of the gelling agents on the textural properties of that lipogel / hydrogel semisolid mixture. This study was based on the response surface methodology with a central composite design.

Texture can be regarded as a manifestation of the rheological properties of a product. It is an important attribute that affects processing and handling, shelf-life and consumer acceptance of products. Textural analysis is widely used for the mechanical characterization of food products. It has been also used on the pharmaceutical and cosmetic area [1,6]. In this technique, an analytical probe is depressed into the sample, at a defined rate to a desired depth. From the resultant force-distance curve, the mechanical parameters firmness and adhesiveness may be derived. Firmness is usually correlated with the maximum force and adhesiveness with the negative area. Firmness is defined as the force necessary to attain a given deformation and adhesiveness is regarded as the work necessary to overcome the attractive forces between the surfaces of the sample and the surface of the probe with which the sample comes to contact [7].

2. MATERIALS AND METHODS

2.1 Preparation of hydrogels and lipogels

Polyacrylic acid (Carbopol ® 934, BF Goodrich) and triethanolamine were purchased from J. Vaz Pereira (Portugal)
Sorbitan monostearate (Span® 60) and sweet almond oil were purchased from Roig Farma (Spain).
The hydrogels were obtained by dispersing the gelling agent in water with a mechanical stirrer. After full dispersion, it was added the neutralizing agent (triethanolamine) in a proportion of 2.14/1 (triethanolamine / Carbopol® 934) with gentle stirring.
On the lipogels preparation, sorbitan monostearate was added to sweet almond oil at a temperature of approximately 60ºC under magnetic agitation (300 r.p.m.) The lipogels were stored at 20ºC for 8 days to ensure full maturation.

2.2 Preparation of bigels

This study was based on the response surface methodology with a central composite design. There were 12 experiments carried out accordingly to an experimental matrix (Table 1) generated by the STATISTICA® program (5.0 version, Statsoft Inc., 1996).
The bigels were prepared by mixing 90% of hydrogel with 10 % of lipogel with mechanical stirring during 10 minutes, at room temperature.

2.3 Textural analysis

The textural analysis was performed in the compression mode in a texturometer (Stable Microsystems TA-XT2*i*, U.K.), by carrying out a penetration test using a cylindrical probe of 25 mm, a depth of 10 mm and velocities of 3 mm/s. After penetrating the sample, the probe returned to a position 30 mm above the platform surface. The textural parameters firmness and adhesiveness were calculated from the curves Force *vs* Distance obtained.

Table 1 – Experimental matrix used on this study

Experiment	Carbopol ® 934 %	Sorbitan monostearate %
1	0.57	17.40
2	0.93	17.40
3	0.57	19.60
4	0.93	19.60
5	0.75	18.50
6	0.75	18.50
7	0.50	18.50
8	1.00	18.50
9	0.75	17.00
10	0.75	20.00
11	0.75	18.50
12	0.75	18.50

3. RESULTS AND DISCUSSION

The texture profiles of the different mixtures were qualitatively similar but quantitatively different. By the analysis of the Paretto chart (Fig. 1) it was observed that Carbopol ® 934 concentration (linear term) was the only factor that significantly influenced ($p < 0.05$) the firmness of the mixtures.

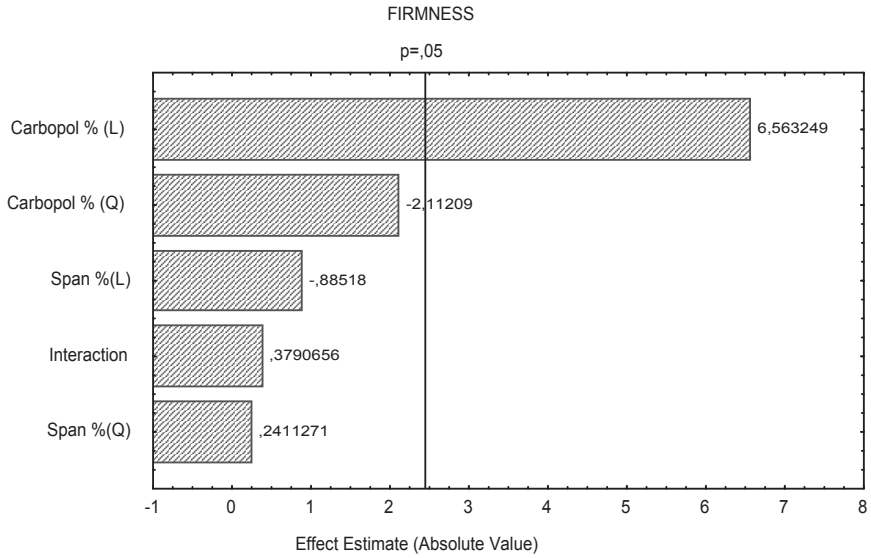

Figure 1 – Paretto chart showing the influence of the gelling agents concentration (linear-L and quadratic- Q terms) on the bigels firmness.

Similar behaviour was found for the adhesiveness of the formulations (Fig. 2). Although it was previously established that the sorbitan monostearate concentration influenced the textural properties of the lipogels [8], in this study it proved to have no influence on the firmness and adhesiveness of the lipogel/hydrogel mixtures, probably due to the low proportion (10%) used.

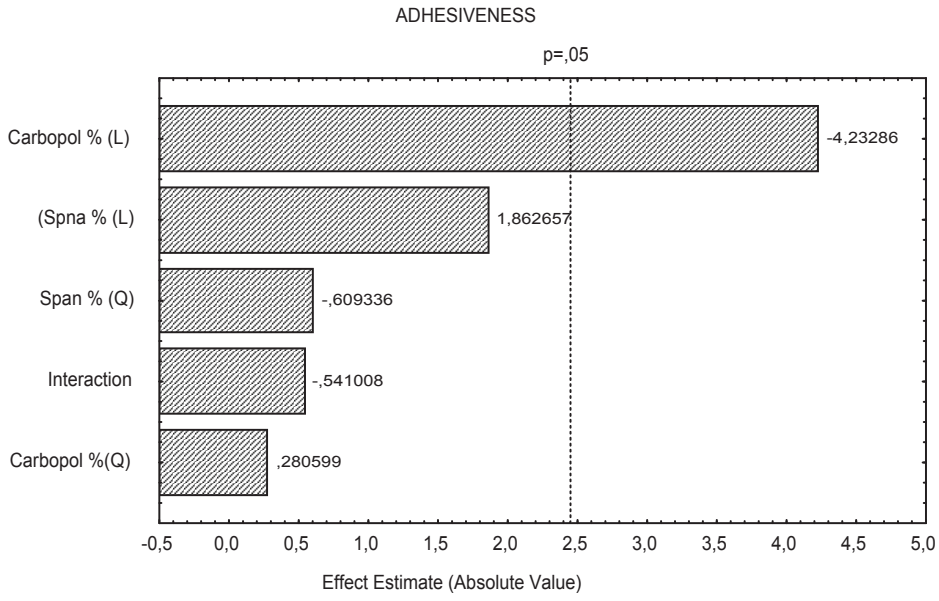

Figure 2 – Paretto chart showing the influence of the gelling agents concentration (linear-L and quadratic- Q terms) on the adhesiveness of the bigels.

4. CONCLUSION

The concentration of sorbitan monostearate had no significant influence on the firmness and adhesiveness of the mixtures. On the other hand, because the concentration of the gelling agent of the hydrogel influenced the textural properties of the lipogel/hydrogel mixture it should be carefully selected considering the intended application in order to maximize its sensorial attributes and efficacy.

REFERENCES

[1] Jones, D.S.; Lawlor, M.S. and Woolfson, A.D. Rheological and Mucoadhesive Characterization of Polymeric Systems Composed of Poly(methylvinylether-co-maleic anhydride) and Poly(vinylpyrrolidone), Designed as Platforms for Topical Drug Delivery. J Pharm Sci 2003; 92(5): 995-1007.
[2]Terech, P. and Weiss, R.G. Low Molecular Mass Gelators of Organic Liquids and the Properties of Their Gels. Chem Rev 1997; 97(8): 3133-3159.
[3]El laithy HM and El-Shaboury KF. The Development of Cutina Lipogels and Gel Microemulsion for Topical Administration of Fluconazole. AAPS Pharmscitech. 2003; 3(4): article 35.
[4]Henmi, T. *et al.* Application of an Oily Gel Formed by Hydrogenated Soybean Phospholipids as a Percutaneous Absorption-Type Ointment Base. Chem Pharm Bull 1994; 42(3): 651-655.
[5]Willimann, H. *et al.* Lecithin Organogel as a Matrix for Transdermal Transport of Drugs. J Pharm Sci 1992; 81 (9): 871-874
[6] Jones,D.S.; Lawlor, M.S. and Woolfson, D. Examination of the flow rheological and textural properties of polymer gels composed of poly(methylvinylether-*co*-maleic anhydride) and poly(vinylpyrrolidone): Rheological and mathematical interpretation of textural parameters. J Pharm. Sci 2002; 91(9): 2090-2110.
[7] M.C. Bourne, Texture Profile Analysis. Food Tech 1978; 32: 62-72.
[8] I.F Almeida; M.M., Alves; M.C. Nunes; Raymundo, A. and Bahia, M.F. Optimisation of an oleogel of sorbitan monostearate and sweet almond oil. Proceedings AERC 2003. p21. September 2003.

MECHANICAL CHARACTERIZATION OF BIGELS (OLEOGEL/ HYDROGEL) SYSTEMS

P. Barrocas; M. Domingues; R.S. Lima; J. das Neves; J. Silva; I.F. Almeida; P. Costa, M.F. Bahia*

Pharmaceutical Technology Department, Faculty of Pharmacy, Oporto University
Rua Aníbal Cunha, nº164, 4050-047 Porto, Portugal
Phone +351 222078949 Fax +351222003977
*ifalmeida@ff.up.pt

Keywords: bigels, texture, rheology.

ABSTRACT

Bigels are systems obtained by the mixture of hydrogels with oleogels. These systems could be promising vehicles for topical formulations. In this study, four different gels were prepared, namely two hydrogels (Hydroxypropylmethylcellulose (HPMC) 3 wt % and Carbopol® 934 0.7 wt %) and two oleogels (Sorbitan monostearate 19 wt % and sweet almond oil (SM-SAO) and Cholesterol 3.5 wt % and liquid paraffin (Ch-LP)). Four bigels (10% oleogel /90% hydrogel) were prepared by the mixture, at ambient temperature, of the gels mentioned above in all possible combinations. The mechanical characterization of these new systems was carried out by using textural and rheological tests.
The textural profile was quali and quantitatively similar between bigels obtained with the same hydrogel. The experimental results showed that the Carbopol® based bigels presented higher firmness and adhesiveness than the bigels obtained with HPMC hydrogel. All the bigels tested presented shear-thinning behaviour.
It is possible to conclude that the mechanical properties of the bigels tested are mainly dependent on the nature and concentration of the gelling agent of the hydrogel. All the formulations presented mechanical behaviour appropriated for topical application, being the bigels based on Carbopol® better suited for bioadhesive dosage forms.

1. INTRODUCTION

Bigels are systems obtained by mixing aqueous gels (hydrogels) with organic gels (oleogels). This mixture is performed at room temperature and without the addition of other ingredients, which can be considered as a technological advantage over other multiphase pharmaceutical/cosmetic dosage forms. Furthermore, hydrogels and oleogels are also easy to prepare.
Bigels can be prepared from different hydrogels and oleogels, allowing the preparation of products ranging from viscous liquids to semisolid. The bigels selected for this study are white, opaque formulations that are easy to spread and provide a coolness sensation on the skin, which are important features considering consumer acceptability. Mechanical properties are also important features considering potential application as dermatological formulations. It is accepted that the clinical and nonclinical performances of gels are dependent on their mechanical/rheological properties [1]. Formulations which have been designed for skin application must exhibit acceptable mechanical characteristics, e.g. ease of application and low firmness. Considering topical use, formulations should have good retention at the site of application. Firmness is related with the ease of product removal from a container, ease of

application onto a substract, whereas adhesiveness, a property related with bioadhesion describes the relative adhesive properties of a formulation [2].
The aim of this study is to characterize the mechanical properties of these bigels in order to access the feasibility of their application as vehicles for topical formulations. This characterization was performed by carrying out textural and rheological measurements.

2. MATERIALS AND METHODS

2.1 Preparation of Hydrogels

Polyacrylic acid (Carbopol ® 934, BF Goodrich) and triethanolamine were purchased from J. Vaz Pereira (Portugal).
Sorbitan monostearate (Span 60®), Cholesterol, Liquid paraffin and Sweet almond oil were purchased from Roig Farma (Spain). Hydroxypropylmethylcellulose (Methocel® E4M Premium EP, Colorcon) was a gift of Multiquímica (Portugal).
The composition of the hydrogels is described on table I.

Table I - Composition of the hydrogels

Polyacrylic acid Gel	Hydroxypropylmethylcellulose Gel
Carbopol®934 ……... 0.7% Triethanolamine ……. 4.5 g Purified water ……. e.q. 300 g	Methocel® ……. 3% Purified water ..... e.q. 300 g

For the manufacturing of the hydrogels, the polymer was dispersed in water under mechanical stirring. For the polyacrylic acid gel, after full dispersion of the polymer, triethanolamine was slowly added with continuous and gentle stirring. These gels were stored at 20ºC before the preparation of the bigels.

2.2 Preparation of Oleogels

The composition of the oleogels, one of cholesterol and liquid paraffin (Ch-LP) and another of sorbitan monostearate (Span 60®) and sweet almond oil (SM-SAO), is shown in table II.

Table II - Composition of the oleogels

Ch-LP Gel	SM-SAO Gel
Cholesterol ……. 3.5% Liquid paraffin ……. e.q. 50 g	Span 60® …… 19% Sweet almond oil ….. e.q. 50 g

The oleogels were prepared by dispersing the organogelator in the liquid phase, with stirring (300 rpm, 10 minutes) and heating (Ch-LP gel 90ºC; SM-SAO gel 60ºC).
Both gels were stored at 20ºC for 8 days to ensure full maturation.

2.3 Preparation of the Bigels

The bigels were prepared by mixing with mechanical stirring for 10 minutes, 90% hydrogel with 10% oleogel. Following this procedure, four bigels were obtained (table III).

Table III – Bigels evaluated on this study

Bigel A	Carbopol 934® gel SM-SAO gel
Bigel B	Carbopol 934® Ch-LP gel
Bigel C	Methocel® SM-SAO gel
Bigel D	Methocel® Ch-LP gel

2.4 Mechanical characterization

The textural analysis was performed in the compression mode in a texturometer (Stable Micro Systems TA-XT2*i*, U.K), by carrying out penetration test using a cylindrical probe of 25 mm of diameter, a penetration depth of 10 mm and velocities of 3 mm/ s. After penetrating the sample, the probe returned to a position 30 mm above the platform surface. From the graphic force *vs* distance obtained, the parameters maximum force (correlated with firmeness [3]) and negative area (correlated with adhesiveness [3]) were calculated. Rheological measurements were performed in a viscometer fitted with concentric coaxial cylinder geometry (Viscotester VT 550, Thermo Electron, Germany). Flow measurements were carried out at 20ºC in the shear rate range from 1 to 400 s^{-1}, with 60 s delay period between measurements. The gels were allowed to rest for 30 min before starting the measurements. All the measurements were performed in triplicate.

3. RESULTS AND DISCUSSION

It was observed that bigels obtained with the same hydrogel presented similar textural profiles, both quanti- and qualitatively The bigels that exhibited the highest firmness and adhesiveness were obtained with Polyacrylic acid hydrogel (Fig. 1).

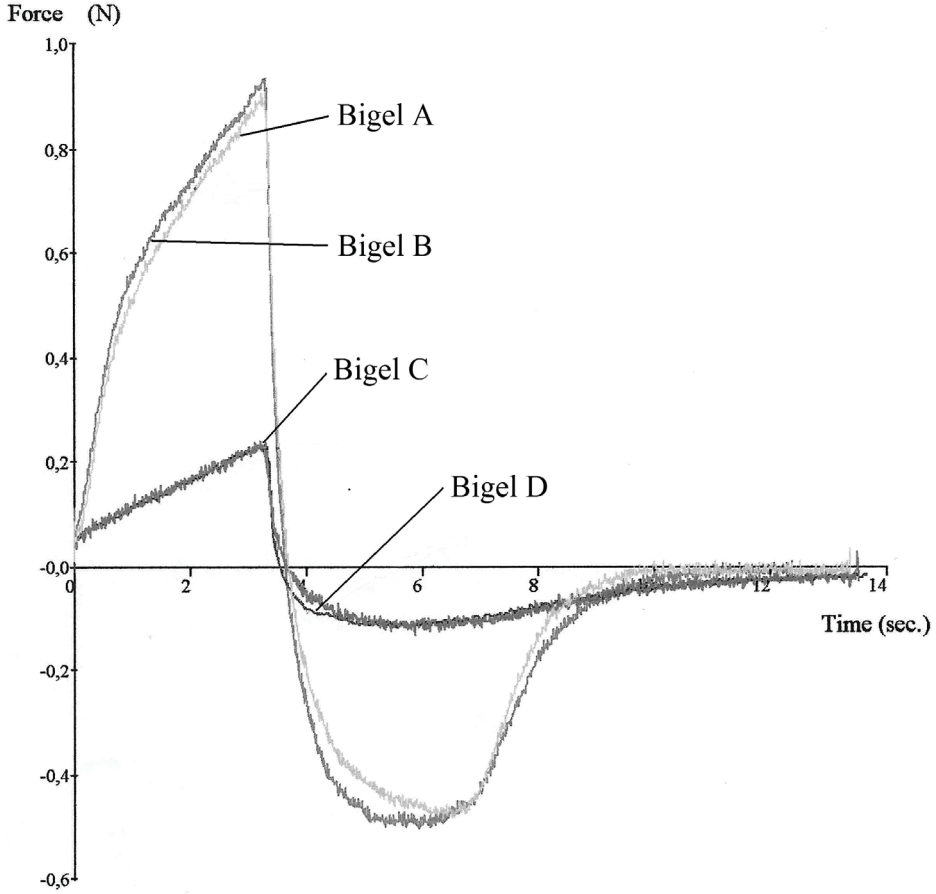

Figure 1 – Textural profiles of the bigels.

The four bigels tested presented shear-thinning behaviour. At low shear rates it was observed that the bigels containing the same hydrogel have similar viscosity (Fig. 2). At shear rates typical of application on the skin (100-10000 s^{-1}) [4], all the formulations presented low viscosities, what may justify the ease of spreading that was subjectively accessed.

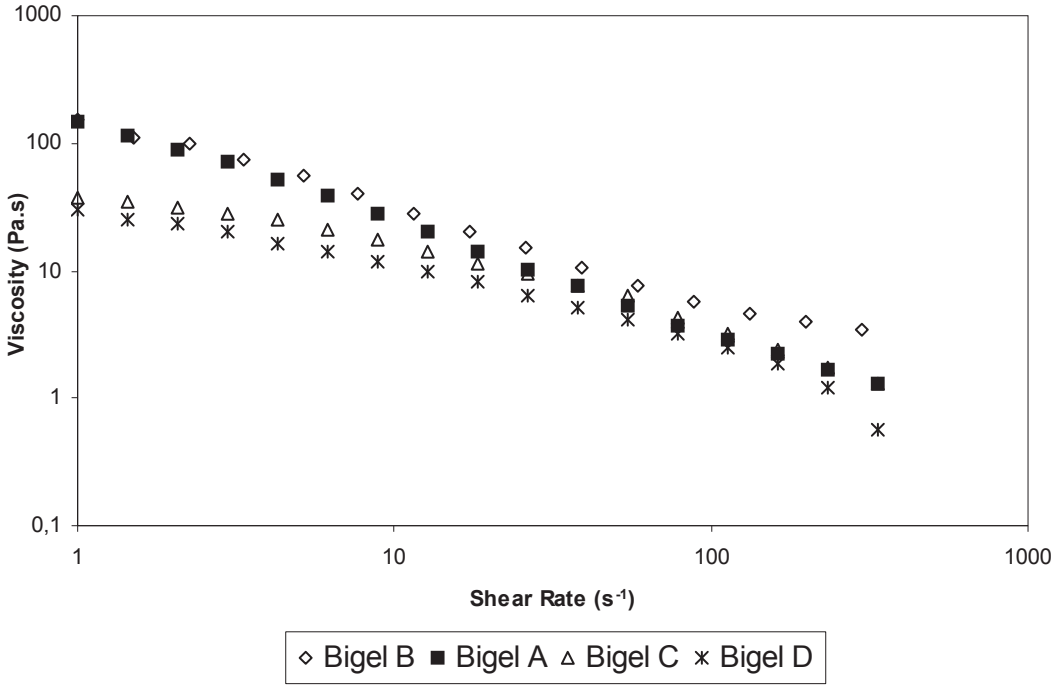

Figure 2 – Flow curves of the bigels.

4. CONCLUSIONS

The mechanical properties of the bigels tested are mainly dependent on the nature and concentration of the gelling agent of the hydrogel. We can generally conclude that, with respect to mechanical properties, these formulations are suitable for topical application as they exhibit a shear-thinning behaviour. The bigels A and B, based on the polyacrylic acid hydrogel, presented higher firmness and adhesiveness and could have particular interest for bioadhesive formulations.

REFERENCES

[1]Jones,D.S.; Lawlor, M. and Woolfson, D. Examination of the flow rheological and textural properties of polymer gels composed of poly(methylvinylether-*co*-maleic anhydride) and poly(vinylpyrrolidone): Rheological and mathematical interpretation of textural parameters. J Pharm. Sci 2002; 91(9): 2090-2110.
[2]Jones, D.S:, Woolfson, A. D. and Brown, A.F. Textural Analysis and Flow Rheometry of Novel, Bioadhesive Antimicrobial Oral Gels. Pharm Res 1997; 14(4): 450-457.
[3]Bourne, M.C. Texture Profile Analysis. Food Tech 1978; 32: 62-72.
[4]Laba, D. The flow of cosmetics and toiletries. In: Laba, D. (edt.) Rheological properties of cosmetics and toiletries. New York: Marcel Dekker; 1993. p. 1-9.

THE EFFECT OF THE DEGREE OF HYDROLYSIS AND CONCENTRATION ON THE HEAT GELLING BEHAVIOUR OF WHEY PROTEIN CONCENTRATE TRYPTIC HYDROLYSATES

D. Torres[1,*], *C.R. Vicente*[2], *J.A.Teixeira*[3], *M.P. Gonçalves*[1]

[1]REQUIMTE, Departamento de Engenharia Química, Faculdade de Engenharia da Universidade do Porto, Rua Dr. Roberto Frias, s/n, 4200-465 Porto, Portugal.
[2] Escola Superior de Tecnologia e Gestão, Instituto Politécnico de Viana do Castelo, Apartado 574, 4900 Viana do Castelo, Portugal
[3]Centro de Engenharia Biológica - IBQF, Universidade do Minho, Campus de Gualtar 4710-057 Braga, Portugal
*Corresponding author-Fax: 351-22 508 1449, Tel: 351-22 508 1684, email: reolog1@fe.up.pt

Keywords: Gelling properties; whey protein hydrolysate; trypsin; rheology

Abstract

Whey proteins have the ability to form heat-induced gels. This property allows their incorporation into solid foods but limits their use in liquid food formulas.

Enzymatic hydrolysis impairs the gelling properties of whey proteins and that can be used to expand their potential food applications. The liberation of specific bioactive peptides during enzymatic hydrolysis also increases the nutritional interest in this kind of ingredients.

In this work, our main objective is to study the gelling properties of whey protein tryptic hydrolysates (WPTH) as a function of the degree of hydrolysis and the protein concentration.

The rheological behaviour of WPTH during heat gelling under small deformation oscillatory shear was investigated using a controlled stress rheometer AR2000 (TA Instruments). According to this study, we can design enzymatic hydrolysates for specific food formulations according to the desired gel (meat, dairy or bakery products) or liquid character (beverages, salad dressings).

1. INTRODUCTION

Bovine whey is the liquid remaining after cheese and casein manufacture. For each kg of bovine cheese, 9 - 11 kg of whey are produced (McIntosh, 1998; TECNINVEST, 2000). Portuguese and world production of whey is increasing (figure 1).

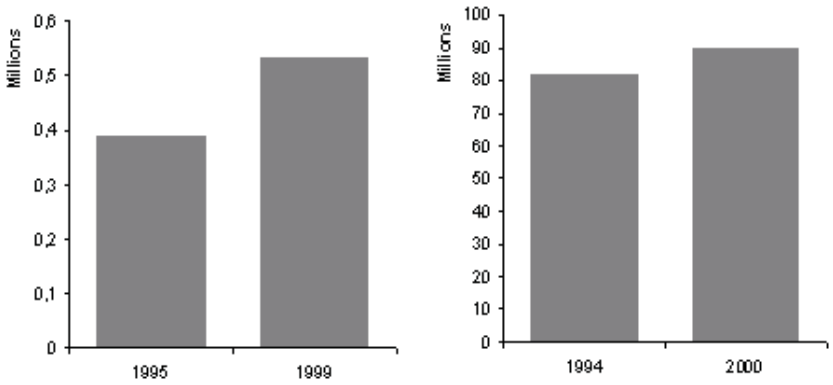

Figure 1. Annual production of liquid whey (millions of ton) in Portugal (1995, 1999) and in the world (1994, 2000). Adapted from McIntosh, 1998 and ANIL, 2002.

Whey contains approximately 20% of the protein and almost all the lactose of the original milk (table 1). These valuable compounds are also responsible for the high putrescibility of whey.

Separation technologies, mainly membrane processes, are being developed to produce protein ingredients. Whey protein concentrates (WPC) and whey protein isolates (WPI) are widely used in food formulation due to their nutritional and functional properties (Turgeon & Beaulieu, 2001; de Wit, 1998). The composition of these ingredients depends on the whey source and on the processing technology. Typical compositions are presented in table 1.

Table 1. Typical composition of milk, whey and derived protein ingredients (%, w/w). Adapted from Smithers et al, 1996; Huffman & Harper, 1999; TECNINVEST, 2000.

			Ingredients		
	Milk	Whey	WPC 34	WPC 80	WPI
Protein	3,6	0,65 - 1,05	34	80	92
Fat	3,7	0,05 - 0,63	3	7	1
Ash	0,7	0,37 - 0,95	7	3	2
Lactose	4,9	4,50 - 5,30	53	6	1
Solids	12,8	6,20 - 7,30	97	96	96

The functional applications include emulsification, gelation and foaming. Gelation is an important functional property of WP that has been extensively studied by different authors (see, for example, Langton & Hermansson, 1992; Le Bon, Nicolai & Durand, 1999; Gosal & Ross-Murphy, 2000; Renard, Robert, Garnier, Dufour & Lefebvre, 2000). Heat-induced gelation is affected by many factors such as pH, concentration, ionic strength, heating rate, and heating temperature.

The ability of whey proteins to form heat induced gels and provide texture is desirable for some “solid like” foods like processed meat, dairy and bakery products. However, this property limits the application of whey proteins in “liquid like” foods including beverages, baby formula and salad dressings (Huang, 1999). Enzymatic hydrolysis impairs the gelation ability and improves the thermal stability of WP and can be used to expand the applications of WP (Doucet, Gauthier & Foegeding, 2001).

From a dietary point of view, the use of whey protein hydrolysates (WPH) instead of the “whole” protein isolates is interesting e.g. to reduce allergenicity or improve digestibility. Milk protein hydrolysates are also an important source of bioactive peptides liberated, from native proteins, during the hydrolysis (Silvestre, 1997). Once liberated, peptides may act as regulatory compounds with hormone-like activity (Pihlanto-Leppälä, 2001).

In this work, a commercial WPC was enzymatically hydrolyzed with trypsin; three hydrolysates with different hydrolysis degree were collected. We have studied, under small deformation rheology, the heat-gelling behaviour of the whey protein tryptic hydrolysates (WPTH) as a function of the degree of hydrolysis and the protein concentration.

2. EXPERIMENTAL

2.1. WPC hydrolysis

A commercial WPC with 70% of protein was used as substrate for trypsin. Samples were prepared by suspending 25 g of WPC in 500 mL of distilled water. The resulting solutions were then heated to the hydrolysis temperature and adjusted to pH 8.0 with concentrate

NaOH. The enzymatic degradations were performed in a 0.5 L stirred, tank-type, batch reactor equipped with pH and temperature control. The pH was kept at 8.0 with NaOH and the temperature was kept constant at 37 ºC. The degree of hydrolysis (DH) achieved was measured by the pH-stat method (Adler-Nissen, 1986). After hydrolysis, the enzyme was inactivated by heating the suspension at 70ºC for 5 min. The resulting suspensions were lyophilised for further analysis using a CHRIST Alpha 2-4 batch freeze-drier (B. Braun Biotech International, Osterode/Harz, Germany).

2.2. Rheology

Sample preparation

Three whey protein tryptic hydrolysates - WPH1, WPH2 and WPH3 - having 1.1, 2.2 and 4.2 DH, respectively, were used. The lyophilised WPHs were hydrated with phosphate buffer (pH 7,0) by slow stirring until the dispersion was complete (3 h). The ionic force was adjusted to 220 mM with NaCl. The protein concentration of the WPH suspensions ranged from 10 to 17%.

Rheological measurements

Rheological measurements were performed with a controlled stress rheometer AR2000 (TA Instruments, Delaware, USA) fitted with a rough acrylic plate geometry (40 mm diameter, gap 500 μm). Before performing the experiments, the samples were covered with a thin layer of liquid paraffin to prevent evaporation.

Each suspension was heated at a rate of 2 ºC.min^{-1} from 20 to 80 ºC. After an equilibration period of 3.5 h at 80 ºC, a frequency sweep ("mechanical spectrum") was recorded over the range 0.06283-62.83 rad.s^{-1}. The sample was then cooled at a rate of 2 ºC.min^{-1} from 80 to 20 ºC and the temperature was maintained during 1 h at 20 ºC. Another frequency sweep (0.06283-62.83 rad.s^{-1}) was recorded at this temperature. Finally, a strain sweep was done. During the temperature, time and frequency sweep experiments, a maximum shear strain of 1 % was stated. Temperature and time sweeps were performed at 6.28 rad.s^{-1}.

3. RESULTS

Figure 1 shows the time evolution of the loss tangent, tanδ (= G''/G'), and of the complex dynamic modulus, G*, at 1Hz, for the three WPH studied at protein concentrations of 13.5% (figure 1A) and 17% (figure 1B).

When tan δ was less than 1 (G'>G''), the systems became gels. For WPH1 and WPH2, values of tan δ gradually decreased during the time sweep at 80 ºC and increased during the cooling stage, suggesting a significant post-gelation restructuring or modification of the network.

For WPH3, gelation occurred only at the end of the time sweep step at 80ºC. During the cooling step (80-20 ºC), modifications of the structure were observed: at a protein concentration of 13,5%, (figure 1A), the WPH3 lost the gel structure whereas, at a protein concentration of 17% (figure 1B), tang δ continued to decrease and a very weak gel was obtained at the end of the experiment.

Figure 2 shows frequency sweeps of the final gels at 20 ºC (protein concentration of 13.5%, figure 1A, and 17%, figure 1B). Only the WPH3 system with 13,5% of protein presented G'<G'' and a high frequency dependence of both modulli which is indicative of a non gel

character (figure 2A). Figure 3A shows the dependence of G' (obtained at 1Hz, from the frequency sweep at 20ºC) on concentration, for each WPH. G' increased as a power law function of protein concentration. It is clear that, for gels WPH1 and WPH2, this dependence increased with DH. We cannot extrapolate this conclusion for WPH3 since it is not a gel for protein concentrations less than 17%. Figure 3B shows the dependence of the rupture strain (%) on concentration. The rupture strain was calculated in the strain sweep step and defined as the strain limit at which the G' variation was less than 5%. A power law function adjusted to the experimental points. Again, the dependence increased with DH.

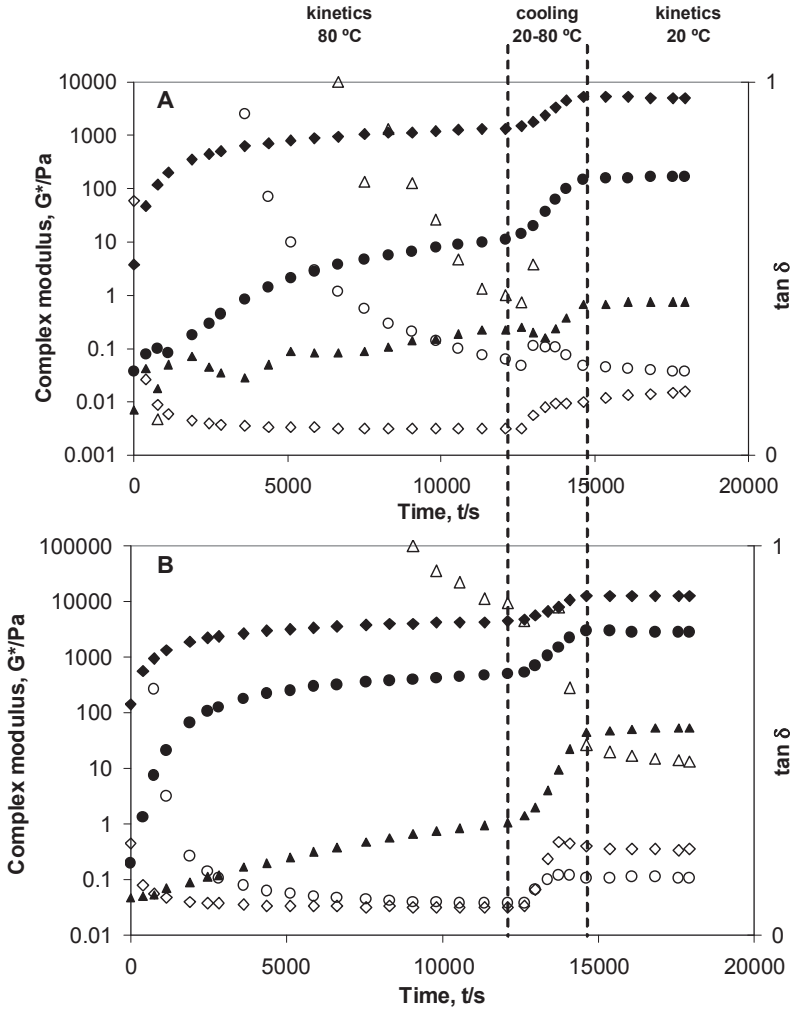

Figure 1. Time evolution of loss tangent (tan δ) and of complex modulus G*. (A) protein concentration 13,5%; (B) protein concentration 17%. WPH1 ♦; WPH2 ●; WPH3 ▲. Filled symbols, G*; empty symbols, tan δ.

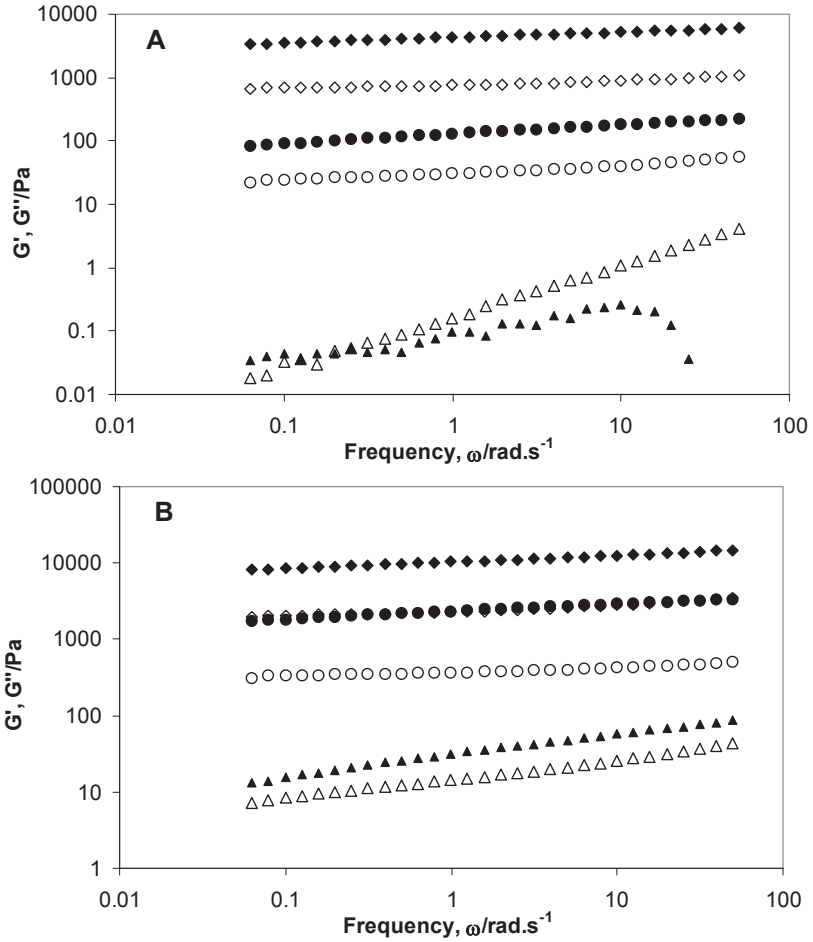

Figure 2. Mechanical spectra of the gels at 20 ºC, strain 1%. (A) protein concentration 13,5%; (B) protein concentration 17%. WPH1 ♦; WPH2 ●; WPH3 ▲. Filled symbols, G'; empty symbols, G''.

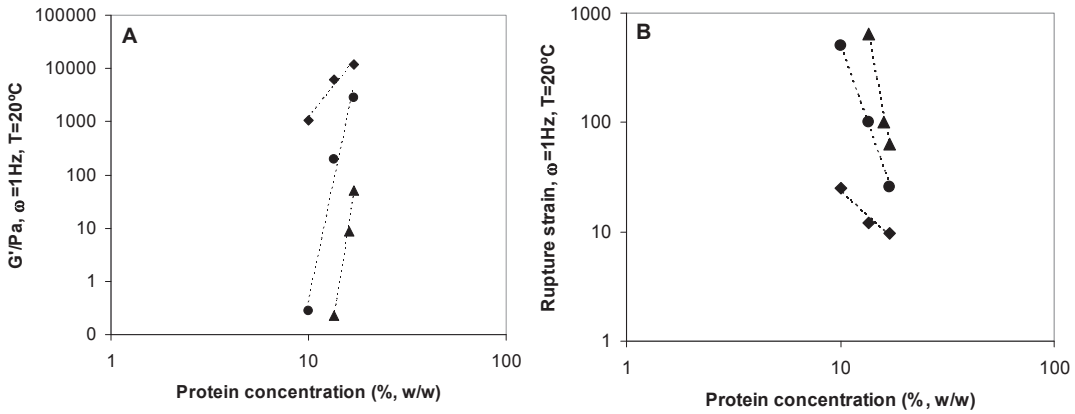

Figure 3. G' (A) and rupture strain (B) vs protein concentration.
WPH1 ♦; WPH2 ●; WPH3 ▲.

As expected, hydrolysis impaired the gelling ability of whey proteins. By carefully controlling the hydrolysis degree, it is possible to improve their functionality for specific applications (Huang, 1999). In the present work, results suggest that WPH3 could be an interesting ingredient for a high protein beverage while WPH1 could be used in dairy desserts or processed meat products.

ACKNOWLEDGEMENTS

This work received financial support from Fundação para a Ciência e a Tecnologia (Project POCTI/2000/QUI/36452).

REFERENCES

- Adler-Nissen, J. (1986). *Enzymic hydrolysis of food proteins*. London, U.K.: Elsevier Applied Science Publishers.
- de Wit, J.N. (1998). Nutritional and functional characteristics of whey proteins in food products. *Journal of Dairy Science*, 81, 597-608.
- Doucet, D., Gauthier, S. F., & Foegeding, E. A. (2001). Rheological Characterization of a Gel Formed During Extensive Enzymatic Hydrolysis. *Food Engineering and Physical Properties,* 66, 711-715.
- Gosal, W.S., & Ross-Murphy, S.B. (2000). Globular protein gelation. *Current Opinion in Colloid & Interface Science*, 5, 188-194.
- Huang, X. L., Catighani, G. L., Swaisgood, H. E. (1999). Modification of rheological properties of whey protein isolates by limited proteolysis. Nahrung, 2, S79-85.
- Huffman, L. M., Harper, W. J. (1999). Maximizing the value of milk through separation technologies. *Journal of Dairy Science*, 82, 2238-2244.
- Langton, M., & Hermansson, A-M. (1992). Fine-stranded and particulate gels of beta-lactoglobulin and whey protein at varying pH. *Food Hydrocolloids*, 5, 523-539.
- Le Bon, C., Nicolai, T., & Durand, D. (1999). Kinetics of aggregation and gelation of globular proteins after heat-induced denaturation. *Macromolecules*, *32*, 6120-6127.
- McIntosh, H. G., Royle, P. J., Le Leu, R. K., Regester, G. O., Johnson, M. A., Grinsted, R. L., Kenward, R. S., Smithers, G. W. (1998). Whey proteins as functional ingredients. *International Dairy Journal*, 8, 425-434.
- Pihlanto-Leppälä, A. (2001). Bioactive peptides derived from bovine whey proteins: opioid and ace-inhibitory peptides. *Trends in Food Science and Technology*, 11, 347-356.
- Renard, D., Robert, P., Garnier, C., Dufour, E., & Lefebvre, J. (2000). Gelation by phase separation in a whey protein system: in-situ kinetics of aggregation. *Journal of Biotechnology*, 79, 231-244.
- Silvestre, M. P. C. (1997). Review of methods for the analysis of protein hydrolysates. *Food Chemistry*, 60, 263-271.
- Smithers, G. W., Ballard, J. F., Copeland, A. D., de Silva, K. J., Dionysius, D. A., Francis, G. L., Goddard, C., Grieve, P. A., McIntosh, G. H., Mitchell, I. R., Pearce, R. J., Regester, G. O. (1996). New opportunities from the isolation and utilization of whey proteins. *Journal of Dairy Science*, 79, 1454-1459.
- TECNINVEST. Estudo de mercado do soro lácteo em Portugal. Relatório T901001/2000. Elaborado para ANIL, Associação Nacional dos Industriais de Lacticínios. 2000.
- Turgeon, S. L., Beaulieu, M. (2001). Improvement and modification of whey protein gel texture using polysaccharides. *Food Hydrocolloids*, 15, 583-591.

STUDY OF THE INFLUENCE OF PRE-HEATING CONDITIONS AND Mg^{2+} CONCENTRATION ON COLD GELATION OF A WHEY PROTEIN ISOLATE

M. Vázquez da Silva[*], *D. Torres, M. P. Gonçalves*
REQUIMTE – Departamento de Engenharia Química, Faculdade de Engenharia da Universidade do Porto, Rua Dr. Roberto Frias s/n, 4200-465, Porto, Portugal

Keywords: protein, whey, gelation, cold-setting, magnesium

ABSTRACT

Heat denatured whey protein isolate (WPI) solutions were used to make ingredients that gel at low temperatures. This study analyses the influence of protein concentration - 4.7 to 10.1 (wt%), holding temperature - 70 to 80 ºC - and time - 10 to 30 min - on the rheology of heat-denatured whey protein solutions. In these experiments, the cold gelation of the denatured protein solutions was induced by the addition of magnesium until 25 mM.

In a second step, the influence of the magnesium concentration (from 25 to 75 mM) on the cold gelation process of a whey protein isolate solution (7.4 wt%), after denaturation at 75 ºC during 20 min, was analysed.

The rheological experiments used to characterize the gels were performed in a controlled stress rheometer, where they were subjected to time, frequency and strain sweep tests.

1. INTRODUCTION

Whey protein isolate is used as a functional ingredient in foods because of its gelation, emulsification and foaming properties. Traditionally, the gels were formed by heating an aqueous solution containing native proteins to a temperature where the globular proteins molecules partially unfolded and then aggregated to form a three-dimensional network that entrapped water through capillary forces[1-3]. More recently, an alternative method has been introduced that allows production of whey proteins gels at low temperatures[4-9]. The cold gelation of whey protein isolate is a promising process because the gelation step occurs at room temperature through the addition of a salt, being specially interesting for applications in the food industry, where heating to high temperatures can be a problem. However, this cold gelation requires a pre-heating step for the protein unfolding, where the environmental conditions are chosen in order to prevent its gelification, which means that the electrostatic repulsion must be such that protein aggregation does not occur. The gelation of the heat-denatured protein is then induced, at room temperature, by the addition of a salt, which screens and disperses charge, leading to a decrease in electrostatic repulsions. In the case of divalent cations, salt addition may also improve the formation of salt bridges between negatively charged groups of proteins. The most common cations used to induce gelation are sodium[3,9], calcium[3,4,6-8] and iron[10]. In this work, we test another option - the magnesium - a divalent cation, which is an important element for the human health.

The physical characteristics of the gels formed depend on the initial characteristics of the heat-denatured whey proteins, as well as the prevailing environmental conditions. Various preparation conditions have been used to produce heat-denatured whey protein solutions used for cold-gelation: holding temperatures have ranged from 70 to 90 ºC, while holding times

[*] Corresponding author-Fax: 22 508 1449, Tel: 22 508 1400 (ext. 2098), email: mvazquez@fe.up.pt

during heating have ranged from 5 to 60 minutes. In almost every previous studies, the pH of the solutions has been hold at 7, but it is possible to obtain gels at other pH conditions[11].

The objective of this study is to analyse the influence of the pre-heating conditions (temperature and time) and the salt concentration on the gelation process. The gels obtained were characterized through rheological experiments made in a controlled stress rheometer, where they were subjected to time, frequency and strain sweep tests.

2. MATERIALS AND METHODS

2.1 Materials

Whey protein isolate powder (LACPRODAN DI-9224, Lot nº 50M160218) was kindly supplied by Arla Foods Ingredients (Videbaek, Denmark). The protein content, determined by the Kjedahl method, was 93.5 %, from which 74 % was β-lactoglobulin. According to the suppliers, the WPI total solids content was 94 % (6 % moisture), the ash content was 4.5 % and the cation content was: sodium, 0.5 %; phosphorus, 0.2 %; chloride, 0.1 %; potassium, 1.2 % and calcium, 0.1 %.

The magnesium chloride, in the form of a hexahydrate salt ($MgCl_2.6H_2O$), the sodium azide and the potassium hydroxide were obtained from Riedel-de-Haën, with weight purity greater than 99, 99 and 85%, respectively. The hydrochloric acid (1 M) was provided by Pronalab.

2.2 Sample preparation

Whey protein solutions of 5.1, 7.9 and 10.8 wt%, which means 4.7, 7.4 and 10.1 wt %, respectively, in terms of total protein (or 3.5, 5.5 and 7.5 wt% in β-Lg), were prepared by dispersing a known amount of the powder into a beaker and bringing to final weight with distilled water and 1M KOH and/or HCl to pH 7. NaN_3 was added to a final concentration of 0.02 (wt %) to prevent bacterial degradation. Each solution was kept under gentle stirring, at room temperature, during at least 3 hours. Covered test tubes (to prevent evaporation) with the protein solution were heated at different temperatures (70, 75 and 80 ºC) and holding times (10, 20 or 30 min) in a water bath. Afterwards, they were immediately immersed in an ice bath and kept for rest at room temperature for 24 hours. Before adding the salt, the protein solutions were degassed.

A 2 M salt solution was prepared by dissolving the appropriate amount of magnesium chloride in distilled water and kept at room temperature.

2.3 Rheology measurements

The rheological measurements were performed with a controlled stress rheometer Carri-Med CSL 50, using a cone-and-plate geometry (2^o cone angle, 40 mm diameter, 55 μm gap). The temperature was controlled by the apparatus (‘Peltier’ system) connected to a recirculation water bath.

The correct amount of salt solution was added to each protein solution in order to obtain the desired concentration of Mg^{2+}, i.e., 25 mM. Since the cold gelation process starts immediately after the salt addition, the samples were transferred to the rheometer in order to start the rheological measurements as soon as possible.

The samples were covered with a layer of paraffin oil to prevent evaporation after having been placed into the measuring device.

The gelation process was monitored by measuring G' and G" at 1 Hz under a 1% strain amplitude, at 25 ºC, for at least 18 hours. Afterwards, a mechanical spectrum was performed from 0.01 to 100 Hz, under a 1 % strain amplitude, at 25 ºC. The strain was within the linear viscoelastic region of the material as determined by a strain sweep done between 0.02984 and 29.84 Pa, at 25 ºC, and frequency of 1 Hz.

3. RESULTS AND DISCUSSION

3.1 Effect of pre-heating conditions

Different whey protein isolate (WPI) solutions were subject to several denaturation conditions, namely, holding temperature and holding time. After denaturation, each solution was kept at room temperature overnight. The samples were characterized according to the following classification:

G - the sample gelled after denaturation and before the salt addition;
√ - the sample did not gel after denaturation, but gelled after the salt addition;
NG - the sample did not gel, even after the salt addition.

Table 1 shows the experimental conditions – protein concentration, holding temperature and time - and the characterization of the samples after denaturation, according to the above classification.

Table 1 – Preliminary results of the cold gelation of WPI solutions.

Protein conc.	**4.7 (wt%)**			**7.4 (wt%)**			**10.1 (wt%)**		
Temp. / time	70 ºC	75 ºC	80 ºC	70 ºC	75 ºC	80 ºC	70 ºC	75 ºC	80 ºC
10 min	NG	NG	NG	NG	NG	NG	NG	√	G
20 min	NG	NG	NG	NG	√	√	√	G	G
30 min	NG	NG	√	NG	√	√	√	G	G

The samples that did not gel after denaturation, but that gelled after the salt addition were subjected to rheological measurements, namely time, frequency and strain sweeps. In Figure 1, the results of the time sweep experiments are shown, through the presentation of the G* modulus.

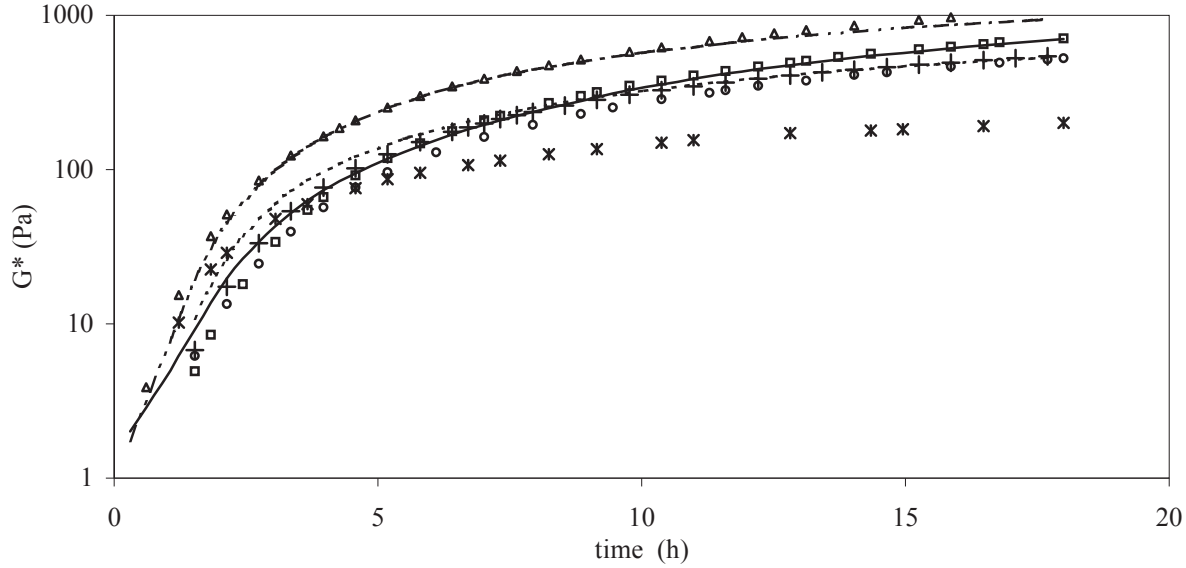

Figure 1 – Time sweep results for different protein concentrations and denaturation conditions.
Legend: —— 10.1% 10min 75ºC; + 10.1% 30min 70ºC; ○ 10.1% 20min 70ºC; Δ 7.4% 30min 80ºC;
−--− 7.4% 20min 80ºC; □ 7.4% 30min 75ºC; --- 7.4% 20min 75ºC; * 4.7% 30min 80ºC

The mechanical spectra (frequency sweeps) results are presented in Figure 2, being possible to easily understand that the samples have the typical behaviour of a gel, since both G' and G'' values are almost unaffected by frequency modifications, and the ratio G'/G'' is about 7.5-10.

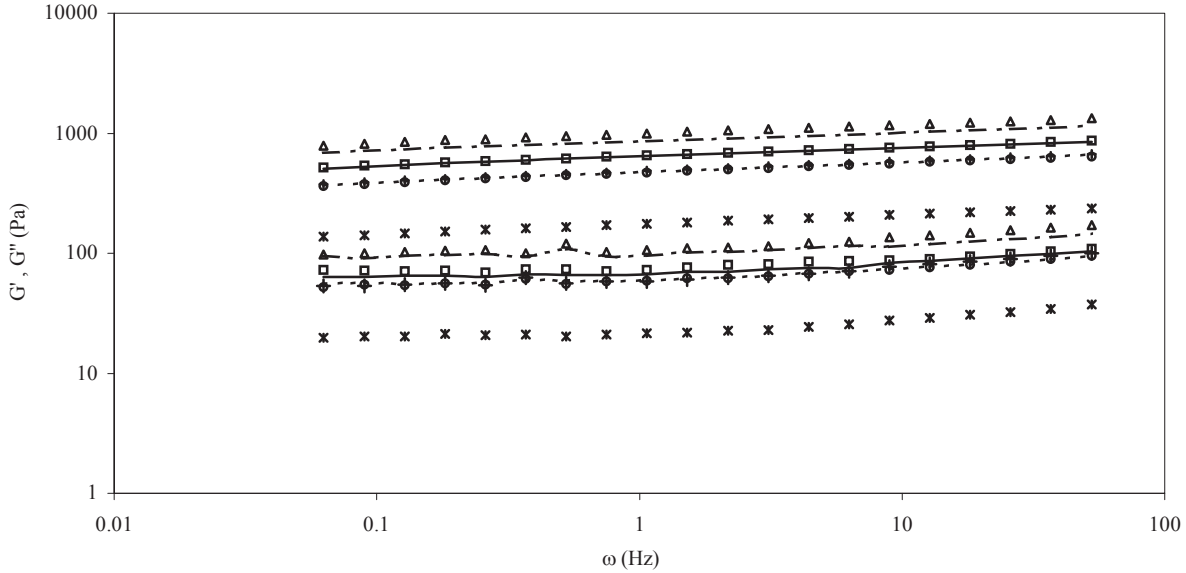

Figure 2 – Mechanical spectra results for different protein concentrations and denaturation conditions.
Legend: —— 10.1% 10min 75ºC; + 10.1% 30min 70ºC; ○ 10.1% 20min 70ºC; Δ 7.4% 30min 80ºC;
−--− 7.4% 20min 80ºC; □ 7.4% 30min 75ºC; --- 7.4% 20min 75ºC; * 4.7% 30min 80ºC
Note: For the same conditions G' > G''.

After the mechanical spectra, the samples were subjected to a strain sweep, with the stress ranging from 0.02984 to 29.84 Pa. The obtained values of G' and G'' are presented in Figure 3, and it is possible to verify that for strains between 0.1 and 5%, the gels are in the linear viscoelastic region.

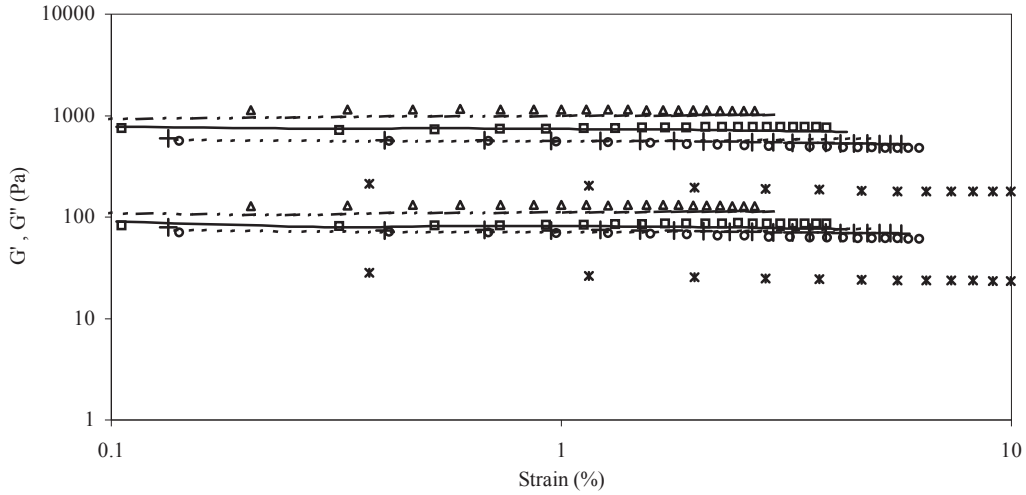

Figure 3 – Strain sweep results for different protein concentrations and denaturation conditions.

Legend: —— 10.1% 10min 75ºC; + 10.1% 30min 70ºC; ○ 10.1% 20min 70ºC; Δ 7.4% 30min 80ºC; −--− 7.4% 20min 80ºC; □ 7.4% 30min 75ºC; --- 7.4% 20min 75ºC; * 4.7% 30min 80ºC
Note: For the same conditions G' > G''.

3.2 Effect of salt concentration on cold gelation

The above results let us conclude that it is possible to obtain gels with different characteristics through the addition of magnesium to WPI solutions denatured under different conditions. Afterwards, the influence of the salt concentration on the gelation process was studied. The solutions of WPI had a concentration of 7.4 (wt%) and were denatured at 75 ºC during 20 minutes. The cold gelation was induced by different concentrations of magnesium in order to understand the role of the salt in the gelation mechanism. The preliminary results obtained until now are shown in Figure 4. This figure shows the G* values for gels produced through the addition of 25, 50 and 75 mM of salt.

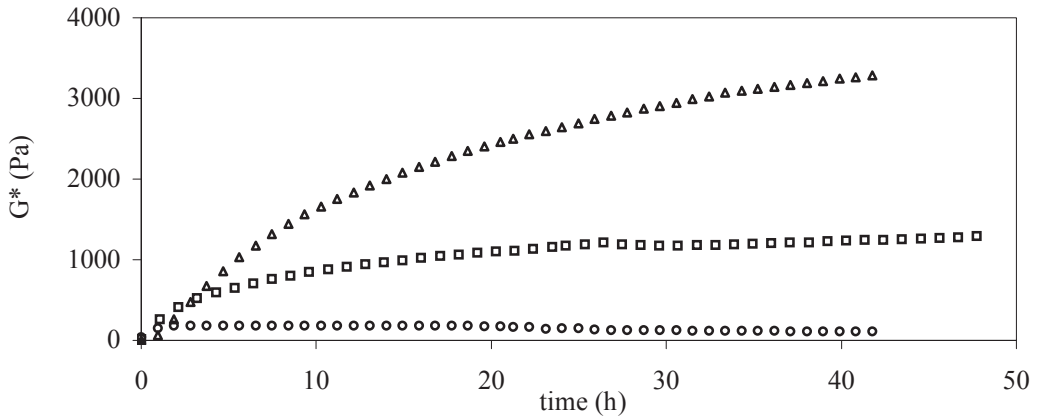

Figure 4 –Time sweep results for different salt concentrations. Legend: Δ 25mM; □ 50 mM; ○ 75 mM.

In a very first analysis, it can be said that the higher is the salt concentration the lower is the gel strength. Nevertheless, this conclusion must be confirmed with further experiments and a more detailed study for a better understanding of the cold-gelation mechanism.

4. CONCLUSIONS

According to the results obtained, it can be verified that is possible to induce the gelation of pre-heated whey protein isolate solutions by the addition of magnesium. This kind of gels is of special interest for food industry because the gelation process occurs at room temperature which is very important regarding that most of the natural products are thermo degradable. This study shows that it is possible to produce gels with different characteristics according to the applied treatment. This fact allows us to choose the most suitable conditions in order to obtain the 'optimum' gel for the desired application.

REFERENCES

[1] Mulvihill, D.M.; Donovan, M.; Whey proteins and their thermal denaturation-A review; Irish J. Food Sci. Tech., 11, 1987, 43-75
[2] Mulvihill, D.M.; Kinsella, J.E.; Gelation characteristics of whey proteins and β-lactoglobulin; Food Tech., 41, 1987, 102-111
[3] Mulvihill, D.M.; Kinsella, J.E.; Gelation of β-lactoglobulin: effects of sodium chloride and calcium chloride on the rheological and structural properties of gels; J. Food Sci., 53, 1988, 231-236
[4] Barbut, S.; Foegeding, E.A.; Ca^{2+} induced gelation of pre-heated whey protein isolate; J. Food Sci., 58, 1993, 867-871
[5] McClements, D.J.; Keogh, M.K.; Physical properties of cold-setting gels formed from heat-denatured whey protein isolate; J. Sci. Food Agric., 69, 1995, 7-14
[6] Barbut, S.; Effects of calcium level on the structure of pre-heated whey protein isolate gels; Lebensm.-Wiss. u.-Technol., 28, 1995, 598-603
[7] Roff, C.F.; Foegeding, E.A.; Dicationic-induced gelation of pre-denatured whey protein isolate; Food Hydrocolloids, 10, 1996, 193-198
[8] Hongsphrabhas, P.; Barbut, S.; Protein and salt effects on Ca2+-induced cold gelation of whey protein isolate; J. Food Sci., 62, 1997, 382-385
[9] Marangoni, A.G.; Barbut, S.; McGauley, S.E.; Marcone, M.; Narine, S.S.; On the structure of particulate gels - the case of salt-induced cold gelation of heat-denaturated whey protein isolate; Food Hydrocolloids, 14, 2000, 61-74
[10] Remondetto, G.E.; Paquin, P.; Subirade, M.; Cold Gelation of b-lactoglobulin in the presence of iron; J. Food Sci., 67, 2002, 586-595
[11] Bryant, C.M.; McClements, D.J.; Optimizing preparation conditions for heat-denatured whey protein solutions to be used as cold-gelling ingredients; J. Food Sci., 65, 2000, 259-263

SHORT-TERM AGEING OF O/W EMULSIONS HOMOGENISED IN A COLLOID MILL PILOT PLANT: A RHEOLOGICAL AND LASER DIFFRACTION STUDY

J. Muñoz[1]; I. Zapata[1]; M.C. Alfaro[1]; M. Berjano[1], V. Flores[1], J. de la Fuente[2], M.Ruíz[2]*

[1]Departamento de Ingeniería Química. Facultad de Química. Universidad de Sevilla. C/ Prof. García González, 1. 41012 Sevilla. España. Phone: (34)954557179, Fax: (34)954556447, E-mail: jmunoz@us.es.
[2]Departamento de Ingeniería Química. Escuela Universitaria Politécnica. Universidad de Sevilla. C/ Virgen de Africa s/n. 41011 Sevilla. España.

Key words: food emulsions, rheology, viscoelasticity, homogenisation, emulsion stability

ABSTRACT

The aim of this project was to set up an experimental design to monitor possible physical changes of highly concentrated O/W emulsions homogenised in a colloid mill at pilot plant scale. The effect of emulsion storage at room temperature was compared with that of storage under refrigerated conditions. Small amplitude oscillatory shear experiments and droplet size distribution (DSD) measurements by laser diffraction were used as experimental techniques. Rheokinetic experiments shortly after emulsion manufacture and frequency sweeps tests at longer time were conducted to study the ageing effect on the rheological properties of emulsions.
The results obtained revealed that the thermal inertia after homogenisation was rather important. However, under the specific manufacture conditions used, emulsions kept at room temperature exhibited G' and G'' values at 20ºC which remained constant between 5 and 336 hours after preparation, showing the same weak gel properties. As far as the DSDs are concerned, they slightly shifted towards a high mean diameter between 24 and 48 hours. After that, the DSDs did not exhibit significant differences along the whole ageing time allowed for this study.
When the emulsion was kept in cold storage, neither the DSD nor the dynamic viscoelastic properties significantly change with ageing in the same period of time. Interestingly, their G' and G'' values were slightly higher than those of the emulsion kept at room temperature. These rheological results were consistent with the lower mean oil droplet diameters of the former, due probably to the fact that coalescence occurring immediately after homogenisation, as a consequence of the high energy input required, was kinetically controlled.

1.INTRODUCTION

Highly concentrated oil in water emulsions exhibit profitable commercial applications in cosmetics and in the food industry. The commercial success of this type of emulsions not only relies on sensorial properties but also on the right consistency as well as on the expected microbiological, chemical and physical stability. The latter should be monitored by different methods, taking into account the different physical instability mechanisms, which may take place even simultaneously (1). Rheology assisted by further techniques has been recently reported that provide useful information concerning the ageing effects on emulsions (Tadros, 2004).
This works focuses on the study of short-time stability of food emulsions on account of consumers' preference trends for fresh stuffs, the interest of researchers and emulsion manufacturers to study the occurrence of possible kinetic effects shortly after emulsion processing.
Rheokinetic experiments in small amplitude oscillatory shear shortly after manufacture and mechanical spectra at longer ageing time were used along with droplet size distribution

measurements to describe the physical stability of the emulsion kept either at room temperature or in cold storage.

2. EXPERIMENTAL

The oil in water (O/W) emulsion studied in this work was formulated on the basis of 76% (wt) sunflower oil, a food grade spray-dried emulsifier containing 30,2% (wt) proteins and typical ingredients usually found in mayonnaise.

The emulsion was manufactured in a Delmix VK7 (Fryma-Koruma) colloid mill pilot plant. First of all, the components of the aqueous phase were added from the liquid hopper through a ball valve to the main vessel. Secondly, the pre-mixed solid ingredients were fed from the solid hopper through another ball valve, starting the agitator and the colloid mill motor. The suspension was pre-homogenized for a short time before feeding the required amount of oil. Finally, a further controlled homogenisation time of about 50s was allowed. A vacuum pressure of (-50kPa) was chosen. The emulsion temperature did not exceed 29ºC during the manufacture process thanks to the cooling jacket, which was fed by water at room temperature.

Samples kept in cold storage were at about 4ºC in separated flasks until one hour before characterization.

Two CS rheometers from Thermo-Haake, Rheostress RS100 and Rheostress RS150 were used. Plate and plate geometry with serrated surface was used to carry out all the small amplitude oscillatory shear experiments. The PPR35 and PPR60 sensor systems were chosen, which have 35mm and 60mm diameter, respectively. A gap of 1mm was always fixed. A silicon oil sealing fluid was used to prevent samples from moisture losses. All the rheological measurements were done at 20ºC. The mechanical spectra results are the average of at least two replicates.

Oil droplet size distribution (DSD) was determined by laser diffraction in a Malvern Mastersizer X (Malvern Instruments). The sunflower oil refraction index was 1.4694 and the corresponding absorption index used was 0.1. The experimental protocol was designed to avoid the occurrence of flocculation during the DSD measurements.

3. RESULTS AND DISCUSSION

Figure 1 shows the results obtained when conducting small amplitude oscillatory shear rheokinetic experiments shortly after emulsion manufacture. In practice, they consisted of a time sweep at fixed frequency and at a strain amplitude which guaranteed a linear viscoelastic response. The strain amplitude value was 0,001 as determined by preliminary results. The fact that both moduli (G’ and G’’) remained essentially constant with the oscillation time supported the linear viscoelasticity condition.

It is noteworthy the high thermal inertia exhibited by the emulsion after its manufacture. Special care was taken to guarantee that the measurement temperature for the rheological experiments, 20ºC, was actually reached before conducting any test.

Rheokinetic experiments are better suited than mechanical spectra to cope with possible fast changes in sample microstructure since the time scale to complete a reasonable mechanical spectrum may be longer or of the same order of magnitude as the characteristic time of the structural change. Figure 1 also shows that neither G’ nor G’’ exhibited a definite trend between 5h and 8,5 h ageing. This supports the lack of significant coalescence along that ageing time. However, the results obtained were slightly different. This may be attributed to the expected variability of the technique coupled with the heterogeneous nature of emulsions. In fact, the viscoelastic response must be sensitive to the polidisperse oil droplet distribution (Table 1) showed by this emulsion, like many other commercial samples. Size polidispersity

implies that oil droplet flocs will probably be slightly heterogeneous. However, as many flocs are included in the sampling volume for rheological characterization the actual problem of sample being heterogeneous at microscopic scale is dampened.

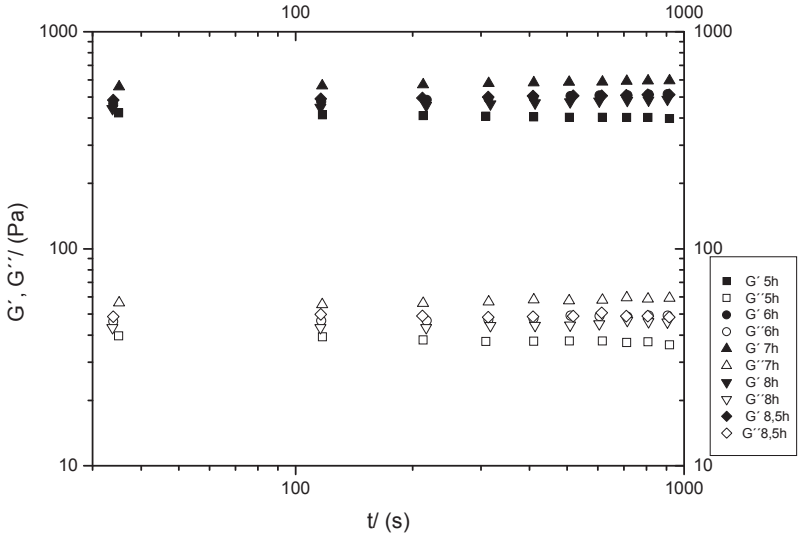

Fig.1. Rheokinetic experiments as a function of ageing at short time after emulsion manufacture. Time dependence of G' and G''at 1Hz (γ^o = 0.001). Temperature: 20ºC.

Once the lack of fast structural changes in the samples was checked, mechanical spectra were obtained as a function of ageing time, since they provide far more information than the oscillation time sweeps at only one frequency. Figure 2 shows that once again the viscoelastic properties did not change with ageing for roughly two weeks.

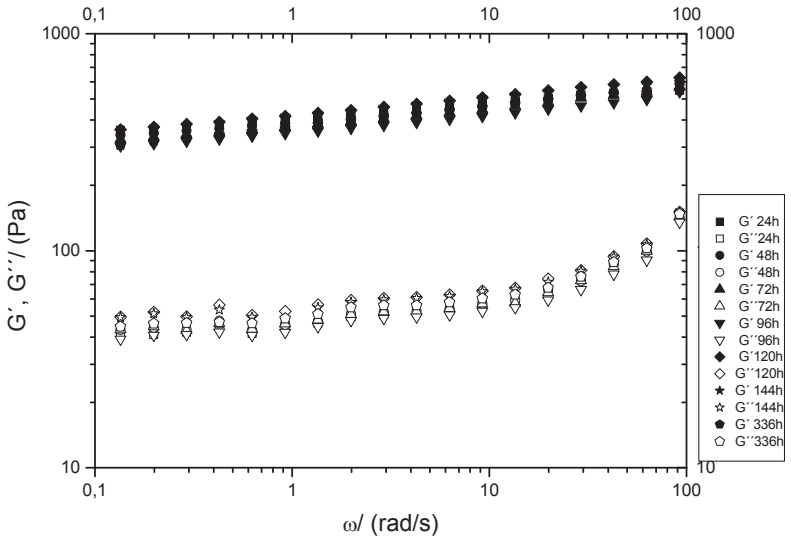

Fig.2 Influence of ageing time on the mechanical spectra at 20ºC (γ^o=0.001)

The concentrated emulsion prepared can be considered as a highly flocculated emulsion. Its high oil volume fraction clearly exceeds the critical value for the formation of a close packing network, resulting in viscoelastic behaviour with weak gel properties.
In order to collect the results obtained with the rheokinetics and mechanical spectra experiments, the G' and G'' results at 1Hz are plotted in figure 3. As can be clearly observed, G' and G'' values were not significantly influenced by ageing during the period of ageing time covered. The G' values are sensitive to the average number of contacts among droplets and to the strength of contacts. Therefore, increasing G' values may be attributed to a flocculation process, while decreasing G' values may be related to coalescence. In any case, this interpretation should be considered with caution if both phenomena take place at the same time or if Ostwald ripening occurs at well. For this reason, the assistance of laser diffraction to detect coalescence is vital for a correct interpretation of these rheological results.

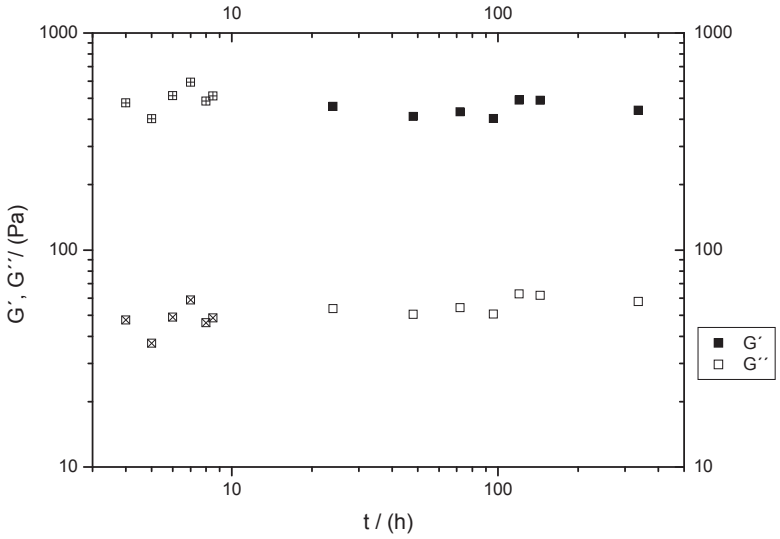

Fig. 3. Influence of ageing time on G' (crossed square: from rheokinetics; closed square: from mechanical spectra) and on G'' (square with x inside: from rheokinetics; opened square: from mechanical spectra). 1Hz. Temperature: 20ºC. (γ^o=0.001). Emulsion kept at room temperature.

Ageing time (h)	D (3,2)	D (4,3)	Span
24	6.43	21.83	2.580
48	7.17	26.41	2.572
72	7.20	26.06	2.644
96	7.55	27.58	2.629
120	7.64	28.93	2.542
144	7.25	27.34	2.563
336	7.41	28.99	2.795

Table 1 Ageing effect on the Sauter's diameter, D (3,2), volumetric diameter, D (4,3) and Span of the droplet size distribution for the emulsion kept at room temperature

Table 1 shows that the mean diameters exhibited a trend to increase from 24 hours to 48 hours ageing which is not significant from a statistical point of view. In fact, no consequences were observed in the dynamic viscoelastic response.
A similar experimental protocol was set up to study the effect of ageing on samples kept in cold storage. Figure 4 summarises the rheokinetic and mechanical spectra results obtained.

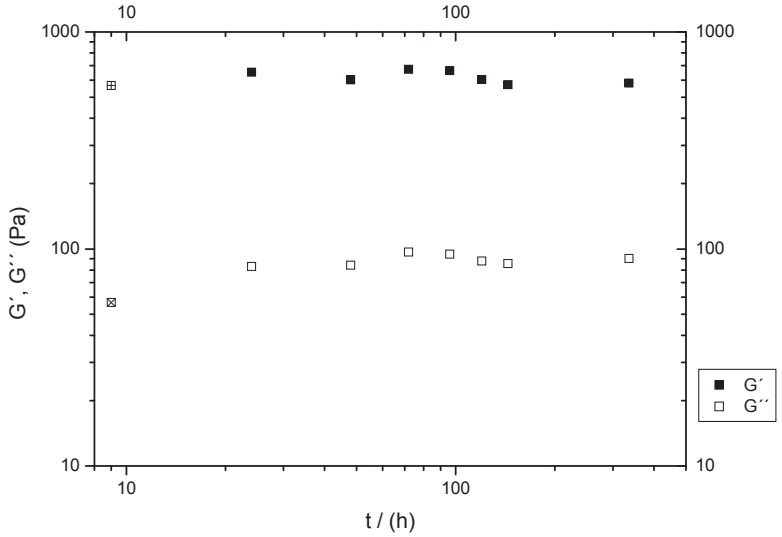

Figure 4. Influence of ageing time on G' (crossed square: from rheokinetics; closed square: from mechanical spectra) and on G'' (square with x inside: from rheokinetics; opened square: from mechanical spectra). 1Hz. Temperature: 20ºC. (γ^o=0.001). Emulsion kept in cold storage (4ºC).

Ageing did not influence the G' and G'' values of the emulsion kept in cold storage. The mechanical spectra were not affected either. With regards the ageing effect on DSD results of emulsions kept in cold storage (Table 2), we did not observe even a trend to increase the mean diameters from 24h to 48 h as it was the case for the emulsion kept at room temperature. In fact, all the relevant parameters describing the DSD and the whole distribution itself (not shown) exhibited an excellent stability during the ageing time covered in this study.

tiempo (h)	D (3,2)	D (4,3)	Span
24	5.69	17.85	2.380
48	5.78	18.48	2.343
72	6.30	20.65	2.403
96	6.31	20.24	2.373
120	6.25	19.71	2.364
144	6.76	22.82	2.376
336	6.41	21.36	2.508

Table 2. Ageing effect on the Sauter's diameter, D (3,2), volumetric diameter, D (4,3) and Span of the droplet size distribution for the emulsion kept in cold storage

Interestingly, the G' and G'' values of the emulsion kept in cold storage were slightly higher than those of the emulsion kept at room temperature. These rheological results were consistent with the lower mean oil droplet diameters of the former, due probably to the fact

that coalescence occurring immediately after homogenisation, as a consequence of the high energy input required, was kinetically controlled when temperature was, in practice, smoothly decreased from 29ºC to room temperature and then kept in a refrigerator.

4. CONCLUSIONS

A highly flocculated O/W emulsion containing 79% (wt) sunflower oil, manufactured in a cooled colloid mill pilot plant, exhibited an excellent physical stability for at least two weeks. No indication of creaming or coalescence was observed regardless the storage temperature. This foresees a good long-term physical stability. Rheokinetic tests under oscillatory shear, mechanical spectra and droplet size distribution measurements clearly supported the conclusions drawn from the experimental results, since neither the storage modulus values nor the loss modulus values were influenced by ageing. In addition, the mechanical spectra, which showed typical weak gel properties, turned out to be also stable for ageing during at least two weeks. The results obtained indicated that it is not necessary to wait for several days to start a rheological characterization since any possible structural rebuilding process, after the high energy-input applied during homogenisation, may be quite fast. As a matter of fact, the emulsion is ready to be studied or delivered from a factory after resting for 48 hours if we consider the droplet size distribution results obtained for samples kept at room temperature. Storage at low temperature, let's say at about 4ºC, "freezes", i.e. kinetically controls, the coalescence occurring immediately after homogenisation as a consequence of the high energy input required. Therefore, under cold storage the emulsion is ready for characterization just 10 hours after its manufacture.

ACKNOWLEDGMENTS

This work is part of the project AGL2002-03898, which has been funded by the Spanish Ministerio de Ciencia y Tecnología (MCYT) and the European FEDER program. The authors gratefully acknowledge the financial support received.

6. REFERENCES

1.Mc Clements D.J. Food Emulsions. Principles, Practice and Techniques. CRC Press. Boca Raton. USA (1999).

2.Tadros, T. Application of rheology for assessment and prediction of the long-term physical stability of emulsions. Adv. Colloid Interface Sci. 108-109, 227-258 (2004).

DEVELOPMENT STUDIES OF SHAMPOOS CONTAINING DIFFERENT SURFACTANTS

*V. Grilo, A. Raposo, H. M. Ribeiro**

UCTF - Faculdade de Farmácia da Universidade de Lisboa
Av. Forças Armadas, 1600 Lisboa, Portugal
Tel: 00.351.217 946 400; Fax: 00.351.217 937 703
helena.ribeiro@ff.ul.pt

Introduction

The primary fuction of a shampoo is to clean both hair and scalp of soils and dirt. Modern shampoos must display detergent, wetting, emulsifying, and foaming properties, thereby ensuring cleaning the hair, while leaving it soft, supple, lustrous and easy to manage.
Mixed solutions of anionic and zwitterionic surfactants are used in various detergent formulations because of their superior properties in comparison to the properties of individual surfactants. In addition, the mixed solutions often have improved foaming, emulsifying and rheological properties, at the same total surfactant concentration, which are important for their applications [(1-4)].
Alkylbetaines and their derivatives represent a class of zwitterionic surfactants, which are electro-neutral inner salts in a wide pH range, with a positive charge on the nitrogen atom and a negative charge on the carboxyl group. Alkylbetaines are among the most widely used co-surfactants in mixtures with anionic surfactants, such as sodium laureth sulfate and various mixtures of sodium laureth sulfates with fatty alcohols especially in shampoos and liquid detergents, because they have a pronounced foam/lather boosting, antistatic, and hair conditioning effects [(5)].
Viscosity is an important aspect of shampoo formulation. Products must have sufficient viscosity to stay on the palm of the hand prior to application but must not come out of the bottle as a globular lump. Anionic systems may be thickened by the addition of electrolytes or non-ionic compounds or by betaines. Sodium chloride and cocamidopropyl betaine are the materials of common choice but others, such as cocoamide DEA, are worth consideration [(6)].

The main purpose of this work was to develop and characterise the physicochemical properties of shampoos containing different surfactants (sodium laureth sulfate, mixtures of sodium laureth sulfates with fatty alcohols and cocoamidopropyl betain) with thickening agents (cocamide MEA and sodium chloride) and preservatives.

Materials and methods

Three shampoos were prepared using different concentrations of surfactants: 12:0:0 (reference); 9:3:0 (formulation 1); 6:2:4 (formulation 2), sodium laureth sulfate (Texapon N70®, Cognis, Dusseldorf, Germany), cocamidopropyl betaine (Tego Betaína L7® , Degussa, Goldschmidt Ag, Germany) and mixtures of sodium laureth sulfates with fatty alcohols (Texapon ASV®, Cognis, Dusseldorf, Germany) sodium laureth sulfate, magnesium laureth sulfate, sodium laureth-8 sulfate, magnesium laureth-8 sulfate, sodium oleth sulfate, magnesium oleth sulfate, as shown on table 1.
Cocamide DEA (Comperlam KD®, Cognis, Dusseldorf, Germany) (3%) and sodium chloride (2%) were added as thickening agents.

Table 1: Shampoos formulations

FORMULATION	SURFACTANT sodium laureth sulfate, cocamidopropyl betaine and mixtures of sodium laureth sulfates with fatty alcohols (%)	NaCl (%)	Cocamide DEA (%)
reference	12:0:0	2.5	0.0
1	9:3:0	--	3,0
2	6:4:2	2,0	1,3

Some physical and chemical properties of the shampoos were evaluated: *pH:* A potenciometric method (Methrom Herisau, pH meter E 516) was used on shampoos; *Rheology:* A Brookfielfd viscometer (Model DVII, SSA, SPD nº 27 at 25 °C) was used to determine the apparent viscosity and the reograms; *Foam expansion*: the ratio between the volume of foam and the volume of liquid from which the foam is generated; *Percentage of active substance:* according to the NP 1204 [7].

Results and Discussion

All the results are shown on table 2.

The pH value for the reference was very low: 3,45. The shampoos must be as neutral as possible, so as not to interfere with other preparations. So, this data is not acceptable for shampoos and can also interfere with other hair care preparations. The formulations made with mixed anionic and anphoteric surfactants (formulation 1 and 2) reveal more acceptable values (5- 5,4).

Table 2. : Physicochemical characterization of the shampoos

FORMULATION	APPEARANCE OF SHAMPOOS	pH*	FOAM EXPANSION (cm)*	APPARENT VISCOSITY (mPa)	% ACTIVE SUBSTANCE*
Reference	▪ Colourless ▪ Clear ▪ Fluid	3,45 (± 0,01)	2,7 (± 0,20)	15500 (± 152,3)	11 (± 0,58)
1	▪ Colourless ▪ Clear ▪ Thick	5,00 (± 0,05)	4,1 (± 0,36)	20700 (± 118,6)	8,0 (± 1,53)
2	▪ Colourless ▪ Clear ▪ Thick	5,40 (± 0,06)	3,8 (± 0,46)	21500 (± 190,0)	9,0 (± 1,73)

*** n = 3**

The amount of foam generated by all the surfactants and the foam stabilizers was very different comparing the reference with formations 1 and 2. Foam is also a function of the primary surfactant and few materials can compete sodium laureth sulfate for quick flash foam. Amphoteric surfactants (cocamidopropyl betaine) and cocamide DEA make the foam creamier and stabilise it.

Continuous shear experiments measure the ability of each system to resist structural breakdown during the standardised shearing procedure. The flow curves obtained for the

reference and formulation 2 presented Newtonian flow behaviour. Formulation 1 was in the form of clockwise hysteresis loops, indicating shear thinning.
Representative plots are shown in figure 1 with apparent viscosity values calculated at the 12,24 s^{-1} also shown in the figure. Apparent viscosity values provide a comparison of the resistance to structural breakdown between the shampoos and the loop areas compare the amount of structure that fractures in the standardised cycle. Measurements with mixed surfactant solutions showed that their viscosity rapidly increased. This data is related with micelle diameter and solution viscosity [5, 8].

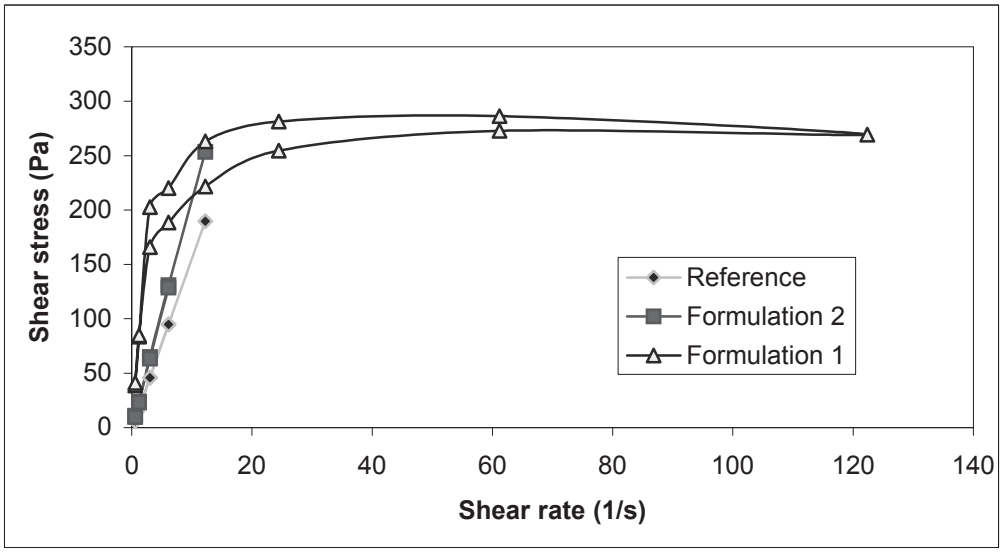

Figure 1: Shampoos' Rheograms

The mechanisms of hair cleansing are complex. Undamaged hair has a hydrophobic surface to which lipids are strongly adsorbed. When hair is shampooed anionic surfactants are adsorbed to hair by their hydrophobic tails and the negatively charged heads orientate outwards. The fibre surface is thus wetted and non-polar materials are displaced. Semi-polar materials are solubilised into micelle structures and are removed by rinsing. Surfactants are a wide group of chemicals exhibiting different application properties. The percentage of active substance showed a variation from 8 to 11%. The daily shampoos are based on very mild anionic and anphoteric surfactants, such as mixtures of sodium laureth sulfates with fatty alcohols and cocamidopropyl betaine. The reference reveal the highest value which can be aggressive to the hair [9].

Conclusions:
The physicochemical and characterisation of these shampoos showed that the mixed preparations were more acceptable than the shampoos containg only anionic surfactants (reference) or aninic and amphoteric surfactant (formulation 1). Foaming, rheological properties and mild detergency was present in the shampoo formulated with sodium laureth sulfates, cocamidopropyl betaine and sodium laureth sulfate. It has superior properties when compared with the other formulations.

References:

1. Lomax, E. G., Ed. *Amphoteric Surfactants*, Surfactant Science Series, **59**; Marcel Dekker: New York, 1996.
2. Domingo, X. In *Amphoteric Surfactants*, Surfactant Science Series, **59**; Lomax, E. G., Ed.; Marcel Dekker: New York, 1996;
3. Tsujii, K. *Surface Activity: Principles, Phenomena, and Applications*; Academic Press: New York, 1998.
4. Basheva, E. S., Ganchev, D., Denkov, N. D., Kasuga, K., Satoh, N., Tsujii, K., *Role of Betaine as Foam Booster in the Presence of Silicone Oil Drop,.* Langmuir (2000), **16,** 1000-1013.
5. N. C. Christov, N. D. Denkov, P. A. Kralchevsky, K. P. Ananthapadmanabhan, A. Lips, *Synergistic Sphere-to-Rod Micelle Transition in Mixed Solutions of Sodium Dodecyl Sulfate and Cocoamidopropyl Betaine*, Langmuir **20** (2004) 565-571.
6. Duarte, A.T., Silva, L.T., Salústio, P., Ribeiro, H.M., *Abordagem do comportamento reológico de champôs contendo diferentes espessantes*, Ver. Port. Farm., vol. II, **1**, supl 124, (2003).
7. Norma Portuguesa 1204, 1976
8. Ribeiro, H. M., Morais, J. A., Eccleston, G. M. *Structure and rheology of emulsions o/w containing different polymers*, Int. J. of Cosmetic Science, 2004, **26**, 47-59
9. Barata, E., "Cosméticos – Arte e Ciência", Lidel, Lisboa, 2002, 92-95.

RHEOLOGICAL BEHAVIOUR OF HIGH-VISCOSITY EMULSIONS: A COMPARISON BETWEEN THE PREDICTIVE CAPABILITIES OF SEVERAL THEORETICAL MODELS

*J. M. Silva, A. V. Machado and J. M. Maia**

Department of Polymer Engineering , University of Minho, Campos de Azurém, 4800 Guimarães, Portugal, email: jmaia@dep.uminho.pt

Keywords: Emulsions models; polymer blends; linear viscoelastic behaviour.

Synopsis

Several models (Palierne, Bousmina (1999) and Lee-Park models) for describing the rheological behaviour of emulsions of polymers are compared. For characteristic values of blends of immiscible polymers, the Palierne and Bousmina models give predictions approximately similar for linear viscoelastic data. The Doi-Otha and Lee-Park models are able, in principle, to describe the behaviour of polymer blends for any type of flow and are usually used to predict the transient response of emulsions. In this work we compare the Lee-Park model and an extension of the Doi-Otha model to include fluids with different viscosities with the Palierne model for linear viscoelastic proprieties.

I. INTRODUCTION

In last years, the importance of blends of immiscible polymers has increased with a large number of studies about relationships between rheology and morphology having been developed. In fact, the rheological behaviour of a blend depends not only on the properties and proportion of the neat polymers, but also on its morphology and the interfacial tension between polymers. Palierne derived an equation for predicting the molten immiscible polymer blend behaviour when subject to small amplitude oscillatory flow:

$$G_B^* = \frac{1+3\sum_i \phi_i H_i^*(\omega)}{1-2\sum_i \phi_i H_i^*(\omega)} G_M^*(\omega) \tag{1}$$

with

$$H_i^*(\omega) = \frac{4\left(\alpha/R_i\right)\left[2G_M^*(\omega)+5G_I^*(\omega)\right]+\left[G_I^*(\omega)-G_M^*(\omega)\right]\left[16G_M^*(\omega)+19G_I^*(\omega)\right]}{40\left(\alpha/R_i\right)\left[G_M^*(\omega)+G_I^*(\omega)\right]+\left[2G_I^*(\omega)+3G_M^*(\omega)\right]\left[16G_M^*(\omega)+19G_I^*(\omega)\right]} \tag{2}$$

where G_M^* is complex modulus of the matrix, G_I^* is complex modulus of the dispersed phase, α is the interfacial tension and ϕ_I is the volume fraction of particles with radius R_i.

Starting from the Kerner model, Bousmina derived another expression for G^*

$$G_B^* = G_m^* \frac{2\left(G_I^*+\alpha/R\right)+3G_M^*+3\phi\left(G_I^*+\alpha/R-G_M^*\right)}{2\left(G_I^*+\alpha/R\right)+3G_M^*-2\phi\left(G_I^*+\alpha/R-G_M^*\right)} \tag{3}$$

where R is the mean radius of dispersed phase.
A new model was proposed for Doi and Otha and later modified by Lee and Park to account for a mismatch in the viscosities of polymers. They proposed the following constitutive equation:

$$\sigma_{ij} = \left(1 + \frac{6(\eta_I - \eta_M)}{10(\eta_I + \eta_M)}\phi\right)\eta_M \dot{\gamma}_{ij} - \alpha q_{ij} - P\delta_{ij} \tag{4}$$

where the anisotropy tensor is given by

$$\frac{\partial}{\partial t} q_{ij} = -q_{ik} d_{kj} - q_{jk} d_{ki} + \frac{2}{3}\delta_{ij} d_{lm} k_{lm} - \frac{Q}{3}\left(d_{ij} + d_{ji}\right) + \frac{q_{lm} d_{lm}}{Q} q_{ij} - \lambda \frac{\alpha}{\eta_M} Q\, q_{ij} - \lambda \nu \frac{\alpha}{\eta_M}\left(\frac{q_{lm} q_{lm}}{Q}\right) q_{ij} \tag{5}$$

$$\frac{\partial}{\partial t} Q = -d_{ij} q_{ij} - \lambda \mu \frac{\alpha}{\eta_M} Q^2 - \lambda \nu \frac{\alpha}{\eta_M} q_{ij} q_{ij} \tag{6}$$

where λ is total relaxation parameter, μ size relaxation , ν shape relaxation. The μ parameter is associated to coalescence, so, it can be considered zero in small amplitude oscillatory flow because deformation of dispersed phase is small. Other considerations suggested $\nu = 1 - \phi$, for the same flow type.

II. INFLUENCE OF EMULSION PARAMETERS IN THE PALIERNE MODEL

We considered a two fluids emulsion. We suppose that both fluids behaviour of Maxwellian mode, according to

$$G^* = \frac{i\omega\eta}{1 + i\omega\lambda} \tag{7}$$

with $\lambda_M = \lambda_I = 0.1s$. We suppose that: matrix and inclusions have the same viscosity ($\eta_M = \eta_I = 10^6$ Pa.s), the interfacial tension is 10 mN/m, the volume fraction is 0.2 and all droplets have same radius, $R = 1\mu m$. Then, we change some parameters value.

A. Radius of dispersed phase

Figure 1 show that the plateau modulus in G' decrease with increasing of radius of particles of dispersed phase. The effect of interfacial tension is opposite since eq 2 depends on α / R_i .

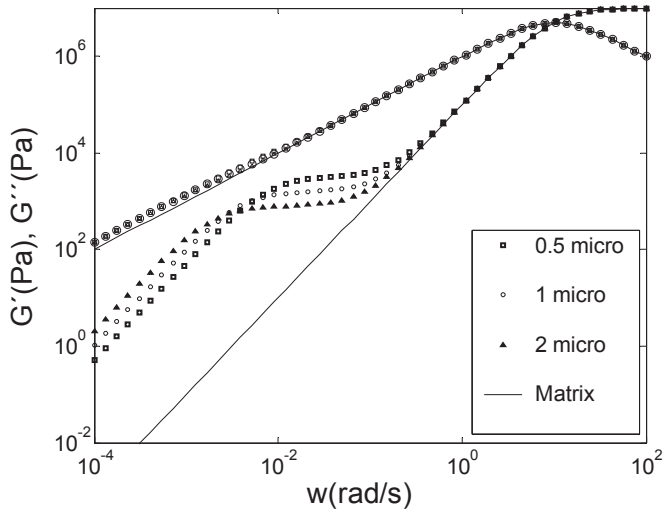

Figure 1 - Dynamic moduli vs frequency. Effect of variation of radius of inclusions. (micro = μm)

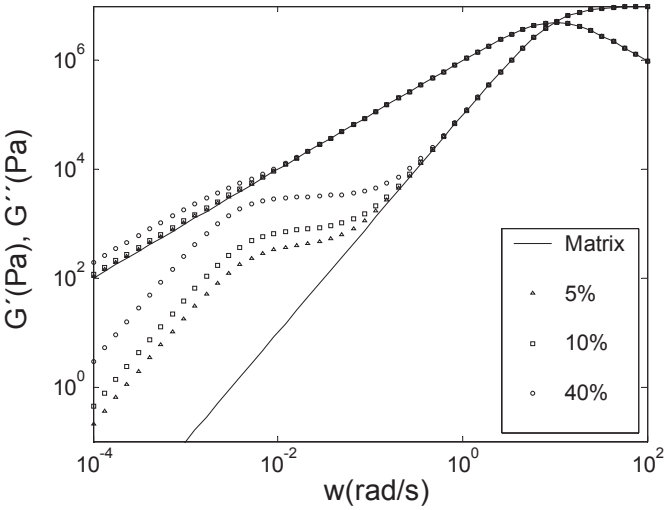

Figure 2 - Dynamic moduli vs frequency. Effect of variation of volume fraction of disperse phase.

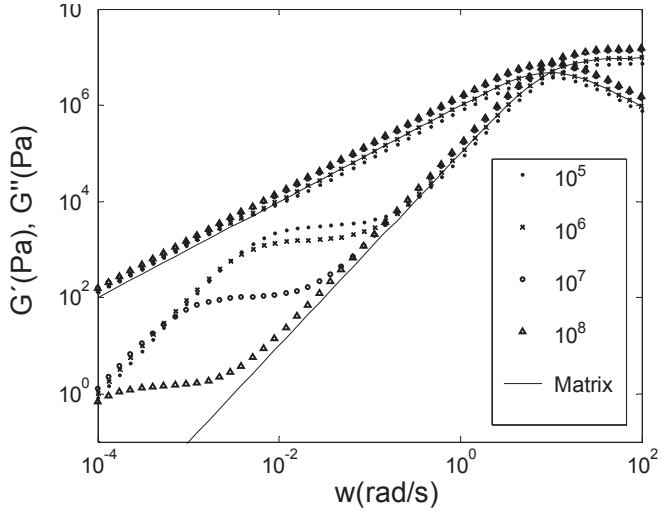

Figure 3 – Dynamic moduli vs frequency. Effect of the zero-shear viscosity of the dispersed phase.

B. Volume fraction of the dispersed phase

The increase of volume fraction of dispersed phase leads to an increase of the $G^{'}$ plateau; figure 2 also shows a slight increase of $G^{''}$ to low frequencies.

C. Viscosity ratio

From the analysis of figure 3 we conclude that plateau modulus in $G^{''}$ decreases with increasing of viscosity ratio between the dispersed phase and the matrix.

D. Relaxation time of the dispersed phase

When the relaxation time of the dispersed phase increases the plateau modulus in $G^{''}$ also increases (Figure 4).

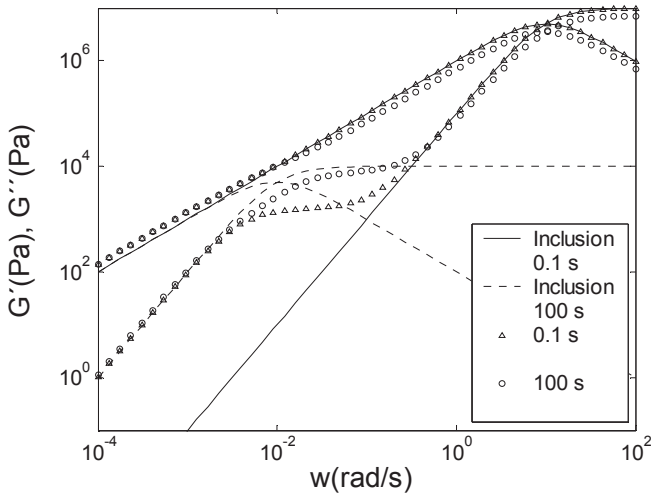

Figure 4 - Dynamic moduli vs frequency. Effect of relaxation time of dispersed phase.

III. COMPARISON BETWEEN PALIERNE AND LEE-PARK MODELS

The Bousmina and Palierne models give very similar predictions for typical values of the parameters, which is not the case with the predictions of the Lee-Park model. We compared these models varying different parameters.

A. Radius

In the Lee-Park model the interfacial area, Q, appears and is related to the particle radius by:

$$Q = \frac{6\phi}{R} \tag{8}$$

Figure 5 shows, for both radii, that the plateau modulus in $G^{''}$ predicted for by the Lee-Park model is higher than that predicted by Palierne model.

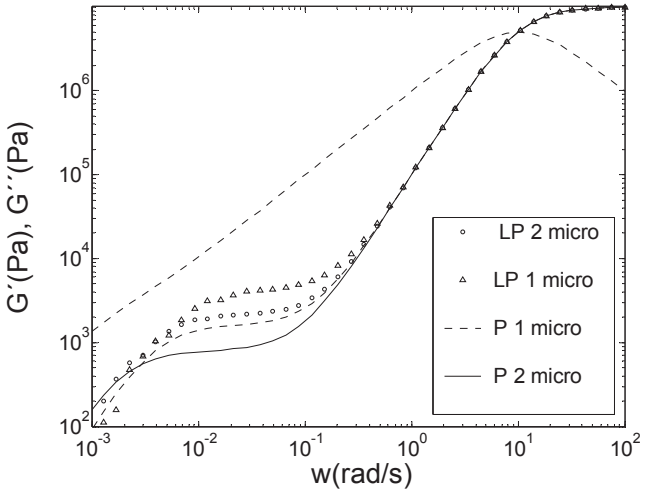

Figure 5 - Dynamic moduli vs frequency. Comparation of models predictions for different radius of inclusions. ($micro = \mu m$, PL- Lee-Park model, P- Palierne model, $\lambda = 0.6$)

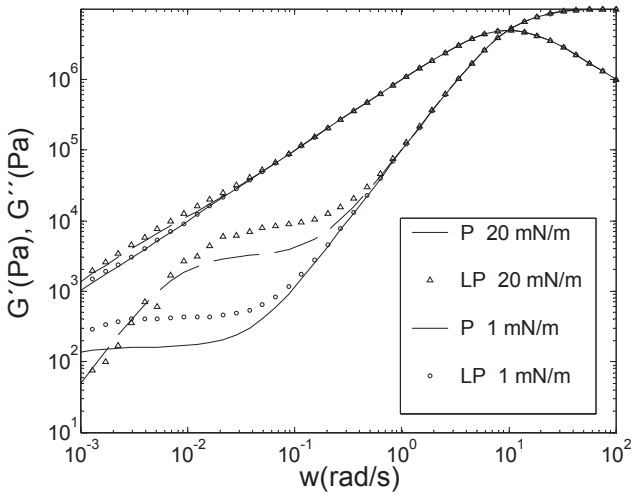

Figure 6 - Dynamic moduli vs frequency. Comparation of models predictions for different values of interfacial tension. (PL- Lee-Park model, P- Palierne model, $\lambda = 0.6$)

B. Interfacial tension

The Lee-Park model predicts a higher value for plateau in $G^{'}$, for different values of interfacial tension (Figure 6).

C. Another parameters

The Lee-Park model shows low sensibility to variations of viscosity ratio and volume fraction of dispersed phase.

IV. CONCLUSIONS

The Palierne and Bousmina models give quantitatively similar predictions for $G^{'}$ and $G^{''}$ of blends in small amplitude oscillatory flows. The Doi-Otha family of models, on the other hand, present an great advantage: they can, in principle, be used for predict behaviour of

a blend in any type of flow, namely, in transient experiences. The Lee-Park model is applicable to blends with any viscosity ratios and predicts higher values for the plateau in G' than the Palierne model.

References

Palierne, J. F. (1990). "Linear Rheology of Viscoelastic Emulsions with Interfacial-Tension." Rheol Acta **29**(3): 204-214

Doi, M. and T. Ohta (1991). "Dynamics and Rheology of Complex Interfaces .1." J Chem Phys **95**(2): 1242-1248

Lee, H. M. and O. O. Park (1994). "Rheology and Dynamics of Immiscible Polymer Blends." J Rheol **38**(5): 1405-1425

Lacroix, C., M. Aressy, et al. (1997). "Linear viscoelastic behavior of molten polymer blends: A comparative study of the Palierne and Lee and Park models." Rheol Acta **36**(4): 416-428

Bousmina, M. (1999). "Rheology of polymer blends: linear model for viscoelastic emulsions." Rheol Acta **38**(1): 73-83

Graebling, D., R. Muller, et al. (1993). "Linear Viscoelastic Behavior of Some Incompatible Polymer Blends in the Melt - Interpretation of Data with a Model of Emulsion of Viscoelastic Liquids." Macromolecules **26**(2): 320-329

RHEOLOGICAL AND MICRO-STRUCTURAL CHARACTERISTICS OF OVINE WHEY GELS

C.D. Pereira[1], A. Cobos[2], O. Diáz[2]
[1]Instituto Politécnico de Coimbra- Escola Superior Agrária, Portugal
[2] Universidad de Santiago de Compostela, Spain
cpereira@mail.esac.pt

Keywords: ovine, whey, rheology, micro-structure.

ABSTRACT

Ovine cheese whey was ultrafiltered (UF) or clarified by thermocalcic precipitation (TP) followed by microfiltration (MF) with different membrane pore sizes (0.65 and 0.20 μm). The MF filtrates were diafiltrated with 9 volumes of water. The procedure gave rise to 5 types of products that were freeze dried: the conventional UF retentate powder (UFRP), the MF retentate powders obtained with both types of membranes (MFRP 0.65 and 0.20 μm) and the correspondent diafiltration powders (DFRP 0.65 and 0.20 μm). The dried products showed different compositions especially in what concerns to their protein contents.

Thermally induced gels were prepared with 10 and 20 % (m/v) solutions of the products, at pH 4 and pH 7, heated at 90ºC during 30 minutes. Rheological determinations of matured gels included stress sweep and frequency sweep tests at 15 and 60ºC. Micro-structural observations were made by scanning electron microscopy (SEM) at 1500 magnifications.

10% solutions of UFRP and MFRP were not able to produce gels. MFRP 0,20 μm gels produced with 20 % solutions at pH 7, showed the highest elastic modulus (G'). These gels were also less affected by pH variations.

At pH 7, 10% solutions of diafiltration powders (DFRP 0.65 and 0.20 μm) originated very strong spongy structures with low ability for water retention.

UFRP and MFRP 0,65 μm gels showed a granular structure as a result of the formation of globular protein aggregates. MFRP 0,20 μm showed similar, but more compact, structure. DFRP gels showed different structures based on a three-dimensional matrix with holes of less than 10 μm, in which water could have been retained.

1. INTRODUCTION.

In several European Countries, the production of sheep's whey is not negligible and, although in some cases whey is further processed in order to obtain other end products such as *Ricotta* cheese, in most of them it is lost.

Due to their high levels of β-Lg (1,2,3), ovine whey powders can be interesting concerning to functional properties such as foaming and gelation due to the significant correlation between these properties and the content of that protein (4). Therefore, market for milk and whey powders of ovine origin presents some potentialities.

2. MATERIALS AND METHODS.

Ovine cheese whey was concentrated by ultrafiltration (**UF**) or clarified by thermocalcic precipitation (**TP**) followed by microfiltration (**MF**) with different membrane pore sizes (0.65 and 0.20 μm). The **MF** filtrates were diafiltrated with 9 volumes of water. The procedure gave rise to 5 types of products that were freeze-dried: the conventional **UF** retentate powder (**UFRP**), the **MF** retentate powders using a 0.65 and 0.20 μm pore size membranes (**MFRP 0.65 and 0.20**) and the diafiltration retentate powders (from the diafiltration of **MF** filtrates) using the two **MF** membranes (**DFRP 0.65 and 0.20**). Details of the production process are described elsewhere (5)

Gels were prepared by solubilizing the powders in water (20% and 10% w/v) and, adjusting the pH to 7 and 4 with NaOH or Hcl 0,1N, stirring for 1 hour at room temperature and finally heating at 90ºC for 30 min followed by rapid cooling to 8ºC. The gels prepared were maturated at 8º C for 15 h.

The dynamic rheological tests were performed with a Haake Rheostress™ RS 100 rheometer (Fisons) fitted with a cone-and-plate device (gap of 140 μm, angle of 4º and a cone diameter of 35 mm). Stress-sweep tests were conducted at a frequency of 1 Hz to determine the linear viscoelastic range.

The complex viscosity (η*), the storage modulus (G') and the loss modulus (G'') were determined between frequencies 0.428 - 42.80 rads s^{-1}, at 20 Pa, in the linear range. Measurements were made at 15ºC and, at 60º C, after heating and maintaining the samples for 3 h at the latter temperature.

Micro structural observations were made at 1500 magnifications by means of a scanning electron microscope JEOL™ model JSM-T220A.

3. RESULTS.

3.1. Composition of powders.

The dried products showed different compositions especially in what concerns to their protein and mineral contents, as it can be observed in Table I.

Table I. Average values for the proteic and mineral composition of the products evaluated.

	UFRP	*MFRP 0,65*	*MFRP 0,20*	*DFRP 0,65*	*DFRP 0,20*
PROTEIN	40,61[a]	21,34[b]	35,80[a]	66,85[c]	22,39[b]
(±)	4,29	0,99	5,77	5,09	1,01
ASH	30,08[a]	31,55[a]	28,08[a]	9,28[b]	28,93[a]
(±)	0,12	1,54	3,52	2,71	3,77

a,b,c Average values in the same line with different letters in superscript, differ significantly ($p < 0.05$).

3.2. Rheology.

10% (m/v) solutions of UFRP and MFRP were not able to produce gels due to protein levels below critical values needed to promote gelation (*i.e.* < than 5% m/v of protein in solution).

MFRP 0.20 gels produced with 20% (m/v) solutions showed the highest elastic modulus (G') at pH 7 (Fig.1.e). These gels were also less affected by variations in pH than UFRP and MFRP 0.65 gels produced in the same conditions.
In all cases the kinematic viscosity (η*) decreased with increased frequency (ω). The elastic module (G') increased while the viscous module (G'') showed little dependency of frequency. These facts are indicative of the presence of well organized tri-dimensional structures (6,7). The elastic modulus was superior to the viscous module at any given frequency, which is a characteristic of visco-elastic solids.
At pH 7, 10% (m/v) solutions of DFRP 0.65 and DFRP 0.20 originated very strong and spongy structures with low ability for water retention. Rheological measurements were only possible for DFRP 0,65 at pH4 (Fig.1.g).

3.3. Micro-Structural observations.

UFRP and **MFRP 0.65** gels showed a closed and bonded granular structure as a result of the formation of globular protein aggregates. These aggregates appear to be connected by means of a continuous fracture surface. However, in the case of **UFRP** this surface presents a more uniform aspect (Fig.2.a and b). In the case of **MFRP 0.20**, the structure was similar but showing smaller and more compact granules (Fig. 2.c). This fact might be due to the higher protein content of these products.
The structure of the gels obtained with solutions of **DFRP 0,65** at 20 (m/v) concentrations (Fig.2.d) was clearly different from the ones observed with **UFRP** and **MFRP**. In this case, the typical globular aggregates were not observed. This structure appeared as a compact three - dimensional matrix with holes, in which, air or water could have been entrapped. This fact reflects the strong spongy structures with low ability for water retention observed at naked eye.
In the case of **DFRP 0,20**, the structures appeared more similar to the ones of **MFRP**. (Fig.2.e) The differences between both **DFRP** might be due to their protein and mineral contents.

4. CONCLUSIONS

Whey powders of ovine origin produced by conventional **UF** or by thermocalcic precipitation followed by **MF** were able to produce gels at concentrations of 20% (m/v). Conventional retentate **UF** powders and retentate **MF** powders showed some similarity in what concerns to their rheological properties as well as to micro structural aspects. In the case of **MF** filtrates those properties were clearly different.

References

(1) Casper J.L., Wendorff W.L., Thomas, D.L. (1998). Seasonal changes in protein composition of whey from commercial manufacture of caprine and ovine specialty cheeses. *J. Dairy Sci.,* 81: 3117-3122.
(2) Pereira C., Cobos A., Ocampo S., Diaz O. (1999). Characterisation of bovine and ovine whey lipoproteins separated by microfiltration. Proceedings of the INRA/IDF seminar *"New applications of membrane technology in the dairy industry"* , pp 55. St. Malo. France.
(3) Pintado M.E., Lopes da Silva J.A., Malcata F.X. (1999). Comparative characterization of whey protein concentrates from ovine, caprine and bovine breeds. *Lebensm.-Wiss. u.-Technol.,* 32: 231-237.

(4) Kim Y.A., Chism G.W., Mangino M.E. (1987). Determination of the β Lactoglobulin, α Lactalbumin and BSA of whey protein concentrates and their relationship to protein functionality. *J.Food Sci.*, 52 (1): 124-127.
(5) Pereira C., Cobos A., Diaz O. (2002). Valorization of by-products from ovine cheese manufacture: clarification by thermocalcic precipitation/microfiltration before ultrafiltration. *Int. Dairy. J.,* 12 (9): 773-783.
(6) Mleko S (1997). Rheological properties of milk and whey protein desserts. *Milchwissenschaft,* 52 (5): 262-265.
(7) van Vliet T., Luyten H., Walstra P. (1991). Fracture and yelding of gels. In *Food Polymers, Gels and Colloids*. Ed. Dickinson E..Royal Society of Chemistry. London.
(8) Langley K.R., Green M.L. (1989). Compression and impact strenght of gels prepared from fractionated whey proteins in relation to composition and microstructure. *J. Dairy Res*., 56: 275-284.

ACKNOWLEDGMENTS

This work was supported by "Consellería de Educación e Ordenación Universitaria da Xunta de Galicia" (XUGA26202B97) and by project *Agro* nº 312 of the Portuguese Ministry of Agriculture. Funding for author C.D.P. was provided by a Ph.D. fellowship (BD 19672/99) issued within the framework "PRAXIS XXI", administered by JNICT, Portugal.

Fig 1. Rheological parameters of ovine whey gels: a) UFRP pH 7; b) UFRP pH4; c) MFRP 0,65 pH7; d) MFRP 0,65 pH4; e) MFRP 0,20 pH7; f) MFRP 0,20 pH4; g) DFRP 0,65 pH4.

(a)

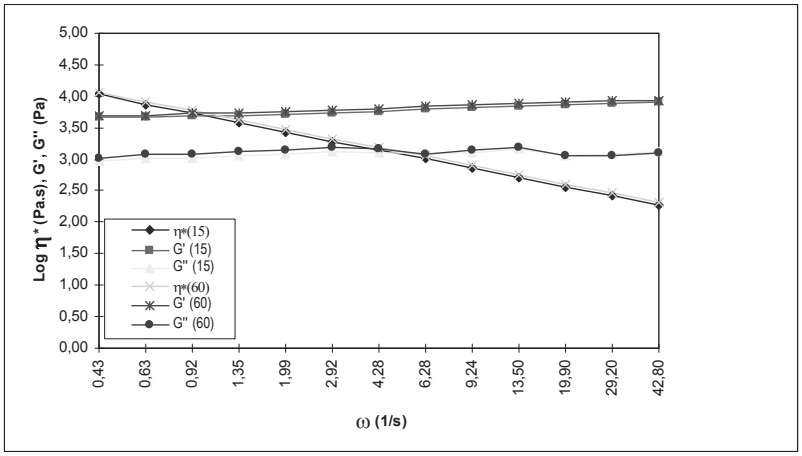

(b)

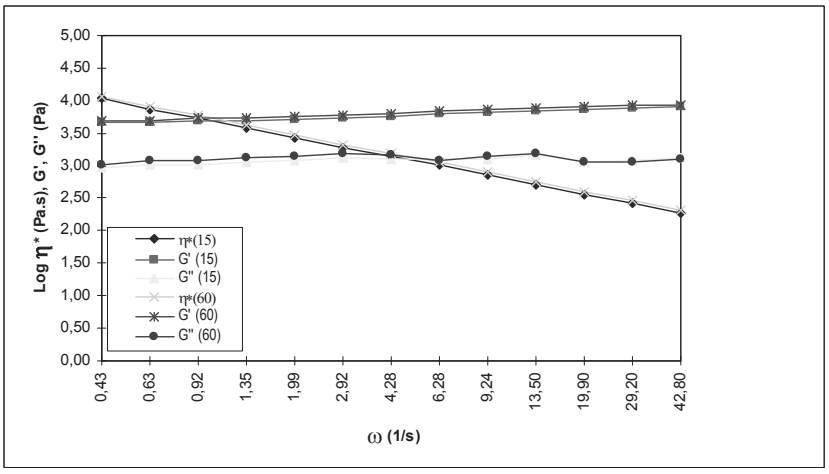

(c)

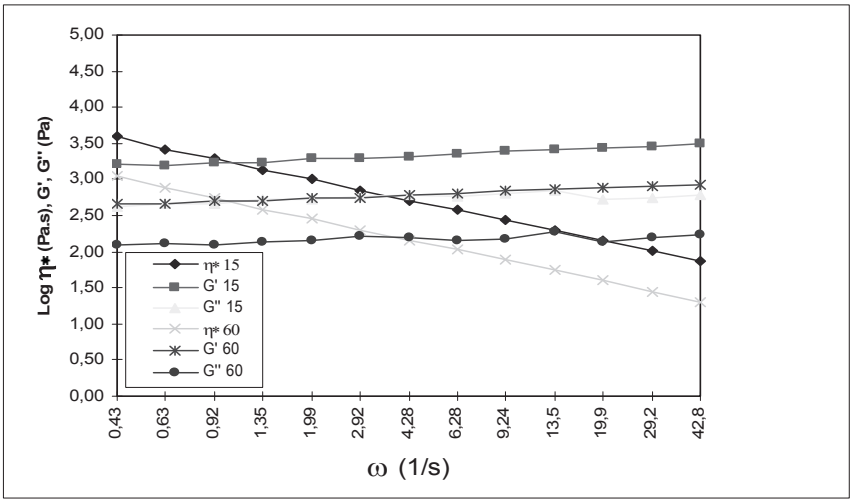

(d)

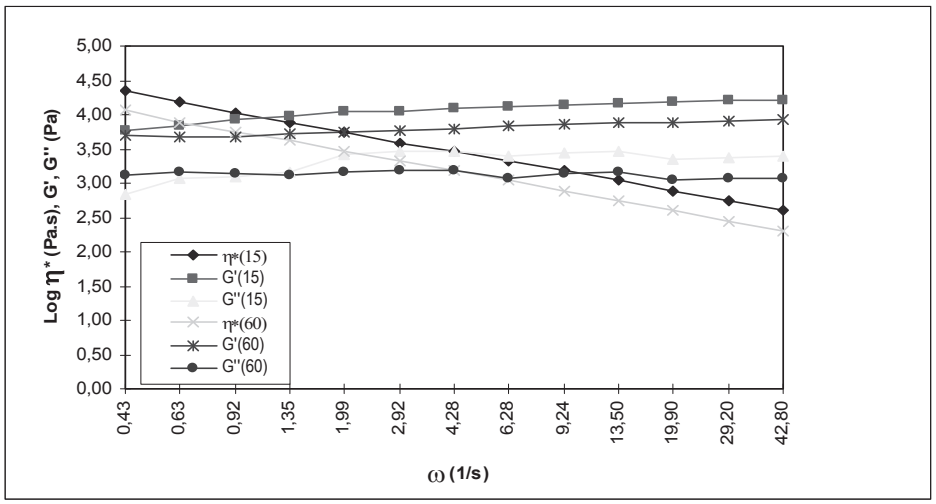
Log η* (Pa.s), G', G'' (Pa)
5,00
4,50
4,00
3,50
3,00
2,50
2,00
1,50
1,00
0,50
0,00
η*(15)
G'(15)
G''(15)
η*(60)
G'(60)
G''(60)
0,43
0,63
0,92
1,35
1,99
2,92
4,28
6,28
9,24
13,50
19,90
29,20
42,80
ω (1/s)

(e)

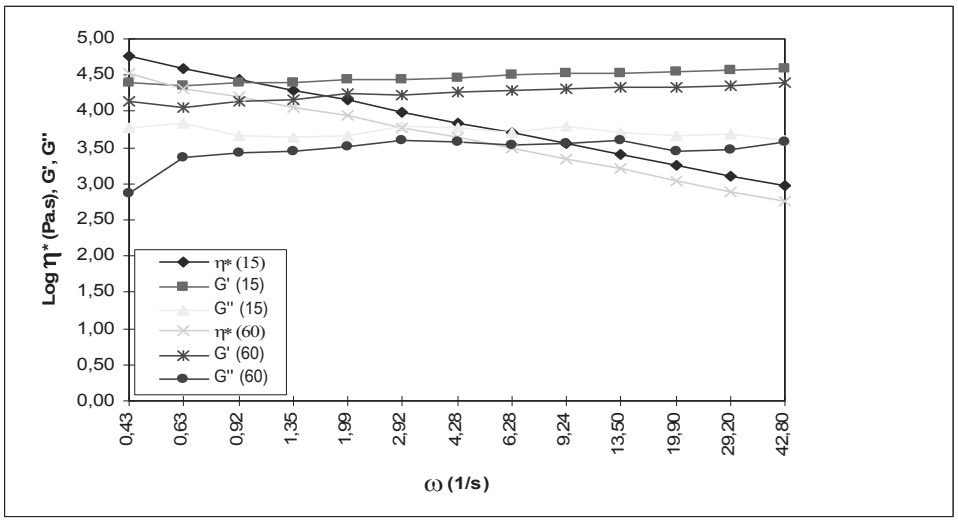
Log η* (Pa.s), G', G''
5,00
4,50
4,00
3,50
3,00
2,50
2,00
1,50
1,00
0,50
0,00
η* (15)
G' (15)
G'' (15)
η* (60)
G' (60)
G'' (60)
0,43
0,63
0,92
1,35
1,99
2,92
4,28
6,28
9,24
13,50
19,90
29,20
42,80
ω (1/s)

(f)

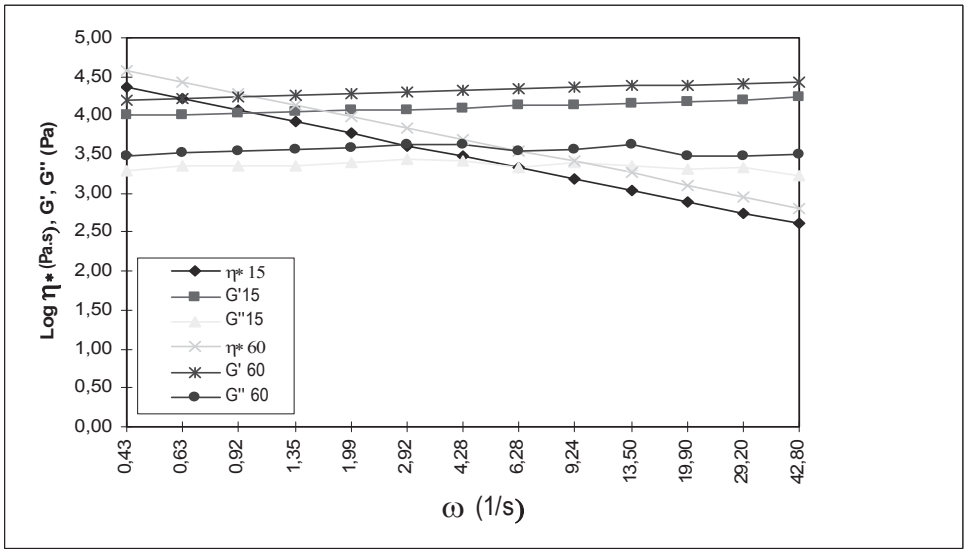
Log η* (Pa.s), G', G'' (Pa)
5,00
4,50
4,00
3,50
3,00
2,50
2,00
1,50
1,00
0,50
0,00
η* 15
G'15
G''15
η* 60
G' 60
G'' 60
0,43
0,63
0,92
1,35
1,99
2,92
4,28
6,28
9,24
13,50
19,90
29,20
42,80
ω (1/s)

(g)

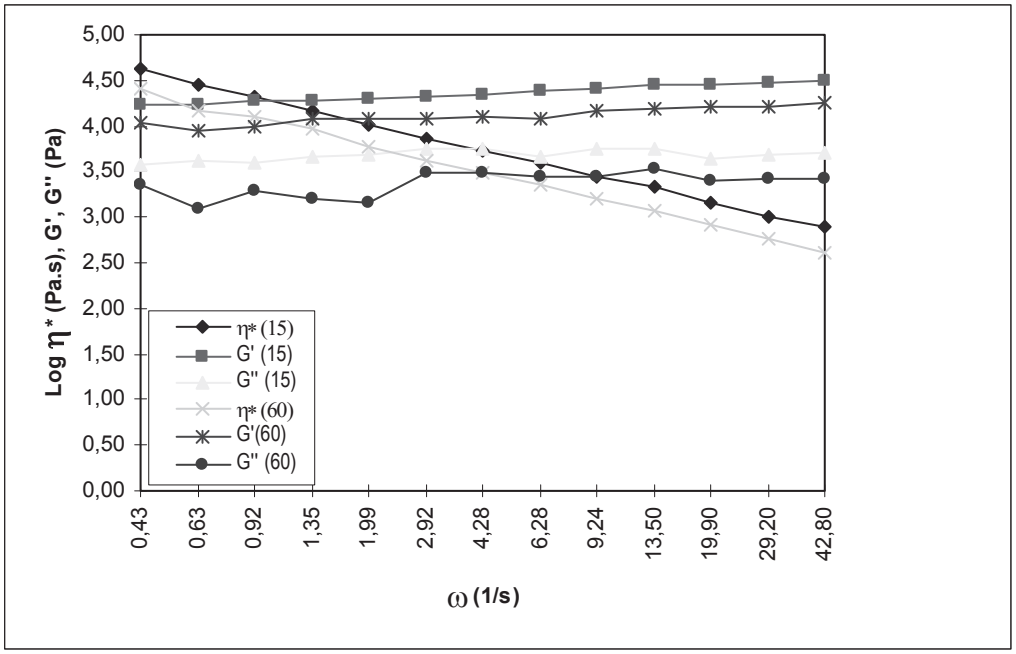

Fig 2. Micro-structural aspects of ovine whey gels: a) UFRP; b) MFRP 0,65; c) MFRP 0,20; d) DFRP 0,65; e) DFRP 0,20.

(a)

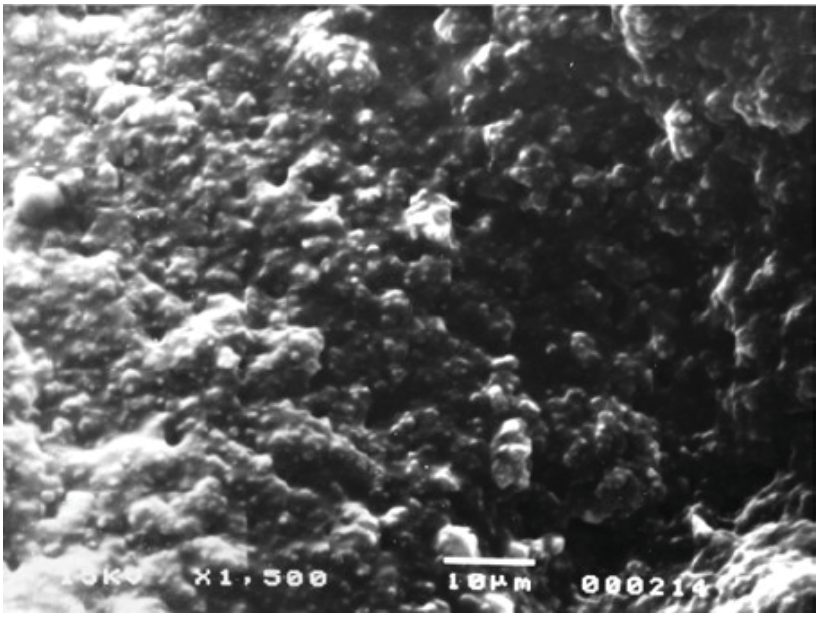

(b)

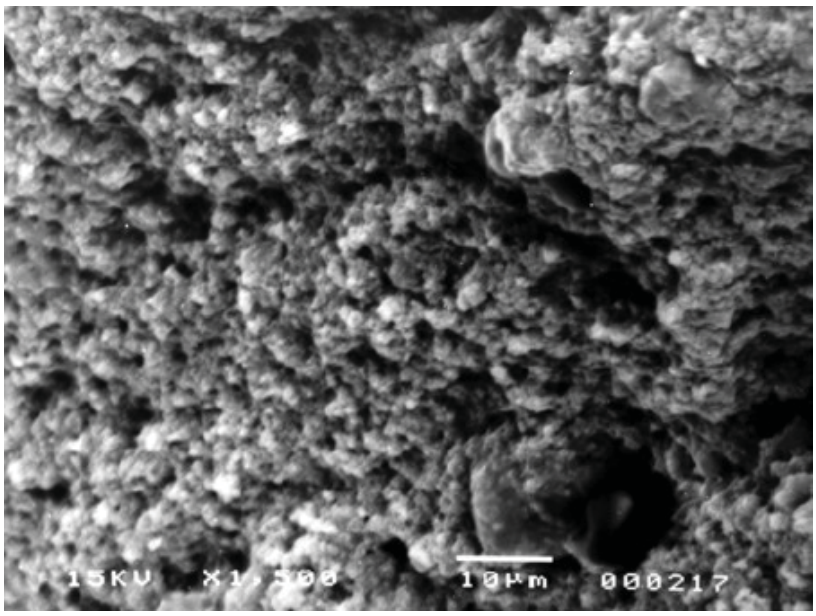

(c)

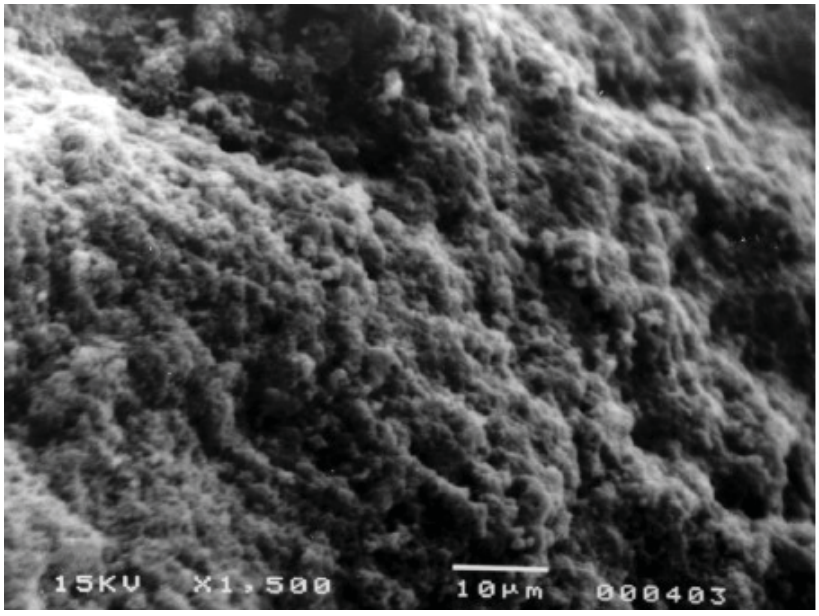

(d)

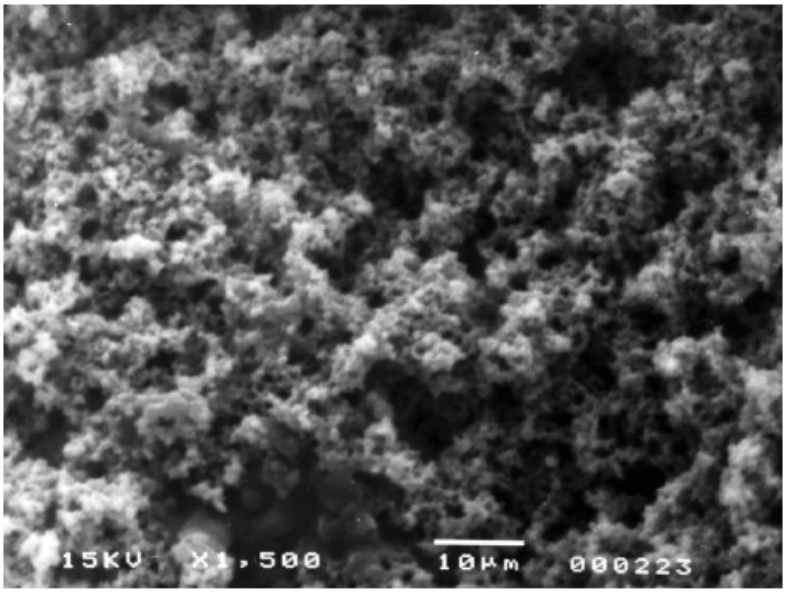

(e)

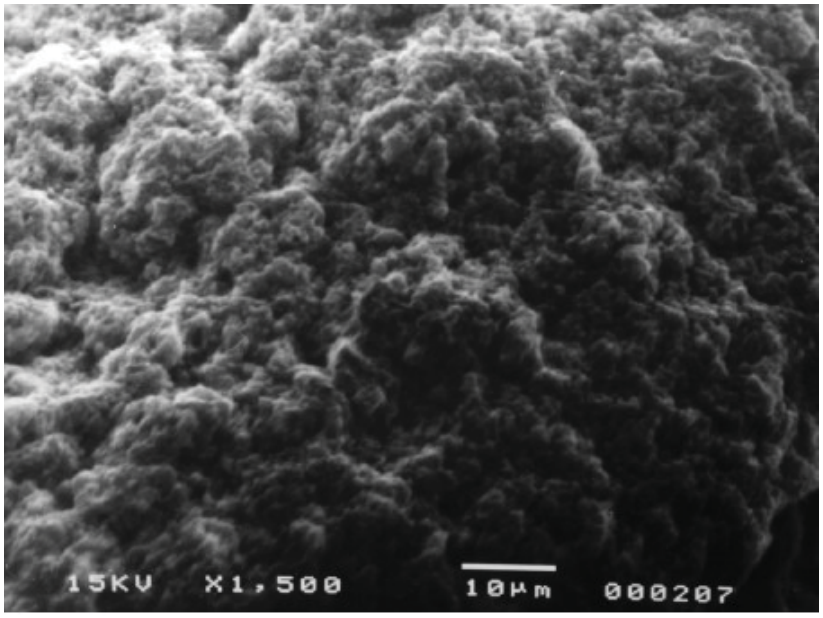

3. COLLOIDS & SUSPENSIONS

A CONTRIBUTION TO THE UNDERSTANDING OF THE RHEOLOGY OF CERAMIC GLAZES

[1] M.G. Rasteiro*, [1] E. Simões, [1]L. Santiago and [2]T. Gassman

[1]Chem Eng Dep, Coimbra University, Pólo II, Pinhal de Marrocos, 3030-290 Coimbra, Portugal
Fax: 239798703, mgr@eq.uc.pt
[2] Colorobbia Portugal

Keywords: Suspensions rheology, glazes, ageing of glazes, ceramics, oscillatory rheometry

Abstract: The rheological behaviour of glaze suspensions for the ceramic industry has to be closely controlled to obtain adequate final product characteristics. In fact, the rheology of these suspensions depends on several factors, such as particle size and concentration, frit and kaolin composition and on the presence of several other additives common to the preparation of ceramic glazes (CMC, de-flocculants etc.). In this work we have studied several glaze suspensions produced with a range of industrial frits and kaolin. Moreover, we were interested in establishing a correlation between changes in rheological behaviour with the ageing of the suspension, trying to relate these deviations with modifications in the ionic composition of the liquid phase, as a consequence of frit dissolution. Thus, we have compared the behaviour of industrial glazes of known composition, with the behaviour of simulated glazes produced with inert silica and known amounts of different cations. The rheological tests allowed an insight into the structures that must be developing in the particulate phase. These structures are strongly dependent on the frit composition that is on the ions dissolving into the liquid. Frits releasing significant amounts of Ca, B, Ba and Pb can pose serious handling problems.

1 INTRODUCTION

The preparation of ceramic glaze suspensions requires that an adequate flow behaviour is reached. For that, several parameters have to be rigorously controlled: particle size and solids concentration, composition of the suspension, ionic charge of the liquid, pH, temperature, etc. On the other hand, it is quite usual in the ceramic industry for the glaze suspension to loose its suitable flow characteristics with time. That can be caused by the dissolution of the glaze or by the sedimentation of the particles, which result in agglomeration or de-agglomeration of the solids. This can pose difficult problems to industry, mainly when the process is irreversible [1]. Recently, some authors started to study the relation between the release of cations by the frit and the alterations detected on the rheological behaviour of the glaze [2,3].

In this work we want to implement a strategy to control the flow behaviour and stability of ceramic glaze suspensions. We have studied the ageing process of several ceramic glazes, with different compositions, prepared with a range of industrial frits and a specific kaolin (Galiza kaolin). The rheological behaviour of the suspensions was analysed, for different ageing times, using a controlled stress rheometer with a cylindrical spindle (both flow and dynamic tests). Moreover, we were interested on establishing a correlation between changes in rheological behaviour with the age of the suspension and modifications in the ionic composition of the liquid, as a consequence of frit dissolution, dependent on frit composition. The ionic composition of the liquid phase was determined by atomic absorption spectroscopy. PH and conductivity of the glaze suspensions were also monitored. Furthermore, the concentration and the particle size of the solid phase were measured for each glaze.

The rheological tests, namely the oscillatory tests, allow an insight into the structures that develop, with ageing time, among the particulate phase. These structures are strongly dependent on frit composition that is on the type of ions that are dissolving into the liquid phase. Furthermore, a strategy was developed to isolate the effect of each ion on glaze

rheology. For that, simulated frits made up of inert silica, kaolin and CMC were prepared, which were additivated with a salt of the ion to be studied and compared with the industrial glazes. We have studied the isolated effect, on suspension rheology, of K^+, Na^+, Ca^{2+}, Ba^{2+}, Pb^{2+} and B^{3+}as well as of combinations of these cations.

2 RHEOLOGY OF SLURRIES

2.1 Flow Tests

When a fluid or slurry is subjected to a deformation, by applying a tangential stress (shear stress, τ) different behaviours can be observed. The resistance offered by the fluid element to deformation can, usually, be related to the fluid viscosity (μ) and more generally, to the rheological behaviour of the fluid.

The form of the function depends on the nature of the fluid that is on its rheological behaviour. The simplest case is the Newtonian fluid that corresponds to a linear relation. However, when analysing slurries, the Newtonian behaviour is rarely found, unless the solids' concentration is very low. The rheological tests that allow us to characterise the fluid in this way are Flow Tests that supply the shear stress versus shear rate curve. Moreover, there are fluids that exhibit a shear stress versus shear rate curve dependent on time. These fluids show a hysterisis loop when they are subjected to an ascendant shear ramp followed by a descendant one. That was the case for all the suspensions tested. These fluids can be either thixotropic or rheopetic, depending on whether viscosity decreases or increases with time.

However, in many situations involving slurries we are not dealing with pure viscous fluids, being faced with viscoelastic materials that possess, simultaneously, the viscous properties of the liquids and the elastic properties of the solids. These materials, when subjected to a deformation, possess the capacity to store energy and to dissipate it through viscous losses. The relation between the viscous and the elastic properties of each material is a characteristic of that material and influences its rheological behaviour. The flow tests do not supply this type of information about the material and dynamic tests, making use, for instance, of oscillatory rheometry, have to be performed to achieve a more detailed characterisation.

2.2 Oscillatory Rheometry

When applying a sinusoidal tension to a viscoelastic material, deformation (strain) occurs, but the rate of strain will vary with time. However, the two functions (stress and strain) can differ and their maximum does not have to occur at the same time. The lag between these two functions (ϕ) is a characteristic of the material.

The complex stress can be defined as follows:

$$\tau^* = \tau_0 \exp(j\,\omega\,t) \quad (1)$$

and the corresponding complex strain as:

$$\gamma^* = \gamma_0 \exp(j\,(\omega\,t - \phi)) \quad (2)$$

The complex material modulus can then be defined as:

$$G^*(\omega) = \frac{\tau^*}{\gamma^*} = G'(\omega) + jG''(\omega) \quad (3)$$

where $j = (-1)^{1/2}$, τ_0 and γ_0 are the amplitudes of the stress and strain functions, respectively.

G* is determined experimentally by oscillatory rheometry through frequency sweep tests for a fixed stress. In equation (3) G' (ω), the real part of the complex modulus, is the storage modulus, which is related to the elastic properties of the material and gives the in-phase stress/strain ratio. G'' (ω) is the loss modulus, related to the viscous losses and giving the in-quadrature stress/strain ratio:

$$G''(\omega) = G^*(\omega)\,sen\Phi \qquad G'(\omega) = G^*(\omega)\cos\Phi \quad (4)$$

These parameters are important to characterise each material varying according to material structure. The relation between the two modules is strongly dependent on that structure.

3 EXPERIMENTAL

In this work we have studied three different glazes based on three frits (transparent, opaque and mat, see Table 1 for compositions) and on a pre-fixed kaolin used as suspending medium (Galiza kaolin). The glazes had also a small percentage of CMC acting as binding agent.

Table 1. Frits' composition

Frit	Chemical Composition (weight %)										
	Na_2O	K_2O	MgO	CaO	ZnO	B_2O_3	PbO	Al_2O_3	SiO_2	BaO	ZnO_2
FTAE 7424	1	5	1	13	10	3	--	8	59	--	--
FOAE 8030	--	5	3	10	12	4	--	6	52	--	8
FMP 3505	4	1	--	19	--	13	2	5	53	3	--

We have also studied suspensions made of pure silica, kaolin and CMC, which will be called simulated glazes. The percentages of the three constituents on both the real and the simulated glazes have been kept constant (92.4% w/w of silica referred to the total solids content and 38.8% w/w of water in the suspension). All the suspensions were prepared through wet grinding in a pilot ball mill, but the grinding time had to be adjusted so that the residue was always around 5% in a 45 μm sieve (see Table 2). The particle size distribution was measured by laser diffraction spectroscopy (LDS). Table 2 summarises the average values of the particle size distributions obtained (d_{10}, d_{50}, d_{90}). For each suspension we have measured and adjusted the suspension density (25ºC), so that it falls between 1600 and 1800 g/l.

In order to isolate the influence, on the rheological behaviour of the glaze, of the different cations usually released by the real frits during processing, we have additivated the inert simulated glazes with salts of those cations. In this way we have studied the influence of K^+, Na^+, Ca^{2+}, Ba^{2+}, Pb^{2+} and B^{3+}, on the suspension behaviour. Three different concentrations of the cations have been tested: 10^{-3}, 10^{-2} and 10^{-1} M (referred to the total suspension volume). PH of the simulated glazes was adjusted to the values typical of the industrial glazes (9 to 10).

Table 2. Suspension characteristics

Suspension		Density (g/l)	d_{10}(μm)	d_{50}(μm)	d_{90}(μm)	Grinding time (h)
FTAE 7424 glaze		1765	2.40	16.14	47.69	23
FOAE 8030 glaze		1791	1.82	16.42	41.81	26
FMP 3505 glaze		1638	2.97	16.83	42.98	22
FTAE 7424+water		1723	1.99	16.77	63.47	19
FOAE 8030+water		1786	1.78	16.65	44.95	20
FMP 3505+water		1425	1.68	16.21	61.92	18
Simulated glaze	K^+	1781	2.59	17.68	52.55	3.5
	Na^+	1780	2.07	16.88	57.42	3.5
	B^{3+}	1792	2.59	17.68	52.55	3.5
	Ca^{2+}	1716	2.59	17.68	52.55	3.5
	Pb^{2+}	1785	1.99	15.38	36.35	4
	Ba^{2+}	1790	2.13	17.7	60.55	4

The ageing of the suspensions was controlled for the following times: 0, 24, 48, 96 and 192 hours. We have checked, for the different ageing times, the conductivity and the rheological behaviour of the suspensions. The rheological tests were performed using a controlled stress rheometer from Haake, with a cylindrical sensor, which allowed a close temperature control (25ºC). For each suspension we have performed both flow tests and dynamic tests (a stress sweep to identify the linear viscoelastic region and a frequency sweep, in that region, to obtain information about the suspension structure). For the simulated glazes the tests were performed only for 0 and 48 hours. Since the glaze suspensions have also got other materials besides the frit (kaolin and CMC), we have checked the effect of the cations studied on these additives (CMC, kaolin and CMC+kaolin).

Moreover, in order to monitor frit dissolution we have analysed the ionic composition of the supernatant water from the glaze, as time passed. For that, we have prepared, through grinding, suspensions made up of just frit and water. The grinding time was adjusted so that the particle size was similar to the one of the glazes, as can be seen in Table 2. The ionic composition was measured by Atomic Absorption Spectroscopy.

4 RESULTS

4.1 Real Glazes

Figures 1 to 3 show both the flow tests (ageing times 0, 48 and 192 hours) and the dynamic frequency sweep tests (0 and 192 hours) for two of the glazes studied. Looking at the shear stress versus shear rate curves it is obvious that the suspensions are thixotropic. Moreover, viscosity is higher for the suspension of frit FTAE7424. As far as the frequency sweep is concerned all the frits show a paste like behaviour, with G''and G' approximately parallel but G''>G'. The behaviour of the glaze approaches a liquid behaviour as frequency increases. For frit FTAE7424 the viscous and elastic modules are closer in the low frequencies region, agreeing with the higher viscosity of this glaze, due to stronger interactions between the particles. Moreover, the absolute value of the modules increases slightly with ageing time. Viscosity and hysterisis area do also increase slightly with time. Frit FMP3505 is the one exhibiting the lower viscosities as can be seen from the flow tests. Simultaneously, it is the one exhibiting a liquid like behaviour, in the frequency sweep test, for lower frequencies. Moreover, the absolute values of the modules decrease slightly with ageing time, though both viscosity and hysterisis area remain approximately unchanged with time. The glaze produced with frit FOAE8030 is also a low viscosity glaze, with a low hysterisis area. Moreover, both viscosity and hysterisis area decrease slightly with ageing time.

Figure 4 summarises how suspension conductivity varied with time for the three glazes tested. Generally speaking conductivity is higher at t=0 hours, decreasing for t=24 hours and increasing, after that, with ageing time, due to frit dissolution. The high initial conductivity results from the high cation release during the grinding step, cations being rearranged afterwards by adsorption around the particles. The analysis of the dissolution results shows that, generally speaking, the concentration of the cations increases with ageing time, revealing the existence of a dissolution process, as indicated previously by the conductivity measurements. In some cases concentration decreases after the first 24 hours, increasing only after that time, in agreement with the conductivity results. Frit FMP3505 shows a lower dissolution. Frits FTAE7424 and FOAE8030 are very similar, both in composition and in the dissolution results. Generally speaking, the more soluble metals are: Ca^{2+}, K^{+}, Na^{+} and B^{3+}.

If we analyse now the rheological behaviour of the different glazes taking into consideration the dissolution and conductivity results, it is possible to establish some correlation between the two parameters. In fact, a higher dissolution and thus ionic concentration, corresponds to higher viscosities and an increased importance of the elastic forces, as happens with frit FTAE7424. Moreover, in this case, viscosity and hysterisis area increase with ageing time, denoting the building of interactions between the particles, in accordance with the dissolution results and Stern theory. Frit FOAE 8030 is very similar to frit FTAE7424, though with a slightly lower dissolution rate, and a conductivity that does not vary much with time. This may justify the lower viscosities obtained for this frit and the apparent weak influence of ageing. Frit FMP3505 shows the lowest dissolution rate and ion concentration, which correspond, simultaneously, to the lowest viscosities and a higher similitude with a liquid like behaviour for low frequencies (high predominance of viscous forces).

4.2 Simulated Glazes

For the simulated suspensions made of silica, kaolin (Galiza), CMC and water, additivated with the cations referred previously (K^+, Na^+, Ca^{2+}, Pb^{2+}, Ba^{2+}, B^{3+}) we have performed both flow and dynamic rheological measurements, as for the real glazes. Only results for the flow tests for the suspensions additivated with K and Ca and for the three concentrations tested will be shown as examples here (see Figure 5) but only for t=0 h since no variation with time was detected. Table 3 summarises the viscosity values for infinite shear rate, for all the simulated glazes tested. From the analysis of Figure 5 it is apparent that the effect of Ca^{2+}, on rheological behaviour, is much more pronounced than the effect of K^+. However, it can be stated for all the cations tested that as ion concentration increases the rheological behaviour of the suspension changes. In fact, as the concentration of K^+ increases the suspension assumes a paste like behaviour for all the frequencies tested and both viscosity and hysterisis area increase. For the simulated glaze additivated with Ca^{2+}, the changes on rheological behaviour resulting from an increase on concentration are much more notorious, the suspension behaving like a gel for the highest concentration tested, 10^{-1}M, with a clear predominance of the elastic forces, even for very low frequencies. These structural alterations resulting from the addition of Ca^{2+} are also notorious on the flow tests (Figure 5 b) with a clear increase of viscosity (Table 3) and hysterisis area as the Ca^{2+} concentration increases. The same was verified for the suspensions additivated with Pb^{2+}. Na^+ showed the weakest influence on the rheological behaviour of the suspension. The suspensions additivated with Ba^{2+} and B^{3+} have very similar behaviour, intermediate between the Ca^{2+} and Na^+ additivated suspensions.

Table 3. Suspensions viscosity at infinite shear rate

Glaze		μ_∞ (Pa s) t=0 h	t=24 h	t=48 h	t=96 h	t=192 h
FTAE 7424		0.8	0.94	0.98	1.15	1.06
FOAE 8030		0.15	0.13	0.12	0.12	0.10
FMP 3505		0.092	0.10	0.099	0.099	0.061
Simulated+K^+	10^{-3}M	0.36				
	10^{-1}M	0.89				
Simulated+Ca^{2+}	10^{-3}M	0.11				
	10^{-1}M	2.41				
Simulated+B^{3+}	10^{-3}M	0.35				
	10^{-1}M	1.36				
Simulated+Na^+	10^{-3}M	0.15				
	10^{-1}M	0.30				
Simulated+Ba^{2+}	10^{-3}M	0.27				
	10^{-1}M	1.79				
Simulated+Pb^{2+}	10^{-3}M	0.29				
	10^{-2}M	0.79				

It is also apparent from the comparison of Figures 1 and 5, that the simulated glazes behave similar to the real glazes for the lowest salt concentration tested (10^{-3}). We have also checked, for the simulated glazes, the conductivity of the suspensions, conductivity depending, of course, on salt concentration, but without varying with time. For the lowest salt concentration tested the conductivity of the simulated glazes was similar to the one of the real glazes.

5 CONCLUSIONS

The results presented allow us to conclude that in the real glazes there is a dissolution process of the frit, as time passes, that can alter the rheological behaviour of the glaze. That ageing process, which is a consequence of the dissolution of the frit, can lead to the building up of microstructures of particles which can cause: changes in the relation between the viscous and elastic modules of the materials; changes on the viscosity of the suspension and on thixotropic behaviour, that is on the hysterisis area.

The oscillatory rheometry tests represent an adequate way of perceiving modifications on suspension structure and characteristics.
It has been proved that $Ca^{2+}$and Pb^{2+} are the cations with stronger influence on the rheology of the suspension. However, the presence of the other cations in high concentrations (10^{-1}) can also affect the rheological behaviour of the suspension. Na^{+} is the one with a lower influence.

REFERENCES

1. RAVAGLIOLI, A., (1992), in *Nuevos Produtos y Tecnologias de Esmaltes e Pigmentos Cerámicos*, ed. J. M. Rincón et al., Castellón Faenza Ed. Iberica, pp.49.
2. NEGRE,F., FELIU,C.,MORENO,A., SANCHEZ, E., BOU, E.,(1996), *Br. Ceramic Trans. J.*,95,2, pp.53.
3. MORENO, A., SÁNCHES, E., (2002), *Ceramica Industrial*, 7, 6, pp19.

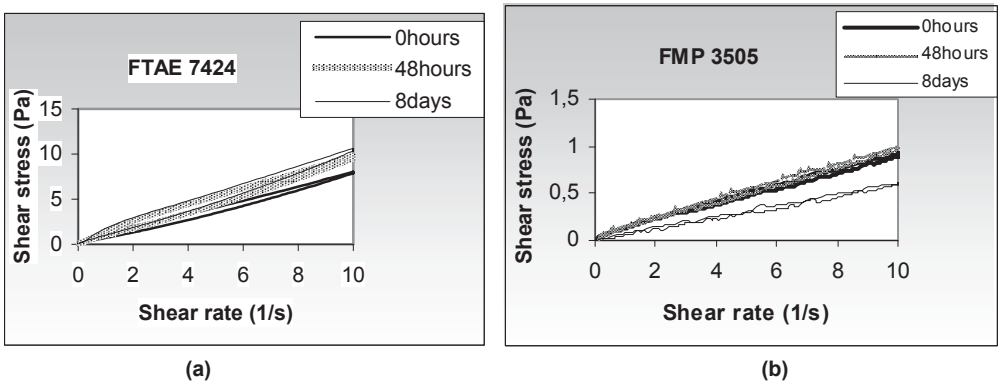

(a) (b)

Figure 1. Flow tests- real glazes

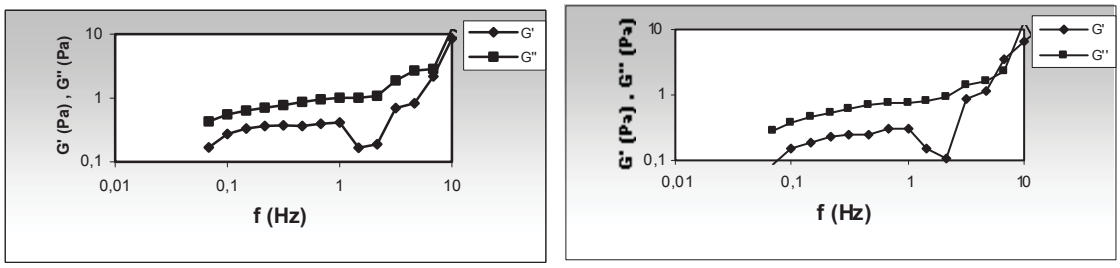

(a)- t= 0 h (b)- t= 8 days

Figure2. Frequency sweep results- FTAE7424

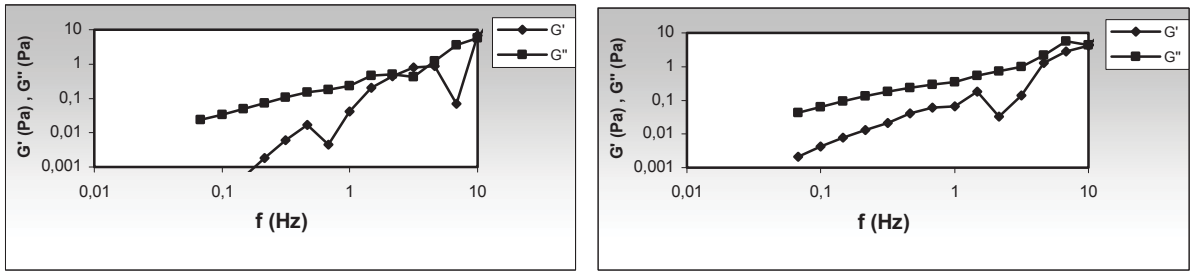

(a)- t= 0 h (b)- t= 8 days

Figure 3. Frequency sweep results- FMP3505

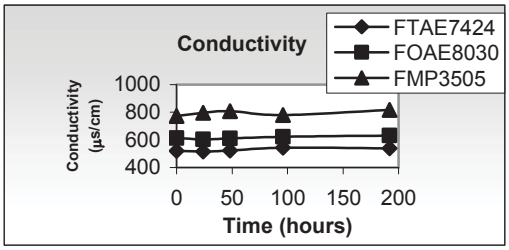

Figure 4. Glaze conductivity as a function of ageing time

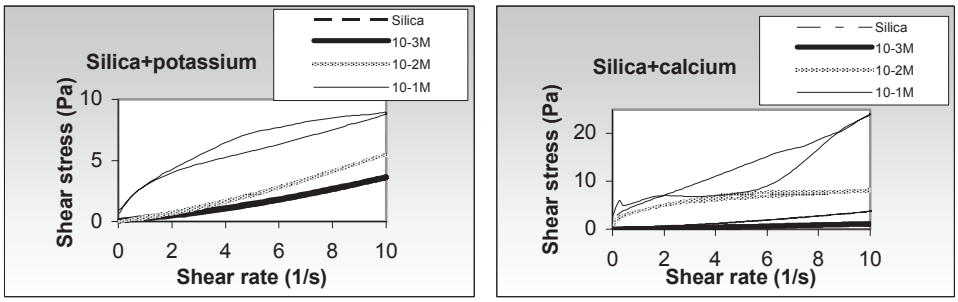

(a) **(b)**

Figure 5. Flow tests- simulated glazes (t= 0 hours)

RHEOLOGICAL PROPERTIES OF PIGMENT SUSPENSIONS: THE INFLUENCE OF PARTICLE SHAPE AND SOLID CONTENT

*S. I. Conceição [1], N. F. Santos[2], J. M. F. Ferreira [3] and J. L. Velho * [1]*

[1]Department of Geosciences, University of Aveiro, 3810-193 Aveiro, Portugal, jvelho@clix.pt
[2]Department of Chemical and Environmental Eng., Polytechnic Institute of Tomar, 2300-313 Tomar
[3]Department of Ceramics and Glass Engineering, University of Aveiro, 3810-193 Aveiro, Portugal

Keywords: Pigments; Coating colours; CMC; Kaolinite; Calcite.

ABSTRACT
The influence of particle shape and solids content of mineral pigment on rheological properties of coating colours was analysed. The effect of molecular weight and concentration of CMC and concentration of two pigments (ground calcium carbonate and kaolin) on rheology of suspension was studied. The adsorption model proposed for CMC molecules, that anticipate different polymer configurations, depending on molecular weight and solids loading, enables a higher comprehension level of the relationships between the macroscopic responses of the colours and the interactions occurring at microscopic or molecular levels.

1. INTRODUCTION

Rheology of suspensions is a very complex matter. In what concerns to paper coating applications, coating colour is a concentrated aqueous suspension where the mineral pigment is the main component [1,2,3,4]. Paper industry uses different pigments in coating applications, kaolin and calcium carbonates (ground, GCC and precipitated, PCC) are the most important. All of them have different intrinsic characteristics, namely, particle shape, surface charge, surface electrical distribution and particle size distribution. Their interactions with the second main constituent of a coating colour, the co-binder or rheological modifier, are always different and complex.

The main goal of this research is to study the influence of one of the main important properties that influence rheology, pigment particle shape. For that, different pigments were selected: kaolin and a ground calcium carbonate. In coating colours formulations, these pigments were added with different solids contents, from 30- to 50-vol.%. As co-binder, we selected two types of CMC (CMC35 and CMC250) were added in two concentration levels, 0.1-wt% and 0.2-wt%.

2. EXPERIMENTAL PROCEDURE

For this study, Standard Porcelain (ECC International, UK) kaolin was selected, with average particle size 4.95 μm (measured by using a laser diffraction instrument, Coulter, LS230). The solid contents were held at 30-, 35- and 40-vol%. The suspensions were prepared by adding 0.4-wt% (relative to dry solids) of an ammonium polycarbonate (Targon 1128, BK Ladenburg, Germany), as dispersing agent in distilled water. A high purity (>99.5-wt.%) ground calcium carbonate (GCC), having an average particle size (d_{50}=1.8 μm) suitable for paper coating was used as pigment. The solid contents were held at three levels, 30-, 40- and 50-vol.%, respectively, 54-, 64- and 73-wt.%. The suspensions were prepared by first adding 0.7-wt.% of the dispersing agent, an ammonium polycarbonate (Targon 1128, KK Ladenburg, Germany), to distilled water. This dispersant is very effective in dispersing calcium carbonate slurries, enabling to obtain very high solids volume. [5,6]

Two CMC grades, CMC35, M_w=35,000 g and CMC250, M_w=250,000 g, were added separately and also mixed in a 1:1 ratio, in total amounts of 0.1-wt% and 0.2-wt% relative to

dry mass of the pigment. Rheological measurements were performed in a rotational stress controlled rheometer (Carri-med 500 CSL, UK) at a strictly controlled temperature of 20ºC. The measuring configuration adopted was a cone and plate, and stress sweep and multi-step shear measurements were performed in the shear rates range from 0.1 s^{-1} up to 1,300 s^{-1}. One can find a complete description of rheological conditions in [5].

3. RESULTS

3.1. Kaolin

Figures 1 and 2 show the flow curves of the coating colours for the two CMC concentration levels, 0.1-wt% and 0.2-wt%, respectively. In the shear range from 0.1 to about 1,200 - 1,300 s^{-1} all colours exhibit Bingham plastic behaviour showing apparent extrapolated yield stress values, which tend to increase with increasing concentrations of solids and CMC binders. The shear stress values required to deform samples increase with increasing solids volume fraction as well as with molecular weight and total added amount of CMC. The difference is much more pronounced when passing from 35- to 40-vol% solids due to the closer proximity of the critical solids content for which viscosity becomes infinite.

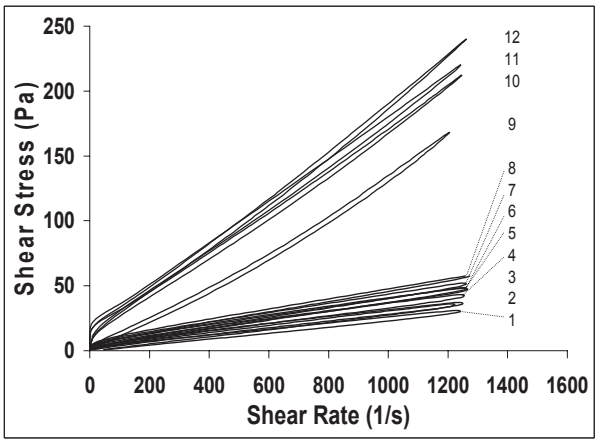

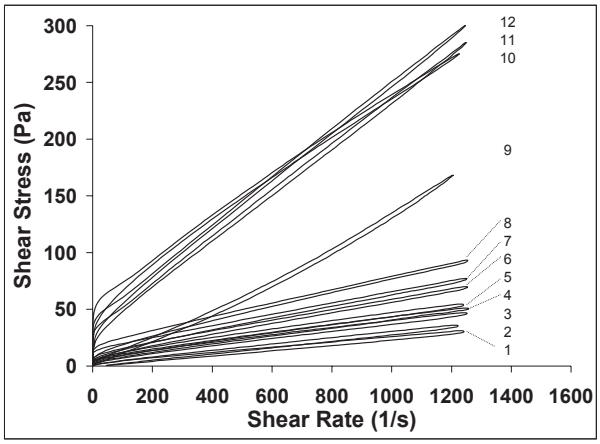

1-30-wt.% without CMC; 2-35-wt.%, without CMC; 3-30-wt.%, CMC35; 4-30-wt.%, CMC35+CMC250; 5-30-wt.%, CMC250; 6-35-wt.%, CMC35; 7-35-wt.% CMC35+CMC250; 8-35-wt.% CMC250; 9-40-wt.%, without CMC; 10-40-wt.%, CMC35+ CMC250; 11-40-wt.%, CMC250; 12-40-wt.%, CMC35.

Figure 1. Effect of solids concentration and molecular weight of CMC (for a total added amount of 0.1-wt%) on the flow curves of kaolin suspensions in the presence of 10-wt.% Latex + 1-wt.% Acrosol.

Figure 2. Effect of solids concentration and molecular weight of CMC (for a total added amount of 0.2-wt%) on the flow curves of kaolin suspensions in the presence of 10-wt.% Latex + 1-wt.% Acrosol.

For 0.1-wt% CMC, there is not a clear difference in the shear stress/shear rate curves between 30- and 35-vol% solids concentration. At these two solids concentrations, the sequence of the flow curves is the same, CMC35, CMC35+CMC250 and CMC250. These results suggest that the co-binder molecules will remain preferentially in the solution rather than adsorbed at the particles' surface. The sequence is changed when the system becomes more concentrated. CMC35 seems to have more accentuated thickening properties, while the mixture gives the less viscous CMC containing systems, with CMC250 in the intermediate position.

With increasing the total added amount of CMC to 0.2-wt%, flow curves for 35-vol% can be individualized from those at 30-vol%, but their sequence still remains the same at these two solids loading. For 40-vol%, the stronger thickening effect is observed for the mixture,

followed by CMC35 and, finally, CMC250. However, the results at this solids loading should be regarded with care because the suspensions became too viscous and sticky, thus likely leading to less reproducible coating properties.
Figures 3 and 4 show the steady state viscosity curves of the coating colours as a function of shear rate in the shear range from 0.1 to about 1,200-1,300 s^{-1} for the two CMC concentration levels, 0.1-wt% and 0.2-wt%, respectively. All the curves show shear-thinning behaviours along the low shear rate range followed by near Newtonian plateaus. The sequences of the curves are essentially the same already observed in Figures 1 and 2, respectively.

3.2. Ground calcium carbonate

Figures 5 and 6 show the flow curves of the coating colours for the two CMC concentration levels, 0.1-wt.% and 0.2-wt.%, respectively. In the shear rate range from 0.1 to about 1,000-1,200 s^{-1} all studied colours show approximate Bingham plastic behaviour having apparent yield stress values. The yield stress reflects the energy that is required in order to get the colours into flow being affected by the structure of the colour at rest, which depends on the interactions between calcium carbonate particles, processing additives and water. A stronger attractive network will correspond to a higher yield stress.

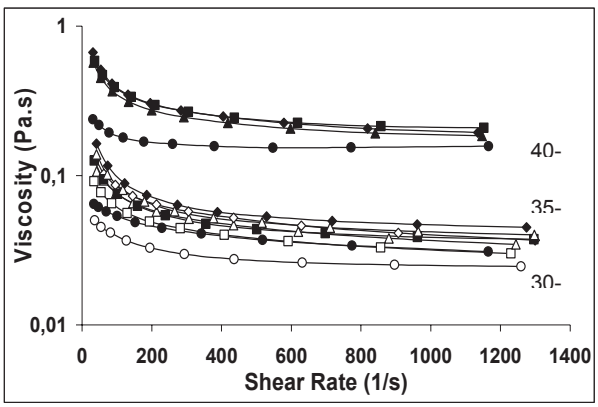

Figure 3. Effects of kaolin concentration and of molecular weight of CMC (for a total added amount of 0.1-wt%) on the steady shear viscosity curves of kaolin suspensions in the presence of 10-wt.% Latex + 1-wt.% Acrosol. Open symbols: 30-vol%; full symbols: 35-40-vol%; (●,○ without CMC; ■,□CMC35; ▲,△ CMC35-250; ◆,◇CMC250).

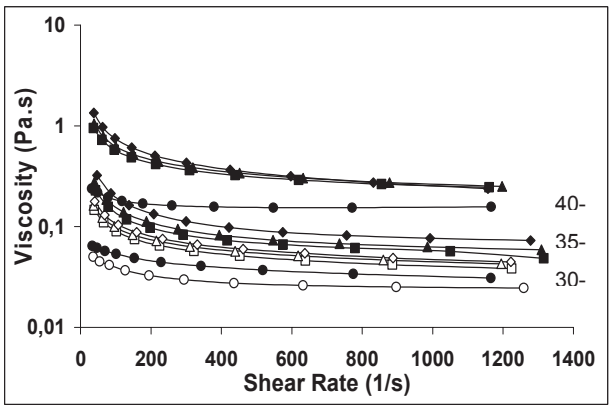

Figure 4. Effects of kaolin concentration and of molecular weight of CMC (for a total added amount of 0.2-wt%) on the steady shear viscosity curves of kaolin suspensions in the presence of 10-wt.% Latex + 1-wt.% Acrosol. Open symbols: 30-vol%; full symbols: 35-40-vol%; (●,○ without CMC; ■,□CMC35; ▲,△ CMC35-250; ◆,◇CMC250).

At given solids loading, the flow curves are affected by M_w and the total added amount of CMC, but in a less straightforward manner. These additives seem to play two different roles, as thickeners and as deflocculants, the predominance of one or the other role depends on interplay among M_w, added amount and solids volume fraction. For a total added amount of 0.1-wt.%, the thickening role seems to prevail at the two lower solids loadings (30- and 40-vol.%), being surprisingly stronger for the lower M_w CMC35, while the curves corresponding to the higher M_w CMC250 or to the mixture CMC35+CMC250 appear almost superimposed.
The sequence of the flow curves is changed when the system becomes more crowded (50-vol.% solids). The suspension without CMC offers more resistance to flow than the one with CMC35, which acts as deflocculant, while the thickening effect seems to be determined by the higher M_w CMC250. This picture significantly changes with increasing the total amount

of added CMC to 0.2-wt.% at which, the stronger thickening effect is observed for the lower M_w CMC35 followed by the higher M_w CMC250, while the mixture of both acts as deflocculant.

These sequences are contrary to those already observed with kaolin suspensions. Differences might relay on different affinities of the ionised CMC molecular chains to dissimilar surface properties of the two materials. In fact, GCC particles usually exhibit an apparent isoelectric point close to pH 8 and a low surface charge density at higher pH values [7], while kaolinite particles are known to possess an uneven surface charge distribution with the basal surfaces presenting high density negative charge along all pH range and the edges behaving like oxide surfaces with an isoelectric point in the neutral pH region. [8]

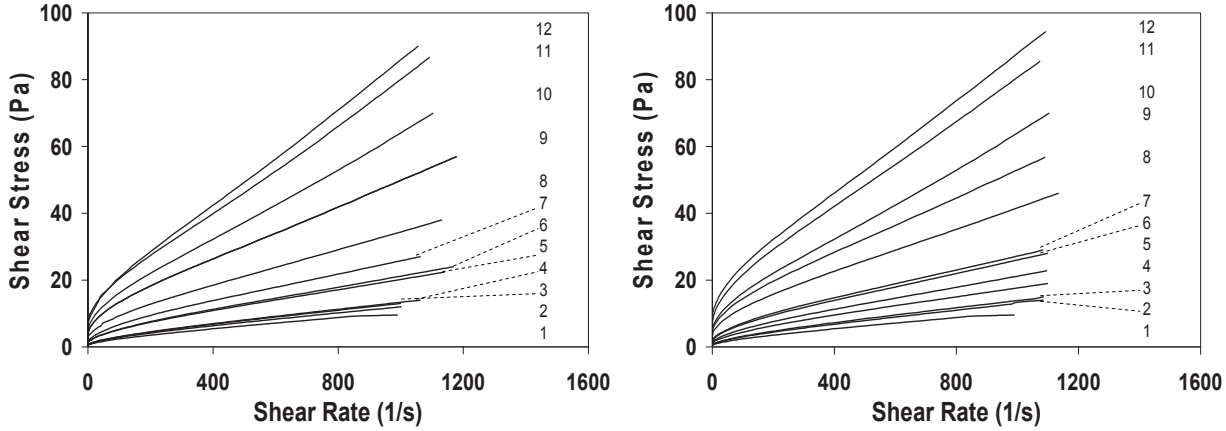

1-30-wt.% without CMC; 2-30-wt.%,CMC250; 3-30-wt.%,CMC35+CMC250; 4-30-wt.%,CMC35; 5-40-wt.% without CMC; 6-40-wt.%,CMC35+CMC250; 7-40-wt.%,CMC250; 8-40-wt.%,CMC35; 9-50-wt.%,CMC35+CMC250; 10-50-wt.% without CMC; 11-50-wt.%,CMC250; 12-50-wt.%,CMC35.

Figure 5. Effects of solids load and molecular weight of CMC (for a total added amount of 0.1-wt%) on the flow curves of $CaCO_3$ suspensions in the presence of 10-wt% Latex + 1-wt% Acrosol.

Figure 6. Effects of solids load and of molecular weight of CMC (for a total added amount of 0.2-wt.%) on the flow curves of $CaCO_3$ suspensions in the presence of 10-wt.% Latex + 1-wt.% Acrosol.

Figures 7 and 8 show the steady viscosity curves of the coating colours as a function of shear rate in the shear rate range from 0.1 to about 1000-1200 s^{-1} for the two CMC concentration levels, 0.1-wt.% and 0.2-wt.%, respectively. All the curves exhibit shear-thinning behaviours at the lower shear rate range (up to about 200 s^{-1}) followed by near Newtonian plateaus. Such behaviours are typical of suspensions containing polymeric binder/thickening agents that help forming a weak network structure, which is gradually disrupted under the applied shear stress field and aligns the particles along the flow direction. The sequences of the curves are essentially the same already observed in Figures 5 and 6, respectively.

Adsorption of polymeric chains with some associated solvent at the surface of GCC particles would result in an increase of their effective volume. The polymeric CMC chains may form different configurations upon adsorbing onto the GCC particles' surface as sketched in Figure 9. A more airy-like conformation would be expected for the low M_w CMC35 (Figure 9a-d), while the longer CMC250 chains would probably adsorb through several segments forming loops and tails less extended to the solution (Figure 9e-f). In fact, the solvency of the water towards CMCs is improved as the M_w decreases. The thickness of the adsorbed layers, the relative affinity of the adsorbing species to the surface, their solvency in the media and the adsorbed amount are all strongly interrelated [7,8,9]. At 0.1-wt.% CMC35, the polymeric chains

might be able to bend and partially align according to the flow direction (Figure 9b). When particles have to approach to closer distances (50-vol.%), such polymer configuration would also exert some steric hindrance at the lower polymer concentration thus enhancing the flowing ability of the suspension, as observed. Increasing the amount of CMC to 0.2-wt.% would lead to a higher degree of surface coverage and a denser adsorbed layer (Figure 9c).

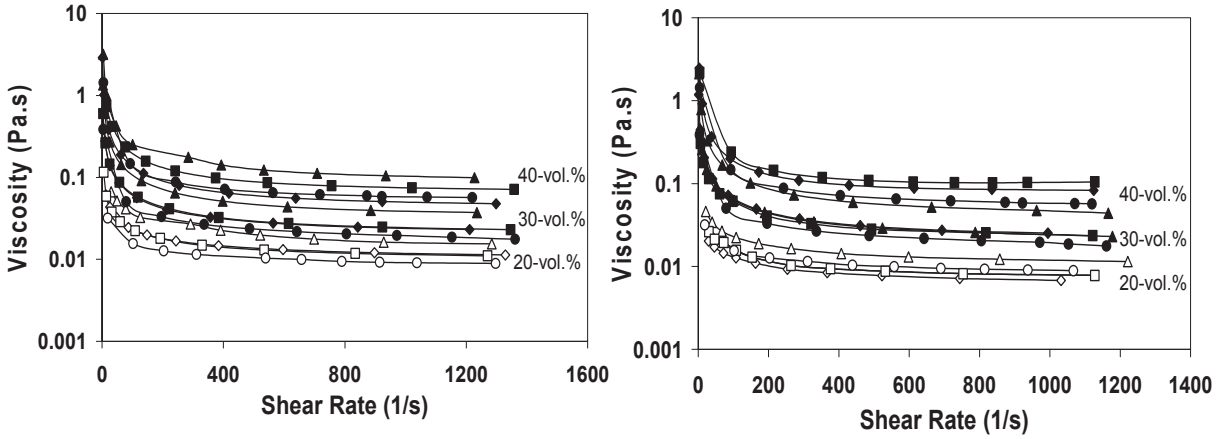

Open symbols: 30-vol%; full symbols: 40-50-vol%; (●,○ without CMC; ▲,△ CMC35; ◆,◇ CMC35-250; ■,□ CMC250).

Figure 7. Effects of solids load and of molecular weight of CMC (for a total added amount of 0.1-wt.%) on the steady shear viscosity curves of $CaCO_3$ suspensions in the presence of 10-wt.% Latex + 1-wt.% Acrosol.

Figure 8. Effects of solids load and of molecular weight of CMC (for a total added amount of 0.2-wt.%) on the steady shear viscosity curves of CaCO3 suspensions in the presence of 10-wt.% Latex + 1-wt.% Acrosol.

Since the predicted effective size of particles will be smaller in the case of CMC250 and the extent of particle bridging will be low at the lower solids volume fractions where the average distance among particles is large, one should expect a lower resistance to flow, as observed. However, at the higher solids concentration (50-vol.%), particles have to approach each other closer than in the previous situations so that the longer polymeric chains of the CMC250 might adsorb at the surface of different neighbouring particles, especially under a low degree of surface coverage (0.1-wt.% CMC250), thus promoting bridging flocculation (Figure 9e), which seems to be the predominant factor responsible for the more pronounced thickening effect observed with added 0.1-wt.% CMCs. Increasing the amount of CMC250 to 0.2-wt.% will enhance the surface coverage and reduce the probability of one polymeric chain to adsorb in more than one particle and, therefore, the trend for bridging flocculation. Again, the possibility for some polymeric chains to remain in the solution cannot be discarded, enhancing the viscosity of the liquid phase (Figure 9f). This explains why at 0.2-wt.% CMC the higher M_w CMC250 imparts a less pronounced shear thickening character in comparison with the lower M_w CMC35. On the other hand, concerning the CMC mixtures, the kinetics of adsorption would be faster for the shorter CMC35 chains, although some competition for adsorbing places at the surface of particles and some partial displacement of the shorter chains by the longer ones along the time can be expected [5,6,7].

CONCLUSIONS

The shorter polymeric chains of CMC35 adsorb faster and tend to form airy-like configurations at the surface of GCC particles increasing their apparent size, thus exerting a

more pronounced thickening effect at lower pigment concentrations compared with the longer ones of CMC250 under the same conditions.
Adding separately 0.1-wt.% of each CMC to high pigment concentrations enabled the shorter molecules of CMC35 to act as deflocculant and the longer ones of CMC250 to promote bridging flocculation for GCC particles. Adding separately 0.2-wt.% of each CMC to high GCC concentrations enabled the shorter molecules of CMC35 to form thick adsorbed layers whose interpenetration enhanced the rheological properties of the coating colours. Contrarily, the higher degree of surface coverage achieved at this CMC concentration hindered the longer molecular chains of CMC250 to promote bridging flocculation.
In respect to kaolinite, due to its lamellar particle shape, which influences surface charge distribution, CMC chains are adsorbed by kaolinite particles in such a way that we may consider it as the opposite relatively what happens with calcite particles.

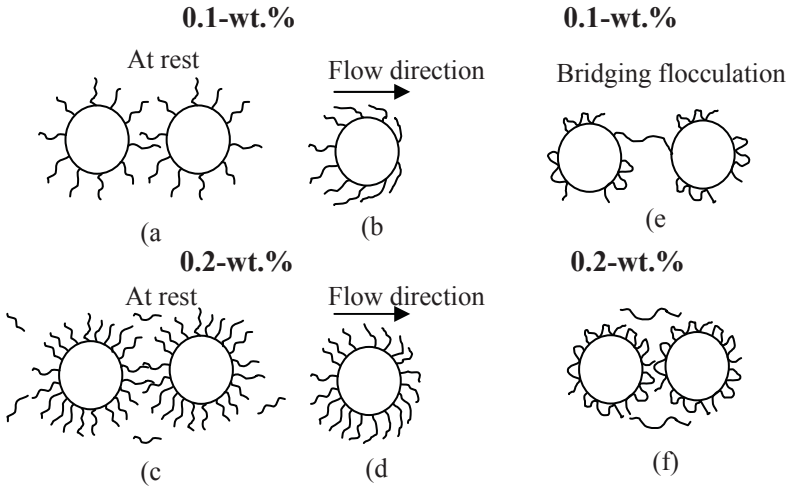

Figure 9. Proposed models for adsorption and conformation
of the different CMC binders onto the particles' surface of GCC.

ACKNOWLEDGEMENTS

Thanks are due to Fundação para a Ciência e a Tecnologia (FCT) for financial support (Project POCTI/45364) and to RAIZ for lab facilities.

REFERENCES

1-Triantafillopoulos,N."Paper Coating Viscoelasticity and its Significance in Blade Coating". Tappi, Atlanta (1996).
2-Gron, J. and Dahvik, P. "Effect of Coating Colour Chemistry and Temperature on Runnability and Coated Paper Properties". *J. Pulp and Paper Sci*., 23, (1997), J422-J427.
3-Willenbacher, N., Hanciogulari, H. and Wagner, H. "High Shear Rheology of Paper Coating Colors – More Than Just Viscosity". *Chem. Eng. Techn*., 20, (1997), 557-563.
4-Fadat, G. and Rigdahl, M. "Viscoelastic Properties of CMC/Latex Coating Colors". *Nordic Pulp and Paper Res. J*., 1, (1987), 30-38.
5-Conceição, S., Velho, J. and Ferreira, J. "Influence of Delaminating Procedure and of Adding Different Molecular Weight Carboxyl Methyl Cellulose Binders on Rheological Behaviour of Kaolin Suspensions". *Applied Clay Science*, 23 (5-6), (2003), 257-264.
6-Conceição, S., Olhero, S., Velho, J. and Ferreira, J. "Influence of Shear Intensity During Slip Preparation on Rheological Characteristics of Calcium Carbonate Suspensions". *Ceramics International*, 24, (1998), 527-532.

7-Tarì, G. and Ferreira, J. M. F., "Colloidal Processing of calcium Carbonate", *Ceramics International*, 24, (1998), 527-532.
8-Tari, G., Fonseca, A. and Ferreira, J. M.F, "Influence of Kaolinite Delamination on the Rheological Properties and Sedimentation Behaviour of Ceramic Suspensions", *Brit. Ceram. Trans*., 97 (6), (1998), 259-262.
9-Page, A., Carreau, P., Moan, M. and Heuzey, M.-C., "Rheological Behavior of Coating Colors : Influence of Thickener ", *The Canadian J. of Chem. Eng*., 50 (12) (2002), 1181-1188.

INFLUENCE OF ADDING CARBOXYMETHYL CELLULOSE ON RHEOLOGICAL PROPERTIES OF PRECIPITATED CALCIUM CARBONATE SUSPENSIONS

S. I. Conceição [1], N. F. Santos [2], J. M. F. Ferreira [3] and J. L. Velho [1]*

[1] Dep. of Geosciences, Univ. of Aveiro, 3810-193 Aveiro, Portugal, fax:234370605 jvelho@clix.pt
[2] Dep. of Chemical and Environmental Engineering, Polytechnic Institute of Tomar, 2300-313 Tomar, Portugal, naterciasantos@ipt.pt.
[3] Dep. of Ceramics and Glass Engineering, University of Aveiro, 3810-193 Aveiro, Portugal, jmf@cv.ua.pt

Keywords: CMC; PCC; Rheology; Slip casting.

ABSTRACT
Rheological properties of precipitated calcium carbonate (PCC) suspensions have been investigated in the presence of different amounts of two carboxymethyl cellulose (CMC) co-binder/thickening agents. The effect of solids volume fraction used during ball-milling on rheological properties of the as-prepared suspensions, or other diluted slurries derived from the more concentrated (35-vol.%) one by adding the required amounts of water (diluted systems), was also studied. The experimental results revealed that, at given solids loading, diluted systems are less viscous than non-diluted ones indicating that high intensity of shearing during slip preparation enhances dispersion and deagglomeration of suspended powders in the range of solids concentration studied (25-35-vol.%). Slip casting experiments were also performed in order to correlate the flow characteristics of the suspensions with their ability towards packing.

1. INTRODUCTION

The demand for synthetic calcium carbonate powders has been rapidly growing in recent years in various fields of industry including pharmaceuticals, elastomers, foodstuffs, food colorants, toiletries, processing of rubbers and plastics, preparation of inks, paints, sealants and other useful products. Precipitated calcium carbonate (PCC) is also a widely used mineral pigment for worldwide paper production.[1-3] Furthermore, PCC can be produced with several crystalline habits (aragonite, rhombohedral, and scalenohedral) and with different size of particles, depending on the specific reaction process that is used.[2-4] These characteristics enable to control the rheological properties of the coating slurries and the reinforcing performance of the filler. PCC is porous and has more surface area than a ground limestone block of the same size, which will display simple structure, or will resemble a single smooth rhombohedal crystal. The very complex surface effect of the precipitated crystal flock, will tend to scatter more light and yield more opacity. However, it is likely that will consume more binder than the ground limestone.[5-6] This observation motivated the present study, which aims to evaluated the effects of solids loading and the concentration and molecular weight of carboxymethyl cellulose (CMC) co-binders on the rheological properties of PCC suspensions and particle packing ability, evaluated by slip casting.

2. EXPERIMENTAL PROCEDURE

The PCC used in this work is a commercial product with a scalenohedral habit. It has an average particle size d_{50}=3.13 μm, measured by using a laser diffraction instrument (Coulter, LS230, UK). Stable suspensions with 20-, 25-, 30- and 35-vol.% of solids contents were prepared by adding 0.7 wt% (relative to dry solids) of the dispersing agent - an ammonium polycarbonate (Targon 1128, BK Ladenburg, Germany) to distilled water. Stirring for 20

minutes performed the mixings. The suspensions were transferred to a cylindrical polyethylene container and deagglomeration was performed by ball milling, using silicon nitrite balls as grinding media (diameter = 1.5 cm), for 24 h. All suspensions were left to deairing by rolling them into the milling container, without balls, for another 24 hours period. From the suspension containing the highest volume fraction of PCC (35-vol%), portions were taken, accurately weighted, and diluted to 20, 25, and 30-vol% solids by adding the required amounts of distilled water. These suspensions will be referred to as "diluted" to distinguish them from those that have been prepared from the beginning with the same required amounts of PCC. Two different molecular weights carboxymethyl cellulose co-binders (CMC35 - M_W = 35 000 g, CMC250 - M_W = 250 000 g) were added separately, or mixed in a 1:1 ratio in total amounts of 0.1 or 0.2-wt% relative to the solids. These co-binders were added to the suspensions after the 24 h deagglomeration step, which were then let to homogenise during the following 24 h rolling and deairing period. Rheological measurements were performed in a rotational controlled stress rheometer (Carri-med 500 CSL, UK) after the 24 h slip-deairing step at a strictly controlled temperature of 20°C. The measuring configuration adopted was a cone and plate (∅=4 cm, 2º, gap=53 μm) and stress sweep and multi-step shear measurements (10 points, max. equilibrium time of 1 min) were performed in the shear rates range from 0.1 s^{-1} up to about 1,300 s^{-1}. Before starting a measurement, pre-shearing was performed at high shear rate for 1 min followed by a rest of 2 min, in order to transmit the same rheological history to whole suspension being tested. The deaired suspensions were poured into plastic rings with 25 mm diameter based on an adsorbent plaster plate. Tree cylindrical samples were prepared form each suspension with a thickness of about 12 mm. The green bodies were first dried at room temperature for 24 h, demoulded, and then put in an oven at 100ºC for another 24 h period. The density of green bodies was measured according to the Archimedes method by immersion in mercury. The relative density was calculated assuming a theoretical density of calcium carbonate of 2.71 g/cm^3 as measured before.[7-8]

3. RESULTS AND DISCUSSION

The flow curves of the diluted and non-diluted suspensions containing different volume fractions of PCC (in the range of 20-35-vol.%) are displayed in figure 1, while figure 2, shows the steady shear viscosity curves.

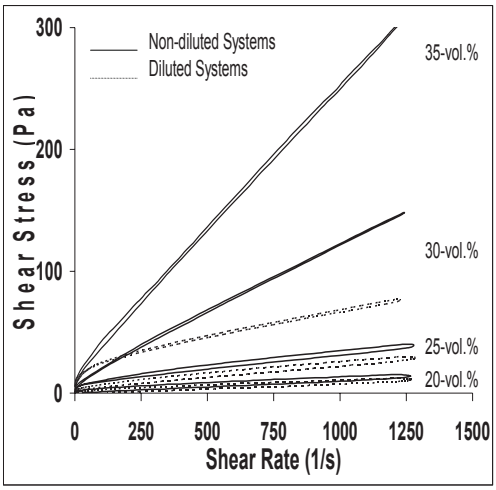

Figure 1. Effects of solids load and the suspension preparation procedure on the flow curves of PCC suspensions.

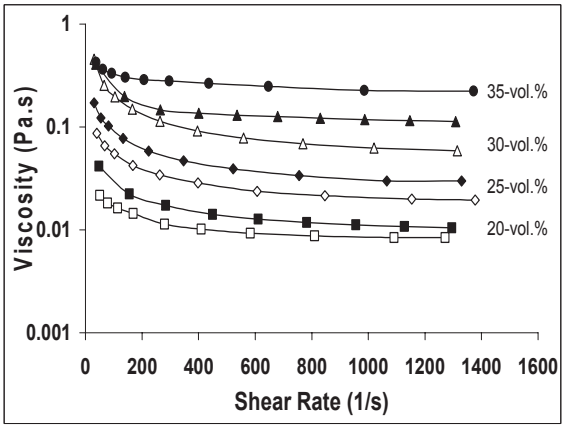

Figure 2. Effects of solids load and the suspension preparation procedure on the steady shear viscosity curves of PCC suspensions. Open symbols: diluted systems; Full symbols: non-diluted systems (■,□ 20% Vol.; ◆,◇ 25% Vol.; ▲,△ 30% Vol.; ● 35% Vol.;).

All the suspensions exhibit a shear thinning behaviour within the lower shear rate range (up to about 400 s^{-1}), and a near Newtonian flow behaviour for higher shear rates. The slopes of the flow curves increased significantly as solids volume fractions passed from 20-25-vol.% to 30-35-vol.%. Diluted systems require lower stress values for flowing under shear, compared with non-diluted ones. The diluted systems have been prepared from a stock suspension containing 35-vol.% solids, corresponding to the maximum achievable solids volume fraction, while keeping good pouring and flowing properties of the suspensions. The best dispersing degree would have been obtained for this suspension. In fact, one would expect that the intensity of the shear forces generated during the deagglomeration step would increase as the average distance among dispersed particles decreases up to a limit, beyond which the flowing properties will be gradually lost and the intensity of shearing will decrease [9]. Figures 3 and 4 show the influence of the molecular weight of CMCs, added in total amounts of 0.1-wt% and 0.2-wt%, respectively, relative to the mass of solids, on steady shear viscosity curves of non-diluted suspensions.

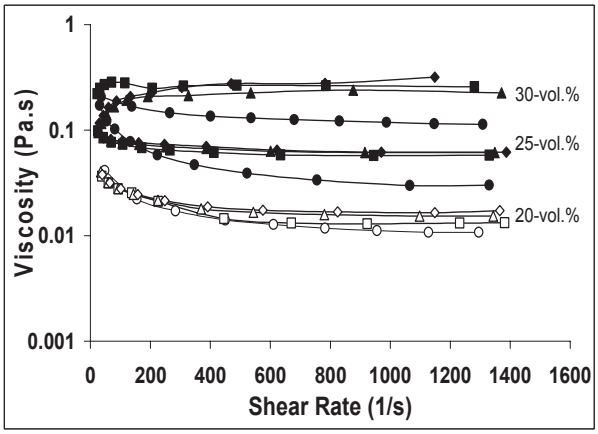

Figure 3. Influence of the molecular weight of CMC on steady shear viscosity curves of non-diluted PCC suspensions (20-30-vol%) in the presence of a total amount of 0.1-wt.% CMC. Open symbols: 20-vol%; Full symbols: 25- and 30-vol%; (●,○ without CMC; ■,□ CMC35; ▲,△ CMC35-250; ◆,◇ CMC250).

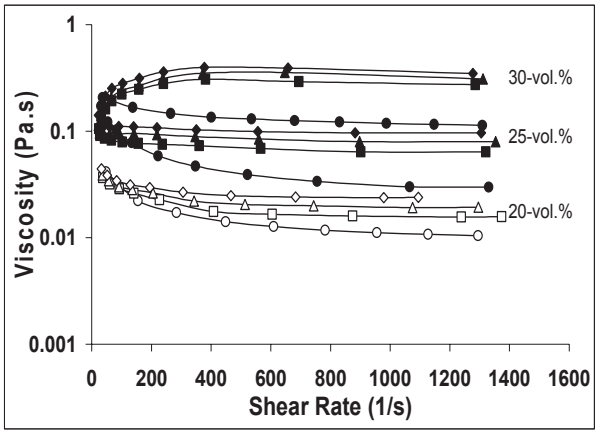

Figure 4. Influence of the molecular weight of CMC on steady shear viscosity curves of non-diluted PCC suspensions (20-30-vol%) in the presence of a total amount of 0.2-wt.% CMC. Open symbols: 20-vol%; Full symbols: 25- and 30-vol%; (●,○ without CMC; ■,□ CMC35; ▲,△ CMC35-250; ◆,◇ CMC250).

At a given solids volume fraction, the curves corresponding to different binder formulations are almost superimposed in the presence of 0.1-wt% CMC, whilst appear better discretized in the presence of 0.2-wt% CMC. The shear thickening flow behaviour is typical of well-dispersed and high concentrated suspensions and will be aggravated in the presence of particle agglomerates[10] or when thick adlayers are adsorbed at the particles surface.[8,11] The sequence of the curves is the same for both systems, being the less viscous the suspensions without CMC, followed successively by those containing CMC35 alone, the mixture CMC35-250, and CMC250 alone.

Figures 5 and 6 show the influence of the molecular weight of CMCs, added in a total amount of 0.1-wt% and 0.2-wt%, respectively, relative to the mass of solids, on steady shear viscosity curves of diluted suspensions. Compared with the non-diluted systems, the diluted ones are

less viscous and more Newtonian-like fluids, especially at the higher solids volume fraction, according to the results presented in Figures 2 and 3. The only exception is observed for the suspensions containing 30-vol.% solids and 0.2-wt.% CMC35, which exhibits a shear-thickening effect in the low shear rate range. This shear-thickening effect can be attributed to an airy-like configuration of the lower molecular weight polymeric chains adsorbed onto the particles surface, thus increasing the apparent size of the dispersed particles. In the presence of 0.1-wt.% CMC, the adsorption density seems to be enough to enhance dispersion, but not so high to hinder the alignment of the polymeric chains along the flow direction under the applied shear stresses. The adsorption density would increase with the CMC concentration, making the alignment of adsorbed molecules according to the flow direction more difficult, especially at lower shear rates, thus imparting the observed shear thickening characteristics.[12]
The longer CMC250 polymeric chains might adsorb through several segments, thus forming loops and tails, which do not extend so far into the solution as the shorter CMC35 chains. The possibility for them to adsorb at the surface of different neighbouring particles, especially under low degree of surface coverage (0.1-wt.%), is likely to occur, leading to a kind of bridging flocculation.
The increasing of CMC250 concentration to 0.2-wt.% will reduce the probability of one polymeric chain to adsorb in more than one particle and, therefore, the trend for bridging flocculation. On the other hand, the different polymer configuration leads to thinner adsorbed layer. This explains why at 0.2 wt%, CMC250 acts as deflocculant in comparison with the lower molecular weight CMC35.

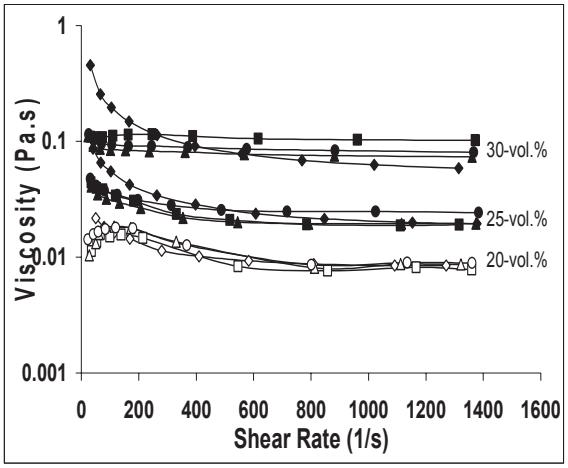

Figure 5. Influence of the molecular weight of CMC on steady shear viscosity curves of diluted PCC suspensions (20-30-vol%) in the presence of a total amount of 0.1-wt.% CMC. Open symbols: 20-vol%; Full symbols: 25- and 30-vol%; (●,○ without CMC; ■,□ CMC35; ▲,△ CMC35-250; ◆,◇ CMC250).

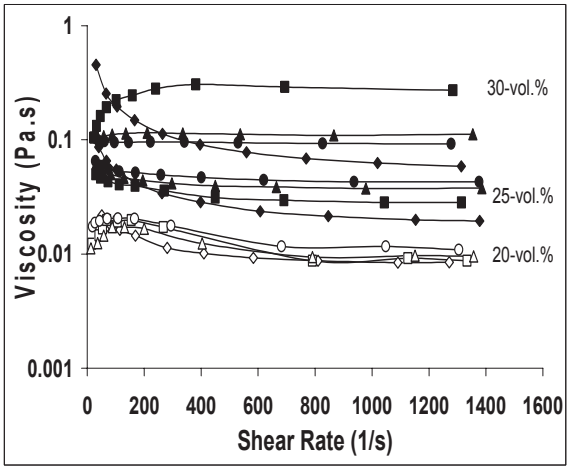

Figure 6. Influence of the molecular weight of CMC on steady shear viscosity curves of diluted PCC suspensions (20-30-vol%) in the presence of a total amount of 0.2-wt.% CMC. Open symbols: 20-vol%; Full symbols: 25- and 30-vol%; (●,○ without CMC; ■,□ CMC35; ▲,△ CMC35-250; ◆,◇ CMC250).

The higher capability of CMC250 chains to immobilize water molecules is the main factor responsible for their enhanced thickening properties. This also explains why the CMC mixtures exhibit an intermediate thickening efficiency. The only exception to this rule, observed in the presence of 0.2-wt.% CMC35, could be understood considering the bulkier airy-like configuration of the shorter polymeric chains.

Slip casting experiments were carried out to evaluate the effects of the intensity of shear forces during the slip preparation on the state of dispersion and deagglomeration of the PCC. Table 1 shows the relative density of the green bodies of non-diluted and diluted PCC suspensions, at different solid loads in absence of CMC binders.

Table 1. Effect of solids loading on green density of slip cast bodies of PCC.

Systems →	Solids volume (weight) fraction							
	Non-diluted [vol% (wt%)]				Diluted [vol% (wt%)]			
Green density	20 (40)	25 (47)	30 (54)	35 (59)	20 (40)	25 (47)	30 (54)	35 (59)
ρ (g/cm^3)	0.89	0.88	0.92	0.94	0.87	0.89	0.90	-
% TD	33%	33%	34%	35%	32%	33%	33%	-

For both diluted and non-diluted suspensions, the density increases with increasing solids loading, reaching a maximum value of 35% of the theoretical density at the highest solids volume fraction for the non-diluted systems. The packing density tends to be lower for the diluted systems, in apparent contradiction with a better deagglomeration degree achieved under these conditions. However, it is worthwhile to note that the more fluid suspensions are also more prone to particle segregation by both gravity and clogging effects[13-14] in absence of thickening agents, thus decreasing the packing density. Tables 2 and 3 show the effect of molecular weight of the co-binders on green density of slip cast bodies prepared from non-diluted and diluted suspensions. The theoretical densities of the green bodies derived from non-diluted and diluted systems tend to increase with increasing solids loading. These differences are much smaller in diluted systems compared with the non-diluted ones.

Table 2. Effect of molecular weight of CMC on green density of slip cast bodies for 0.1-wt% CMC.

Additives →		CMC 35 [vol% (wt%)]			CMC 250 [vol% (wt%)]			CMC35+CMC 250 [vol% (wt%)]		
Systems ↓	Green density ↓	20 (40)	25 (47)	30 (54)	20 (40)	25 (47)	30 (54)	20 (40)	25 (47)	30 (54)
Non-diluted	ρ (g/cm^3)	0.80	0.77	0.93	0.81	0.78	0.93	0.80	0.79	0.90
	% TD	29.5%	28%	34%	30%	29%	34%	29.5%	29%	33%
Diluted	ρ (g/cm^3)	0.88	0.88	0.92	0.90	0.92	0.93	0.89	0.90	0.96
	% TD	32%	32%	34%	33%	34%	34%	33%	33%	35%

Table 3. Effect of molecular weight of CMC on green density of slip cast bodies for 0.2-wt.% CMC.

Additives →		CMC 35 [vol% (wt%)]			CMC 250 [vol% (wt%)]			CMC35+CMC 250 [vol% (wt%)]		
Systems ↓	Green density ↓	20 (40)	25 (47)	30 (54)	20 (40)	25 (47)	30 (54)	20 (40)	25 (47)	30 (54)
Non-diluted	ρ (g/cm^3)	0.82	0.81	0.91	0.81	0.81	0.93	0.80	0.81	0.93
	% TD	30%	30%	33.5%	30%	30%	34%	30%	30%	34%
Diluted	ρ (g/cm^3)	0.91	0.93	0.96	0.92	0.93	0.94	0.92	0.91	0.94
	% TD	33.5%	34%	35%	34%	34%	35%	34%	33.5%	35%

The green densities obtained from diluted systems are generally higher than those achieved from the non-diluted ones, contrarily to the observations in absence of CMC binder/thickening agents, being even better in the presence of a total amount of 0.2-wt.% of

these additives, irrespective to their molecular weight. These results prove that the better dispersion and deagglomeration degrees have been achieved in the diluted systems, being in close agreement with a previous report on kaolin.[12] The shear stresses involved in the deposition stage should probably be too small to reveal any difference in rheological behaviour of the suspensions, namely, the shear thickening character of the suspension containing 30-vol.% solids and 0.2-wt.% CMC35. Therefore, the generality of the packing density data are in good agreement with the rheological results discussed above.

4. CONCLUSIONS

The rheological characteristics of PCC suspensions, and their packing ability during slip casting preparation were shown to be strongly dependent on the intensity of shear during slip preparation, as controlled by solids volume fraction. These characteristics were enhanced with increasing solids loading, conferring better performance to diluted systems. The efficiency of dispersion can be accessed by rheological measurements and complemented by slip casting experiments. The green density of slip cast bodies seems even more reliable in the evaluation of the dispersion degree. Adding CMC co-binders might play different roles in terms of rheology, depending on the interplay between the polymeric chain lengths (molecular weight, and chain conformation), and the added amount, and the suspension concentration.

ACKNOLEDGEMENTS

Thanks are due to Portuguese Foundation for Science and Technology (FCT) for the financial supported in the frame of the contract No. POCTI/2002 – CTM 45364.

5. REFERENCES

1-Delgado, H. M. S., "Carbonatos de Cálcio na Indústria do Papel. Estudos Aplicados em Rochas Carbonatadas Portuguesas", Tese de Doutoramento, Universidade de Aveiro, (1991).
2-Krogerus, B., "Precipitated Calcium Carbonate (PCC)" in *Papermaking Chemistry,* Cap. 6, Ed. Tappi Press, (1999), 128-129.
3-You, K.J., "Process for Producing Ultrafine Particles of Colloidal Calcium Carbonate", *Patent No: GB 2309691, UK Patent Application,* (1998).
4-Virtanen, P., "Process for Preparing and Modifying Calcium Carbonate ", *Patent No: WO 99/36361, World Patent,* (1999).
5-Drukenbrod, M., "Calcium Carbonate – Types, Uses and Limitations", *Paint and Coatings,* (2001).
6-Imppola, O., "Precipitated Calcium Carbonate – PCC" in *Pigment Coating and Surface Sizing of Paper,* Cap. 9, Ed. Tappi Press, (2000).
7-Tarì, G. and Ferreira, J. M. F., "Colloidal Processing of Calcium Carbonate", *Ceramics International*, **24** (1998), 527-532.
8-Conceição, S. I., Olhero, S., Velho J. L. and Ferreira J. M. F., "Influence of Shear Intensity During Slip Preparation on Rheological Characteristics of Calcium Carbonate Suspensions", *Ceramics International*, **29**, (4) (2003), 365-370.
9-Kloow, G., "Carboxy Methyl Cellulose" in *Pigment Coating and Surface Sizing of Paper,* Cap. 9, Ed. Tappi Press, (2000).
10-Tarì, G., Fonseca, A. T., and Ferreira, J. M. F., "Influence of Kaolinite Delamination on the Rheological Properties and Sedimentation Behaviour of Ceramic Suspensions", *Brit. Ceram. Trans*. **97** (6) (1998) 259-262.
11-Sandås, S. E. & Salminem, P. J., "The Influence of the Molecular Weight of Carboxymethyl Cellulose (CMC) on Rheology, Dewatering and Coating Performance", in *Nordic Pulp and Paper Research Journal* **5** (1) (1993), 184-188.
12-Conceição, S., Velho, J. L. & Ferreira, J. M. F., "Influence of Delaminating Procedure and of Adding Different Molecular Weight Carboxylmethyl Cellulose Binders on Rheological Behaviour of Kaolin Suspensions", *Applied Clay Science,* **23**, (5-6) (2003), 257-264.

13-Ferreira, J. M. F. "Role of the Clogging Effect in the Slip Casting Process", *J. Europ. Ceram. Soc*., **18** (1998) 1161-1169.
14-Olhero, S.M. and Ferreira J. M. F., "Particle Seggregation Phenomena Occurring During Slip Casting Process", *Ceramics International*, **28** (4) (2002) 377-386.

HYDROXYL ETHYL CELLULOSE (HEC) AS RHEOLOGICAL MODIFIER IN COATING COLOURS FOR PAPER APPLICATIONS

*S. I. Conceição [1], N. F. Santos[2], J. M. F. Ferreira [3] and J. L. Velho * [1]*

[1]Department of Geosciences, University of Aveiro, 3810-193 Aveiro, Portugal, jvelho@clix.pt
[2]Department of Chemical and Environmental Eng., Polytechnic Institute of Tomar, 2300-313 Tomar
[3]Department of Ceramics and Glass Engineering, University of Aveiro, 3810-193 Aveiro, Portugal

Keywords: HEC; Rheology; Coating colours; PCC.

ABSTRACT
Precipitated calcium carbonate (PCC) is a very important pigment especially for paper coating applications. One of the most exigent applications of PCC is in paper coating where suspension rheology is a critical property. Carboxyl methyl cellulose (CMC) is a very common co-binder applied in coating colour formulations. New co-binders are positioning as an alternative to CMC. One of them is hydroxyl ethyl cellulose (HEC). The main goal of this research is to analyse the potentialities of this co-binder as possible alternative to CMC in order to improve rheology of PCC suspensions. Two PCC pigments were selected: one, with scalenohedral habit, calcitic (PCC-C); the other, with acicular particles, aragonitic (PCC-A). The results show a clear difference between rheological characteristics of PCC-C and PCC-A slurries due, essentially, to particle shape effects. Rheological properties of coating colours with added HEC show interesting results which confer this additive a high potential for paper coating applications.

1. INTRODUCTION

Paper industry, namely the one that is involved in the production of coated papers, is very exigent in terms of rheological control of coating colours. In fact, there is an influence of rheology on paper properties, namely, thickness, optical, structural and print properties [1,2]. The importance of using rheological modifiers in order to control viscosity is a critical matter. Carboxyl methyl cellulose (CMC) is a common one, and, despite the research done on this rheological modifier, there is still research to be done, especially relatively to the interactions between pigment particle and polymeric chains of CMC. [3]
New rheological modifiers are appearing in the market and one of them is HEC (hydroxyl ethyl cellulose). Is very common in USA and Japan but has limited share in Europe. This fact is the main reason for this research. The main goal was to investigate its potential application as rheological modifier in coating colours for paper coating applications.

2. EXPERIMENTAL PROCEDURE

Two pigments were selected for this research. Both of them are precipitated calcium carbonate (PCC), a pigment that is doing some inwards on paper coating despite its market, as filler is very common. These PCC pigments have different particle shape. One is of calcitic nature, with scalenohedral habit (PCC-C); the other of aragonitic nature, with acicular particles (PCC-A), having average particle sizes of 0.637 μm and 0.643 μm, respectively, measured by using a laser diffraction instrument (Coulter LS230).
The suspensions containing PCC-C were prepared with 50-vol% of solids, while suspensions containing PCC-A were prepared at 48-vol% of solids loading. Two CMC grades with different molecular weights (M_w) were used: CMC35 with a M_w=35,000 g/mol and CMC250 with M_w=250,000 g/mol. As an alternative to CMCs, a new co-binder is used, HEC with M_w=115,000 g/mol. All these co-binders have been added separately in a fixed amount of 0.1 and 0.2-wt.% relative to dry mass of PCC. After adding the co-binders, each suspension was

transferred to a cylindrical polyethylene container and left rolling in a rotating system for 24 hours for homogenising and deairing.
Rheological measurements were performed in a rotational controlled stress rheometer (Bohlin C-VOR, USA) after the 24 h slip-deairing step at a strictly controlled temperature of 20°C. The measuring configuration adopted was a cone and plate (∅=40 cm, 4º, gap=150 μm). For flow behaviour and viscosity tests, stress sweep and multi-step shear measurements (20 points, max. equilibrium time of 1 min) were performed in the shear rates range from 0.1 s^{-1} up to about 1,100 s^{-1}, while oscillatory tests were carried out with a constant frequency of 0.1 Hz and variable shear stress (from 0.01 to 100 Pa).

3. RESULTS

The flow curves of the coating colours for the two pigments, PCC-C and PCC-A, are shown in Figures 1 and 2 (PCC-C) and 3 and 4 (PCC-A). It can be seen that all the curves exhibit shear thinning behaviours. The flow curves are affected by the type and the M_w of co-binders.

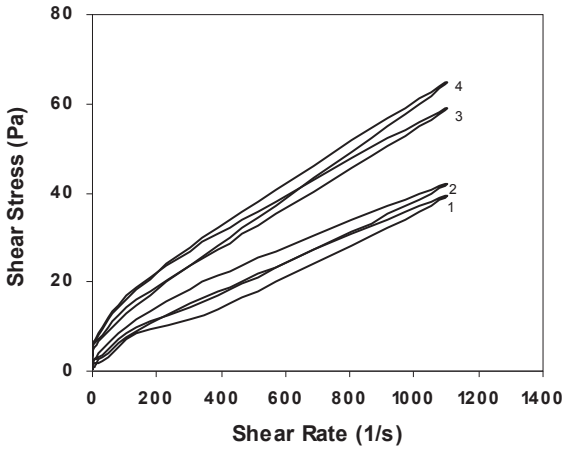

Figure 1. Effect of solids concentration and molecular weight of co-binders (for a total added amount of 0.1-wt%) on the flow curves of PCC-C suspensions in the presence of 10-wt% Latex + 1-wt% Acrosol.

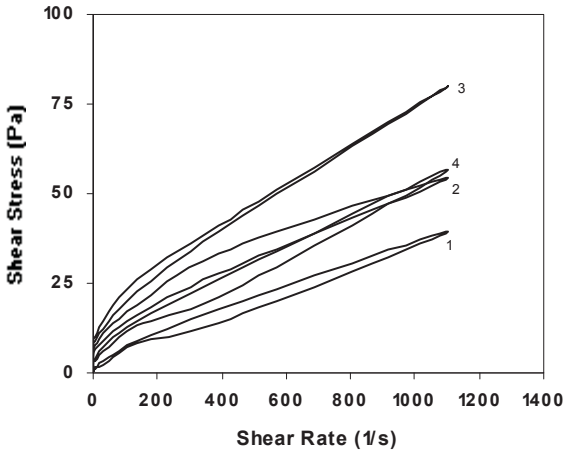

Figure 2. Effect of solids concentration and molecular weight of co-binders (for a total added amount of 0.2-wt%) on the flow curves of PCC-C suspensions in the presence of 10-wt% Latex + 1-wt% Acrosol.

Legend: 1-Without co-binder; **2**-With HEC; **3**-With CMC250; **4**-With CMC35.

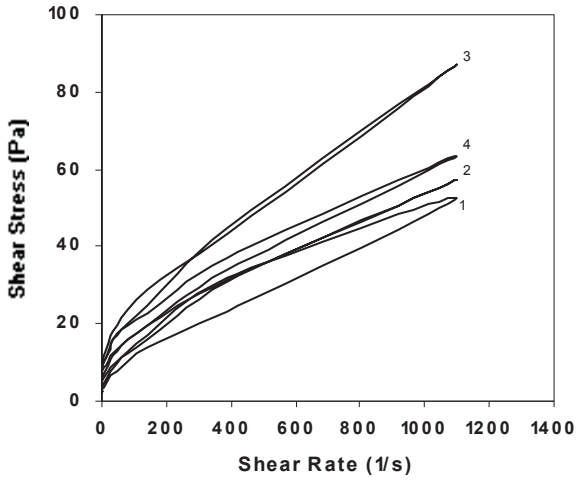

Figure 3. Effect of solids concentration and molecular weight of co-binders (for a total added amount of 0.1-wt%) on the flow curves of PCC-A suspensions in the presence of 10-wt% Latex + 1-wt% Acrosol.

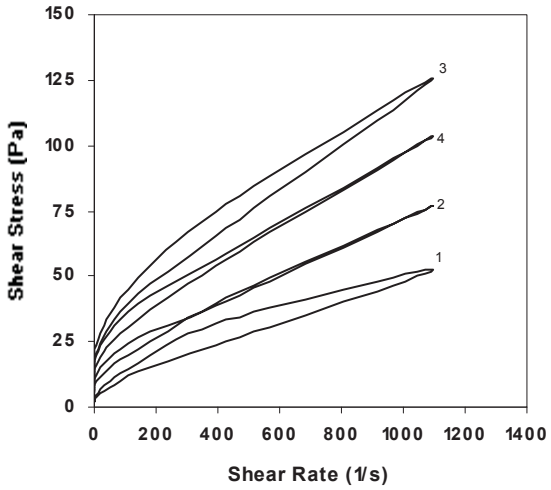

Figure 4. Effect of solids concentration and molecular weight of co-binders (for a total added amount of 0.2-wt%) on the flow curves of PCC-A suspensions in the presence of 10-wt% Latex + 1-wt% Acrosol.

These additives seem to play two different roles, namely, as thickeners of the dispersing liquid media, increasing its viscosity; and as surface active agents. The predominance of one or the other role seems to depend on the interplay among the type and M_w of co-binders, and the particle shape of pigments.

In all cases, the shear stress values required for the systems to flow at a given shear rate increase, relatively to the situations in absence of co-binders, which exhibit the more fluid-like behaviour. Furthermore, the hysteresis loop of the flow curves is also sensitive to the type and M_w of the added co-binders.

The sequence of the curves is the same for the two PCC pigments except for the PCC-C (0.1wt.%). It is interesting to note that HEC with a M_w=115,000 g/mol has a lower thickening effect than CMC35 (M_w=35,000 g/mol). This might be due to different polymer configurations when adsorbed at the particles surface as well as to different specific interactions between polymers and solid surfaces.

The shorter molecules of CMC35 are more prone to form an airy-like conformation, thus increasing more the apparent volume of the dispersed particles when compared to the other longer polymer chains, which might adsorb through small segments, forming loops and tails less extended to the solution. Another interesting feature of the flow curves obtained in the presence of the higher M_w co-binders is the relatively narrow hysteresis loop, i.e. a less accentuated tendency for particles structuration after shear (tixotropy). This can be understood considering that the total added amount of 0.1-wt.% and 0.2-wt.% would enable a good surface coverage by the polymeric chains to avoid bridging flocculation effects.

PCC-A is responsible for higher yield values and higher shear stress values than that of PCC-C. Acicular particles, probably due to their higher packing ability, they show an higher resistance to flow. PCC-C have a natural tendency to develop structure, it means that these particles are in clusters (soft aggregates). Despite these aggregates, the packing ability of these aggregates is weak and so, the resistance to flow is low. Despite these differences between PCC-C and PCC-A, is interesting to see that HEC behaves in the same manner and despite its medium molecular weight is the best of all co-binders in terms of shear stress.

The steady viscosity curves of the coating colours for the two pigments, are shown in figures 5 and 6 (PCC-C) and in figures 7 and 8 (PCC-A). The shear-thinning behaviour is confirmed for all the curves up to shear rates of about 300 s^{-1} followed by near Newtonian plateaus. Such behaviours are typical of suspensions containing polymeric binder/thickening agents that help forming a weak network structure, which is gradually disrupted under the applied shear stress field and aligns the particles along the flow direction. The sequences of the curves are essentially the same already observed in Figures 1 to 4, respectively.

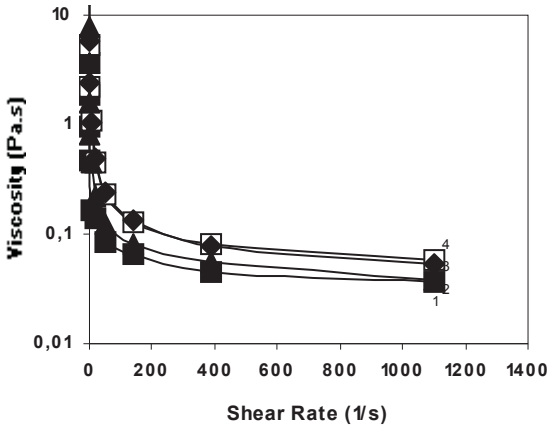

Figure 5. Effects of co-binder (for a total added amount of 0.1-wt.%) on the steady shear viscosity curves of PCC-C suspensions in the presence of 10-wt.% Latex + 1-wt.% Acrosol.

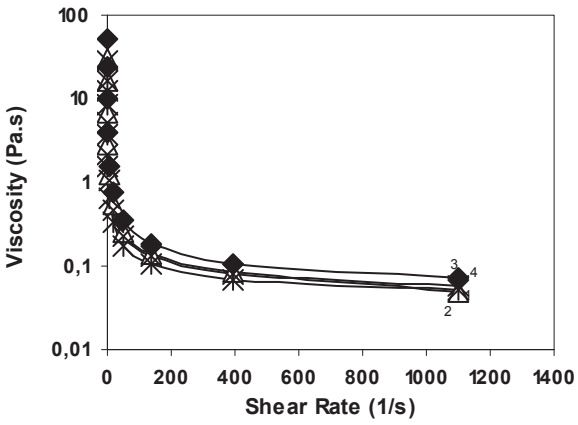

Figure 6. Effects of co-binder (for a total added amount of 0.2-wt.%) on the steady shear viscosity curves of PCC-C suspensions in the presence of 10-wt.% Latex + 1-wt.% Acrosol.

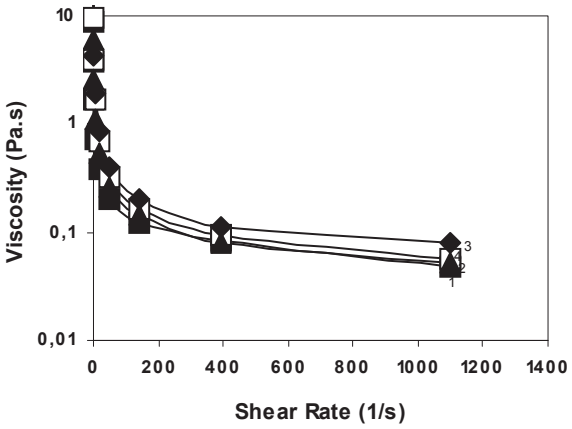

Figure 7. Effects of co-binders (amount of 0.1-wt.%) on the steady shear viscosity curves of PCC-A suspensions in the presence of 10-wt.% Latex + 1-wt.% Acrosol.

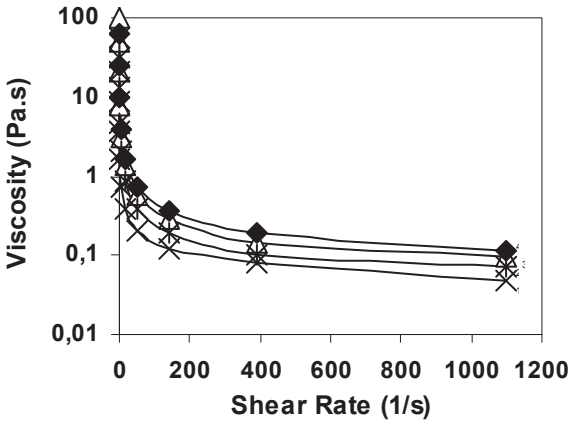

Figure 8. Effects of co-binders (amount of 0.2-wt.%) on the steady shear viscosity curves of PCC-A suspensions in the presence of 10-wt.% Latex + 1-wt.% Acrosol.

An amplitude sweep was used to characterise the consistency at rest with regard to dispersion stability during long-term storage. Figures 9 and 10 show the oscillatory curves of PCC-C colours in the absence and in the presence of 0.1-wt.% and 0.2-wt.% CMC co-binders, while Figure 11 and 12 compares the oscillatory curves of the same pigment suspensions but in the presence of 0.1-wt.% and 0.2-wt.% CMC35 and HEC.

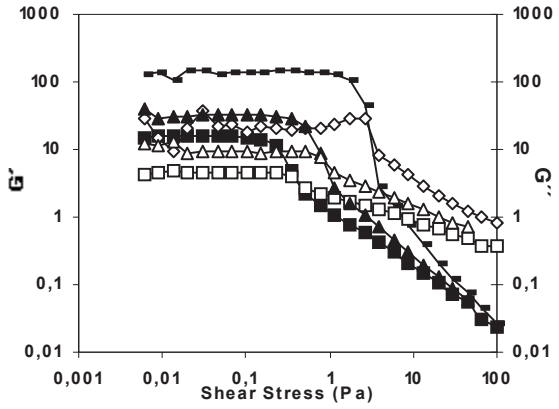

Figure 9. Dynamic moduli for PCC-C suspensions, with 0.1-wt% of CMC35 and HEC.

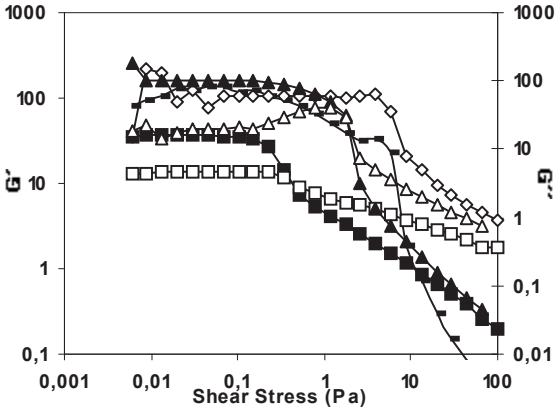

Figure 10. Dynamic moduli for PCC-C suspensions, with 0.2-wt% of CMC35 and HEC.

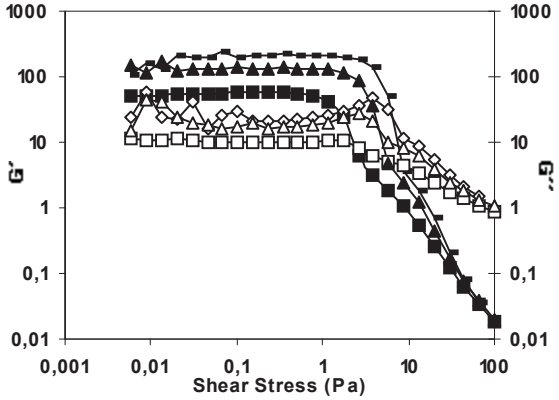

Figure 11. Dynamic moduli for PCC-A suspensions, with 0.1-wt% of CMC35 and HEC.

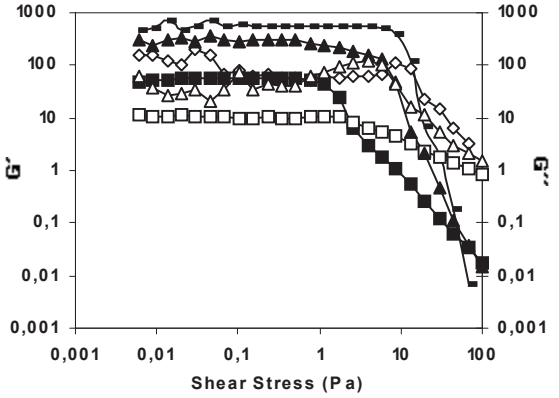

Figure 12. Dynamic moduli for PCC-A suspensions, with 0.2-wt% of CMC35 and HEC.

Legend: ■.G'-Latex; □.G''-Latex;▲.G'-HEC; Δ.G''-HEC; -.G'-CMC35; ◊.G''-CMC35

G' represents the elastic (reversible deformation) behaviour of the sample. G'' is a measure of the deformation energy used up in the sample during the shear process and lost to the sample afterwards thus, representing the viscous (irreversible deformation) behaviour of the sample.
It can be seen that G´ exhibits a more or less extended plateau, revealing that the analysis included the linear viscoelastic (LVE) range. The extent of the plateau increases with decreasing co-binders M_w. This means that the crossover point where the viscous character dominates over the elastic one occurs at increasing shear stress values as M_w of co-binders decreases.
Regarding the influence of different added co-binders, the oscillatory curves of PCC-A exhibited the same trends as observed with PCC-C. However, the acicular form of PCC-A particles resulted in measured G´ values, which were almost one order of magnitude greater than those observed for the scalenohedral PCC-C particles. Such differences are significant, especially if one considers the lower solids loading of PCC-A colours. In a consistent way, the crossover point also occurs for higher shear stress values for the acicular PCC particles in the presence of co-binders.

The difference of crossover point between CMC35 and HEC is greater for PCC-C than for PCC-A which means that for PCC-A, due probably to their acicular (discrete) particles, the role of the two co-binders is almost the same. But, for the scalenohedral (structured) particles of PCC-C, the less M_w of CMC35, with shorter polymeric chains, they are responsible for a longer reversible deformation.

Between 0.1-wt% and 0.2-wt% co-binders concentration there are interesting aspects to be analysed. For PCC-C pigment, data for G' is almost the same, which means that the structured particles can absorb efficiently co-binders chains. The shear stress correspondent to the crossover point is effectively influenced by by co-binder concentration. For PCC-A pigment, there is an evident influence of the co-binder concentration. In fact, not only G' and G'' increase but also the shear stress correspondent to the crossover point is influenced by co-binder concentration.

Furthermore, the comparison of the figures 9 to 12 suggests that the colours with added HEC co-binder would exhibit a better stability at rest since the G´ plateaux are more flat than with CMC35. In other words, the same suitable rheological properties might be achieved with smaller added amounts of these additives.

In figures 13 to 16, the storage and loss moduli in the linear regime are presented as functions of the frequency for PCC-C and PCC-A suspensions with CMC35 and HEC. In what regards to PCC-C, again we notice that the storage modulus is considerably larger than the loss modulus. Both moduli increase with HEC concentration, specially G'', while, in respect to CMC35, G'' shows an increase greater than G'. Both G' and G'' are constant at low frequency and increases slightly at higher frequencies. Therefore, the suspensions display a typical viscoelastic, solid-like behaviour, as shown by [4-6].

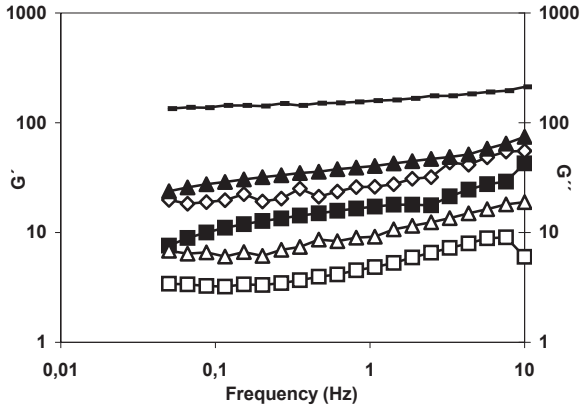

Figure 13. Dynamic moduli for PCC-C (0.1-wt% of co-binder) as function of frequency.

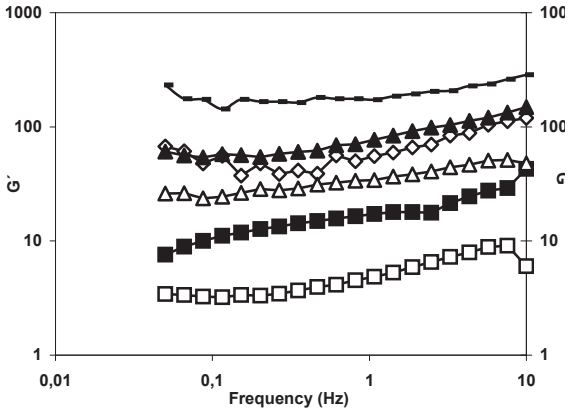

Figure 14. Dynamic moduli for PCC-C (0.2-wt% of co-binder) as function of frequency.

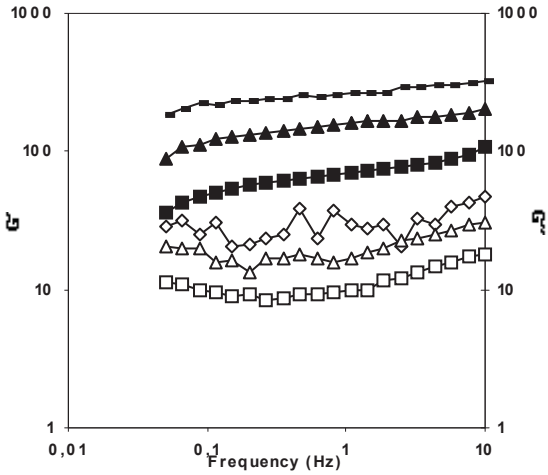

Figure 15. Dynamic moduli for PCC-A (0.1-wt% of co-binder) as function of frequency.

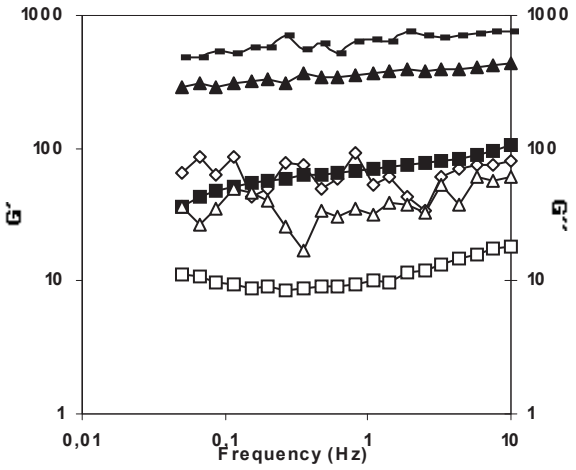

Figure 16. Dynamic moduli for PCC-A (0.2-wt% of co-binder) as function of frequency.

Legend: ■.G'-Latex; □.G''-Latex;▲.G'-HEC; Δ.G''-HEC; -.G'-CMC35; ◊.G''-CMC35

In what respect to PCC-A pigment, we can see that both moduli increase, as expected, with co-binder concentration. The storage modulus G' is nearly independent of the frequency, while the loss modulus G'' show a very irregular pattern, specially for a co-binder concentration of 0.2-wt%. HEC is responsible for lower G' and G'' values, when compared to CMC35 at different frequencies.

CONCLUSIONS

The results presented in this work show that co-binder HEC is a good alternative to the more commonly used CMC one since it imparts good flow behaviour. On the other hand, the morfology of the pigment particles plays the most relevant role in determining the rheological properties. Elongated particles are more prone to structural regeneration after shear due to the easy bridging of the particles by the adsorbed co-binder molecules.

ACKNOWLEDGEMENTS

Thanks are due to Portuguese Foundation for Science and Technology (FCT) for the financial supported in the frame of the contract No. POCTI/2002 – CTM 45364.

REFERENCES

1-Conceição, S.I., Santos, N.F., Velho, J.L., Kholkin, A. & Ferreira, J.M.F., "Relationship between Coating characteristics and Printability", WPP – Chemical Technology of Wood Pulp Paper, Proceedings of WPP'2003, 17-19 September 2003, Bratislava-Slovakia, (2003), 161-166.

2-Lehtinen, E., "Coating binders – general", in *Pigment coating and surface sizing of paper*, chap. 13, ed. tappi press, (2000), 189-195.

3-Young, T. S. & Fu E., "Associative behaviour of cellulosic thickeners and its implications on coating structure and rheology", *Tappi Journal*, April, (1991), 197-207.

4-Carreau, P., De Kee, D. and Chhabra, R., "Rheology of polymeric systems: Principles and applications", hanser, Munich (Germany) (1997).

5-Yziquel, F., Moan, M. Carreau, P. and Tanguy, P., «Nonlinear viscoelasticity behavior of paper coating colors", *Nordic Pulp and Paper Research Journal*, 14(1), (1999), 37-47.

6-Carreau, P. and Lavoie, P., "Coating colors: A rheologist point of view ". In Proceeding of TAPPI Coating Conference, Atlanta, (1991), 203-212.

4. BIOPOLYMERS & BIOLOGICAL MATERIALS

EFFECTS OF PROCESSING ON THE RHEOLOGICAL PROPERTIES OF WHEAT GLUTEN BIOMATERIALS

Jerez, A.[1], Partal, P.[1], Martínez, I.[1], Gallegos, C.[1] and Guerrero, A.[2]*

[1] Departamento de Ingeniería Química. Facultad de Ciencias Experimentales. Campus el Carmen, Universidad de Huelva, 21071 (Huelva), Spain.
[2] Departamento de. Ingeniería Química. Facultad de Química, Universidad de Sevilla, 41012 (Sevilla), Spain.

Keywords: Wheat gluten, bioplastics, rheology, viscoelasticity, processing.
(*) Author to whom correspondence should be addressed, e-mail: abel.jerez@diq.uhu.es

Abstract

Vegetal proteins, due to its characteristics, could be considered a suitable raw material for the production of new biodegradable plastic, which could replace synthetic polymers in certain applications, reducing the environmental problems caused by their use. The present article focus on the study of the effect of formulation and processing on the rheology of bioplastics composed mainly by gluten and glycerol. Gluten proteins and glycerol, as plasticizer, mixtures were prepared with this aim, both by physico-chemical and mechanical procedures. The physco-chemical method consists in the addition of sodium disulphite to a solution of proteins in an ethanolic solvent, and finally mixing with the plasticizer agent at a controlled pH. The solution obtained was then casted on to a plain surface and submited to a drying process. The mechanical method of preparation consists in the mixing of a dough-like material based on gluten and plasticizer undergoing shear and temperature controlled conditions. The evolution of the linear viscoelastic behaviour, of the gluten / glycerol mixture, during the stages of preparation and the effect of the process conditions, have been evaluated in stress controlled rheometers. The thermal behaviour of the material has also been tested, between 25º and 160º C, by 2º C/min temperature ramp, at controlled strain and at a fixed frequency. The results obtained show that during the mechanical processing of gluten an increase on the value of the viscoelastic moduli takes place, showing a weak gel-like behaviour, with higher values of the elastic moduli than the viscose one. This behaviour is observed too in the plastic prepared by the physico-chemical method.

1. Introduction

An increasing interest in the use of natural biopolymers has been notice during the last twenty years. The different uses of these new biomaterials go from biodegradable packing, edible and non-edible, and plastic films to adhesives. Proteins, lipids and polysaccharides have been used as biopolymers to obtain new biomaterials. Proteins derived from plants are a class of renewable materials that are produced at a kiloton scale per annun, e.g. wheat gluten, soy and pea [1,2]. In addition, these new materials present the advantage of biodegradability, wheat gluten biomaterials degradation rates have proved to be among the rates of fast degrading polymers, completely degrading in 50 days when buried in farmland soil [3]. These properties become a great opportunity for adding value to a material which is often obtained as an agricultural by-product of the food processing industry. Moreover, the importance of new biodegradable materials is not only that they help to reduce waste materials but they could help to preserve petroleum reserves by substituting synthetic polymers [4].

Wheat gluten contains two main groups of proteins, gliadin, also known as prolamin, and glutenin. Gliadin exhibits viscous flow properties without significant elasticity. accounting for the extensionability of wheat flour dough and acts as a filler diluting glutenin interactions. Glutenin is one of the largest natural molecules, consisting of polymers made from polypeptide chains linked end-to-tail by disulfide bonds [5].

A plasticizer is a major component, required to overcome film brittleness and helping to avoid chipping and cracking of films during subsequent handling and storage. Plasticizers are molecules with low molecular weight, low volatility, which modify the three-dimensional structure of proteins. Wheat gluten films without a plasticizer become brittle and difficult to handle. The plasticizer reduces intermolecular forces and increase polymeric chains mobility. Moreover, the plasticizer reduces the glass transition temperature of the thermoplastic wheat gluten proteins [1; 6]. The Tg of wheat gluten has been studied as a function of water, glycerol, and sorbitol contents.

Processing films, coatings or other materials based on polymers of agricultural origin requires three main steps: breaking of intermolecular bonds (non-covalent and covalent, if necessary) that stabilize polymers in their native forms by using chemical or physical rupturing agents; arranging and orienting mobile polymer chains in desired shape; and, finally, allowing formation of new intermolecular bonds and interactions to stabilize the three-dimensional network. The shape obtained in the second step is mainly maintained by eliminating agents used in the first step to break intermolecular bonds. Active sites for bond formation become free and close enough to each other to create new interactions, hydrogen bonds, hydrophobic interactions and disulfide bonds, forming a new three-dimensional network.

Wheat Gluten has been proved to be an excellent film-forming agent. Other authors have obtained films by dispersing wheat gluten in an ethanolic solvent containing a plasticizer and acetic acid, then casting the film forming solution and finally drying it [7]. The *casting method* of film processing is based on the above mentioned three steps, using a chemical reactant to disrupt disulfide bonds, dispersing, solubilizing proteins and finally drying it. Previous authors who have studied film formation by the casting method have processed 50 μm thick samples, obtaining good quality films which could be used for food packaging in view of the properties they posses such as opacity, water vapour, oxygen and carbon dioxide permeability, and mechanical properties. However, the use of these films in other applications in which they could substitute synthetic polymers is limited [7;8].

Another way of processing wheat gluten biomaterials is the *mixing method*, or thermo-plastic processing, which consist of mixing proteins and plasticizer to obtain a dough like material. Contrary to thermo-plastic polymers, gluten viscosity does not decrease upon heating but rather level off or increase due to cross-linking reactions. Therefore, the extrusion of proteins is, in general, only possible in a limited window of operating conditions and the material properties of extrudates depend on the processing conditions in a complex way [9-10].

The aim of this work was to compare the linear viscoelastic behaviour of bioplastic prepared by casting method and thermoplastic processing. Thus, the material rheology during its processing has been analysed.

2. Materials and Methods

Wheat gluten was provided by RIBA S.A. Protein content was 83 wt. %, lipids 1.5 to 2 wt. %, and ashes 0.7 to 0.8 wt. %. Its moisture content was 8 wt. % on dry basis.

Wheat gluten biomaterials were prepared by the casting method according to a slightly modified procedure used by other authors [8, 11-12]. Wheat gluten was premixed with water and sodium sulphite (3 mg / g wheat gluten) to disrupt S-S bonds. Afterwards, ethanol was added as solvent. Then the plasticizer was added, 0.5 g plasticizer / g gluten (G/WG). The pH of the forming solution was adjusted between 4 and 5, according to Gontard's studies on the influence of main process variables on film casting [13].

The solution was then mixed during 30 minutes at 500 rpm, with an IKA RW-20 Mixer (Germany), in a thermostatic bath at 60º C, in order to remove air from the solution and to concentrate the solution in wheat gluten proteins by eliminating ethanolic solvent. After the mixing stage, 0.5 g/cm^2 of solution was poured and casted onto a petri disc. This method allowed to obtain a controlled thickness between 1 and 1.2 mm. The material was dried at room temperature, evaporating continuously, increasing protein concentration of the biomaterial and allowing the formation of a new three-dimensional network. The biomaterial thickness was then measured and verified at several positions with a slide gauge before the experiments were carried out.

The mixing method was carried out in a torque-rheometer which consists of a batch mixer fitted with two counter-rotating rollers, turning with different angular velocities with a ratio of 3:2 (Rheocord, Haake, Germany). Torque and product temperature were recorded during the mixing process. The mixing chamber can be considered adiabatic, as it was not cooled. Volume of the chamber (310 cm^3) was filled with approximately 245 g of sample, corresponding to 80% filling ratio. The content of plasticizer was fixed to 0.5 g glycerol/g wheat gluten, and three different mixing speed were tested (15, 50, and 90 rpm).

Oscillatory shear tests, from 0.01 to 100 rad/s, at a constant stress within the linear viscoelastic region, were conducted, at 25ºC, for each sample in a controlled stress rheometer Rheoscope (Haake, Germany), using serrated parallel plate geometry, 20 mm diameter, and 1-3 mm gap. Previously, stress sweep test at 6.28 rad/s were carried out in order to obtain the linear viscoelastic region of the material.

Temperature sweep test, from 25 to 170º C, were conducted in a controlled rate rheometer ARES (Rheometrics Sci., U.S.A.), using a serrated parallel plate geometry, 25 mm diameter and 1-2 mm gap. Measurements were performed at constant frequency (6,28 rad/s) and strain (within the linear viscoelastic region), selecting a 2º C/min temperature ramp.

3. Results and Discussion

3.1 Casting Method

Stress sweep tests were run to determine the linear viscoelastic domain. The results obtained show that drying time has a large influence on the rheological properties of the material, so that as drying time is longer the value of the viscoelasticity moduli are higher and the linear viscoelastic region becomes wider in stress values.

The evolution of the storage and loss moduli with frequency as a function of the drying time is shown in Figure 1. Both moduli show a remarkable increase with drying time. The storage modulus G' is always higher than the loss modulus G'' within the experimental frequency range, as corresponds to a gel-like structural network. Hence, the gluten film shows a predominantly elastic response, although a crossover point appears in the high-frequency regime at lower drying times.

In addition, a plateau region in G' is also observed at intermediate frequencies. The plateau region has been extensively described in polymer rheology in terms of an entanglement network among polymer chains in which the motion of molecules is constrained by the neighbouring molecules [14]. As may be seen, a plateau region develops at low drying time. Nevertheless, the plateau region shifts to lower frequencies as the drying process takes place. This fact would indicate higher terminal relaxation times during solvent evaporation and, therefore, improved elastic characteristics of the material.

As a result, two time periods showing different rheological behaviour can be found along drying in Figure 1A. At the first period of drying (below ten days) the mechanical spectrum shows a well defined plateau region, characterised by a slight frequency dependence for the

storage modulus and a minimum for the loss modulus. As a result, loss tangent (tanδ = G''/G') for this region shows a strong dependence on frequency (Figure 1B). The second period, which takes place above ten days, is characterised by a gel behaviour, with a mechanical spectrum in which G' is higher than G'', both showing similar slopes with frequency (Figure 1A). The complex modulus tends to a plateau value and tanδ decreases with time in the whole frequency window (Figure 1B).

The initial drying period (0-10 days) follows the development of a three-dimensional network structure, and involves a number of different physical interactions among chain segments. However, the presence of noncovalent bonds may complicate the microstructural description of the network, because their number and position can fluctuate with drying time [15].

Subsequently, the trend to reach a constant value in G^* and tan δ, between 10 and 90 days, would be caused by further chemical crosslinking paralleled by annealing processes, such as a rearrangement of crosslinks and lateral chain aggregation, leading to the formation of covalent bonds among different polymer chains [16]. Moreover, above 30 days, the values of the viscoelastic functions of these samples do not change significantly with drying process and can be considered as properties of the final material for comparison with other concentrations and processing conditions.

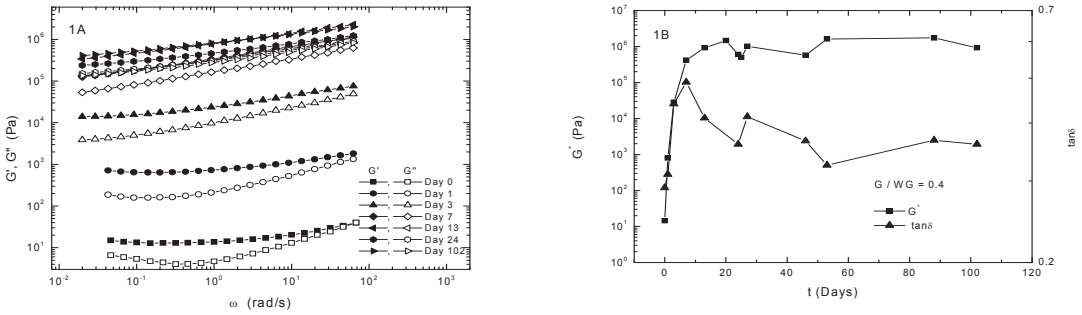

Figure 1. A) Stress sweep tests during drying process at 25ºC. B) Critical stress and strain dependences with drying time.

3.2 Mixing Processing

Plasticizers decrease the glass transition temperature of thermoplastic wheat gluten proteins. This result is interesting and allows one to consider thermoplastic formation like extrusion for processing wheat gluten based materials, avoiding blushing and thermal degradation [1;17].

Figure 2A shows the evolution of torque and temperature during the mixing process for a 0.5 glycerol/gluten ratio sample. Three regions may be observed. The first region, at which no significant increase in torque was observed, corresponds to an induction period that takes place at low mixing times. The time required for this induction period decreases as mixing speed is raised. In the second region, torque undergoes an exponential increase up to a maximum, showing lower values of torque and time for the peak as mixing speed increases, which also gives rise to an increase in the slope of this zone. Finally, a sudden torque decay is observed in the last region.

In addition, three different temperature zones are also found along the mixing process, which are related to the above described torque regions. Thus, the almost isothermal step, up to 30ºC, is followed by an exponential increase, with a slope that also increases with larger mixing speeds. In this way, the temperature reached at the peak of torque is higher as mixing speed increases. This fact may explain the lower values of torque observed with higher

mixing conditions. Furthermore, the final observed torque decay coincides with a slight increase in temperature.

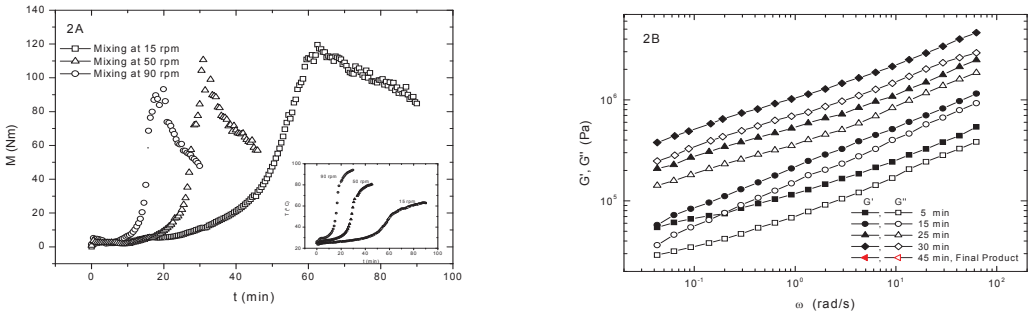

Figure 2. A) Torque and temperature evolutions during thermoplastic processing. B) Mechanical spectrum, at 25ºC for samples at different stages during mixing at 50 rpm.

In order to know the rheological properties of the material in the above described regions and to compare them with those obtained using the casting method, the linear viscoelastic behaviour of glycerol/gluten samples at different stages of the mechanical processing (at 50 rpm) is shown in Figure 2B. The mechanical spectrum of these samples show predominantly elastic characteristics, with values of the storage modulus, G', higher than the loss modulus, G", in the whole frequency range. However, the mechanical spectrum observed in the first region of processing, below 30ºC, is characteristic of a weak gel-like network, showing a trend to a plateau region in G' at low frequency (slope log G' vs. log frequency of 0.23). In the first region, the material presents a consistency typical of a concentrated suspension. Above 30ºC, the plateau region vanishes and the slope of G" decreases in the high frequency regime from 0.42 to 0.35. The frequency dependence of the viscoelastic moduli during processing shows an intermediate behaviour between a permanent network and a temporary entangled network [15].

The development of a gel-like behaviour and, therefore, the elastic characteristics would not be only related to the rearrangement of polymeric proteins and creation of new interactions but rather to the growth of clusters due to polymerizaton reactions [9].

3.3 Thermal effects

The influence of thermomechanical and chemical treatments on the development of the gluten network structure are compared for a selected concentration, 0.5 glycerol / gluten ratio, in Figure 3, –which shows the dependence of two viscoelasticity functions (G' and tanδ) with temperature, at constant frequency (6.28 rad/s). The evolution of the viscoelastic functions was always similar for all the concentrations studied, showing three regions as temperature is raised.

Between 20º and 80º C, G' and G'' decrease due to thermal agitation, down to a plateau region which would result from an increase in protein-protein interactions. The plateau region tends to appear at lower temperature as glycerol content increases. Between 80º and 140º C, the viscoelastic moduli undergo a remarkable increase and tanδ a dramatic decrease, which could be attributed to proteins crosslinking reactions, which occur under thermomechanical severe conditions [5]. Finally, above 120º C, a decrease in the slope of both moduli growth is noticed and a minimum in tanδ takes place.

The thermal and mechanical histories seem to produce significant differences in the type of gel network formed. Thus, As may be seen, the biomaterial obtained by mixing shows a higher thermal susceptibility. Thus, at 25ºC, the values of G' are higher than those

corresponding to the casting method. On the contrary, the thermomechanical procedure leads to lower values for the minimum of G' and higher values for the maximum in loss tangent. Moreover, after a temperature ramp, bioplastic obtained by the casting method, shows higher values of G' and the minimum in tanδ appears at higher temperature.
The formulation of the final molecular network involves the dissociation and unfolding of protein molecules, which allow them to recombine and crosslink through specific linkages [10]. From previous results, we may deduce that the casting method provides protein based materials with higher thermosetting and crosslinking potentials, since physicochemical processing leads to partially denaturated proteins with active sites for bond formation.

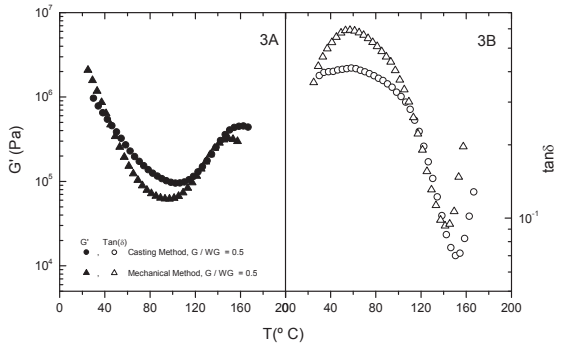

Figure 3. Dynamic temperature ramps (at 6.28 rad/s) performed on biomaterials prepared by different methods.

4. Conclusions

The viscoelasticity functions during processing shows an evolution from a viscoelastic behaviour characterised by a well defined plateau region (typically found for entangled polymer solutions) to a gel behaviour either upon drying or mixing. For the later case the plateau vanishes at the earliest stages of mixing. The final behaviour observed at 25º C presents enhanced elastic characteristics, showing a similar slope for G' and G'' (ca. 0.35).
The frequency dependence of the dynamic moduli exhibits intermediate behaviour between a permanent network and a temporary, entangled network. Thus, the number and position of non-covalent bond change during processing and the formation of covalent bonds among different polymer chains depends on processing conditions. Thus, although at 25º C both casting and mechanical methods of preparation display similar mechanical spectra, their dependences on temperature reveal remarkable differences. Mechanical processing leads to a material with higher thermal susceptibility. This effect may be related to thermal history during thermoplastic processing and the presence of active sites by the addition of chemical breaking agents. The presence of both partial denaturated proteins and active sites would increase polymerization reactions and lead to a higher structuration during thermal denaturation.

Acknowledgements

This work is part of a research project sponsored by the MCYT-FEDER programme (AGL2002-01106). The authors gratefully acknowledge its financial support.

References

[1] J. Irissin-Mangata, G. Baudin, B. Boutevin, N. Gontard. New plasticizers for wheat gluten. Eur. Polym. J. 37 (2001) 1533-1541

[2] L. A. De Graaf. Denaturation of Proteins from a non-food perspective. J. Biotechnol. 79 (2000) 299-306
[3] S. Domenek, P. Feuilloley, J. Gratraud, M-H. Morel, S. Guilbert. Biodegradability of Wheat Gluten based bioplastics. Chemosphere 54 (2004) 551-559.
[4] L. A. De Graaf, P. Kolster. Industrial proteins as a green alternative for 'Petro' polymers : Potencials and limitations. Macromol. Symp. 127 (1998) 51-58
[5] A. Gennadios. Protein-Based Films and coatings. CRC Press, New York (2002) 69-115.
[6] Y. I. Matveev, V. Y. Grinberg, V. B. Tolstoguzov. The plasticizing effect of water on proteins, polysaccharides and their mixtures. Glassy state of biopolymers, food and seeds. Food Hydrocolloids 14 (2000) 425-437.
[8] N. Gontard, S. Guilbert, J.L. Cuq. Water and Glycerol as Plasticizers Affect Mechanical and Water Vapor Barrier Properties of an Edible Wheat Gluten Film. J Food Sci. 58, No 1, (1993) 206-211
[10] T. J. Herald, R. Gnanasambandam, B. H. McGuire, K. Hachmeister. Degradable Wheat Gluten Films: Preparation, properties and applications. J Food Sci. 60, 5, (1995), 1147-1156
[13] A. Redl, M. H. Morel, J. Bonicel, B. Vergnes, S. Guilbert. Rheological properties of gluten plasticized with glycerol: dependence on temperature, glycerol content and mixing conditions. Rheol. Acta 38 (1999) 311-320
[14] A. Redl, S. Guilbert , M. H. Morel. Heat and shear mediated polymerisation of plasticized wheat gluten protein upon mixing. J. Cereal Sci. 38 (2003) 105-114
[16] N. Gontard, R. Thibault, B. Cuq, Guilbert S. Influence of relative humidity and film compositon on oxygen and carbon dioxide permeabilities of edible films. J Agric Food Chem. 44 (1996) 1064-1069
[17] V. Micard, M. H. Morel, J. Bonicel, S. Guilbert. Thermal properties of raw and processed wheat gluten in relation with protein aggregation. Polymer. 42 (2001) 477-485
[19] N. Gontard, Guilbert S., J. L. Cuq. Edible wheat gluten films: Influence of the main process variables on film properties using response surface methodology. J Food Sci. 57, No 1, (1992) 190-199
[21] F. D. Ferry Viscoelastic Properties of Polymers, 3rd ed. Wiley, New York, (1980)
[23] S. B. Ross-Murphy. Structure-property relationships in food biopolymer gels and solutions. J. Rheol. 39(6) (1995), 1451-1463
[24] R. Lapasin, S. Pricl. Blackie Academic and Professional, Chapman and Hall, London,UK (1995).
[25] A. Redl, M. H. Morel, J. Bonicel, B. Vergnes, S. Guilbert. Extrusion of wheat gluten plasticized with glycerol: Influence of process conditions on flow behaviour, rheological properties, and molecular size distribution. Cereal Chem. 76(3) (1999) 361-370

MODELLING KINEMATIC VISCOSITIES OF AQUEOUS SOLUTIONS OF SUGAR + SODIUM CHLORIDE INVOLVING CONCENTRATION AND TEMPERATURE

F. Chenlo, R. Moreira, G. Pereira*

Departamento de Enxeñería Química, Universidade de Santiago de Compostela, Rúa Lope Gómez de Marzoa, 15782 Santiago de Compostela, Spain. Phone: 00 34 981 563 100 Fax: 00 34 981 528 050
E-mail: eqchenlo@usc.es

Keywords: Kinematic viscosity, aqueous solutions, empirical model, osmotic dehydration

ABSTRACT
In this paper an equation to model experimental data of kinematic viscosities of aqueous solutions commonly employed in osmotic dehydration is proposed. The binary and ternary systems are constituted by water as solvent and by sugars (sucrose, glucose and lactose) and glycerol with or without sodium chloride as solutes. The range of concentration of all systems studied covers the typical experimental conditions of interest in this type of processes and temperature varied from 20 to 50 ºC. The parameters of the equation proposed for each system were optimized and the resulting expression adjusted experimental data with deviations less than 3.0%.

1-INTRODUCTION

This work is concerned with the reological aspects of aqueous solutions employed in osmotic dehydration, and particulary, with modelling kinematic viscosities. The dehydration operation is a common method of food materials preservation. Important contributions during last years have been made to improve the quality and economics of the global process, particularly, using combined methods where one step is constituted by osmotic dehydration.

Osmotic dehydration consists on the partial removal of water by direct contact of a wet material with a hypertonic medium, i.e. a high concentrated sugar or salt solution. During osmotic dehydration there are complex mass transfer phenomena which have been defined as dewatering-impregnation-soaking of a food material in concentrated solutions. These processes are commonly studied considering a global resistance to component transport in the bulk of the body of the food material neglecting the external resistance (this assumption is difficult to accept for osmotic systems).

For rigorous models the mass transfer resistance in the fluid phase must be taken into account, and, in this way, the viscosity of the solutions must be known. The choice of osmotic agents depends on taste, cost, water activity lowering capacity and also viscosity values of the solutions (these values are high especially when disaccharides are employed). As the composition of the food material is changing during osmotic process one of the goals is to control the solids gain that strongly depends on desired final product characteristics and also can be related with the viscosity of the solution (1).

Additionally, osmotic dehydration is an effective way to reduce overall energy requirements (2) operating at ambient conditions, but agitation power is necessary and depends directly on osmotic media viscosity. Working at low temperatures colour and flavour retention are favoured (3).
Rheological properties of these solutions are function of physicochemical characteristics of the solutes, composition and temperature of solutions and must be determined experimentally.

In previous papers kinematic viscosity data of binary and ternary aqueous solutions with several solutes as sodium chloride and sucrose (4), and glucose (5), glycerol (6), and lactose (7) were experimentally determined and correlated by mean of several single equations.

The aim of this work is to establish a unique equation for modelling overall experimental data of kinematic viscosities of systems above mencioned for both single and two solutes commonly employed in osmotic dehydration.

2-MODELLING

For modelling, first the binary solutions viscosity experimental data was adjusted, ν_i ($m^2 \cdot s^{-1}$), with salt and sucrose, glucose, glycerol and lactose, separately. In this way, the follow expression was obtained:

$$\nu_i = \nu_w \cdot (1 + F_i) \quad [1]$$

where i = 1 is a sugar o glycerol and i = 2 is sodium chloride, ν_w ($m^2 \cdot s^{-1}$) is the kinematic viscosity of water as function temperature given by (4):

$$\nu_w = 0.09607 \cdot 10^{-6} \cdot \exp\left(\frac{2.90}{T_R^3}\right) \quad [2]$$

and T_R the reduced temperature:

$$T_R = \frac{T}{273.1} \quad [3]$$

where T (K) is the absolute temperature; and F_i is the term that involves the effect of the concentration m_i (molality) of the solute as:

$$F_i = a \cdot m_i \cdot \exp\left(b \cdot m_i^c\right) \quad [4]$$

where *a*, *b* and *c* are parameters. The parameters *a* and *c* don't appreciably change with temperature, and the following simple mathematical dependence of the parameter *b* with the temperature was found:

$$b = \frac{1}{d \cdot T_R^3 + e} \quad [5]$$

where *d* and *e* are new parameters for optimizing.

The experimental kinematic viscosity data for ternary solutions of several sugars or glycerol and sodium chloride were adjusted using an equation that involves the previous expressions for binary systems and an additional term where the inter-action of both solutes is included. The equation has the following form:

$$\nu_{1+2} = \nu_w \cdot \left[1 + F_1 + F_2 + f \cdot m_1 \cdot m_2 \cdot \exp\left(g_1 \cdot m_1\right) \cdot \exp\left(g_2 \cdot m_2\right)\right] \quad [6]$$

where F_1 and F_2 are the particullary form of equation [4], and *f*, g_1 and g_2 are new parameters.

To obtain the parameters *f* and g_1 and g_2 (the last two are practically constant with temperature and a mean value is used) and *f* shows a dependence with temperature that can be modelled as:

$$f = j \cdot \exp\left(k \cdot T_R^3\right) \qquad [7]$$

where *j* and *k* are new parameters. Taking into account the previous considerations, and general equation is obtained:

$$\nu_{1+2} = \nu_w \left[1 + F_1 + F_2 + j \cdot m_1 \cdot m_2 \cdot \exp(g_1 \cdot m_1) \cdot \exp(g_2 \cdot m_2) \cdot \exp\left(k \cdot T_R^3\right)\right] \qquad [8]$$

Statistical analysis of experimental data and non-linear fittings were carried out using the program TableCurve 3D®. After optimization of the values of parameters, equation [8] allows reproducing the experimental kinematic viscosity data of ternary solutions of several sugars, glycerol and sodium chloride with high accuracy (deviations less than ±3.0%) using parameters values shown in Table 1, where subscript 1 refer to sugar or glycerol and subscript 2 to the sodium chloride in all cases.

Table 1 Parameters of the model for kinematic viscosities of binary and ternary aqueous solutions.

Binary systems				
Solute	a (m^{-1})	c	d (m^c)	e (m^c)
Sucrose	0.762	1.12	2.430	-1.001
Glucose	0.325	0.89	3.730	-1.689
Lactose	0.720	1.00	1.768	-1.000
Glycerol	0.125	0.22	2.291	-1.000
Sodium Chloride	0.014	0.20	-0.127	0.909
Ternary systems				
Solutes	j (m^{-2})	k	g_1 (m^{-1})	g_2 (m^{-1})
Sucrose + NaCl	0.851	-2.130	0.600	0.073
Glucose + NaCl	0.261	-1.644	0.241	0.072
Lactose + NaCl	0.117	-1.000	0.256	0.235
Glycerol + NaCl	0.028	-0.866	0.076	0.136

Figures 1, 2 and 3 shows, as example and respectively, both experimental and calculated data with the equation proposed for solutions of lactose, sodium chloride and lactose + sodium chloride. Figure 4 show experimental data versus calculated values of kinematic viscosity for all ternary systems of glucose with sodium chloride at 25 ºC, as example.

3-CONCLUSIONS

Proposed equations for binary and ternary systems were tested with several solutions of interest in osmotic dehydration that allow to estimate the kinematic viscosity in the working typical range as a function of concentration and temperature of solution. Equations for ternary systems involve the parameters of the corresponding binary systems and with an additional term are successfully able to fit experimental data (with maximum deviations of 3.0%). In this way, just an equation form can predict the kinematic values of typical osmotic media.

ACKNOWLEDGEMENTS

The authors acknowledge to the MCYT and the FEDER the partial support with the project (AGL2002-00255).

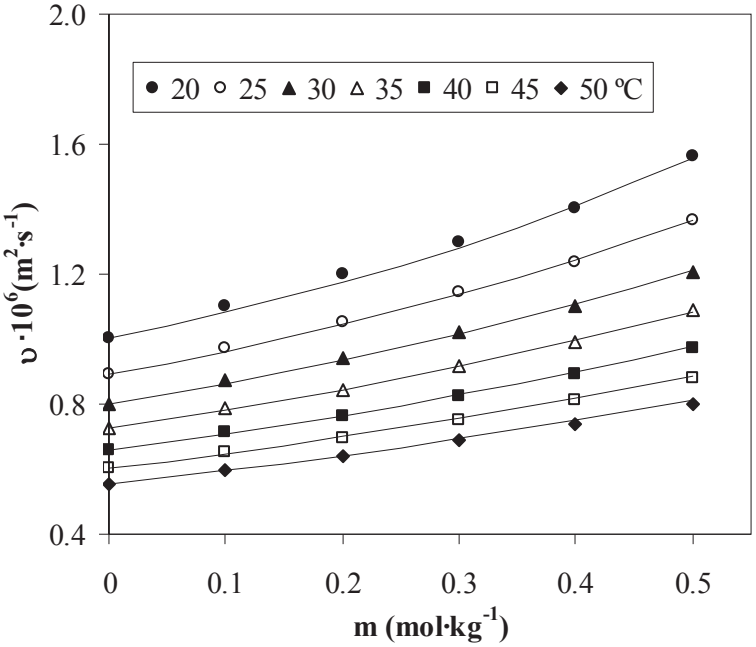

Figure 1. Experimental and calculated values of kinematic viscosity of lactose aqueous solutions at several temperatures and concentrations.

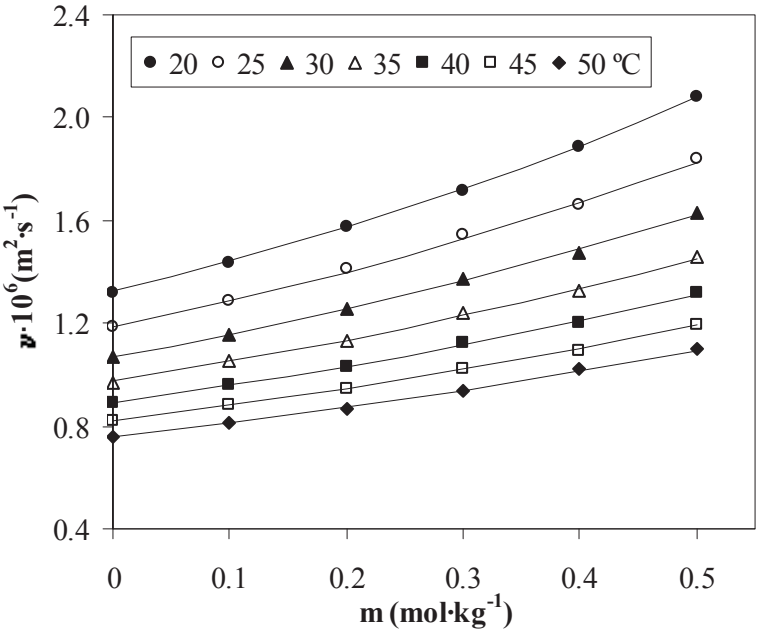

Figure 2. Experimental and calculated values of kinematic viscosity of sodium chloride solutions 4.0 molal at different concentrations of lactose and temperatures.

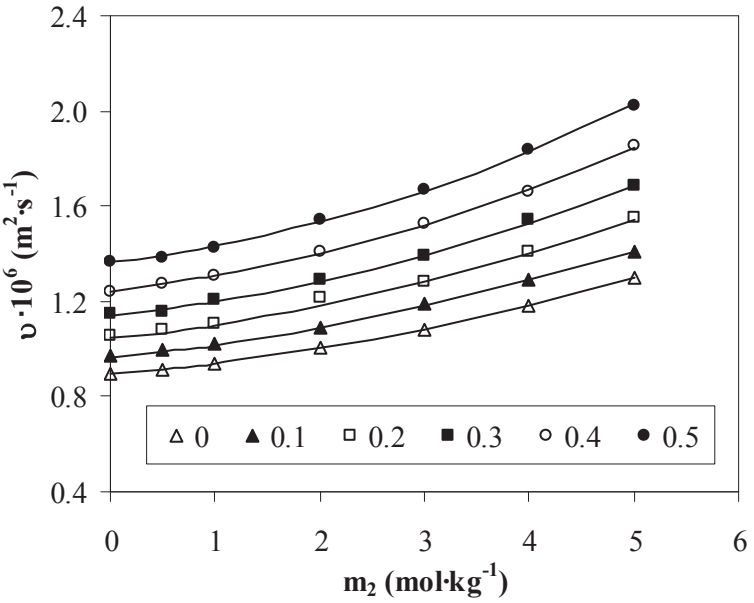

Figure 3. Experimental and calculated values of kinematic viscosity of aqueous solutions with different molality concentrations of sodium chloride (2) and lactose at 25 ºC.

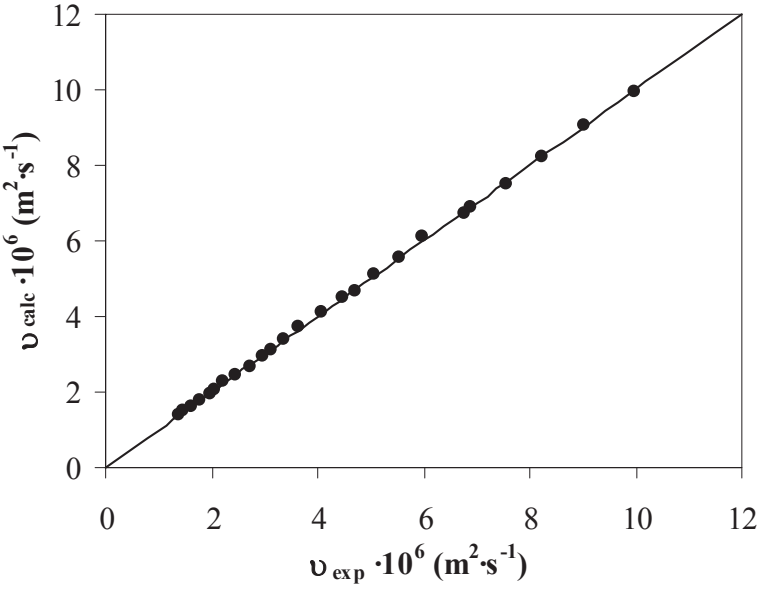

Figure 4. Experimental data versus calculated values of kinematic viscosity of all aqueous solutions of glucose + sodium chloride at 25 ºC.

REFERENCES

(1) Giraldo, G.; Talens, P.; Fito, P.; Chiralt, A. Influence of sucrose solution concentration on kinetics and yield during osmotic dehydration of mango. J. Food Eng., *58*, 33 – 43, 2003.

(2) Grabowski, S.; Marcotte, M. ; Poirier, M. ; Kudra, T. Drying characteristics of osmotically pretreated cranberries-energy and quality aspects. Drying Technol., *20* (10), 1989-2004, 2002.

(3) Ponting, J.D. Osmotic dehydration of fruits – Recent modifications and applications. Proc. Biochem., *8*, 18-23, 1973.

(4) Chenlo, F.; Moreira, R.; Pereira, G.; Ampudia, A. Viscosities of aqueous solutions with sucrose and sodium chloride of interest in osmotic dehydration processes. J.Food Eng., *54* (4), 347-352, 2002.

(5) Moreira, R.; Chenlo, F.; Pereira, G. Viscosities of ternary aqueous solutions with glucose and sodium chloride employed in osmotic dehydration operation. J. Food Eng., *57* (2), 173-177, 2003.

(6) Chenlo, F.; Moreira, R.; Pereira, G.; Bello, G. Kinematic viscosity and water activity of aqueous solutions of glycerol and sodium chloride. European Food Res. Tech., (in press).

(7) Chenlo, F.; Moreira, R.; Pereira, G.; Bello, G. An equation for modeling the kinematic viscosities of binary and ternary solutions with sugars and sodium chloride as a function of concentration and temperature. Experimental data of solutions with lactose. Int. J. Food Prop., (in press).

ESTUDIO DE LA VISCOSIDAD APARENTE DE DISOLUCIONES ACUOSAS DE DIFERENTES ESPESANTES ALIMENTARIOS

F. Chenlo[a],, Mª J. Vazquez-Vila[b] , G. Pereira-Gonçalves[b] y Mª D. Torres-Perez [b].*

Departamento de Ingeniería Química, Universidade de Santiago de Compostela, España.
[a] E.T.S.E. Rúa Lope Gómez de Marzoa 15782, Santiago de Compostela. [b] Facultad de Ciencias, Lugo.
E-mail: eqchenlo@usc.es

Palabras clave: Viscosidad, espesantes, comportamiento reológico, mezclas.

RESUMEN
Se ha determinado experimentalmente la viscosidad aparente de disoluciones acuosas de xantano, garrofín y carboximetilcelulosa sódica, así como de sus mezclas binarias. En todos los casos las medidas se realizaron con un viscosímetro rotacional con diferentes velocidades de cizalla, para varias concentraciones y temperaturas de las disoluciones, y en el caso de los sistemas binarios, con diversas proporciones de los solutos. Los resultados indican que las disoluciones de xantano son siempre las más estables, pues su viscosidad no varía ni con el tiempo de medida ni presentan ciclos de histéresis y en todos los casos los valores máximos de viscosidad se logran en las disoluciones binarias con igual proporción de los solutos.

1. INTRODUCCIÓN

El xantano es un polisacárido extracelular formado por varias especies de Xanthomonas, con una estructura formada por una cadena lineal de glucosa, y una ramificación formada por una manosa acetilada, un ácido pirúvico y una manosa terminal, Figura 1. El garrofín se encuentra en la semilla del algarrobo, estando su estructura formada por una cadena lineal de manosa con ramificaciones monomoleculares de galactosa. Por su parte, la carboximetilcelulosa sódica se obtiene químicamente a partir de la celulosa.

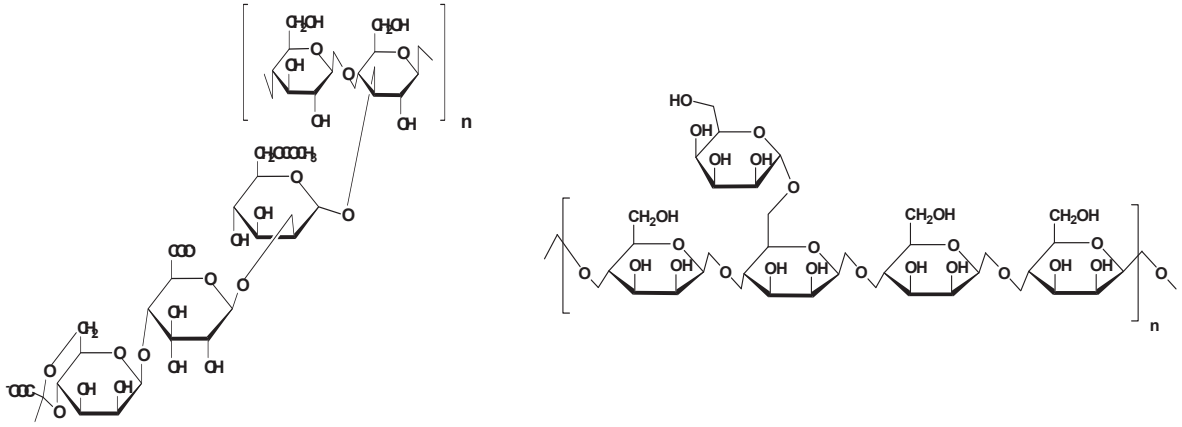

Figura 1 Estructuras moleculares del Xantano y del Garrofín.

Las aplicaciones de estos espesantes son múltiples (1) y los principios que guían su utilización se sitúan en diversos niveles, entre lo que se puede citar la modificación de las propiedades reológicas de un fluido, su estabilidad temporal, características en la transmisión de calor, etc. Particularmente, en la industria alimentaria y a nivel organoléptico se emplean para modificar la apariencia y la textura de los alimentos, de ahí que se usen habitualmente en la industria de congelados, postres, helados, salsas y productos lácteos, entre otros, en donde, además, se emplean para evitar la aparición de cristales de hielo, la formación de grumos, el adecuado

enfriamiento y calentamiento, etc, características todas ellas estrechamente relacionadas con la viscosidad de los sistemas y su estabilidad.

2. SISTEMAS ESTUDIADOS

La determinación de la viscosidad aparente de las disoluciones acuosas de xantano (X), garrofín (G) y carboximetilcelulosa sódica (CMC), así como de sus mezclas binarias, se llevó a cabo en un viscosímetro rotacional de cilindros concéntricos ST-DIGIT L.

Así, se analizó la influencia de la velocidad de cizalla del husillo sobre la viscosidad de las disoluciones, y se estudió la posible existencia de ciclos de histéresis, para velocidades entre 10 y 200 rpm. La concentración total de las disoluciones se modificó del 0,1 al 2,0 por ciento en peso, y en las mezclas las proporciones de los solutos empleadas fueron 1/4, 2/3, 1/1, 3/2 y 4/1. Además, se analizó la estabilidad de las disoluciones tomando medidas a 1, 24 y 48 horas, y para temperaturas de 25, 30, 35, 40 y 45 ºC

3. RESULTADOS EXPERIMENTALES

En las disoluciones acuosas de un soluto, la viscosidad aparente aumenta con la concentración de los solutos, siendo siempre las disoluciones de xantano las más viscosas, tal y como puede verse, a modo de ejemplo, en la Figura 2 para una concentración ensayada y 25 ºC.

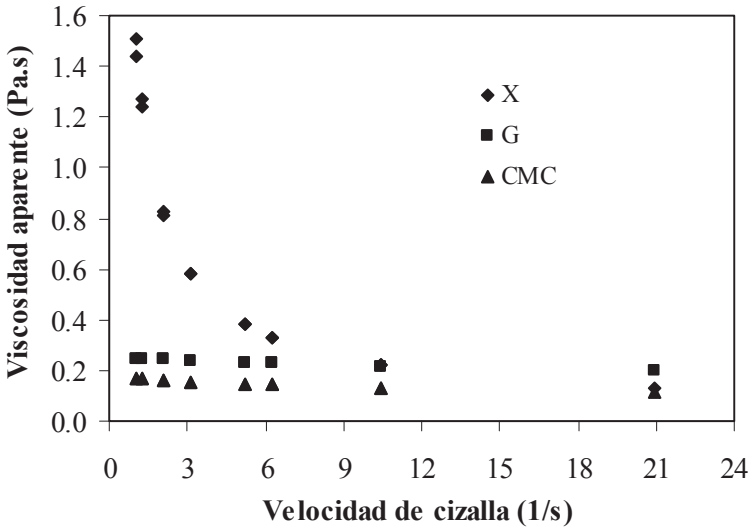

Figura 2. Viscosidad aparente en disoluciones al 0,1% en peso de los solutos y 25 ºC.

En las disoluciones de xantano el mayor aumento de viscosidad tiene lugar a concentraciones bajas; en las disoluciones de garrofín el aumento más acusado se da para concentraciones en torno al 1% en peso, y en las disoluciones de CMC el aumento de viscosidad es siempre menor que para los otros solutos. En las disoluciones de garrofín los resultados parecen indicar la existencia de ciclos de histéresis, si bien la influencia de dichos ciclos sobre la viscosidad aparente es mucho menor que la correspondiente al cambio de concentración.

En el caso de las disoluciones de dos solutos, y para la misma concentración total, la viscosidad es siempre mayor en los sistemas con dos espesantes que en los individuales, siendo las disoluciones con xantano las más viscosas, tal y como puede verse en la Figura 3 para las disoluciones al 0,1% en peso y proporción 1/1 de los solutos. En ningún caso se ha observado la presencia de ciclos de histéresis.

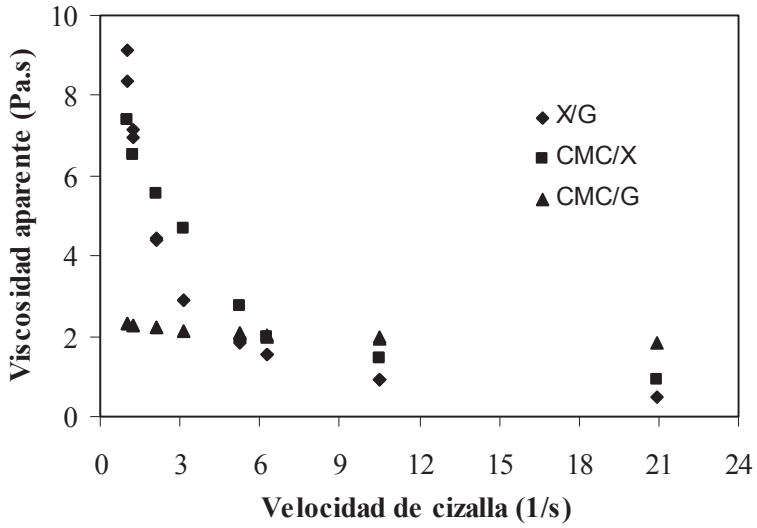

Figura 3 Viscosidad aparente de las disoluciones ternarias de concentración total 0,1% en peso, proporción de los solutos 1/1 y 25 ºC.

Al modificar la relación de concentración de los espesantes en los sistemas ternarios, se ha comprobado que las viscosidades más elevadas se obtienen siempre cuando los solutos están en proporción 1/1, tal y como refleja la Figura 4.

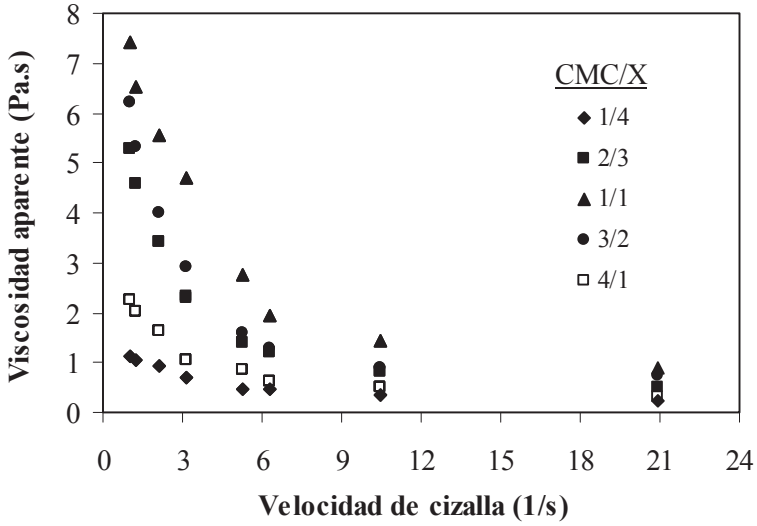

Figura 4. Viscosidad de disoluciones de xantano+CMC de concentración total 0,1% en peso a 25 ºC. Influencia de la proporción relativa de los solutos.

Al analizar la influencia del tiempo sobre la viscosidad, los resultados indican que en los sistemas de un soluto la viscosidad disminuye con el tiempo solamente en el caso de las disoluciones de garrofín. En las disoluciones ternarias el tiempo solamente influye sobre el sistema G/CMC, mientras que para X/G dicha variación no tiene lugar.

En cuanto a la influencia de la temperatura, en todos los casos la viscosidad disminuye al aumentar la temperatura, si bien en los sistemas con xantano y CMC esta variación es mucho menor que para los sistemas con garrofín.

4. MODELIZACIÓN

En la bibliografía existen numerosas ecuaciones para modelizar el comportamiento reológico de un fluido (1, 2, 3). Para un valor dado de la concentración, el efecto conjunto de la velocidad de cizalla, γ (1/s), y de la temperatura, T (K), sobre la viscosidad aparente, η (Pa·s), puede ser representado mediante una combinación del modelo de Ostwald de Waele-Nutting y de la ecuación de Arrhenius, según la expresión de Harper y el Sahrigi:

$$\eta(T,\gamma) = A\exp\left(\frac{E}{RT}\right)\gamma^{n-1} \tag{1}$$

donde E/R representa la energía de activación, A es un factor preexponencial y n es el índice de comportamiento del fluido a cualquier temperatura.

Por su parte, el efecto conjunto de la temperatura y de la concentración, C (% peso), sobre la viscosidad aparente, para una velocidad de cizalla dada, pueden ser expresados mediante la relación:

$$\eta(T,C) = D\exp\left(\frac{E}{RT}\right)C^{B} \tag{2}$$

Por otra parte, diversos autores proponen la siguiente expresión para representar el efecto conjunto de las tres variables sobre la viscosidad aparente:

$$\eta(T,C,\gamma) = K\exp\left(\frac{E}{RT} + BC\right) \tag{3}$$

Se han empleado, entonces, las tres expresiones anteriores para modelizar el comportamiento reológico de todas las disoluciones de este trabajo, y se ha comprobado que en todos los casos es la ecuación (1) la que proporciona los mejores resultados, tanto para las disoluciones de un soluto como para los sistemas ternarios.

En la Tabla 1 se muestran para algunos de los sistemas ensayados los valores del índice de comportamiento en el caso de las disoluciones de un soluto. Se observa el carácter pseudoplástico de las disoluciones, y que su valor disminuye al aumentar la concentración.

Tabla 1. Parámetros de ajuste obtenidos para disoluciones de un soluto.

Soluto	Xantano			Garrofín			CMC		
Concentración (% en peso)	n	E_a/R (K)	A (Pa·s^n)	n	E_a/R (K)	A (Pa·s^n)	n	E_a/R (K)	A (Pa·s^n)
0,50	0,251	-347,4	4,11	0,963	2906,7	$1{,}5\cdot10^{-5}$	0,921	10076	$4\cdot10^{-16}$
0,75	0,172	-352,6	10,64	0,882	2655,9	$1{,}6\cdot10^{-4}$	0,831	705,96	0,129
1,00	0,075	-1139,9	160,6	0,793	2225	$2{,}8\cdot10^{-3}$	0,765	671,37	0,053

Destacan las grandes diferencias numéricas en los valores de los parámetros de la correlación según la naturaleza de los solutos. Para la totalidad de los sistemas ensayados las desviaciones entre los datos experimentales y los calculados mediante las ecuaciones de ajuste son inferiores al 4%. A modo de ejemplo, en la Figura 5 se muestran los datos experimentales y las líneas de correlación para uno de los sistemas.

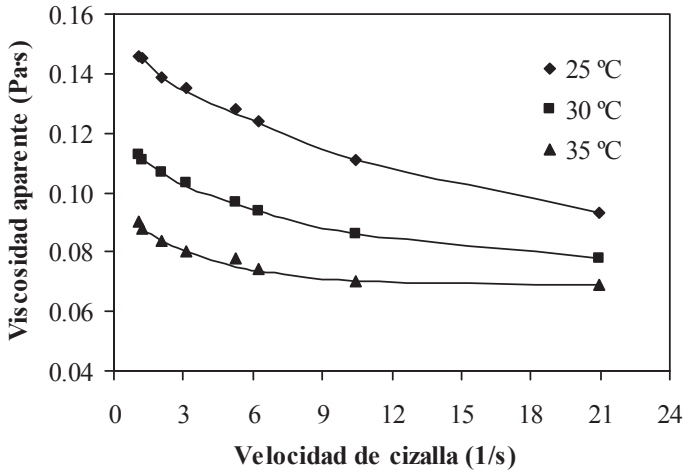

Figura 5. Valores experimentales y calculados de la viscosidad aparente para la disolución de CMC al 0,2% en peso y varias temperaturas.

En las disoluciones de dos solutos, el valor de los parámetros de correlación de la ecuación (1) no siguen una tendencia clara con la proporción de cada soluto, tal y como se muestra en la Tabla 2 para algunos de los sistemas estudiados, pero el ajuste de los datos experimentales a la ecuación sigue siendo satisfactorio, tal y como puede verse en la Figura 6 para el sistema xantano/garrofín de concentración total 0,1% en peso.

Tabla 2. Ejemplo de los parámetros de ajuste obtenidos para las disoluciones ternarias.

Sistema	CMC/X			CMC/G			X/G		
Proporción (%)	n	E_a/R (K)	A ($Pa \cdot s^n$)	n	E_a/R (K)	A ($Pa \cdot s^n$)	n	E_a/R (K)	A ($Pa \cdot s^n$)
1/4	0,384	27,77	1,091	0,676	-53,00	0,820	0,243	157,81	1,514
1/1	0,494	357,70	2,359	0,928	149,42	1,4	0,082	386,32	2,561
4/1	0,348	144,39	1,453	0,627	-62,84	0,789	0,188	62,11	1,220

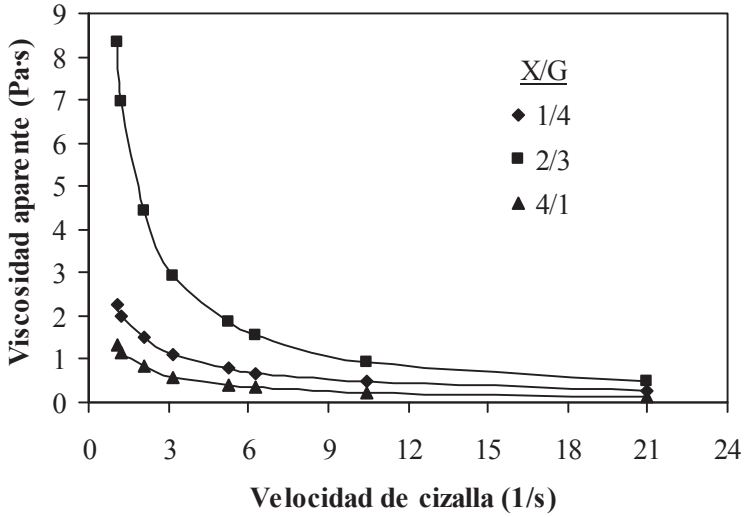

Figura 6. Valores experimentales y calculados de la viscosidad aparente para las disoluciones de xantano+garrofín al 0,1% en peso total y varias proporciones de los solutos.

5. CONCLUSIONES

Se ha determinado experimentalmente la viscosidad aparente de disoluciones acuosas de xantano, garrofín y carboximetilcelulosa sódica, a diferentes concentraciones, temperaturas y velocidades de cizalla; los mismos ensayos se han realizado para mezclas binarias de los solutos, variándose entonces la concentración total de la disolución y la proporción de cada soluto.

Las disoluciones acuosas de xantano, garrofín y carboximetilcelulosa sódica presentan comportamiento pseudoplástico, pero así como para xantano y CMC la viscosidad no varía con el tiempo, en las disoluciones de garrofín aparecen ciclos de histéresis. En cualquier caso, la viscosidad aparente disminuye al aumentar la temperatura y aumenta al hacerlo la concentración.

Para las disoluciones acuosas con dos solutos, aquéllas en las que participa el xantano presentan elevada viscosidad aparente aún para concentraciones bajas, y en ningún caso varían con el tiempo debido al carácter estabilizante del dicho soluto. Además, la viscosidad aparente de todas las disoluciones varía con la temperatura y con la proporción de cada soluto presente en la misma, si bien en todos los casos la máxima viscosidad se obtiene para la relación de concentraciones 1/1.

Debido al diferente comportamiento de los espesantes, especialmente en el caso del garrofín, y a la dispersión de los parámetros de ajuste obtenidos al correlacionar mediante varios modelos bibliográficos los valores experimentales de la viscosidad aparente, se está trabajando en la búsqueda de una ecuación empírica única que permita reproducir el comportamiento de todos los sistemas estudiados.

6. BIBLIOGRAFÍA

(1) Muller, H. G., *Introducción a la reología de los alimentos*, Ed. Acribia, Zaragoza, España (1978).

(2) Steffe, J. F., Ph. D., P.E., *Rheological methods in food process engineering*, Ed. Freeman Press, Second Edition, East Lansing (1996).

(3) Bourne, M., *Food texture and viscosity*, Ed. Academic Press, Second Edition, New York (2002).

Agradecimientos

Los autores agradecen al MCYT y al FEDER el financiamiento parcial por medio del proyecto (AGL2002-00255).

EFFECT OF CONCENTRATION ON THE RHEOLOGY OF TARA GUM AND LOCUST BEAN GUM AQUEOUS SOLUTIONS

W. Sittikijyothin, D. Torres and M.P. Gonçalves

REQUIMTE, Departamento de Engenharia Química, Faculdade de Engenharia da Universidade do Porto, Rua Dr. Roberto Frias, s/n, 4200-465 Porto, Portugal.

The rheological behaviour in steady shear and in oscillatory shear for two types of galactomanans - tara gum (TG) and locust bean gum (LBG) - in aqueous solution was investigated within the concentration range of 0.25 - 1.29 wt%, at 25 ºC, using a controlled stress rheometer AR2000 (TA Instruments) fitted with a cone-and-plate geometry.

Variations of the specific viscosity at zero shear rate as a function of the coil overlap parameter, $C[\eta]$, revealed a similar behaviour for both gums. Shear rate / apparent viscosity data were well described by Carreau and Cross models.

The mechanical spectra were typical of macromolecular solutions. The generalized Maxwell model with four elements and the Friedrich – Braun model were employed to describe the experimental results. The correlation between dynamic and steady shear properties (Cox-Merz rule) was satisfactory for both galactomannans.

Keywords: Rheological properties; Tara gum; Locust bean gum

*Corresponding author-Fax: 351-22 508 1449, Tel: 351-22 508 1684, email: pilarg@fe.up.pt

MECHANICAL PROPERTIES OF SELECTED BIOLOGICAL MATERIALS: ANALYSIS OF EXPERIMENTAL DATA USING A NEW SOFTWARE TOOL

M. Vázquez da Silva[*], *L. Mayor, M.A. Lemos, W. Sittikijyothin, M. P. Gonçalves, A. M. Sereno*

REQUIMTE – Departamento de Engenharia Química, Faculdade de Engenharia da Universidade do Porto, Rua Dr. Roberto Frias s/n, 4200-465, Porto, Portugal

Keywords: texture, modelling, software, food, gel

ABSTRACT

The characterization of the mechanical properties of biological materials is not an easy task because of their heterogeneity. It also requires the use of a large number of samples combined with several types of experimental tests. Furthermore, the experimental data obtained do not give concise information about the mechanical properties under study. To obtain this information it is necessary to transform the data into other physical parameters by the application of mathematical models of differing complexity.

In this work, is presented a computer program, written in FORTRAN 99, for the analysis of data obtained from four mechanical tests: compression tests (with and without failure), compression-relaxation tests, Texture Profile Analysis (TPA) and puncture tests.

In this study are presented some examples of application of the developed software to mechanical data obtained from different biological materials, namely, vegetables (pumpkins) and cold-set whey protein gels.

1. INTRODUCTION

The measurement of mechanical properties of materials is important in the understanding and prediction of their rheological behaviour. In foods and other heterogeneous materials this is not an easy task, as it requires the use of a large number of samples as well as several types of experimental tests. These tests are usually performed in devices called Universal Testing Machines, where the samples are compressed or tensed and data of force, distance and time are collected. In order to obtain parameters with physical significance is necessary to apply mathematical models to the experimental data, since these data by themselves do not give any particular information.

The use of simple software has proved to be a helpful tool for the analysis of raw data and the application of rheological models [1,2]. For this purpose, a software tool, written in FORTRAN 99, was implemented and used in the analysis of mechanical data obtained from different biological materials, namely, vegetables (pumpkins) and cold-set whey protein gels.

2. MATHEMATICAL MODELS

The software tool developed allows the application of some mathematical models applied to three compression tests: uniaxial compression (with and without failure), compression-relaxation and Texture Profile Analysis (TPA). Concerning to the data obtained from uniaxial compression tests, three parameters were determined: Hencky strain, stress and toughness. Maxwell and Peleg models were applied to experimental data obtained from the

[*] Corresponding author-Fax: 22 508 1449, Tel: 22 508 1400 (ext. 2098), email: mvazquez@fe.up.pt

compression-relaxation tests. In TPA tests several parameters were calculated: cohesiveness, gumminess, chewiness, fracturability, stringiness and springiness. Finally, puncture test allows the determination of the fracturability, the puncture resistance and the rigidity of a material [3]. The models and definitions used in the analysis of mechanical data from the aforementioned tests are presented bellow.

2.1 Basic concepts

Strain: $$\varepsilon = \frac{\Delta L}{L_0} \qquad (1)$$

Hencky strain: $$\varepsilon_H = -\ln\left(1 - \frac{\Delta L}{L_0}\right) \qquad (2)$$

Stress: $$\sigma = \frac{\text{Force}}{\text{area}} \qquad (3)$$

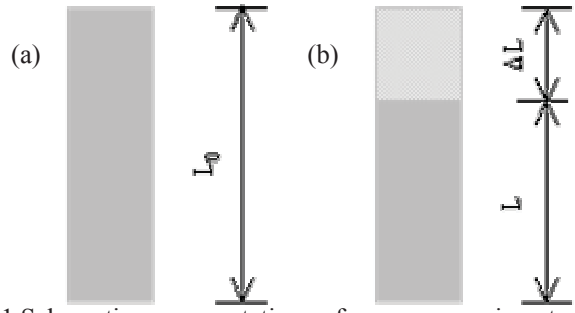

Figure 1.Schematic representation of a compression test. Before (a) and after (b) a predetermined deformation.

2.2 Compression tests

During compression tests the material was submitted to compression until a predetermined degree of deformation. This deformation can lead to the failure of the material, being in such case a failure compression test. As well as the concepts defined in section 2.1, other parameters are also obtained:

Elasticity constant, defined as the slope, k_2, of the initial linear zone of *stress vs. Hencky strain* curve

$$\sigma = k_1 + k_2\,\varepsilon_H \qquad (4)$$

Toughness represents the area under the curve *stress vs. Hencky strain*, until the rupture stress

$$\text{Toughness} = \int_0^{\varepsilon_H^{rupt}} \sigma\, d\varepsilon_H \qquad (5)$$

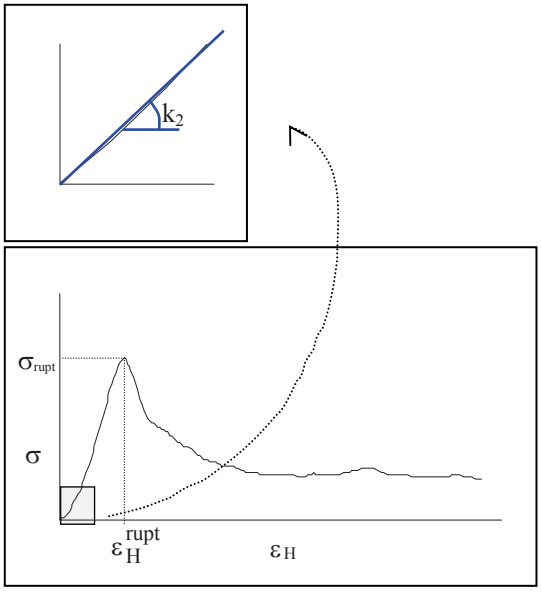

Figure 2. Typical representation of a compression test with rupture of the material.

2.3 Compression-relaxation tests

In these tests, samples were submitted to a constant deformation, and the response of the material was analysed measuring the resulting stress *versus* time.

Maxwell model

$$\sigma = \sigma_e + (\sigma_0 - \sigma_e)\exp\left(-\frac{t}{\tau_{rel}}\right) \qquad (6)$$

where σ_0 (Pa) and σ_e (Pa) represent the initial and the equilibrium stress, respectively, and τ_{rel} (s) is the relaxation time.

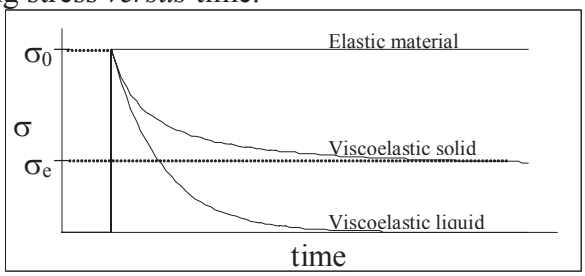

Figure 3. Typical relaxation curves for different types of materials.

Peleg model

$$\frac{\sigma_0 \, t}{\sigma_0 - \sigma} = c_1 + c_2 t \qquad (7)$$

where σ_0 (Pa) represents the initial stress, and c_1 (s) and c_2 are two model parameters.

2.4 Texture Profile Analysis

The purpose of TPA tests is to simulate the mastication of the food material to be analysed. Two consecutive compressions were applied, with a deformation big enough to ensure the rupture of the material. *Force vs. time* data are gathered and several parameters were determined [3].

Fracturability (N) is the force at the first peak in the *force vs time* curve. The material can be classified as crumbly, crunchy or brittle, depending on the fracturability value.

Hardness 1 (N) is the force at maximum compression during the 1st compression. According to this, the material can be named as soft, firm or hard.

Adhesiveness (N.s) represents the area 3.

Stringiness (m) is the extended distance of the material before it breaks away from the compression plates.

Hardness 2 (N) is the force at maximum compression during the 2nd compression.

Springiness (m) is the length of the compression cycle during the 2nd compression. The material can be classified as plastic or elastic.

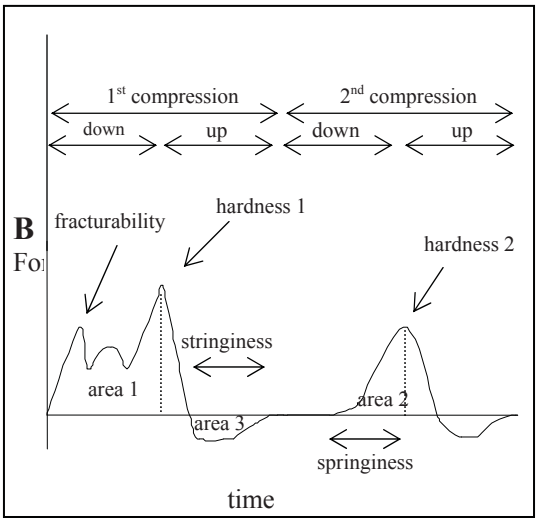

Figure 4. Typical TPA test.

Cohesiveness is the ratio *area 2 / area 1*.

Gumminess (N) is the product of *hardness 1* by *cohesiveness*. Common terms to describe gumminess are short, mealy, pasty and gummy.

Chewiness (J) is the product of *gumminess* by *springiness*

2.5 Puncture tests

In these tests the material was submitted to the penetration of a probe, and data of force and distance were recorded, in order to determinate the parameters:

Fracturability (N) is the force at the first peak in the *force vs distance* curve.

Rigidity ($N.m^{-1}$) is defined as the ratio between force and distance, in the fracturability point.

Puncture resistance (N) is the force at the second peak in the *force vs distance* curve. If there is no second peak, the puncture resistance is equal to fracturability.

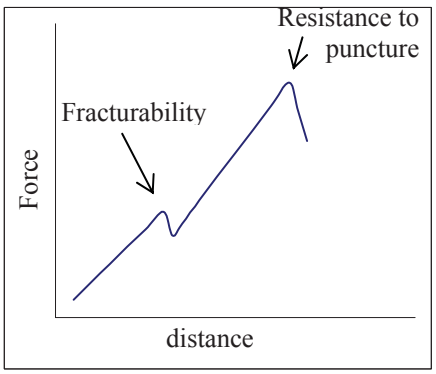

Figure 5. Typical puncture test.

3. SOFTWARE

The computer program presented was developed in FORTRAN 99, and is able to make the necessary calculations for the texture data analysis. The program needs some input data, which contain important information, namely, experimental data file name, name for the results file, sample characteristics, type of test and inherent variables. In the special case of the relaxation tests, the model parameters that better fit the experimental data were determined by an optimisation procedure, according to the method of Roth-Meyer [4], based in the second order Levenberg-Marquadt algorithm [5] to minimize an objective function that was chosen by the user.

The output file of the program, collates the main input data and all the results of the calculation process, namely, characteristics of the sample, model parameters, deviation of the parameters, and others.

4. EXAMPLES OF APPLICATION

4.1 Compression tests

Pumpkin (*Cucurbita Pepo L.)* was used in the compression tests. Cylinders (15 mm diameter, 15 mm length) of parenchymatic pumpkin tissue were made using a metallic cork borer and a cutter. The tests were performed until the rupture of the material. In Figure 6 is shown an example of an input and output file, related to a pumpkin compression test.

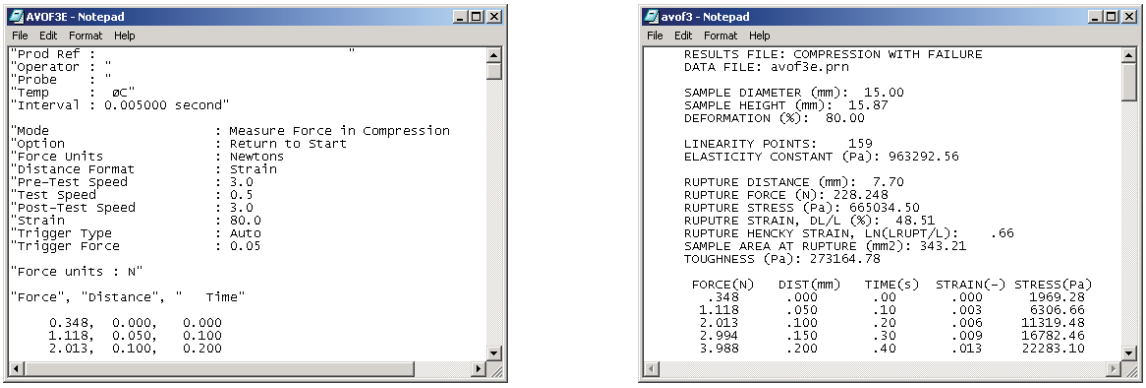

Figure 6. Example of an input (left) and output (right) file of a compression test preformed with pumpkin.

4.2 Compression-relaxation tests

Pumpkin cylinders with the same characteristics of compression tests were used to perform the compression-relaxation tests. In this case two different models were used in the data analysis. In Figure 7 is presented the input file and the corresponding output file, using the Maxwell model. On the other hand, Figure 8 shows the same input file, but being the output file the result of the application of Peleg model.

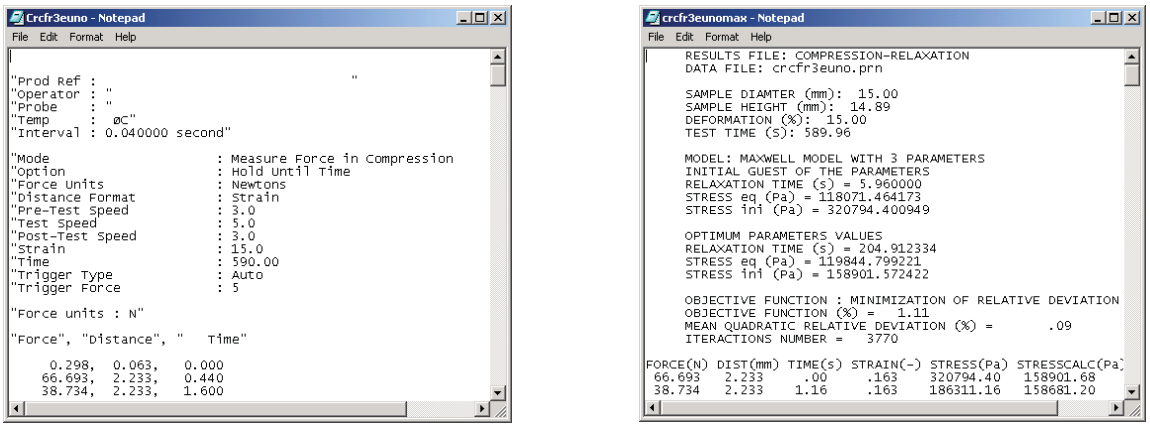

Figure 7. Example of an input (left) and output (right) file of a compression-relaxation test with the application of the Maxwell model.

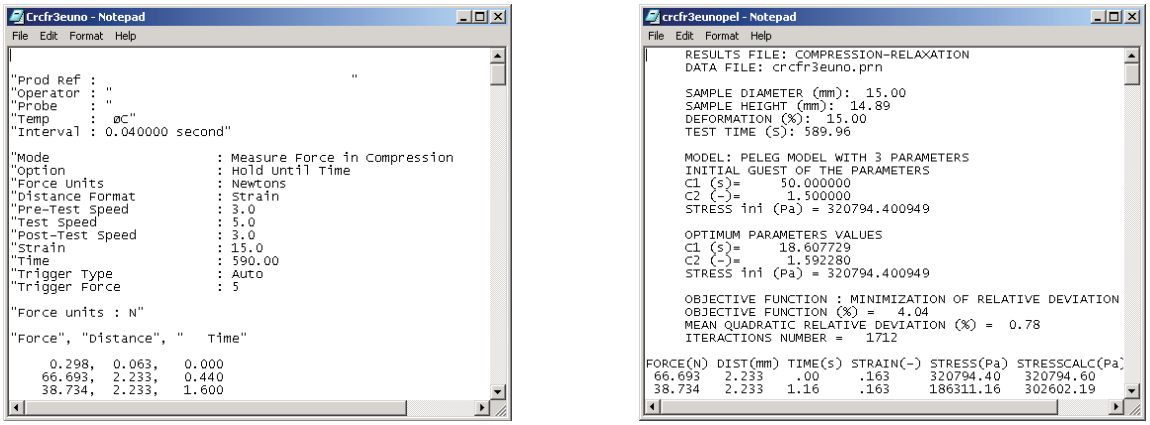

Figure 8. Example of an input (left) and output (right) file of a compression-relaxation test with the application of the Peleg model.

4.3 TPA tests

The TPA tests were performed with whey protein concentrate (WPC) gel cylinders (15 mm diameter), obtained by a cold –gelation process. The gels had a protein concentration of 7.5 (wt%), at pH 7, and were produced in two steps: first, the protein solutions were heat-denatured and, second, the gelation was induced by the addition of magnesium, at room temperature. The input and output files are presented in Figure 9.

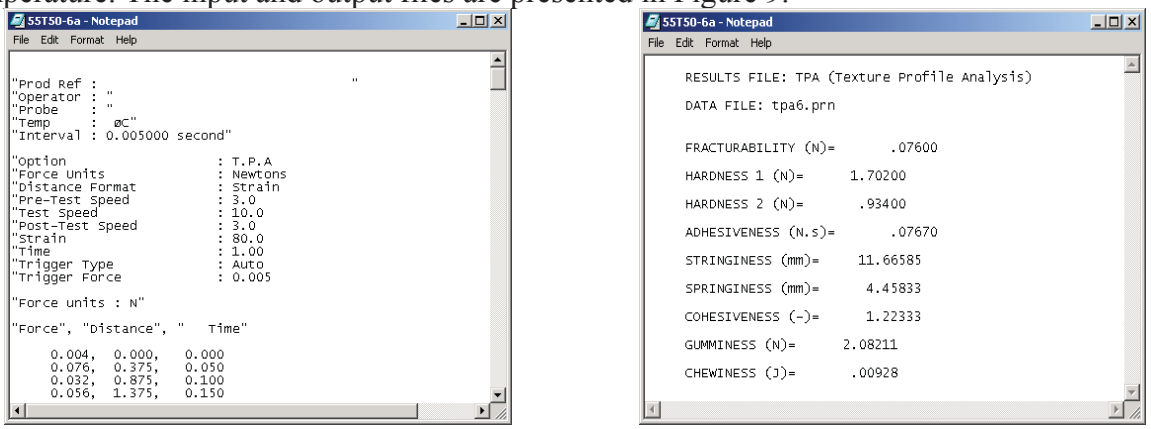

Figure 9. Example of an input (left) and output (right) file of a TPA test performed with WPC gel cylinders.

4.4 Puncture tests

The gels used in these tests were produced in the same way as described in the previous section. Nevertheless, in this case, the protein solutions were placed in beakers, where the puncture tests were performed. Figure 10 shows an example of an input file and the corresponding output file.

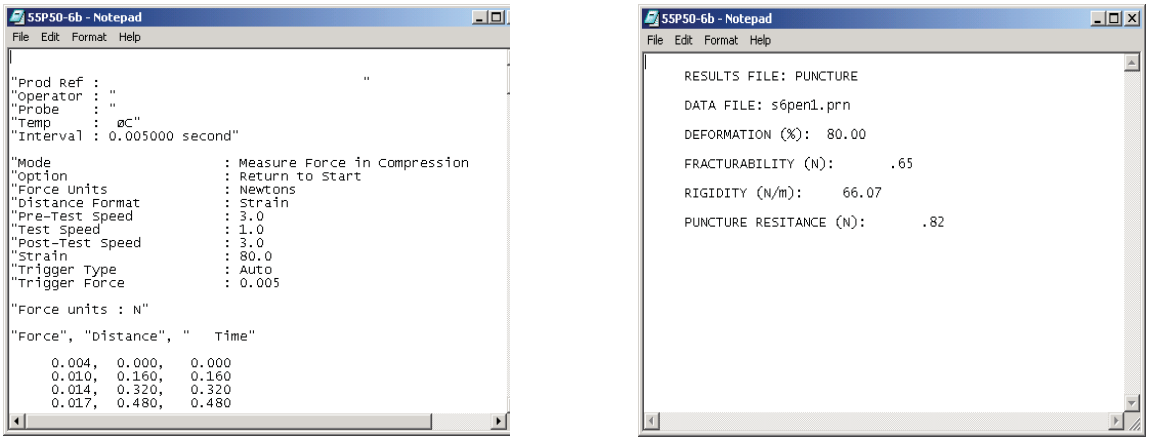

Figure 10. Example of an input (left) and output (right) file of a puncture test performed with WPC gel.

5. CONCLUSIONS

The presented program was found to be very useful, not only because the simplicity of its utilization, but also because it minimizes the time consumed for data analysis and avoids the errors produced by manual calculations.

6. REFERENCES

[1] Miller, B.D.F., Peleg, M.D., Normand, R.H., Gonter, R.H., Klein, E., A computer aided method for the characterization and classification of solid food materials. J. Food Sci., 51 (1), 1986, 123-127, 134.

[2] Roberts, G.P., Barnes, H.A., Mackie, C., Using the microsoft excel “solver” tool to perform non-linear curve fitting, using a range of non-Newtonian flow curves as examples. *Applied Rheology*, 11, 2001, 271-276.

[3] Steffe, J.F., Rheological methods in food process engineering, (2nd edition), Freeman Press, USA. ISBN 0-9632036-1-4, 1996.

[4] Wolfe, M.A., Numerical methods for unconstrained optimisation: An introduction, Van Nostrand Reinhold Co., New York, 1978.

[5] Gill, P.E., Murray, W., Wright, M.H., Practical optimisation, Academic Press, London, 1981.

EFFECT OF GALACTOMANNANS ON THE MICROSTRUCTURE AND FLOW PROPERTIES OF β-LACTOGLOBULIN SOLUTIONS AT pH 4.6

*W.Sittikijyothin and M.P. Gonçalves**

REQUIMTE, Departamento de Engenharia Química, Faculdade de Engenharia da Universidade do Porto, Rua Dr. Roberto Frias, s/n, 4200-465 Porto, Portugal. (Tel: 351-22 508 1684, Fax: 351-22 508 1449, e-mails: wancheng@fe.up.pt and pilarg@fe.up.pt)

Keywords: Tara gum; Locust bean gum; β-lactoglobulin; Rheological properties; Microstructure

ABSTRACT

In the present work, the microstructure and rheological properties of galactomannan (tara or locust bean gum) / β-lactoglobulin aqueous systems was investigated in the conditions of the lowest compatibility (near the isoelectric point of the protein). The rheological experiments were carried out with a controlled stress rheometer AR2000 (TA Instruments), at 20 ºC. The flow behaviour of the mixed systems was compared to that of each biopolymer alone, at the same concentration as in the mixture. For pure galactomannan solutions, the Cross model described well the flow curves whereas the Bingham model was applied for the pure β-lactoglobulin solution and the mixtures. Confocal laser scanning microscopy (CLSM) was used to observe the microstructure of the mixed systems. It showed that these were two-phase, with a β-lactoglobulin enriched continuous phase.

1. INTRODUCTION

Proteins and polysaccharides are present together in many kinds of systems and both contribute to the structure, texture and stability through their thickening or gelling behaviour. Presently, it is generally accepted that the phase state of such systems determines to a large extent their functional properties. When the possibility of intermolecular complexes formation is excluded, the most common behaviour is thermodynamic incompatibility, inducing phase separation, except in dilute solutions. Globular protein/ neutral polysaccharide aqueous mixed systems generally undergo segregative phase separation above a certain concentration threshold [1]. The rheological behaviour of these systems depends on the phase state and on the rheology and microstructure of the phases. Some work on whey proteins (or β-lactoglobulin) / neutral polysaccharides mixed systems, in the gel state or in conditions of changing temperature, is reported in the literature [2, 3]; few studies dealt with systems in the liquid state. At our knowledge, the structure of such systems has never been considered.

We present here results obtained with mixed systems of β-lactoglobulin and galactomannans, in the liquid state, in the conditions of the lowest compatibility (near the isoelectric point of the protein). The effect of the concentration of the neutral polysaccharide, tara gum (TG) or locust bean gum (LBG), on the flow behaviour of the globular protein was assessed. The microstructure of the systems was observed using confocal laser scanning microscopy.

2. MATERIALS AND METHODS

2.1. Materials

The commercial sample of β-lactoglobulin (PSDI 2400) was kindly supplied by Arla Foods, Denmark. Its protein content was 85.6 wt %, as determined by the Kjeldahl method using a nitrogen factor of 6.35. Commercial samples of locust bean gum (LBG, H01091-990) and tara gum (TG, REF 1760), were kindly supplied by Degussa Texturant Systems (France) and Carob S.A. (Spain), respectively. Their mannose to galactose ratios (M/G) were 3.63 ± 0.09 and 3.03 ± 0.07, respectively, as determined by the method of Coimbra et al. [4]. Their intrinsic viscosities were 11.76 and 16.94 dL/g, respectively, at 20°C, as determined from Huggins and Kraemer extrapolations. Tara gum sample was purified by precipitation with isopropanol, as previously described [5].

2.2. Methods

Preparation of the solutions

β-lactoglobulin stock solutions (14 wt %) were prepared by dispersing a known amount of the powder in distilled water, under gentle stirring, at room temperature. Locust bean gum and tara gum solutions (1.1 wt %) were prepared by gradually adding the required amount of gums to distilled water. The solutions were vigorously stirred for 1 h, at room temperature, followed by heating the dispersion at 80 ºC in a water bath for 30 min, under continuous stirring. The pH of stock solutions was then adjusted to 4.6 ± 0.1 by careful addition of HCl solution. After pH adjustment, the stock solutions were centrifuged for 2 h at 35,000 g, at 20 °C, to remove insoluble matter. Then, protein and polysaccharide concentrations were checked using Bradford assay and dry matter analysis, respectively. In all cases, sodium azide was added (5 ppm) in order to prevent bacterial degradation.

Mixtures were prepared with a constant 6.5 wt % β-lactoglobulin concentration and with different concentrations of both galactomannans, by careful mixing of the required amounts of the stock solutions.

Rheological measurements

Viscosity measurements were performed using the controlled stress rheometer AR2000 (TA Instruments), at 20 °C. A cone-and-plate geometry (2° cone angle, 40 mm diameter, 54 μm gap) was used for all tests. Flow curves were recorded using logarithmic ramps of shear stresses from 0.1 Pa till 5 or 50 Pa, depending on sample concentration.

Confocal laser scanning microscopy

β-Lactoglobulin was stained with the fluorescent dye Rhodamine Isothiocyanate (RITC). Mixtures with galactomannans were prepared as described above, poured on a concave slide, covered with a glass cover slip and hermetically sealed to prevent evaporation. The microstructure of the samples was examined immediately after preparation of the slides, by using a Leica TCS SP2AOBS (Germany) confocal laser scanning microscope, in the fluorescence mode. The light source was a HeNe laser. TRITC was excited at 543 nm and the emission fluorescence was detected between 548 and 631 nm. The 20X objective was used.

3. RESULTS AND DISCUSSION

Figure 1 displays the flow curves obtained for solutions of β-lactoglobulin (6.5 wt %), LBG (0.33 and 0.44 wt %) and their mixtures. Results for tara gum solutions and their mixtures with β-lactoglobulin were qualitatively similar and are not shown.

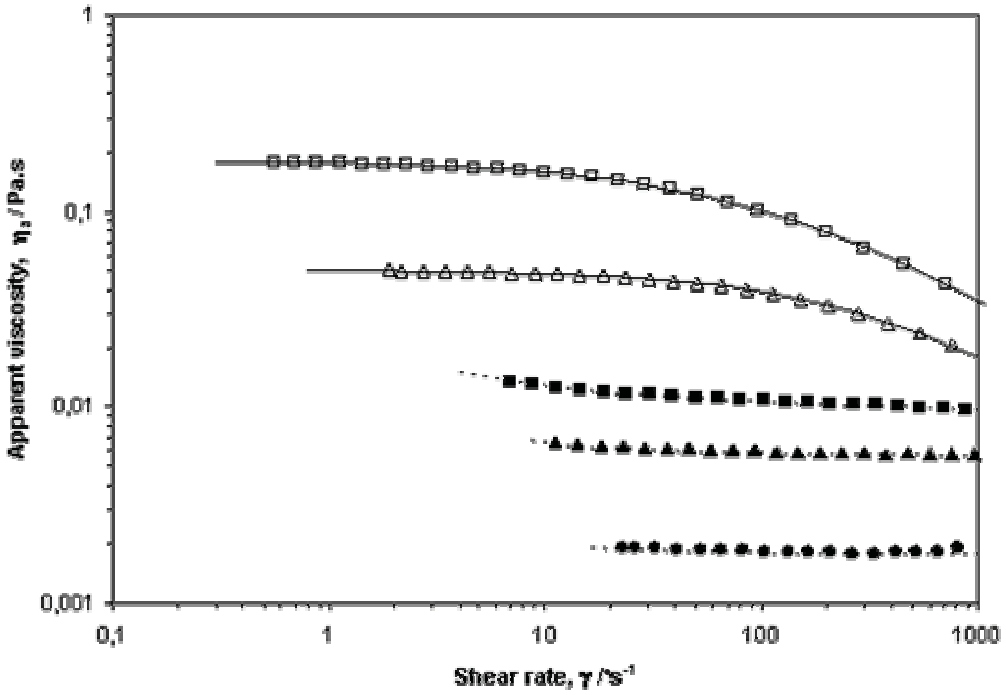

Figure 1 Flow curves for pure LBG, pure β-lactoglobulin and their mixed solutions at pH 4.6 and 20 °C. Symbols: 0.33%LBG (Δ), 0.44%LBG (□), 6.5%β-Lg+0.33%LBG (▲), 6.5%β-Lg+0.44%LBG (■) and 6.5%β-Lg (●); Full lines represent predictions of the Cross model and dotted lines those of the Bingham model.

LBG exhibits the expected shear thinning behaviour and its flow curves can be fitted by the Cross model:

$$\eta_a = \eta_\infty + \frac{(\eta_o - \eta_\infty)}{\left[1 + (\tau \dot{\gamma})^m\right]} \tag{3.1}$$

where $\dot{\gamma}$ is the shear rate (s^{-1}), η_a is the apparent viscosity (Pa.s), η_0 is the zero-shear rate viscosity (Pa.s), η_∞ is the infinite shear rate viscosity (Pa.s), τ (s) is a characteristic time related to the longest relaxation time of the system, and m is a dimensionless exponent related to the power law exponent n by m = 1-n, for the case where $\eta_\infty << \eta_a << \eta_0$. Since the high shear rate Newtonian viscosity was never approached in our study, the above equations were simplified (only three adjustable parameters), assuming $\eta_0 >> \eta_\infty$. The Cross parameters obtained from data fitting are reported in Figure 1 and Table 1: as expected, η_0 and τ values increased with increasing concentration; similar m values were obtained for all samples showing that the concentrations of the two galactomannans reside in the same zone of concentration regime. These characteristics are in good agreement with previous results obtained for galactomannans [6].

Table 1 Magnitudes of the Cross model parameters for steady simple shearing, obtained for locust bean gum (LBG) and tara gum (TG) solutions

Samples	Conc.(wt %)	η_0 (Pa.s)	τ (s)	m	RE*
LBG	0.33	0.0506	0.0022	0.7657	0.0028
	0.44	0.1820	0.0075	0.7158	0.0065
TG	0.23	0.0576	0.0058	0.7630	0.0102
	0.31	0.2062	0.0208	0.7383	0.0122
	0.47	1.1977	0.0772	0.7655	0.0150

*RE, relative deviation error = $\sum_{i=1}^{n} \left| \frac{x_{\exp,i} - x_{cal,i}}{x_{\exp,i}} \right| \Big/ n$

β-lactoglobulin solution exhibits a Newtonian behaviour in the shear rate range of the experiment. Mixed systems behave differently of the individual components. The viscosity of these systems, for all the shear rate range studied, lies between those of the protein and of the galactomannan alone, at the same concentration as in the mixture. The shape of the flow curves is completely different from that of the corresponding galactomannan, at the same concentration, and approaches that of the protein. But, as the concentration of the galactomannan increases, an apparent yield stress appears at low shear rates. These curves can be fitted by the Bingham (Eq. 3.2) model:

$$\eta_a = \eta_p + \frac{\sigma_0}{\dot{\gamma}} \tag{3.2}$$

where η_p is the plateau viscosity (Pa.s) and σ_0 is the apparent yield stress (Pa). As shown (Figure 1, Table 2), the model fits the data well, as illustrated by the magnitudes of RE (relative deviation error).

Table 2 Parameters of the Bingham model for steady simple shearing, obtained for β-Lg solution and the mixed systems

Systems	σ_0 (Pa)	η_p (Pa.s)	RE*
6.5% β-Lg	0.0027	0.0018	0.0117
6.5% β-Lg + 0.33%LBG	0.0086	0.0059	0.0152
6.5% β-Lg + 0.44%LBG	0.0130	0.0107	0.0619
6.5% β-Lg + 0.23%TG	0.0069	0.0063	0.0190
6.5% β-Lg + 0.31%TG	0.0150	0.0125	0.0419

*RE, relative deviation error = $\sum_{i=1}^{n} \left| \frac{x_{\exp,i} - x_{cal,i}}{x_{\exp,i}} \right| \Big/ n$

The η_p and σ_0 values increased with increasing galactomannan concentration in the mixture.

When we compare the flow behaviour of both galactomannans, alone or in the mixed systems, for the same "reduced concentration", $C[\eta]$, we see that they behave quite similarly. In figure 2 and for the sake of clarity, only the systems with 0.31 wt % TG and 0.44 wt % LBG are presented.

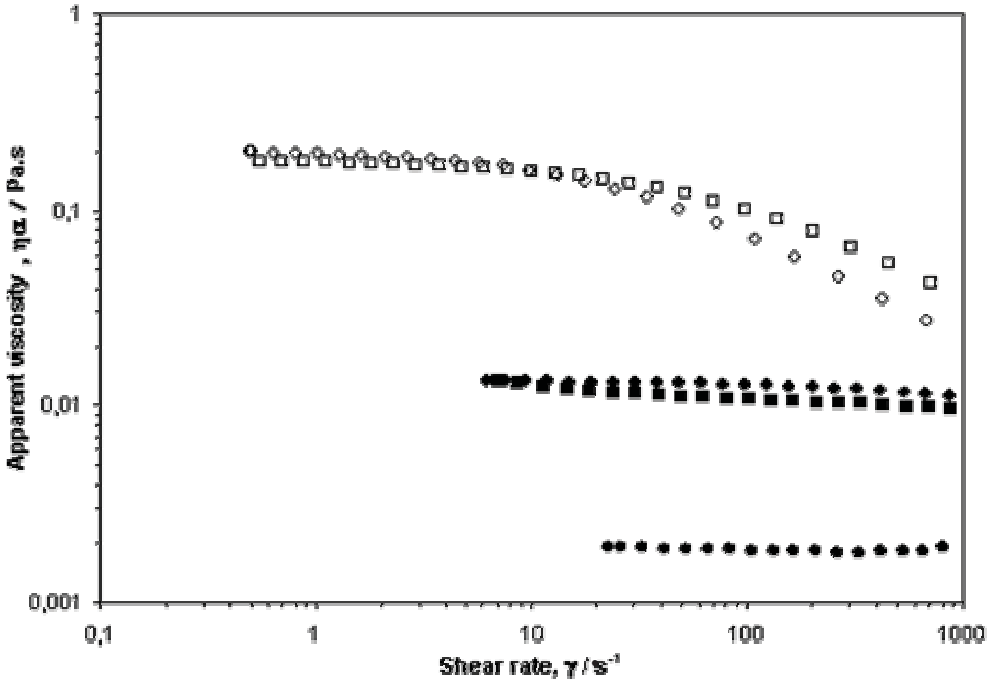

Figure 2 Flow curves for pure galactomannans, pure β-lactoglobulin and their mixtures at pH 4.6 and 20 °C. Symbols: 0.31%TG (◇), 0.44%LBG (□), 6.5%β-Lg+0.31%TG (◆), 6.5%β-Lg+0.44%LBG (■) and 6.5%β-Lg (●).

The predicted parameters from the Cross (Table 1) and Bingham (Table 2) models reflect this similarity (for 0.23 wt % TG - 0.33 wt % LBG and 0.31 wt % TG - 0.44 wt % LBG).

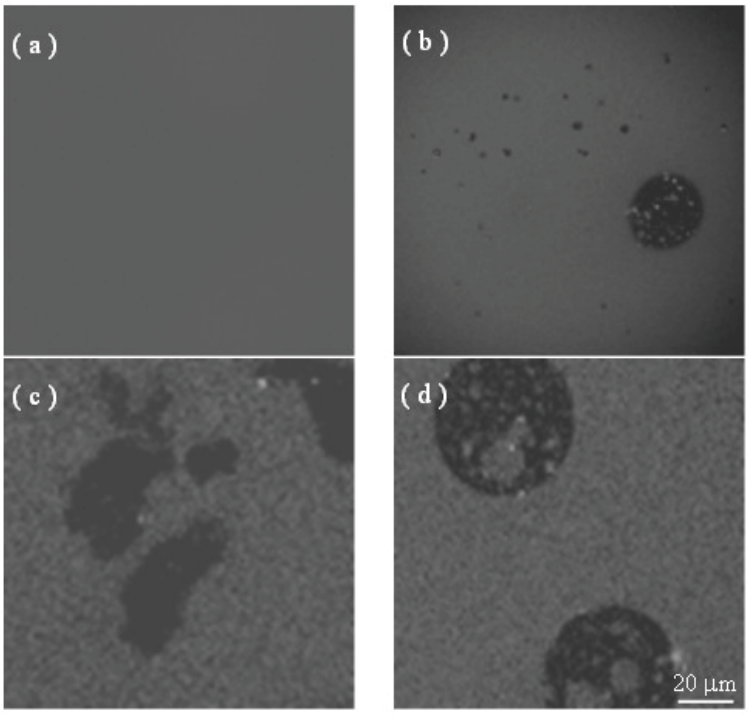

Figure 3 CLSM micrographs, at 20X magnification, of samples in aqueous system at pH 4.6 and 20 °C: 6.5%β-lg (a), 6.5%β-lg+ 0.23%TG (b), 6.5%β-lg+ 0.44%LBG (c) and 6.5%β-lg+ 0.31%TG (d).

The microstructure was analysed using CLSM in the fluorescence mode. Clear areas correspond to the fluorescence of the label (RITC) bound to the protein. The results show that, whereas β-lactoglobulin solutions are homogeneous, the mixed systems are two-phase (Figure 3). Moreover, they are emulsions of a β-lactoglobulin continuous phase containing galactomannan inclusions. These results sustain the observed flow behaviour of the mixtures which approaches that of the continuous phase.

4. CONCLUSIONS

Segregative phase separation was observed for β-lactoglobulin/galactomannan aqueous systems, in the liquid state, at 20 ºC, in the concentration range studied. The two-phase systems lie in the region of the phase diagram where β-lactoglobulin is the enriched continuous phase. The flow curves of these systems can be described by the Bingham model. Similar flow behaviour was found for β-lg / LBG and β-lg / TG mixed systems where the "reduced concentration", $C[\eta]$ of both galactomannans was similar.

ACKNOWLEDGEMENTS

We are indebted to Dr. P. Sampaio from Instituto de Biologia Molecular e Celular da Universidade do Porto (IBMC) for performing the CLSM experiments.

This work was financially supported by Fundação para a Ciência e a Tecnologia (project POCTI / 2000 / QUI / 36452). The author W. Sittikijyothin is indebted to Fundação para a Ciência e a Tecnologia for the PhD grant nº SFRH / BD / 6041 / 2001.

REFERENCES

[1] Doublier J.L., Garnier C., Remard D., Sanchez C., "Protein-polysaccharide interactions" *Current Opinion in Colloid & Interface Science,* (2000) 5, 202-214.

[2] Gonçalves M.P., Torres D., Andrade C.T., Azero E.G., Lefebvre J., "Rheological study of the effect of *Cassia javanica* galactomannans on the heat-set gelation of a whey protein isolate at pH7" *Food Hydrocolloids*, (2004) 18, 181-189.

[3] Olsson C., Stading M., Hermansson A.M., "Rheological influence of non-gelling amylopectins on β-lactoglobulin gel structures" *Food Hydrocolloids*, (2000) 14, 473 - 483.

[4] Coimbra M.A., Delgadillo I., Waldron K.W., Selvendran R.R., "Isolation and Analysis of Cell Wall Polymers from Olive Pulp" *in: Linskens HF. Jackson JF (Eds). Modern Methods of Plant Analysis,* (1996) vol.17 - Plant Cell Wall Analysis. p. 19. Springer-Verlag. Berlin – Heidelberg.

[5] Lopes da Silva J. A., Gonçalves M.P., "Studies on a purification method for locust bean gum by precipitation with isopropanol" *Food Hydrocolloids,* (1990) *4*, 277-287.

[6] Lazaridou A., Biliaderis, C.G., Izydorczyk M.S., "Structural characteristics and rheological properties of locust bean galactomannans: A comparison of samples from different carob tree populations" *Journal of the Science of Food and Agriculture,* (2000) *81,* 68-75.

RHEOLOGICAL AND INTERFACIAL PROPERTIES OF TARA GUM AS ADDITIVE OF REDUCED-CALORIE MAYONNAISE

J. Muñoz[1]; M.C. Alfaro[1]; M. Ruiz[2]; J. De la Fuente[2]; M. Martínez[1]; D.P. Torres[3]; M.P. Gonçalves[3]*

[1]Departamento de Ingeniería Química. Facultad de Química. Universidad de Sevilla. C/ Prof. García González,1. 41012 Sevilla. España. Phone: 34954557179, Fax: 954556447, jmunoz@us.es
[2]Departamento de Ingeniería Química. Escuela Universitaria Politécnica. Universidad de Sevilla. C/ Virgen de Africa s/n. 41011 Sevilla. España. Phone: 34954552846, manuela@us.es
[3]REQUIMTE, Departamento de Engenharia Química. Faculdade de Engenharia da Universidade do Porto. C/ Roberto Frías 4200-465. Porto. Portugal. Phone: 351225081684. Fax: 351225081449, pilarg@fe.up.pt

Keywords: rheology, food gums, food hydrocolloids, interfacial properties, mayonnaise

ABSTRACT
The rheology of O/W emulsions as reduced-calorie mayonnaise (RCM) is controlled by its semisolid continuous phase, which must exhibit weak gel rheological properties. In all cases, the continuous phase of commercial RCM contains starch as thickener. Modified starches can be used alone to provide a commercially acceptable physical stability to RCMs. However, it is interesting to search for synergistic blends with other food gums, which result in enhanced rheological properties, longer shelf life and creamier texture of the corresponding RCMs.
The aim of this contribution is to show different aspects of the use of both tara gum (E-417) and a highly cross-linked waxy maize hydroxypropyl distarch phosphate (E-1442) as stabilisers of RCM.
The results obtained suggest that purified tara gum shows significant interfacial properties and may assist egg yolk components as emulsifier. In fact, tara gum alone or competing with a low molecular-mass emulsifier (1-monostearin) decreased the surface tension at the air-water interface. The drop in surface tension was also noticeable when either acetic acid or NaCl at different concentrations were added. In order to form the continuous phase, the key step is the gelation of the starch/tara aqueous suspension used. This process was studied at different starch/tara mass ratio values by conducting temperature ramps under small amplitude oscillatory shear. The influence of frequency on the dynamic viscoelastic functions did not support the Winter's criterion for the onset of a gel-like behaviour in these systems. G' increased with temperature showing a higher slope as frequency was raised, regardless the presence of tara in the starch suspension. The gelation process was also studied by optical microscopy photomicrographs obtained simultaneously to temperature ramps conducted under small amplitude oscillatory shear. Microphotographs showed different microstructures as the gelation process was carried out.

1. INTRODUCTION

Reduced calorie mayonnaise basically consists of an O/W emulsion containing a low oil concentration and a semisolid continuous phase formulated with starch and, in some cases, further hydrocolloids, like food gums. A gelation process is compulsory for the starch-based continuous phase to get its functional properties as stabiliser (1). Even though food gums are usually associated with thickening and gelation behaviour, they also may exhibit some interfacial properties (2).

The aim of this contribution was to gain a deeper insight into the role of both tara gum and a highly cross-linked waxy maize starch (E-1442) as stabilisers of RCM, paying special attention to the interfacial properties of tara and the gelation process of the tara gum/modified starch in aqueous dispersions containing sugar.

2. EXPERIMENTAL

Aqueous dispersions containing sugar, modified starch and tara gum were prepared in a composition range derived from typical compositions of these materials in low-oil content mayonnaise. The actual composition and nomenclature of the systems studied in this work are shown in Table 1.

Ingredients	K00	K04
Standard tara gum	0.0	0.70
Modified Starch	7.10	6.38
Deionized water	85.45	85.45
sugar	7.45	7.45

Table 1. Composition (%wt) and nomenclature of starch-based gels

A stabilised, highly cross-linked starch with a high amylopectin/amylose ratio, namely a waxy maize hydroxypropyl distarch phosphate (E-1442), C* Polar Tex 06748 and standard tara gum were used as received for the rheological tests. They were kindly supplied, respectively, by Cerestar Ibérica, S.A. (Barcelona) and Carob, S.A. (Mallorca). Tara gum was purified with isopropanol, acetone and ether before conducting surface tension measurements.

The aqueous dispersion of tara gum, modified starch (MS) and sugar was achieved following a strict protocol to guarantee, first of all, the right dispersion, hydration and homogenisation of tara gum in water. Then a blend of MS and sugar was dispersed in the tara solution using a magnetic stirrer.

Surface tension measurements were run at room temperature in a Sigma-701 tensiometer, using the Wilhelmy plate technique. The influence of purified tara gum concentration on the surface tension at the air-solution interface at steady-state was studied between 0,5% (wt) and 10^{-5}% (wt). These experiments were repeated in the presence of a low-molecular weight emulsifier, 1-monostearin (0.0806mg). The effect of adding typical ingredients of mayonnaise, sodium chloride and acetic acid was also considered.

The gelation of the starch-sugar and the tara gum-starch-sugar aqueous dispersions were studied by conducting temperature sweep experiments in small amplitude ($\gamma°$=0.01) oscillatory shear (SAOS), using a multiwave protocol. In this way, dynamic viscoelastic data were obtained at 0.5, 2.4, 4.3, 6.2, 8.1 and 10 Hz . Temperature was increased from 20 to 80ºC at a rate of 2.0 ºC min^{-1}. These experiments were performed in a CS rheometer AR2000 (TA Instruments), using a serrated plate & plate sensor system (diameter:25mm, gap:1.0mm).

In addition, a CS rheometer Rheoscope RO1 (Thermo-Haake) with a cone & transparent plate sensor system (diameter:70mm, angle:1º, gap:0.052mm) was used to take photomicrographs at the same time a SAOS temperature sweep was carried out as detailed above but at 1Hz.

All the rheological experiments were at least done twice and always using a silicon-oil fluid to avoid evaporation, sealing the sample-air interface.

3. RESULTS AND DISCUSSION

3.1. Interfacial properties

All the surface tension data obtained are shown in Figure 1. The addition of tara gum resulted in a clear drop of surface tension. In fact surface tension decreased with tara concentration, regardless the presence of 1-monostearin, even though at the highest tara concentration

studied (0.5%wt) a change of trend was observed. The latter may be attributed to the high viscosity of the subphase, which probably hinder the diffusion of tara macromolecules to the solution-air interface. 1-monostearin yielded a dramatic fall in surface tension due to its amphiphilic structure (Figure 1B). Interestingly, when used with tara gum a synergistic effect occurred since the surface tension values were lower than those shown by either 1-monostearin or tara alone. Sodium chloride did not significantly influence the interfacial properties as expected, on account of the non-ionic character of tara gum. It must be also pointed out that the increase of surface tension at 0.5% tara gum is dampened or even eradicated at the highest acetic acid concentration studied (5%wt), indicating that partial hydrolysis may occur. The reduction in the average size of tara macromolecules enhance their diffusion to the interface.

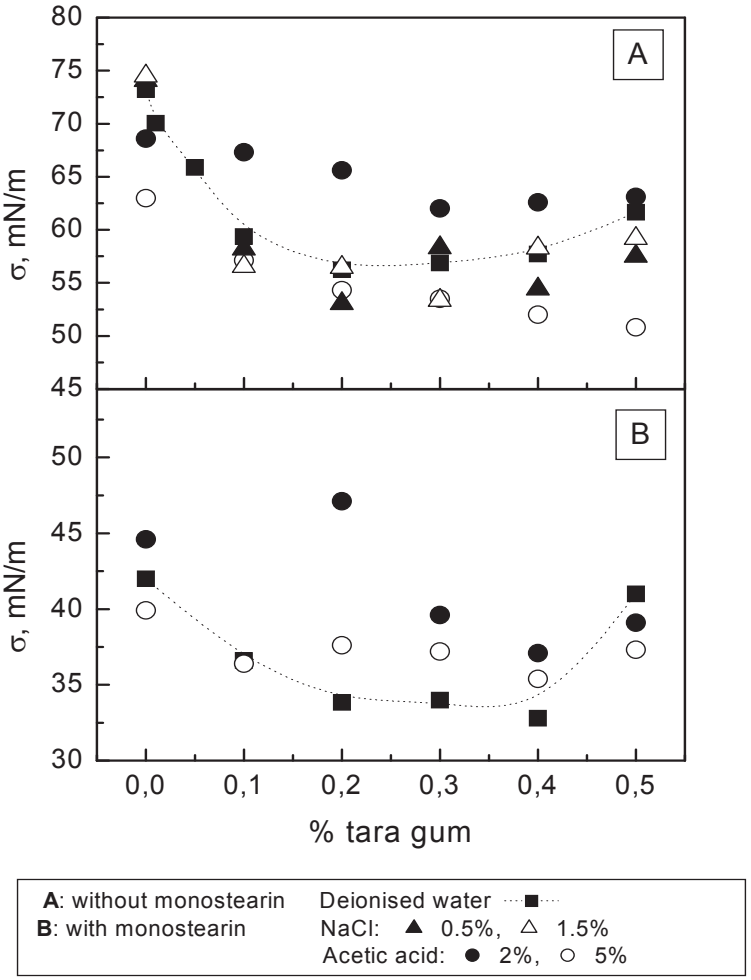

Fig. 1. Influence of tara gum concentration on the surface tension at room temperature of solutions without (A) or with (B)1-monostearin at different sodium chloride and acetic acid concentrations

3.2. Rheological characterization

Multiwave SAOS data corresponding to the system K04, obtained from a temperature ramp are shown in Figure 2, where G' and G'' are plotted against temperature at several frequencies. The same qualitative behaviour was observed regardless the applied frequency. Both G' and G'' went down with temperature from 20ºC up to a first critical T_1 temperature,

G'' remaining slightly higher than G' since the viscoelastic behaviour was still typical of a fluid-like suspension of starch granules in a viscous continuous phase of tara gum dispersed in a solution of sugar in water. Above T_1 the values of both moduli went sharply up so that G' values crossed over those of G'' at an upper critical temperature, T_2. The latter was considered to be the gelatinisation temperature of the starch-based dispersions studied, although it should be better associated with a narrow temperature range given that not all the granules begin to gelatinise at the same temperature (3). In fact, T_2 values ranged from 56ºC to 60ºC.

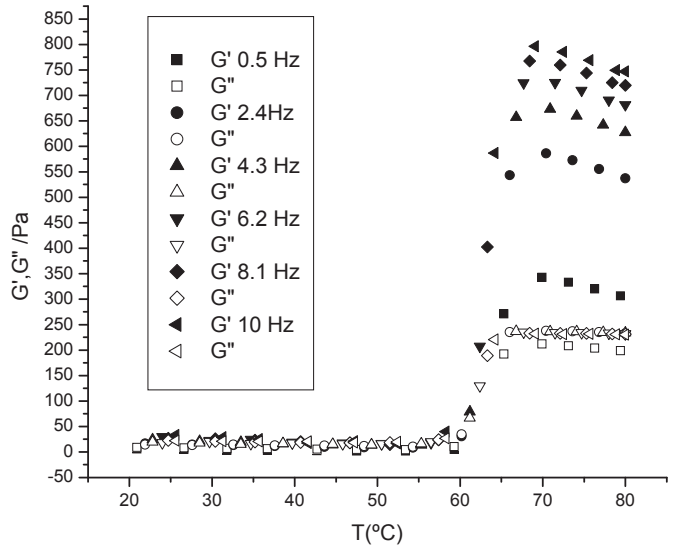

Fig. 2. Multiwave SAOS temperature sweep showing the formation of the K04 starch-tara gum gel at 0.5Hz, 2.4Hz, 4.3Hz, 6.2Hz, 8.1Hz and 10Hz. (γ°=0.01). Closed symbols: G', opened symbols: G''.

As temperature was raised from around 60ºC to 70ºC, the systems studied evolved from a fluid-like suspension to a weak gel, as illustrated by the dramatic increase in G' compared to that of G''. On the whole G'' levelled off at high temperature while G' reached a peak value between 65ºC and 70ºC. The fall of the elastic component was attributed to coleaching of amylopectin to the continous matrix (4) and linked to granule softening and disintegration (5). However, our optical microscopy photomicrogaphs, taken simultaneously to a SAOS temperature ramp at 1Hz, revealed that the disintegration of granules was practically completed before the peak G' value was reached. Figure 3 illustrates the onset of the K04 dispersion gelatinisation at around 62ºC, where the collapse of molecular order within some starch granules was found to occur while, at the same time, other granules remained essentially unaltered. Figure 4 shows the weak gel microstructure formed by K04 at about 65ºC, which will be responsible for the long-term stability of low-oil content mayonnaise formulated with these biopolymers and will basically control its rheology.

With regard to the influence of frequency along the whole temperature range studied, G' increased with frequency, as expected, turning out to be much more sensitive to frequency than G'', indicating a transition from a fluid-like suspension to a weak gel. Furthermore, G' increased more rapidly with temperature than G'' before and after forming the weak gel structure (Figure 2).

Similar results were obtained for system K00, although the response showed a limited reproducibility probably as a consequence of starch suspension instability.

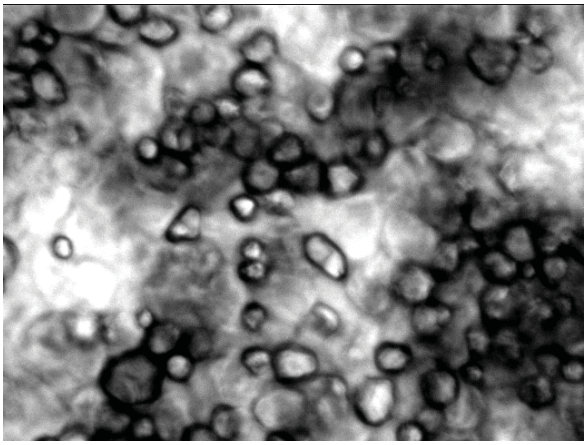

Fig.3 Rheoscope RO-1 photomicrograph of system K04 taken at 62ºC while conducting a SAOS temperature sweep at 1Hz (γ =0.01) and showing the onset of gelatinisation

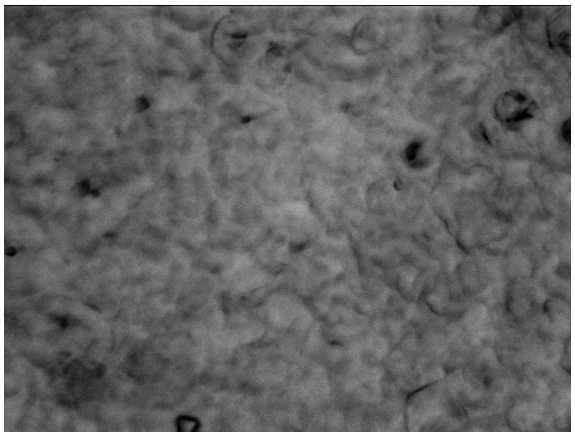

Fig.4 Rheoscope RO-1 photomicrograph of system K04 taken at 65ºC while conducting a SAOS temperature sweep at 1Hz (γ =0.01) and showing a continuous weak gel structure

A further objective of this work was to check if the Winter's criterion to define the so called critical gelation time could provide useful information concerning the onset of gelatinization in these starch-based systems. Therefore, the loss tangent was plotted at different frequencies against the time associated to every temperature in the ramps, using a semilogarithmic scale (Figures 6). In order to obtain accurate results, these SAOS temperature ramps were run at fixed frequencies at 1Hz, 5Hz and 10Hz. The Winter's criterion was not useful to define the gelation time or critical temperature for K04, as can be deduced from Figure 6, since the values of the loss tangent depended on frequency along the whole temperature range. In other words, a single time exhibiting a constant loss tangent could not be either found or interpolated when frequency was varied. Similar results were obtained for K00, although showed some noise at the lower temperatures. For this reason, we took up the temperature at which G' crossed over G''as rheological criterion to define the onset of gelatinisation.

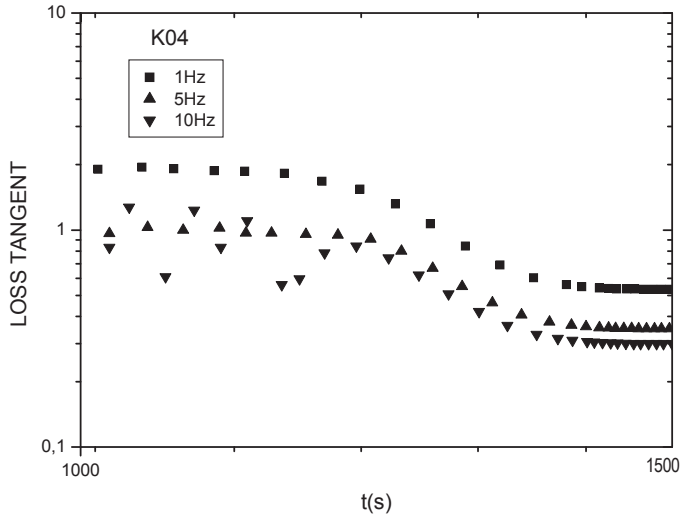

Fig. 6. Loss tangent versus time at different frequencies along the SAOS temperature ramp of K04

4. CONCLUSIONS

To sum up, tara gum exhibits measurable interfacial properties which are also noticeable when competing at the air-solution interface with a low-molecular mass surfactant, 1-monostearin. A multiwave temperature ramp under oscillatory shear was used to illustrate the influence of frequency on the gelation of starch/tara gum aqueous dispersions. The Winter's criterion to define the gelation time was not useful; therefore G' crossing over G'' was taken up as criterion to define the onset of gelatinisation. The whole gelation process was also characterised by photomicrographs showing the evolving optical microscopy microstructure under oscillatory shear.

ACKNOWLEDGEMENTS

This work is part of a project (HP2001-0067) sponsored by the Portuguese-Spanish "Acciones Integradas"program. The authors gratefully acknowlege the financial support received.

5. REFERENCES

1. Martínez I., Partal P., Muñoz J., Gallegos, C. Influence of thermal treatment on the flow of starch-based food emulsions. Eur Food Res Technol, 217, 17-22 (2003).
2. Dickinson E. Hydrocolloids at interfaces and the influence on the properties of dispersed systems. Food Hydrocoll, 17, 25-39 (2003).
3. Thomas D.J., Atwell W.A. Starches. Eagan Press. St. Paul, Minnesota, USA (1997).
4. Hansen L.M., Hoseney R.C., Faubion J.M. Oscillatory rheometry of starch-water systems: effect of starch concentration and temperature. Cereal Chem. 68, 347-351 (1991).
5. Tattiyakul J., Rao M.A. Rheological behavior of cross-linked waxy maize starch dispersions during and after heating. Carbohydr. Polym. 43, 215-222 (2000).

PEA PROTEIN- KAPPA-CARRAGEENAN MIXTURES: PHASE BEHAVIOUR, RHEOLOGY AND MICROSTRUCTURE UNDER IONIC STRENGTH EFFECT

R.M. Musampa[1], M.M. Alves[2], J.M. Maia[1]*

[1] IPC – Institute for Polymers and Composites, Department of Polymer Engineering, University of Minho, Campus de Azurém, 4800-058 Guimarães, Portugal
[2]CERTA/ISEIT, av. 25 de Abril, 5370-202 Mirandela, Portugal

Keywords: phase separation, pea protein, κ - carrageenan, confocal microscope and rheology.

ABSTRACT

The phase diagrams of pea protein and κ -carrageenan mixtures have been established at pH 7, 60ºC and two different ionic strengths (0,05M and 0,2M). These systems led to phase separation probably due to depletion-flocculation mechanism. In the same conditions, rheology and microstructure by confocal laser scanning microscopy (CLSM) of these systems in monophasic and biphasic regions have been investigated. CLSM showed the formation of pea protein aggregates network in presence of κ-carrageenan. Marked differences between mixtures in two-phase region and one component solutions have been evidenced in flow and viscoelastic properties. The results showed that the rheological behaviour is governed by the protein enriched, continuous phase.

1 -INTRODUCTION

The important feature of food systems is their multicomponent nature. These systems are made up of two major kinds of biopolymers, protein and polysaccharide. To understand the mechanisms of structure formation processes in food systems, many investigations focused into protein-polysaccharide interactions [1, 3, and 4]. Most systems exhibited phase separation due to their limited thermodynamic compatibility in common aqueous solvent. The knowledge and understanding of phase behaviour of the protein-polysaccharide mixtures, in particular, is of great importance in the development of products with new and specific properties.

In this work, the phase behaviour of a globular protein, pea protein isolate, and an anionic polysaccharide, κ-carrageenan, under the influence of ionic strength is investigated. Biopolymer mixtures were studied at 60ºC, pH 7 and two different ionic strengths, at 0,05M and 0,2M. The phase diagrams are established according to the biopolymer concentrations under the above conditions. In order to characterise the behaviour of mixtures, rheological measurements were performed in the monophasic region as well as in the biphasic one. In addition, the structure of the systems was observed by Confocal Laser Scanning Microscopy (CLSM).

[*]Corresponding author : Tel. (351)253-510-328, Fax (351) 253-510-339
e-mail jmaia@dep.uminho.pt

2 - MATERIALS AND METHODS

Pisane®, pea protein isolate (PPI) (10%, w/w) dispersions were prepared in phosphate buffer (pH 7, I=0,05M or I=0,2M) at room temperature and then centrifuged. Pea protein supernatants ($PPS_{0,05}$ and $PPS_{0,2}$) were obtained. Kappa-carrageenan (κ-C) (Satiagel™ AMP45) solutions were prepared in appropriate buffer phosphate. $PPS_{0,05}$ or $PPS_{0,2}$ - κ -C mixtures were prepared at appropriate ratios and then kept by stirring in a controlled water bath at 60ºC for 45min and then, centrifuged at 26.000 rpm for 45min at 60ºC. Phase diagrams were established according the phase-volume-ratios method [5]. Rheological measurements were performed in both the biphasic and monophasic regions using a controlled stress rheometer (Paar Physica MCR 300) in a steady and oscillatory shear with plate-plate geometry (25mm diameter, gap 0,5mm) at 60ºC in the angular frequency range of 6,28-62,8 rad/s and shear rate ($d\gamma/dt$) from 10^{-3} to $103s^{-1}$.

The Confocal Laser Scanning Microscopy was performed at 60ºC with a Bio-Rad MCR 600 microscope (emission at 585nm and excitation at 598nm). The pea protein was stained with Rhodamine B. The images from the one-phase to two-phase regions were taken.

3 - RESULTS AND DISCUSSION

The phase diagrams (fig 1 and fig 2) of the pea protein and κ -carrageenan mixtures showed strong similarities in phase separation between biopolymers because of their limited co-solubility in the aqueous solvent. The phase diagram at high ionic strength showed a slight increase in the compatibility than at low ionic strength indicating the effect of the ionic strength. The role of the ionic strength should be regarded as a factor eliminating electrostatic repulsion between proteins by shield effect and thus, favouring the self-association.

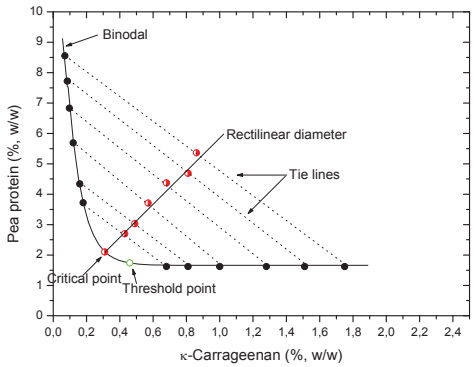

Figure1. Phase diagram of the PPS0,05 - k-C mixture at pH 7, 60ºC and I = 0,05M

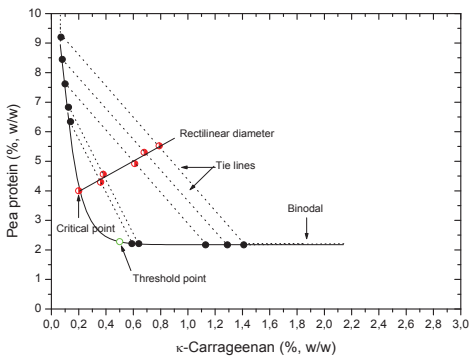

Figure2. Phase diagram of the $PPS_{0,2}$ - k-C mixture at pH 7, 60ºC and I = 0,2M.

In relation to CLSM observations, a phase separation of $PPS_{0,05}$ and $PPS_{0,2}$ – κ -C mixtures and the formation of proteins network in presence of polysaccharide are clearly showed (fig 3a-b). In both systems, the two-phase regions correspond to the pea protein continuous phase with large aggregates at high ionic strength. In this case, depletion-flocculation could be evoked as the mechanism through the phase separation occurs.

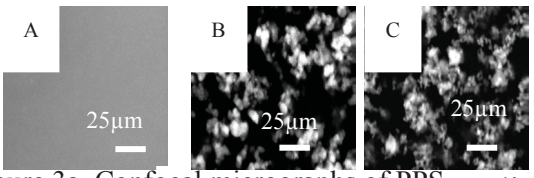

Figure 3a. Confocal micrographs of $PPS_{0,05}$ - κ -C mixtures:(A)4,7wt%$PPS_{0,05}$, (B)4,7wt%$PPS_{0,05}$+0,81wt% κ -C, (C)1wt%$PPS_{0,05}$ +0,81wt% κ -C.

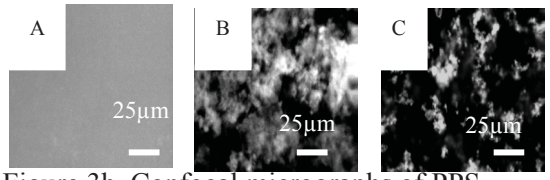

Figure 3b. Confocal micrographs of $PPS_{0,2}$ - κ-C mixtures:(A)5,5wt%$PPS_{0,2}$ (B)5,5wt%$PPS_{0,2}$+0,8wt% κ -C, (C)1,5wt%$PPS_{0,2}$+0,8wt% κ -C.

These results are evidenced in the rheological properties (fig 4a-b and fig 5a-b). Rheological behaviour of the mixtures in two-phase regions differed from the one-phase regions and particularly from the individual macromolecule solutions [2]. A marked viscous character of the medium is observed and is governed particularly by the continuous phase which is protein enriched. This may ascribed to the formation of protein aggregates network.
In conclusion, as showed by experiments, mixed pea protein and κ -carrageenan led to the thermodynamic incompatibility arise from the depletion-flocculation mechanism. The interactions between biopolymers governed the viscoelastic properties and the structural organisation in the medium.

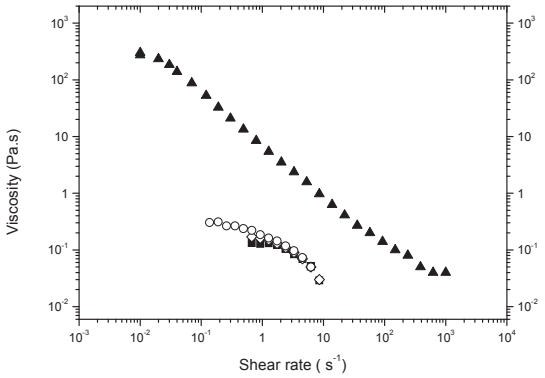

Figure4a. Viscosity/shear rate profiles for $PPS_{0,05}$ - κ-C mixtures:4,7wt%$PPS_{0,05}$+0,81wt% κ -C(▲), 1wt%$PPS_{0,05}$+0,81wt% κ -C(■), 4,7w%$PPS_{0,05}$(◊) and 0,81% κ -C(○).

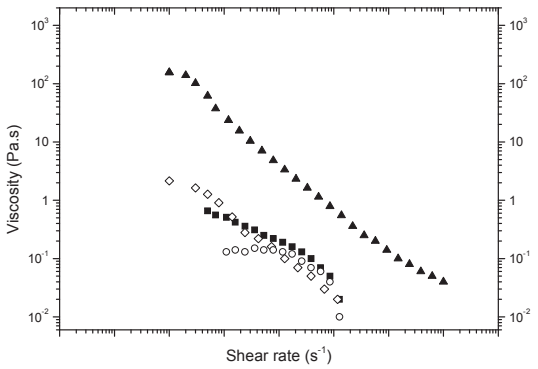

Figure4b. Viscosity/shear rate profiles for $PPS_{0,2}$ - κ-C mixtures:5,5wt%$PPS_{0,2}$+0,8wt% κ -C(▲), 1,5wt%$PPS_{0,2}$+0,8wt% κ -C(■), 5,5w%$PPS_{0,2}$(◊) and 0,8% κ -C(○).

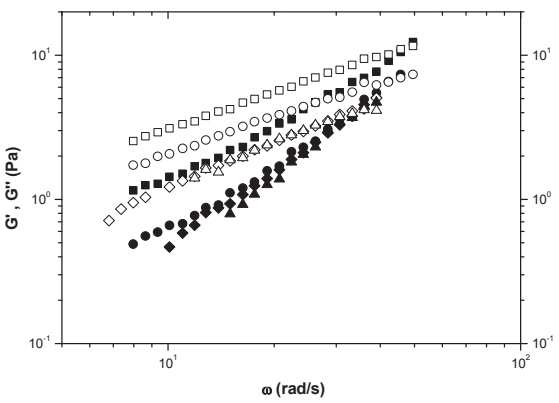

Figure5a. Viscoelastic properties of a 4,7%$PPS_{0,05}$ (strain amplitude 30%; G':♦, G'':◊), a 0,81w% κ -C solution (strain amplitude 20%; G':▲, G'':Δ) and a 4,7w%$PPS_{0,05}$+0,81w% κ -C(strain amplitude 30% ; G':■, G'':□) ; 1w%$SPP_{0,05}$+0,81w% κ -C (strain amplitude 30% ; G':●, G'':○)

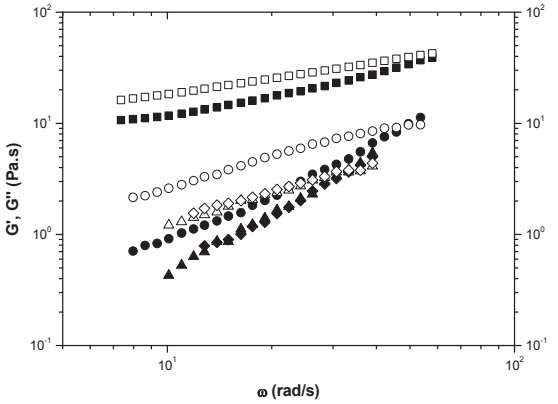

Figure5b. Viscoelastic properties of a 5,5w%$PPS_{0,2}$ (strain amplitude 30%; G':♦, G'':◊), a 0,8w%κ-C solution (strain amplitude 30%; G':▲, G'':Δ) and a 5,5w%$PPS_{0,2}$+0,80w% κ -C (strain amplitude 40% ; G':■, G'':□); 1,5w%$PPS_{0,2}$+0,8w% κ -C (strain amplitude 40%; G':●, G'' :○)

REFERENCES

[1] Doublier, J-L., Garnier, C., Renard & D., Sanchez, C., Protein-polysaccharide interactions. Current opinion in Colloid and Interface Sciences, 5, 202-214, 2000.

[2] Silva, J.A.L. & Rao, M.A. (1992). Viscoelastic properties of food hydrocolloid dispersions. In M.A., Rao & J. F. Steffe (Eds.), *Viscoelastic properties of food* (pp.285-315). Elsevier Applied Science, London & New-York.

[3] Tolstoguzov, V.B. (1986). Functional properties of protein-polysaccharide mixtures. In J.R.Mitchel & D.A. Ledward (Eds.), *Functional properties of food macromolecules*, (pp.385-415). Amsterdam: Elsevier.

[4] Tolstoguzov, V.B., Functional properties of food proteins and role of protein-polysaccharide interaction. Food Hydrocolloids, 4(6), 429-468, 1991.

[5] Polyakov, V.I., Grinberg, V.Ya. & Tolstoguzov, V.B., Application of phase-volume-ratio method for determining the phase diagram of water-casein-soybean globulins. Polymer Bulletin, 2, 757-760, 1980.

INFLUENCE OF XANTHAN GUM AND LOCUST BEAN GUM ON THIXOTROPIC BEHAVIOUR OF FOOD EMULSIONS CONTAINING MODIFIED STARCH

M. J. Hernández[*1], *M.Dolz*[1], *J. Delegido*[1], *M. C. Alfaro*[2], *J. Muñoz*[2]

[1]Departament de Termodinàmica. Fac. Física i Farmàcia. Univ. València. 46100 Burjassot, Valencia (Spain). Phone: 0034 963544902, FAX: 00 34 963543385, e-mail: M.Jesus.Hernandez@uv.es
[2]Departamento de Ingeniería Química. Facultad de Química. Universidad de Sevilla. 41012 Sevilla (Spain). Phone: 0034 954557179, FAX: 0034 954556447, e-mail: jmunoz@us.es

Keywords: thixotropy, emulsions, starch, gums, hydrocolloids

ABSTRACT
Low oil content mayonnaises are food emulsions which exhibit thixotropic behaviour. They include generally modified starch in their formulation. In this work we analyze the effect of substituting part of this starch by other natural gums, such as xanthan gum or locust bean gum, on this rheological property. The aim of the study is to demonstrate if these gums, or a synergistic combination of them, can modify the stability of the emulsions in relation to stirring.
In order to compare the possible influence, the hydrocolloid gels prepared previous to the final emulsification have also been analyzed. Rheological measurements, between 1 and 100 s^{-1}, of up curves and down curves after different agitation times have been carried out at room temperature.
All the systems, both the gels and the emulsions, are shear thinning fluids, following the Herschel-Bulkley model. The emulsions containing the greatest percentage of gums presented a yield stress much bigger than the corresponding gels. However, in the systems containing the expected synergistic mixtures, with less amount of gums, σ_0 was smaller for gels than for emulsions. Analysis of this time dependence of consistency, together with the relative thixotropic areas calculated by integration, showed that the substitution of starch by gums led to an increase of emulsions thixotropy.

1. INTRODUCTION

An emulsion becomes thermodynamically unstable basically due to the high interface area, which leads to the spontaneous aggregation of drops. Emulsion stability can be increased by adding emulsifiers to reduce interfacial tension or hydrocolloids to increase viscosity, thereby reducing drop mobility. Mayonnaises are food emulsions that normally contain about 70-80% oil. When they are formulated with less amount of fat the introduction of hydrocolloids is absolutely necessary in order to assure the stability of the emulsion [1].
Studying the flow behaviour of food emulsions from a practical perspective implies considering a yield stress, σ_0, i.e., a finite amount of stress needed to initiate flow [2]. This yield stress can be considered to impart stability to the emulsion in low-stress situations such as storage or transportation. At higher shear stresses, most food emulsions show shear thinning behaviour. The flow behaviour of these emulsions is also time dependent, so analysing their thixotropic behaviour permits to control their stability in relation to the stirring time [3,4].
Generally the commercial low calorie mayonnaises, include modified starch in their formulation. This hydrocolloid has also thixotropic behaviour [5]. In this work we have compared a reference emulsion containing only modified starch, with other four formulations that substitute part of the starch for xanthan gum, locust bean gum and two synergistic blends

[*] To whom correspondence should be adressed. E-mail: M.Jesus.Hernandez@uv.es

of them. The aim of the study is to analyse how the addition of these gums modify the flow and thixotropic behaviour of the final emulsion.

2. EXPERIMENTAL

2.1. Materials

Acetylated distarch adipate, commercially C*Tex 06214, was acquired from its manufacturer Cerestar (Cargill, Barcelona). Xanthan gum was provided by Jungbunzlauer Ges.m.b.H. (Quimidroga, Barcelona) and locust bean gum was obtained from Industrial Garrofera Valenciana (Ingavasa, Valencia). Pasteurised liquid salted egg yolk, sunflower oil and wine vinegar (equivalent acetic acid concentration: 10%) were kindly supplied by Hijos de Ybarra (Seville). Commercial salt and sugar, preservatives (potassium sorbate and sodium benzoate) and deionised water were also used.

2.2. Emulsion manufacture

Emulsion formulation was adapted from the commercial composition of low oil content mayonnaise containing 4 wt% of modified starch (MS) as stabilizer and 34 wt% of vegetable oil. The total content of stabilizer was maintained at 4 wt%, the MS fraction being partially replaced by xanthan gum, locust bean gum or a mixture of both gums. Table 1 indicates the hydrocolloid content in the different formulations tested, together with the notation used in the text below to refer to each of the emulsions.

Table 1. Systems notation, both gels and emulsions, and the hydrocolloid content in each case

System notation	Hydrocolloid content (wt)
MS	4 % modified starch
LBG	3.6 % MS + 0.4 % locust bean gum
XG	3.6 % MS + 0.4 % xanthan gum
0.03 (LB+X)	3.94 % MS + 0.03 % locust bean gum + 0.03 xanthan gum
0.1 (LB+X)	3.8 % MS + 0.1 % locust bean gum + 0.1 xanthan gum

The final manufacture method chosen consisted of two steps: the first dealt with the hydrocolloid gel formation and the second with the emulsion manufacture.
In the first stage, the solid ingredients (sugar, salt, preservatives and hydrocolloid power) were mixed, dispersed in water (stirring for 5 min at room temperature) and heated to 95ºC while stirring for 15 min in order to ensure homogeneous gelation of the starch.
After cooling to room temperature, the gels were kept at 5ºC during 24 hours.
Finally, the liquid egg yolk was added to the gel and emulsification was carried out using a rotor-stator Ultraturrax T-50 homogenizer (Ika, Germany). This process was performed at 10ºC, with a homogenization speed of 5000 rpm during 7 min. Oil was added slowly during the first 3 minutes and vinegar added at the end.
The final emulsions prepared were stored at 5ºC until measurement.

2.3. Viscosity measurements

The experimental values of shear stress were determined with a RS1 (Haake), using a serrated plate (35 mm diameter) and working in controlled rate mode. The flow curves were performed between 1 and 100 s^{-1}, in 20 steps logarithmically distributed (10 s each).
The thixotropy loops were designed following the Weltmann method [5]. The sample was relaxing during 20 min before the up curve was obtained. After different agitation times (1, 2, 3, 5, 10, 20 min) at the maximum shear rate, the different down curves were performed.

3. RESULTS AND DISCUSSION

All systems exhibited shear thinning behaviour with an apparent yield stress for both up and down flow curves. As a consequence of the thixotropy of both gels and emulsions, a decrease in viscosity was observed for the down curves obtained after stirring. These phenomena is shown for the reference systems (starch gel and starch emulsion), as an example, in Figure 1 (A and B respectively).

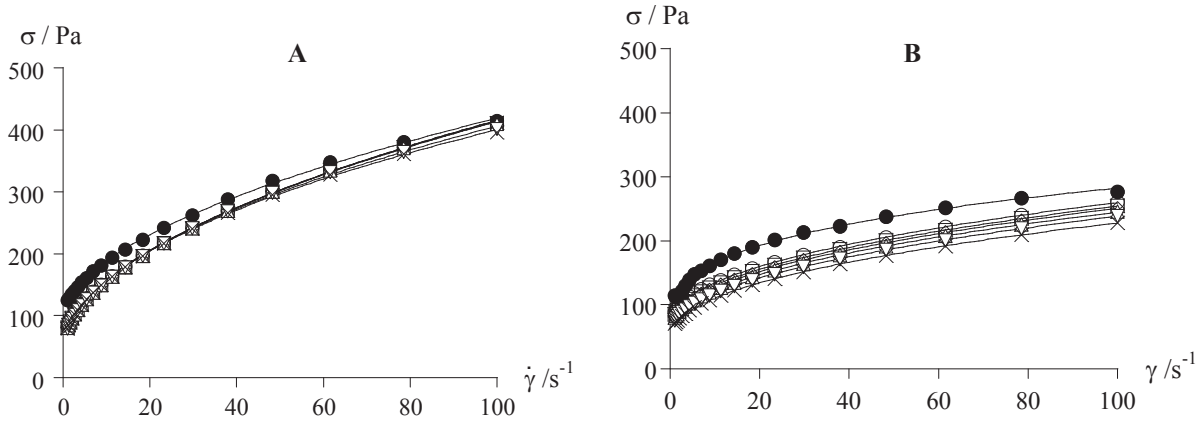

Figure 1. Flow curves for the MS systems **(●)** Up curve and down curves after agitation: **(○)** 1 min, **(□)** 2 min, **(◇)** 3 min, **(△)** 5 min, **(▽)** 10 min and **(×)** 20 min. . **A**: gel, **B**: emulsion.

The rheograms fitted very well ($r^2 > 0.998$) to the Herschel-Bulkley model.

$$\sigma = \sigma_0 + K\dot{\gamma}^n \quad (1)$$

Table 2 shows the values obtained for the yield stress and power law index, with the corresponding uncertainties. In order to simplify, an unique value of σ_0 an n was considered for all the down curves of each system.

Table 2. Yield stress, σ_0, and power law index, n, for all the systems studied

	Gels				**Emulsions**			
	Up curve		**Down curves**		**Up curve**		**Down curves**	
	σ_0 / Pa	**n** ± 0.01	**σ_0 / Pa**	**n** ± 0.01	**σ_0 / Pa**	**n** ± 0.01	**σ_0 / Pa**	**n** ± 0.01
MS	79 ± 2	0.47	33.5 ± 0.5	0.47	76 ± 1	0.47	54 ± 3	0.47
LBG	108 ± 4	0.37	32.1 ± 0.5	0.37	194 ± 30	0.36	59 ± 1	0.36
XG	78 ± 1	0.25	42 ± 4	0.25	197 ± 3	0.43	107 ± 3	0.43
0.03(LB+X)	105 ± 2	0.48	48.2 ± 0.7	0.48	91 ± 6	0.45	56 ± 3	0.45
0.1(LB+X)	166 ± 8	0.49	37.0 ± 0.5	0.42	105 ± 2	0.45	68 ± 5	0.45

The values of the power law index were the same for the up and the down curves. The only exception was the 0.1(LB+X) system, as the gel up curve was fitted with a slightly higher n (about 7%). The shear thinning behaviour was quite similar for the systems MS, 0.03(LB+X) and 0.1(LB+X), what indicated that starch was dominating the rheological behaviour of these systems. This was not the case of the LBG systems and the XG gel, which were more shear dependent.

Regarding the yield stress it was observed that both in gels and emulsions, σ_0 decreased when the system was stirred. This effect is about 80% for the 0.1(LB+X) gel. The highest values of σ_0 corresponded to the up curves of XG and LBG emulsions, approximately twice the value corresponding to the XG and LBG gels. For the rest of the systems, σ_0 was higher in gels than in emulsions. However, for the down curves, in all cases yield stresses of emulsions were higher than yield stresses of gels. This could be interpreted as emulsions being more structured systems.

Table 3 shows the values obtained for the consistency, K, for both gels and emulsions. For the down curves, K decreased with agitation time (Figure 2), so it was fitted to an equation analogous to the thixotropic Weltmann model for shear stress [4].

$$K(t) = A - B \ln t \qquad (2)$$

where t was expressed in min, and K in Pa s^n. Values of parameters A and B are also shown in table 3.

Table 3. Consistency, K, for all the systems studied

	Gels			**Emulsions**		
	Up curve	**Down curves** $K = A - B \ln t$		**Up curve**	**Down curves** $K = A - B \ln t$	
	K_0 / Pa s^n	**A/ Pa s^n**	**B/ Pa s^n**	**K_0 / Pa s^n**	**A/ Pa s^n**	**B/ Pa s^n**
MS	38.2 ± 0.4	43.0 ± 0.1	0.35 ± 0.08	19.2 ± 1.9	21.8 ± 0.1	1.34 ± 0.03
LBG	83.1 ± 1.5	89.3 ± 0.1	3.77 ± 0.07	31 ± 3	49.5 ± 0.1	4.01 ± 0.07
XG	81.4 ± 0.2	95.4 ± 0.2	1.35 ± 0.11	23.9 ± 0.8	34.8 ± 0.1	2.43 ± 0.08
0.03(LB+X)	37.2 ± 0.5	44.4 ± 0.2	1.35 ± 0.11	19 ± 2	23.7 ± 0.1	1.24 ± 0.05
0.1(LB+X)	28 ± 5	51.0 ± 0.3	1.49 ± 0.16	21.0 ± 1.7	26.3 ± 0.1	1.89 ± 0.07

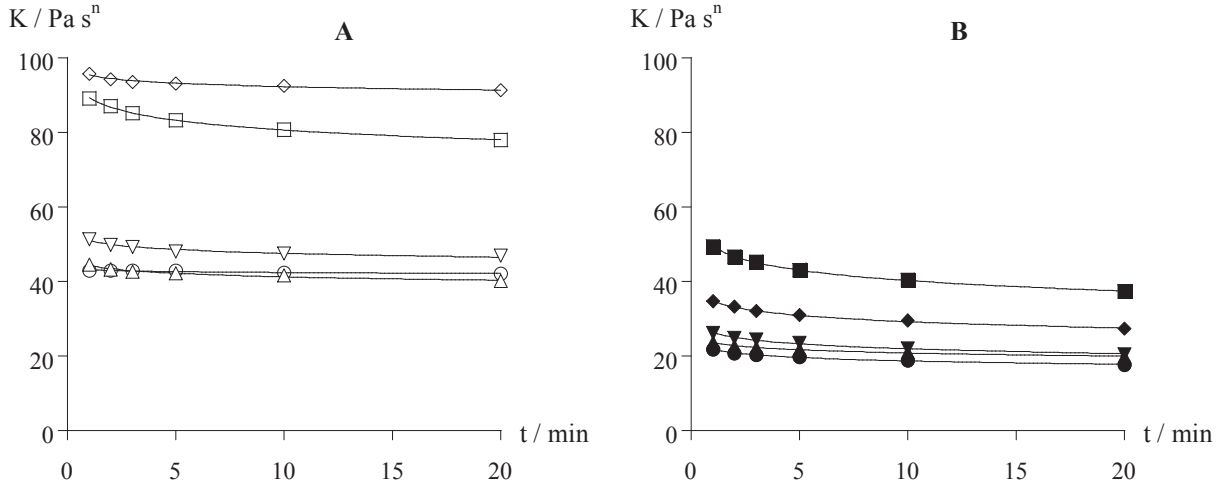

Figure 2 Consistency for down curves as a function of agitation time: **A (gels)**: (○) MS, (□) LBG, (◇) XG, (△) 0.03(LB+X), (▽) 0.1(LB+X) gel, **B (emulsions)** (●) MS, (■) LBG, (◆) XG, (▲) 0.03(LB+X), (▼) 0.1(LB+X).

Consistencies for up curves, K_0, and for t = 1 min, K = A, were much bigger for the gels than for the emulsions. When comparing the different systems, two groups were observed. MS systems were similar to those containing the blends, while the XG and LBG gels and emulsions were significantly more consistent.
On the other hand, analysing the values of B allowed us to characterize variation of consistency with agitation time, as it could be compared with the thixotropic breakdown coefficient proposed by Weltmann-Tung.
The three gels containing xanthan gum presented a similar behaviour, while we could say that the gel LBG was three times more thixotropic. The lowest value of B corresponds to the MS gel, what could indicate less thixotropy after the first minute of agitation. However, an important decrease in shear stress wass observed when comparing up and down flow curves (Figure 1). As equation 2 worked only for t >1 min, B did not reflect this effect.
Regarding to the emulsions, the tendency was not the same than for the gels. Parameter B for the XG emulsion was not comparable to the value for the other emulsions containing xanthan gum. We could say that XG and LBG emulsions were more thixotropic, and then less stable, especially the LBG emulsion.

On the other hand, in order to verify the conclusions obtained from the previous analysis, we calculated thixotropic areas from the loops performed. This method allowed us to consider also the thixotropic breakdown during the first minute, and include the influence of the differences in the power law index. To compare all the systems behaviour more properly, relative thixotropic areas were obtained. The following expression, what meant integrating the equations obtained after fitting flow curves [3], was applied.

$$S_R = 100\frac{S_{tix}}{S_{up}} = 100\frac{\int_1^{100}(\sigma_{0_{up}} + K_{up}\dot{\gamma}^{n_{up}})d\dot{\gamma} - \int_1^{100}\left[\sigma_{0_{dw}} + (A - B\ln(t))\dot{\gamma}^{n_{dw}}\right]d\dot{\gamma}}{\int_1^{100}(\sigma_{0_{up}} + K_{up}\dot{\gamma}^{n_{up}})d\dot{\gamma}} \quad (3)$$

The values calculated for S_R for all the emulsions are plotted as a function of time in figure 4.

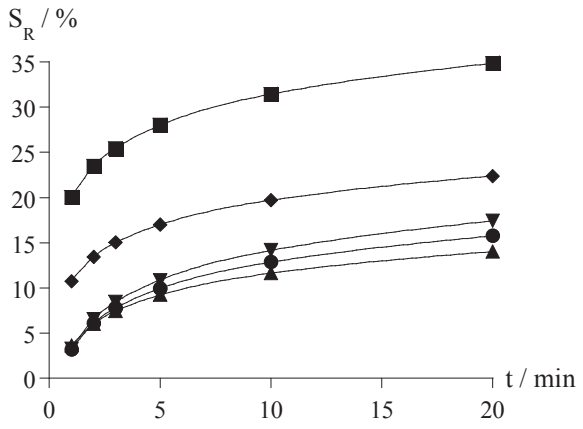

Figure 4. Relative thixotropic areas of the emulsions as a function of agitation time: (●) MS, (■) LBG, (◆) XG, (▲) 0.03, (▼) 0.1.

It is clear that the substitution of part of the starch by natural gums provoked an increase of the relative thixotropy. The emulsions containing the blends of gums exhibited quite a similar behaviour, with S_R between approximately 3 and 12 % in the range of agitation times studied.

However, addition of a higher percentage of gums increased the thixotropy, as S_R varied between 10 and 20% for the XG emulsion and arrived to 35% for the LBG emulsion. These results were in agreement with those obtained from the analysis of K(t) = f(t).

4. CONCLUSIONS

Both the gels and the corresponding emulsions fitted the Herschel Bulkley model, with n<0.5. The emulsions containing the greatest percentage of gums presented a yield stress much bigger than the corresponding gels. However, in the systems containing the expected synergistic mixtures, with less amount of gums, σ_0 was smaller for gels than for emulsions. Consistency, K, exhibited a logarithmic dependence with agitation time. Analysis of this dependence, together with the relative thixotropic areas calculated by integration, showed that the substitution of starch by gums led to an increase of the thixotropy, what implies that the resulting emulsions are less stable in relation to stirring.

5. ACKNOWLEGMENTS

This work is part of the project CTIDIA/2002/136. Financial support of Agencia Valencia de Ciència i Tecnologia (Generalitat Valenciana) is gratefully acknowledged.

6. REFERENCES

1. Franco, J.M.; Berjano, M.; Gallegos, C. (1997). “Linear viscoelasticity of salad dressing emulsions”. Journal of Agricultural & Food Chemistry. 45(3):713-719.

2. Kiosseoglou, A.; Papalamprou, E.; Makri, E.; Doxastakis, G.; Kiosseoglou, V. (2003). “Functionality of medium molecular weight xanthan gum produced by Xanthomas Campestris ATCC 1395 in batch culture”. Food Research International, 36(5), 425-430.

3. Dolz, M.; Hernández, M. J.; Delegido, J.; Cabeza, C. (2002). “Influence of different hydrocolloids in relative thixotropic areas of low-oil content salad dressings”. In Progress in Rheology. Theory and Applications, Martínez Boza F. J. et al. eds. GER, Sevilla.

4. Juszczak, L.; Fortuna, T.; Kosla A. (2003). “Sensory and rheological properties of Polish commercial mayonnaise”. Nahrung-Food. 47(4)232-235.

5. Dolz, M.; Hernández, M. J.; Pellicer, J.; Delegido, J. (1995). “Shear stress synergism and relative thixotropic area”. Journal of Pharmaceutical Science, 84(6), 728-732.

6. Weltmann, R. N. (1943). “Breakdown of thixotropic structure as function of time”. Journal of Applied Physics, 14, 343-350.

MECHANICAL PROPERTIES OF CHITOSAN MEMBRANES – EFFECT OF THE BIOPOLYMER STRUCTURE

*C. Santos, J.A. Lopes da Silva**

Departamento de Química, Universidade de Aveiro, 3810-193 Aveiro, Portugal.
Tel.: +351-234370360; Fax: +351-234370084

*Corresponding author - email: jsilva@dq.ua.pt

Keywords: chitosan, acetylation degree, molecular weight, mechanical properties, stress relaxation

Abstract
β-Chitin was extracted from squid pens and chitosan samples with different acetylation degree (DA) and molecular weight (MW) were obtained by controlled deacetylation and depolymerisation. Chitosan membranes were obtained by a casting/solvent evaporation method. Static tensile stress-strain deformation measurements and stress-relaxation studies were performed to assess the mechanical behaviour of these membranes, as a function of molecular weight and acetylation degree of the biopolymer. The results indicate that the DA has a significant influence on the tensile properties. The Young's modulus, elongation, and tensile strength increase as the degree of acetylation decreases. In contrast, the MW within the range analysed, seems to only affect positively the yield and ultimate tensile strengths of the chitosan membranes, not showing any significant effect on the Young's modulus and elongation. The tensile stress relaxation curves were fitted with an exponential decay model composed by a spring and two Maxwell elements in parallel. The relaxation rate was very similar for all the samples, what is in accordance with the lack of significance observed for the effect of DA and MW on the relaxation times. However, both chitosan properties had significant influence on the limiting (residual) relaxation modulus, increasing this property as the DA decreases or the MW increases.

1. INTRODUCTION

Chitosan is a co-biopolymer consisting of β-(1→4)-2-acetamido-2-deoxy-D-glucose and β-(1→4)-2-amino-2-deoxy-D-glucose units, obtained from the natural occurring polysaccharide chitin. Due to its film-forming properties, biocompatibility and antimicrobial properties, chitosan has extensive application in different areas [1], such as the biomaterials, biotechnology, food packing, pharmaceuticals, and as a cationic flocculent
Most of the physical and chemical properties of this biopolymer depend greatly on the degree of acetylation and on the molecular weight, including its film forming properties [2,3].
In this study, β-chitin was extracted from squid pens, and deacetylated under controlled conditions. A sample with intermediate degree of acetylation was depolymerised to obtain chitosan samples with different molecular weights. We have then studied the effect of the acetylation degree and molecular weight on the mechanical and viscoelastic properties of chitosan films.

2. EXPERIMENTAL

2.1. Materials and sample preparation

Chitosan with different degrees of acetylation (DA) was obtained from deacetylation of chitin from squid pens. The controlled deacetylation process was performed with sodium hydroxide 40% (m/v), at 70 ºC under stirring and N_2 atmosphere, during different times. Different samples were obtained, with DA ranging from 0 to 27%. The DA was determined by infrared spectroscopy using the relationship (A_{1655}/A_{3450})x115, proposed by Baxter *et al* [4]. Chitosan samples with different molecular weight (MW), ranging from 600 to 2500 kDa, were obtained by oxidative depolymerisation, according to Tommeraas *et al* [5]. The MW was determinate based on the Mark-Houwink-Sakurada equation proposed by Kasaai *et al*. [6]. The relative viscosities in 0.25 M acetic acid/0.25 M sodium acetate were measured using a Cannon-Fenske capillary viscometer and the intrinsic viscosities were calculated using the Huggins and Kraemer equations.
Films were prepared from 1% chitosan solutions (different DA and different MWs) in 0.1 M acetic acid and 0.5% glycerol. The solution was degassed and casted on a glass plate (17x17 cm) and the solvent allowed to evaporate in an oven at 35ºC. The films were peeled form the plates, neutralised in 0.1 M NaOH, and dried again. All films were conditioned at room temperature (25±2ºC) for 2 days in an environmental chamber set at 50% (±1%) relative humidity (RH), before testing. All mechanical tests were done on 9x1 cm rectangular film strips. Thickness ranged from 28 μm to 38 μm.

2.2. Mechanical properties

Mechanical properties in tension were evaluated using a texture analyser equipment (model TA.Hdi, Stable Micro Systems, England) equipped with fixed grips lined with thin rubber on the ends. The initial grip separation was set at 50 mm, and the crosshead speed was 0.5 mm/s. Young's modulus, percentage elongation, yield strength and tensile strength, were determined from stress-strain curves obtained from uniaxial tensile tests to membrane failure. Uniaxial tensile stress-relaxation experiments were conducted at 25ºC (±1ºC) / 50% (±2%) RH. Membrane strips were pulled initially at a rate of 0.5 mm/s up to a final strain of 2%. This strain was held constant and the tensile force was recorded as a function of time.

2.3. Modelling

Considering the material as a viscoelastic solid, with the tensile relaxation modulus $E(t)$ approaching a finite value with time (E_e), we have used a generalised mechanical model with two Maxwell elements and a spring in parallel,

$$E(t) = E_e + E_1 e^{(-t/\tau_1)} + E_2 e^{(-t/\tau_2)} \qquad \text{(I)}$$

where $E(t)$ is the tensile relaxation modulus, E_e the limiting value for the relaxation modulus ($t \to \infty$), E_1 and E_2, and the τ_1 and τ_2, are the elastic modulus component and the relaxation times, respectively, of each Maxwell component. The fit was performed by nonlinear regression using Statistica software (v. 6.0, StatSoft Inc.).

3. RESULTS & DISCUSSION

3.1. Stress-strain response to failure

Typical stress/strain curves for membranes prepared from chitosans with different acetylation degrees and MWs are shown in Figure 1. The acetylation of the amino group of the chitosan glucosamine units was found to have a significant influence on the tensile properties.
The film's ability to stretch, measured as the strain value for which the film breaks (% elongation), increases as the degree of acetylation decreases, contrarily to that previously reported [2]. At lower acetylation degrees the chitosan films can absorb a larger amount of energy before breaking. The yield point, or the point where the first sign of a non-elastic deformation occurs, is clearly more evident at low acetylation degree. Both the yield strength and the tensile strength increase as the degree of acetylation decreases (Table 1). Therefore, increasing the degree of acetylation originates chitosan membranes more brittle and less stress resistant.
The Young's modulus, or the modulus of elasticity, was measured as the ratio of stress to strain over the range for which this ratio is constant. It also increases when the acetylation degree decreases (Table 1), meaning that the intrinsic stiffness of the chitosan membranes increases as the acetylation degree decreases.

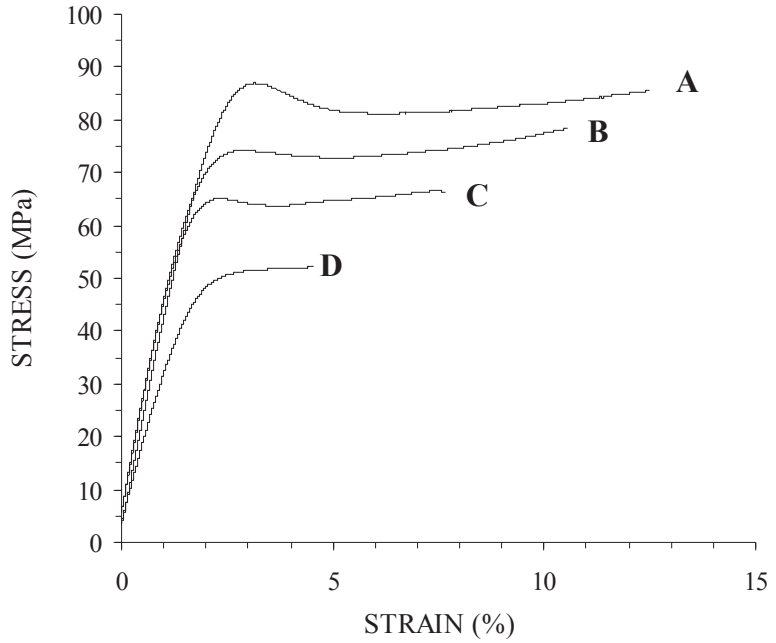

Figure 1 – Representative stress-strain curves obtained from uniaxial tensile experiments, until failure of the membrane strip. Samples are a low (**A**) and high (**D**) acetylated chitosan, with high MW, and a high (**B**) and (**C**) low MW sample, with intermediate degree of acetylation.

In contrast, the MW, within the range analysed, has not showed any significant influence on the Young's modulus and elongation of the membranes (Table 2). Only the yield and ultimate tensile strengths were positively affected by the increasing in the chitosan MW, in accordance with previously reported results [2]. Contradictory results have been reported for the effect of MW on the elongation degree. Chen and Hwa [7] reported that elongation % of chitosan films increased with the chitosan MW, but others [2] have reported that elongation % decreased with increasing MW.

Table 1 – Tensile mechanical properties obtained from stress-strain curves – the effect of the DA of chitosan

	Young's modulus (MPa)	Elongation (%)	Yield strength (MPa)	Tensile strength (MPa)
Low DA	37.7 ^{a}	12.4 ^{a}	82.1 ^{a}	85.8 ^{a}
Intermediate DA	33.3 ^{b}	8.6 ^{b}	64.8 ^{b}	71.3 ^{b}
High DA	25.3 ^{c}	3.2 ^{c}	51.4 ^{c}	51.6 ^{c}

* Averaged results (n=6) with different superscripts are significantly different at $p<0.05$

Table 2 – Tensile mechanical properties obtained from stress-strain curves – the effect of MW of chitosan

	Young's modulus (MPa)	Elongation (%)	Yield strength (MPa)	Tensile strength (MPa)
Low Mw	36.8 ^{x}	8.7 ^{x}	62.3 ^{x}	63.2 ^{x}
High Mw	37.3 ^{x}	10.5 ^{x}	77.2 ^{y}	77.4 ^{y}

* Averaged results (n=6) with different superscripts are significantly different at $p<0.05$

3.2. Tensile stress relaxation properties

Representative stress relaxation curves for membranes prepared from chitosans with different acetylation degrees and MWs are shown in Figures 2 and 3, respectively. The mechanical model selected (Eqn. I) was found to yield good degree of fit, with r^2 values ranging from 0.988 to 0.994, yet providing a size balanced model (5 parameters). The parameters obtained by fitting the model are shown in Tables 3 and 4.

Qualitatively the relaxation behaviour was quite similar, exhibiting the typical exponential stress decay versus time. The relaxation rate was very similar for all the samples, what is in accordance with the lack of significance observed for the effect of DA and Mw on the relaxation times (Tables 3 and 4). However, both chitosan properties had significant influence on the limiting relaxation modulus (E_e), increasing this property as the DA decreases or the MW increases, meaning that the membranes prepared from chitosans with lower DA or higher MW have a more pronounced solid character, dissipating less stress from the initial value, associated to the applied strain.

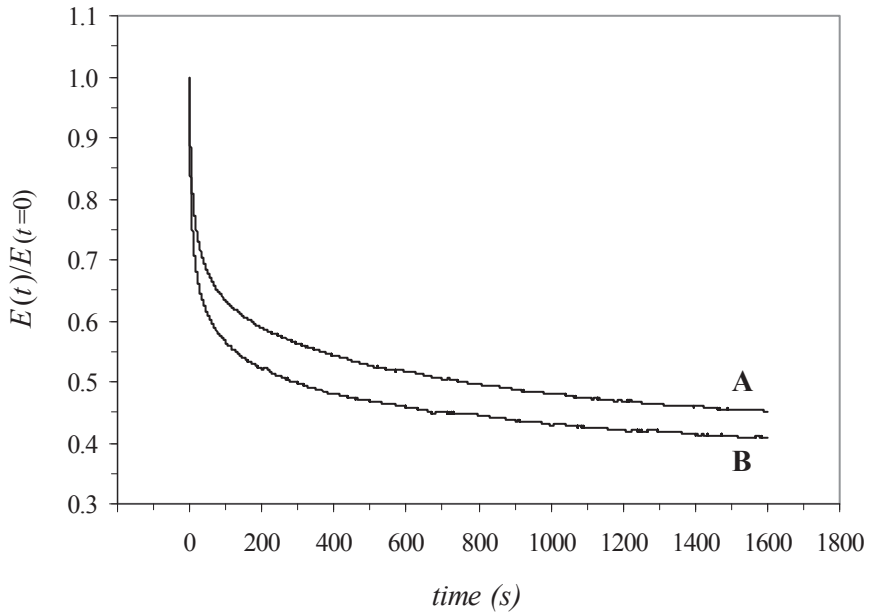

Figure 2 – Representative stress relaxation curves (normalised modulus, average of three experiments) obtained for membranes prepared from a low (**A**) and high (**B**) acetylated chitosan. Results obtained at 2% tensile strain (25 ºC (±1 ºC)/50 %(±2 %) RH).

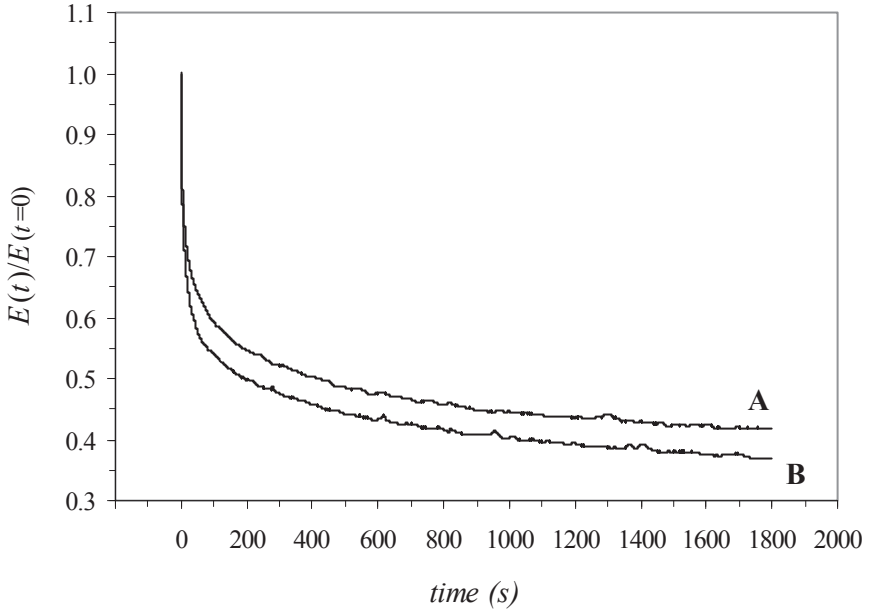

Figure 3 – Representative stress relaxation curves (normalised modulus, average of three experiments) obtained for membranes prepared from a low (**A**) and high (**B**) MW chitosan. Results obtained at 2% tensile strain (25 ºC (±1 ºC)/50 %(±2 %) RH).

Table 3 - Relaxation modulus coefficients and relaxation times for chitosans with different DA - generalised Maxwell model (Eqn.I)

	E_e (MPa)	E_1 (MPa)	E_2 (MPa)	τ_1 (s)	τ_2 (s)
Low DA	1381 [a]	716 [a]	666 [a]	30 [a]	595 [a]
Intermediate DA	1005 [b]	740 [a]	687 [a]	33 [a]	583 [a]
High DA	867 [c]	517 [b]	353 [b]	27 [a]	553 [a]

* Averaged results (n=4) with different superscripts are significantly different at $p<0.05$

Table 4 - Relaxation modulus coefficients and relaxation times for chitosans with different MW - generalised Maxwell model (Eqn.I)

	E_e (MPa)	E_1 (MPa)	E_2 (MPa)	τ_1 (s)	τ_2 (s)
Low Mw	1095 [a]	804	608	26	569
High Mw	1350 [b]	771	657	29	551

* Averaged results (n=4) with different superscripts are significantly different at $p<0.05$

4. ACKNOWLEDGEMENTS

We thank FCT (Portugal) for financial support through the programmes POCTI and FEDER (project POCTI/AGR/34804/2000).

5. REFERENCES

[1] Hirano S (1977) *Applications of Chitin and Chitosan*, Ed. Goosen MFA, Technomic, Muscat, pp 31-54.

[2] Hwang KT, Kim JT, Jung ST, Cho GS, Park HJ (2003) Properties of chitosan-based biopolymer films with various degrees of deacetylation and molecular weights. *J Appl Polym Sci*, **89**, 3476-84, 2003.

[3] Chen XG, Zheng L, Wang Z, Lee CY, Park HJ (2002) Molecular affinity and permeability of different molecular weight chitosan membranes. *J Agric Food Chem*, **50**, 5915-5918.

[4] Baxter A, Dillon M, Taylor KDA, Roberts AF (1992) Improved method for i.r. determination of the degree of *N*-acetylation of chitosan. *Int J Biol Macromol*, **14**, 166-169.

[5] Tommeraas K, Varum K, Chritensen B, Smidsrod O (2001) Preparation and characterization of oligosaccharides produced by nitrous acid depolymerisation of chitosans. *Carbohydr Res*, **333**, 137-144.

[6] Kasaai MR, Arul J, Charlet G (2000) Intrinsic viscosity-molecular weight relationship for chitosan. *J Polym Sci Part B: Polym Phys*, **38**, 2591-2598.

[7] Chen RH, Hwa H-D (1996) Effect of molecular weight of chitosan with the same degree of deacetylation on the thermal, mechanical, and permeability properties of the prepared membrane. *Carbohydr Polym*, **29**, 353-358.

INFLUENCE OF PENTOSANS ON THE VISCOELASTICITY AND MOLECULAR DYNAMICS OF GLUTEN NETWORKS

*D.M.J. Santos, A.M.P. Gil, J.A. Lopes da Silva**

Departamento de Química, Universidade de Aveiro, 3810-193 Aveiro, Portugal.
Tel.: +351-234370360; Fax: +351-234370084

*Corresponding author: email: jsilva@dq.ua.pt

Keywords: gluten, pentosans, viscoelastic properties, solid state NMR

Abstract: In this work, we have studied the effect of water-soluble pentosans on gluten viscoelasticity and molecular dynamics. Viscoelastic behaviour was assessed by dynamic rheological tests at low strain amplitude – oscillatory frequency sweeps after sample preparation and temperature sweeps during heating and cooling of the samples. Selected samples were also characterised by ^{1}H magic-angle-spinning (MAS) NMR as a function of heating and cooling. The addition of pentosans to the unheated gluten caused a general increase in the viscoelastic moduli (*G'*, *G"*) and an increase of the viscous character of the system (tan δ increases), an effect more pronounced as the amount of pentosans increases. During the heating and cooling cycle (20-80-20ºC), the presence of pentosans hindered the irreversible changes taking place within the protein network above 60ºC, besides the general increase in the moduli. The ^{1}H MAS spectra revealed a slight decrease in resolution in the presence of pentosans what may reflect a less overall molecular mobility induced by pentosans, probably by competition for water. Analysis of the T_2H relaxation times shows that the presence of pentosans induces a reduction on protein mobility and the formation of a network in which the water is held more rigidly. This is consistent with pentosans causing a decrease of available water for hydration and plasticization of the gluten. The effect of the heating-cooling cycle on both samples was found to be apparently reversible showing an increase in spectral resolution which reflects an increase in general molecular mobility at high temperatures. By cooling back to 20ºC, after heating to 80ºC, the two initial dynamically distinct protein populations are converted into a single dynamically uniform population, which may be related to the observed irreversible increase in *G'*. The smaller dynamic changes observed in the presence of pentosans are also consistent with the smaller changes observed for *G'*.

1. INTRODUCTION

Gluten is considered to be the main wheat flour component responsible for the viscoelastic properties of dough and for most of the end-use quality attributes of wheat [1]. Therefore, understanding the factors affecting gluten properties is very important. Despite their low concentration in wheat flour, pentosans have an important role in dough properties and bread-making quality of flours [2]. Most of their effects on baking have been related to their high water affinity [3]. Recently [4], it was shown that besides the water extractable pentosans compete with gluten for water, resulting in an increased resistance of gluten against extension, they may also interfere directly with gluten through ferulic acid mediated interactions between pentosans and protein.

The aim of this work was to contribute to a better understanding of the role of pentosans on gluten viscoelastic behaviour, using fundamental dynamic rheological tests in shear, complemented with solid NMR experiments. The effect of heat treatment on gluten viscoelasticity and how this effect depends on the presence of WSP were also studied.

2. EXPERIMENTAL

2.1. Materials

Wheat flour from a Portuguese wheat cultivar *Sorraia* was provided by *Estação Nacional de Melhoramento de Plantas* (Elvas, Portugal). This flour was defatted and fractionated into 3 main components (starch, gluten and water-solubles), as previously described [5]. The gluten fraction was then freeze-dried and ground to a power. Water-soluble pentosans (WSP) were obtained from the water-solubles fractions according to the procedure described previously [5], modified to decrease the relatively high protein content of the WSP. After removal of the water-soluble proteins, and after heat inactivation of the α-amylase used to remove starch, the WSP were treated by clay, filtered and then precipitated at 80% ethanol. The precipitated was washed with ethanol and ketone, and dried overnight at 40ºC.

2.2. Sample preparation

The study was conducted at 50 % (w/w) water content for added pentosan levels between 0 and 10% (gluten dry weight basis). The required amounts of water were added to previously prepared dry blends of gluten and WSP, taking into consideration the moisture content of each solid sample. Mixtures were prepared at room temperature, under controlled mechanical input (3 min), and then transferred to the rheometer measuring device or to the NMR rotor.

2.3. Rheological measurements

The rheological properties where monitored using a controlled-stress rheometer (AR-1000, TA Instruments). The hydrated samples were studied using a parallel plate configuration (2 cm diameter, 1.5 mm gap), covered with sandpaper to prevent slipping of the dough. The water loss was minimized by placing a low viscosity mineral oil on the exposed edge of the samples. Temperature control was performed (±0.1 ºC) by a Peltier element at the bottom plate. Oscillatory frequency and temperature scans where done under small deformation amplitude, within the linear range of viscoelastic behaviour of the samples.

2.4. Solid state NMR

Proton magic-angle-spinning (MAS) experiments were carried out on a Bruker DRX 4000 NMR spectrometer operating at 400 MHz, using a 4 mm CP/MAS Bruker probe. Proton MAS spectra were obtained with a recycle delay of 2-5 s and a 90º pulse length of ca. 3-5 μs. Proton T_2 relaxation times were measured through the Carr-Purcell-Meiboom-Gill pulse sequence with delays between pulses in the 0.05-300 ms range. ^{1}H MAS spectra were obtained at 20ºC, after heating the sample to 80ºC, and after cooling back to 20ºC. Temperature control was performed (±0.2 ºC) by an external B-VT Bruker 2000 temperature control unit.

3. RESULTS AND DISCUSSION

3.1. Samples after hydration and mixing at room temperature

The viscoelastic behaviour of the hydrated gluten sample is typical of a transient network, approaching the plateau zone at low frequencies. It can be noticed (Fig. 1) that at low frequencies both moduli decrease their dependence on frequency and that the loss tangent (tan δ) tends to reach a minimum. The effect of the presence of WSP is more pronounced as the amount of pentosans increases. For 1% pentosans the effect on the viscoelastic behaviour is not significant. For 10% WSP the effect is clearly evident as illustrated in Fig. 1. Both viscoelastic moduli increase with the addition of WSP, but the loss modulus (*G''*) increases more than the storage modulus (*G'*), thus increasing tan δ and the viscous character of the system. The presence of WSP also increases the dependency of *G'* upon frequency, meaning that now more rearrangements can take place within the period of the oscillatory deformation, among the units building the network.

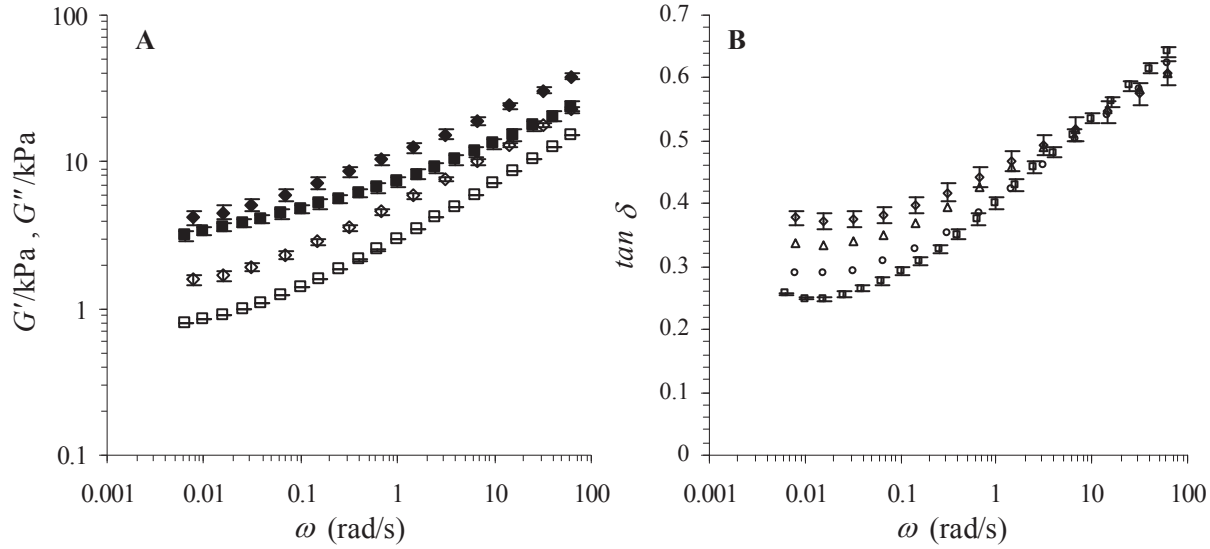

Figure 1 – Viscoelastic behaviour of gluten and gluten+WSP samples (50% w/w water), at 20ºC, strain amplitude 0.01. A – Storage (filled symbols, *G'*) and loss (open symbols, *G''*) moduli plotted logarithmically against frequency (*ω*); B – Loss tangent (tan δ=*G''*/*G'*) against frequency. Average values from triplicate measurements with standard deviations in Y bars.
□ -0% WSP, ○ - 1% WSP, △ - 5% WSP, ◇ - 10% WSP.

3.2. Effect of temperature on viscoelasticity

Dynamic rheological measurements during heating the gluten sample, in the absence of WSP, between 20 and 80ºC, indicated that *G'* first decreases as temperature increases, reaching a minimum around 61ºC, and then increases (Fig. 2). Up to 50 ºC the decrease in *G'* is essentially reversible (results not shown) and thus may be related to the increase of molecular motion and rupture of reversible intermolecular interactions (e.g. hydrogen bonds and electrostatic interactions). Above 60ºC the changes in the viscoelastic behaviour are no longer reversible. The observed increase in *G'* is associated to irreversible protein denaturation; it has been related to chemical modifications affecting the polymer size distribution through SH-SS exchange reactions [6]. It must be noted that the irreversible changes affect essentially

the mechanisms of storing energy within the network, since the changes in loss modulus remain practically reversible during the heating-cooling cycle.
The presence of WSP had an important effect on the gluten thermal behaviour, an effect also more pronounced as the amount of pentosans increased. An example is shown in Figure 2. The WSP reduce the viscoelastic changes taking place above *ca*. 60ºC, and the effect of heating became essentially reversible. Figure 3 compares the mechanical spectra obtained after heating to 80ºC and cooling back to 20ºC to those measured at 20ºC before heating. The amplitude of the irreversible changes occurring within the gluten network is much higher in the absence of the WSP. The spectra recorded before and after heating are qualitatively similar, but in the absence of WSP the increase in *G'* is much more pronounced.

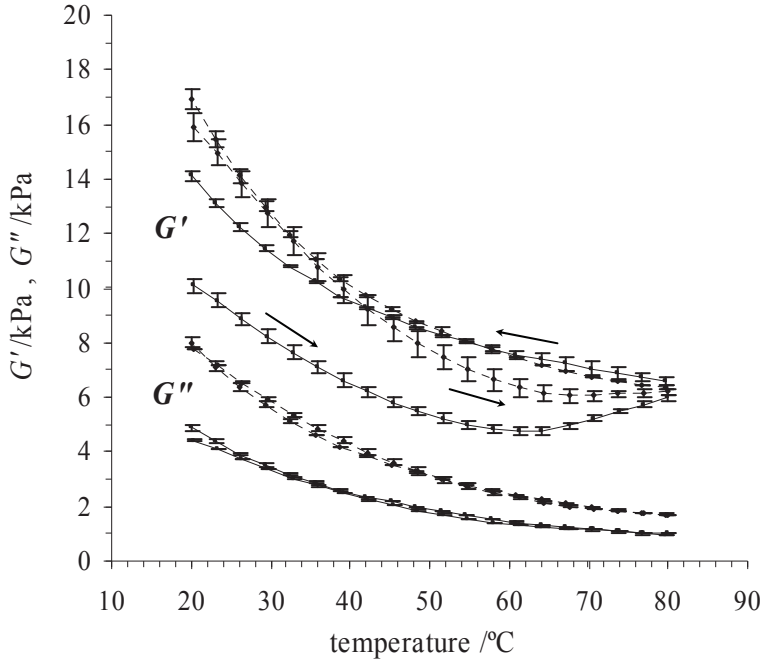

Figure 2 – Changes in the storage (*G'*) and loss (*G''*) moduli with temperature, for gluten (continuous lines) and gluten+10%WSP samples (dotted lines). Results obtained by heating (20-80ºC) and cooling (80-20ºC) at 1ºC/min, 1% strain amplitude and frequency 0.5 Hz. Average values from triplicate measurements with standard deviations in Y bars.

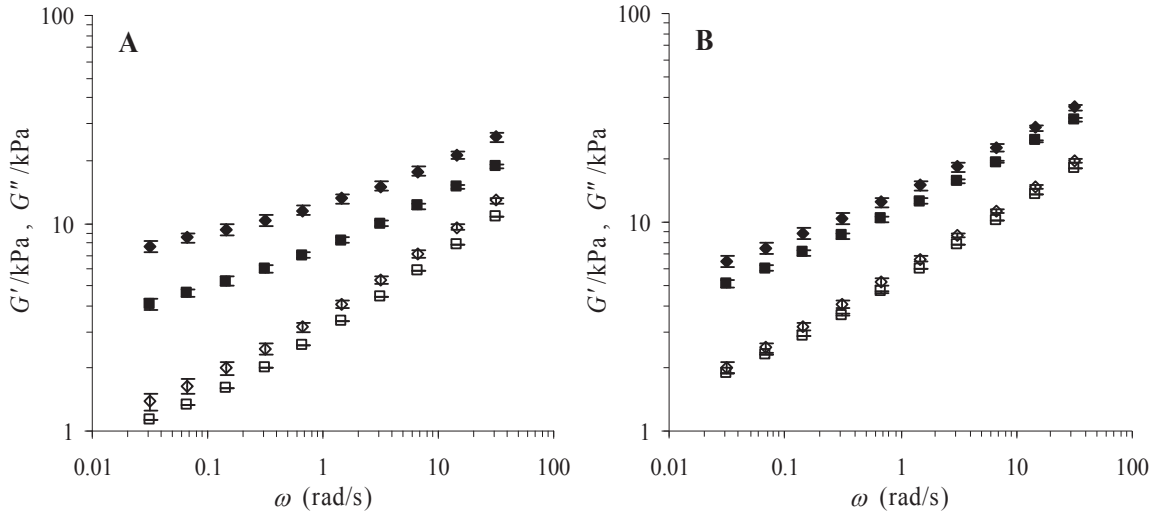

Figure 3 – Mechanical spectra of (A) gluten and (B) gluten+10%WSP samples (50% w/w water) obtained before and after heating at 80ºC. Filled symbols denote for *G'* and open symbols for *G''*. ■,□ - At 20ºC before heating,◆,◇ - At 20ºC after heating to 80ºC and cooling to 20ºC.

3.3. Complementary information obtained by NMR T_2H measurements

The ^{1}H NMR study of samples of gluten and gluten/WSP gives information about the changes in molecular dynamics of the protein and water. Figure 4 shows the ^{1}H MAS NMR spectra of a sample of hydrated gluten and a sample of hydrated gluten+1%WSP. A slight decrease in resolution is seen in the presence of pentosans and this may be interpreted tentatively as a reflection of less overall molecular mobility induced by pentosans.

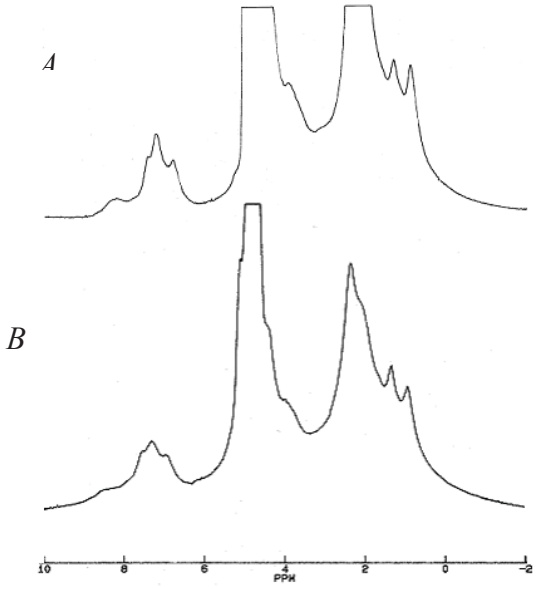

Figure 4 – ^{1}H/MAS spectra of (A) gluten and (B) gluten+1%WSP, 50% (w/w) D_2O. Spinning rate 10 kHz, 40 scans.

Proton transverse relaxation times, T_2H, were measured for each peak in the spectra. For gluten alone at 20ºC, protein peaks (Table 1) arise from 2 protein populations with

comparable magnitude (40-50%) and with different mobility: a rigid population with T_2's of 0.2 ms and a mobile population with T_2's of 4-6 ms. The presence of pentosans induces the formation of only one protein population with relatively low mobility (0.5 ms) and in which the water is held more rigidly (T_2 of water is 1,6 ms instead of 11 ms for the gluten sample). This is consistent with pentosans causing a decrease of available water for hydration and plasticization of the gluten.

Heating the samples increases the T_2 values, reflecting the expected increase in general mobility for all components (Table 1). Upon cooling, the gluten sample shows a single dynamic population for the protein, indicative that all protein in now forming a uniform network, in which the protein retains a relatively high mobility (T_2H 2-3 ms), along with the water present (T_2H 10 ms). This reflects an increase of 12 xs compared to the initially hindered population existing in the gluten sample. This conversion between 2 dynamically distinct populations into a single dynamically uniform population may be related to the observed irreversible increase in *G'*.

In the presence of 1% pentosans, the protein remains mainly on one single population for which the mobility increases slightly (x4) with heating-cooling, probably reflecting some re-adjustment of the network and/or some water re-distribution between pentosans and gluten. The smaller dynamic changes observed in this sample are consistent with the smaller changes in *G'* observed in the presence of WSP.

Table 1 Proton transverse relaxation times (T_2H/ms) for gluten and gluten+1%WSP, calculated from ^{1}H/MAS spectra obtained for 50% (w/w) D_2O hydrated samples at different temperatures.

		Gluten					
ppm	*Assignment*	20ºC		80ºC		20ºC	
		T_2A/ms	T_2B/ms	T_2A/ms	T_2B/ms	T_2A/ms	T_2B/ms
4.8	water	10.9±0.4	--	0.10±0.03	9.6±0.1 (89%)	0.33±0.09	9.6±0.1 (91%)
6.9	-NH_2 side-chains	0.15±0.05	6.9±1.7 (40%)	0.66±0.12	11±1 (63%)	2.8±0.4	--
7.4		0.20±0.05	3.9±0.5 (54%)	0.27±0.03	12±1 (85%)	2.3±0.3	--
7.6		0.22±0.05	6.6±0.6 (52%)	--	--	3.1±0.4	--
8.4	-NH backbone	1.77±0.04	--	0.48±0.14	7±1 (60%)	0.8±0.2	--
		Gluten+1%WSP					
ppm	*Assignment*	20ºC		80ºC		20ºC	
		T_2A/ms	T_2B/ms	T_2A/ms	T_2B/ms	T_2A/ms	T_2B/ms
4.8	water	1.6±0.3	--	7.7±0.1	--	1.1±0.8	6.7±0.2 (96%)
6.9	-NH_2 side-chains	0.45±0.04	--	0.8±0.1	7±1 (35%)	2.0±0.4	--
7.4		0.46±0.05	--	0.6±0.1	11.4±0.9(65%)	1.8±0.3	--
7.6		0.49±0.04	--	10.5±0.7	--	0.19±0.03	3.4±0.8 (29%)
8.4	-NH backbone	0.27±0.02	--	0.18±0.04	4.9±0.3 (66%)	0.56±0.07	--

4. ACKNOWLEDGEMENTS

We thank the Estação Nacional de Melhoramento de Plantas (Elvas, Portugal) for providing the wheat flours.

5. REFERENCES

1. MacRitchie, F. 1999. Wheat proteins: Characterization and role in flour functionality. *Cereal Food World*, **44**, 188-193.
2. Michniewicz, J., Biliaderis, C.G., Bushuk, W. 1991. Effect of added pentosans on some physical and technological characteristics of dough and gluten.*Cereal Chem.*, **68**, 252-258.
3. Rouau, X., Moreau, D. 1993. Modification of some physicochemical properties of wheat flour pentosans by an enzyme complex recommended for baking. *Cereal Chem*., **70**, 626-632.
4. Wang, M., Hamer, R.J., van Vliet, T., Oudgenoeg, G. 2002. Interaction of water extractable pentosans with gluten protein: effect on dough properties and gluten quality. *J. Cereal Sci*., **36**, 25-37.
5. Santos, D.M.J., Gama, A.C., Lopes da Silva, J.A. 2002. A rheological study of wheat starch-water soluble pentosan mixtures under hydrothermal gelling conditions. *J. Food Sci*., **67**, 3372-3380.
6. Lefebvre, J., Popineau, Y., Deshayes, G., Lavenant, L. 2000. Temperature-induced changes in the dynamic rheological behavior and size distribution of polymeric proteins for glutens from wheat near-isogenic lines differing in HMW glutenin subunit composition. *Cereal Chem*., **77**, 193-201.

NON-NEWTONIAN VISCOSITY OF DILUTE POLYMER SOLUTIONS

J. García de la Torre, J.G. Hernández Cifre, M.C. López Martínez, R. Pamies*

Dpto. Química Física, Facultad de Química, Universidad de Murcia, 30071 Espinardo, Murcia (Spain). Fax: +34 968 364148 Phone: +34 968 3674420

e-mails: jgt@um.es, jghc@um.es, clopez@um.es, rpamies@um.es

* - Corresponding author

Keywords: bead-spring model , Brownian dynamics simulation, non-Newtonian fluid

Abstract
The non-Newtonian behaviour, i.e. the dependence of the viscosity on the shear rate, is a basical characteristic of polymer solutions. Polymer and solvent features such as excluded volume (EV), hydrodynamic interaction (HI) and finite extensibility (FE) play an important role in this kind of behaviour. The use of numerical and computational methods allow for the study of the polymer dynamics avoiding approximations necessary in theoretical approaches. In this work we study the influence of the foregoing effects by using the Brownian Dynamics simulation technique. The polymer chain is modeled as a sequence of beads and springs. EV effects are modeled by means of a Lennard-Jones potential and HI between beads is taken into account by means of the Rotne-Prager-Yamakawa tensor. In order to perform Brownian Dynamics simulations, a predictor-corrector algorithm based on that of Ermak and McCammon was used. In our simulations we observe the typical Newtonian plateau at low shear rates and the strong potential decay of the viscosity at large share rates (*shear thinning*), which is caused by the finite extensibility of the chain. However, at moderate shear rate, when viscosity decreases up to half of its zero-shear rate value, HI and EV have a great influence on the shear rate viscosity dependence.

1. THEORY AND METHODOLOGY

The study of the non-Newtonian behaviour of polymer solutions has become a classical problem in polymer rheology. Statistics and dynamics of the polymer chain play an important role in this kind of behaviour. Thus, since the beginning experimental (1) and theoretical (2,3) research has been carried out to elucidate the influence of the polymer/solvent characteristics (excluded volume (EV), hydrodynamic interaction (HI) and finite extensibility (FE)), on the non-Newtonian behaviour. However, there are experimental difficulties to reach large shear rates, and theoretically model simplifications are too crude; thus, there are not too much results in the non-Newtonian regime. The use of numerical and computational methods such a Brownian Dynamics avoid approximations in the models and allow for the simulation of the polymer dynamics at any shear rate.

In this work we study the behaviour of a dilute polymer solution subjected to simple shear. The polymer chain is modeled with the well-known bead-and-spring model: a sequence of beads (representing interaction units) and springs (representing the chain elasticity). In order to account for the finite extensibility of the real polymer chain, FENE (finite extensible non-linear elongational) springs were employed. These springs follow the force law,

$$F = \frac{HQ}{1-(Q/Q_{\max})^2} \tag{1}$$

where H is the spring constant, Q the spring elongation and Q_{max} the maximum spring length. EV effects are modeled by means of the Lennard-Jones potential. By choosing appropriate values of the Lennard-Jones parameters, one can mimic all kind of solvent conditions (good, theta and bad). HI between beads is taken into account by means of the Rotne-Prager-Yamakawa (or modified Oseen) tensor. In order to perform Brownian Dynamics simulations, the predictor-corrector Brownian algorithm of Iniesta and García de la Torre was used. A description of this methodology as well as examples for the simulation of non-Newtonian behaviour can be found in (4) and references therein.

2. RESULTS

In our simulations we observed, as expected, the typical Newtonian plateau at low shear rates and the strong potential decay of the viscosity at large shear rates (*shear thinning*). This decay is caused by the finite extensibility of the chain, represented here by the use of FENE springs. However, at moderate shear rate, when viscosity decreases upto half of its zero-shear rate value, HI and EV have a great influence on the shear rate viscosity dependence. In our simulations we can at will either include or not these effects in order to elucidate the role of each of them. Figure 1, a log-log plot of the dimensionless intrinsic viscosity, $[\eta]^*$, vs. the dimensionless shear rate, β, is a clear example of the non-Newtonian behavior due exclusively to the finite extensibility of the springs (HI and EV effects were disabled) as obtained in our simulations. In Figure 2 we appreciate the joint effect of HI and EV on the viscous behaviour. In order to avoid the FE influence, Hookean springs were used, so that there is not shear thinning at high shear rate.

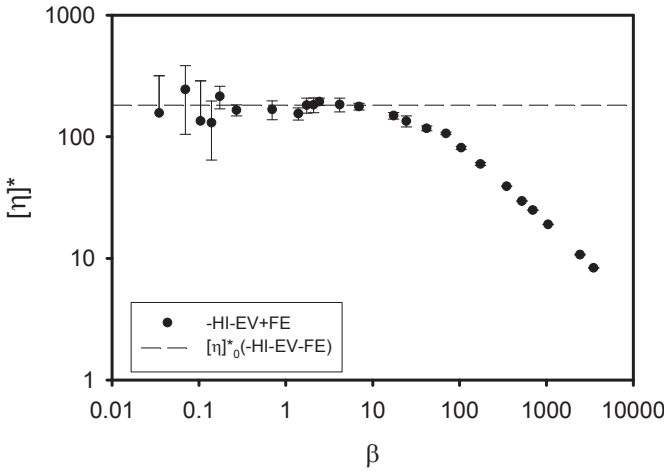

Figure 1 – Typical flow curve of a polymeric material in steady shear flow.

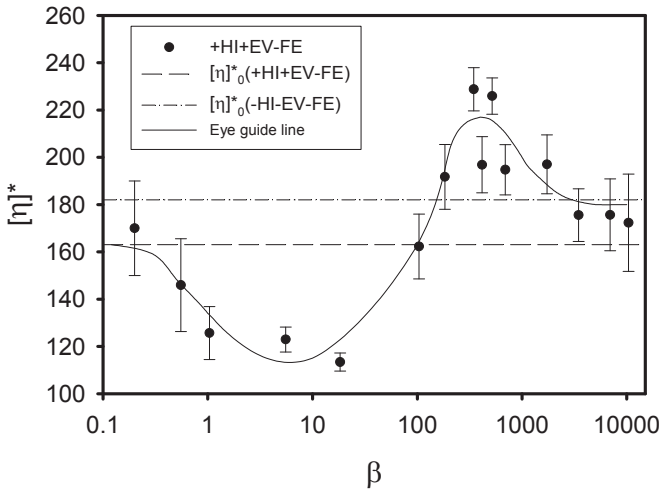

Figure 2 – Effect of HI and EV on the flow curve.

Straight lines show the values of the zero-shear intrinsic viscosity in abscence and presence of HI and EV as indicated in the legend. As observed, at high shear rate, EV and HI effects tend to dissapear. We also tried to compare our simulation results with experimental data. Figure 3 is a linear plot representing the evolution of the relative intrinsic viscosity, $[\eta]/[\eta]_0$, with the shear rate.

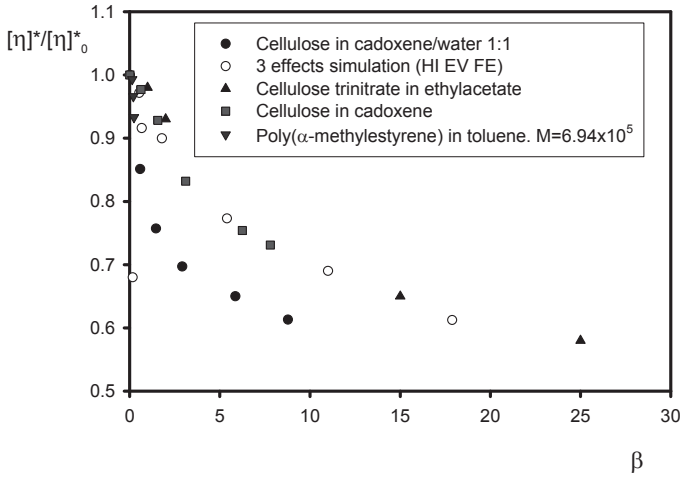

Figure 3 – Comparison of experimental and simulation data.

It is shown that simulation is able to reproduce experimental data. As already commented, it is difficult to reach high shear rates in experiments, therefore the viscosity decreases about 50% at the most. In this region, results present large error bars.

3. ACKNOWLEDGEMENTS

This work was funded by DGICYT, Proj. BQ2000-0229. JGHC is the recipient of a Ramón y Cajal research contract by MEC.

4. REFERENCES

[1] E. Riande and J.M. Pereña, "Non-Newtonian behavior of cellulose solutions", *Makromol. Chem*., 175, 1974, 2923-2938
[2] J.A. Subirana, "Solvent effects on the non-Newtonian viscosity of dilute solutions of flexible linear macromolecules", *J. Chem. Phys.*, 41, 1964, 3852-3856
[3] M. Fixman, "Polymer dynamics: non-Newtonian intrinsic viscosity", *J. Chem. Phys.*, 45, 1966, 793-803
[4] J.J. López Cascales and J. García de la Torre, "Shear-rate dependence of the intrinsic viscosity of bead-and-spring chains: hydrodynamic interaction and excluded-volume effects", *Polymer*, 32, 1991, 3359-3363

5. FOOD RHEOLOGY & PROCESSING

STUDY OF THE EFFECT OF FREEZING ON THE VISCO-ELASTIC PROPERTIES OF STRAWBERRIES

Fundo, J., Brandão, T.R.S., Quintas, M. and [*]*Silva, C.L.M.*

Escola Superior de Biotecnologia, Universidade Católica Portuguesa
Rua Dr. António Bernardino de Almeida
4200-072 Porto, Portugal
tel: 225580058 fax: 225090351
[*]crislui@esb.ucp.pt

Keywords: strawberry; visco-elastic properties; freezing

ABSTRACT

The objective of this work was to study the influence of freezing on the visco-elastic properties of strawberries.
Food structure plays an important role in food quality and functionality. It is important for the consumers to find an identical sensation when they eat a fresh strawberry and when the strawberry is defrosted. The visco-elastic properties of a food product are an indirect measure of its structure. Experimental measurements of these properties may correlate to changes on the physical attributes of the product.
In this work, a dynamic mechanical analyser was used to assess changes on loss (E'') and storage (E') modulus, applying a compressive test with a Ø1.5 cm parallel plate geometry.
Strawberries were acquired in a local market and frozen in a blast and fluidized bed freezer at –30 ºC for 1 hour. Samples were stored at –30 ºC in freezing chambers.
Analyses were performed on fresh strawberries, after freezing and during storage. The samples were cut in small cylinders (1.5cm x 1.5cm) and left to relax during 1 hour at room temperature.
Preliminary tests were performed in order to evaluate the linear visco-elastic region and the loss and storage modulus were determined. A dynamic frequency sweep test was also performed.
Results showed that the behaviour of fresh strawberry sample varies significantly when compared with a defrosted sample. The influence of the storage still cannot be evaluated and is currently under study.
Overall, it can be concluded that the freezing process greatly influenced the visco-elastic properties of the strawberries.

INTRODUCTION

In our days, consumers are demanding more attractive food products that look and taste excellent, are easy to prepare and are nutrition balanced. Freezing is a simple and common method of food preservation. This process delays food deterioration and growth of microorganisms, and extends the product shelf life whistle maintaining its original characteristics [1]. However, when a food product freezes, several changes occur: water is transformed into ice, there is a volume expansion and the ice crystals may incite the rupture of cellular walls. This process is responsible for structural changes, which directly affect texture. This is especially critical for high water content foods (fruits and vegetables are examples), and may result in extensive irreparable cell wall damages.

Texture is a very complex property to define, involving a great number of food characteristics somehow associated with fracture and particle size. It clearly plays a basic role in food appreciation and perceived characteristics. Food products' attributes are detected by mechanical, tactile, visual and auditory receptors by the consumer [2], and texture is dynamically evaluated throughout consumption [3].

Rheological measurements may help to explain some aspects related to food texture. Although it is not possible to quantify this perception, results from rheological experiments can be used to explain structure changes occurring when a food product is submitted to different processing conditions.

The knowledge of foods' rheological behaviour is also important in process design, since it allows the minimisation of the degree of damage by optimisation of the applied stress and/or strain [4]. A relation between structural mechanics of the food material and the observed mechanical behaviour plays also an important role in quality control [5].

Dynamic mechanical tests are indicated when analogies between food physical properties and human sensory is the objective to achieve [6]. Dynamic tests are usually applied in studies of visco-elastic properties of materials, such as foods in the linear visco-elastic region. The materials are subject to a deformation or stress varying harmonically with time, including direct stress or strain measurements. These tests can be carried out using either rotational or compression/elongation equipment, with controlled stress or strain.

In compression/elongation testing, the elastic properties of a material can be evaluated on the basis of the elastic or storage modulus (E'), which is the ratio of elastic stress to strain, meaning the ability of a material to store energy elastically. The viscous properties are measured by the viscous or loss modulus (E''), that is the ratio of viscous stress to strain, representing the ability of a material to dissipate energy. The sum of storage and loss modulus is called "Young's Modulus" or modulus of elasticity and is represented by E [6,7].

The tangent of the phase angle (tan δ) between the applied oscillatory strain and the oscillatory stress response is the ratio of the loss to the storage modulus and is a measure of the damping property of the material. [6,7].

The use of rheological measurements in foodstuffs, especially in fruits, is limited by one major difficulty, that is the assurance of material isotropy. This drawback can be minimised by the proper choice of fruit samples and/or by cutting samples within the pulp. The natural heterogeneity of the fruit pieces should not be forgotten when testing these products, and replicates must be carried out.

The objective of this work was to study the influence of freezing on the visco-elastic properties of strawberries, using a dynamic mechanical analyser.

MATERIALS AND METHODS

Sample preparation

Fragaria ananassa strawberries, acquired in a local market, were frozen in a blast and fluidized bed freezer (Armfield FT36) at –30ºC for 1 hour and stored at –30ºC in freezing chambers (Fitoterm, S550 BT), simulating industrial processing. This storage temperature

was selected based on previous studies with strawberries, with the objective of assessing quality retention during frozen storage [8,9].
Before analysis, the samples were cut in small cylinders (1.5cm x 1.5cm) and left to relax for 1 hour at room temperature to eliminate any state of stress caused to the sample due to the pressures caused by cutting.

Rheological measurements

Rheological analyses were performed on fresh strawberries, after freezing (day 0) and during storage time (days 7, 14, 21, 29, 35 and 49).

A Dynamic Mechanical Analyser, DMA (Rheometrics® Solid Analyser II) was used to measure the visco-elastic properties of samples in compression, using parallel plates (ϕ1.5 cm). The DMA used in this work was strain-controlled and an oscillatory strain was applied to the sample. Resulting sinusoidal stress of the sample was measured, and the viscous and elastic properties were analysed.

Tests were performed in order to evaluate the linear visco-elastic region, estimate both loss and storage modulus within the region and determine the strain to be applied in further testing. To achieve this goal, a dynamic strain sweep test was carried out, using 1 Hz frequency and at constant temperature (20ºC).

A dynamic frequency sweep test, with constant strain (2.5×10^{-4}) and temperature (20ºC) was also carried out.
Three replicates were analysed for each condition, and the values of loss and storage modulus were calculated from the average of the experimentally obtained results.

RESULTS AND DISCUSSION

Preliminary results of the dynamic strain sweep test (Figure 1) showed a similar interval of visco-elasticity both for fresh and defrosted strawberries. According to these results, the value of strain chosen for the frequency sweep test was the same for all tested samples and equal to 2.5×10^{-4}.
In Figure 2 it is shown a typical example of fresh and defrosted strawberries samples result of a frequency sweep test. It can be observed that storage and loss modulus are constant with time of observation (frequency). Although large differences in the loss and storage modulus occurred between fresh and defrosted samples, E' is higher than E'' in both cases. This is due to the fact that strawberries behave more like a solid than a liquid, and although the freezing process dramatically changes the structure of strawberries, this characteristic is maintained.

Results show evidence that the freezing process drastically affects the visco-elastic properties of strawberries. It is possible to observe the great reduction on the values of storage and loss modulus from the fresh to the defrosted samples. This can also be confirmed by visual inspection of strawberries, that became softer and without consistency after the freezing process.

Comparing a fresh sample with a defrosted one, it is possible to observe that the ratio E' to E'' was also modified, i.e. E'' suffered a greater reduction that E'. This may indicate that during the freezing process, the samples lost more "ability to store elastic energy than to dissipate it".

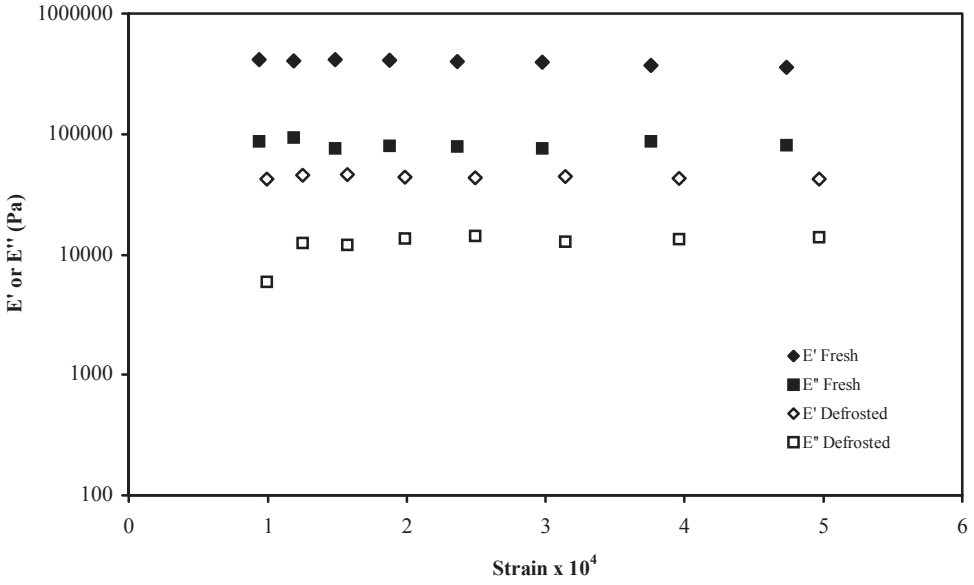

Figure 1. Results of a dynamic strain sweep test in both fresh and defrosted samples.

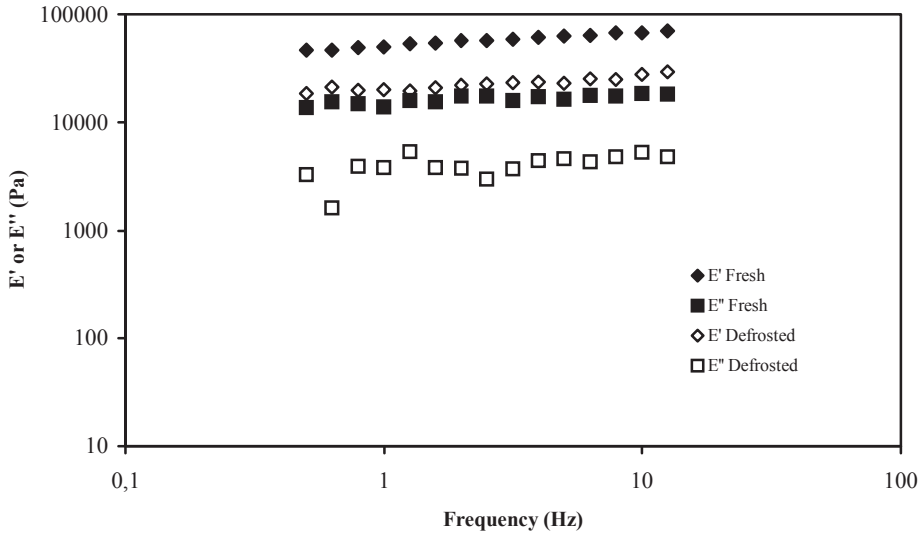

Figure 2. Typical result of a frequency sweep test for fresh and defrosted samples.

No significant changes occurred in the visco-elastic properties of the samples during storage at –30ºC (Figure 3). This is probably due to the fact that this temperature has been selected based on previous studies, being the lowest storage temperature [8,9] for reducing quality loss. This could indicate that –30ºC was below the glass transition temperature. However, a published work referred a value equal to –51.3ºC for *Fragaria ananassa* strawberries [10]. This fact can lead to two major conclusions: i) the time of storage under study was not enough

to perceive significant changes and/or ii) if the selected storage and freezing temperature was lower than –30ºC, a greater quality retention could be observed.

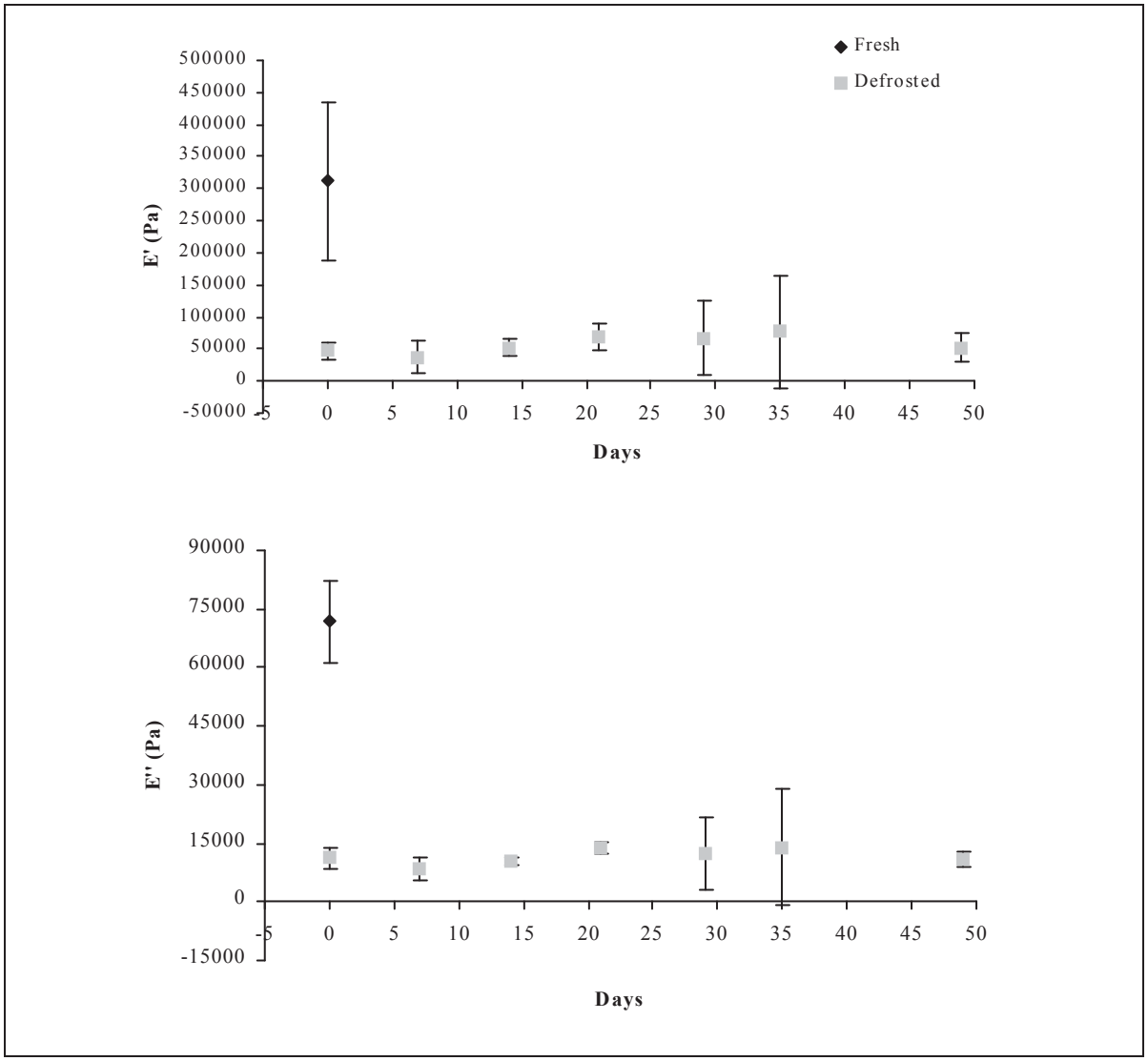

Figure 3. Storage and loss modulus as function of days of storage at –30ºC (results were obtained using strain equal to 2.5×10^{-4}).
The bars indicate the standard deviation of the experimental values.

CONCLUSIONS

From rheological measurements it was observed that strawberries' characteristics resemble behaviour closer to a solid material. Although the "solid like" characteristic is maintained, the freezing process greatly affects the visco-elastic properties of strawberries. After freezing, a decrease in E' and E'' was observed, which can be related with the visual observation of softening and lost of firmness.
During frozen storage at –30 ºC no significant changes occurred in the samples visco-elastic behaviour.

REFERENCES

1 George, R. M. (1993). Freezing processes used in the food industry. Trends Food Sci. Technol. 4 (5), 134-138.

2 Borwankar, R.P. (1992). Food texture and rheology: a tutorial review. J. of Food Eng. 16, 1-16.

3 Bourne, M.C. "Texture, Viscosity and Food", Cornell University, New York State Agricultural Experiment, Station and Institute of Food Science, Geneva, New York.

4 Morrow, C.T. and Moshenin, N.N. (1966). Considerations of selected agricultural products or viscoelastic materials. J. Food Sci. 31 (5), 686-698.

5 Morrow, C.T. and Moshenin, N.N. (1968). Dynamic viscoelastic characterization of solid food materials. J. Food Sci. 33 (5), 646-651.

6 Steffe, J. F. (1992). "Rheological Methods in Food Engineering", Freeman Press, East Lansing, MI, USA.

7 Ferry, J. D. (1980). "Viscoelastic Properties of Polymers", John Wiley and Sons, New York, USA.

8 Silva, C.L.M. (2003). "Melhoria da Qualidade de Horto-fruticolas Congelados: Novos Pré-Tratamentos e Efeito de Abusos de Temperatura na Cadeia de Distribuição". Final Report of Project POCTI/BIO/43624/2000.

9 Teixeira, I., Gonçalves, E.M., Abreu, M., Brandão T.R.S. and Silva, C.L.M. (2003). Studies on the Temperature Effect on Coulor and Vitamin C Contents of Frozen Storage Strawberries (*Fragaria* ^{x}*ananassa Duschesne*). Poster presented at X Congresso Nacional de Biotecnologia (BIOTEC'2003), Lisboa, Portugal, 6 to 8 December.

10 Moraga, G., Martinez-Navarrete, N., Chiralt, A. (2004). Water sorption isotherms and glass transition in strawberries: influence of pretreatment. J. Food Eng. 62, 315-321.

DETERMINATION OF RIPENING TIME OF "TERRINCHO" CHEESE USING TEXTURE AND COLOR PARAMETERS

I.M.P.LV.O. Ferreira[1] , O. Pinho[1,2], M. M. Alves[3],

[1] REQUIMTE, Serviço de Bromatologia, Faculdade de Farmácia, Universidade do Porto, Rua Aníbal Cunha, 4050-047 – Porto, Portugal; isabel.ferreira@ff.up.pt
[2] Faculdade de Ciências da Nutrição e Alimentação da Universidade do Porto, Rua Dr. Roberto Frias, 4200-465 Porto, Portugal.
[3] Instituto Piaget, I.S.E.I.T.-Mirandela, C.E.R.T.A., Av. 25 de Abril, 5370-202 Mirandela, Portugal.

Key words: Texture Profile Analysis, ewe cheese, hardness, chewiness.

ABSTRACT

"Terrincho" ewe cheese is a typical product of the North-Eastern region of Portugal it is manufactured from raw ewe's milk of the race "Churra da Terra Quente" and bears the status of PDO cheese. The area and conditions for its production is well established. It undergoes a minimum of 30 days of ripening.
In this type of cheese the estimation of ripening time is important, because it is made from raw ewe's milk and for food safety reasons "Terrincho" cheese must not be sold with less than 30 days of ripening.
A multiple linear regression analysis with stepwise variable selection involving 14 variables was carried out with the aim of estimate ripening time. The general formula of the estimation equation is $y = a_1 x_1 + a_2 x_2 + \ldots + a_n x_n$ where y is cheese ripening time and x_1, x_2, … x_n are texture and color parameters. The statistical treatment of results showed that the product ripening time could be estimated with 6 variables, L* (e), L* (i), b* (i), hardness, a* (i) and chewiness, and a constant. The equation obtained was y= 257.782 -1.160 x L* (e) – 1.655 x L* (i) + 3.376 x b* (i) + 0.01067 x hardness + 9.750 x a* (i) – 0.01919 x chewiness SE = 4.2 R=0.972 n=89 $p< 0.001$, with an estimation error of 4.2 days. Good correlation was obtained between the measured and estimated values.
This regression equation was applied with success to confirm the ripening time of 10 "Terrincho" cheeses from 5 different dairy plants.

INTRODUCTION

"Terrincho" ewe cheese is a typical product of the North-Eastern region of Portugal and is manufactured from raw ewe's milk of the race "Churra da Terra Quente" according to the specifications of its Denomination of Origin Regulatory Board D.N. (1). Thus the, area and conditions for "Terrincho" ewe cheese production are well established. It undergoes a minimum of 30 days of ripening and its consumption has increased over the past few years.
In this type of cheese the estimation of ripening time is important, because it is made from raw ewe's milk and for food safety reasons reasons"Terrincho" cheese must not be sold with less than 30 days of ripening.
The rheological properties of a cheese depend upon its structure. The three major constituents of cheese are casein, fat and water. The structural differences between various types of cheese result from the effects of the differences in manufacturing procedures on the structure (2).
Easily determinable texture parameters can be useful in the testing of the product and in the evaluation of ripening conditions as described by Bara-Herczegh (3) when analyzing ewe cheeses mechanical parameters determined with a Texture Profile Analyzer.

The parameters that have an effect on the physical properties of the curd are the milk composition, and the amount of rennet. During cheese manufacturing, the curd is cut into small pieces so that serum can drain away. The granules formed are pressed and aggregated making a more compact and homogeneous structure with its own rheological properties.

The role of pH in cheese texture is particularly important because changes in pH are related directly to chemical changes in the protein network of the cheese curd. The influence of the water activity and salt content on the rheological properties of cheese is indirect. Decreases in water activity greatly decrease the rate of proteolytic activity in cheese. A high concentration of salt increases the osmotic pressure, diverting a significant quantity of water from the structural bonds of the casein network (4).

With regard to the visual aspect, quality control involving color evaluation is carried out in numerous ways. Color perception differs from person to person, and depends upon lighting and numerous other factors; many industries rely on human vision coupled with an instrumental system of color measurement. These instruments attempt to simulate the manner in which the average human eye sees the color of an object, under specified illumination conditions.

The aim of this work was to establish a multiple linear regression equation with texture and color parameters that enable determinations of ripening time of "Terrincho" cheese.

MATERIAL AND METHODS

Cheese samples

A batch of 18 "Terrincho" ewe cheeses, used to study the chemical, textural and color parameters, during ripening. From this batch groups of 3 cheeses were picked with 0, 6, 12, 20, 30 and 60 days of ripening.
During ripening the cheeses were stored in a ripening chamber at 10-12ºC and air relative humidity of 88-89%. All the samples were ripened by the respective manufacturers, at each time, cheeses were sent to the laboratory in refrigerated boxes and analyzed immediately to monitor the changes.
Ten cheeses manufactured on 5 different dairy plants with 30 days of ripening were also analysed, to confirm there ripening time.

Methods

Physico-chemical analysis

The determination of acidity was performed according to AOAC method (5).
The water activity was determined by a special apparatus (AW Sprint TH-500, Novasina, Swiss), pH-value was determined at room temperature using a penetrometric eletrode (Mettler- Toledo). Dry matter was evaluated using Scaltec Instruments GmbH. Germany.

Texture analysis

In recent years, multifunctional texture test instruments have been developed which are easy to use and suitable for both imitative and empirical tests. In this work, the textural analysis was performed in a texturometer TA-Xt2i (Stable Micro Systems, U.K.), with a load cell of 5 Kg, by carrying out texture profile analysis (TPA).

Sample preparation- prior to TPA test a layer of 0.5cm was removed from cheese upper surface, to obtain a regular surface for probe penetration.

Testing conditions – Penetration tests were performed, at 20 ± 2°C, using a plastic cylindrical probe of 13 mm ∅, a penetration depth of 20 mm and 1 mm/s of crosshead speed; this tests were done 5 times on each sample (one on de middle and four on different parts of cheese surface) and performed in triplicate.
Mechanical parameters - from the force *versus* time texturograms were obtained 8 parameters: hardness (g), fracturability (g), adhesiveness (g.s), springiness, cohesiveness, gumminess, chewiness and resilience.

Color Measurement
Color analyses were performed using a colorimeter CR 300 (Minolta, Japan).
L^*, a*, b* color parameters were determined according to the CIELAB color space, were L^* corresponds to light/dark chromaticity (changing from 0%, dark, to 100%, light), a* to green/red chromaticity (changing from -60, green, to 60%, red) and b* to blue/yellow chromaticity (changing from -60, blue, to 60%, yellow). The instrument was calibrated with a white tile (L^* = 97.10, a* = -4.88, b*=7.04) before the measurements.
Color determinations were made 5 times, one on de middle and four on different parts of cheese surface, before and after removing a layer of 0.5 cm of upper surface.

Statistical Analysis
The averages and standard deviations were calculated for each parameter.
Descriptive statistics, analysis of variance (ANOVA), pairwise comparisons of mean values with Turkey test, principal component analysis (PCA) and multiple regression were performed with SPSS for Windows version 11.5 (SPSS Inc, Chicago, IL).

RESULTS AND DISCUSSION

Changes in physico-chemical and texture characteristics during "Terrincho" cheese ripening.

Physico-chemical characteristics
"Terrincho" cheese samples from M dairy plant used for studies during ripening had an average protein, fat content, NaCl, ash, of 40g/100g dry matter (DM), 50g/100g (DM) 5.5 g/100g (DM) and 1.5 g/100g of cheese, respectively.
Moisture and water activity showed significant differences, during 60 days of ripening (Fig.1). These parameters greatly influence proteolytic activity in cheese.

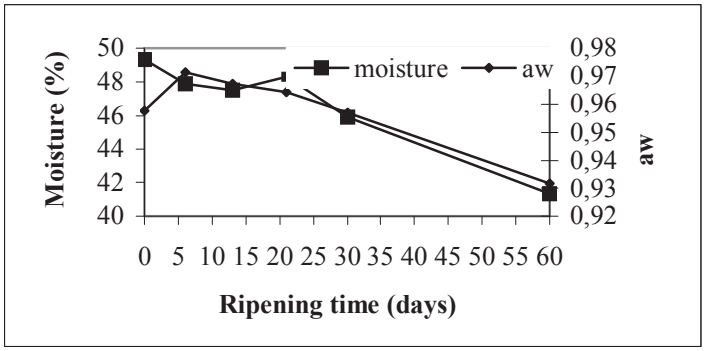

Fig.1 Changes of moisture and aw during 60 days of ripening.

Acidity increased during ripening, and pH decreased up to 30d and increased slightly between 30 and 60 days. Thus, confirming the important metabolic activity of lactic acid bacteria (Fig.2). The decrease of pH values is related with texture parameters, because no fusion of curd particles occurs until near pH 5.8 (6).

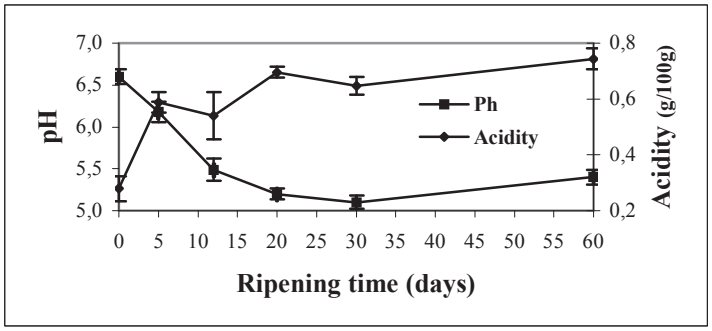

Fig.2 Changes of acidity and pH during 60 days of ripening.

Texture attributes of TPA analysis

The mean values obtained for texture attributes of TPA analysis during ripening together with ANOVA results are presented in Table 1.

Table1-Texture profile analysis, and Colour measurement, with ANOVA results during 60 days of ripening time

Texture and Colour attributes	**Ripening Time (days)**						**ANOVA results**	
	0	6	12	20	30	60	F	*p*
Hardness (g)	915.4 ± 65.1 a	1417.0 ± 58.9 α	1578.1 ± 145.6 a	2871.4 ± 677.7 b,c	1926.3 ± 392.5 b,c	1810.8± 291.7 a	9.933	0.001
Fracturability (g)	846.9 ± 77.8 a	1107.3 ± 258.1 a,b	1491.0± 103.1 a,b	2394.4± 458.4 c	1730.3± 303.5 b,c	1549.2 ± 164.4 a,b	11.656	10^{-4}
Adhesiveness (g.s)	-1393.8± 285.9 a	-887.7 ± 103.1a	-1230.4 ± 65.3 a	-2778.4 ± 496.3 b,c	-2448.1 ± 493.2 b	-3495.4 ± 53.2 c	24.966	10^{-4}
Springiness	0.98± 0.00 a	0.97 ± 0.0 a	0.81 ± 0.14 a	0.97 ± 0.01 a	0.98± 0.01 a	0.84 ± 0.14 a	2.709	0.078
Cohesiveness	0.49± 0.0 1a,c	0.44± 0.01 b	0.45± 0.01 b	0.43 ± 0.0 b	0.45± 0.01 a,b	0.52 ±0.01 c	20.911	10^{-4}
Gumminess	444,5± 38.3 a	617.8 ± 35.1 a	707.4 ± 86.3 a	1254.2 ± 322.9 b	871.5± 154.4 a,b	941.2 ± 165.5 a,b	8.003	0.002
Chewiness	435.7± 38.6 a	598.9 ± 34.4 a	671.3 ± 30.0 a	1221.4 ± 320.7 b	857.1 ± 157.4 a,b	891.7 ± 145.4 a,b	8.209	0.002
Resilience	0.09± 0.01 a	0,10± 0.00 a	0.09 ± 0.01 a	0.08± 0.00 a,b	0.05± 0.00 b,c	0.05± 0.00 c	20.043	10^{-4}
L*(i)	87.19 ± 0.21 a	86.61 ± 0.1 a	86.60 ± 0.96 a	83.42 ± 0.40 a	82.61 ± 1.04 b	79.63± 1.67 c	33.594	10^{-4}
a*(i)	-6.96± 0.08 a	-7.24 ± 0.09 a,b	-7.28± 0.14 a,b	-7.33 ± 0.09 a,b	-7.83 ± 0.23 b	-7.03 ± 0.59 a	9.098	0.009
b*(i)	16.38 ± 0.05 a	16.66 ± 0.04 a	17.79 ± 0.19 a,b	18.12 ± 0.54 a,b	20.66 ± 1.09 c	19.76 ± 2.23 b,c	13.778	0.001
L*(e)	84.63 ± 0.58 a	84.50 ± 0.32 a	84.23 ± 1.47 a	83.36 ± 0.50 a	76.87 ± 2.51 b	59.46 ± 1.94 c	108.29	10^{-4}
a*(e)	-6.24± 0.02 a,b	-7.40± 0.08 c	-6.63 ± 0.44 a,c	-6.50 ± 0.19 a,c	-5..50 ± 0.55 b	-4.31± 0.09 d	27.979	10^{-4}
b*(e)	17.97 ± 0.34 a	19.88 ± 0.30 a	21.31 ± 1.18 a	22.26 ± 0.85 a	28.43 ± 3.92 b	20.86 ± 0.70 a	11.691	10^{-4}

a-d Means in lines without common superscripts are significantly different ($p<0.05$; n=18)
L* (e), a* (e), and b* (e) correspond to parameters measured on cheese surface (external) and L* (i), a* (i), and b* (i) corresponded to parameters measured on cheese surface after removing a layer of 0.5 mm (inside cheese).

Texture profile analysis revealed significant changes for fracturability, adhesiveness, cohesiveness and resilience during 60d of ripening as shown by F and *p* values of ANOVA (Table 1).

Hardness, fracturability, gumminess and chewiness increased up to 20 days of ripening and afterwards decreased. A significant increase was observed between 12 and 20 days of ripening. Important changes on texture occurred after 20 days of ripening. At this time pH decreased to 5.5. As the pH of cheese curd decreases there is a concomitant loss of colloidal calcium phosphate from the casein submicelles and, below about pH 5.5, a progressive dissociation of the submicelles into smaller casein aggregates (7).
Cohesiveness decreased at the beginning of ripening, maintained up to 30 days of ripening, and a significant increase was noted between 30 and 60 days. It is described a maximum cohesiveness for pH between 5.2 and 5.8 (6).

In general, our results concerning texture changes during ripening were in good agreement with those described by Lawrence (6). Two distinct phases in texture development took place during cheese ripening. Initially, rubbery texture of young cheese curd was converted into a smoother, more homogeneous product. After 20d, a gradual change in texture was observed, as caseins suffer higher hydrolysis.

Color measurement
The mean values obtained for L*, a*, b* parameters are also shown in Table 1 and presented considerable changes during ripening. L* (e), a* (e), and b* (e) correspond to parameters measured on cheese surface (external) and L* (i), a* (i), and b* (i) correspond to parameters measured on cheese surface after removing a layer of 0.5 mm (inside cheese).

L* decreased significantly during ripening, this was prominent on exterior surface (F=108.3) than on interior surface (F=33.6).

An increase on yellowish b* (i) and b* (e) was observed up to 30 days of ripening, however, at 60 days cheeses were less yellow.

These results were in agreement with other authors that described a decrease in lightness and a slight increase on both reddish (a) and yellowish (b) during cheese ripening (8).

Estimation of "Terrincho" cheese ripening time

"Terrincho" cheese ripening time was estimated with stepwise variable selection involving the 14 variables by multiple linear regression analysis. The general formula of the estimation equation is $y = a_1 x_1 + a_2 x_2 + \ldots + a_n x_n$ where y is cheese ripening time and x_1, x_2, … x_n are texture and color parameters. The correlation between the measured and estimated values is shown in Fig.3.
The product ripening time can be estimated with 6 variables, L* (e), L* (i), b* (i), hardness, a* (i) and chewiness, and a constant. The estimation error is 4.2 days.
The estimation of the cheese age on the basis of texture parameters during similar period of time was made by other authors (2) with an accuracy of about 15-16 days. The use of 2 texture and 4 color parameters greatly improved the estimation error.
This regression equation was applied with success to confirm the ripening time of Terrincho cheese from 5 different dairy plants.

CONCLUSIONS

Changes in moisture, aw, pH, acidity, texture and color were monitored during "Terrincho" cheese ripening. Two phases were distinguished: the first, up to 20 days was characterized by

a slow decrease of moisture and aw. During this period pH decreased from 6.6 to 5.4 resulting an increase in hardness, fracturability, gumminess, chewiness and yellow color. After 20 days the decrease of moisture and aw was more prominent and the pH increased slightly, this second phase was characterized by an increase in cohesiveness and decrease of hardness and fracturability, because caseins suffer higher hydrolysis in to small peptides.

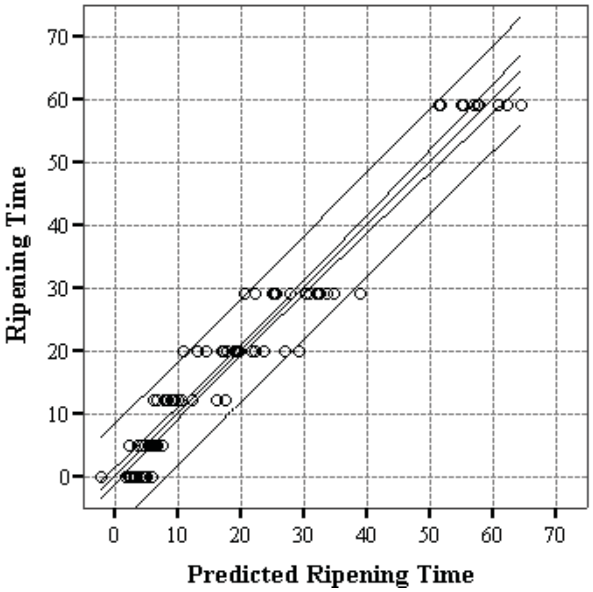

Figure 4- Estimation of cheese ripening time Y = ripening time, x = texture and color parameters, SE = standard error. Y= 257.782 -1.160 x L* (e) – 1.655 x L* (i) + 3.376 x b* (i) + 0.01067 x hardness + 9.750 x a* (i) – 0.01919 x chewiness SE = 4.2 R=0.972 n=89 $p< 0.001$

Estimation of ripening time using 2 texture and 4 color parameters and a constant was possible with a standard error of 4.2 days. This regression equation was applied with success to confirm the ripening time of Terrincho cheese from 5 different dairy plants.

Acknowledgements: This work received financial support from Agro nº 26 (Medida 8 Acção 8.1.)

REFERENCES

(1) Despacho Normativo 293/93 from 1 October 1993, D. R. I Série B- nº 231

(2) Bara-Herczegh, O., Horváth-Almássy, K., Csanádi, J. and Orsi, F. 2002. Suitability of Texture Parameters for Characterization of Hajdú Cheese Ripening. Acta Alimentaria. 3:149-159.

(3) Bara-Herczegh, O., Horváth-Almássy, K., Fenyvessy, J. and Orsi, F. 2001 Suitability of Texture Parameters for Characterization of Trappist cheese ripening. Acta Alimentaria. 30:127-143.

(4) Prenticle, J. H. 1991. Cheese rheology in: Hui, Y. H. (Ed.) Encyclopedia of food science and technology, Vol. 1. John Wiley & Sons, Inc. New York, pp. 348-369.

(5) AOAC (2000). 33.7.14 AOAC Official Method 920.124 Acidity of Cheese.

(6) Lawrence, R.C. Creamer, L.K. and Gilles, J. 1987. Symposium cheese ripening Technology - Texture Development During Cheese Ripening, Journal of Dairy Science Vol. 70: 8: 1748-1760.

(7)Lebecque, A., Laguet, A., Devaux, M.F. and Dufour, E. 2001. Delineation of the texture of Salers cheese by sensory analysis and physical methods. Lait. 81: 609-623.

(8)Pillonel, L., Badertscher, R., Butikofer, M., Casey, M., Dalla Torre, M. Lavanchy, P. Meyer, J., Tabacchi, R. 2002. Analytical methods for the determination of the geographic origin of Emmental cheese. Main framework of the project; chemical, biochemical, microbiological, color and sensory analyses. Eur. Food Res. Technol. 215: 260-267.

STUDY OF BEER FOAM PROTEINS: CORRELATION WITH HIDROPHOBICITY AND SIGMA VALUE

*L.C. Nogueira[1], M.F. Martins[2], I.M.P.L.V.O. Ferreira[2], L.C. Trugo[1]

[1]Laboratório de Bioquímica Nutricional e de Alimentos, Instituto de Química, Universidade Federal do Rio de Janeiro, Brasil. e-mail: luciana.nogueira@ig.com.br
[2]REQUIMTE, Serviço de Bromatologia, Faculdade de Farmácia, Universidade do Porto, Rua Aníbal Cunha, 4050-047 – Porto, Portugal.

Keywords: beer, foam proteins, hidrophobicity.

ABSTRACT

Foaming property is one of the most conspicuous aspects of beer quality. Extensive research has been carried out on chemical compounds in beer to elucidate the mechanisms of formation and to enhance beer foam stability. The proteins and polypeptides present in beer are generally regarded as making the single greatest contribution to beer foam quality. It seems that foam stability is a function of hydrophobic character and molecular weight; that is, the higher the molecular weight and the higher the hydrophobic character, the best is the foam quality. However, there are many factors which affect, directly or indirectly the ability of proteins to stabilise the interface. Variations in the ingredient composition of beers may affect the foaming behaviour, increase the ethanol content can result in a decrease in foam stability. The objective of this study was to apply the technique of RP-HPLC in the hydrophobic interaction mode and the Sigma value determination in order to evaluate the profile of beer proteins and to establish correlations with the quality of the foam. Three different beers (low alcohol beer made with 100% malt; 6% (v/v) of alcohol beer made with 100% malt and a beer made with part of adjuncts, all Pilsen type) were used. Statistical analysis was made by ANOVA, considering $p < 0,05$. Our results demonstrated that the increase of ethanol concentration resulted in a decrease in foam stability. The beer made with part of adjuncts had foam with less hydrophobic proteins compared with the other two. And the values of the low alcohol beer foam had the best results compared with the others. The beers made with 100% malt had the best results of Sigma and hydrophobic proteins compared with the beer made with adjuncts. We conclude that exists a positive correlation with the Sigma values and the quantity of hydrophobic proteins in beer foam.

INTRODUCTION

It has been a matter of major interest to establish the chemical nature of those materials in beer that contribute to the stability of the foam. Besides proteins, which are considered to be very important factor for foam and colloidal stability of beer, other beer constituents such as iso-alpha acids, peptides, amino acids, proteinase, fatty acids and melanoidins are suggested to influence foam properties (1). Brewing material variables such as barley varieties, malt types, hop usage, yeast strains, and malting and brewing processes influences the contents of these constituents in beer. Many methods have been tried in the isolation and characterization of these foam-positive beer proteins. Proteins and polypeptides make an important contribution to foam quality, although the role they play is not clearly defined. Fractionation of beer components on the basis of hydrophobicity and size has been used to identify key surface of polypeptides. The hypothesis that is hydrophobicity, which is the primary determinant of foam stabilizing ability in beer polypeptides, has been reported by a series of

papers by Onish and coworkers (2-4). In general, fractions of greater hydrophobicity have the greatest foaming potential, as do those of higher molecular mass (> 5000 Da) (5).

The protein content of beer has been estimated to be 0.5 gL^{-1}. Most beer proteins and polypeptides have been shown to originate from the malt and are the product of proteolytic and chemical modifications that occur during brewing process (6-12). It has also been demonstrated that yeast proteins are present in beer, albeit as minor constituents.

As the heterogeneity of barley proteins is further increased by modification during malting and brewing, it is not surprising that few proteins have been purified to homogeneity. The best characterized is protein Z, an 40000 Da protein found in barley, which remains virtually unchanged throughout the malting and brewing process and which has been estimated to make up 20-170 mgL^{-1} of beer protein. Another protein, associated with foam formation, is a barley lipid transfer protein 1 (LTP1), which has a molecular weight of 9700 Da.

The appearance of stable foam on beer influences consumer's preconceptions about the quality of that beer, knowing that the perception of foam is different between nationalities, age groups and sexes. Beer foam quality is characterized by its stability, adherence to glass, and texture, which are inherently determined by the quality of the barley and hop raw materials used for beer production (7). In addition, beer production processes, addition of foam palliatives, packaging and method of dispense influence the basic foam quality determined by the raw materials.

Different methods have been used to study beer proteins such as chromatography (2,6), electrophoresis (8) and immunochemical techniques (4, 9, 10).

Hydrophobic interaction chromatography is a technique for isolating proteins and polypeptides. It relies on the affinity of hydrocarbon side-chains on a Sepharose matrix for hydrophobic areas located on the surface of the polypeptide.

The objective of this study was to apply the technique of RP-HPLC in the hydrophobic interaction mode and the Sigma value determination in order to evaluate the profile of beer proteins and to establish correlations with the quality of the foam. Statistical analysis was made by ANOVA, considering $p < 0,05$.

MATERIALS AND METHODS

Beer samples

Three different beers (low alcohol beer made with 100% malt; 6% (v/v) of alcohol beer made with 100% malt and a beer made with part of adjuncts, all Pilsen type) were used. The beers were produced in controlled conditions, so the quantity and type of each compound was noted.

The beer (200mL) was sparged with air through a stainless steel HPLC aerator frit until 1 L of foam had been formed in a 2 L Erlenmeyer at 20ºC. The foam was allowed to drain for 15 minutes before the beer liquid was removed. The foam was then allowed to collapse and was collected for further HPLC analysis.

Instrumentation

The chromatographic analysis was carried out in an analytical HPLC unit (Jasco) equipped with a quaternary pump type PU 1580, a type 7125 Rheodyne Injector with a 500μL loop, a Jasco multiwavelength diode array detector MD-910 and a Borwin PDA Controller Software were also used. The column was a Chrompack P 300 RP, which contains a polystyrenedivinylbenzene copolymer-based packing (8 μm, 300 μm, 150 x 4.6 i.d.). The column heater used was a type 7981 – Jones.

Separations conditions

The RP – HPLC was performed at 45ºC temperature. Gradient elution was carried out with a mixture of two solvents. Solvent A consisted of 0.1% trifluoroacetic acid (TFA) in water and solvent B consisted of 0.1% TFA in 80% aqueous acetonitrile, 〔v/v〕. Proteins were eluted with a linear gradient increasing the proportion of solvent B, from 60% to 100% over 30 min, and returning to initial condition within 5 min. The analysis was monitored at 280 nm.

Sigma value method (Σ)

Foam was generated by pouring beer into a special foam funnel. Beer collected in the funnel was drained away at a rate such that only foam is present in the funnel 90 seconds after the end of pouring. At a stage (t secs) which must be 225-230 secs after the first drainage period, the volume of beer drained from the foam (b) and the volume of beer still in the foam (c) are measured.

$$\Sigma = t / \{2.303 \log\left[(b + c) / c\right]\}$$

Σ values of 105 secs, 95 – 105 secs and < 95 secs describe good, average and poor foams respectively.

RESULTS AND DISCUSSION

The purpose of our research was examine beer proteins of differing hidrophobicity in order to determine their relative contributions to foam stability and the correlation with Sigma value, that is a measure of the average life-time of a foam bubble.

Table 1 shows the retention times (TR), the areas average and the areas sommatory of the beer foam proteins.

The Sigma values for beer foams were: 106, 104 and 71 secs for low alcohol beer, 6% alcohol beer and beer with adjuncts, respectively.

Table1 – Proportions of differently polypeptides in beer foam proteins

		Retention times (TR) and areas					Total areas
		12 min.	13 min.	14 min.	15 min.	16 min.	
Beer	Low alcohol beer	nd	nd	201960	nd	529385	731345
	6% alcohol beer	1218	66225	140598	nd	628704	836746
	Beer with adjuncts	nd	nd	82216	nd	304799	387016
Foam	Low alcohol beer	nd	61402	134107	103248	461113	759872
	6% alcohol beer	nd	56475	123987	nd	384661	676874
	Beer with adjuncts	32179	78887	nd	427603	nd	538670

nd: not detectable.

As beer is a mixture of surface-active compounds, these will compete for places in the bubble walls, which may result in foams of stability other than might be expected. Isolation of a substance from beer which gives a stable foam by itself need not necessarily imply that it stabilises the foam in poured beer (1). Variations in the ingredient composition of beers makes comparison of the foaming behaviour of one beer with another difficult. In addition, there are a wide range of methods available for measuring foaming properties, some of which are endorsed and used by the brewing industry, others of which are not (13).

Of the many factors that contribute to beer foam stability, one of the most important is polypeptide content (1, 6, 14). Beer polypeptides consist of a wide range of molecules, which vary both in molecular weight and hydrophobicity. Previous work has shown that hydrophobic polypeptides to be concentrated in the foam, evidencing their importance to beer foam stability (1, 2, 5, 7, 15). Sigma values were highly correlated with total area of foam hydrophobic peptides, Pearson correlation was 0.921. However, there are many other factors which affect, directly or indirectly the ability of proteins to stabilise the interface. The high concentration of ethanol in one of the beers studied, resulted in a decrease in foam stability, owing to a decrease of foam total hydrophobicity when is compared with the beer itself. But, when we compare with the foam of beer with adjuncts, the hidrophobicity and the Sigma value results was higher. It can be explained by the fact that the beer with high content of ethanol and the low alcohol beer were made with 100% malt. So, they have more quantity of proteins when compared with the beer with adjuncts. Besides this, the quantity of hops that was put in the low alcohol beer and the beer with high content of alcohol was higher than the other made with adjuncts.

It seems that unhopped beers have poor *foamability*, which is increased by hops, soft resins and humulones (α-acids), though not by lupulones (β-acids) or non-resinous components of hops, e.g. essential oils (16). Apparently, the degree of foam formation is related to the ability of a substance to lower the surface tension of beer, which seems to depend on the number of hydrophobic side-chains on the molecule.

CONCLUSIONS

The stabilisation of beer foam structures appears to be heavily dependent on the occurrence of hydrophobic interactions and exists a positive correlation between the Sigma values and the quantity of hydrophobic proteins in foam.

ACKNOWLEDGEMENT

This work received financial support from Reitoria da Universidade do Porto (project "Influência da fracção proteica, hidratos de carbono, e ácidos orgânicos na estabilidade da espuma da cerveja"), Brew Tech, CAPES, FAPERJ and CNPq.

REFERENCES

1. Bamforth, C.W. The foaming properties of beer. J.Inst. Brew. 91, 370-383, 1985.
2. Onish, A., and Proudlove, M. O. Isolation of beer foam polypeptides by hydrophobic interaction chromatography and their partial characterization. J. Sci. Food Agric. 65: 233-240, 1994.
3. Hughes, P., Mills, C., Kauffman, J., Brierley, E. , Dickie, K., Proudlove, M., Onishi, A ., and Wilde, P. The foaming and interfacial behavior of beer polypeptides: The effect of hidrophobicity. Monogr. Eur. Brew. Conv. 27: 129-140, 1998.
4. Mills, E. N.C., Kauffman, J.A., Morgan, M.R.A., Field, J.M., Hejgaard, J., Proudlove, M. O. , and Onish, A . Immunological study of hidrophobic polypeptides in beer. J. Agric. Food Chem., 46: 4475-4483, 1998.
5. Yokoi, S., Yamishita, K., Kunitake, N., and Koshimo, S. Hydrophobic beer proteins and their function in beer foam. J. Am. Soc. Brew. Chem. 52: 123-126, 1994.
6. Slack, P. T., and Bamforth, C. W. The fractionation of polypeptides from barley and beer by hydrophobic interaction chromatography: The influence of their hidrophobicity on foam stability. J. Inst. Brew. 89: 397-401, 1983.
7. Sorensen, S.B., Bech, L.M., Muldbejerg, M., Beenfeldet, T., and Breddam, K. Barley lipid transfer protein 1 is involved in beer foam formation. Tech. Q. Master Brew. Assoc. Am. 30: 136-145, 1993.
8. Curioni, A . , Pressi, G., Furegon, L., and Peruffo, D.B. Major proteins of beer and their precursors in barley: Electrophoretic and immunological studies. J. Agric. Food Chem. 43: 2620-2626, 1995.
9. Kauffman, J. A ., Mills, E. N.C., Brett, G.M., Fido, R.J., Tatham, A . S., Shewry, P.R., Onish, A . , Proudlove, M.O . , and Morgan, M. R.A . Immunological characterization of barley polypeptides in lager foam. J. Sci. Food Agric. 66: 345-355, 1994.
10. Hejgaard, J., Kaersgaard, P. Purification and properties of the major antigenic beer proteins of barley origin. J. Inst. Brew. 89, 402-410, 1983.
11. Brandt, A ., Sevendsen, I., and Hejgaard, J. A plant serpin gene structure, organization and expression of the gene encoding barley Z4. Eur. J. Biochem. 194: 499-505, 1990.
12. Evans, D.E., and Sheehan, M.C. Don't be fobbed off: The substance of beer foam – a review. J. Am. Soc. Brew. Chem. 60 (2): 47-57, 2002.
13. Brierley, E.R., Wilde, P.J., Onishi, A ., Hughes, P.S., Simpson, W.J. and Clark, D.C.
14. Lusk, L.T., Goldstein, H. and Ryder, D. J. Am. Soc. Brew. Chem. 53: 93-103, 1995.
15. Maeda, K., Yokoi, S., Kamada, K. and Kamimura, M. J. Am. Soc. Brew. Chem. 49: 14-18, 1990.
16. Asano, K. and Hashimoto, N. Report Research Laboratory Kirin Brew. Co., 19: 9, 1976.

INFLUENCE OF TEMPERING AND COCOA BUTTER ON RHEOLOGICAL PROPERTIES OF DARK CHOCOLATE

A. Pereira, J. Dias, N.B. Alvarenga, J. Canada*

ADCTA, Escola Superior Agrária de Beja, Rua de Pedro Soares, 7801-902 Beja, PORTUGAL
Tel. +351 284314300 Fax: +351 284388207
Email: joao.dias@esab.ipbeja.pt

Keywords: Chocolate, Tempering, Viscosity, Colorimeter, Cocoa butter

Abstract
The influence of tempering profile and addition of cocoa butter to dark chocolate was studied. The experimental methodology was close to similar studies on chocolate and included the evaluation of yield stress and plastic viscosity in chocolate at 40ºC. Three different profiles of tempering were tested in a viscometer at constant shear rate and using a water bath for temperature control. Samples of tempered chocolate were moulded in polycarbonate moulds for evaluation of force to fracture, in a texturometer, and colour, in a colorimeter. In general, the addition of cocoa butter influenced plastic viscosity ($p<0.05$), decreasing from 0.89 Pa.s (0% added cocoa butter) to 0.4 Pa.s (10% added cocoa butter). Also, yield stress was affected by the addition of cocoa butter ($p<0.05$), decreasing from 23.48 Pa (0% added cocoa butter) to 7.52 Pa (10% added cocoa butter). The results of the testing in small samples of moulded chocolate have showed a significant influence of added cocoa butter on force to fracture ($p<0.05$), decreasing from 2.78 N (0% added cocoa butter) to 2.03 N (10% added cocoa butter). The colour of chocolate was also influenced by the addition of cocoa butter, shifting to a yellowish colour. The results concluded that the tested tempering levels didn't present significant effects over any depending variable.

1. INTRODUCTION

Chocolate is eaten more for pleasure than for nutrition, therefore consumer appeal is the key to selling such a product successfully. In central Europe this is influenced by only a few parameters: the flavour needs to be creamy, sweet, and slightly cocoa with a harmonious aftertaste; no sandiness must to be perceivable; chocolates have to melt tenderly and quickly in the mouth without being sticky [1]. The majority of chocolate is produced via conventional routes, that is, the process is based on roasting, mixing, grinding, winnowing, refining and conching [2, 3]. These two last operations are crucial for a good quality: refining must achieve the correct particle size, while conching influences both flavour and flow properties [1]. Together with the right ingredients, processing technology is just as important for achieving this desired quality.

Cocoa butter is the main fat used for chocolate and is also a determinant factor for the properties of the final product, contributing for achieving the intended properties: good flavour, good texture, smooth texture and glossy appearance [4]. The triacylglycerol (TAG) composition of a fat is one of the most important parameters since it governs the physical properties as well as the polymorphic behaviour of the fat. Polymorphism is defined as the ability of a TAG molecule to crystallize in different molecular packing arrangements corresponding to different unit cell structures, typically characterized by X-ray diffraction spectroscopy [5]. Cocoa butter TAG can crystallize into 6 different polymorphic forms, usually denoted either by Greek letter or Roman numeral (or both). The melting points of each polymorph of cocoa butter are summarized in table 1.

Table 1. Melting point of different polymorphic forms of cocoa butter, by different authors

Vaeck	Duck	Willie and Lutton	Huygherbaert and Hendrickx	Lovegren et al.	Davis and Dimick
[ºC]					
18.0 (γ)	17.0 (γ)	17.3 (I)	14.9 – 16.1 (I)	13.0 (VI)	13.1 (I)
23.5 (α)	21 – 24 (α)	23.3 (II)	17.0 – 23.2 (II)	20.0 (V)	17.1 (II)
28.0 (β'')	28.0 (β'')	25.5 (III)	22.8 – 27.1 (III)	23.0 (IV)	22.4 (III)
-	33.0 (β')	27.3 (IV)	25.1 – 27.4 (IV)	25.0 (III)	26.4 (IV)
34.5 (β)	34.4 (β)	33.8 (V)	31.3 – 33.2 (V)	30.0 (II)	30.7 (V)
		36.3 (VI)	33.8 – 36.0 (VI)	33.5 (I)	33.8 (VI)

Source: [5]

One of the most important steps for producing chocolate of good quality is to achieve Form V, the correct crystalline structure of cocoa butter. The presence of any lower melting polymorphs lowers the quality of the final product in a number of ways [6]:

- Chocolate softens easier at room temperature. Chocolate melts over a range, and the presence of lower polymorphs will mean that a greater fraction the cocoa butter will be liquid at room temperature
- Chocolate is less easier to demould
- Lower polymorphs subsequently recrystallise into large form V or form VI crystals, causing "fat bloom" and decreasing the acceptance by the consumer

It is difficult, however, to achieve Form V by simple cooling of chocolate. Most large-scale chocolate production employs a tempering stage prior to moulding where a carefully controlled programme of shear and temperature generates seed crystals in Form V. This is a nucleation process which is highly dependent on the process parameters used [6]. In practice, tempering involves four steps: (1) complete melting of the chocolate to about 50ºC, which removes most or all of the crystalline material; (2) cooling to the point of crystallization; (3) maintaining a holding temperature for crystallization for about a minute; and (4) reheating to melt out unstable crystals. During this process, temperature control is very critical, and the shear applied within the process is also a crucial parameter [3].

The principal effect of tempering is to develop a population of seed crystals that are sufficient to avoid heterogeneous crystallization during cooling [7]. To be effective, tempering must provide a seed concentration between 0.1 to 1.15% of cocoa butter mass [8]. Other studies, however, concluded that larger amounts, 2 to 5% of cocoa butter, of seeds were needed for good temper. This difference may be due to differences in seed size, which affects the number of seed crystals. Von Drachenfels *et al*. specified the importance of crystal size [9]. The smaller and more regular the size of seed crystals, the glossier the chocolate and the greater its bloom resistance. On the other hand, if the crystal size is too large, the crystals tend to re-crystallize during the storage. Both effects could promote further bloom. Homogenous heat release, which occurs through the inside as well from the outerlayer, is the best way to avoid any tension on the chocolate surface and consequently, reduce subsequent bloom [10].

2. METHODOLOGY

For these experiments, dark chocolate "callets" Ref. 811 and cocoa butter ref. CB-666 from Callebaut were used. Experiments were carried out on chocolate, including determination of viscosity in three different tempering levels (figure 2), based in other studies [14], and in three different concentrations of additional cocoa butter: 0%, 2.5% and 10%.

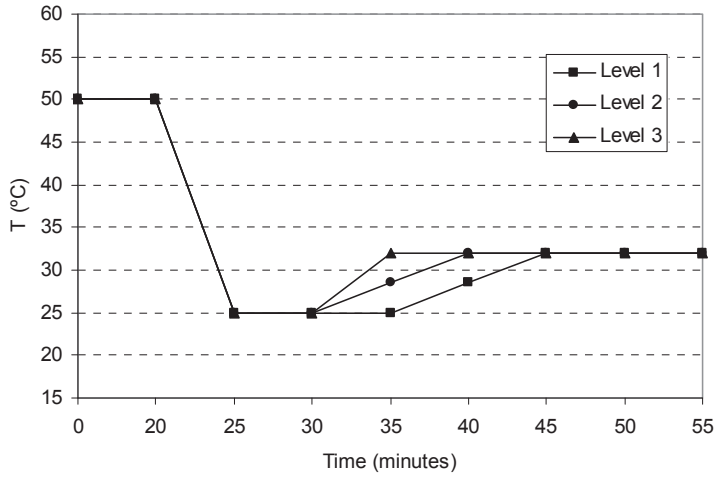

Figure 1: Tempering levels

As shown in figure 1, all tested tempering levels started melting the chocolate at 50ºC for 20 minutes, then cooled down to 25ºC. During tempering "Level 1", the temperature of chocolate was kept at 25ºC for 10 minutes, then was re-heated to 32ºC in 10 minutes and was kept inside the rheometer at this temperature for 10 minutes, prior to moulding. In tempering "Level 2", the temperature of chocolate was kept at 25ºC for 5 minutes, then was re-heated to 32ºC in 10 minutes and was kept inside the rheometer at this temperature for 10 minutes. Finally, in "Level 3", the temperature of chocolate was kept at 25ºC for 10 minutes, then was re-heated to 32ºC in 5 minutes and was kept at this temperature for 10 minutes, prior to moulding.

Viscosity measurements were carried out with a ThermoHaake VT 550 (Gebr. HAAKE GmbH, Germany) using a DIN 53019 sensor system (MV – DIN) and a water bath Grant with controlled temperature, including cooling and heating. This determination was performed at 40ºC, accordingly to OICCC standards [11]. The parameters of Casson model - plastic viscosity (η_P) and yield stress (τ_C) - were determined using the tangencial viscosity, for different shear rates.

The yield stress (τ_C) value was previously obtained by fitting the experimental data to the Casson model (Eq. 1) and calculating the square of the ordinate intercept in the Casson plot. Apparent viscosity values were obtained with the expression (Eq. 3).

$$\sigma = \sigma_0 + K\dot{\gamma}^{n} \qquad \text{Eq. 1}$$

$$\sigma^{0.5} = \sigma_0^{0.5} + K\dot{\gamma}^{0.5} \qquad \text{Eq. 2}$$

$$\eta_{ap} = \frac{\sigma_0}{\dot{\gamma}} + K\dot{\gamma}^{n-1} \qquad \text{Eq. 3}$$

For the testing of the tempering levels, 90g of chocolate "callets" were weighted into the MV cup and the chocolate was melted at 50ºC for 20 minutes, in a Clifton water bath with

temperature control. Afterwards, the cup was placed in the viscometer, and the apparent viscosity was measured, at shear rate (γ) $1s^{-1}$. The determination of force to fracture was carried out in a texturometer TAHDi® from Stable Micro Systems, using a 2mmØ cylindrical probe. The fracture force was considered to be the highest peak of the texturogram. The samples consisted in small chocolate discs 24mm Ø x 1mm height, maintained at 15ºC. The chocolate samples were produced using tempered chocolate, at 32ºC, poured into a polycarbonate mould, pre-heated at 30ºC. The chocolate colour was determined using a colorimeter Minolta CR-300 and was calibrated using a Minolta calibration plate (Y=92.7, x=.3134, y=.3195). The equipment presents the results accordingly to the L*, a* and b* system.

The effects of tempering and added cocoa butter in chocolate analysed by ANOVA. The Scheffé's ANOVA post hoc comparisons was used to evaluate the ability for discriminations. All calculations were carried out with the Statsoft STATISTICA 6.0 software.

3. DISCUSSION

The rheograms obtained in this study were similar to results obtained in other studies [12, 13]. The shear stress was plotted as a function of shear rate for each concentration of added cocoa butter (Figure 2). The addition of cocoa butter to chocolate decreased considerably the values of shear stress and yield stress. By the other hand, increasing values of cocoa butter in chocolate shown a lower relation between shear stress and shear rate, thus decreasing the measured values of plastic viscosity.

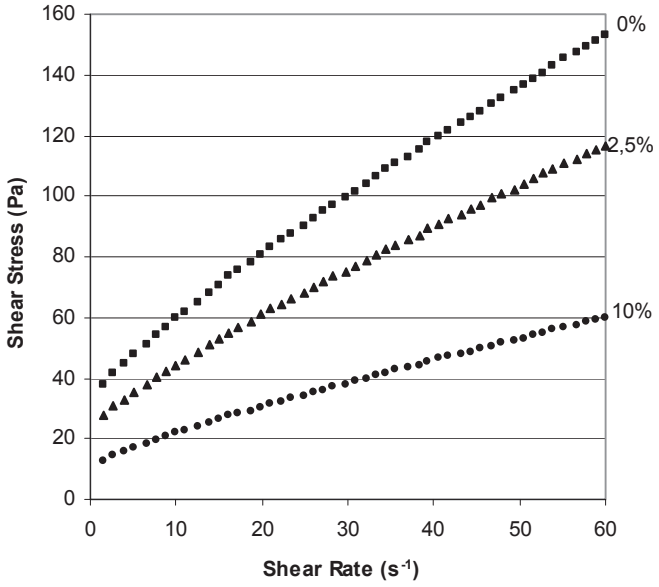

Figure 2: Rheogram of dark chocolate at 40ºC

The results of tempering profile of chocolate present a reduced influence on chocolate apparent viscosity (figure 3). Nevertheless, the measured apparent viscosity on tempering "Level 2" using 0% additional cocoa butter (figure 3b) presented lower viscosity values than tempering "Level 1" and "Level 3". The apparent viscosity of chocolate with 2.5% added cocoa butter presented similar evolution on tempering "Level 1" and "Level 2" but lower values on "Level 3", bellow 25 Pa.s (figure 3c). The apparent viscosity of chocolate with 10%

added cocoa butter presented the similar evolution on all tempering levels, and presented values of apparent viscosity around 10-13 Pa.s.

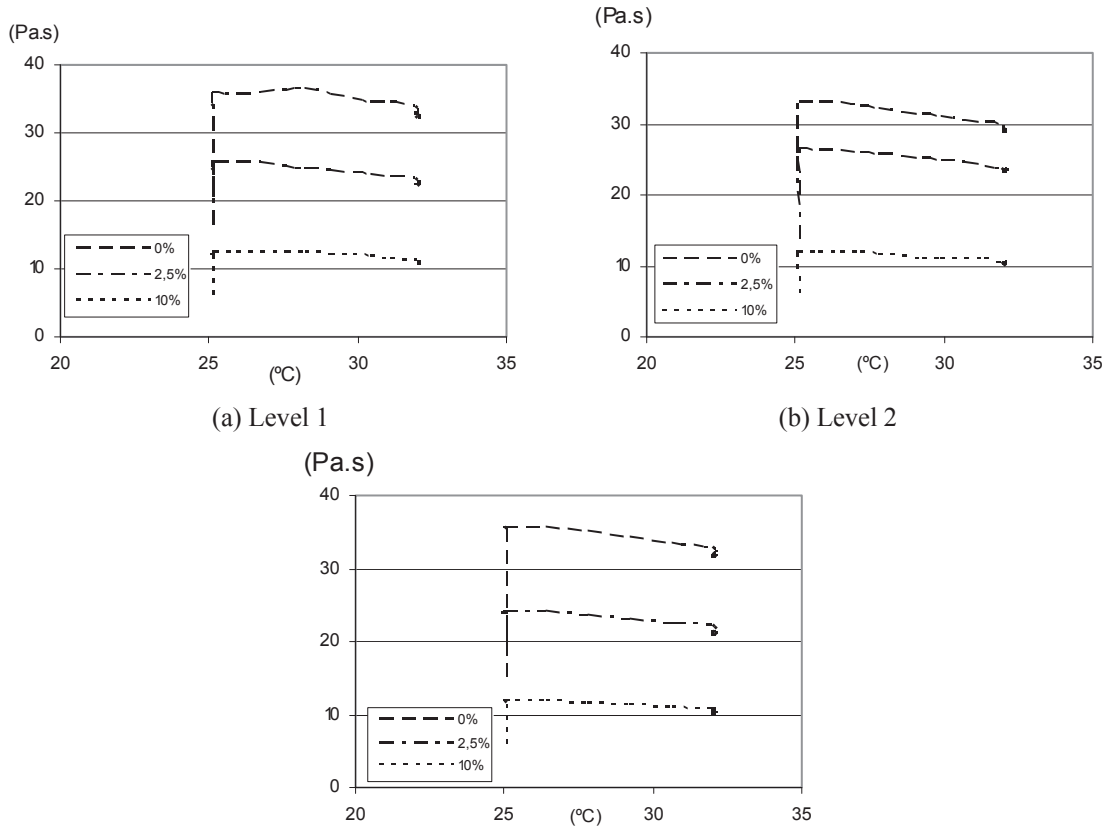

(a) Level 1 (b) Level 2

(c) Level 3

Figure 3: Apparent viscosity during chocolate tempering ($\gamma = 1s^{-1}$).

The two factors ANOVA concluded that tested tempering levels didn't present significant effects over any depending variable ($p<0.05$), however the addition of cocoa butter to chocolate presented a significant effect over yield stress (τ_C), plastic viscosity (η_P), force to fracture and parameter b* of colour ($p<0.05$). The interaction between tempering level and added cocoa butter did not present a significant effect over any dependant variable. The Scheffé's post hoc comparisons was used to evaluate the ability for discriminations and the results are presented in table 2.

Table 2: Average values on different cocoa butter concentrations and results of Scheffe's ANOVA post hoc comparisons

Added cocoa butter	Casson parameters		Force to fracture (N)	Colour		
	τ_C (Pa)	η_P (Pa.s)		L*	a*	b*
0%	23.48^a	0.89^a	2.78^a	31.85^a	4.76^a	3.44^b
2.5%	16.7^b	0.77^b	2.37^{ab}	31.46^a	4.78^a	3.88^{ab}
10%	7.52^c	0.4^c	2.03^b	31.01^a	4.76^a	4.11^a

Cocoa butter concentration presents a significant influence over Casson parameters and over force to fracture ($p<0.05$). The increasing values of cocoa butter concentration lowers the yield stress (τ_C), plastic viscosity (η_P) and force to fracture (table 2). This is due to a lubrification effect of the cocoa fat on the matrix, has stated in other studies [12].

The results of colorimeter conclude that only parameter b* is affected by cocoa butter concentration ($p<0.05$). The increasing concentration of cocoa butter increases the value of parameter b*, shifting to the yellowish region, typical colour of cocoa butter.

4. ACKNOWLEDGMENTS

The authors would like to thank the contribution of Mr. Vitor Nunes (BakeMark).
The authors would like to thank the contribution of Prof. Silvina Ferro Palma and Eng. Manuela Costa (ESAB).

5. REFERENCES

[1] Bolenz, S.; Thiessenhusen, T.; Schape, R. (2003). "Fast conching for milk chocolate" in *Eur. Food Res. Technol*. **218**: 62 - 67
[2] Minifie, B. (1980). *Chocolate, cocoa and confectionery: science and technology*. 2nd Edition. AVI Publishing Company, Inc., Westport, USA
[3] Fryer, P.; Pinschower, K. (2000). "The materials science of chocolate" in *MRS Bulletin*, December. In *http://www.mrs.org/publications/bulletin* (visited 27th April 2004)
[4] Rebelo, R. (2000). *A manteiga de cacao e a gordura do leite na indústria*. Relatório do trabalho de fim de curso de Engenharia Agro-Industrial. Instituto Superior de Agronomia, Universidade Técnica de Lisboa.
[5] Lonchampt, P.; Hartel, R. (2004). "Fat bloom in chocolate and compound coatings" in *Eur. J. Lipid Sci. Technol.* **106**: 241 - 274
[6] Tewkesbury, H.; Stapley, A.; Fryer, P. (2000). "Modelling temperature distributions in cooling chocolate moulds" in *Chemical Engineering Science* **55**: 3123 - 3132
[7] Giddey, C.; Clerc, E. (1961). "Polymorphism of cocoa butter and its importance in the chocolate industry" in *Rev. Int. Choc*. **16:** 548–554. Cit. in Lonchampt and Hartel (2004)
[8] Loisel, C.; Lecq, G.; Keller, G.; Ollivon, M. (1997). "Fat bloom and chocolate structure studied by mercury porosimetry" in *J. Food Sci*. **62:** 781–788. Cit. in Lonchampt and Hartel (2004)
[9] Von Drachenfels, H.; Kleinert, J.; Hanssen, E. (1962). "A new method of preventing fat bloom" in *Rev. Int. Choc*. **XVII:** 409–410. Cit. in Lonchampt and Hartel (2004)
[10] Kleinert, J. (1962). "Studies on the formation of fat bloom and methods of delaying it" in *Rev. Int. Choc.* **16:** 201–219. Cit. in Lonchampt and Hartel (2004)
[11] OICCC (2000). *Standard 10/1973. Viscosity of cocoa and chocolate products*. Ed. Office International du Cacao, du Chocolat et de la Confiserie
[12] Beckett, S. (2004). *The science of chocolate*. The Royal Society of Chemistry, Cambridge.
[13] Steffe, J. (1996). *Rheological methods in food process engineering*. 2nd Edition. Freeman Press, East Lansing
[14] Smith, R. e Nelson, R. (no date). *The tempering and rheological profile of chocolate.* In Loughborough University: *http://www.lboro.ac.uk* (visited 24th May 2004)

INSTRUMENTAL AND SENSORY PROPERTIES OF MASHED POTATOES AT DIFFERENT TEMPERATURES

M.D. Alvarez,[1] Cristina Fernández,[1] Wenceslao Canet,[1] M.E. Tortosa[2]*

[1]Department of Plant Foods Science and Technology, Instituto del Frío-CSIC, José de Novaís nº 10, E-28040 Madrid, Spain. Tel: +34 91 5492300; Fax: +34 91 5493627; Email: ifrat44@if.csic.es
[2]Department of Plant Physiology and Biology, Escuela Técnica Superior de Ingenieros Agrónomos, Ciudad Universitaria s/n, E-28040 Madrid, Spain

Keywords: Sample temperature; TPA test; Firmness test; Sensory analysis; Structure

Abstract Sample temperature effect on textural and firmness parameters and sensory attributes of fresh and frozen/thawed natural and commercial mashed potatoes was studied. SEM was used to obtain information on the structure of potato cells and how this is affected by processing. Instrumental parameters or sensory attributes were found to increase at 55 °C, which could be related to gelatinisation of the remaining starch in the products. In natural mashed potato, TPA and firmness parameters were lower in processed than in fresh samples, indicating a weakening of the structure, as confirmed by microphotographs. In commercial mashed potato, TPA parameters at 55 and 65 °C and firmness parameters at 25 °C were higher in the processed samples, indicating enhanced structural strength as confirmed by microphotographs. Firmness per gram of product was the best instrumental parameter for measuring texture in these products. The results of the different analyses indicated that 55 °C was the preferred sample temperature for consumption of mashed potatoes.

1. INTRODUCTION

Fresh mashed potato and flakes stood at opposite extremes in terms of stickiness, firmness and coarseness irrespective of treatments. The product with most preferred texture, fresh mashed potato, was the least sticky while flake product, which was the least preferred, was the stickiest [1]. After cooking or reconstitution, mashed potato may be subjected to thermal treatments. Freezing reduced the G', G" and η* values of mashed potatoes made from flakes, measured at 20 °C, as compared with freshly made product [2]. Recent studies have described the effect of individual and mixtures of hydrocolloids on the quality of frozen and thawed cooked potato purees [3, 4]. Rheological characterisation of semisolid foods usually entails viscosity and viscoelastic measurements [5]. Instrumental objective tests used for measuring the texture of solid food may be perfectly valid for semisolid products, with the advantage that they provide a rapid means of ascertaining and characterising product texture. The purposes of the present study were (i) to characterise the texture of natural and commercial mashed potatoes, instrumentally by Texture Profile Analysis (TPA) and firmness tests, and by sensory analysis; and (ii) to determine the effects of sample temperature and freezing/thawing on instrumental parameters and sensory attributes. Correlations between the structures and the physical characteristics of the obtained products were sought.

2. MATERIALS AND METHODS

2.1 Preparation of samples

For preparation of natural mashed, fresh tubers (cv. Kennebec) were selected. Tubers were manually washed, peeled and diced. Mashed was prepared from 395 g of potatoes, 150 ml of milk, 100 ml of water and 5 g salt using a Thermomix TM 21. Ingredients were cooked

(20 min/100 °C), and the liquid evaporated was determined by weighing the ingredients before and after boiling. This was compensated by addition of boiling water, and the ingredients were again cooked (5 min/100 °C). The mash was triturated for 40 s. The product was homogenised through a stainless steel sieve (diameter 1.5-mm). For preparation of commercial mashed potato, aseptically packed commercial dehydrated potato flakes were used and mashed prepared according to label instructions. Following preparation, half of each sample was packed in polyethylene plastic, sealed under light vacuum (-0.05 MPa) on a Multivac packing machine and immediately frozen to –80 °C. The packs were then kept for 1 week in a freezer at –80 °C. Determinations were made on frozen samples after these had thawed overnight in a domestic refrigerator. Temperatures of 25, 35, 45, 55 and 65 °C were reached in the fresh and frozen/thawed samples by placing them in a CB60VS waterbath (-30 to +110 °C) with a constant product weight:water volume ratio of 1:20. Water and product temperatures were monitored by K-type thermocouples using a hardware and software system developed by Rico *et al*. [6].

2.2 Instrumental texture measurements

TPA and firmness tests were performed with a TA.HDi Texture Analyzer (Stable Micro Systems Ltd, Godalming, UK) using a 250 N load cell and the application program Texture Expert for Windows^{TM}, version 2.61. During the tests, the different sample temperatures were maintained using a Temperature Controlled Peltier Cabinet (XT/PC) coupled to a heat exchanger and PID control unit (Fig. 1). For performance of the TPA tests, a flat 35-mm diameter aluminium plunger (SMS P/35) was used to penetrate a 60-mm diameter stainless steel cylinder containing 50±1 g of mashed potatoes (Fig. 1A). The experimental conditions were: deformation rate (180 mm min^{-1}), compression level (33.3 %), and a rest period of 5 s between cycles. The software automatically calculates the hardness (N), adhesiveness (N s), springiness, cohesiveness and gumminess (N) from the curve generated by such a test.

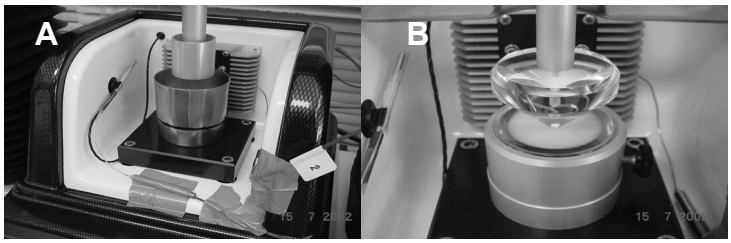

Figure 1 Attachments used with the TA.HDi texturometer in the instrumental measurements: A - cylinder probe and container used for TPA tests; B - spreadability rig used for firmness tests.

For performance of the firmness tests, a spreadability rig was used (Fig. 1B), consisting of a 45° conical perspex probe (P/45 C) that penetrates a conical sample holder containing 7±0.1 g of mashed potatoes. Deformation rate was of 180 mm min^{-1}. The force time curve was used to calculate the firmness (N), the area under the curve force versus time (N s), the firmness per g of product (N g^{-1}), the area under the curve per displaced volume (N s mm^{-3}) and the average force (N).

2.3 Sensory analysis

A five-member panel trained specifically in mashed potato conducted sensory texture profile analysis. Texture profile [7] was modified to evaluate frozen mashed vegetables. Scores for attributes were based on a 9-point descriptive intensity scale that was converted to

a 0-9 numerical scale for statistical analysis, with 0 = not detectable and 9 = extremely intense. Mashed samples were also subjected to an overall acceptability test in respect of all sensory attributes (texture, colour, taste) on a 9-point hedonic scale (9 = like extremely, 1 = dislike extremely).

2.4 Microscopic examination

SEM using a Hitachi model S-2500 microscope examined microstructure. Mashed potatoes were air-dried, then mounted and sputter-coated with platinum (400-A) in a P-S1 diode sputtering system metallizer. Microphotographs were taken with a Mamiya camera (Mamiya America Corporation, Elmsford, NY) using Ilford 6x9 cm FF-4 film (Ilford Imaging Group, Madrid, Spain). Films were processed following the standard method.

2.5 Statistical analysis

Statgraphics® software version 5.0 (STSC Inc., Rockville, MD) was used to perform analysis of variance and least significant difference (l.s.d.) tests. Confidence levels were 99% for instrumental parameters and 95% for sensory attributes.

3. RESULTS AND DISCUSSION

3.1 Instrumental parameters

Table 1 Sample temperature effect on textural parameters: natural and commercial mashed potatoes*

Temperature (°C)	Hardness (N)	Adhesiveness (N s)	Springiness	Cohesiveness	Gumminess (N)
Fresh natural mashed potatoes					
25	2.154 (0.140) a, b	-3.529 (0.523) a	0.972 (0.009) a	0.784 (0.030) a	1.681 (0.054) a
35	1.966 (0.066) b, c	-3.415 (0.215) a	0.924 (0.021) b	0.725 (0.043) a	1.430 (0.049) b, c
45	1.811 (0.039) c	-3.500 (0.195) a	0.891 (0.020) b	0.739 (0.022) a	1.338 (0.023) c
55	2.312 (0.131) a	-3.806 (0.442) a	0.920 (0.020) b	0.749 (0.037) a	1.723 (0.086) a
65	1.918 (0.081) b, c	-3.434 (0.388) a	0.915 (0.016) b	0.791 (0.037) a	1.516 (0.048) b
LSD (1%)	0.239	0.902	0.043	0.083	0.134
Frozen/thawed natural mashed potatoes					
25	0.697 (0.088) a	-0.535 (0.037) a	0.518 (0.014) a	0.806 (0.018) a	0.555 (0.033) a
35	0.986 (0.017) b	-1.242 (0.092) b	0.800 (0.050) b	0.740 (0.030) b, c	0.727 (0.017) b
45	1.017 (0.081) b	-1.565 (0.082) b	0.844 (0.018) b, c	0.711 (0.027) c	0.725 (0.019) b
55	1.355 (0.100) c	-2.667 (0.175) c	0.890 (0.014) c	0.799 (0.010) a	1.083 (0.085) d
65	1.137 (0.062) b	-2.984 (0.258) c	0.904 (0.015) c	0.789 (0.017) a, b	0.896 (0.035) c
LSD (1%)	0.181	0.363	0.063	0.052	0.108
Fresh commercial mashed potatoes					
25	1.712 (0.205) a	-2.552 (0.138) a	0.875 (0.078) a	0.923 (0.062) a	1.451 (0.191) b
35	2.422 (0.197) b, c	-2.421 (0.203) a	0.781 (0.048) a, b	0.744 (0.063) b, c	2.116 (0.122) a
45	2.051 (0.119) a, b	-2.437 (0.123) a	0.825 (0.070) a	0.871 (0.056) a, b	1.593 (0.127) b
55	2.682 (0.175) c	-1.707 (0.255) b	0.644 (0.058) b	0.614 (0.056) c, d	1.551 (0.088) b
65	1.928 (0.118) a	-1.423 (0.265) b	0.639 (0.032) b	0.569 (0.058) d	1.087 (0.148) c
LSD (1%)	0.402	0.494	0.143	0.142	0.336
Frozen/thawed commercial mashed potatoes					
25	4.892 (0.058) a	-0.704 (0.123) a	0.505 (0.040) a	0.403 (0.007) a	1.973 (0.081) a
35	1.551 (0.104) b, c	-0.518 (0.015) a	0.507 (0.046) a	0.499 (0.010) b	0.774 (0.058) c
45	0.865 (0.062) d	-0.818 (0.012) a	0.588 (0.066) a	0.651 (0.034) c	0.562 (0.033) d
55	1.436 (0.089) c	-2.477 (0.250) b	0.806 (0.069) b	0.937 (0.033) d	1.352 (0.052) b
65	1.683 (0.159) b	-3.301 (0.176) c	0.894 (0.018) b	0.897 (0.035) d	1.506 (0.096) b
LSD (1%)	0.244	0.356	0.123	0.065	0.163

*Mean (s.d.) of four determinations. [a,b,c,d] Different letters in the same column indicate significant differences $P < 0.01$.

In fresh natural mashed, temperature significantly affected hardness, springiness and gumminess (Table 1). Hardness and gumminess were highest at 55 °C. In frozen/thawed

natural mashed, temperature significantly affected all textural parameters evidencing as temperature affected processed samples more significantly than fresh samples. In frozen/thawed natural mashed, all parameters except cohesiveness increased with increasing temperature, indicating that higher temperature reinforced structural strength. Again, hardness and gumminess were highest at 55 °C. For natural mashed, all TPA parameters except cohesiveness were lower in the processed than in the fresh samples, which suggests that the product structure was weakened by freezing and thawing. In fresh and frozen/thawed commercial mashed (Table 1), sample temperature again significantly affected all textural parameters. In fresh samples, adhesiveness, springiness and cohesiveness decreased significantly with increasing sample temperature. In frozen/thawed commercial samples, adhesiveness, springiness and cohesiveness increased with increasing sample temperature. Hardness and gumminess decreased up to 45 °C, increasing again at 55 and 65 °C. Values of most textural parameters were higher in processed than in fresh samples at both 55 and 65 °C. Sample temperature affected significantly all the firmness parameters in fresh and frozen natural and commercial mashed (Table 2). In fresh mashed, the highest parameters were recorded at 55 °C. Values of all parameters were lowest at 65 °C, indicating loss of structural strength when a high temperature was reached. In processed mashed, firmness values were also higher at 55 °C than at 45 and 65 °C. Mashed potato is a starchy food, and it has been proposed that rheological properties of starch dispersions be based on the mass fraction of starch granules [8]. Gelatinisation of potato starch occurs in a temperature range of 50-60 °C [9, 10]. Results suggest that at the higher temperatures (chiefly 55 °C), there was some gelatinisation of the starch remaining in the products, which could account for the increase in the values of both TPA and firmness parameters at this temperature.

Table 2 Sample temperature effect on firmness parameters: natural and commercial mashed potatoes*

Temperature (°C)	Firmness (N)	Area (N s)	Firmness/product g (N g^{-1})	Area/disp vol (N s mm^{-3})	Average force (N)
Fresh natural mashed potatoes					
25	3.784 (0.139) a	4.037 (0.198) a	0.533 (0.013) a	5.372E-04 (2.64E-05) b	0.524 (0.026) a
35	3.070 (0.104) b	3.313 (0.201) b	0.429 (0.010) b	4.407E-04 (2.67E-05) c	0.430 (0.026) b
45	3.006 (0.137) b	3.208 (0.183) b	0.417 (0.015) b	4.270E-04 (2.44E-05) c	0.416 (0.024) b
55	4.426 (0.172) c	4.950 (0.353) c	0.606 (0.024) c	6.587E-04 (4.70E-05) a	0.642 (0.046) c
65	2.708 (0.224) b	2.765 (0.157) b	0.380 (0.033) b	3.682E-04 (2.09E-05) c	0.359 (0.020) b
LSD (1%)	0.387	0.552	0.050	0.0001	0.071
Frozen/thawed natural mashed potatoes					
25	3.378 (0.161) a	2.307 (0.149) a	0.467 (0.020) a	3.072E-04 (1.99E-05) a	0.299 (0.019) a
35	2.359 (0.197) b	2.125 (0.204) a, b	0.331 (0.026) b	2.830E-04 (2.72E-05) a, b	0.276 (0.027) a, b
45	1.644 (0.111) c, d	1.526 (0.100) c, d	0.233 (0.017) c, d	2.035E-04 (1.33E-05) c, d	0.198 (0.013) c, d
55	1.803 (0.083) c	1.858 (0.131) b, c	0.250 (0.013) c	2.472E-04 (1.75E-05) b, c	0.241 (0.017) b, c
65	1.438 (0.066) d	1.463 (0.110) d	0.203 (0.008) d	1.950E-04 (1.46E-05) d	0.190 (0.014) d
LSD (1%)	0.320	0.346	0.043	0.0001	0.045
Fresh commercial mashed potatoes					
25	8.835 (0.451) a	7.273 (0.359) a	1.227 (0.052) a	9.687E-04 (4.83E-05) a	0.943 (0.046) a
35	6.552 (0.309) b	6.116 (0.361) b	0.924 (0.043) b	8.140E-04 (4.78E-05) b	0.792 (0.047) b
45	2.478 (0.290) d	2.249 (0.302) d	0.351 (0.045) d	2.992E-04 (4.02E-05) d	0.291 (0.039) d
55	3.959 (0.219) c	3.584 (0.239) c	0.552 (0.037) c	4.772E-04 (3.18E-05) c	0.464 (0.031) c
65	2.681 (0.187) d	2.345 (0.178) d	0.373 (0.020) d	3.122E-04 (2.37E-05) d	0.304 (0.023) d
LSD (99%)	0.734	0.713	0.098	0.0001	0.092
Frozen/thawed commercial mashed potatoes					
25	12.244 (0.750) a	9.433 (0.313) a	1.692 (0.086) a	12.575E-04 (4.32E-05) a	1.220 (0.041) a
35	3.079 (0.160) b	2.566 (0.086) b	0.440 (0.023) b	3.418E-04 (1.15E-05) b	0.333 (0.011) b
45	1.856 (0.102) c	1.610 (0.079) c	0.258 (0.012) c	2.145E-04 (1.05E-05) c	0.209 (0.010) c
55	2.832 (0.347) b	2.528 (0.282) b	0.402 (0.051) b	3.368E-04 (3.76E-05) b	0.328 (0.037) b
65	2.403 (0.112) b, c	2.175 (0.102) b	0.331 (0.014) b, c	2.895E-04 (1.35E-05) b	0.282 (0.013) b
LSD (99%)	0.921	0.483	0.112	0.0001	0.062

*Mean (s.d.) of four determinations. [a,b,c,d] Different letters in the same column indicate significant differences $P < 0.01$.

In processed natural mashed, the lowest values for all firmness parameters were again found at 65 °C, indicating fluidification of the product at that temperature. Firmness

parameters indicated weakening of the gel structure of both fresh and processed natural mashed when a given temperature threshold was passed, and they were lower in processed than in fresh samples. In both commercial samples, values for all parameters decreased with increasing temperature, indicating fluidification with increasing temperature. In this product also, parameter values were higher at 55 °C than at 45 or 65 °C; again, this could be connected with gelatinisation of the remaining starch. Firmness parameters at 25 °C, like TPA parameters at 55 and 65 °C, were also higher in processed than in fresh samples, indicating that freezing and thawing of commercial mashed led to the creation of a coarsely aggregated structure.

3.2 Sensory analysis

In fresh natural and frozen/thawed commercial mashed, granularity decreased and moisture increased significantly with increasing temperature (Table 3). In frozen/thawed natural product, granularity again decreased significantly with increasing temperature. In fresh commercial mashed, granularity decreased and moisture increased, although the effect of temperature was less significant in commercial mashed. Scores for both attributes were higher in the processed samples than in the fresh samples, indicating that processing rendered granularity and moisture more appreciable. In all the samples, temperature significantly affected attributes perceived on putting the sample in the mouth, except for moisture in frozen natural samples (Table 4).

Table 3 Sample temperature effect on sensory attributes perceived before putting the sample in the mouth: fresh and frozen/thawed natural and commercial mashed potatoes*

	Fresh natural mashed potatoes		Fresh commercial mashed potatoes	
Temperature (°C)	Granularity	Moisture	Granularity	Moisture
25	2.100 (0.529) a	2.433 (0.153) a	2.067 (0.503) a, b	3.267 (1.332) a, b
35	0.900 (0.265) b	6.733 (0.379) c	2.867 (1.617) a	3.333 (1.102) b
45	0.900 (0.300) b	5.400 (0.300) b	1.300 (0.361) b	5.567 (1.079) c
55	0.766 (0.252) b	5.633 (0.651) b	2.133 (0.306) a, b	1.567 (0.252) a
65	0.600 (0.100) b	6.866 (0.907) c	0.900 (0.436) b	4.000 (0.520) b, c
LSD(95%)	0.583	0.998	1.474	1.723
	Frozen/thawed natural mashed potatoes		Frozen/thawed commercial mashed potatoes	
25	6.800 (0.778) a	7.133 (1.196) a	7.533 (0.451) a	1.833 (0.551) a
35	6.567 (0.783) a	7.466 (1.339) a	7.067 (0.924) a	3.467 (0.907) b
45	1.333 (0.836) b	5.633 (1.682) a	6.467 (0.611) a	7.200 (0.700) c
55	1.200 (0.432) b	6.267 (1.434) a	2.200 (0.755) b	6.600 (0.872) c
65	0.766 (0.905) b	5.567 (1.737) a	0.400 (0.200) c	6.533 (0.208) c
LSD(95%)	0.646	1.939	1.162	1.266

*Mean (s.d.) of five panellist's scores. [a,b,c] Different letters in the same column indicate significant differences $P < 0.05$.

Scores for commercial mashed is not shown. In general terms, these attributes increased with increasing temperature and scored highest at 55 and 65 °C. Results suggest that the panellists also detected gelatinisation of potato starch remaining in the samples at these temperatures. In fresh and frozen/thawed natural mashed, cohesiveness and adhesiveness significantly increased and fibrosity decreased with increasing temperature (Table 5). The effect of sample temperature on these attributes was less significant in fresh commercial mashed, where fibrosity was highest in samples at 55 °C. In frozen/thawed commercial mashed, cohesiveness and adhesiveness also increased significantly with increasing temperature.

Table 4 Sample temperature effect on sensory attributes perceived at the time of putting the sample in the mouth: fresh and frozen/thawed natural mashed potatoes*

Fresh natural mashed potatoes					
Temperature (°C)	Adhesiveness	Denseness	Homogeneity	Moisture	Firmness
25	1.667 (0.681) a	4.333 (1.234) a, b	6.000 (0.557) a	2.133 (0.379) a	2.333 (0.586) a
35	4.567 (0.737) b	3.200 (0.520) a	7.533 (0.208) b	6.900 (0.557) b	4.700 (0.781) b
45	5.067 (0.981) b	5.167 (1.069) b, c	7.567 (0.404) b	6.200 (0.200) b	4.933 (0.757) b
55	5.000 (1.323) b	5.300 (0.600) b, c	7.800 (0.100) b	6.600 (0.361) b	6.500 (0.436) c
65	5.133 (0.802) b	6.300 (0.346) c	7.267 (0.551) b	6.433 (0.945) b	5.533 (0.503) b, c
LSD(95%)	1.700	1.504	0.741	1.002	1.142
Frozen/thawed natural mashed potatoes					
25	2.700 (1.125) a	2.367 (0.721) a	2.433 (0.848) a	6.567 (0.721) a	2.867 (0.684) a
35	2.000 (1.125) a	2.467 (0.935) a	4.033 (1.875) a	7.333 (1.473) a	3.100 (1.187) a
45	5.200 (1.286) b	5.367 (0.935) b	5.100 (1.532) a	6.800 (0.890) a	5.500 (0.697) b
55	4.933 (1.183) b	5.433 (0.640) b	7.567 (0.836) a, b	7.533 (0.811) a	5.867 (1.328) b
65	5.333 (0.547) b	6.133 (0.684) b	7.600 (0.605) b	7.500 (0.952) a	6.100 (0.793) b
LSD(95%)	1.225	0.679	1.557	1.089	1.041

*Mean (s.d.) of five panellist's scores. [a,b,c] Different letters in the same column indicate significant differences $P < 0.05$.

Table 5 Sample temperature effect on sensory attributes perceived at the time of preparing the sample for swallowing: fresh and frozen/thawed natural and commercial mashed potatoes*

	Fresh natural mashed potatoes			Fresh commercial mashed potatoes		
Temperature (°C)	Cohesiveness	Adhesiveness	Fibrosity	Cohesiveness	Adhesiveness	Fibrosity
25	3.167 (0.971) a	3.267 (1.021) a	1.233 (0.351) a	4.533 (0.709) a	4.200 (0.985) a	1.033 (0.635) a
35	3.567 (1.250) a	5.400 (1.323) b	1.167 (0.289) a	7.433 (0.577) c	6.733 (0.603) c	0.767 (0.379) a
45	3.267 (0.611) a	5.730 (0.115) b	0.733 (0.231) a, b	5.433 (0.416) a	4.400 (0.400) a, b	1.533 (0.473) a, b
55	5.867 (0.666) b	5.900 (0.656) b	0.900 (0.346) a	6.733 (0.666) b, c	6.967 (1.102) c	2.100 (0.608) b
65	6.033 (0.702) b	6.000 (0.608) b	0.367 (0.153) b	5.600 (0.985) a, b	5.867 (1.137) b, c	1.200 (0.200) a
LSD(95%)	1.590	1.545	0.517	1.267	1.628	0.884
	Frozen/thawed natural mashed potatoes			Frozen/thawed commercial mashed potatoes		
25	2.333 (0.836) a, b	1.900 (1.056) a	1.400 (0.793) a, b	3.567 (0.513) a	2.300 (0.700) a	1.700 (0.346) a, b
35	2.100 (0.697) a	2.000 (1.321) a	1.933 (1.361) b	1.633 (0.404) b	1.533 (0.404) a	2.867 (1.701) b
45	3.267 (0.848) b	4.933 (1.189) b	1.767 (0.836) b	1.433 (0.764) b	1.600 (0.436) a	4.900 (1.652) c
55	6.133 (1.403) c	6.267 (1.403) b, c	1.100 (0.632) a, b	6.167 (1.650) c	4.733 (0.289) b	1.800 (0.300) a, b
65	5.800 (0.778) c	6.400 (0.532) c	0.600 (0.697) a	5.567 (0.751) c	6.133 (0.603) c	0.633 (0.321) a
LSD(95%)	0.987	3.042	0.916	1.687	0.924	1.983

*Mean (s.d.) of five panellist's scores. [a,b,c] Different letters in the same column for each type of puree indicate significant differences $P < 0.05$.

In fresh natural mashed, the panellists found the 55 °C samples the most acceptable (Table 6). In frozen/thawed natural and commercial mashed, the panellists scored the 65 ºC samples highest for overall acceptability. In fresh commercial mashed, panellists scored the 45 ºC samples highest for overall acceptability. Results of instrumental measurements and sensory analysis, combined with the overall acceptability tests, show that preferred temperature for consumption was 55 °C or 65 °C.

Table 6 Sample temperature effect on sensory attributes perceived during the final and residual phases of mastication and on *overall acceptability*:fresh and frozen/thawed natural and commercial mashed potatoes

	Fresh natural mashed potatoes				Fresh commercial mashed potatoes			
T[a] (°C)	Easy to swallow	Palate coating	Fibrosity	*Overall acceptability*	Easy to swallow	Palate coating	Fibrosity	*Overall acceptability*
25	6.367 (0.757) a	4.800 (0.700) a	0.900 (0.100) a	5.333 (0.473) a	5.800 (0.436) a, b	5.300 (1.300) a	2.533 (0.651) a	4.067 (0.850) a
35	6.867 (0.833) a	7.333 (0.351) b	0.867 (0.252) a	6.666 (0.643) b	5.267 (1.069) b	5.967 (0.379) a, b	2.367 (0.252) a, b	4.300 (0.300) a
45	7.267 (1.021) a	6.733 (0.115) b	0.567 (0.208) a	5.633 (0.577) a	6.967 (0.351) a	6.967 (0.321) b	1.667 (0.252) b, c	6.200 (1.212) b
55	6.600 (0.656) a	6.867 (0.651) b	0.700 (0.173) a	7.500 (0.608) b	1.733 (0.252) c	2.600 (0.173) c	1.667 (0.702) b, c	5.367 (0.814) a, b
65	6.467 (0.569) a	7.167 (0.252) b	0.667 (0.289) a	7.267 (0.208) b	6.767 (0.808) a	6.467 (0.666) a, b	1.167 (0.252) c	6.100 (0.693) b
LSD(95%)	1.424	0.859	0.390	0.957	1.198	1.264	0.856	1.506
	Frozen/thawed natural mashed potatoes				Frozen/thawed commercial mashed potatoes			
25	6.267 (1.393) a	1.900 (1.298) a	1.867 (1.361) a, b	2.500 (1.056) a	3.433 (1.041) a	6.467 (0.451) a, b	1.500 (0.473) a	0.467 (0.473) a
35	6.100 (1.490) a	6.633 (0.753) b	2.367 (1.529) a	2.867 (0.905) a	2.267 (0.252) a	6.233 (0.777) a, b	2.867 (0.351) b	1.267 (0.351) a
45	6.867 (0.945) a	6.533 (1.098) b	1.867 (0.738) a, b	5.167 (1.458) b	6.400 (1.153) b	5.067 (1.222) a	6.000 (1.124) c	3.233 (1.124) b
55	5.800 (1.885) a	6.267 (1.690) b	1.200 (0.532) a, b	6.300 (1.386) b, c	6.933 (0.850) b	7.433 (0.473) b	1.167 (1.007) a	6.167 (1.007) c
65	7.233 (1.183) a	7.067 (1.240) b	0.800 (1.040) b	6.733 (1.075) c	6.533 (1.301) b	7.200 (0.721) b	0.700 (1.159) a	6.933 (1.159) c
LSD(95%)	1.816	1.530	1.297	1.407	1.800	1.420	0.982	1.621

*Mean (s.d.) of five panellist's scores. [a,b,c] Different letters in the same column indicate significant differences $P < 0.05$.

3.3 Microstructure examination

In fresh natural mashed, cooked cells were still firmly bound together by degraded cementing materials and by starch gel released from damaged cells and forming cell aggregates (Fig. 2A). In the reconstituted product, more cells embedded in starch gel appear separated from one another (Fig. 2C). Natural mashed contains more cell aggregates, which could give it greater mechanical strength; this would account for the fact that the mechanical parameters are higher in natural than in commercial mashed. In both potato cells, the surface is rough; the cell walls show wrinkles and folds (Figs. 2B, 2D).

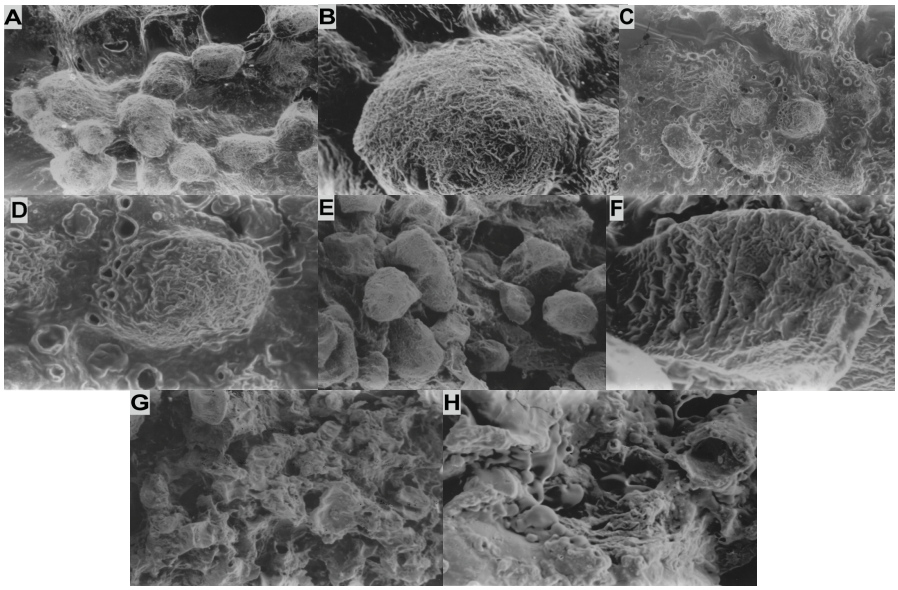

Figure 2 Microphotographs of mashed potato products: A, B fresh natural (1 cm = 250 μm and 1 cm = 70 μm respectively); C, D fresh commercial (1 cm = 250 μm and 1 cm = 70 μm respectively); E, F frozen/thawed natural (1 cm = 250 μm and 1 cm = 25 μm respectively); G, H frozen/thawed commercial (1 cm = 454 μm and 1 cm = 70 μm respectively).

After freezing/thawing of natural mashed, some cells still formed cell aggregates, but a comparison of Figs. 2A and 2E explains why instrumental parameters are lower in frozen than in fresh natural mashed. Ice crystals were formed outside and inside the cells, leaving most of them visibly shrunken (Figs. 2E, 2F). The starch gel also retrograded more fully under freeze-thaw conditions [11]. In the frozen/thawed commercial mashed all the cells appear broken, torn apart and embedded in a retrograded starch gel. That appears be the cause of a hard final product, explaining why instrumental parameters are higher in the frozen than in the fresh commercial mashed (Figs. 2G, 2H).

References

1. Novais, A., Hanson, S.W. & Ryley, J. The texture of mashed potatoes in catering I. The background. The contribution of hedonic texture to overall preference. Lebensm Wiss und-Technol, 15, 295-302 (1982).
2. Alvarez, M.D. & Canet, W. Rheological properties of mashed potatoes made from dehydrated flakes: effect of ingredients and freezing. Eur Food Res and Technol, 209, 335-342 (1999).
3. Downey, G. Quality changes in frozen and thawed, cooked puréed vegetables containing hydrocolloids, gums and dairy powders. Int J Food Sci and Technol, 37, 869-877 (2002).
4. Downey, G. Effects of cryoprotectant mixtures on physical properties of frozen and thawed puréed cooked potatoes: some introductory studies. Int J Food Sci and Technol, 38, 857-868 (2003).
5. Alvarez, M.D. & Canet, W. Influence of cooking and freeze-thawing cycles on viscoelastic properties of vegetable purees. Lebensm Wiss und-Technol, 34, 549-555 (2001).
6. Rico, R., Alvarez, M.D. & Canet, W. Sistema de adquisición y análisis de datos. Eurofach Electrón, 18, 60-65 (1995).
7. UNE 87025 *Manual de análisis sensorial. Tomo I – Alimentación* (edited by Aenor). Pp. 167-186. Madrid: Aenor (1996).
8. *Rao, M.A. Flow and functional models for rheological properties of fluid foods. In*: Rheology of Fluid and Semisolid Foods. Principles and Applications *(edited by G.V. Barbosa-Cánovas). Pp. 25-59. Maryland: Aspen Publishers Inc (1999).*
9. Briant, A.M., Personius, C.J. & Cassel, E.G. Physical properties of starch from potato of different culinary quality. Food Res, 10, 437-444 (1945).
10. Suzuki, A., Shibanuma, K., Takeda, Y., Abe, J. & Hizukuri, S. Structures and pasting properties of potato starches from Jaga Kids Purple '90 and Red '90. J Applied Glycosci, 41, 425-432 (1994).
11. Moledina, K.H., Fedec, P., Hadziyev, D. & Ooraikul, B. Ultrastructural changes in potato during potato granule process as viewed by SEM. Starch/Stärke, 30, 191-199 (1978).

METHODS FOR MEASURING YIELD STRESS IN FRESH AND FROZEN NATURAL AND COMMERCIAL POTATO PUREES

C. Fernández, M.D. Alvarez, W. Canet*

Department of Plant Foods Science and Technology, Instituto del Frío-CSIC, José de Novaís nº 10, E-28040 Madrid, Spain. Email: ifrat44@if.csic.es

Keywords: Steady shear; Dynamic rheological test; Flow curve; Yield stress; Freezing

ABSTRACT

Seven methods for determining yield stress of concentrated suspensions were applied to fresh and frozen natural and commercial purees at different temperatures. Since potato puree was consistent with Herschel-Bulkley flow behaviour, yield stress was more reliably determined by extrapolation of the flow curves assuming the Herschel-Bulkley model than Bingham and Casson models. Methods for determining yield stress by dynamic rheological tests were tedious and are not always applicable. Given the high correlation between Herschel-Bulkley yield stress and that as determined by Bohlin option (R^2 = 0.8735), Bohlin's "Yield stress option" appears to be highly useful for direct measurement of this property in potato puree. Temperature influenced yield stresses more in frozen than in fresh purees, both natural and commercial. At equal temperatures, processing reduced yield stresses in natural puree but increased them in commercial puree, showing that their structures were not affected in the same way.

1. INTRODUCTION

Many commercially valuable foods like apple sauce and tomato paste are concentrated dispersions of insoluble matter in aqueous media. Their rheological behaviour, especially yield stress, is important for industrial handling, storage, processing and transport of concentrated suspensions [1]. Yield stress means the stress that must be exerted simply to move one fluid layer past another [2], and it plays a role in the coating of solid surfaces. In terms of the strength of the coherent network structure, it is the force per unit area required to achieve breakdown of the structure followed by the cleavage of network bonds or linkages connecting the flow units [3, 4]. Several methods have been employed for the determination and comparison of the yield stress of food suspensions, but most magnitudes of yield stress are determined by extrapolation of shear rate-shear stress data according to several flow models such as those of Casson, Herschel-Bulkley and Mizrahi-Berk [4-6]. With the availability of automated rheometers, dynamic rheological tests can also be used to determine yield stresses of food and non-food suspensions [4, 7-11]. The main objectives of the present study were (1) to determine, compare and correlate the yield stresses of two different potato puree types obtained by seven established methods, and (2) to study the effect of sample temperature and freezing on the magnitudes of the yield stresses.

2. MATERIALS AND METHODS

2.1 Preparation of samples

For preparation of natural puree, fresh tubers (cv. Kennebec) were selected. Tubers were manually washed, peeled and diced. Natural potato purees were prepared from 395 g of potatoes, 150 ml of milk, 100 ml of water and 5 g salt using a Thermomix TM 21. Ingredients were cooked (20 min/100 °C), and the liquid evaporated was determined by weighing the ingredients before and after boiling. This was compensated by addition of boiling water, and

the ingredients were again cooked (5 min/100 °C). The mash was triturated for 40 s. The product was homogenised through a stainless steel sieve (diameter 1.5-mm). For preparation of commercial puree, aseptically packed commercial dehydrated potato flakes were used and mashed prepared according to label instructions. Following preparation, half of each sample was packed in polyethylene plastic, sealed under light vacuum (-0.05 MPa) on a Multivac packing machine and immediately frozen to –80 °C. The packs were then kept for 1 week in a freezer at –80 °C. Rheological measurements of frozen samples were made after samples had been allowed to thaw overnight in a domestic refrigerator.

Rheological behaviour was evaluated on the samples with temperature ranging from 25 to 65 °C. Temperatures were reached in the fresh and frozen/thawed samples by placed them in a CB60VS waterbath with a constant product weight:water volume ratio of 1:20. Water and product temperatures were monitored by K-type thermocouples using a hardware and software system developed with the LabWindows/CVI package for automation of the thermal process control [12].

2.2 Rheological measurements

A Bohlin CVR 50 controlled-stress rheometer was used to conduct steady shear and small amplitude oscillatory shear experiments (SAOS) using a plate-plate sensor system with 2-mm gap (PP40, 40 mm) and a solvent trap to minimize moisture loss during tests. Samples were allowed to relax 5 min before conducting rheological measurements such as equilibration time after loading the sample on the sensor system. Temperature control was carried out with a Peltier Plate system (-40 to +180 °C). Each curve presented is a typical one out of two run.

2.3 Steady shear and yield stress data

Flow curves were obtained at shear rates of 0.1-100 s^{-1} approximately, which is the range of interest in food texture studies [13]. Data were fitted to the Bingham (1), Casson (2) and Hershel-Bulkley (3) models [4]. Bingham, Casson and Herschel-Bulkley yield stresses were obtained respectively by extrapolation of shear rate-shear stress data according to flow models (1)-(3).

$$\sigma - \sigma_{0B} = \eta' \dot{\gamma} \quad (1)$$

$$\sigma^{0.5} = K_{0c} + K_c(\dot{\gamma})^{0.5} \quad (2)$$

$$\sigma - \sigma_{0H} = K_H(\dot{\gamma})^{nH} \quad (3)$$

Bohlin also obtained yield stress using Bohlin “Yield stress option” (σ_{0BO}) through the viscometry stress ramp test, which involves applying a gradually increasing stress and monitoring the instantaneous viscosity for an inflexion of the curve: i.e. the onset of flow (Fig. 1a). Besides, yield stress was obtained by direct extrapolation of the straight-line portion of shear rate-shear stress data (σ_{0BM}) in accordance with Michaels and Bolger [14] (Fig. 1b). This way of obtaining yield stress is known and is referred to as the Bingham method in this work.

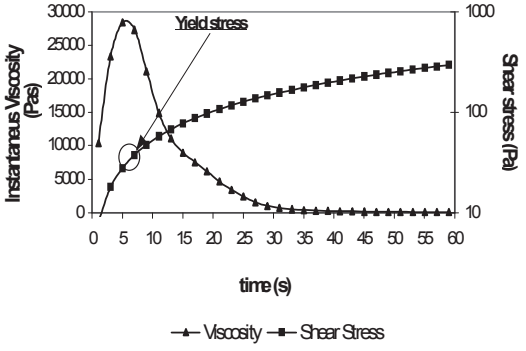

Fig. 1a Yield from the Bohlin "Yield Stress Option"

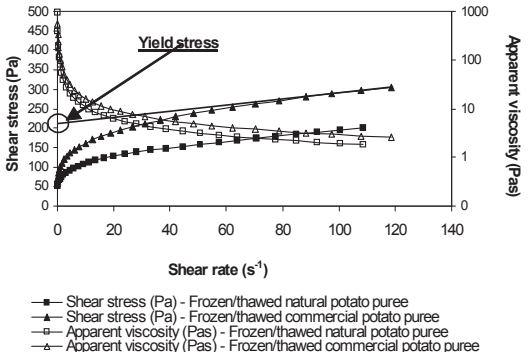

Fig. 1b Yield from the Bingham Method

2.5 Yield stress from dynamic shear data

Magnitudes of storage modulus G' and loss modulus G" were determined for each sample from stress sweeps at 1 rad.s^{-1}. As the strain was increased, G' and G" remained relatively constant until at a critical value of strain the magnitude of G' decreased sharply and that of G" increased sharply (Fig. 2a). The magnitude of G' at the critical strain value was recorded as the experimental yield value (σ_{Ge}) [15].

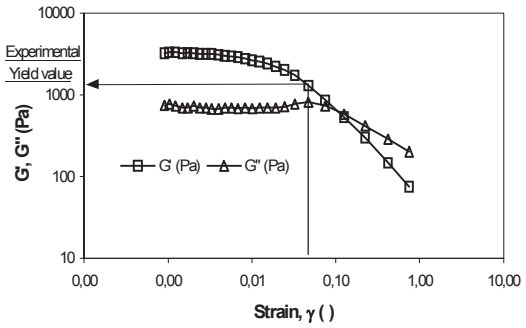

Fig. 2a Yield from dynamic rheological test, Method I

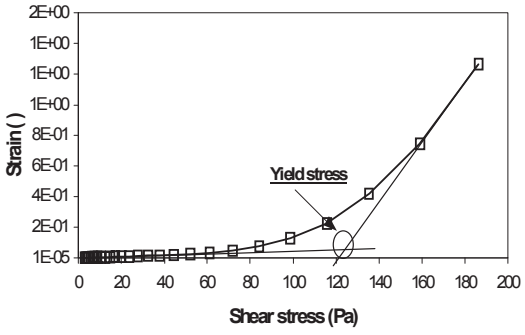

Fig. 2b Yield from dynamic rheological test, Method II

For some of the potato purees studied, a modified Cox Merz rule was found to be applicable to:

$$\eta^*(\alpha\omega) = \eta(\dot{\gamma})\big|_{\omega=\dot{\gamma}} \quad (4)$$

In separate experiments, frequency sweeps over the range 0.1-100 rad.s^{-1} were conducted in the linear viscoelastic domain, and shift factors (α) for Cox-Merz plots were determined from plots of steady shear viscosity shear rate and complex viscosity frequency data as described earlier [15]. The product of the Cox Merz shift factor (α) and σ_{Ge} was calculated to obtain the corrected dynamic yield stress, which in this study is designated dynamic yield stress from method I, σ_{DRI}. It is also possible to determine yield stresses from dynamic tests by plotting strain versus shear stress (Fig. 2b). The shear stress corresponding

to the intersection of the tangents and the two distinct segments of the strain-shear stress curve is considered to be the yield stress and in this study is called the dynamic yield stress from method II, σ_{DRII}. Therefore, a total of seven different methods were applied to obtain yield stresses for the two types of potato purees studied.

2. RESULTS AND DISCUSSION

Tables 1 and 2, respectively, show the magnitudes of yield stresses obtained for fresh and for frozen/thawed natural and commercial potato purees using the different methods applied at the different sample temperatures studied.

Table 1 Magnitudes of yield stress (Pa) in natural potato puree using different methods

Temp (°C)	Bingham yield stress, σ_{0B}	Casson yield Stress, σ_{0C}	Herschel Bulkley yield stress, σ_{0H}	Yield stress from Bohlin Option, σ_{0BO}	Yield stress from Bingham Method, σ_{0BM}	Experimental yield stress, σ_{Ge}	Cox-Merz rule shift factor, α	Dynamic yield stress (I), σ_{DRI}	Dynamic yield stress (II), σ_{DRII}
Fresh natural potato puree									
25	201.7	164.1	105.5	32.6	345	9089.4	0.008	72.7	200
35	169.0	147.6	111.2	60.7	228	11930	0.005	59.6	199
45	169.7	166.0	117.8	61.4	175	10305	0.009	92.7	167
55	127.0	116.5	100.9	33.0	145	10899	0.005	54.5	240
65	182.4	164.1	151.8	33.5	215	14076	0.007	98.5	193
Frozen/thawed natural potato puree									
25	226.6	211.1	75.9	12.9	302	6406.6	-	-	250
35	74.6	56.3	11.1	8.3	120	2397.6	-	-	39
45	68.9	51.1	25.8	8.0	116	2287.2	-	-	29
55	113.4	73.8	33.5	11.9	217	3785.3	0.008	30.3	40
65	84.7	63.9	41.4	8.4	121	2282.8	0.014	31.9	37

In fresh natural puree, the temperature did not appear to affect the yield stress values obtained from the Bingham model, σ_{0B}. However, in frozen/thawed natural potato puree, σ_{0B} was clearly higher at 25 °C than at the other sample temperatures. In natural potato puree, except for 25 °C, σ_{0B} values were lower in the processed than in the fresh samples, indicating that freezing decreased the strength of the network structure of the samples. The effects of both temperature and processing on Casson yield stresses σ_{0C} were similar to those found for Bingham yield stresses. For natural puree exhibiting non-linear plastic behaviour (Fig. 1b), the correlation coefficients of the fits to the Casson model were higher than those corresponding to the Bingham model for all temperatures. In fresh natural puree, Herschel-Bulkley yield stress values, σ_{0H}, exhibited a non-identifiable trend with sample temperature, whereas in processed samples, the σ_{0H} value was higher at 25 °C than at the other temperatures. From the σ_{0B}, σ_{0C} and σ_{0H} yield stresses, it would appear that the effect of temperature was more pronounced in processed than in fresh samples. In natural puree, σ_{0H} values were also lower in the processed than in the fresh samples at all temperatures, more clearly evidencing fluidification of the product with processing. As was to be expected from the shape of the flow curves of potato puree (Fig. 1b), of the models used, the Herschel-Bulkley equation was the one for which fits gave the highest correlation coefficients.

In both fresh and frozen/thawed natural purees (Table 1), yield stresses obtained from the Bohlin option, σ_{0BO}, followed a non-identifiable trend with sample temperature and, as was found for σ_{0H}, σ_{0BO} values were also clearly lower in frozen/thawed than in fresh samples

at all temperatures. Bingham method yield stresses, σ_{0BM}, decreased with sample temperature up to 55 °C in fresh natural puree, whereas in frozen/thawed natural puree, σ_{0BM} decreased with temperature up to 45 °C. Except for 55 °C, σ_{0BM} values were lower in frozen/thawed than in fresh samples. It must be considered that even if the extrapolation is performed carefully, the yield values obtained by the Bingham method are somewhat uncertain for potato purees that exhibit a pronounced non-linear shear stress-shear rate ratio.

In frozen/thawed natural puree at 25, 35 and 45 °C, σ_{DRI} could not be obtained; relationships between complex and steady viscosities in these samples were non-linear and therefore it was not possible to multiply experimental yield stresses by the Cox-Merz rule shift factor for these temperatures. In contrast, in fresh natural puree, relationships between complex and steady viscosities were linear at all temperatures. σ_{DRI} values in fresh natural puree exhibited a non-identifiable trend with sample temperature. In natural puree, dynamic yield stresses (II), σ_{DRII}, were lower in processed than in fresh samples for all the temperatures except 25 °C. In fresh samples, temperature had a non-identifiable influence on σ_{DRII} values, while in processed samples the values corresponding to 25 °C were higher than those for other temperatures.

In fresh commercial puree (Table 2), σ_{0B} was lowest at 65 °C, while in frozen/thawed commercial puree, σ_{0B} at 25 °C was clearly higher than at other temperatures. At 35, 45 and 55 °C, σ_{0B} values were lower in processed than in fresh samples. As in the case of natural puree, the effect of both temperature and processing on σ_{0B} and σ_{0C} yield stresses in commercial puree was similar. Again, correlation coefficients were higher in the Casson model fits than those corresponding to the Bingham equation, indicating that a non-linear model is more suitable for characterization of potato puree flow behaviour. σ_{0H} was higher in the frozen/thawed samples than in the fresh samples at all temperatures, indicating that the processing of commercial puree led to the formation of a coarsely aggregated structure.

Table 2 Magnitudes of yield stress (Pa) in commercial potato puree using different methods

Temp (°C)	Bingham yield stress, σ_{0B}	Casson yield stress, σ_{0C}	Herschel Bulkley yield stress, σ_{0H}	Yield stress from Bohlin Option, σ_{0BO}	Yield stress from Bingham Method, σ_{0BM}	Experimental yield stress, σ_{Ge}	Cox-Merz rule shift factor, α	Dynamic yield stress (I) σ_{DRI}	Dynamic yield stress (II) σ_{DRII}
Fresh commercial potato puree									
25	193.9	159.8	20.7	62.6	311	2705.6	-	-	300
35	237.0	185.9	22.6	49.1	395	2163.8	-	-	97
45	167.7	124.2	19.6	11.9	268	1611.8	-	-	62
55	232.2	156.1	29.0	12.9	463	1721.5	-	-	123
65	58.4	43.7	5.7	8.1	96	1233.2	-	-	53
Frozen/thawed commercial potato puree									
25	629.4	564.2	387.6	212.0	750	15552	0.020	311	590
35	199.1	174.7	38.6	37.5	261	4944	0.015	74.2	267
45	65.0	47.0	23.6	8.0	120	1517.5	-	-	45
55	126.9	94.2	30.8	9.7	190	1766.8	0.020	35.4	70
65	121.3	87.6	30.6	8.7	203	13956	0.020	279.1	59

The temperature effect was more clearly apparent in the processed samples where σ_{OBM} was higher at 25 °C than at other temperatures. In fresh commercial puree at all temperatures, and in frozen/thawed puree at 45 °C, it was not possible to obtain dynamic yield stresses (I), σ_{DRI}, since in these samples the relationships between complex and steady viscosities were

also non-linear. In frozen/thawed commercial puree, σ_{DRI} was much lower at 55 °C than at 25 °C, indicating a temperature effect.

In order to quantify the differences between the magnitudes of the yield stresses obtained by the different methods, linear correlations from data for both puree types were established between the yield stress values produced by six applied methods (Table 3).

Table 3 Equations and R^2 for linear correlation between yield stresses of potato purees obtained by six different methods

	Bingham yield stress, σ_{0B}	Casson yield stress, σ_{0C}	Herschel Bulkley yield stress, σ_{0H}	Yield stress from Bohlin Option, σ_{0BO}	Yield stress from Bingham Method, σ_{0BM}	Dynamic yield stress (II), σ_{DRII}
σ_{0B}	1					
σ_{0C}	$\sigma_{0C} = 0.91\sigma_{0B} - 13.96$ ($R^2 = 0.9913$)	1				
σ_{0H}	$\sigma_{0H} = 0.63\sigma_{0B} - 29.11$ ($R^2 = 0.7978$)	$\sigma_{0H} = 0.70\sigma_{0C} - 21.94$ ($R^2 = 0.8447$)	1			
σ_{0BO}	$\sigma_{0BO} = 0.36\sigma_{0B} - 23.08$ ($R^2 = 0.9147$)	$\sigma_{0BO} = 0.40\sigma_{0C} - 18.13$ ($R^2 = 0.9422$)	$\sigma_{0BO} = 0.50\sigma_{0H} - 1.51$ ($R^2 = 0.8735$)	1		
σ_{0BM}	$\sigma_{0BM} = 1.16\sigma_{0B} + 44.63$ ($R^2 = 0.9376$)	$\sigma_{0BM} = 1.23\sigma_{0C} + 67.55$ ($R^2 = 0.8905$)	$\sigma_{0BM} = 1.35\sigma_{0H} + 133.67$ ($R^2 = 0.6268$)	$\sigma_{0BM} = 2.81\sigma_{0BO} + 133.50$ ($R^2 = 0.7867$)	1	
σ_{DRII}	$\sigma_{DRII} = 0.97\sigma_{0B} - 19.02$ ($R^2 = 0.8157$)	$\sigma_{DRII} = 1.08\sigma_{0C} - 8.00$ ($R^2 = 0.8643$)	$\sigma_{DRII} = 1.41\sigma_{0H} + 36.32$ ($R^2 = 0.8459$)	$\sigma_{DRII} = 2.64\sigma_{0BO} + 46.96$ ($R^2 = 0.8486$)	$\sigma_{DRII} = 0.73\sigma_{0BM} - 30.02$ ($R^2 = 0.6593$)	1

There was very good linear correlation (R^2 = 0.9913) between Casson and Bingham yield stresses. However, Bingham yield stresses were higher in magnitude than Herschel-Bulkley yield stresses, and were higher by a factor of 2.5 than the yield stress values obtained from the Bohlin option. This would indicate that, if the flow curves for potato purees do not follow Bingham behaviour, yield values will be seriously overestimated by use of this model. In certain cases, the Bingham yield value can be higher by a factor of 4-5 than the value obtained by non-linear extrapolation [16].

There was good linear correlation (R^2 = 0.9422) between Casson yield stresses and yield stresses from the Bohlin option. The highest magnitudes of yield stress were clearly produced by the Bingham method. These were almost 3 times higher than those obtained from the Bohlin option. The highest linear correlation of Herschel-Bulkley yield stresses was with yield stresses from the Bohlin option (R^2 = 0.8735), the former being nearly twice the latter. Although yield stresses from the direct Bohlin option were the lowest, the Herschel-Bulkley model was the one that best characterised the flow behaviour of potato puree, and so this direct method would appear to be a reliable technique for measuring yield stresses in potato puree.

We certainly think that if linear correlations between different yield stresses were established between different potato puree groups separately (that is, between fresh and frozen natural and commercial potato puree, or between fresh natural and commercial puree and frozen natural and commercial puree, or even between fresh natural puree, frozen natural puree, fresh commercial puree and frozen commercial puree, separately), comparisons of the ratios between different yield stresses could help us understand the differences between potato puree structures and how they are affected by processing.

3. CONCLUSIONS

The experimental results indicated that the methods applied to the determination of yield stress constitute a complementary set of techniques that are useful in studying the

rheology of natural and commercial potato purees, either fresh or frozen/thawed. The effects of sample temperature and freezing on yield stresses as determined by different methods are comparable. The influence of sample temperature on yield stresses was greater in the processed purees. In natural potato purees, yield stresses decreased with processing, indicating a weaker structure, whereas in commercial potato purees yield stresses increased with processing, indicating greater strength. The behaviour of potato puree was consistent with the Herschel-Bulkley model, which is therefore more reliable for determination of yield stress than the Bingham and Casson models. Determination of yield stress from dynamic rheological tests is extremely tedious, is not always applicable and is more uncertain. Nevertheless, the high linear correlation found between Bohlin and Herschel-Bulkley yield stresses would suggest that the Bohlin "yield stress option" is a suitable tool for the direct measurement of yield stress in potato puree.

References

1. Rao, M. A. (1987). Predicting flow properties of food suspensions of plant original. *Food Technology, 41*(8), 85-88.
2. Charm, S. E. (1962). The nature of role of fluid consistency in food engineering applications. *Advances in Food Research*, 11, 356-435.
3. Durán, L., & Costell, E. (1982). Rheology of apricot puree : characterization of flow. *Journal of Texture Studies*, 13, 43-58.
4. Qiu, C. G., & Rao, M. A. (1988). Role of pulp content and particle size in yield stress of apple sauce. *Journal of Food Science*, 53(4), 1165-1170.
5. Missaire, F., Qiu, C. G., & Rao, M. A. (1990). Yield stress of structured and unstructured food suspensions. *Journal of Texture Studies*, 21, 479-490.
6. Rao, M. A., & Cooley, H. J. (1983). Applicability of flow models with yield for tomato concentrates. *Journal of Food Process Engineering*, 6, 159-173.
7. Hoffmann, H., & Rauscher, A. (1993). Aggregating systems with a yield value. *Colloid and Polymer Science*, 271, 390-395.
8. Steffe, J. F. (1992a). Yield stress: phenomena and measurement. In R. P. Singh, & A. Wirakartakusmah, *Advances in Food Engineering*, (pp. 363-376). FL, USA: CRC Press, Boca Ratón.
9. Steffe, J. F. (1992b). *Rheological Methods in Food Process Engineering*. East Lansing, MI, USA: Freeman Press.
10. Yoo, B., Rao, M. A., & Steffe, J. F. (1995). Yield stress of food dispersions with the vane mehod at controlled shear rate and shear stress. *Journal of Texture Studies*, 26, 1-10.
11. Yoshimura, A. S., Prud'homme, R. K., Princen, H. M., & Kiss, A. D. (1987). A comparison of techniques for measuring yield stress. *Journal of Rheology*, 31(8), 699-710.
12. Rico, R., Alvarez, M. D., & Canet, W. (1995). Sistema de adquisición y análisis de datos para la automatización y control de procesos térmicos. *Eurofach Electrónica*, 18, 60-65.
13. Bistany, K. L., & Kokini, J. L. (1983). Dynamic viscoelastic properties of foods in texture control. *Journal of Rheology*, 27(6), 605-620.
14. Michaels, A. S., & Bolger, J. C. (1962). The plastic behaviour of flocculated kaolin suspensions. *Industrial & Engineering Chemistry Fundamentals*, 1, 153-162.
15. Yoo, B., & Rao, M. A. (1995). Yield stress and relative viscosity of tomato concentrates: effect of total solids and finisher screen size. *Journal of Food Science*, 60(4), 777-779, 785.
16. Nguyen, Q. D., & Boger, D. V. (1983). Yield stress measurement for concentrated suspensions. *Journal of Rheology*, 27(4), 321-349.

EFFECT OF MILK FAT CONTENT ON THE FLOW BEHAVIOUR OF CUSTARD DESSERTS

*A. Tárrega , L. González-Tomás and E. Costell**

Laboratory of Physical and Sensory Properties
Instituto de Agroquímica y Tecnología de Alimentos (CSIC)
PO Box 73, 46100 Burjassot, Valencia (Spain)
Phone: +34-96-3900022
Fax.: +34-96-3636301
e-mail: ecostell@iata.csic.es

Keywords: Dairy desserts, milk fat content, starch gelatinisation, flow behaviour

ABSTRACT
The effect of milk fat content on the starch gelatinisation and on the flow behaviour of dairy custard desserts was investigated. Six custard samples with fixed amounts of sucrose, vanilla aroma and colorant and varying in starch concentration (2.5, 3.25 and 4%) and in the fat content of milk (skim milk and whole milk) were prepared. Viscosity profiles during thermal treatment (heating and cooling) were recorded using a Rapid Visco^{TM} Analyser. The samples were stored at 4ºC during 24 h and then their flow behaviour was measured at 5±0.5ºC using a Haake rheometer RS1 with parallel plates (diameter= 6 mm, gap = 1 mm) geometry. The hysteresis loop was obtained by registering shear stress at shear rates from 1 to 200 s^{-1} in 60 s and down in 60 s. Viscosity profiles during thermal treatment showed that fat content didn´t modify the swelling temperature of the starch in the systems measured. The samples with whole milk showed higher viscosity at the end of the cooling period. All samples showed time-dependent flow and this dependence was higher in samples with whole milk. Steady shear data of samples fitted well to the Herschel and Bulkley model ($0.947 \leq R^2 \leq 0.997$). The yield stress values, obtained by fitting experimental data to the Casson model, the consistence index values and the pseudoplasticity increased with starch concentration and were significantly higher for samples with whole milk.

1. INTRODUCTION

The "natillas", semisolid dairy dessert of wide consumption in Spain, are composed of milk, starch, hydrocolloids, sugars, colorants and aromas. Their rheological and sensory properties are strongly influenced by the particular characteristics of each ingredient and by their crossed interactions. Wide information can be found in the literature on the rheological behaviour of water-starch pastes (1,2,3) as well as on the effects produced on this behaviour by substituting milk instead of water in starch dispersions (4,5). However, only a few papers deal with the rheological characterisation of commercial dairy desserts (6,7,8), or their corresponding model systems (9,10). The different types and concentrations of crosslinked starches presumably present in the commercial products, might be responsible in great part for the differences in rheological behaviour of these systems although other factors such as differences in milk fat content could probably affect the system structure and modify their rheological behaviour.

The objective of this study was to investigate the effect of milk fat content on the starch gelatinisation and on the flow behaviour of dairy custard desserts with different starch concentrations.

2. MATERIALS AND METHODS

2.1. Sample preparation

Six custard samples with fixed amounts of sucrose (8%), colorant Vegex NC 2c (CHR Hansen S.A.) (0,052%) and vanilla aroma 37548A (Lucta S.A.) (0,016%) were prepared varying in the concentration of modified waxy maize starch C*PolarTex® 06741 (Cerestar Ibérica, Spain) (2.5, 3.25, 4% w/w) and in the fat content of milk (skim milk with 0.1% fat and whole milk with 3.12% fat). Both skim milk and whole milk were prepared 24 h in advance by dissolving 12% (w/w) milk powder (Central Lechera Asturiana, Asturias, Spain) in deionised water.

2.2.Thermo-mechanical treatment

A Rapid Visco-Analyser (RVA) (Newport Scientific, Warriewood, Australia) was used to evaluate pasting properties of samples. RVA Custard Power Pasting Method (Method 20, version 5) (Newport Scientific, 1998) was applied as follows: each sample was rapidly stirred at 960 rpm for 10 s, while heated at 50ºC, before the shear input was switched to 160 rpm for the rest of the process. Temperature was held at 50ºC up to 1 min. Then the samples were heated from 50ºC to 95ºC during 3 min 42 s, and the temperature held at 95ºC for 5 min. They were cooled down to 30ºC in 5 min and 48 s, and then held at 30ºC for 4.5 min. Viscosity and temperature data were recorded over time; data gathering and analysis were performed using the Thermocline for Windows software, provided by the instrument's manufacturer. Each analysis was done in duplicate.

2.3. Rheological measurements

After the thermo-mechanical or preparation process, the samples were kept at 4-5 ºC for 24 hours. Then the flow behaviour of each system was measured. Measurements were carried out in a controlled stress rheometer RS1 (Thermo Haake, Karlsruhe, Germany), using parallel plates geometry of 6 cm diameter and 1mm gap, monitored by a RheoWin software package (version 2.93, Haake). A temperature of 5 ±0.5ºC was kept during measurements with a water circulator device Phoenix P1 Circulator (Thermo Haake). Samples were allowed to rest for 15 minutes before measurements were done and a fresh sample was loaded for each measurement. Up and downward curves were recorded. Custard samples flow was measured by recording shear stress values at increasing shear rates from 1 to 200 s^{-1} in 60 s and down in reverse sequence in the same time. Data from the upward segment of the shear cycle were fitted to Herschel-Bulkley model (Eq. 1) using the Rheowin Pro software (version 2.93, Haake). The yield stress (σ_0) value, used in the Herschel-Bulkley's model, was previously obtained by fitting the experimental data to the Casson model (Eq. 2) and calculating the square of the ordinate intercept in the Casson plot (7) and the apparent viscosity values were obtained with the expression (Eq. 3).

$$\sigma = \sigma_0 + K\dot{\gamma}^{n} \qquad \text{(Eq.1)}$$

$$\sigma^{0.5} = \sigma_0^{0.5} + K\dot{\gamma}^{0.5} \qquad \text{(Eq.2)}$$

$$\eta_{ap} = \sigma_0/\dot{\gamma} + K\dot{\gamma}^{n-1} \qquad \text{(Eq.3)}$$

2.4. Statistical analysis

The effects of starch concentration and milk type on the flow parameters were analysed by ANOVA including three factors with interactions. The Fisher test (α=0.05) was used to calculate the minimum significant difference. All calculations were carried out with the Statgraphics Plus 4.1 software.

3. RESULTS AND DISCUSSION

3.1. Viscosity-temperature profiles

All viscosity profiles of the studied systems showed a similar pattern. The viscosity increased during the heating period at constant temperature (95ºC), continued to increase during cooling and the profile finalized with a plateau region for samples with skim milk, corresponding to their particular final viscosity, while samples with whole milk showed a slightly decreasing trend at the last two minutes of processing (Figure 1)

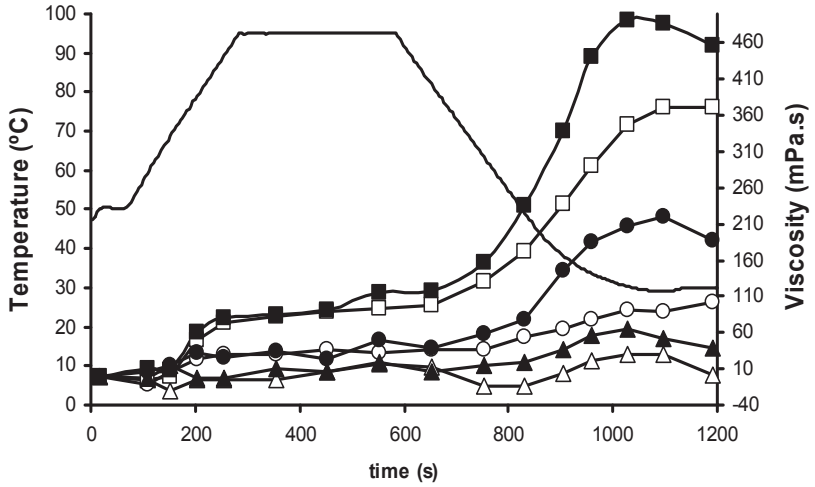

Figure 1. Viscosity profiles during thermal treatment of 4% (squares), 3.25% (circles) and 2.5% (triangles) starch concentration in skim milk (empty symbols) and in whole milk (filled symbols) custard systems. Temperature profile (—)

No differences in the swelling temperature, taken as that at which consistency began to increase, were observed among samples with different milk fat content. The viscosity value registered at the end of heating period, the slope of the increase in viscosity during cooling and the final viscosity at the end of cooling period increased with starch concentration, due to an increase in the volumetric fraction of the starch granules in the dispersion. At the same starch concentration, all three parameters showed higher values for whole milk samples, which is attributable to the higher viscosity of the dispersing phase, due to the higher fat content (5).

3.2. Flow behaviour

Rheograms (up and down curves) of custard dessert samples were recorded. All samples exhibited time dependent non-Newtonian flow (Figure 2). A similar behaviour was observed in commercial samples of vanilla dairy desserts of seven different brands (7). Substitution of whole milk for skim milk in the studied samples originated an increase in the registered shear stress values and in the hysteresis loop area. This effect was higher for 3.5% starch samples than for higher (4%) or lower (2.5%) starch concentration samples.

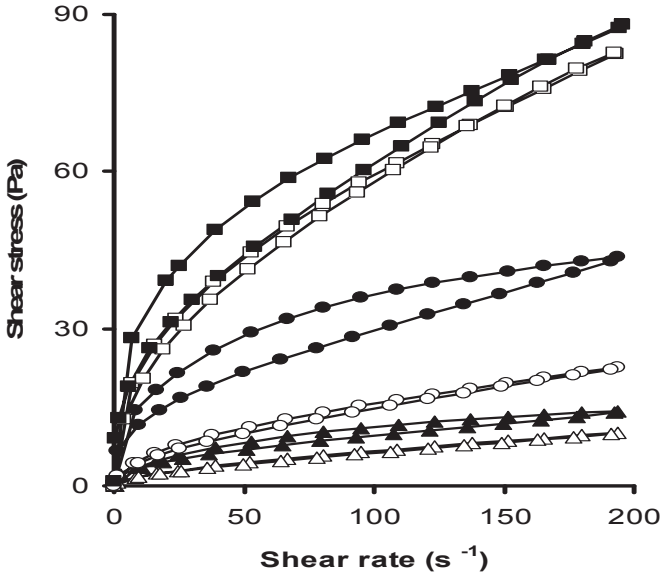

Figure 2. Flow curves of 4% (squares), 3.25% (circles) and 2.5% (triangles) starch concentration in skim milk (empty symbols) and in whole milk (filled symbols) custard systems.

Characterisation of the flow behaviour of samples was based on the experimental data obtained in the upward rheogram. Yield stress was calculated using the Casson model equation. Flow data were fitted to the Herschel-Bulkley model, obtaining R^2 values between 0.947 and 0.997. As expected, in both skim milk and whole milk starch dispersions the consistency coefficient (K) and the yield stress (σ_0) values increased with starch concentration while the flow index (n) values slightly decreased, thus indicating an increase in shear-thinning behaviour. At the same starch concentration, it should be noticed that both K and σ_0 showed higher values for whole milk samples while n values were lower (Table 1).

A two-way ANOVA with interaction was used to study the combined effects of the type of dispersion medium (skim milk or whole milk) and the starch concentration (2.5, 3.25 and 4%) on the variations in yield stress (σ_0), apparent viscosity at $1s^{-1}$ (η_1) and flow index (n). The corresponding binary interaction was significant ($\alpha \leq 0.05$) for the three parameters (F_{int}=14.00 for σ_0, F_{int}=12.32 for η_1 and F_{int}=6.99 for n), indicating that the effect of substituting whole milk with skim milk on plasticity (σ_0 values), apparent viscosity (η_1 values) and pseudoplasticity (n values) was different, depending on starch concentration.

Starch (%)	Milk Type	σ_0 (Pa)	K (Pa.s^{-1})	n
2.5	skim milk	0.80	0.21	0.71
	whole milk	2.50	0.46	0.62
3.25	skim milk	2.91	0.62	0.66
	whole milk	10.47	1.55	0.56
4	skim milk	13.09	2.41	0.63
	whole milk	22.16	2.92	0.59

Table 1. Flow behaviour of custard dessert samples at 5ºC. Average values of Herschel-Bulkley parameters.

Apparent viscosity at 1s $^{-1}$ was higher in whole milk model systems, the increment being relatively bigger for 3.25% starch concentration than at the other two starch concentrations (Figure 3).

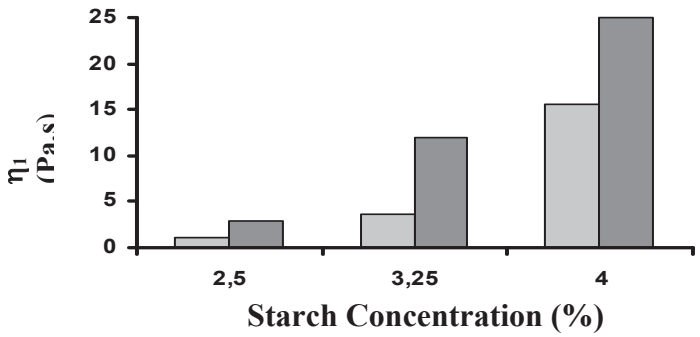

Figure 3. Values of apparent viscosity at 1s $^{-1}$ of custard desserts with different starch concentration and with skim milk ( ) and with whole milk ( ).

These results followed the same trend than those obtained by others authors in dispersions of native starches (5). They observed that the apparent viscosity of 6% wheat starch pastes at 2.2 s^{-1} increased by 15% using high fat (3 %) milk, as compared with using skim milk (0.2% fat), and concluded that besides the effect of milk on the increase in rigidity of the starch granules, the three-dimensional fat polymers contributed to the increase in apparent viscosity of starch milk pastes.

4. ACKNOWLEDGEMENTS

To MCyT of Spain for the financial support (Project AGL 2003-0052) and for the fellowship awarded to author Tárrega and to CHR Hansen S.A. and Lucta S. A for providing free samples of colorant and aroma.

5. REFERENCES

1. Tecante, A., & Doublier, J. L.(1999). Steady flow and viscoelastic behavior of crosslinked waxy cornstarch-k-carrageenan pastes and gels. *Carbohydrate Polymers*, 40, 221-231.

2. Rosalina, I. & Bhattacharya, M., (2002). Dynamic rheological measurements and analysis of starch gels. *Carbohydrate Polymers*, 48, 191–202.

3. Nayouf, M., Loisel, C., & Doublier, J. L. (2003). Effect of thermomechanical treatment on the rheological properties of crosslinked waxy corn starch. *Journal of Food Engineering*, 59, 209-219

4. Matser, A. M. & Steeneken, P. A. M. (1997). Rheological properties of highly cross-linked waxy maize starch in aqueous suspensions of skim milk components. Effects of the concentration of starch and skim milk components. *Carbohydrate Polymers*, 32, 297-305.

5. Abu- Jdayil, B., Mohameed, H. & Eassa, A. (2004). Rheology of wheat starch-milk-sugar systems: effect of starch concentration, sugar type and concentration, and milk fat content. *Journal of Food Engineering*, 64, 207-212.

6. Batista, P., Nunes, M. C. & Sousa, I. (2002). Physical characterisation of commercial dairy desserts. In F.J.Martínez Boza, A. Guerrero, P.Partal, J.M. Franco & J. Muñoz., *Progress in Rheology Theory and Applications* (pp. 449-452). Sevilla: Publicaciones Digitales S.A.

7. Tárrega, A., Durán, L. & Costell, E. (2004a). Flow behaviour of semi-solid dairy desserts. Effect of temperature. *International Dairy Journal*, 14, 345-353.

8. Tárrega, A., Durán, L. & Costell, E. (2004b). Rheological characterization of semisolid dairy desserts. Effect of temperature. *Food Hydrocolloids*, in press.

9. Wischman, B., Norsker, M., & Adler-Nissen, J. (2002). Food product models developed to evaluate strach as food ingredient. Narung/Food, 46, 167-173

10. Depypere, F., Verbeken, D., Thas, O. & Dewettinck, K. (2003). Mixture design approach on the dynamic rheological and uniaxial compression behaviour of milk desserts. *Food Hydrocolloids*, 17, 311-320.

FREEZING/THAWING IMPACT ON THE RHEOLOGICAL PROPERTIES OF EWE CHEESE

[1]*Alvarenga, N.*;* [1]*Fernandes, O. and* [2]*Sousa, I. M. N.*

[1] ADCTA, Escola Superior Agrária de Beja, Rua Pedro Soares, 7801-902 Beja, Portugal, mail: bartolomeu.alvarenga@esab.ipbeja.pt
[2] SCTA/DAIAT - Instituto Superior de Agronomia, Tapada da Ajuda, 1349-017 Lisboa, Portugal, mail: isabelsousa@isa.utl.pt

Keywords: cheese, ewe's milk, texture, rheology, freezing

ABSTRACT
Preservation by freezing started to be implemented by cheese manufacturers to regulate the market offer, to reduce the impact of season dependence of ewe's milk production on cheese. Therefore, the impact of freezing on cheese texture, rheology and chemical properties needs to be studied.
This is a preliminary study, where samples from the same cheese production lot were submitted, during different periods of time of 0, 3, and 12 month, to freezing temperatures (-10ºC). Although this is a common temperature for the cheese manufacturers freezers, it is well above the temperature of glass transition (Tg) of this material, that was determined to be around –20ºC.
Texture was measured by a TAHDi texture analyser from Stable Micro Systems (UK) and expressed in terms of hardness, cohesivity and adhesiveness. Viscoelastic parameters, G' and G'' were determined in a controlled stress rheometer RS 75 from Haake (Germany). Chemical parameters, pH, fat, total and soluble nitrogen and moisture were also evaluated.
The first 3 month of freezing reduced moisture of about 3 % and increased hardness from 6.2 N up to 10.9 N. After 12 month of freezing, hardness increased to 11.8 N. This effect was also seen on the mechanical spectra of the cheeses, with an increase on the magnitude of the storage modulus G'_{1Hz} from 11.7 up to 19.7 kPa in the first 3 month. However, a significant decrease ($P<0.05$) of the storage modulus occurred after 12 month of freezing, down to 14.0 kPa. This can be explained by the activity of proteolytic enzymes, even at –10ºC, since the material, at this temperature, is still at the "rubbery state", where biological reactions can take place at considerable rates. The other critical step, which can have and additional contribution to this explanation is thawing, where this proteolysis can be enhanced by internal mechanical damages produced by previous water crystal growth that will induce higher contact between enzymes and proteins.

1- INTRODUCTION

Freezing is a suitable procedure to prolong stability and shelf-life of cheeses, although Fennema (1972) pointed out the lack of unanimity on the extent of damage to cheese caused by freezing [1]. Damage depends on the type of cheese involved (composition and manufacturing procedures), the freezing conditions and the parameters chosen to evaluate the damage.
Several authors have studied the changes in texture, and proteolysis of frozen Mozzarella cheese [2], previously Cervantes et al. (1983) working on low moisture, part-skim Mozzarella cheese, concluded that, after one week of frozen storage, the samples were not significantly affected by freezing or thawing, as assessed by compression and sensory evaluation [3]. Bertola *et al* (1996 a, b) concluded that Mozzarella could be frozen and then stored at 20ºC without quality loss as long as the final product undergoes a period of ageing of at least 14 to 21 days before being consumed [4,5].

Cheeses can be classified as soft, semi-soft and hard paste, not in terms of texture, but as a function of moisture, referred to non-fat moisture calculation [6]. Studies of Mozzarella melting behaviour under extensional rheology can be extended to soft and semi-soft cheeses, in order to get a better characterization of the material properties, in terms of fundamental rheology.
Califano *et al*. (1998) studied the vacuum package of low moisture Mozzarella cheese samples, subjected to a freeze - thaw (-20/4ºC) process before ageing. Nine organic acids were analyzed each week. They were only affected by ripening time [7].
Alvarenga & Sousa (2000) developed and evaluated an instrumental method to measure Serpa cheese texture and concluded that, from the texture parameters studied, cheese hardness was the best parameter to characterize semi-soft cured cheese texture [8]. In addition, hardness showed to be well correlated with cheese ripening time henceforth, it would be able to discriminate cheeses and/or monitor cheese ripening evolution [9].
During freezing, complex food materials undergo a second order physical transition known as the glass transition [10]. The molecules are kept at very low levels of mobility, in an amorphous state, without the order of the crystal reached by pure substances. This glassy state has many advantages, mainly on increasing shelf life, as chemical and biological reactions are dramatically delayed. This physical transition is temperature dependent and it is a function of the material composition. The presence of small molecules, such as water, fat, etc. increases the mobility of the systems and lowers the glass transition temperature (Tg). This temperature can be determined by several methods, being DSC (Differential Scanning Calorimetry) one of the most commonly used. The storage of cheese below Tg will guarantee a minimum of changes at biological, chemical and structural levels, that will be reflected on the preservation of the sensory attributes at the texture and flavour levels.
In Spain, Canet *et al*. (1995) studied the freezing impact on ewe cheese. Although this study didn't used the recent application of the Tg concept in preservation technologies, allowed the development of freezing technologies in Spanish dairies [11].

2- MATERIAL AND METHODS

In this preliminary study samples from the same cheese allotment were submitted to the same freezing temperature, -10ºC, during different periods of time, namely: 0, 3 and 12 month. Although this is a common temperature used on the cheese manufacturers freezers, it is well above the temperature of glass transition (Tg) of this material, that was determined[1] to be around –20ºC. The physic-chemical composition was analyzed, namely: pH, fat, total nitrogen, water-soluble nitrogen and moisture (standard routine methods). The texture was analyzed by a texture analyser TAHD*i* of Stable Microsystems UK (Alvarenga and Sousa 2000). Rheological measurements were performed using a controlled-stress rheometer (RS-75, Haake, Germany) using serrated paralel plate geometry (20 mm). A constant shear stress of 50 Pa, within the linear viscoelastic region of the material, was used in all measurements. Frequency sweeps were conducted at 20ºC, with oscillation frequencies ranging from 0.001 to 100 Hz.

3-RESULTS AND DISCUSSION

Figure 1 shows the average texturograms for samples without any freezing time (A), 3 months of freezing (B), and 12 month of freezing (C).

[1] Aknowledgements: Prof. J.A. Martins from Universidade do Minho for Tg determinations by DSC.

In the first freezing period (0-3 month) the moisture decrease about 3%(m/m) and hardness (fig.1) increased from 6.2N to 10.9N. After 12 month of freezing, hardness increased up to 11.8N.

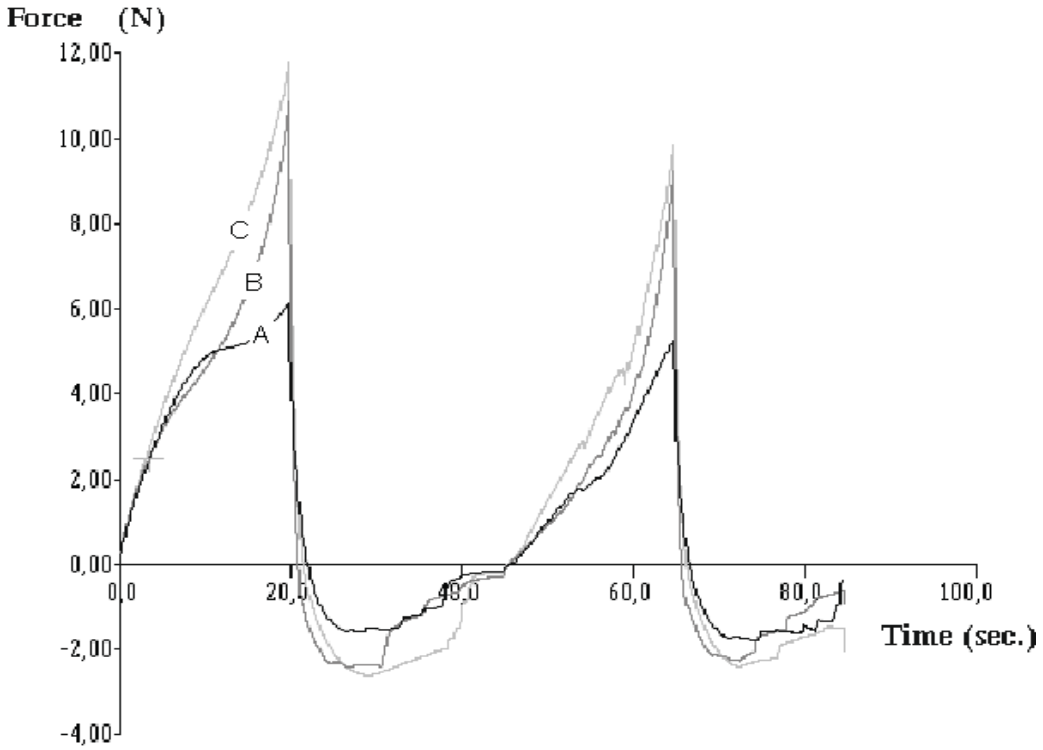

Figure 1 – Average texturograms of samples without freezing (A) and with 3 (B) and 12 months (C) of freezing.

Table 1 shows the average results for hardness, G' at 1Hz, and physical-chemical composition, of samples without freezing and with 3 and 12 months of freezing.

Table 1 – Average results and standard deviations for hardness, G'-1Hz, and physical-chemical composition

	0 month	3 months	12 months
pH	5.3 ± 0.1	5.3 ± 0.1	5.7 ± 0.0
Fat (g/100g)	24.0 ± 1.3	25.0 ± 0.0	26.2 ± 1.0
Total nitrogen (g/100g)	3.17 ± 0.12	3.32 ± 0.04	5.75 ± 0.27
Water soluble nitrogen (g/100g)	1.16 ± 0.17	0.84 ± 0.07	1.00 ± 0.02
Moisture (g/100g)	51.6 ± 1.1	48.5 ± 0.8	48.26 ± 0.9
FTS (g/100g)	49.6 ± 1.9	47.6 ± 0.7	50.8 ± 2.6
MCNF (g/100g)	67.9 ± 0.2	64.7 ± 1.1	65.5 ± 2.0
Hardness (N)	6.18 ± 1.53	10.88 ± 3.73	11.82 ± 0.68
G'-1HZ (kPa)	11.668 ± 4.609	19.700 ± 5.458	13.983 ± 2.178

FTS – Fat in Total Solids; MCNF – Moisture on Cheese no Fat.

The mechanical spectra on fig.2 features a viscoelatic material with a low level of structure similar to the weak gel behaviour with close values for G' and G" and a strong dependence of these on frequency.

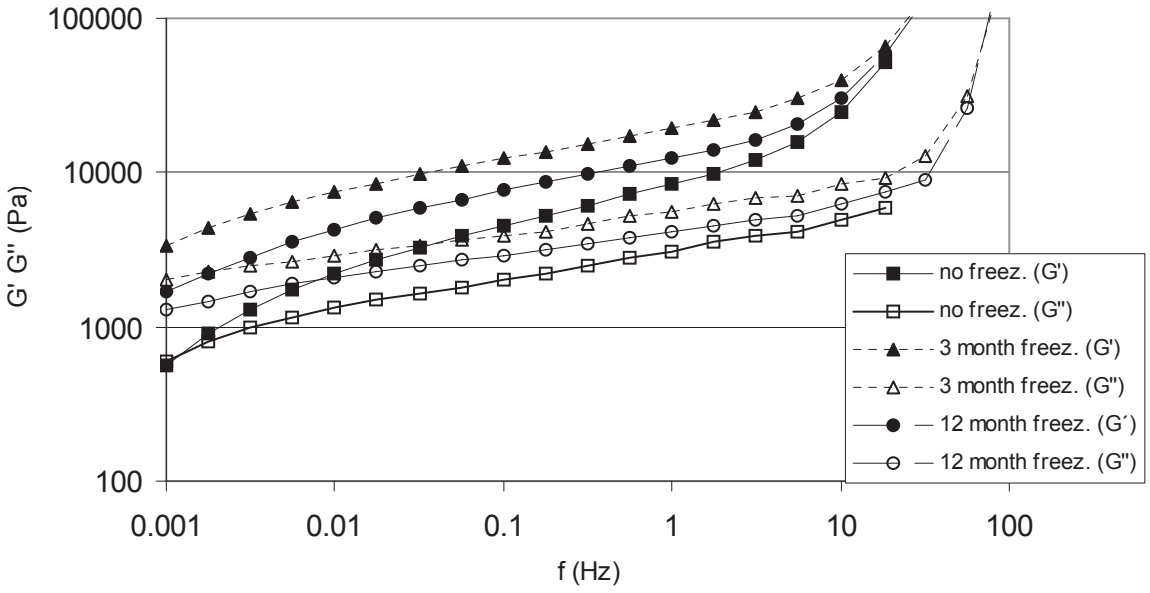

Figure 2 – Mechanical spectra of cheese paste without freezing (square symbols) and with 3 (triangle) and 12 months (circle) of freezing.

The cheese not subjected to freezing (squares in fig. 2) shows the weakest structure with the crossing point at the left of the graph. The relatively highest structure level corresponds to the 3 month freezing cheese (triangles in fig.2). If we translate the spectra into a single number-G'(1Hz), one can see that it closely compaires with hardness. The first increase on hardness and viscoelastic parameters can be explained by the loss of moisture, but the subsequent softening, showed by the cheese with freezing time of 12 month, can only be understood if proteolysis occurred at these low temperatures. These results suggest two different processes: (1) moisture loss with time, resulting in hardness increase and higher values for the viscoelastic parameters, (2) a proteolytic process, with protein damage, resulting in cheese paste softening. In fact, proteolysis may continue at the freezing temperature used and proteolitic activity may even increase during thawing. Storage temperature was far above the Tg for these cheeses. This can explain the progress of proteolytic enzymes, even at –10ºC, since the material is at the "rubbery state" where biological reactions can take place, at considerable rates. The other critical step is thawing, where this proteolysis can be enhanced by internal mechanical damages produced by water crystal growth that will induce higher contact between enzymes and proteins.

4- REFERENCES

[1] Fennema, O. (1972). Freezing of cheese - pros and cons. Western milk ice cream news, 20 October, Leete, Greenbrae, CA.

[2] Diefes, H.A. Rizvi, S.S.H. Bartsh, J.A. (1993). *Rheological behaviour of frozen and thawed low-moisture part skim, Mozzarella cheese*. Journal of Food Science, 58, 764-769.

[3] Cervantes, M.A.; Lund, D.B.; Olson, N.F. (1983). *Effects of salt concentration and freezing on Mozzarella cheese texture*. Journal of Dairy Science, 66, 204-213.
[4] Bertola, N.C. Califano, A.N.; Bevilacqua, A.E.; Zaritzky, N.E. (1996a). *Effect of freezing conditions on functional properties of low moisture Mozzarella cheese*. Journal of Dairy Science, 79, 185-190.
[5] Bertola, N.C.; Califano, A.N.; Bevilacqua, A.E.; Zaritzky, N.E. (1996b). *Textural changes and proteolysis of low moisture Mozzarella cheese frozen under various conditions*. Lebensmittel Wissenschaft und Technologie, 29, 470-474.
[6] Portaria nº 73/90 (1990). *Regulamenta as características, classificação, acondicionamento, rotulagem e condições de conservação do queijo*. Diário da República de 1 de Fevereiro de 1990 - 1ª Série.
[7] Ak, M.M. & Gunasekaran, S. (1995). *Measuring Elongational properties of Mozzarella Cheese*. Journal of Texture Studies, 26, 147-160.
[8] Califano, A.N. & Bevilacqua, A.E. (1998). *Freezing low moisture Mozzarella cheese: changes in organic acid content*. Food Chem, 64, 193-198.
[9] Alvarenga, N.B.M.G & Sousa, I. (2000). *Evaluation of texture measurements of soft cheese*. Proceedings of the XIIIth International Congress on Rheology, IV volume, Cambridge, UK, pp. 392-394.
[10] Alvarenga, N.B.M.G., Raymundo, A.; Sousa, I. (2001). *Evolução da Textura e da Composição Físico-química do Queijo Serpa ao Longo da Maturação*. Proceedings of the "5º Encontro de Química dos - Alimentos da Sociedade Portuguesa de Química". Escola Superior de Biotecnologia - Universidade Católica Portuguesa.
[11] Blanshard, J. & Lillford, P. (Ads.) (1993). *The glassy state in foods*. Nottingham University Press, Nottingham, UK, pp 103-122.
[12] Canet, W.; Acevedo, H.M. & Juárez, M. (1995). *Estudo de la influencia de la congelación y de la conservación al estado congelado in Reología y Textura de Productos* Alimentarios de Interés Industrial. Grupo Español de Reología – Real Sociedad Española de Química.

ESTUDO DA DETERMINAÇÃO DA CAPACIDADE DE RETENÇÃO DE ÁGUA EM LOMBO DE PORCO PRETO

Costa, M.[1]; Ferro Palma, S.[1]; Alvarenga, N.B; Garcia, C[2].*

1-ADCTA Escola Superior Agrária de Beja, Tel.+351284314300 Fax: + 351284388207
2- Universidad de Extremadura, Faculdad de Veterinária, Tel. +34927257122
Email: lela.costa@esab.ipbeja.pt

Palavras chave: Capacidade de Retenção de Água, Pistométrico, Texturómetro, Centrifugação.

Abstract:
The Water-Holding Capacity (WHC) was determined in a sample of an entire pork loin and a sample of crushed, using three different methods as follows: the pistometric method, the centrifugation method only applies to the entire sample and the texturometer method using two different forces. From these determinations we draw the conclusion that the most reliable method is the method of centrifugation applied to the entire sample, followed by the (TI2385) method and the (PI) method, which show results in order of the 30% and such a value seems to be closer to the real and the most prevailing in the different method.
The method selected was the (PI), since it is the one with the best performance, with a lower economic investment and with WHC values quite acceptable.

1. INTRODUÇÃO

O objectivo deste trabalho é a selecção de um método de Capacidade de Retenção de Água mais eficaz e que apresente melhores resultados.
A Capacidade de Retenção de Água (CRA) é a propriedade mais estudada na Tecnologia de Alimentos e dela dependem outras, tais como a cor, dureza e rugosidade dos produtos cárneos. É importante em qualquer produto cárneo, já que determina dois importantes parâmetros económicos: as perdas de peso nos processos de transformação e a qualidade dos produtos obtidos [1].
A carne pode em função do seu Poder de Retenção de Água, absorver mais ou menos água. Esta faculdade de absorção de água extrínseca designa-se por "Poder de Inchamento". Poder de Retenção de Água e Poder de Inchamento da carne, são dois factores intimamente ligados, sendo um determinante do outro. Para que a carne possa absorver a água, é preciso que a fibra se liberte, ao máximo, do seu sarcolema. Uma vez efectuada esta operação, a carne terá pelo menos ao nível das proteínas miofibrilhares, um comportamento coloidal frente à água [2].
Uma estrutura fortemente reticulada, em consequência das interacções entre a actina e a miosina, dificilmente incha; a estrutura rígida opõe-se à acção da água. Uma estrutura frouxa, absorve mais facilmente a água.
Os 75% de água do músculo estão repartidos em 5% a 10% de água ligada e 90 a 95% de água livre. A água livre está associada às substâncias dissolvidas. Compreende a água imobilizada nos espaços extracelulares (20% de água livre), a água retida pelas miofibrilhas (70% de água livre) por causa da configuração das proteínas musculares e a água retida pelo retículo sarcoplasmático (10% de água livre). É a água livre que intervém na Capacidade de Retenção de Água [3].

A Capacidade de Retenção de Água evolui regularmente no músculo, no decorrer da sua transformação em carne, podendo distinguir-se dois períodos: o período que vai do abate até ao fim da rigidez cadavérica e o período de maturação propriamente dito. Se os fenómenos

que afectam a capacidade de retenção de água são bem conhecidos no decorrer do primeiro período, é raro encontrar estudos sobre a sua evolução no decorrer da maturação [3].

Pode-se no entanto ainda referir um período que antecede os dois atrás citados, o qual corresponde ao repouso do animal antes do abate, evitando que ele entre em stress, e que pode influenciar esta capacidade.

Quando o objectivo da medida é comparar a capacidade de retenção de água de diferentes amostras de carne, é importante que uma pressão alta, adequada e constante, se aplique sobre circunstâncias standard. A capacidade de retenção de água deveria ser expressa, não como água libertada, mas como a água retida, isto é, a diferença entre a água total e a água libertada [4].

2 - MATERIAL E MÉTODOS

2.1 - Material

Foram analisados 5 lombos de porco de raça Ibérica indiscriminadamente direito e esquerdo, provenientes da salsicharia F40 em Pedrogão, distrito de Beja.
Estas amostras foram recolhidas em Janeiro e foram transportadas numa mala térmica, uma vez que a quantidade e as distâncias não justificaram o uso de outros equipamentos de transporte, até ao laboratório.

2.2 Métodos

2.2.1 - Método Pistométrico
2.2.1.1 Em lombo inteiro (PI) [5] (modificado).
Pesa-se a amostra de lombo filetiado (0,3g inteiro) (m), a qual é inserida entre as duas folhas de papel de filtro. A amostra é depois submetida a uma determinada pressão durante 5 minutos através de um pistão de peso 2385g numa superfície nivelada. Por último retira-se a amostra prensada e pesam-se os dois papéis de filtro com a água que ficou retida (P2). O resultado é expresso em percentagem.
2.2.1.2 - Em Lombo Moído (PM).
Pesa-se a amostra de lombo (5g moído) (m), a qual é inserida entre as duas folhas de papel de filtro. A amostra é depois submetida a uma determinada pressão durante 5 minutos através de um pistão numa superfície nivelada. Por último retira-se a amostra prensada e pesam-se os dois papéis de filtro com a água que ficou retida (P2). O resultado é expresso em percentagem.
2.2.2 – Método por Centrifugação (C) em lombo inteiro à velocidade de 20000 rotações por minuto (rpm) durante 15 minutos [6] (modificado).
Pesa-se a amostra de lombo (1g inteiro) (m),para os papéis de filtro anteriormente pesados, a qual é inserida num tubo de vidro sem homogeneizar centrifugando-se a 20000 rpm durante 15 minutos.
Por último retira-se a amostra centrifugada e pesam-se os dois papéis de filtro com a água que ficou retida (P2). O resultado é expresso em percentagem.

2.2.3 – Método pelo Texturómetro
2.2.3.1 – Em Lombo inteiro com a aplicação de uma força 2385g (TI2385).
O aparelho utilizado para a realização do teste foi o Texturómetro TA-Hdi Stable Microsystem. Este, está ligado a um computador e é controlado por um programa informático Texture Expert [7].
Pesa-se a amostra de lombo (0,3g inteiro) (m), a qual é inserida entre as duas folhas de papel de filtro. Depois de escolhida a sonda e de definir as condições de teste coloca-se a amostra por baixo e ao centro da sonda fazendo-se correr o teste.
A amostra é submetida a uma determinada força (2385g).
Por último retira-se a amostra prensada e pesam-se os dois papéis de filtro com a água que ficou retida (P2). O resultado é expresso em percentagem.
2.2.3.2 – Em Lombo inteiro com a aplicação de uma força 5000g (TI5000).
Pesa-se a amostra de lombo (0,3g inteiro) (m), a qual é inserida entre as duas folhas de papel de filtro. Depois de escolhida a sonda e de definir as condições de teste coloca-se a amostra por baixo e ao centro da sonda fazendo-se correr o teste.
A amostra é submetida a uma determinada força (5000g)
2.2.3.3 – Em Lombo moído com a aplicação de uma força 2385g (TM2385)
Pesa-se a amostra de lombo (5g moído) (m), a qual é inserida entre as duas folhas de papel de filtro. Depois de escolhida a sonda e de definir as condições de teste coloca-se a amostra por baixo e ao centro da sonda fazendo-se correr o teste.
A amostra é submetida a uma determinada força (2385g)
Por último retira-se a amostra prensada e pesam-se os dois papéis de filtro com a água que ficou retida (P2). O resultado é expresso em percentagem.
2.2.3.4 – Em Lombo moído com a aplicação de uma força 5000g (TM5000)
Pesa-se a amostra de lombo (5g moído) (m), a qual é inserida entre as duas folhas de papel de filtro. Depois de escolhida a sonda e de definir as condições de teste coloca-se a amostra por baixo e ao centro da sonda fazendo-se correr o teste.
A amostra é submetida a uma determinada força (5000g).
Por último retira-se a amostra prensada e pesam-se os dois papéis de filtro com a água que ficou retida (P2). O resultado é expresso em percentagem.

Para cada método foi determinado o DP (Desvio Padrão) (S) e a Média através do programa Microsoft Excel 97 nos 5 lombos (10 repetições de cada amostra de lombo).
Seguidamente calculou-se o erro, fez-se a identificação dos valores aberrantes pelo teste de Grubbs, eliminando-os no caso de existirem, e por último fez-se o cálculo da repetibilidade e da avaliação da capacidade de discriminação.

3. RESULTADOS E DISCUSSÃO

Nas figuras 1 e 2 podem observar-se as médias da Capacidade de Retenção de Água nos diferentes métodos aplicados à amostra moída e à amostra inteira

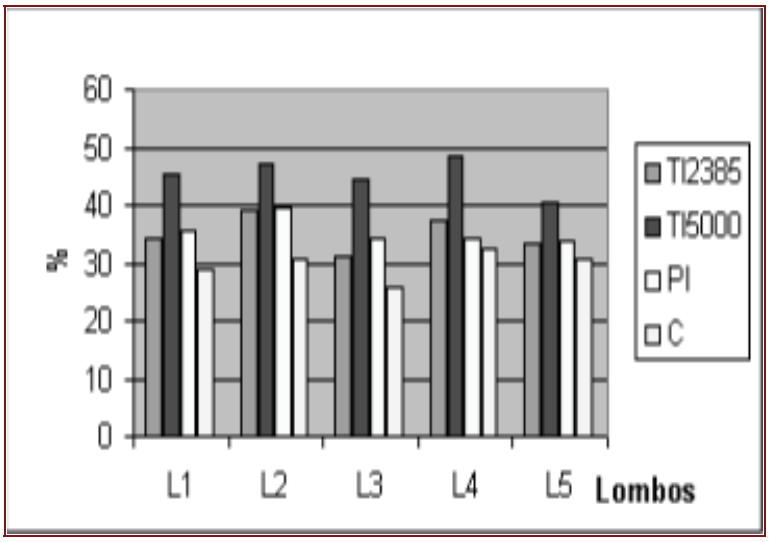

Figura 1 - Médias da determinação da C.R.A obtidas nos diferentes métodos em Lombo Inteiro

TI 2385 = Método pelo texturómetro com uma força 2385g para lombo inteiro
TI 5000 = Método pelo texturómetro com uma força 5000g para lombo inteiro
PI = Método pistométrico lombo inteiro
C = Método por Centrifugação

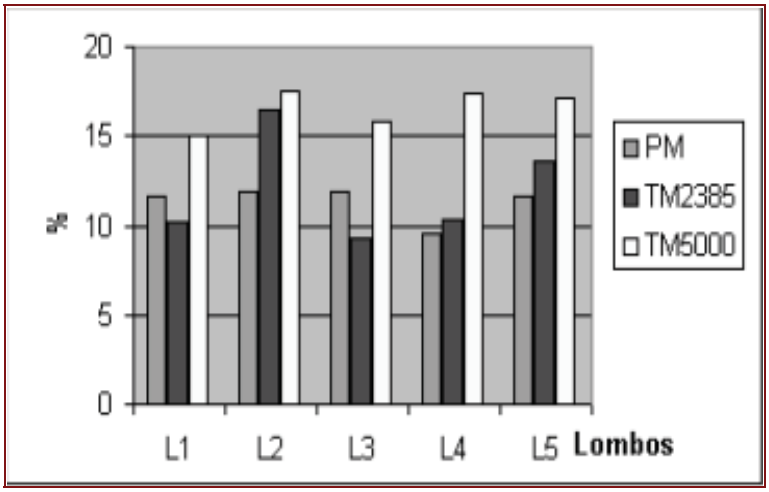

Figura 2 - Médias da determinação da C.R.A obtidas nos diferentes métodos em Lombo Moído

TM 2385 = Método pelo texturómetro com uma força 2385g para lombo moído
TM 5000 = Método pelo texturómetro com uma força 5000g para lombo moído
PM = Método pistométrico lombo moído

Grau-Hamm, Kauffman *et al* modificado por Ribeiro [8] usaram o método da compressão para 0,3g de amostra inteira (à semelhança destes métodos) e determinaram a CRA através do cálculo da área da mancha impressa no papel de filtro.
Utiliza este mesmo método e regista valores aproximados de 35% de CRA em carne fresca de ovinos [9].

À semelhança de outros autores os três métodos utilizados neste trabalho que obtiveram valores próximos dos esperados são os que utilizaram a amostra inteira.

Como se pode verificar pela análise da figura 1, o método que obteve maior percentagem de Capacidade de Retenção de Água foi o método do texturómetro para a amostra inteira (TI5000), seguido do método do texturómetro para a amostra inteira (TI2385), que apresentam resultados em todas as amostras acima dos 40% e 35%, respectivamente. No entanto, estes resultados são anormalmente elevados, julgando-se que também foi arrastada gordura da amostra ou até possivelmente ocorreu rompimento no tecido celular. Este rompimento, pode provocar perdas de líquido intracelular, induzindo a erro os resultados obtidos.
Em relação ao método da centrifuga e do pistão aplicado à amostra inteira, pode verificar-se que são os métodos que aparentemente se julgam dar melhores resultados, uma vez que todos os lombos apresentam uma percentagem de Capacidade de Retenção de Água na ordem dos 30%.

Como se pode verificar pela análise da figura 2, os métodos que apresentam Capacidade de Retenção de Água mais baixa são os métodos do pistão (PM) e texturómetro (TM2385 e TM5000) variante f= 2385g e f=5000g, para a amostra moída, pois apresentam resultados abaixo dos 20% em todas as amostras, provavelmente devido a perdas de água na moenda.
O método do Pistão para a amostra moída é o que apresenta um erro médio e repetibilidade média menor de 0,64% e 0,72%, respectivamente. Por outro lado, o método do Pistão para a amostra inteira é o que apresenta um erro médio e repetibilidade média mais altos com 4,34% e 15,48%, respectivamente.
Ainda convém salientar que o método do Texturómetro na variante f=2385g, relativamente ao método do texturómetro variante f=5000g, é o que apresenta valores médios de repetibilidade e erro mais altos, tanto para a amostra inteira como para a amostra moída.

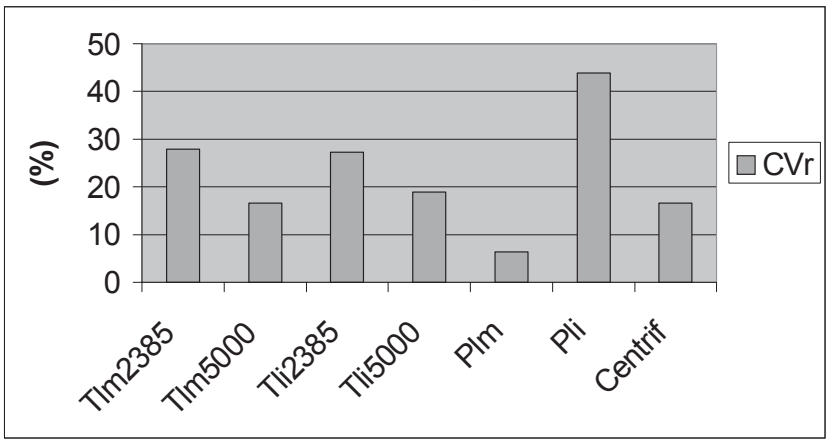

Figura 3 – Valores médios do coeficiente de variação da repetibilidade para os diferentes métodos nos lombos

Tlm 2385 = Método pelo texturometro com uma força 2385g para lombo moído
Tlm 5000 = Método pelo texturometro com uma força 5000g para lombo moído
Tli 2385 = Método pelo texturometro com uma força 2385g para lombo inteiro
Tli 5000 = Método pelo texturometro com uma força 5000g para lombo inteiro
Plm = Método pistométrico lombo moído
Pli = Método pistométrico lombo inteiro
Centrif = Método por Centrifugação

Da observação da figura 3 podemos concluir que o método do pistão para a amostra moída (Plm) é o que apresenta melhor repetibilidade, uma vez que, o coeficiente de variação da repetibilidade é menor (6,37%), seguido dos métodos da centrifugação e do texturómetro para a amostra moída f=5000 (Tlm 5000) que apresentam um coeficiente de variação da repetibilidade igual de 16,64%.
No entanto convém referir que apesar do método do pistão para a amostra moída (PM) apresentar melhor repetibilidade apresenta valores de CRA baixos.
Por outro lado, os métodos que apresentam pior repetibilidade são o método do pistão para a amostra inteira (Pli) e o método do texturómetro variante f=2385g para a amostra moída (Tm2385) e para a amostra inteira (Tli2385), uma vez que apresentam valores de coeficiente da repetibilidade elevados 43,94%, 27,32% e 27,81%, respectivamente.

4. CONCLUSÃO

A Capacidade de Retenção de Água da carne (CRA) aparece como uma característica complexa difícil de dominar. Ela contribui com a cor, sabor e a maciez para a qualidade gustativa da carne.

Depois de uma análise imediata dos resultados obtidos podemos ser levados a crer que o Método pelo texturómetro (TI5000) é que apresenta valores mais elevados de Capacidade de Retenção de Água. No entanto e pelo anteriormente referido na discussão, a acreditação deste método obriga a estudos mais aprofundados por forma a compreender melhor os resultados obtidos.

Os três métodos que utilizaram a amostra moída (Pistão, Texturómetro f=5000g e 2385g), apresentam piores resultados de Capacidade de Retenção de Água que os métodos que utilizaram a amostra inteira.

É de notar que a quantidade de amostra moída utilizada foi de aproximadamente 5g enquanto que, para os métodos que utilizaram amostra inteira foi de aproximadamente 0,3g, pelo que pode estar aqui um factor de variabilidade, uma vez que a amostra ao ser moída pode perder água.

Após a discussão dos resultados do presente trabalho, o método que nos dá resultados mais confiantes na determinação da Capacidade de Retenção de Água no Lombo de porco é o Método da Centrifugação (C), seguido do método do Texturómetro (TI2385g) aplicado à amostra de lombo inteiro que apresentam resultados na ordem dos 30%, valor que nos parece mais perto do real e predominante dos diferentes métodos.

Frente a estes resultados, é difícil determinar qual o melhor método para a CRA, visto que os três métodos que utilizam amostra inteira apresentam valores muito próximos, mas correspondentes a diferentes coeficientes de variação da repetibilidade. Os métodos da centrifugação e do texturómetro (TI2385) apresentam menores coeficientes de variação da repetibilidade, contudo pela fácil execução do método do pistão (PI), pelo fraco investimento económico e pela obtenção de valores de CRA bastante aceitáveis, seriamos levados a seleccionar este método, apesar de ter um coeficiente de variação de repetibilidade superior.

6. BIBLIOGRAFIA

1. Torre, G.L., García, B.M.C. (1991). *Manual de Bioquímica Y Tecnologia de la Carne.* Editorial Acríbia, S.A. Zaragoza (España).
2. Girard, J.P. (1991). *Tecnologia de la Carne y de los Productos Cárnicos*. Editorial Acríbia, S.A. Zaragoza (España).
3. Rosset, R., Lameloise,P. (1983). *Le Pouvoir de Retencion d' Eau de la Viande*. Editorial Acríbia S.A. Zaragoza (España). **7.** Pederson, J.W. (1994). Água. *Ciência de la Carne Y de los Productos Carnicos*. Editorial Acríbia, S.A. Zaragoza (España)
4. Pederson, J.W. (1994). Água. *Ciência de la Carne Y de los Productos Carnicos*. Editorial Acríbia, S.A. Zaragoza (España).
5. Grau, R. And Hamm, R. 1953. Eine einfache Methode zur Bestim-mung der Wasserbindung im Muskel. Naturwissenschaften *40*, 29.
6. Bouton, P. E., Harris, P. V. and Shorthose, W.R. 1971. Effect of ultimate pH upon the water holding capacity and tenderness of mutton. J. Food Sci. *36*, 435**.**
7. Alvarenga, N. B. M. G.(2000). *Estudos em textura de queijo Serpa*. Dissertação para Obtenção do Grau de Mestre em Ciência e Tecnologia dos Alimentos. Universidade Técnica de Lisboa.
8. Ribeiro, M.G.T.S.P.C.P. (1998). Textura de Queijo – *Um Estudo de Variáveis de Processamento*. Dissertação para a Obtenção do Grau de Mestre em Ciência e Tecnologia dos Alimentos. Universidade Técnica de Lisboa.
9. Silva, J.M.B.S. (1997), *Contributo para o Estudo do Crescimento, das Características das Carcaças e da Qualidade da Carne de Borregos das Raças Serra da Estrela, Merino Branco e Churro da Terra Quente em Sistemas Intensivos de Produção.* Doutoramento em Engenharia Agronómica. Universidade Técnica de Lisboa. Instituto Superior de Agronomia

PRACTICAL RHEOLOGICAL MEASUREMENTS IN YOGHURT

Cardoso A, Cruz MB, Gonçalves MA, Ribeiro RR & Sousa IMN

e-mail: isabelsousa@isa.utl.pt
SCTA/DAIAT - Instituto Superior de Agronomia,Universidade Técnica de Lisboa, Tapada da Ajuda, 1349-017 Lisboa, Portugal

Abstract

The yoghurt is a biologically active dairy product, therefore it presents a relatively reduced shelf life.
The main effect of yoghurt biological activity is the reduction on pH with acid production. This should have an impact on the yoghurt gel structure, since sineresis is common with yoghurt ageing. This gel structure variation with time must be detected by rheological measurements.
The objective of this practical study, was to investigate which method proved to be able to discriminate between a yoghurt "before expiring date" and an "off the shelf life period" yoghurt. This study was set up with a simple protocol within the scope of the practical classes of the Rheology course.
Two package of yoghurt from a set of four were tested, one of them was kept in the refrigerator and the other was left at room temperature (23 – 26 ºC) for five days. Measurements with the Texturometer TAX – T2 from Stable Microsystems; the Viscometer Brookfield and the Rheometer RS 75 from Haake Germany were taken with four replicates in the texturometer and Rheometer and three for the viscometer. The statistical tool one way ANOVA/MANOVA with “post hoc comparisons” by the Scheffé test was used to analyze the results.
Dynamic measurements gave viscoelastic parameters using the rheometer and these were not able to differentiate the two yoghurts the viscosity by the Brookfield was also not able to distinguish the two materials, but the texturometer was able to discriminate the two yoghurts for firmness.

1-Introduction

The gel structure of yoghurt contributes strongly to its characteristic texture, which is an important organoleptic property perceived by the consumer. The gel is, however, highly shear-sensitive, and the rheology and texture of a yoghurt are thus strongly dependent on the amount of mechanical processing which it receives between gel formation and eventual consumption. There are two types of yoghurt, stirred and set. Set yoghurt is inoculated, filled and incubated in the retail container itself. This process usually forms a firm gel. It is important to be able to understand the factors which govern the rheology of yoghurt and to be able to predict the changes which will occur during processing, as this will allow the selection of processing plant which allows development of the best possible product texture, for the example the elimination of pumps which gives excessive shear.
Rheological analysis of yoghurt is thus necessary for the production of material with organoleptic properties acceptable to the consumer, and for the design of correct processing equipment and procedures. Ideally, it should be possible to use quality assurance (QA) data to modify and control process conditions to produce a product with quality attributes acceptable to the consumer (1).
In an attempt to quantify the effect of shear on the structure of the gel can be quantified in terms of changes in G’ and G’’, the storage and loss moduli it was concluded (1) that at low

strains, yoghurt is primarily elastic, i.e G'>G'', but at high strains the gel structure breaks down, and the material becomes viscous, G''>G'.
The objective of this practical study was to investigate which method proved able to discriminate between a yoghurt "before expiring date" and a yoghurt passed it's shelf life period. The following parameters were determined and compared: the conservative and dissipative moduli (Rheometer), flow and consistency (Brookfield Viscometer), firmness and adhesivity (Texturometer).

2-Material and methods

Two package of yoghurt from a set of four were tested, one of them was kept in the refrigerator and the other was left at room temperature (23 – 26 ºC) for five days, to reduce the shelf life.

Dynamic measurements

Rheological measurements were performed using a controlled-stress rheometer (RS – 75, Haake, Germany) using a serrated parallel plate sensor (35 mm) with 1 mm gap, at 25 ºC± 1 ºC.
Stress sweep tests were performed to determine the linear viscoelastic region. The stress range applied was of 0,1- 2000 Pa, with a constant frequency of 1 Hz.
The frequency sweep tests were set up inside the viscoelastic region, in a frequency range of 10^{-2} -10^{2} Hz. The constant stress applied to the "out of the expire date" yoghurt was 30 Pa, and 10 Pa to the other one.
The determinations were replicated four times.

Flow measurements

The Brookfield Viscometer was used to determine the consistency and the flow index. The spindle nº 25 was used and three replicates were made. The rotation speed ranged from 0,5 up to 100 rpm. The outer cylinder's radius was 9,5 mm, and the inner cylinder was 2,39 mm.
The power law equation was used to fit the results and consistency in $Pa.s^n$ and flow index was obtained from linearization of the results.

Texture measurements

The textural variables, firmness and adhesiveness, were obtained from the textural profile analysis carried out in a texturometer TA-XT2 (Stable Micro Microsystems, UK). Penetration tests were performed in the commercial package of the yoghurt (50 mm diameter and 60 mm height), using a cylindrical probe of 10 mm diameter (25 mm of penetration and 1 mm/s of crosshead speed). These determinations were conducted at 20 ºC ± 1 ºC and replicated four times.

Statistical Analysis

The statistical tool one way ANOVA/MANOVA with "post hoc comparisons" by the Scheffé test was used to analyze the results.

3-Results and Discussion

From the dynamics measurements in the controlled stress rheometer a set of results were obtained as follows.

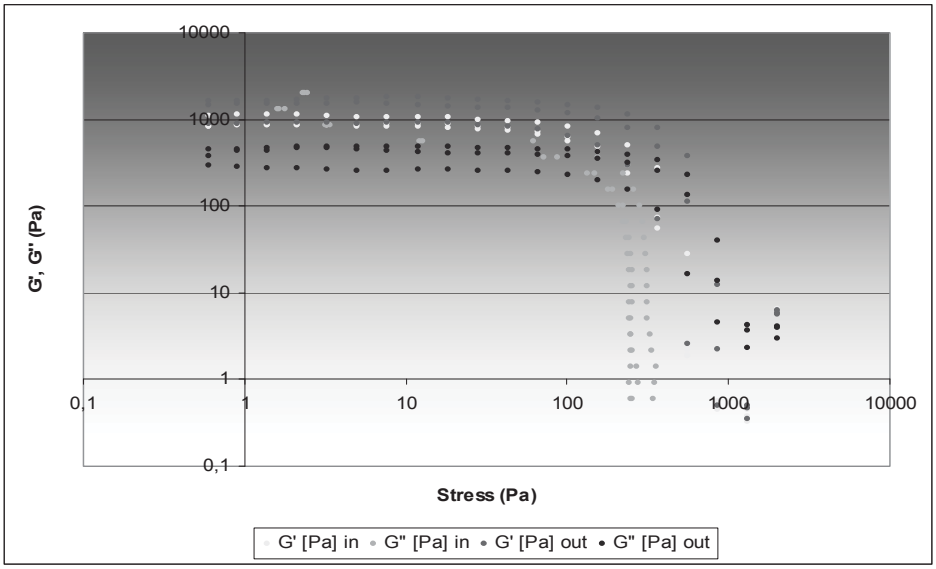

Fig. 1 – Stress sweep for the two yoghurts

The yoghurt's linear viscoelastic zone goes up to 10 Pa (before expiring date), and 30 Pa (off the shelf life period) as it can be seen in Fig. 1.

A bigger extension of the linear viscoelastic zone may be interpreted into a higher material structuration level, since it reflects a higher resistance to higher tensions.

It is not possible to discriminate between the two yoghurts with the stress sweep, since both present similar behaviors.

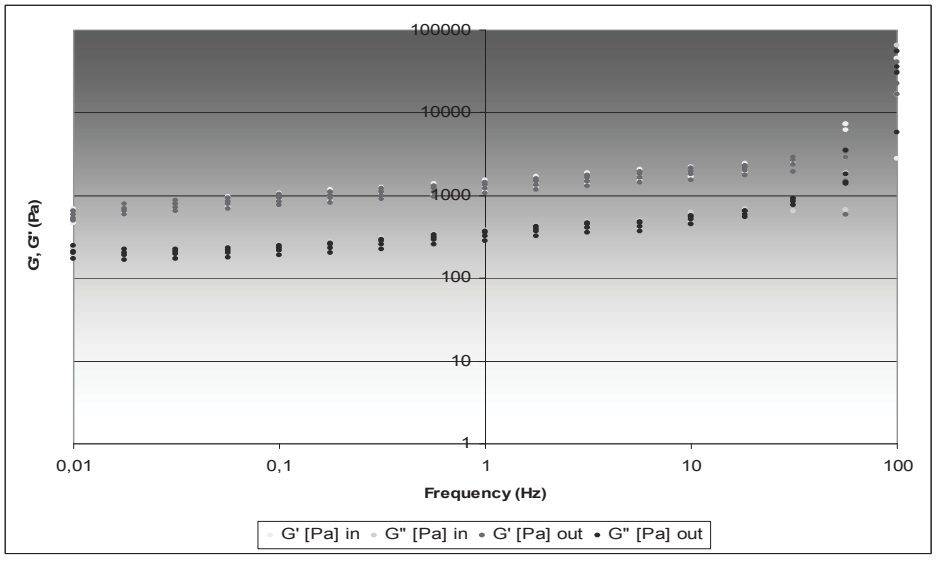

Fig. 2 –Frequency sweep for the two yoghurts

From the mechanical spectra of the two yoghurts, as one can observe in Fig. 2, the G´ values are always superior to G'', which represents a predominance of the elastic component over the viscous component, as it was expected since at lower tensions, the yoghurt is essentially elastic, i.e., G´>G´´.

Here it is also impossible to differentiate both yoghurts as the behavior of G' and G" with frequency remains similar for both cases.

From the results obtained in the rotational viscometer, whose power law adjustments are shown in Fig. 3 and Fig. 4. These linearizations permit the calculation of consistency *k* and flow index *n*. Further Scheffé contrasting of these values gave a probability value of 0,544 for the consistency, meaning that values of these parameter for yoghurt in and yoghurt out aren't significantly different; for the flow index the *p-value* was of 0,294 meaning that there are no significantly differences between the two yoghurts.

In this case, the rotational viscometry using high shear where yoghurt performs essentially as a viscous material (1) wasn't able to discriminate the two different yoghurts.

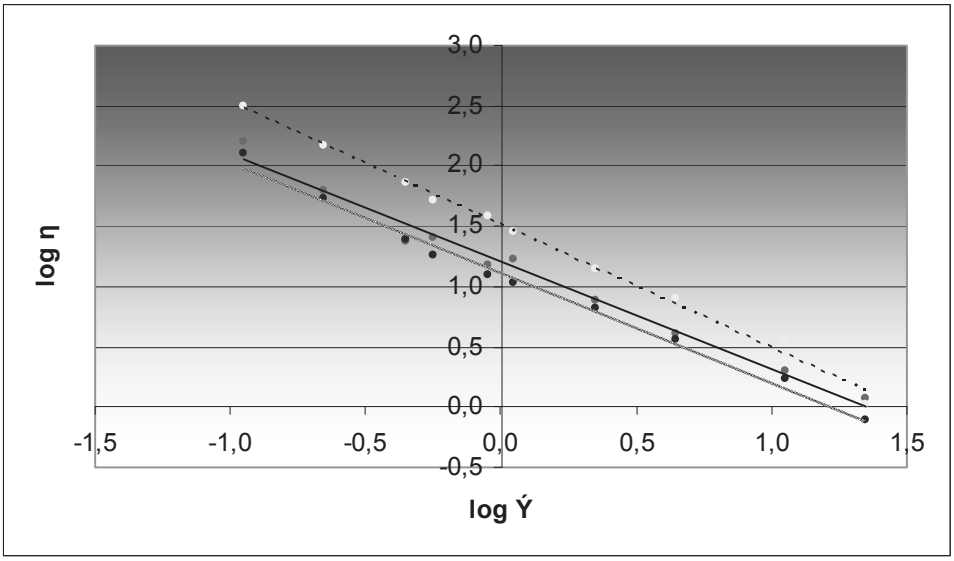

Fig. 3 – Linearization of Brookfield experimental results of three replicates and power law adjustment for yoghurt in

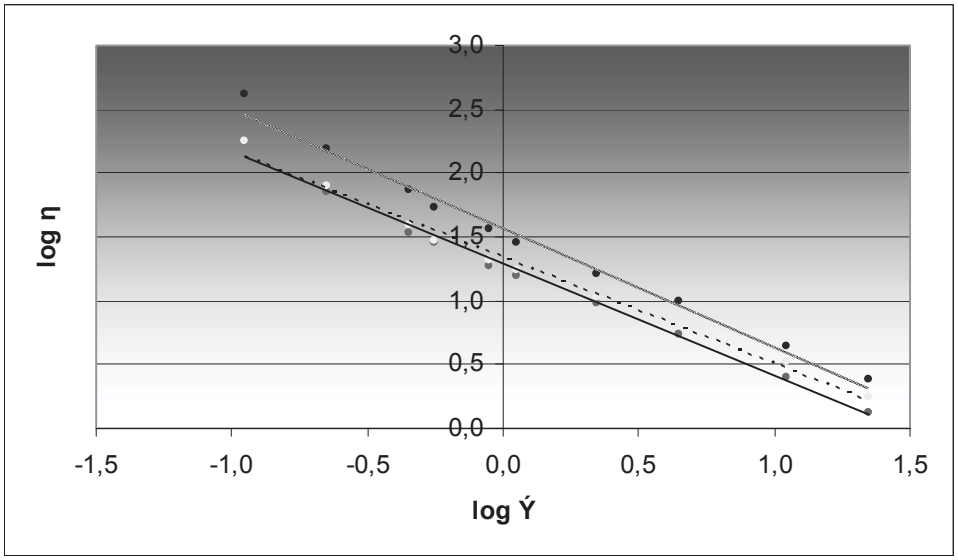

Fig. 4 – Linearization of Brookfield experimental results of three replicates and power law adjustment for yoghurt out

An example of the texturogram resulting from the penetration test in yoghurt can be seen in Fig. 5.

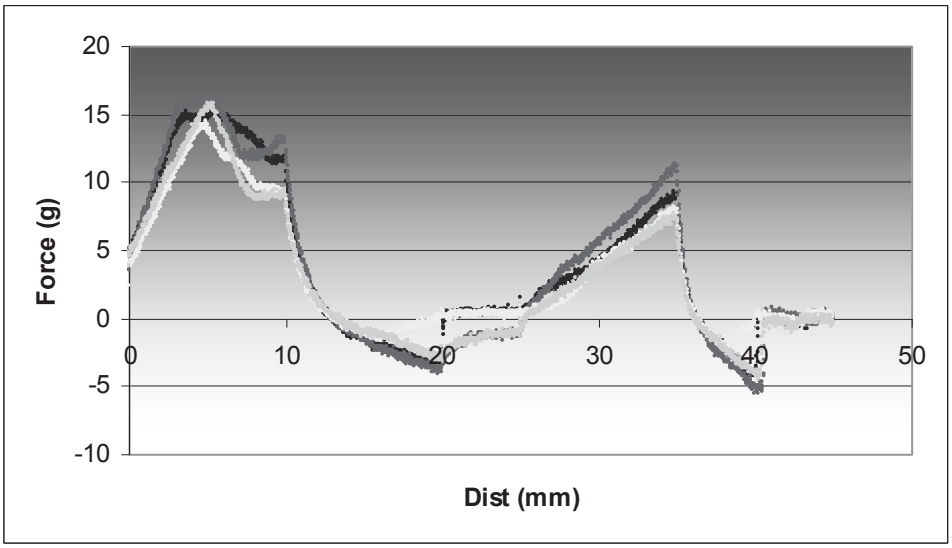

Fig. 5 – Texturogram resulting from four penetration tests

Firmness as the height of the first peak contrasted by the Scheffé method gave a *p-value* of 0,022, i.e. the two yoghurts showed significant different values of firmness. Adhesivity, the negative area of the texturogram did not show significant differences with a *p-value* of 0,369 higher than 0,05.

Texture could only discriminate between yoghurts when the firmness parameter was considered.

Conclusion

- In the present work, only the texturometer gave significant differences for the determinations of firmness. No differences were found on the mechanical spectra at low stress regime or in the high shear regime on the rotational viscometer. This might be showing that the two yoghurts were similar, since the out of date yoghurt was forced by exposing to ambient temperature.
- This needs further investigation with yoghurts not from the same lot of production but with one out of the expiring date. The pH measurements and the quantity of sineresis will give support for the conclusions compairing the data given by the 3 different conditions and testing equipment.

Bibliography

1. Steventon *et* al (1990) cited by Carter, R.E., (1990), *Rheology of food, pharmaceutical and biological material whit general rheology,* Elsevier Applied Science Publishers Ltd, NY

TEXTURE MEASUREMENTS IN BEEF. I. FROSEN IN DOMESTIC FREEZERS

*Lourenço AC, Pereira ML Simões MB & Sousa IMN**

e-mail: isabelsousa@isa.utl.pt

SCTA/DAIAT - Instituto Superior de Agronomia,Universidade Técnica de Lisboa, Tapada da Ajuda, 1349-017 Lisboa, Portugal

Keywords: Meat, Texture, Domestic freezers, Frozen beef

Abstract

Texture is a fundamental attribute for meat quality. The Warner-Bratzler cell is the standard probe to measure meet tenderness. However, the geometry of this blade is relatively complicated, which adds difficulty when interpreting texturograms.
This is a practical work within the scope of the lab. lectures of the rheology course at the I.S.A. and the objective was to determine the discriminating ability of two simple blades for meet texture evaluation when preserved in domestic freezers. The blades were straight, one was sharp and the other was not: HDP/BSG Blade Set with Knife and HDP/BSG Blade Set with Guillotine from the Stable Microsystems (SMS) UK.Ten beef pieces from the same meet cut were used. The first two were measured in a texturometer TA-XT2 (SMS) in penetration mode at 1mm/s at 8mm deep in a controlled room at 20 ± 1ºC. The other beef pieces were kept in 4 different freezers at -6ºC; -8ºC; -26ºC and -31ºC for 15 days. After this period of time, the meet was defrost for one day in the refrigerator and kept at room temperature. Analysis of texture was performed as for the first two pieces. At least 14 replicates were performed for each blade set and for each of the temperatures tested. Anova/manova statistical analysis (Statistica 6.0) with the Post hoc comparisons using the Scheffé test was used to characterise data. The not sharp Blade set, HDP/BSG Blade Set with Guillotine, was not able to distinguish between the 5 different testing conditions but the sharp blade set, HDP/BSG Blade Set with Knife, gave significantly different results ($P<0.05$) for the maximum force in penetration as a measure of meet tenderness. In conclusion the HDP/BSG Blade Set with Knife proved to be very useful when measuring meet tenderness, with texturograms easy to interpret.

1. Introduction

Meat is a highly perishable food, it deteriorates easily by enzymatic and microbial activity, by dehydration or by oxidation. These mechanisms lead to taste, aroma, and colour losses.
In today's day and age, the quotidian habits of modern life stimulate the consumption of products that have been submitted to the freezing processes. The conditions involving the freezing process are of extreme importance in order to maintain the characteristics of the fresh product.
The study of the impact on meat frozen in conditions simulating household procedure becomes a subject of high importance.
Freezing is a way of preserving products for a long period because it leads to molecular immobilization and at the limit make them go into a vitreous state.
The time needed to achieve the vitreous state will determine the quality of the meat after it defrosts.

The velocity at which the ice crystals form and their size depends on the size of the piece of the meat to be frozen, on the freezing conditions and on the package.
If the freezing process is conducted in a fast way the ice crystals formed are of small dimensions as opposed to a slow freezing which leads to the formation of large ice crystals. Fast freezing causes the formation of ice crystals to be mainly in the spaces between muscular fibres, thus the cellular rupture is restricted (1). This way the losses by exudation of the meat after defrost are reduced, resulting in a product of higher quality, higher juiciness and tenderness. When the process of freezing is slow, the fluids in the spaces between the fibre cells are the first to freeze thus; the concentration of solutes inside cells is higher. By osmotic pressure the water leaves the cell causing higher losses by exudation (2).
Meat quality is evaluated by various parameters such as colour, flavour, texture, juiciness and tenderness, being the latest of great importance.
Tenderness is the result of the muscle protein structure and consequently is affected by various zootechnic characteristics (breed, age, gender); anatomic characteristics (muscle type); fat characteristics; handling and feeding characteristics and technological characteristics (electric stimulation) (3).
Sensory analysis, although a useful instrument in food science, presents great difficulties. This fact has led to the development of instruments of objective measure such as the texturometer.
The texturometer allows the determination of texture by analysis of the material's response to a deformation caused by a probe. Different tests can be run in the texturometer. Simple penetration test consist of submitting the sample to a defined length of puncture, at a defined speed, plotting force along with time.
Firmness is a parameter evaluated in texture analysis, given by the maximum force applied to the sample during the test. Tenderness is directly opposed by firmness.

2. Material and Methods

2.1 Samples preparation

Ten pieces of beef from the same meat cut from the back quarter of the carcass were used. The pieces were cut adjacently approximately 2 cm thick. The meat was bought in a butcher shop.
Two of the beefsteaks were analysed immediately, and the others were put in plastic bags and kept at freezing temperatures for 15 days. The beefsteaks were selected randomly, and two pieces of beef were placed in 4 different domestic freezers under different conditions of freezing, as follows:

Table 1. Freezing conditions

Measured Temperature (±1ºC)	***Type of freezer***	***Observation***	
-6	*Freezer(Indesit) **	*Assembled freezer*	*With top*
-8	*freezer **		*Without top*
-26	*Freezer (Fagor) *****	*Independt freezer*	*First drawer*
-31	*Freezer (AEG) *****		*Last drawer*

2.2 Firmness evaluation

Firmness evaluation was carried out using a texturometer TA-XT2, with two simple blades. The blades were straight, one was sharp and the other was not: HDP/BSG Blade Set with Knife (HDP/BSG-K) and HDP/BSG Blade Set with Guillotine (HDP/BSG-G) from the Stable Microsystems (SMS) UK (fig 1).

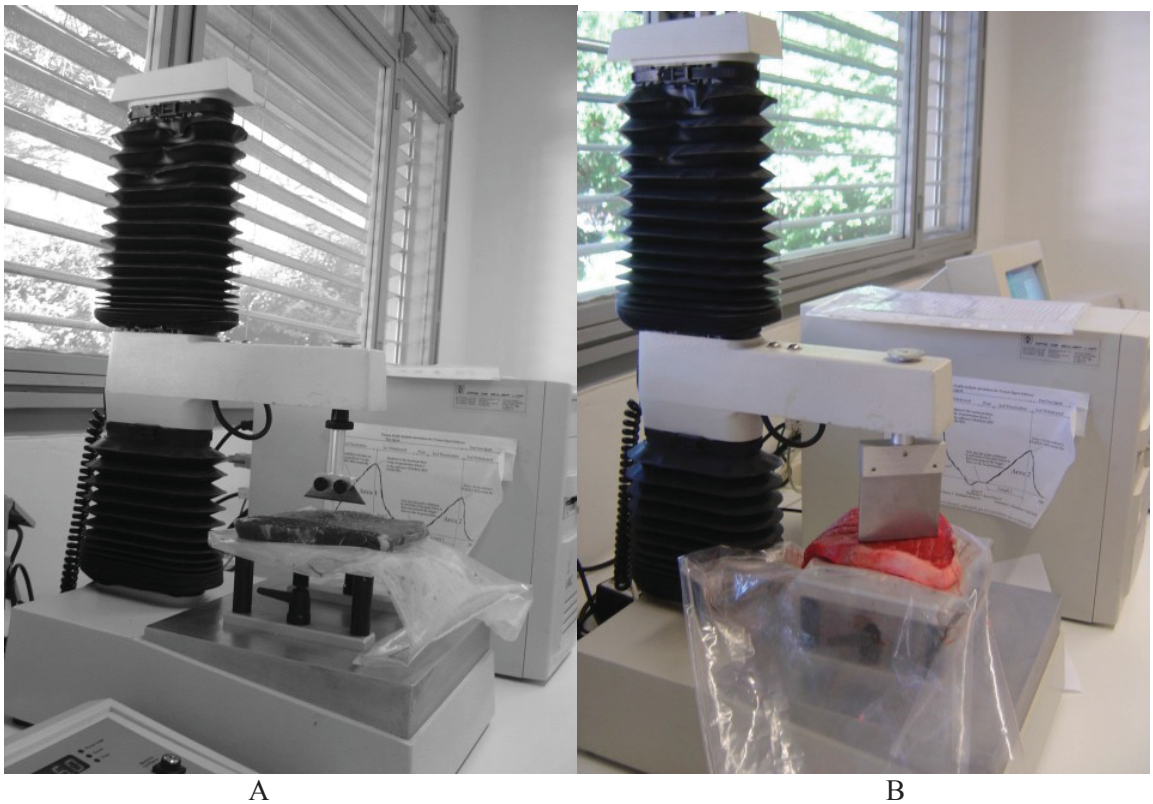

A B

Figure 1. A- HDP/BSG Blade Set with Knife, B- HDP/BSG Blade Set with Guillotine

Tests were conducted at 20ºC ±1ºC in a room with controlled temperature, on freshly cut pieces (reference) and on meat after being defrost in the refrigerator overnight.

In each meat piece 15 cuts were performed at 1mm/s and the resistance to knife penetration at 8mm depth was registered in a texturogram (fig.2).

A

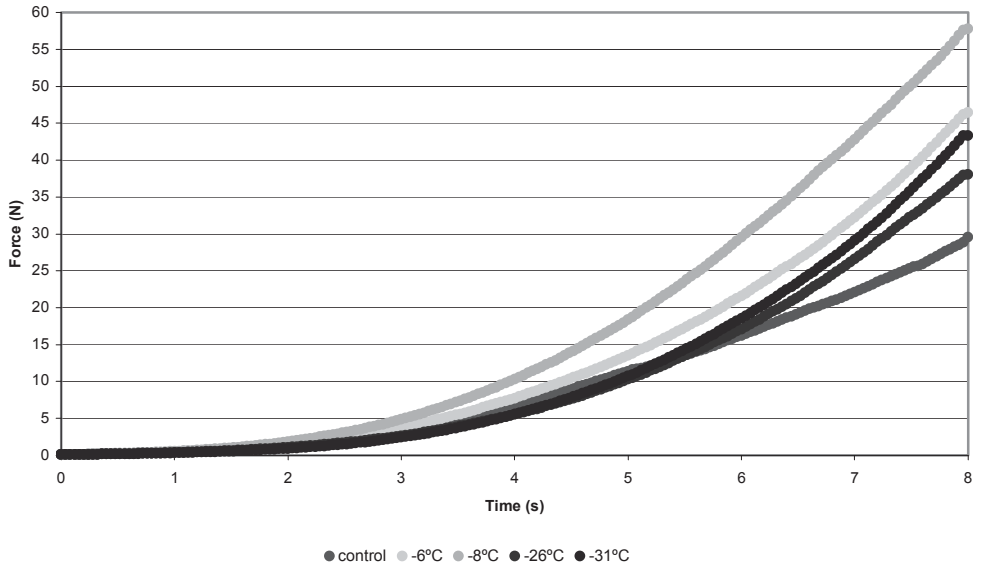

B

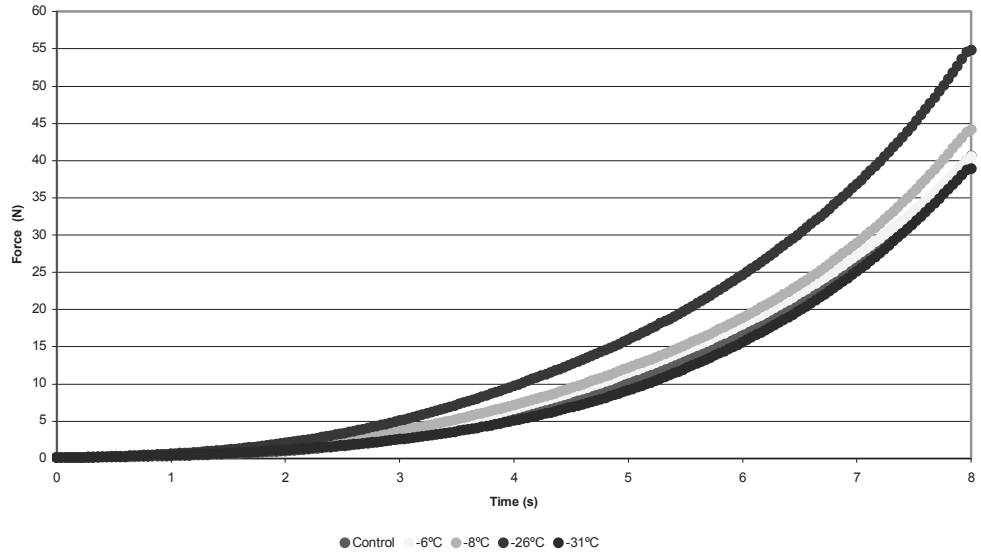

Figure 2. Average texturograms of beef pieces preserved at different temperatures in domestic freezer using the probe A- HDP/BSG Blade Set with Knife, B- HDP/BSG Blade Set with Guillotine

Analysis of the result was performed by Anova/Manova Scheffé test in post hoc comparison for each of the 15 replicates.

To evaluate quality of the results basic statistics with relative error was calculated using the equation:

$$\left(\frac{\delta / \sqrt{n}}{\bar{x}} \times 100 \right) \qquad (1)$$

$\bar{x}$ - average value
δ - standard deviation
n - number of replicates

3. Results and discussion

Table 2 shows the results obtained by penetration of beef pieces (fig1) preserved at different temperatures below 0ºC in four different domestic freezer, using two different blades, a sharp and a non-sharp blade.

Table 2- Average ± standard deviation of firmness determined in TA-XT2by 8mm penetration at 1mm/s of two blades (Sharpe and non-sharp)

	15 Replicates	Reference	-6ºC	-8ºC	-26ºC	-31ºC
Force (N)	Blade HDP/BSG-K	31.68 ± 12.505	46.70 ± 8.488	59.85 ± 9.451	38.77 ± 8.184	43.63 ± 11.094
	Blade HDP/BSG-G	40.59 ± 17.227	40.51 ± 11.082	44.29 ± 12.51	54.96 ± 12.236	38.70 ± 22.646

Comparing the results obtained one can see from table 3 that only the measurements obtained with HDP/BSG Blade Set with Knife were able to differentiate between different temperatures of freezing.

Table 3- Probability values from the Scheffé test contrast for A- HDP/BSG Blade Set with Knife, B- HDP/BSG Blade Set with Guillotine

A	Fresco	- 6ºC	- 8ºC	- 26ºC	- 31ºC
Fresco		0,005715	0,000000	0,548255	0,043673
- 6ºC	0,005715		0,052696	0,256050	0,94925
- 8ºC	0,000000	0,052696		0,000026	0,004562
- 26ºC	0,548255	0,256050	0,000026		0,682779
- 31ºC	0,043673	0,94925	0,004562	0,682779	

B	Fresco	- 6ºC	- 8ºC	- 26ºC	- 31ºC
Fresco		1,000000	0,976353	0,159778	0,998278
- 6ºC	1,000000		0,978135	0,189941	0,998797
- 8ºC	0,976353	0,978135		0,476849	0,912812
- 26ºC	0,159778	0,189941	0,476849		0,104331
- 31ºC	0,998278	0,998797	0,912812	0,104331	

4. Conclusion

From this Short practical work it can be said with statistical confidence of 95% that a blade like HDP/BSG Blade Set with Knife in a penetration test at 1mm/s with 40% penetration depth and 15 replicates will give meaningful results to evaluate tenderness of beef subjected to different temperature conditions in storage for 15 days.

5. References

1. Kaminarskaya, A.K. (1972) Character of crystallisation in animal tissue during freezing under different conditions. *In* "Freezing and storage of fish, poultry and meat". Refrigeration Science and Technology": 229-236.
2. Henrickson, R.L.; Mardsen, J.L. (1994). Carne y productos cárnicos. *In* "Tecnología de los alimentos congelados". Ed. C.P. Mallet. A.Madrid Vicent, Ediciones: 202-211.
3. Blásquez, B.; Huidobro, F.R; Miguel, E.; Onega, E. (2002). Changes in meat quality characteristics of bovine meat during the first 6 days post mortem. Meat Science: 1439-1446.

INFLUENCE OF THE ADDITION OF RESISTANT STARCH ON THE RHEOLOGICAL PROPERTIES OF A BAKERY PRODUCT BATTER

R. Baixauli, A. Salvador and S.M. Fiszman

Instituto de Agroquímica y Tecnología de Alimentos (CSIC)
Apartado de Correos 73, 46100 Burjassot (Valencia)
TEL.:+34 96 390 00 22 FAX:+34 96 363 63 01
e-mail: rbaixauli@iata.csic.es, asalvador@iata.csic.es, sfiszman@iata.csic.es

Keywords: Resistant starch, rheological characteristics, consistency, batter.

ABSTRACT

Resistant starches (RS) are of great interest to the food industry because of their potential benefits to health, as they have similar properties to fibres. Indeed, RS is considered a 'functional fibre'. It may be defined as the starch fraction that is not broken down by enzyme hydrolysis in the small intestine but does ferment in the colon. Because of its low moisture retention, it can be used in intermediate moisture foods such as bakery products. The purpose of this work is to study the influence of the addition of RS (5-15% dry weight) on the rheological properties of a muffin batter. Batter flow was characterised by an adjustment to the Ostwald-de Waele equation. At low RS concentrations no variation in the consistency index (k) was observed but at 10% or higher it fell significantly; the flow index (n) did not vary at the different RS concentrations studied. The dynamic viscoelastic behaviour of the batters was frequency-dependent at 25ºC and practically independent at 85ºC (formation of a stable structure). A significant drop in the elasticity module (G') and the loss module (G'') was only observed at the 15% concentration of RS at 25ºC. It may be concluded that the addition of resistant starch does not alter the rheological properties of this type of batter to any great degree. Therefore, unlike other types of starch, when using resistant starch it will not be necessary to vary the basic formulations or to adapt the machinery employed in processing them.

INTRODUCTION

Resistant starches (RS) are of great interest to the food industry because of their potential benefits to health, as they have similar properties to fibres. Indeed, resistant starch is considered a 'functional fibre' and the AOAC methods for the measurement of dietary fibres (1) include RS in the total dietary fibre. Resistant starch may be defined as the starch fraction that is not broken down by enzyme hydrolysis in the small intestine but does ferment in the colon (2). Given its low water-holding capacity, it can be used in low to intermediate moisture foods such as bakery products. Different studies have employed various sources of fibre in the preparation of good quality bakery products. Grigelmo-Miguel et al. (1999, 2001)(3 and 4), for instance, studied the effects on physical properties and acceptance by consumers of adding dietary fibre from peaches to the ingredients of 'magdalenas' (similar to US muffins). As RS is a novel food component, its study covers various aspects, ranging from analysis to the physiological implications of its consumption (5). The purpose of this work is to study the influence of the addition of RS (5-15% by weight) on the rheological properties of a magdalena batter.

MATERIALS & METHODS

Batter preparation

The batter mix consisted of wheat flour (26, 21, 16 and 11%), resistant starch (HI-MAIZE 1043, National Starch) (0, 5, 10 and 15%), egg white (14%), egg yolk (7%), sugar (26%), milk (13%), oil (12%), bicarbonate of soda (1.03%), citric acid (0.79%) and lemon zest (0.18%). The ingredients were mixed in a Kenwood Major Classic mixer (Kenwood Ltd, UK).

Rheological characterisation of the batter

The flow behaviour of the magdalena batters was studied at 25ºC, using a Physica Rheolab MC120 rheometer for controlled deformation. Viscoelastic characterisation of the samples was performed in a Haake Rheostress1 controlled stress rheometer at 25ºC and 85ºC. In both cases, a 50 mm diameter plate-plate sensor with a 1 mm gap between the plates was used.

RESULTS

Flow behaviour of the batters

The flow curves for the batters at the different resistant starch (RS) concentrations studied are shown in Figure 1.

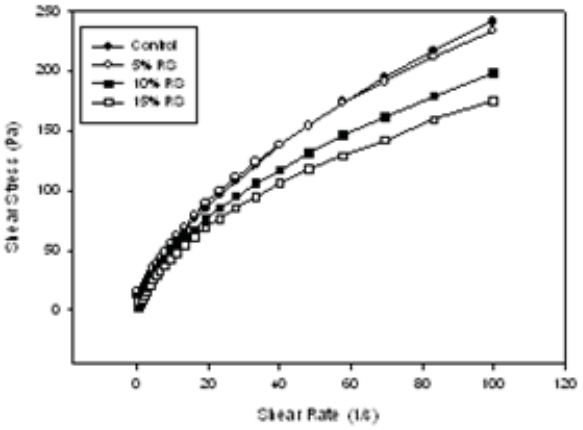

Figure 1. Flow curves at 25ºC of batters with different resistant starch concentrations

The rise in stress observed at the higher shear rates is an indication of pseudo-plastic behaviour. The test results fit the Ostwald de Waele model and the flow behaviour index (n) and consistency index (k) values were calculated. The only variation in n observed for the different resistant starch concentrations was the higher value for 15%. Although no variations in the consistency index were observed at low concentrations, this parameter fell significantly at 10% or above (Figure 2), possibly because of the dilution of the flour.

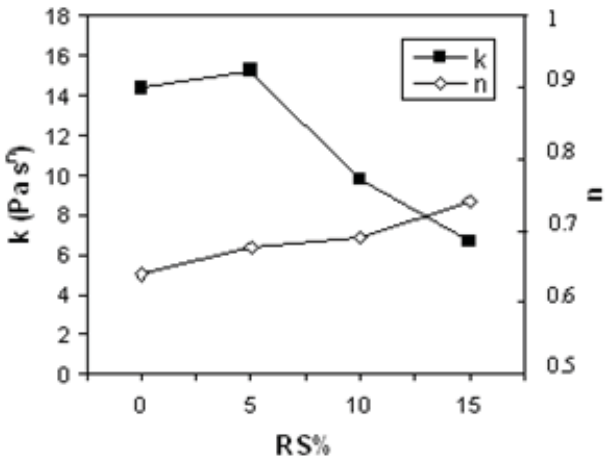

Figure 2. Consistency index (k) and flow behaviour index (n) at 25ºC for resistant starch concentrations

Viscoelastic properties of the batters

The mechanical spectra at 25ºC and 85ºC of the batters with different resistant starch concentrations are shown in figures 3 and 4.

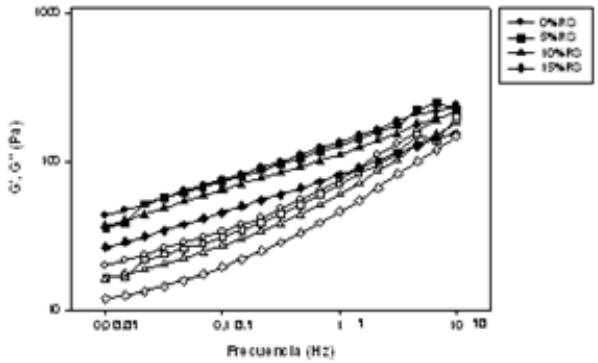

Figure 3. Mechanical spectrum at 25ºC of batters with different resistant starch (RS) concentrations (G': solid circles, G'': empty circles).

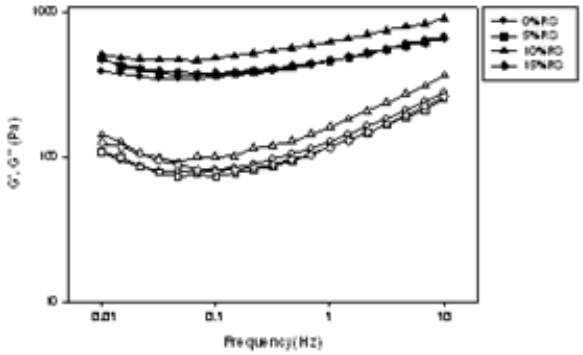

Figure 4. Mechanical spectrum at 85ºC of batters with different resistant starch (RS) concentrations (G': solid circles, G'': empty circles).

Over the frequency range studied, G' (storage module) and G'' (loss module) evolved differently at 25ºC and at 85ºC. At 25ºC the batters were frequency-dependant, whereas at 85ºC they were practically independent of frequency.

At 25ºC, G' and G'' both decreased slightly as the resistant starch concentrations rose. The greatest difference can be seen at the 15% concentration of resistant starch. At 85ºC, however, G' and G'' remained practically the same for all the RS concentrations studied.

ACKNOWLEDGMENTS

The authors are grateful to National Starch for supplying the Hi-maize 1043 resistant starch.

REFERENCES

1. Yue, P. y Waring S. Resistant Starch in Food Applications. *Cereal Foods World* 43 (9), 690-695 (1998).

2. Waring S. Functionality of resistant starch in food applications. *Food Aust.* 50 (12), 615-621 (1998).

3. Grijelmo-Miguel, N., Carreras-Boladeras, E. y Martín-Belloso, O. Development of high-fruit-dietary-fibre muffins. *Eur. Food Res. Technol.* 210, 123-128 (1999).

4. Grijelmo-Miguel, N., Carreras-Boladeras, E. y Martín-Belloso, O. Influence of the Addition of Peach Dietary Fiber in Composition, Physical Properties and Acceptability of Reduced-Fat Muffins. *Food Sci. Technol. Int*. 7 (5), 425-431 (2001).

5. Saura-Calixto, F and Abia, R. Resistant starch: an indigestible fraction of foods. *Grasas y Aceites* 3, 239-242 (1991).

EFFECT OF IRRADIATION ON FUNCTIONAL PROPERTIES OF EGG PRODUCTS

Martins, S.[1]; Ribeiro, R.[1], Botelho, M.L.[2]; Cabo Verde[2], S.; Santana, A.[1];Lima[1] , M. G.*

[1]Escola Superior Agrária de Santarém, S. Pedro, 2001-904 Santarém, Portugal.
[2]Instituto Tecnológico e Nuclear, Estrada Nacional 10, Apartado 21, 2686-953 Sacavém, Portugal
* Corresponding author. Fax: + 351 243 307 301 tel.: +351 243 307 300
e-mail: glima@esa-santarem.pt

Keywords: Eggs irradiation, egg product, dose, Initial Asymptotic Viscosity.

ABSTRACT
Alternative technologies must be developed and implemented considering sanitation and preservation of eggs mainly for risk population. Food irradiation is an alternative to eliminate *Salmonella* spp. and *Campylobacter* spp. from eggs, as a low dose is enough to have a safe product. This study presents the correlation between irradiation dose and some of functional egg properties. Viscosity of non irradiated and irradiated eggs was evaluated by means of VT550 Haake with a NV sensor and co-axes cylinders at 5 °C of temperature. This was developed in two phases:

- At first the applied irradiation doses were 0.5, 2 and 5 kGy. After irradiation at 5 kGy, the yolk color decreased to a pale yellow and the white was modified to a turbid yellow. The Cross equation was utilized to calculate viscosity curves. Initial asymptotic viscosity data showed a tendency to a decrease of yolk viscosity with increasing irradiation doses, at doses superior to 0.5 kGy and a decrease of white egg viscosity as such a Newton behavior (Pinto *et al.*, 2004).
- A second study with irradiation doses of 0.5, 1, 1.5 and 2 kGy. Results indicated that an increase of the irradiation dose corresponds to a decrease of the yolk and a decrease of white egg viscosity as such a Newton behavior.

1. INTRODUCTION

In Portugal, ubiquitous Salmonella like *S. enteritidis* and *S. typhimurium* are responsible for almost 95 % of human cases of Salmonellosis, with eggs and meats playing a major role in Salmonella carriage. A study was performed for Salmonella detection in one hundred of half a dozen eggs sold in local markets in Lisbon. Salmonella was found in 29 samples, corresponding to a calculated prevalence ranging between 9.7% and 29.0% (Bernardo, 1999), being *S. enteritidis* the most frequent serotype found. This problem must be considered a major cause of concerning in eggs market. Although some methodologies were developed at the modern production of poultry products, the incidence of salmonellosis appears to be rising. Eggs are one of the most complete nutritional proteins foods. As so it is necessary to developed and implement methodologies that could guaranty a safety product with preservation of the main properties.

The most usual procedure for inactivation of microorganism is thermal destruction although other energy transfer as ionising radiation is an attractive alternative to heat pasteurisation for eggproducts. Irradiation of eggs with 2 or 3 kGy reduced bacterial contamination to non-detectable levels (2). Recent studies show that a radicidation dose of 1.5 kGy could guarantee sanitation of shell egg and eggproducts (3).

Serrano *et al.* (4) reported that a dose of 1.5 kGy did not affect the colour and the thermal characteristics of whole or liquid eggs. Irradiated liquid egg whites have been reported to have more stable viscosity than thermally pasteurised samples (5). The functional properties of egg white protein, including whipping, emulsifying and gelling properties, were either

maintained or significantly improved with irradiation. There are also studies pointing that gamma irradiation combined with heating might be an effective method of reducing allergenic properties of eggs derived from ovomuciod and ovalbumin (6).
The aim of this study was to develop and compare the methodologies of irradiation (radicidation) and heat (pasteurization) eggproducts. Studies were performed to evaluate the impact on the nutritional and functional properties in order to get a safety product without significant changes.

2. MATERIAL AND METHODS

2.1. Sampling.

Eggproducts (whites and yolks) were collected from an egg industry (DEROVO SA, Pombal, Portugal).

2.2. Irradiation process.

Dosimetry studies were carried out in the gamma facility to find out the best geometry and dose rate for irradiation of egg products. For gamma irradiation, egg products were irradiated in final package and irradiated in a cobalt-60 facility with 47 kCi activity at room temperature, at a dose rate of 1 $kGyh^{-1}$. The range of applied dose was developed in two phases:
1st Phase*: *Dose 0.0, 0.5, 2.0 and 5.0 and pasteurized eggproduct .- The absorbed dose were monitored with routine dosimeters.
2nd Phase*: *Dose 0.0, 0.5, 1.0, 1.5 and 2.0 kGy and pasteurized eggproduct. - The absorbed dose was monitored with routine dosimeters.

2.3. Viscosiety determination.

Viscosity of non irradiated, irradiated and pasteurized egg products was evaluated by means of VT550 Haake with a NV sensor and co-axes cylinders.
1st Phase: Viscosity measures of three replicates of each irradiation dose were performed at 5oC.
2nd Phase: Viscosity measures of six replicates of each irradiation dose were performed at 5oC.
The Cross equation was utilized to viscosity curves.

$$\eta = \eta_\infty + \frac{(\eta_0 - \eta_\infty)}{\left[1 + (\dot{\gamma}/\dot{\gamma}_c)^m\right]} \qquad (1)$$

η - Apparent Viscosity (Pa.s)

η_0 - Initial Asymptotic Viscosity $\qquad$ η_∞ - Final Asymptotic Viscosity

$\dot{\gamma}$ - shear rate (s^{-1}) $\qquad$ $\dot{\gamma}_c$ - critical shear rate

3. RESULTS AND DISCUSSION

3.1. Effect of irradiation and heat-treatment on the viscosity of egg products

Visual evaluation of yolks and whites eggproducts has shown that irradiation induced colour changes - the yolk colour die (pale yellow) and the white egg was modified to a turbid yellow. These alterations were dependent on the irradiation dose and were more significant for an irradiation dose above 2 kGy.

1st Phase: Dose 0.0, 0.5, 2.0 and 5.0 kGy at dose rate of 1.0 kGy/h and pasteurized eggproduct.

In figures 1 and 2 we can see effect of irradiation and heat-treatment on the viscosity of yolks and whites from eggproducts. Viscosity measures of three replicates of each irradiation dose were performed at 5^{o}C. The initial asymptotic viscosity values (η_0) were obtained by application of Cross equation.

Analysis of asymptotic viscosity data suggests that irradiation of eggproduct induce a slight increase in the viscosity of the yolks at 0.5 kGy followed by a decrease in the other dose (Figures 1). Irradiated white egg products also show a decrease in viscosity with increasing dose of irradiation (Figures 2). Pasteurized egg products show a behavior similar to eggproducts irradiated at 2 and 5 kGy dose (Figures 1 and 2). An irradiation dose of 2 kGy, which is sufficient to reduce contamination to non detectable levels, seems to have similar effects as a thermal pasteurisation on the functional properties of white eggproducts as thermal pasteurisation, since in both treatments the viscosity of whites is highly reduced.

Results of asymptotic viscosity for yolk egg products show higher variation. Low dose of irradiation (0.5 kGy) does not seem to affect the viscosity of yolk eggproducts, but results indicate that viscosity decreases with a 2 and 5 kGy irradiation dose (Figure 1).

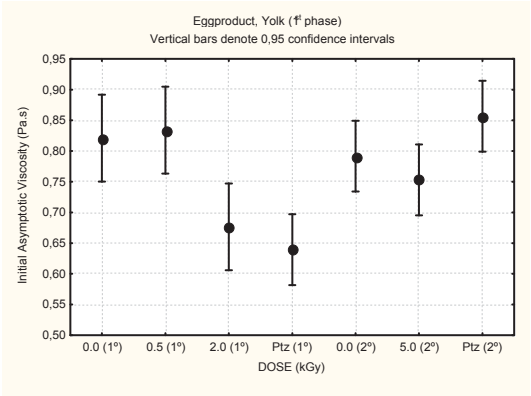

Figure 1: Effect of irradiation and heat-treatment on the viscosity of yolks from eggproducts.

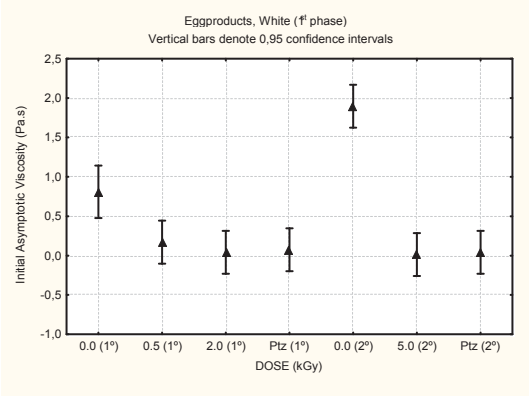

Figure 2: Effect of irradiation and heat-treatment on the viscosity of Whites from eggproducts

The results obtained were not conclusive so further studies were performed.

2nd Phase Dose 0.0, 0.5, 1.0, 1.5 and 2.0 kGy at dose rate of 1.0 kGy/h and pasteurized eggproduct.

In the following figures we can see the effect of irradiation and heat-treatment on the viscosity of yolks and whites from egg products. Viscosity measures of six replicates of each irradiation dose were performed at 5°C. The initial asymptotic viscosity values (η_0) were obtained by application of Cross equation.
Analysis of asymptotic viscosity data suggests that irradiation of eggproduct does not affect the viscosity of the yolks till 1.0 kGy followed by a decrease in higher doses (Figures 3 a) and a decrease in the viscosity of the whites (Figures 4). We can not establish comparisons with pasteurized yolk eggproduct because the sample had a viscosity anomaly high (figure 3 b). Irradiated white egg products also show a decrease in viscosity with increasing dose of irradiation. Pasteurized white egg products show a behavior similar to white egg products irradiated at 1.5 and 2 kGy dose (Figure 4).

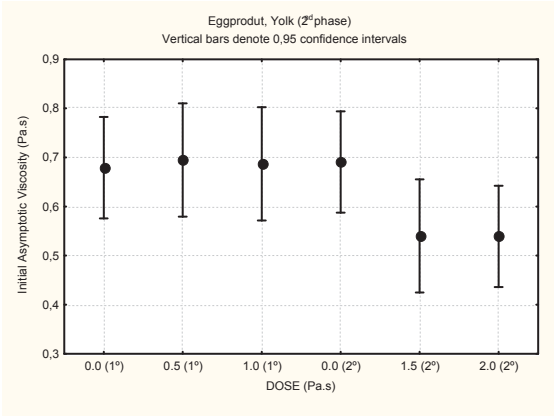

Figure 3 a: Effect of irradiation on the viscosity of yolks from eggproducts.

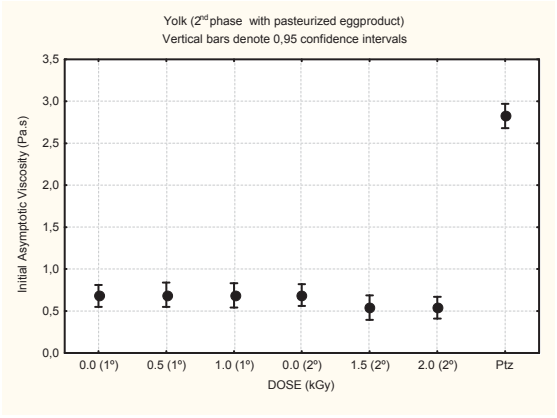

Figure 3 b: Effect of irradiation and heat-treatment on the viscosity of yolks from eggproducts.

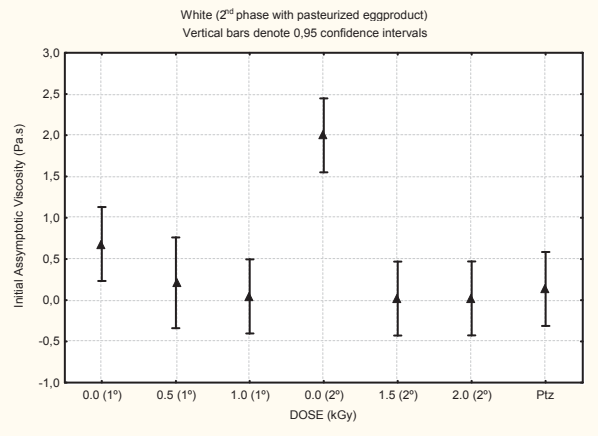

Figure 4: Effect of irradiation and heat-treatment on the viscosity of Whites from eggproducts.

Comparisons between two phases for results in the same dose of irradiation

As we can see in the figures 5 and 6 the results obtained in the two phases of the study are very similar, suggesting that the irradiation dose of 1.5 kGy (enough to obtain a microbiological safe product), seems to induced a slight decrease in the viscosity of yolks and whites. It is important to study industrial processing with irradiated yolks and whites to make sure that the products maintain their functional importance at industrial level.

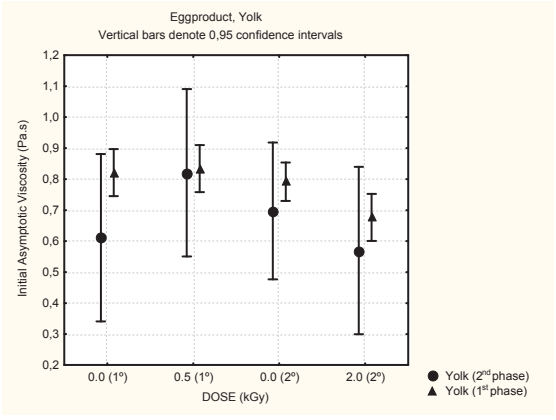

Figure 5: Comparisons of the effect of irradiation on the viscosity of yolks from eggproducts for two phases.

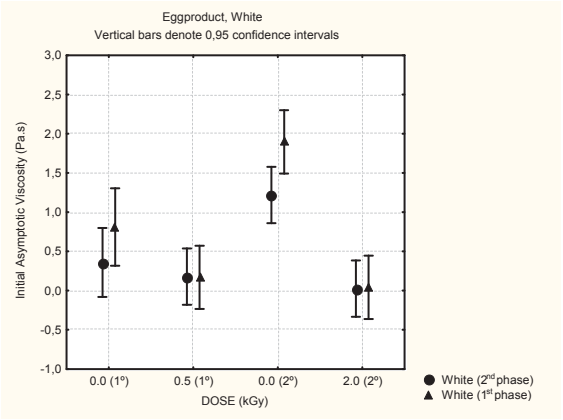

Figure 6: Comparisons of the effect of irradiation on the viscosity of whites from eggproducts for two phases.

ACKNOWLEDGMENTS

We are grateful to DEROVO S.A. (Pombal, Portugal) for the availability of shell egg and egg products.

REFERENCES

(1) Pinto, P.; Ribeiro, R.; Sousa, L.; Cabo Verde, S.; Lima, M. G.; Dinis, M.; Santana, A.; Botelho, M. L. (2004). Sanitation of Chicken eggs by ionizing radiation: functional and nutrional assessment. Radiation Physics and Chemistry (accepted for publication).

(2) Tellez I.G., Trejo, R.M., Sanchez R.E., Ceniceros R.M., Luna Q.P., Zazua P., Hargis B.M. ,1995. Effect o gamma irradiation on commercial eggs experimentally inoculated with *Salmonella enteritidis*. Radiat. Phys. Chem. 46, 789-792.

(3) Cabo Verde, S., Tenreiro, R., Botelho, M. L., 2004. Sanitation of chicken eggs by ionising radiation: HACCP and inactivation studies. Radiation Physics and Chemistry.

(4) Serrano, L.E., Murano E.A., Shenoy K., Olson D.G., 1997. Dvalues of *Salmonlla enteritidis* isolates and quality attributes of shell eggs and liquid whole eggs treated with irradiation. Poult. Sci. 76, 202-206.

(5) Wong, Y.C., Herald, T.J., Hachmeister, K.A., 1996. Comparison between irradiated and thermally pasteurised liquid egg white on functional, physical and microbiological properties. Poult. Sci. 75, 803-815.

(6) Lee J.W.; Lee K.W., Yook, H.S., Lee, S.Y., Kim, H.Y., Jo, C., Byun, M.W., 2002. Allergenicity of hen's egg ovomucoid gamma irradiated and heated under different pH conditions. J. Food Prot. 65, 1196-1199.

(7) Bernardo, F., 1999. Prevalence of Salmonella in eggs with dirty shells sold in Portugal. In: Proceedings of Foodborne Illness Congress, May 28-29, OPorto, Portugal, pp. 30-31

(8) Huang, S., Herald, T.J., Mueller, D.D., 1997. Effect of electron beam irradiation on physical, physiochemical and functional properties of liquid egg yolk during frozen storage. Poult. Sci. 76, 1607-1615.

GLASS TRANSITION IN TRADITIONAL COOKIES WITH DIFFERENT FIBRES

Costa, A. *, *Piteira, F.* *; *Diogo A.C.* ** and *Sousa, I.* *

*Secção de Ciência e Tecnologia dos Alimentos. Instituto Superior de Agronomia. Tapada da Ajuda 1349-017 Lisboa. Portugal, E-mail: isabelsousa@isa.utl.pt
** Instituto Superior Técnico, Dep. Engª Materiais, Av. Rovisco Pais, 1049-001 Lisboa, Portugal

Keywords: D.M.T.A., glass transition, dietary fibre, functional food, cookies, texture.

ABSTRACT
It is known that fibre compounds are considered as multifunctional substances, positively affecting the activity of human body. This work is part of a project to understand the role of fibres from different sources in traditional cookies delectableness.

Crispness of cookies is obviously related to the fact that they stay in the glassy state at room temperature. Therefore the glassy state is determinant for the desired cookies texture. Water, lipids and high molecular mass molecules (e.g. fibres) are crucial for glass relaxation and have opposite contributions.
The aim of this work is the study of the influence of fibre addition on glass relaxation temperature (T_g) in traditional cookies. This relaxation was observed through two different methods: Dynamic Mechanical Thermal Analysis (DMTA), which is focused on the temperature dependence of viscoelastic behaviour, and Differential Scanning Calorimetry (DSC), that measures the enthalpy or heat capacity changes in the sample as it is heated.
Cookies have an amorphous structure in which water and lipids act as plasticizers, fibre has a structuring contribution and they will affect the glass transition. The availability of water can be measure by the water activity (ratio of product moisture at equilibrium with relative humidity), values of a_w were smaller than 0.2±0.010, with moisture contents around 2%. Oat, orange and pea fibres were added at 0, 6 and 8% levels.
DMTA showed a dramatic decrease of the storage modulus, representing the glass transition phenomena, at a range of 40 to 50ºC for all the cookies. The T_g of these cookies by DSC, showed values from 41.5 to 45.8ºC. Texture of all cookies was also measured by penetration tests and hardness results were around 10N, commercial cookies showed hardness values from 4.6 to 12.5 N in 20 different brands.
It was possible to verify that cookies with 6 and 8% of fibre can be produced without changing the essential structural/texture properties.

1. INTRODUCTION

The amount of dietary fibre in the human diet in these days, have been decreasing significantly and claims for attention. A diet low in dietary fibre is associated with a spectrum of degenerative diseases, e.g. constipation, diverticular diseases, diabetes, obesity, coronary heart disease and bull cancer. Now it's well-established that consumption of adequate amounts of dietary fibre reduces the risk of these diseases (1).
Cookies are a product with a strong presence in the market and it's consumed by almost everyone. The incorporation of fibre in cookies it's a simple and easy way to increase de fibre intake of people. This addition gives them same functionality, because of the well known positive effect of fibres in the human body (2).
Fibres are copolymers of simple sugars. Research carried out on the stability of food polymers has shown that they have an amorphous structure in which water acts as a plasticizer (3). The

change from a metastable glassy state to the rubbery state, characterised by a general increase of the free volume, disorder and mobility of the polymer chains is translate in terms of cookies texture in a change from a crisp into a lump cookie(4). This glass transition, strongly dependant on the molecular mobility in the material system brings about a sudden change in their thermal and mechanical properties. Traditionally, it is the discontinuous variation of the calorific capacity (Cp) of amorphous materials according to temperature which is measured by differential scanning calorimetry (DSC) (5). Dynamic rheological techniques, can determine fundamental mechanical properties of materials. In particular oscillatory dynamic testing, in which a sinusoidal small-amplitude strain is imposed onto a sample, to produce a stress out-put, or vice versa, is an alternative technique for examining the fundamental viscoelastic properties (6): stress modules G' accounting for elasticity and loss modulus related to viscosity. A sudden decrease in G' and tanδ peak are characteristic of a transition from glassy-like to a rubbery-like consistence.

As we know, addition of new ingredients may affect the cookies structural/textural properties, so it's of great importance to study this influence (7). The purpose of this work is to understand the phenomena involved with fibre enriched cookies. Three different sources of fibre (pea, oat and orange) were used: cereals, fruits and legumes. Levels of fibre incorporation and the impact on cookies production process and final texture were studied.

Water content determinations (moisture and a_w) were made, texture analysis and T_g determinations. T_g is a characteristic of enormously importance in food stuff like cookies that are characterized by a rigid structure with low molecular mobility and that can pass to a higher mobility state with the increasing temperature(8). The first condition gives the desired crispness of cookies, higher mobility of molecules is responsible for unpleasant texture.

2. MATERIALS AND METHODS

2.1 Material

Cookies were the samples used in this work. They were made in a traditional way, using comercial wheat flour kindly offered by Nacional (Portugal) and fat (palm oil) graciously supplied by Fima-Lever (Portugal). Additions of fibres were made at a level of 6 to 8%. Further incorporation of fibre is limited by machinability of cookies dough. Henceforth 8% was the limiting value for cookies processing. The fibres used were; pea, offered by Cosucra, orange and oat fibre kindly supplied by Rettenmaier & Sohne GmbH+Co (German). Technical data is showed in table 1. Orange fibre is a dietary fibre, produced from carefully dried orange peel with pulp components. Oat fibre is a bright, microfine dietary fibre produced by a special process from oat bran (Vitacel, 2002). Other ingredients used were commercial sucrose (sugar), baking powder and tap water.

Table- 1 Characteristics of Fibres (according to suppliers technical data sheet)

	Fineness (μm)	Water Binder Capacity (gH_2Ogds^{-1})	*Insoluble Dietary Fibre Content (AOAC method)*	Soluble Dietary Fibre Content *(AOAC method)*
Pea fibre	90% < 300	3-5	86.2 %	1,8 %
Oat Fibre	90% < 35	3.2	93 %	3 %
Orange Fibre	87 % < 32	8.6	32 %	28 %

2.2 Methods

The samples were analysed for moisture content, water activity, texture and glass transition temperature by DSC and DMTA.

- For moisture content determinations, 2g of cookies were weighed, in triplicate, in aluminium dishes and dried to a constant weight in a hot air oven at 105±2 ºC.
- For water activity (a_w) determinations, the cookies were manually chopped into small pieces, placed into the cell of a Rotronic-Hygroskop DT, and the average values calculated for three different readings.
- For texture determination hardness the force required to pierce a cookie with a 2 mm diameter cylindrical flat-faced stainless steel probe, with a test speed of 1.00 mm/s was measured using a TA-XT2 Texture Analyser (Stable Micro Systems, Surrey, UK). Twenty readings for each sample, allowed the maximum puncture force required to be measured and averaged.
- DMTA analysis of the cookies was conducted with a Dynamic Mechanical Thermal Analyser MK II (Rheometric Scientific). The samples had the form of rectangular bars with 30 x 11 x 3mm. Were measured in bending mode, clamped rigidly at both ends and its central point was submitted to a sinusoidal stress. The temperature scan was run from 303 to 393 K using a heating rate of 2 K/min at a fixed frequency of 1 Hz. For each material, three samples were tested and during the analysis, it was determined the sample's modulus (G') and tang (Tanδ) as function of temperature.
- In DSC analysis it was used a Shimadzu model DSC 50 (Kyoto, Japan) apparatus with a TA-50 WSI software. The equipment was calibrated with 99.999% indium. The DSC measurements were performed in nitrogen atmosphere at constant pressure, from 293 K to 523 K, with a heating rate of 5 K/min. Aluminium pans were employed. The results are the average of at least three thermograms. An empty DSC pan was scanned, with each sample, as the reference

3. RESULTS AND DISCUSSION

The results obtained with the cookies manufactured with the optimised conditions are showed on Table 2.

Table - 2 Average values of manufactured cookies with oat, orange and pea fibres (analysed by ANOVA/MANOVA post-hoc Scheffé contrasts).

Fibre (g)	*Lipids* (g)	*Cooking Time* (min)	*Moisture* (%)±std	a_w±std	*Hardness* (N)±std	T_g (K)
Range of values measured for 20 different commercial Cookies						
			2.1-5.3	0.08-0.35	4.6-12.5	318.95-332.6
Pea fibre cookies						
6	20	15	1.6_a ±0.70	0.07_a ±0.007	9.5_a±2.03	314.5_a ±1.45
8	20	15	1.5_a ±0.03	0.10_b ±0.010	9.4_a ±2.52	315.0_a ±0.58
Oat fibre cookies						
6	20	15	1.0_a ±0.06	0.07_a ±0.008	10.0_a ±3.60	316.0_a ±2.67
8	20	15	0.7_b ±0.09	0.04_b ±0.003	10.7_a ±2.41	315.2_a ±2.04
Orange fibre cookies						
6	20	15	1.4_a ±0,54	0.07_a ±0.002	9.8_a ±1.75	318.8_a ±0.38
8	20	15	3.8_b ±0,26	0.37_b ±0.014	9.7_a ±1.92	317.6_b±0.38
Cookies without fibre						
0	20	15	1.9 ±0.12	0.07 ±0.00	11.6_a ±4.37	318.1 ±0.61

(All the results had a percentage of error of less than 5%)

3.1 *Effect of fibre addition on cookies properties*

3.1.1 Moisture content and Water activity

The determination of moisture and water activity (a_w) showed low values, with moisture around 2% and a_w smaller than 0.2. But, as we can see in fig. 1 and fig. 2 the orange fibre cookies have higher values (moisture=3.8% and a_w=0.37).

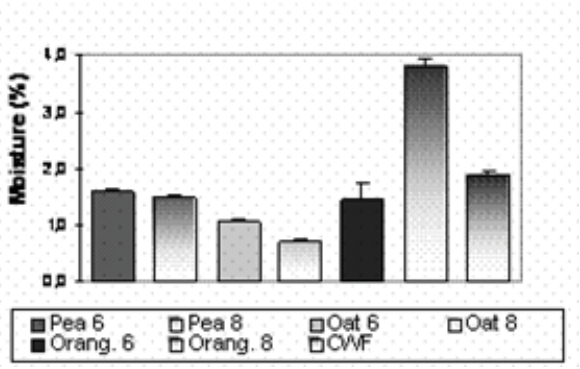

Fig. 1 - Cookies moisture content (%)

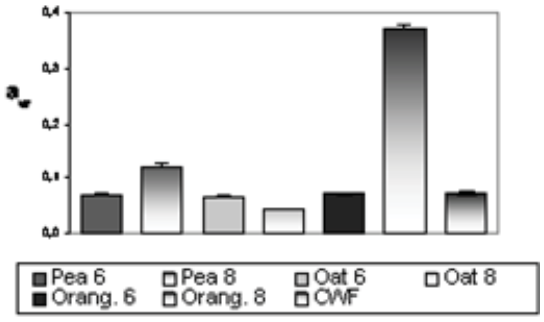

Fig. 2 - Cookies water activity (a_w)

This happens because the orange fibre has a water binding capacity of 8.6g $H_2O.gds^{-1}$ and 28% of soluble dietary fibre, so, more addition of fibre implies addition of water to the recipe and consequently cookies with higher moisture and a_w. The pea and the oat fibre, had low level of soluble fibre (3 and 2% respectively) that means less addition of water for the same level of fibre, compared with the orange fibre cookies.

3.1.2 Texture on cookies with different fibres

Texturometer analyses used to measure hardness, showed that the addition of fibres at these levels (6 and 8%), didn't show much influence on the cookies texture. In general we can say that hardness has not been affected with these levels of fibre addition, the values of all samples remained between 9.4 and 11.6N with no significant difference ($p < 0,005$)

3.1.3 Phase transitions on cookies with different fibres

The glass transition temperatures (T_g) were also measured in order to study the fibre effect on the cookies structure. The change from glassy to rubbery state obtained when the temperature increases, is directly related to the changes in Young modulus.
Thermomechanical changes of fibre additions on cookies, observed in DMTA scans, are reported in fig. 3, 4 and 5.

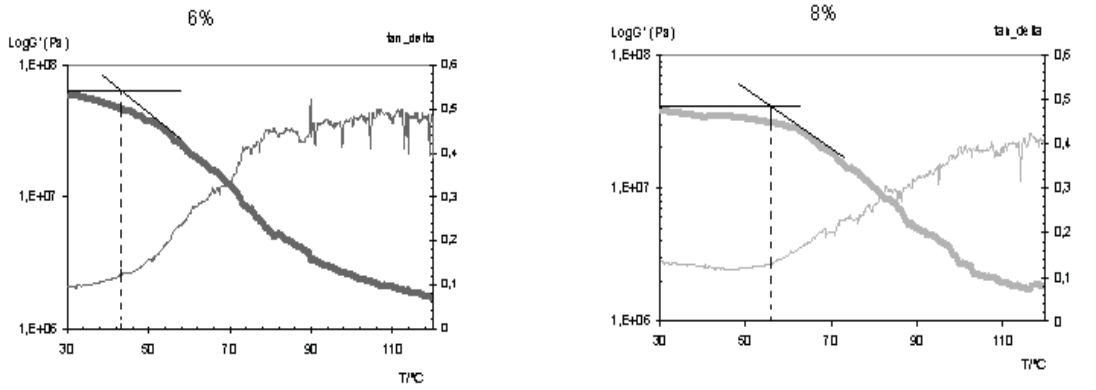

Fig. 3 - DMTA thermograms for cookies with 6 and 8% of **pea** fibre, illustrating T_g.

As we can see in these thermograms fig. 3, 4 and 5, there is a drop of the modulus around the temperature of 323 K and according to (9) the location of the α-relaxation Temperature or T_g can be determined from the drop of the storage modulus.

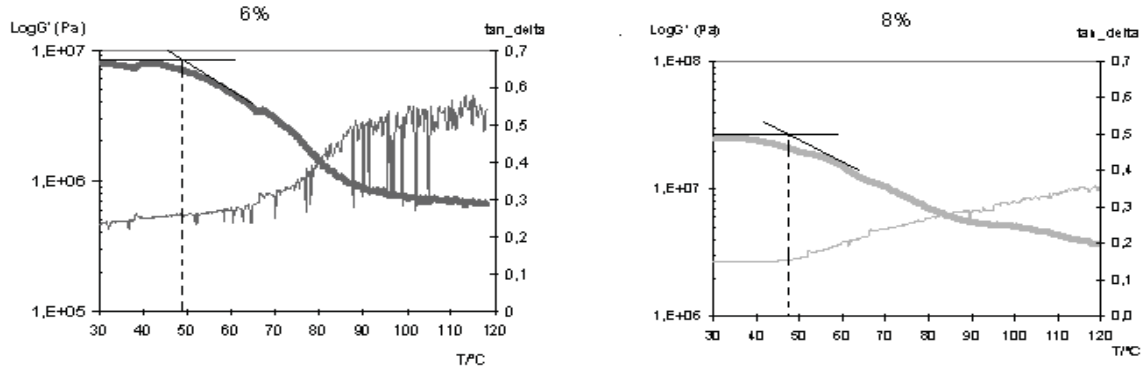

Fig. 4 - DMTA thermograms for cookies with 6 and 8% of **oat** fibre, illustrating T_g.

For all tree types of fibre, orange, oat and pea, the glassy transition temperature was not affected by the fibre incorporation, at least for these levels (6 and 8%) of fibre incorporation.

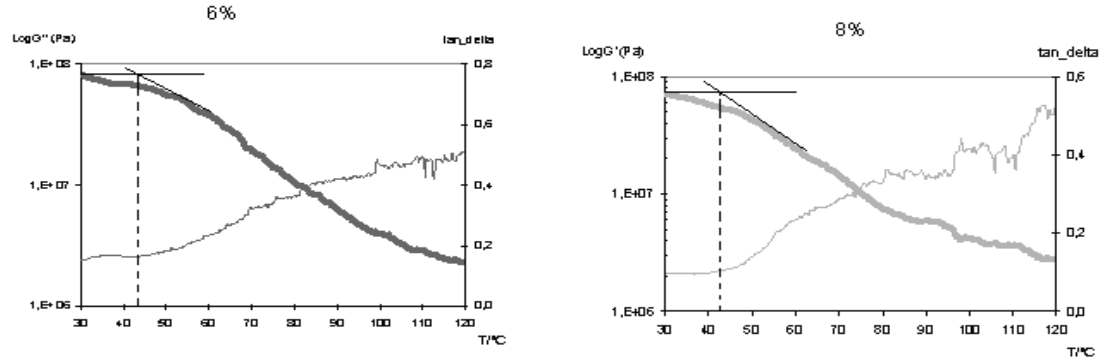

Fig. 5 - DMTA thermograms for cookies with 6 and 8% of **orange** fibre, illustrating T_g.

In DSC measurements the experimental results are expressed in a termogram where we have heat capacity versus temperature. A 2nd order transition like T_g can be observed in DSC as a base line change on the heat capacity flow signal during de temperature scan. In fig. 6 and 7 there are the results obtained with our samples of cookies at 6 and 8% fibre.

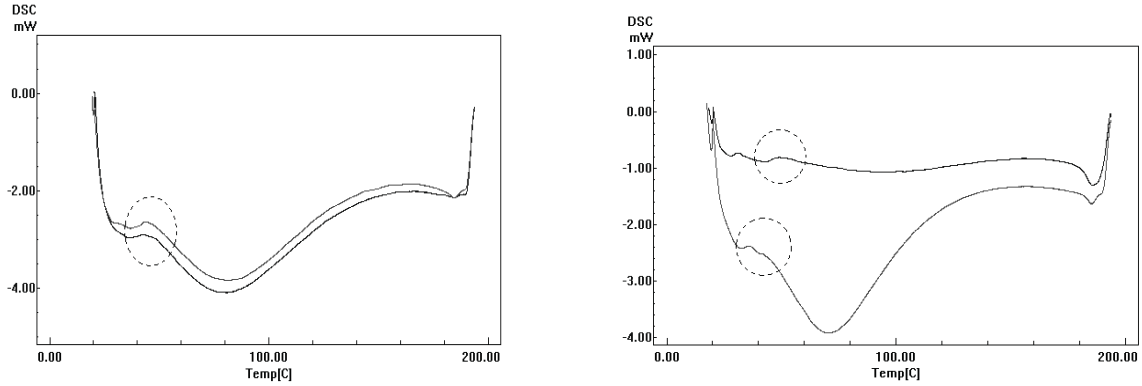

Fig. 6 - DSC thermograms for cookies with _6 and _8% of **pea** and **oat** fibre, illustrating T_g.

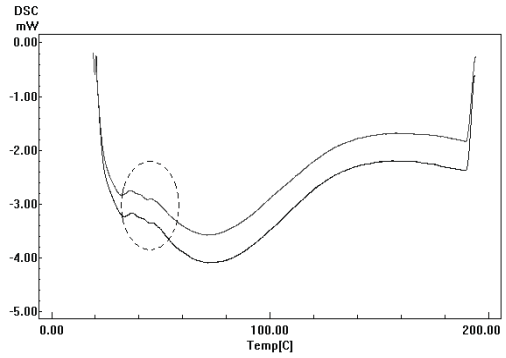

Fig. 7 - DSC thermograms for cookies with _6 and _8% of **orange** fibre, illustrating T_g.

The glass transition temperature is the temperature at the midpoint of the variation of the base line. The values observed go from 314.5 to 318.8 K. The increasing of fibre was not affecting the cookies structure, like we had already seen in DMTA analysis.

4. CONCLUSIONS

In this work it was possible to verify, using DSC and DMTA measures, that the addition of fibres (orange, oat and pea) at levels of 6 and 8%, do not affect significantly the Glass Relaxation Temperature (T_g) of the cookies. Which, mean that fibres can be used in cookies base formulation up to a level of 6 to 8% without changing the essential structure/texture properties. So, it will be possible to provide the consumers with a high level functionality product. The recommendable daily intake of fibre is 25g which means tat if this was the only daily source a simple packet of cookies will do for the 25g.

5. REFERENCES

1-Sidhu, J.; Al-Hooti, S.; Al-Saqer, J. (1999). Effect of adding wheat bran and germ fractions on the chemical composition of high-fiber toast bread. *Food Chemistry*, 67: pp 365-371

2-Behall, K. and Reiser, S. (1986). Effects of Pectin on Human Metabolism. In; Chemistry and Function of Pectins. Eds. Fishman, M. L. and Jen, J. J. *American Chemistry Society Symposium*: pp 248-262

3-Slade, L. and Levine, H. (1993). The Glassy State in Application for the Food Industry with an Emphasis on Cookie and Craker Production. In: The Glassy State in Foods. Nottingham University Press, Loughborough, United Kingdom, pp 333-371.
4-Ferry, I. D. (1980). Viscoelastic Properties, New York, John wily and Sons: pp 280-291.
5-Rouilly, A. Orliac, and O, Silvestre, F. (2001).DSC study on the Therrmal Properties of Sunflowers Proteins, According to their water content. *Polymer*, 45: pp 10111-10117
6-Addo, K.; Xiong, Y.; Blanchard, S. P. (2000). Thermal and dynamic rheological properties of wheat flour fractions. *Food Research International*, 34: pp 329-335
7-Zoulias, E.; Oreopoulou, V.; Tzia, C. (2002) Textural properties of low-fat cookies containing carbohydrate or protein-based fat replacers. *Journal of Food Engineering*, 55: pp 337-342
8-Roos, Y. H. (1995). Phase Transition In Foods. Food Science and Technology. International Series. *Academic Press, London*: 360p
9-Di Gioia, L.; Cuq, B. and Guilbert, S. (1999). Thermal Properties of Corn Gluten meal and its Proteic Components. *International Journal of Biological Macromolecules*, 24: pp 341-350.

6. ACKNOWLEDGMENTS

The authors wish to thanks the Nacional-Companhia Industrial de Transformação de Cereais S.A., FIMA-Lever, J. Rettenmaier & Sohne GmbH+Co and Cosucra S.A. for graciously supplying the materials. We also thank SOPARLIM-Sociedade Panificadora Arraiolense for their technical assistance in cooking processing.

CORRELATION BETWEEN BEER FOAM STABILITY AND ISO-α-ACIDS PROFILE

Lúcia H.M.L.M.Santos[1], K. Jorge[2] , L.C. Nogueira[2], I.M.P.L.V.O. Ferreira[1], L.C. Trugo[2]*

[1] REQUIMTE, Serviço de Bromatologia, Faculdade de Farmácia, Universidade do Porto, Rua Aníbal Cunha, 4050-047 – Porto, Portugal. isabel.ferreira@ff.up.pt
[2]Laboratório de Bioquímica Nutricional e de Alimentos, Instituto de Química, Universidade Federal do Rio de Janeiro, Brasil. e-mails: luciana.nogueira@ig.com.br; lctrugo@iq.ufrj.br

Keywords: beer, iso-α-acids, sigma values, foam stability.

ABSTRACT

An aspect of beer quality generally considered to be of major importance is the presence of a stable and attractive head of foam. Foam stability is the ability of foam, once formed, to resist degradation processes. Beer foam is stabilized by the presence of beer polypeptides and hop bitter acids, but a number of other beer components can also substantially affect beer foam. The composition of the grist for beer production should be critical for the quality of the resultant foam as most of the protein found in foam comes from this source. Besides hop bitter acids and their chemically modified variants, exogenous stabilizers such as propylene glycol alginate and pectins enhance the stability of beer foams. Iso-α-acids, the major source of bitter flavour in beer, are concentrated in beer foam. Studies have shown that the stabilization of the matrix foam takes place as a result of hydrophobic bonding between the side-chains of the hop acid and hydrophobic amino acid residues on the polypeptides. But the presence of foam-negative components which reduce foam stability even in the presence of adequate foam-stabilizing components is a fundamental issue that compromise beer foam quality. The effect of lipids and higher alcohols on beer foam can only be described as disastrous. The objective of our study was evaluate different types of beer with different proportions of malt, adjuncts and alcohol and correlate their foams with the iso-α-acids, analyzed by HPLC method and Sigma value, that is a measure of the average life-time of a foam bubble.

INTRODUCTION

Beer is unique in its use of hops (*Humulus lupulus* L.) to provide an essential part of its characteristic flavour and aroma (1). Hops are thus the one ingredient that distinguishes beer from all other beverages. So, the bitter taste of beer is derived from hops or hop extracts added to the wort during brewing (2). In the boiling process, the hop α-acids or humulones, which are almost tasteless, are isomerized into the bitter-tasting iso-α-acids or isohumulones. These products are not only responsible for the bitter taste of beer, but they also exhibit bacteriostatic properties and furthermore play an essential role in enhancing the foam stability of beer (3). The most widely accepted model for beer foam structure is that of Asano and Hashimoto (4). They proposed that hop-derived compounds, such as iso-α-acids, combine with polypeptides in the foam. This increases the viscosity of the foam liquid regions, thus reducing drainage and improving foam stability (5, 6). But Simpson and Hughes (7) created a new model to describe the chemical interactions that lead to stabilization of beer foam by hop derived bitter acids. In this scheme, they propose that the interactions between the hop acid and the polypeptides are of two types. Firstly, the amino groups of the polypeptide and the

carbonyl groups of the hop acid interact by ion-dipole bonding, i.e. the interaction is not of the strict ion-ion type. Secondly, further stabilization of the foam matrix takes place as a result of hydrophobic bonding between the side chains of the hop acid and hydrophobic amino acid residues on the polypeptides. Chemically-modified iso-α-acids, such as dihydroisohumulone, tetrahydroisohumulone and hexahydroisohumulone enhance foam stability to a greater extent than do iso-α-acids. Chemical reduction of the side-chain carbonyl group and/or cabon-carbon double bounds of such compounds increase the hydrophobicity of their side-chains, enhancing their ability to take part in hydrophobic interactions.
The contribution that many separate components of beer can make, either constructively or destructively to its head has been investigated repeatedly, at times it still seem to be nearer to answering the question of whether stable foams are irretrievably linked to the presence in beer of one or a few special types of foam active substances or alternatively whether the balance of a greater or lesser number of compounds of diverse chemical structure determines foam stability (8). Beer devoid of alcohol can give extremely unstable foams. In the extreme it might be found that alcohol-free beers fail to afford a sufficient degree of foam formation. The addition of ethanol to such beers enhances foamability and foam stability. The foaminess of protein solutions is enhanced at ethanol concentrations up to 1%, declining once more at higher levels (9).
For the analysis of the iso-α-acids in beer, a pre-concentration step is often performed. Enrichment is commonly carried out by liquid-liquid extraction or by solid phase extraction (SPE) on reversed phase material. In this work, an HPLC method that enables simultaneous analysis of iso-α-acids and reduced α-acids in beer without sample preconcentration was used. Beer was only degassed and filtered prior to injection as suggested by Vanhoenacker et al (10).
The objective of our study was to evaluate different types of beer with different proportions of malt, adjuncts and alcohol and correlate their foam stability with the iso-α-acids composition. For that purpose iso-α-acids were analysed by ion-pair HPLC. The stability of beer foam was determined according to the modified Ross & Clark (ASBC) method.

2 - MATERIALS AND METHODS

2.1 - Beer samples

Six commercial beer brands were acquired according to their grist composition. Beers were bought at local stores, kept at room temperature, and freshly opened prior to analysis. Degassing was done by ultrasonication. Table 1 describes sample composition.

Table 1 –Sample labelling

Sample	Alcohol (%vol)	Ingredients mentioned on the label
1	7.2	Water, malt, rice, milho, hop, stabilising (E405)
2	Without alcohol	Water, malt, rice, milho, hop, stabilising (E405)
3	4.6	Water, malt, rice, milho, hop, stabilising (E405)
4	5.4	Water, malt, rice, milho, hop, stabilising (E405)
5	4.8	Water, malt, rice, hop, stabilising (E405), antioxidant (E223)
6	5.4	100% malt – beer without additives

2.2 – Reagents and standards

Iso-α-acids (IAA), Dihydro-iso-α-acids (DHIAA), tetrahydroiso-α-acids (THIAA), hexahydro-iso-α-acids (HHIAA) a were generous gift from Brewtec (Brazil). Each pure bittering agent was diluted at 1:160 proportion in the same solvent of chromatography.

2.3 – Ion pair chromatography of iso-α-acids

The HPLC procedure was based on the method described by Jorge (11). Ion pair chromatography was applied using an isocratic HPLC system, which consisted of a C18 column (5 μm – 250 x 4 mm) column and detection at 254 nm.
The mobile phase was prepared by mixing 360mL of aqueous buffer (3.83 g of 85% phosphoric acid with 42 mL of tetrabutylammonium hydroxide 0.4 mol/L solution and about 900 mL HPLC grade water at pH 7.4) and 840 mL of organic solution (160 mL acetonitrile with 900 mL methanol). The flow-rate was set at 0.4 mL/min at room temperature.

2.4 – Beer foam stability

Ross & Clark introduced the concept of the Sigma (Σ) value (8), a measure of the average life-time of a foam bubble. Foam is generated by pouring beer into a special foam funnel. Beer collecting in the funnel is drained away at a rate such that only foam is present in the funnel 90 seconds after the end of pouring. At a stage (t secs) which must be 225-230 sec after the first drainage period, the volume of beer drained from the foam (b) and the volume of beer still in the foam (c) are measured.

$$\Sigma = t / (2.303 \log (b+c)/c)$$

Σ values of 105 sec, 95-105 secs and <95 sec describe good; average and poor foams respectively.

3 – RESULTS AND DISCUSSION

The most common bittering agent is a mixture of the various geometric isomers and analogs of the iso-α-acids (isohumulones), which are normally produced by addition of hops to boiling wort. The iso-α-acids can be converted to the THIAA by catalytical hydrogenation and can also be formed from beta acids as starting material. An insufficient hydrogenation reaction can result in DHIAA where the double bond adjacent to the carbonyl group remains. The THIAA produced from beta or alpha acids can be converted to the HHIAA, which contains both.
Figure 1 shows the typical chromatographic profile obtained for beer samples analyzed. Similar qualitative profiles were obtained for the six samples, however quantitative differences were observed.

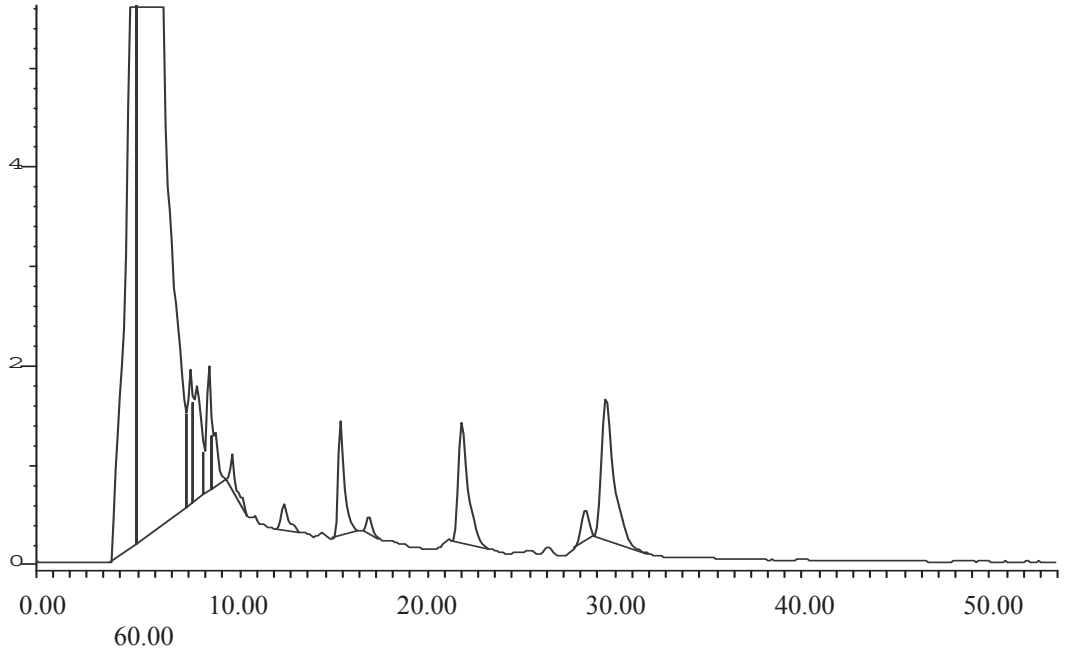

Figure 1- Typical chromatogram obtained for ion-pair HPLC analysis of beer iso-α-acids and reduced iso-α-acids, after direct injection with detection at 254 nm.

Table 2: Data for HPLC analysis and sigma evaluation.

Sample	Sigma	Alcool content(%)	Total iso-α-acids and reduced iso-α-acids (expressed as arbitrary units of area x 10^{-3})
1	121	7.2	4.8
2	109	Without alcohol	4.2
3	107	4.8	4.6
4	102	5.4	4.5
5	106	4.6	4.3
6	93	5.4	4.1

Sample 1 presented the highest sigma value, 121, and total iso-α-acids and reduced iso-α-acids (expressed as arbitrary units of area). On the other hand, sample 6 presented the lowest sigma value, 93, and the lowest total iso-α-acids and reduced iso-α-acids. If we exclude the sample 2, without alcohol, all the other samples presented a positive correlation between sigma value and total iso-α-acids area, as shown in Figure 2.

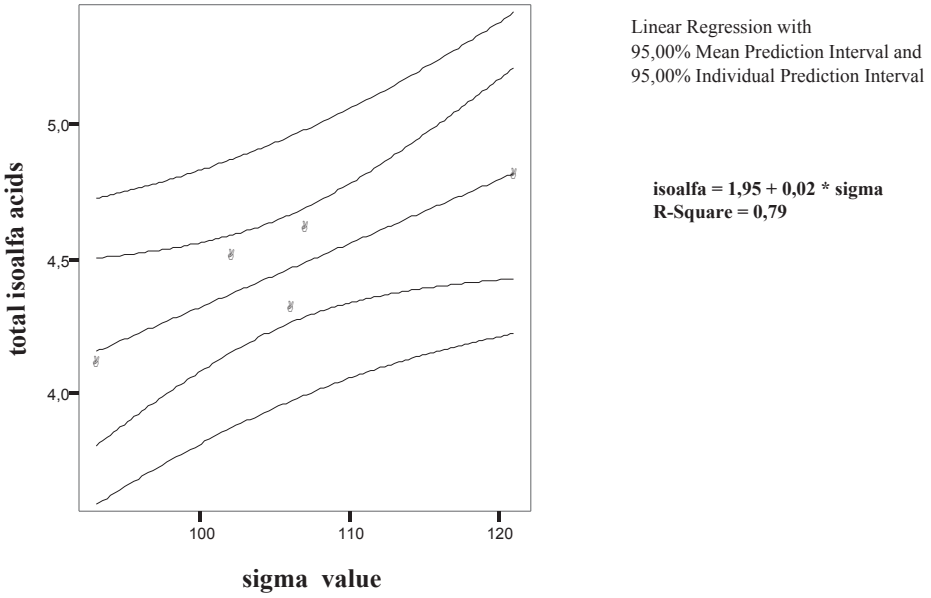

Figure 2 – Correlation between sigma value and total iso-α-acids.

More samples are being analyzed with respect to iso-α-acids profile. However, these results are in good agreement with other from literature, indicating that low hopped beers have poor foamability (8). The degree of foam formation is related to the ability of a substance (in this case hop resins and their precursors) to lower the surface tension of beer, which seems to depend on the number of hydrophobic side-chains on the molecule iso-α-acids and reduced iso-α-acids all give high degrees of foam formation. Hop resins enhance foaming by promoting foam formation, enhancing stability of the foam once formed and thence causing adhesion.

ACKNOWLEDGEMENT

This work received financial support from Reitoria da Universidade do Porto (project "Influência da fracção proteica, hidratos de carbono, e ácidos orgânicos na estabilidade da espuma da cerveja"), Brew Tech, CAPES, FAPERJ and CNPq.

REFERENCES

1. Hughes, P.S. and Baxter, E.D. Beer: quality, safety and nutritional aspects. RSC Paperbacks, p.112, 2001.
2. Verzele, M. J. Inst. Brew. 92, p.32, 1986.
3. D. De Keukeleire, Vindevogel J., Szucs R., Sandra P. Trends Anal. Chem. 11, p.275, 1992.
4. Asano, K. and Hashimoto, N. Contribution of hop bitter substances to head formation of beer. Report of the Research Laboratories of Kirin Brewery Company Ltd., 19, p. 9-16, 1976.
5. Klopper, W.J. On head retention. Journal of the Institute of Brewing, 60, p. 217-222, 1954.
6. Gardner, R.J. Surface viscosity and gushing (of beer). Journal of the Institute of Brewing, 78, 391-399, 1972.

7. Simpson, W.J. and Hugues, P.S. Cerevisia Biotechnol., 19, p.39-44, 1994.
8. Bamforth, C.W. The foaming properties of beer. J. Inst. Brew, 91, p. 370-383, 1985.
9. Bumbullis, W. and Schugerl, K. European Journal of Applied Microbiology, 8, p.17, 1979.
10. Vanhoenacker, G.; Keukeleire, D; Sandra, P.; Analysis of iso-α-acids and reduced iso-α-acids in beer by direct injection and liquid chromatography with ultraviolet absorbance detection or with mass spectrometry. J Chromatography A 1035 (2004) 53-61.
11. Jorge, K.; Trugo, L.C.; Quality control of beer hopped with reduced isomerised products. Archivos Latinoamericanos de Nutricion, vol. 48, 3, 1998, 242-246.

NEW BEER FOAM VISUAL ANALYSIS SYSTEM

K. Jorge (1), I.M.P.L.V.O. Ferreira (2), and L. C. Trugo (3)*

(1,3) Instituto de Química, Universidade Federal do Rio de Janeiro, Rio de Janeiro, Brazil.
(2) REQUIMTE - Serviço de Bromatologia, Faculdade de Farmácia, Universidade do Porto, Porto, Portugal.
(*) Phone: +55-21-33253219; katia_jorge@hotmail.com

Key words: Beer foam; visual analysis; foam stability; foam analysis; foam images

ABSTRACT
In the brewing industry, the quality of the foam created in a glass is an indication of the quality of the beer. The visual impressions of beer foam stability have been only slightly improved. Most of the standard methods for measuring beer foam stability are based on measurements of the weight or volume of the liquid collapsed from the foam. Liquid drainage is only one of the factors related to foam stability. Consequently, values measured by conventional drainage methods can give a misleading evaluation of foam stability. In the present work a different approach for the evaluation of foam stability based on image analysis is described.
In order to collect the foam images a KODAK digital camera DS 300 and the Digital Science 1D software was applied. Commercial beers of different brands were acquired according to their grist composition. The beer foam was generated manually in a Ross & Clark cylinder by simulating a consumer-use situation. The foam of the 14 beer samples were photographed in the times: zero, 30 s, 60 s, …300 s, 600 s, and 900s. The photos were treated by the software KODAK Science 1 D and the Visual Foam Index (VFI) was calculated for each photograph during the collapse time. The VFI helped us to group beer samples according to their foam collapse behavior. The first group at time zero ($VFI_0<10$) had only one beer sample, Chimay, the second group ($10<VFI_0<20$) had eight beers, Voll-Damm, Estrella-Levante, Estrella-Damm, Damm-Classic, A.K.-Damm, Bock-Damm, Erdinger and Cristal, the third group ($35<VFI_0<45$) one beer, Damm-Bier, and the last group ($45<VFI_0<55$) had four beer samples, Tagus, Superbock, Tuborg and Jansen. The results achieved promoted a scientific progress to discriminate the quality of the foam between different beer styles, which could guide more objectively the use of technological processes to really improve beer quality.

INTRODUCTION

Beer foam quality is one of the main characteristics that a consumer uses to judge the quality of dispensed beer. Beer foam quality is defined by a combination of its stability, quantity, lacing (adhesion or cling), whiteness, creaminess and strength (4).
Ronteltap et al (13) provided an excellent investigation into the physics of beer and concluded that foam characteristics are determined by the progress of four key processes: bubble formation, drainage, coalescence, and disproportionation. The number of potential foam-active components is certainly numerous and their interaction is complex. Bamforth (3) states that, “perhaps the biggest need is a decent method for assessing foam quality”. Many methods were developed but none has been worldwide accepted.
Most of the standard methods for measuring beer foam stability are based on measurements of volume of the liquid collapsed from the foam over a fixed time. There are some points that could give a misleading evaluation of the foam stability, beer temperature (20°C), foam generating in a different way from a typical pouring method (robotic and gassing), and liquid drainage alone is insufficient for the evaluation.
The visual impressions of foam stability have been only slightly improved. Most of the standard methods for measuring beer foam stability are based on measurements of the weight

or volume of the liquid collapsed from the foam (2,4,5,6,7,10,14). As demonstrated by Haugsted and Erdal (9), it is possible to utilize an image analysis system to perform the foam assay. According to Evans and Sheehan (7), the best method to access the foam must combine a digital camera, and a software for image analysis, which uses algorithms to reproduce consumers evaluation. Guided by this idea some authors had worked in visual systems of foam evaluation (Constant (6), Hallgren et al (8), Haugsted and Erdal (9), Mulroney et al. (12), Skands et al. (16), Yasui et al (17), Schneider and Raske (15), Jorge et al (11). For these reasons, we decided to develop a visual system to improve practical beer foam evaluation.

EXPERIMENTAL

Beer Samples

The beer samples used in this study were acquired in Portugal and Spain. The 14 beers were: Voll-Damm (Extra Type – 7.2% v/v alcohol; ingredients: water, malt, mais, hops); Estrella-Levante (Premium Type – 4.6 % v/v alcohol; ingredients: water, malt, rice, hops); Damm-Bier (Premium Type – no alcohol; ingredients: water, malt, rice/mais, hops); Estrella-Damm (Premium Export Type – 4.6 % v/v alcohol; ingredients: water, malt, rice/mais, hops); Damm-Classic (Pilsen Type – 4.6% v/v alcohol; ingredients: water, malt, rice/mais, hops), A.K. Damm (Premium Type – 4.8% v/v alcohol; ingredients: water, malt, hops), Bock-Damm (Bock Type – 5.4% v/v alcohol; ingredients: water, malt, rice/mais, hops), Jansen (Pilsen Type – no alcohol; ingredients: water, malt, rice/mais, hops), Tuborg (Extra Type – 7.2% v/v alcohol; ingredients: water, malt, rice/mais, hops), Superbock (Pilsen Type – 5.6% v/v alcohol; ingredients: water, malt, glucose syrup, rice/mais, hops), Tagus (Pilsen Type – 5.4% v/v alcohol; ingredients: water, malt, hops), Chimay (Triple Weissen Type – 8.0% v/v alcohol; ingredients: water, malt, wheat, sugar, hops), Erdinger (Weissen Type – 5.3% v/v alcohol; ingredients: water, wheat, malt, hops), and Cristal (Pilsen Type – 4.8% v/v alcohol).

Analytical Methods

With the objective to develop a visual system of foam analysis, we reproduced a consumer use situation using manual pouring technique. Beer samples were held at 6°C, room temperature 20°C, the foam cylinder used was the same of Ross and Clark (modified Carlsberg method), rinsed with hot water between measurements, the foam amount generated was 800 mL, to reach the upper cylinder's mark. The distance between the beer bottle/can and the cylinder was of 10 cm. The photographs had been made in the times, zero, 30 s, 60 s, 90 s, 120 s, 150 s, 180 s, 210 s, 240 s, 270 s, 300 s, 600 s, and 900 s. We used a KODAK digital camera, KODAK 300 model DS, and the software KODAK Digital Science 1 D, which enabled an easily time lapse picture capture and image analysis. The system consists of an apparatus for holding the foam cylinder, another one to hold the digital camera and the light source. The light source was mounted above the foam cylinder to enable a uniform background. We defined a specific rectangular area at the foam cylinder glass surface to be analysed by the Digital Science software. Kodak Scientific Imaging Systems offers innovative digital imaging and image analysis systems for electrophoresis gels, blots, plates, chemiluminescence, fluorescence, chromogenic, and radio-isotopic samples, and we tried to use it on beer foam analysis. It permits finding lanes on an image. The algorithm determines lane location and accurately calculates the spacing of the lane lines on the image. Once the lanes on the image have been marked and labeled, the software KODAK Digital Science 1D automatically search the defined lanes for bands. When the "Find Bands" command has been executed, the analysis process begins and the software creates a median profile for each lane,

identifies bands and generates statistics for each band. We use the average number of bands of each image as being the VFI

Once a series of images was acquired, we started the treatment of each picture observing the homogeneity of the distribution and size of the CO_2 bubbles. Beer foam samples with distinguished bubbles (middle and big size) give high VFI value (high number of bands), lower image density. The VFI helped us to group beer samples according to their foam collapse behavior.

We also performed the beer foam analysis according to the ASBC procedures (sigma value method) (1). The statistic software used to treat the results was the SPSS, version 5.0.

RESULTS

Table 1: Beer foam analysis results – sigma, T, b and c values.

Beer Samples	T	b	c	sigma	Sigma	sd
Jansen	228/230	43/44	4,2/4,0	94/93	94 [abcdefghi]	0,71
Voll Damm	217/220	76/77	14,9/15,0	120/121	121 [ajklmnopqrst]	0,71
Bock Damm	209/215	56/60	9,3/9,0	107/108	108 [bjuvwxyzA]	0,71
Tuborg	229/230	59/58	10,8/10,5	123/123	123 [kBCDEFG]	0,0
Chimay	223/224	85/85	13,0/13,2	110/112	111 [lHIJKLM]	0,71
Erdinger	220/225	84/85	8,2/8,0	91/92	92 [mNOPQRST]	0,71
Superbock	225/230	58/59	5,8/5,4	94/93	94 [cnuBNUV]	0,71
AK Damm	214/220	65/67	7,7/8,0	95/98	97 [oHWXYZ]	2.12
Tagus	215/225	53/56	5,6/5,5	92/93	93 [dpvCIO12]	0,71
Damm Classic	221/220	40/41	5,6/6,0	105/107	106 [ewDJPUW13456]	1.41
Est. Damm	220/220	53/51	6,9/6,5	102/101	102 [faqxEKQX37]	0,71
Est. Levante	221/219	64/64	9,1/9,5	106/107	107 [gryFLRY489]	0,71
Damm Bier	217/218	49/49	7,5/7,8	107/110	109 [hszSV257810]	2,12
Cristal	230/228	57/56	6,9/7,1	103/104	104 [itAGMTZ6910]	0,71
c Average			8,3			

[a] p=0,002; [b] p=0,011; [c] p=0,081; [d] p=0,075; [e] p=0,016; [f] p=0,060; [g] p=0,002; [h] p=0,033; [i] p=0,009; [j] p=0,005; [k] p=0,048; [l] p=0,039; [m] p=0,018; [n] p=0,023; [o] p=0,058; [p] p=0,029; [q] p=0,024; [r] p=0,002; [s] p=0,023; [t] p=0,005; [u] p=0,061; [v] p=0,056; [w] p=0,017; [x] p=0,044; [y] p=0,000; [z] p=0,061; [A] p=0,005; [B] p=0,003; [C] p=0,090; [D] p=0,063; [E] p=0,081; [F] p=0,039; [G] p=0,042; [H] p=0,012; [I] p=0,007; [J] p=0,018; [K] p=0,013; [L] p=0,074; [M] p=0,060; [N] p=0,030; [O] p=0,083; [P] p=0,035; [Q] p=0,071; [R] p=0,023; [S] p=0,007; [T] p=0,027; [U] p=0,034; [V] p=0,022; [W] p=0,027; [X] p=0,012; [Y] p=0,052; [Z] p=0,044; [1] p=0,015; [2] p=0,057; [3] p=0,010; [4] p=0,010; [5] p=0,047; [6] p=0,007; [7] p=0,049; [8] p=0,015; [9] p=0,090; [10] p=0,018.

According to the beer foam analysis present in table 1, Jansen, Erdinger, Superbock, AK Damm, and Tagus beer samples have the lowest beer foam stability results ($\delta < 100$). Bock Damm, Chimay, Damm Classic, Estrela Damm, Estrella Levante, Damm Bier, and Cristal beer samples have the middle beer foam stability results ($100 \leq \delta \leq 120$) and Voll Damm and Tuborg have the highest ones ($\delta > 120$).

Observing the graph of figure 1 we can see different curves of foam collapse behavior. At time zero, VFI_0, we have four groups: the first group ($VFI_0<10$) had only one beer sample,

Chimay, the second group ($10<VFI_0<20$) had eight beers, Voll-Damm, Estrella-Levante, Estrella-Damm, Damm-Classic, A.K.-Damm, Bock-Damm, Erdinger and Cristal, the third group ($35<VFI_0<45$) one beer, Damm-Bier, and the last group ($45<VFI_0<55$) had four beer samples, Tagus, Superbock, Tuborg and Jansen. Comparing the VFI_0 and sigma value results we can´t find a positive correlation**.** However, observing the graph in figure 1 in an ampler form, we see a clear difference of the foam behavior between Chimay and AK Damm beer.

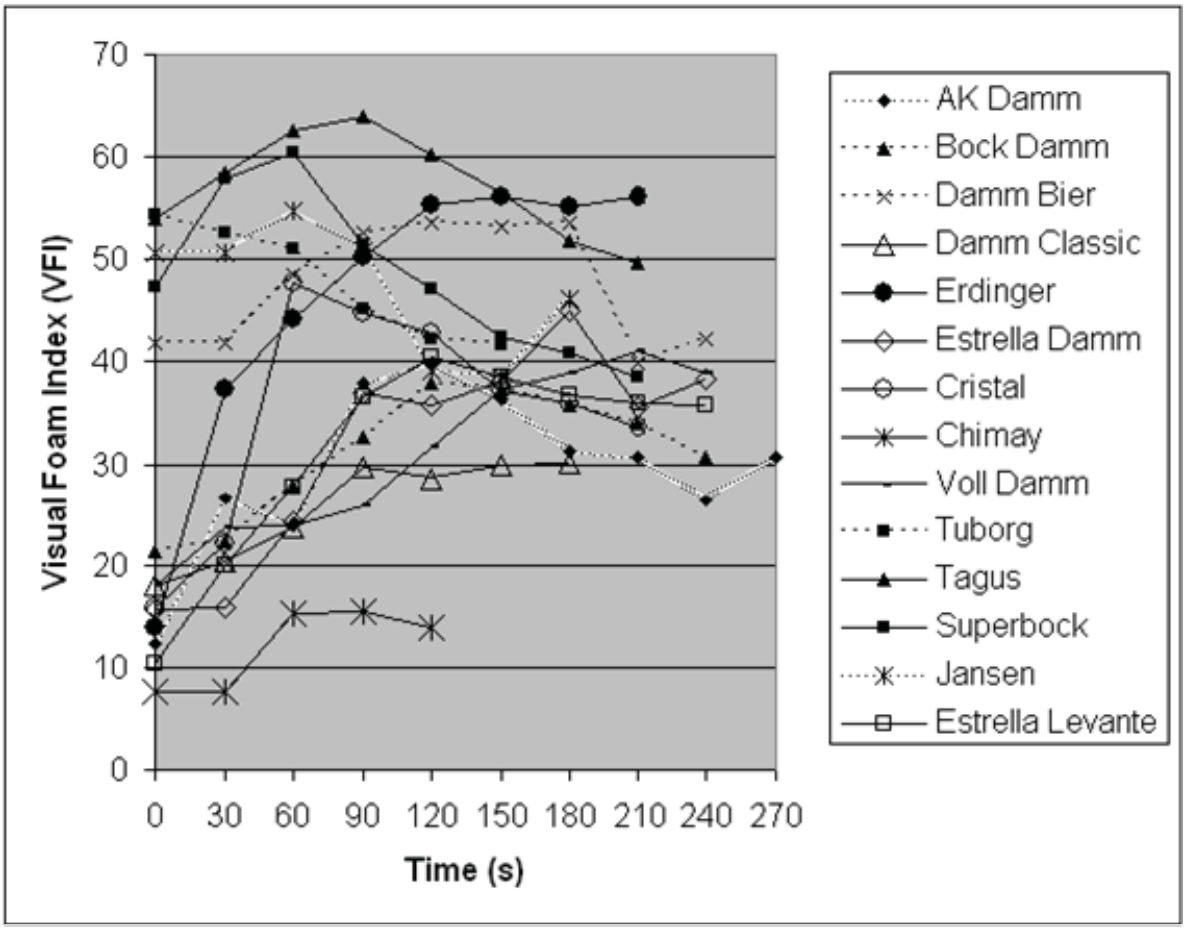

Figure 1: Visual Foam Index (VFI) of beer samples during foam collapse time, from time zero until 270 s.

The Chimay beer, after 120 s, could not have anymore its image analyzed by the 1D software, because its foam did not totally fill the defined visual field for analysis. This beer, then, for its foam instability must have given the lowest result of sigma. What we also perceive is that its c value, used to calculate sigma, is the second bigger value, being only below Voll Damm beer. Calculation of sigma value is favored. As higher the c value is, higher is the sigma value.

$$\text{Sigma } (\delta) = T / \ln (b+c/c)$$

The c value represents the amount of foam that remains adhered on the cylinder after analysis time. This foam is then collected and its volume measured. Analyzing the image at the time of 300 s, we perceive almost none foam adhered on the cylinder walls, but dense amount next to the beer surface.

AK Damm beer sample is the only one that after 270 s still has foam filling the visual field of analysis, demonstrating a higher foam stability. This is not confirmed by its sigma value (δ= 97).
The lowest standard deviation result for VFI values during the time was obtained at the point 150 s, VFI_{150} ± 1. Maybe this point can be considered the best representative image for foam assay. The results are not only easily measured, but also reproducible. The technique can be applied as a quality control tool and may also prove of great help in optimizing foam quality and troubleshooting.

CONCLUSION

We consider that this method has a good correlation with the consumer way of evaluating beer foam, and offers a simple and practical concept for foam analysis. Some studies suggest that improving foam stability alone is not sufficient for overall improvement of foam quality. Foam quality parameters such as clinging, creaminess (foam homogeneity) and foamability are also important. Therefore, we believe that an image analysis equipment is very important to evaluate the whole beer foam quality. The conventional values can´t be isolated from visual impressions.

ACKNOWLEDGEMENT

This work received financial support from Reitoria da Universidade do Porto (project "Influência da fracção proteica, hidratos de carbono, e ácidos orgânicos na estabilidade da espuma da cerveja"), CAPES, CNPq and FAPERJ.

REFERENCES

1- American Society of Brewing Chemists. *Methods of Analysis,* 7th ed. Beer 22A Sigma value method. The Society, St. Paul, MN, 1976.
2- Anger, H.-M., Glaro, L., and Scholz, M. A new process for foam stability measurement. Brauwelt International 3:146-150, 2002.
3- Bamforth, C. W. Bringing matters to a head: The status of research on beer foam. Monog. Eur. Brew. Conv. 27: 10-23, 1999.
4- Bamforth, C. W. The foaming properties of beer. J. Inst. Brew. 91: 370-383, 1985.
5- Blom, J. Investigations on foam. *J. Inst. Brew.* 43:251-262, 1937.
6- Constant, M. A pratical method for characterizing poured beer foam quality. J. Am. Soc. Brew. Chem. 50: 37-47, 1992.
7- Evans, E. and Sheehan, M. C. Don't be fobbed off: the substance of beer foam – a review. J. of ASBC. 60: 47-57, 2002.
8- Hallgren, L., Rosendal, I., and Rasmussen, J. A. Experiences with a new stability analyzer, Sustem Calsberg, J. Am. Soc. Brew. Chem. 49: 78-86, 1992.
9- Haugsted, C., and Erdal, K. Head hunting. Proc. Congr. EBC. 23: 449-456, 1991.
10- Helm, E. Ueber eine Methode zur Schaumbestimmung. *Wochenschr. Brau.* 5:241-243, 1933.
11- Jorge, K., Nothaft, A, and Trugo, L. C. Concept of a Foam Analysis System Using Machine Vision Technologies. MBAA TQ, vol. 40, no. 2, pp. 108-110, 2003.
12- Mulroney, A. R., Wenn, R. V., Oortwyn, J., and Williamson, R. R. The measurement of beer foam using a new laser-based video device. Proc. Congr. EBC 26:615-622, 1997.
13- Ronteltap, A., Hollemans, M. Bisperink, C. G. J., and Prims, A. R. Beer foam physics. TQMBAA. 28: 25-32, 1991.
14- Rudin, A. D. Measurement of the foam stability of beers. *J. Inst. Brew*, 63:506-509, 1957.
15- Schneider, J., and Raske, W. New Method of Foam Analysis by Using Nephelometric Opto-Eletronic Rapid Methods. Monogr. Eur. Brew. Conv. 27: 93-112, 1998.

16- Skandes, B., Lavrsen, L., and Bonfils, L. The Use of a Robot in Assessing Foam Quality. Monogr. Eur. Brew. Conv. 27: 62-68, 1999.
17- Yasui, K., Yokoi, S. Shigyo, T., Tamaki, T., and Shinotsuka, K. J. of ASBC. 56: 152-158, 1998.

TEXTURAL AND SENSORIAL CHARACTERISTICS OF "TERRINCHO" CHEESE

O. Pinho[1,2], E. Mendes[1], M. M. Alves[3], I.M.P.LV.O. Ferreira[1]

[1] REQUIMTE, Serviço de Bromatologia, Faculdade de Farmácia, Universidade do Porto, Rua Aníbal Cunha, 4050-047 – Porto, Portugal; isabel.ferreira@ff.up.pt
[2] Faculdade de Ciências da Nutrição e Alimentação da Universidade do Porto, Rua Dr. Roberto Frias, 4200-465 Porto, Portugal.
[3] Instituto Piaget, I.S.E.I.T.-Mirandela, C.E.R.T.A., Av. 25 de Abril, 5370-202 Mirandela, Portugal.

Key words: Texture Profile Analysis, ewe cheese, ripening and sensory analyses.

ABSTRACT

"Terrincho" ewe cheese is a Portuguese PDO cheese manufactured from raw ewe's milk of the race "Churra da Terra Quente". However, textural and sensorial studies on this cheese are quite scarce.
Cheese texture may be defined as a composite sensory attribute resulting from a combination of physical properties and perceived by the senses of sight, touch, and hearing. In recent years, multifunctional texture test instruments developed for both imitative and empirical tests have been a useful help to study food texture.
The aim of this work was to perform intravarietal comparison of "Terrincho" cheeses from 5 different dairy plants, through its chemical, physical and sensorial characteristics by evaluation of mechanical parameters from Texture Profile Analysis (TPA) and color parameters in terms of CIELAB color space (L*, a* and b*). In addition to mechanical and color tests, composition analyses and sensory tests were performed. A total of 14 samples of "Terrincho" cheeses with 30 days of ripening were evaluated.
Correlation was verified between composition, pH, texture profile analyses, color and related sensory characteristics of "Terrincho" cheeses from 5 different dairy plants. Cheeses with slightly higher fat contents, moisture and a_w and lower sodium chloride contents presented lower hardness, fracturability, gumminess, chewiness.
Color intensity, elasticity when pressing the fingers, fracturability when cutting with a knife, hardness on the mouth, evaluated from sensory analysis, positively correlated with the same instrumental measurements. No correlation was found for adhesiveness.

INTRODUCTION

Especially for "Protected Denomination of Origin" (PDO) cheeses, which often present a large variety of textures and tastes, production of consistently high quality cheeses continues to be a challenge for people involved in the chain of production. Thus, there is an increasing need for characterization of PDO cheeses. Texture and color are important criterions used to evaluate cheese quality.
"Terrincho" ewe cheese is a typical product of the North-Eastern region of Portugal and is manufactured from raw ewe's milk of the race "Churra da Terra Quente". It undergoes a minimum of 30 days of ripening and its consumption has increased over the past few years. Its is marketed as round blocks weighing around 1 kg. Its surface is smooth, flexible, dry or slightly fatty to the touch and uniformly light- yellow in color. Its interior is uniformly light-yellow. It is easy to cut, tender in the mouth. Its taste and smell is characteristically aromatic, succulent, and pleasantly salted.

Cheese texture may be defined as a composite sensory attribute resulting from a combination of physical properties and perceived by the senses of sight, touch, and hearing. Reological mechanical properties are manifested by the reaction of food to a stress applied during consumption (e.g. squeezing between the fingers, manual cutting and mastication). They comprise the following characteristics hardness, cohesiveness, viscosity, springiness, chewiness, and gumminess. The mechanical properties are measured organoleptically by the pressure exerted on the cheese by the finger and knife or teeth, tongue, and roof of the mouth during eating.

The rheological properties of a cheese depend upon its structure. The three major constituents of cheese are casein, fat and water. The structural differences between various types of cheese result from the effects of the differences in manufacturing procedures on the structure (1). A good curd is a prerequisite to obtain a quality cheese, thus, milk coagulation is a major step of cheese manufacturing largely determining the texture of the product (2).

The aim of this work was to perform intravarietal comparison of "Terrincho" cheeses from 5 different dairy plants, through its chemical, physical and sensory characteristics.

MATERIAL AND METHODS

Cheese samples

In agreement with professionals (veterinaries, farmers, cheese makers and marketing agents) 5 dairy plants (B, V, R, T and M) were selected for the quality and regularity of "Terrincho" cheeses production. A total of 19 Terrincho ewe cheeses produced during the same cheese making season (winter) and ripened for 30 days (the minimum recommended ripening time) were analysed. Three cheeses from each dairy plant were used to study the physico-chemical analysis, textural and colour parameters. A fourth cheese within each batch was used for sensory analysis. Only three cheeses were available from R dairy plant.
Cheese samples were coded with a letter (B, V, R, T and M) representing the respective dairy plant where have been manufactured and a number.

Methods

Physico-chemical analysis

The determination of the moisture, fat (3), total protein content, NaCl, ash, and acidity were determined according to AOAC methods (4-7).
The water activity was determined by a special apparatus (AW Sprint TH-500, Novasina, Swiss), pH-value was determined at room temperature using a penetrometric eletrode (Mettler- Toledo). Dry matter was evaluated using Scaltec Instruments GmbH. Germany.

Texture analysis
In recent years, multifunctional texture test instruments have been developed which are easy to use and suitable for both imitative and empirical tests. In this work, the textural analysis was performed in a texturometer TA-Xt2i (Stable Micro Systems, U.K.), with a load cell of 5 Kg, by carrying out texture profile analysis (TPA).

Sample preparation- prior to TPA test a layer of 0.5cm was removed from cheese upper surface, to obtain a regular surface for probe penetration.

Testing conditions – Penetration tests were performed, at 20 ± 2°C, using a plastic cylindrical probe of 13 mm ∅, a penetration depth of 20 mm and 1 mm/s of crosshead speed; this tests were done 5 times on each sample (one on de middle and four on different parts of cheese surface) and performed in triplicate.
Mechanical parameters - from the force *versus* time texturograms were obtained 8 parameters: hardness (g), fracturability (g), adhesiveness (g.s), springiness, cohesiveness, gumminess, chewiness and resilience.

Color Measurement
Color analyses were performed using a colorimeter CR 300 (Minolta, Japan).
L^*, a*, b* color parameters were determined according to the CIELAB color space, were L^* corresponds to light/dark chromaticity (changing from 0%, dark, to 100%, light), a* to green/red chromaticity (changing from -60, green, to 60%, red) and b* to blue/yellow chromaticity (changing from -60, blue, to 60%, yellow). The instrument was calibrated with a white tile (L^* = 97.10, a* = -4.88, b*=7.04) before the measurements.
Color determinations were made 5 times, one on de middle and four on different parts of cheese surface, before and after removing a layer of 0.5 cm of upper surface.

Sensory Analysis
A panel composed of seven members performed sensory analysis. Subjects were selected (2 sessions) for their sensory ability and trained (11 sessions) for descriptive analysis according to the guidelines in the ISO 11036:1994 standard texture profiles. Thus, before tasting the samples, screening and training was carried out in order to verify and discuss the use of texture attributes (8). The attributes whose variations were significantly perceived by the panelists were considered for the purpose of this study.
The following sensory attributes were assessed using a seven-point scale: intensity and homogeneity of color, elasticity, when pressing with the finger, adhesivity and fracturability when cutting with a knife, hardness and adhesiveness when chewing.

Statistical Analysis
The averages and standard deviations were calculated for each parameter.
Descriptive statistics, analysis of variance (ANOVA), pairwise comparisons of mean values with Turkey test, principal component analysis (PCA) and multiple regression were performed with SPSS for Windows version 11.5 (SPSS Inc, Chicago, IL).

RESULTS AND DISCUSSION

The chemical composition, the texture attributes of TPA analyses, and the color parameters of 14 samples of “Terrincho” cheeses with 30 days of ripening from five different dairy plants, (B, V, R, T and M) are listed in Table 2.
In general, cheeses from the five dairy plants presented similar composition, expect for ash content as result of different NaCl content. Especially for dry matter and fat content in dry matter small variability was observed, as shown by low F values of ANOVA analysis, F= 6.12 and 6.26, respectively. Larger variability was observed for protein content in dry matter (F=52.4).

Concerning texture attributes of TPA analysis cheeses from B, V, T and R dairy plants presented similarity with respect to hardness, springiness and chewiness, only cheeses from M dairy plant were significantly different for those attributes.
The attribute that presented greater variability between cheeses from different dairy plants was cohesiveness (F=75,57).
With respect to color attributes no significant differences were observed on L*, a*, b* measured on exterior surface and L* measured on interior of cheeses from (B, V, T, R and M) dairy plants. However, significant differences were observed between a* and b* measured on interior of the same cheeses. Cheeses from M cheeses were the most yellow and V cheeses the less yellow. This results are in agreement with those obtained by Alvarenga (9), b*(i) was the most important parameter to distinguish Serpa cheeses from two different producers.

Table 1- Chemical composition and attributes of texture and color of "Terrincho" ewe cheeses of five dairy plants.

	B	V	R	T	M	F	p
Dry matter	45.52 ± 0.28 a	46.16 ± 0.78 a,b	45.28 ± 1.59 a	47.72 ± 0.91 b	45.85 ± 0.68 a	6.12	0.01
Protein/dry matter (g100 g)	45.46 ± 0.78 a	46.95 ± 0.46 a	46.15 ± 1.84 a	50.73 ± 1.07 b	40.23 ± 1.23 c	52.4	10^{-4}
Fat/dry matter (g100 g)	55.2 ± 0.00 a	53.63 ± 2.47 a,b	53.68 ± 2.50 a,b	53.80 ± 0.78 a	50.88 ± 1.01 b		0.003
Ash content (g100 g)	3.08 ± 0.06 a	3.18 ± 0.11 a	3.62 ± 0.11 b	3.39 ± 003 c	5.52 ± 0.10 d	598	10^{-4}
NaCl/dry matter (g100 g)	2.54 ± 0.20 a	2.03 ± 0.16 c	3.29 ± 0.36 b	2.49 ± 0.31 c	6.26 ± 0.32 d	12.3	0.001
Acidity content (g100 g)	0.792 ± 0.03 a	0.708 ± 0.12 a,b	0.642 ± 0.06 b	1.296 ± 0.12 c	0.648 ± 0.03 a,b	1.29	10^{-4}
aw	0.974 ± 0.001 a	0.972 ± 0.002 a	0.968 ± 0.001 b	0.973 ± 0.001 a	0.957 ± 0.001 c	184	10^{-4}
pH	5.26 ± 0.12 a	4.96 ± 0.04 b	5.08 ± 0.04 b,d	4.86 ± 0.04 c	5.13 ± 0.04 d	77.5	10^{-4}
Hardness (g)	313.9 ± 13.0 a	683.3 ± 48.2 a	497.6 ± 6.1 a	542.0 ± 72.3 a	1926.3 ± 392.5 b	34.5	10^{-4}
Fraturability (g)	0 ± 0 a	467.1 ± 123.8b	0 ± 0 a	239.6 ± 88.2 a,b	1730.3 ± 303,5 c	58.5	10^{-4}
Adhesiveness (g.s)	-1577.5 ± 23.6 a,b	-2158.5 ± 152.5 a,c	-1880.8 ± 149.3 a,b,c	-1355.8 ± 122.2 a,b	-2448.1 ± 493.2 c	8.83	0.004
Springiness	0.96 ± 0.01 a	0.97 ± 0,01 a	0.97 ±0.00 a	0.96 ±0.01 a	0.98 ± 0.01 a	1.92	0.191
Cohesiveness	0.56 ± 0.01 a	0.5 ± 0.01 b	0.57 ± 0.01 a	0.5 ± 0.01 b	0.45 ± 0.01 c	75.5	10^{-4}
Gumminess	174.4 ± 5.7 a	344.1 ±20.7 b	271.2 ± 0.4 a	269.5 ± 31.5 a	871.5 ± 154.4 c	40.6	10^{-4}
Chewiness	168.3 ± 4.3 a	335.3 ± 24.4 a	264.3 ± 127.0 a	259.9 ± 30.2 a	857.1± 158.0 b	37.9	10^{-4}
Resilience	0.05 ± 0.00 a	0.03 ± 0.00 b	0.05 ± 0.00 a	0.04 ± 0.00 b	0.05 ± 0.00 a	30.6	10^{-4}
L*(i)	80,14 ± 0.90 a	81,79 ± 0.90 a,b	81,48 ± 0.68 a,b	81,92 ± 0.05 a,b	82,61± 1.04 b	4.47	0.029
a*(i)	-7,38±0.12 a	-6,52 ± 0.20 b	-6,63 ± 0.05 b	-6,47 ± 0.33 b	-7,83 ± 0.23 a	22.1	10^{-4}
b*(i)	17,34±1.25 a	15,41 ± 0.38 a	15,87 ±0.08 a	15,75 ± 0.81 a	20,66 ±1.10 b	17.5	10^{-4}
L*(e)	69,81± 0.84 a	67,92 ± 2.15 a	67,63 ± 3.16 a	71,86 ± 8.68 a	76,87 ±2.51 a	1.97	0.183
a*(e)	-4,64 ± 0.37 a	-4,80 ± 0.61 a	-5,22 ± 0.57 a	-4,55 ± 0.40 a	-5,50 ± 0.55 a	1.86	0.202
b*(e)	23,43 ± 1.21 a,b	20,57 ± 0.63 a	21,63 ± 2.34 a	18,27±1.38 a	28,43 ±3.92 b	8.99	0.03

a-d Means in lines without common superscripts are significantly different ($p<0.05$; n=15)
L* (e), a* (e), and b* (e) correspond to parameters measured on cheese surface (exterior) and L* (i), a* (i), and b* (i) corresponded to parameters measured on cheese surface after removing a layer of 0.5 mm (interior).

The results from PCA have been depicted on a two-dimensional plot (Fig. 1) that explained 79 % of the total variance. The Dimension 1 (k= 14.1) explained 64% of the variance in data. The negative segment of the plot for Dimension 1 was related with hardness, gumminess, chewiness, ash, springiness, fracturability, L* (e), b* (i), and b* (e) while the positive segment of the plot for that Dimension was mainly related with protein, adhesiveness, cohesiveness, fat, aw, a*(i), and a* (e). The Dimension 2 was basically related to dry matter, and L*(i) (negative coefficient), resilience, acidity and pH (positive coefficient).

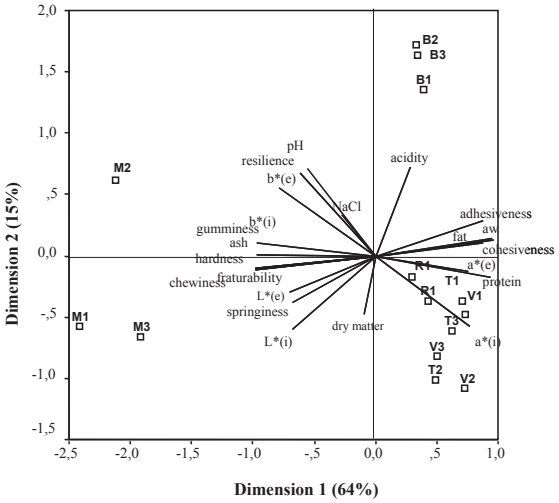

Fig 1 - Principal Component biplot showing relationship between "Terrincho" ewe cheese from B, V, R, T, M, from dairy plants and chemical composition, texture and color.

Differences were observed between cheeses from B and M dairy plants and the cheeses from others dairy plants. As shown in Fig.1 cheeses from R, T and V dairy plant, presented similar chemical composition, texture and color, because they clustered together. Cheeses from B dairy plant separated from the others mainly owing to their lower dry matter, L* (i) and higher pH, resilience, acidity, fat content and water activity. While cheeses from M dairy plant separated from the others, mainly, owing to higher hardness, gumminess, chewiness, fracturability and springiness. This cheeses also presented higher L* (e), b* (i), b* (e), NaCl and ash content. Textural analysis of cheese performed by Chen et al. (10) also refer a positive correlation between cheeses NaCl content and hardness.

Following the same procedure PCA was run on mean values from parameters and mean sensory scores for 4 texture attributes and color intensity of cheeses from the 5 dairy plants and yielded two components that explained 90% and 10% of the variance, respectively, (Fig. 2). The eigenvalue of Dimension 1 is k = 15.3.

Cheese grouping according to TPA analysis, color and sensory attributes was similar to that obtained previously for instrumental analysis of these cheeses (Fig.1)

As expected, panelists noted differences between cheeses from B and M dairy plants and cheeses from the other dairy plants (R, T and V). This last group of three cheeses presented similar chemical and sensory characteristics.

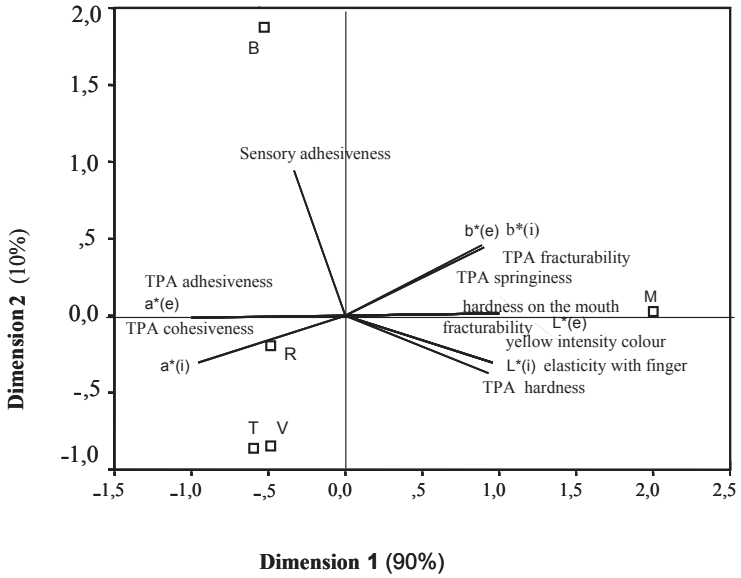

Fig. 2- Principal Component biplot showing relationship between mean values from TPA and color parameters and mean sensory scores from 4 texture attributes and color intensity of cheeses from B, V, R, T, M dairy plants.

Color intensity, hardness on the mouth fraturability when cutting with a knife, and elasticity when pressing with the fingers were positively correlated with b*(e), b (i), TPA hardness, TPA fraturability and TPA springiness. Only sensory adhesiveness was not correlated with TPA adhesiveness.

Acknowledgements: This work received financial support from Agro nº 26 (Medida 8 Acção 8.1.)

REFERENCES

(1) Bara-Herczegh, O., Horváth-Almássy, K., Csanádi, J. and Orsi, F. 2002. Suitability of Texture Parameters for Characterization of Hajdú Cheese Ripening. Acta Alimentaria. 3:149-159.
(2) Lebecque, A., Laguet, A., Devaux, M.F. and Dufour, E. 2001. Delineation of the texture of Salers cheese by sensory analysis and physical methods. Lait. 81: 609-623.
(3) SO. (1972). ISO 3433 Cheese-determination of fat content van Gulik Method Standard. International Organization for Standardization
(4) AOAC (2000). 33.7.07 AOAC Official Method 935.42 Ash of Cheese.
(5) AOAC (2000). 33.7.10 AOAC Official Method 935.43 Chloride (Total) in Cheese.
(6) AOAC (2000). 33.7.12 AOAC Official Method 920.123 Nitrogen in Cheese.
(7) AOAC (2000). 33.7.14 AOAC Official Method 920.124 Acidity of Cheese.
(8) Bárcenas, P., Elortondo, F.J.P., Salmerón, J. and Albisu, M. 2001. Sensory Profile of Ewe's Milk Cheeses. Food Sci. Tech. Int. 7: 4: 347-353.
(9) Alvarenga, N.B., 2000. Estudos em Textura de Queijo Serpa. Dissertação para obtenção do grau de Mestre em Ciência e Tecnologia dos Alimentos. Universidade Técnica de Lisboa.
(10) Chen, A.H., Larkin, J.W., Clarw, C.J., Irwin, W.E. 1979. Textural analysis of cheese. Journal of Dairy Science. 62: 901-907.

VISCOSITY OF PORTUGUESES HONEYS CORRELATION WITH SENSORY ANALYSIS

M.F. Martins[1,3], L.C. Nogueira[2], O. Pinho [1,3], I.M.P.L.V.O. Ferreira[1]*

[1]REQUIMTE - Serviço de Bromatologia, Faculdade de Farmácia, Universidade do Porto, R. Aníbal Cunha, 164, 4099-030 Porto, Portugal; isabel.ferreira@ff.up.pt

[2]Laboratóriode Bioquímica Nutricional e de Alimentos, Instituto de Química, Universidade Federal do Rio de Janeiro, Brasil

[3]Faculdade de Ciências da Nutrição e Alimentação da Universidade do Porto, Rua Dr. Roberto Frias, 4200-465 Porto, Portugal

Key words: Honey, viscosity, crystallization, fluidity, sensory analysis

ABSTRACT

Honey is the natural sweet substance produced by honeybees, it consists essentially of different sugars, predominantly glucose and fructose. The consistency can be fluid, viscous or partly to entirely crystallized. The colour, the flavour and aroma vary, but usually derive from the plant origin.
The present work was conducted to compare the viscosity of Portuguese honeys from different origins, including rosemary honey (*Rosmarinus officinalis* L.), heather honey (*Calluna, Erica* sp.) and eucaliptus honey (*Eucalyptus globules* L.). In addition, honey samples were subjected to a sensory panel to evaluate their organoleptical quality. The colour, consistency, aspect, smell and flavour were qualitatively analysed. Refractive index of honey samples using a refractometer at a constant temperature of 20ºC was also determined and readings converted to moisture content (percent m/m).
The results obtained using these methodologies were analysed by statistical multivariate analysis, such as principal component analysis, in order to understand the differences between honey samples of different origins. Good correlations were obtained between sensory and instrumental analysis.

INTRODUCTION

Honey is the natural sweet substance produced by honeybees from the nectar of blossoms or from secretions of living parts of plants or excretions of plant sucking insects on the living parts of plants, which honey bees collect, transform and combine with specific substances of their own, store and leave in the honey comb to ripen and mature.
Honey production starts immediately after the flower pollen, nectar and honeydew are collected and deposited in the bee's pouch (honey sac). The mixture of raw materials is then given to worker bees in the hive to deposit it in the six-sided individual cells of the honeycomb. The changing of nectar into honey proceeds in the cell in the following stages: water evaporates from the nectar, which then thickens; the content of invert sugar increases through sucrose hydrolysis by acids and enzymes derived from bees, while an additional isomerization of glucose to fructose occurs in the honey sac; absorption of proteins from plant and bees, and acids from the bee's body; assimilation of forage minerals, vitamins and aroma substances; and absorption of enzymes from the bee's salivary glands and honey sacs. When the water content of the honey drops to 16-19%, the cells are closed with a wax lid and

ripening continues, as reflected by a continued hydrolysis of sucrose by the enzyme invertase and by the synthesis of new sugars.
Honey is marketed as a liquid or semisolid product. It is usually oversaturated with glucose, which granulates, i.e. crystallizes, within the thick syrup in the form of glucose hydrate. To stabilize liquid honey, it has to be filtered under pressure to remove the sugar crystals and other crystallization seeds. Heating of honey decreases its viscosity during processing and filling, and provides complete glucose solubilization and pasteurisation. Heating has to be gentle since the low pH of honey and its high fructose content make it sensitive to heat treatment.
Most honeys behave like *Newtonian* fluids. Some, however, show thixotropic properties that are traceable to the presence of proteins, or dilating properties due to the presence of trace amounts of dextran (1, 2) reported that the presence of colloids (0.18-0.8%) in some honeys (such as heather and white clover) contributed to the thixotropic behaviour. Removal of colloids (possibly protein) by heat coagulation from the sample resulted in the loss of this thixotropy and permanent increase in viscosity.
The colour of honey varies from nearly colourless to dark brown. The consistency can be fluid, viscous or partly to entirely crystallized. Viscosity is one of the important properties of honey. This property is particularly critical during storage, handling and processing (3). The flow properties of honey are influenced by several factors, such as composition, temperature and amount and size of crystals. One of the predominant factors is the moisture content. Generally, the viscosity of honey decreases with water content (4). Viscosity is also a key quality factor for consumers and it is important for the choice of package. The taste and aroma vary, but usually derive from the plant origin, they are also important for consumers. Producers are especially concerned with variations in taste with changes in flow behaviour and viscosity. In general, it is known that increases in viscosity substantially decrease taste intensity.
The present work was conducted to investigate the viscosity behaviour of commercial Portuguese honeys from different origins. The rheological nature of honey was evaluated by measuring stress at various strain rates and by measuring the viscosity at 40 ºC. In addition, honey samples were subjected to a sensory panel to evaluate their organoleptic quality. The colour, consistency, aspect, smell and taste were qualitatively analysed. Refractive index of honey samples using a refractometer at a constant temperature of 20ºC was also determined and readings converted to moisture content (percent m/m). The results obtained using these methodologies were analysed by statistical multivariate analysis, in order to understand the differences between honey samples of different origins.

MATERIALS AND METHODS

Sampling

Six brands of commercial honey were randomly purchased from the Portuguese market, including rosemary honey (*Rosmarinus officinalis* L.), heather honey (*Calluna, Erica* sp.) and eucaliptus honey (*Eucalyptus globules* L.) (Table 1).

Table 1 – Classification of honey brands according to the respective label.

Brand	Honey type	package
1	Rosemary (*Rosmarinus officionalis* L.)	Glass bottle
2	Rosemary (*Rosmarinus officionalis* L.) and Erica (*Calluna vulgaris)*	Glass bottle
3	Eucaliptus (*Eucalyptus globules* L.)	Glass bottle
4	Lamiaceae (*Lavandula stoechas* L.)	Flexible Plastic bottle
5	Eucaliptus (*Eucalyptus globules* L.) and tiliaceae (Tilia sp.)	Flexible Plastic bottle
6	Heather (*Calluna vulgaris*, Erica sp.)	Glass bottle

Rheological measurements

The rheological measurements were made using a Brookfield rotatory viscometer, by measuring stress at various strain rates and by measuring the viscosity at 38 ºC.
To ensure reproducibility of the results, special care was taken when choosing spindle, rotational speed, container dimensions, sample temperature and sample preparation. Homogeneity of the sample was quite important, and honey samples were also kept at constant and uniform temperature of 40 ºC that was controlled using a constant-temperature bath.
Concerning sensitivity and accuracy, Brookfield Viscometers are guaranteed to be accurate to within ± 1% of the full-scale range of the spindle/speed combination in use (this percentage, expressed in centipoises values, is equal to the spindle combination with a Factor of 25 would therefore be ± 25 cps). Reproducibility is to within ± 0,2%.

Moisture

Moisture was determined with an Abbe refractometer reading at 20 ºC obtaining the corresponding % moisture from the Chatway Table (5) revised and updated Codex Alimentarius Commission (6).

Sensory analysis

Honey samples were subjected to a sensory panel to evaluate their organoleptic quality. Descriptive analyses were performed. The colour, consistency, aspect, smell and flavour were identified and quantified using 5 panellists who have been specially trained for this purpose. The guidelines contained in the ASTM Special Technical Publication (7,8) and in the ISO standards (9-11) were used. Panellists were asked to give a classification on a 0-7 point scale.

Statistical analyses

Statistical treatment of the data was performed using SPSS for windows version 11.5 (SPSS Inc, Chicago, IL). A principal component (PC) analysis was carried out with sensory data.
The Kaiser criterion was established to select PCs. Factors were rotated using the varimax method for ease of interpretation (12). A Categorial Principal Component Analysis was performed to correlate results from instrumental analyses (viscosity and moisture) with

sensory attributes of texture. Mean values were used. This procedure simultaneously quantified categorical variables while reducing the dimensionality of the data. The optimal-scaling approach allowed to be scaled at different levels.

RESULTS AND DISCUSSION

The results of analysis of viscosity and moisture are summarized in Table 1. The refractive index varied from 1.4971 to 1.4945 and the corresponding moisture content ranged between 15.567% and 16.900%. The honey samples under investigation were similar in moisture content, except sample 1 that presented lower moisture content. These values were within the range found by other researchers and indicate a proper degree of maturity for these honey samples (13). European regulations require <21% moisture for safety from fermentation.
Concerning viscosity measurement, significant differences between samples were observed ($F=853$, $p<10^{-4}$). Samples 2 and 3 presented significant differences when analysed by Post Hoc Tukey.test.

Table 1- Viscosity and moisture of sample honeys.

Brand	Viscosity (cps)	Moisture (%)
1	$4316 \pm 175^{a,b}$	15.567
2	28333 ± 1527^{d}	16.400
3	6950 ± 826^{c}	16.084
4	$4333 \pm 152^{a,b}$	16.084
5	3450 ± 86^{a}	16.900
6	5266 ± 251^{b}	16.484

Values are expressed as mean±standard deviation of ten determinations. $^{a-d}$ means in columns without common superscripts are significantly different ($p<0.05$).

All examined samples of honey behaved like a Newtonian fluid, Fig. 1 shows an example of the flow curves of honey samples measured at 38ºC, where the shear stress linearly varies with the shear rate and passes through the origin.

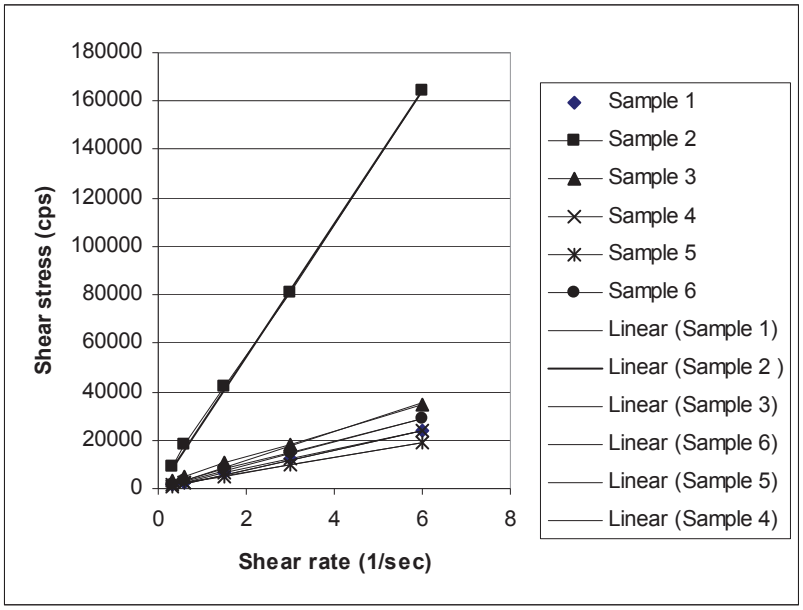

Fig. 1 – Flow curves of honey samples measured at 38 ºC.

PC analysis was applied to sensory attributes (Fig. 2 Table 2). Two PCs accounting for 81.1% of the total variance described the main variation in the texture and taste attributes. Sensory attributes related with texture, such as crystallization, transparency, fluidity in glass and in mouth, showed high positive loadings (> 0.9) with PC1. Positive correlations were observed between lack of crystallization, transparency and fluidity. Accordingly, PC1 was defined as "viscosity factor", and this factor distinguished sample 2 from the others. Intensity and quality of odour, and taste and floral aroma were related with PC2, and, accordingly, this factor was defined as "flavour factor". It distinguished two clusters one obtained with samples 1, 3 and 6 and another with samples 4 and 5.

Table 2 – Principal component loadings for sensory attributes

Rotated Component Matrix[a]

	Component	
	1	2
without cristalization	,924	,186
transparency	,964	,142
fluidity in glass	,945	,094
odor quality	,191	,897
odor inten	,105	,920
aroma quality	,223	,780
aroma intensity	-,049	,834
floral arom	,280	,782
fluidity in mouth	,900	,180

Extraction Method: Principal Component Analysis.
Rotation Method: Varimax with Kaiser Normalization.
a. Rotation converged in 3 iterations.

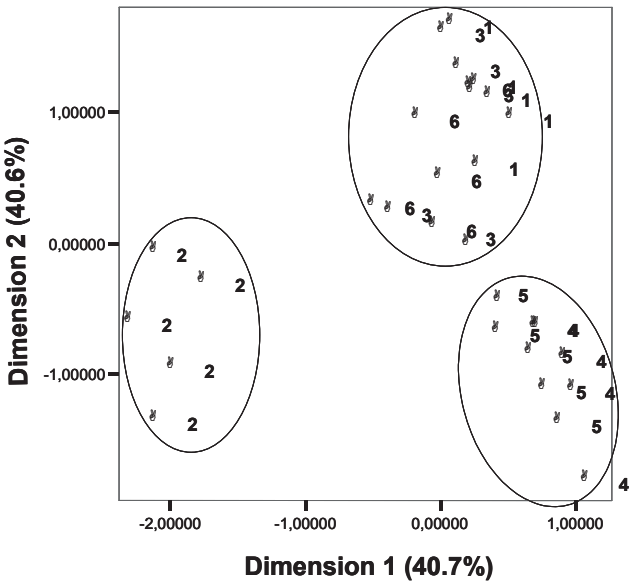

Figure 2 – PCA graphic representation of extracted variables

Good correlations were obtained between sensory and instrumental analysis. The viscosity measured instrumentally was inversely correlated with the sensorial attributes lake of crystallization, transparency, fluidity in glass and fluidity in mouth, Pearson correlation was higher than - 0.9. No correlation was observed between viscosity and moisture content. A biplot with results of Categorial Principal Component Analysis was performed to correlate results from instrumental analyses with sensory attributes of texture (Fig. 3).

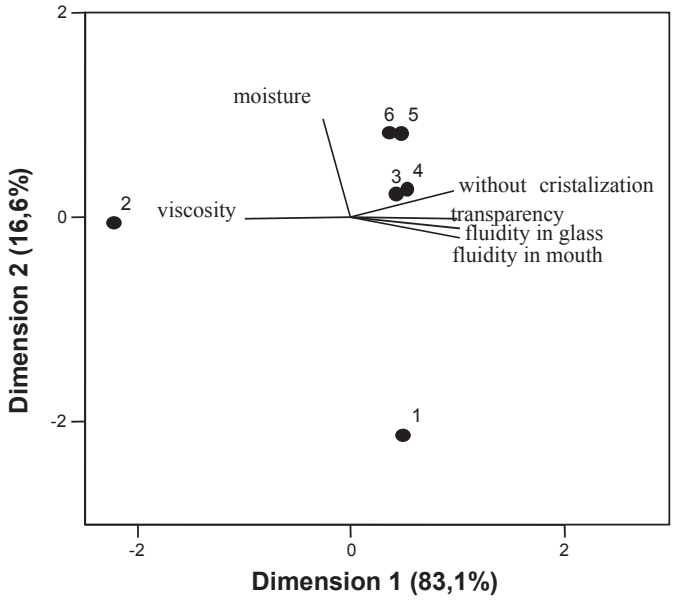

Fig. 3 – Biplot showing relationship between mean values of instrumental analysis and respective sensory texture attributes.

CONCLUSIONS

The honey samples under investigation were similar in moisture content, except sample 1 that presented slightly lower moisture content. Significant differences between samples were observed with respect to viscosity measurement, sample 2 presented the higher viscosity. This sample was different from all the others. Samples 4 and 5 presented lower viscosity, these samples were packaged in plastic flexible bottles and their viscosity was appropriate for the type of packaging.
Reological characteristics of honey were not related with its floral origin but seemed to be related with handling, processing and storage that each honey brand suffered.

REFERENCES

(1) Belitz, H.D., Grosch, W., and Shieberle, P., Food Chemistry, Edited by Springer-Verlag Berlin Heidelberg, 2004.
(2) Munro, J. A. (1943). The viscosity and thixotropy of honey. *Journal of Entomology*, 36, 769-777.
(3) Assil, H. I., Sterling, R., Sponrns, (1991). Crystal control in processed liquid honey. *Journal of Food Science*, 56, 1034-1041.

(4) Basim Abu-Jdayil, Abd Al-MajeedGhzawi, Kamal I.M. Al-Malah, Shahera Zaitoun (2002) Heat effect on rheology of light and dark-colored honey. *Journal of Food Engineering*, 51, 33-38.
(5) Chatway, H.D. (1935). Honey tables showing the relationship between various hydrometer scales and refractive index to moisture content and weight per gallon of honey. Can. Bee J., 43, 215.
(6) Codex Alimentarius Commission-CAC (1981). Vol. II, Ist ed. Codex Stan. 12.
(7) American Society for Testing and Materials, Guidelines for the selection and training of sensory panel members, STP 758, Philadelphia, 1981.
(8) American Society for Testing and Materials, Manual on descriptive analysis testing for sensory evaluation, MNL 13, Philadelphia.
(9) International Organization for Standardization, Sensory Analysis: Methodology General Guidance, ISO 6658.
(10) International Organization for Standardization, Sensory Analysis – Methodology – General guidance for the selection, training and monitoring of assessors – Part 1: Selected accessors ISO 8586-1.
(11) International Organization for Standardization, Sensory analysis – Methodology – Texture profile analysis ISO 11036.
(12) Hair, J.F., Anderson, R.E., Tatham, R.L. & Black, W.C. (1998). Multivariate data analysis, 5th ed London: Prentice-Hall.
(13) Lazaridou, A., Biliaderis, C.G., Bacandritsos, N., Sabatini, A,G. (2004). Composition, thermal and rheological behaviour of selected Greek honeys. *Journal of Food Engineering*, 64, 9-21

OPTIMISATION OF TEXTURE ANALYSIS IN PROCESSED FRUITS

Abreu, M.[a]; Gonçalves, E. M.[a*]; Rossa, A.[b]; Brazão, R.[b]; Alegria, C.[a]; Pinheiro, M. J.[a]; Moldão-Martins, M.[b]; Sousa, I.[b]*

[a] – UTPV/ DTIA/ Instituto Nacional de Engenharia, Tecnologia e Inovação (INETI)
[b] – Instituto Superior de Agronomia

[*] - Corresponding authors: Tel.: +351-21-7127101/53; fax: +351-21-7127162;
E-mail address: marta.abreu@mail2.ineti.pt (M. Abreu); elsa.goncalves@mail2.ineti.pt (E. M. Gonçalves)

Abstract
The health benefits of fruits consumption are well recognized. Fruits are an important source of vitamins, phenolic compounds and fibre in human diet. Fruits during maturation, storage and processing undergo degradation of sensory attributes, namely texture which is highly important for minimally processed and frozen fruits quality. Therefore, excessive softening is the main factor limiting fruit shelf life and storage. The main aim of this work was to find the best test procedure (using the plunger test) to discriminate differences resulting from fruits preservation processes and storage. The three variables affecting puncture tests studied were: probe type (penetration and compression probes) deformation rate (0.5 and 1.0 $mm.s^{-1}$) and depth deformation (5 and 7.5 mm). A randomised full factorial experimental designed was used among variables considered. Two vegetables materials were tested with two degrees of softening: different stages of maturation for *Rocha* pear (firm and ripe samples), and for yellow pumpkin produced by thermal processing in contrast to raw fruit (raw and thermal processed samples). The texturometer was a TA-Hdi texture analyser (Stable Micro Systems). Data were analysed by the factorial ANOVA with post-hoc LSD test, $p<0.05$, using Statistic v.6.1. as software. For *Rocha* pear, a penetration test, using a flat-head stainless steel cylinder probe travelled 5 mm inside the sample, at 0.5 $mm.s^{-1}$, was found to be a more satisfactory test to discriminate firmness results between samples (firm and ripe). For pumpkin, the greatest firmness differences between samples (raw and thermal processed) were achieved for the same probe regardless rate and depth deformation applied.

Key Words: 'Rocha' pear; yellow pumpkin; Optimisation; firmness; Texture analysis.

1. INTRODUCTION

The increasing popularity of fruits and vegetables is based on the increasing recognition of their dietary importance. Published reports link fruits and vegetables intakes with reduced risk of cardiovascular disease and cancer.

The ultimate objective of transformation of fruits and vegetables industry is to satisfy consumers. It is generally agreed that consumer satisfaction is related to product quality.

Texture is a quality parameter witch is critical in determining the acceptability of fruits and vegetables. Often the appearance of the commodity is the most critical factor in the initial purchase (in addition to price) while subsequent purchases may be more related to texture.

Textural attributes of fruits and vegetables are related to the structural, physiological, and biochemical characteristics of the living cells; their changes over time; and their alteration by processes such as minimal processing or freezing. The continuous physiological changes in living cells plus the inherent variability among individual units of the commodity make the assessment of fruit or vegetable texture difficult.

Mechanical properties of fruit products are most conveniently measured with the force-deformation curves. With this curves, a number of mechanical properties can be determined such as maximum force to rupture or puncture. Two methods have been used to obtain such

force-deformation curves (1): i) the compression of fruit by a large flat plate, ii) the compression of the product by a small flat cylindrical die.
Puncture testing is one of the simplest and most widely used methods for objective measurement of the firmness of many food products (2, 3, 4 and 5). The results obtained from puncture test are influenced by probe diameter, loading velocity, cultivars (3), and state of maturity or process (6).
The aim of the present work was to compare different mechanical loading tests (small flat-head cylinder and large flat plate probe), loading velocity and depth deformation, in order to optimise a texture test that gives a greater discriminative response relative to firmness differences of *Rocha* pear and pumpkin, destined to minimal processing and frozen process, respectively.

2. MATERIALS & METHODS

To design this proposal, the following variables were considered: 3 probe types (A= 5 mm diameter flat- head stainless steel cylinder probe; B = 10 mm flat-head stainless steel cylinder probe; C = 100 mm compression platen), 2 deformation rates (v_1= 0,5 mm.s^{-1} and v_2= 1,0 mm.s^{-1}) and 2 deformation depths (p_1= 5 mm and p_2= 7,5 mm). Under these circumstances a randomised factorial experimental design (3 x 2 x 2), with 10 replicates, for each combination of variables was performed.
The instrumental texture analysis of the combined variables was performed in two fruit samples that presented sensory perceived differences, caused by ripening process (*Rocha* pear) or by thermal treatment (pumpkin).
The sample preparation for the texture analysis was depended on the type of the test performed. For penetration test (flat- head stainless steel cylinder probe) both fruits were cut into cross sections (perpendicular to the longitudinal fruit axis) with a constant thickness at approximately 1 cm. For flat plate compression tests, the cross sections prepared as described above were produced to a cylinder-shaped piece of fruit, 1 cm in diameter.

2.1 Fruits

2.1.1 Pear

Rocha pear (*Pyrus communis*) used in this work was obtained from an orchard located in the west centre of Portugal, picked in August 2003 and stored at 1^{o}C.
Fruits of uniform size and maturity stage (based on external colour) were selected and divided randomly in two groups. The pears of the first sampling were kept in refrigeration (1°C) until testing (firm samples). The remaining fruits were kept at room temperature (3 days) to achieve a late ripeness stage and consequently a tissue softening sensory perceived, before testing (ripe samples).

2.1.2 Pumpkin

The pumpkin (*Cucurbita maxima* L.) used in the present study was obtained in a local market in Lisbon. At its arrival to the laboratory, the pumpkin was cut in cylinders 10 mm diameter and 1 cm height. Cylinders from the same fruit were randomised and divided in two groups. One set of fruits cylinders was submitted to blanching process 95°C during 5 minutes (TT samples), the others were kept raw (raw samples), until testing.

2.2 Texture analysis

The influence of the probe type (penetration and compression) at deformation rates of 0.5 and 1.0 mm.s^{-1}, performed at up two different penetration levels (ranging from 50 to 75% of the sample height) on the firmness (N), in the texture analysis of all samples, was examined using a TA-Hdi texture analyser (Stable Micro Systems) with a 50 Kg load cell. All tests were performed on the flat side of each cylinder (2.0 x 1.0 cm) or slice (1 cm height).
Firmness results (N.mm^{-2}) were taken as the maximum peak force (N) in the deformation curve divided by the contact area (mm^2), in order to compare values between different probes. The contact area of cylinder probes, 5 mm (probe A) and 10 mm diameter (probe B) for penetration tests were 19.6 mm^2 and 78.5 mm^2, respectively. For compression platen, 100 mm diameter (probe C) the contact area was 314.2 mm^2, given by the sample cylinder diameter.

2.3 Statistical treatments

Data were analysed by the factorial ANOVA with post-hoc LSD test, $p<0.05$, using Statistic v.6.1. as software.

3. RESULTS AND DISCUSSION

The figures 1 and 2, shows significant differences ($p<0.05$) between samples of *Rocha* pear (firm and ripe), under overall combined tested conditions.

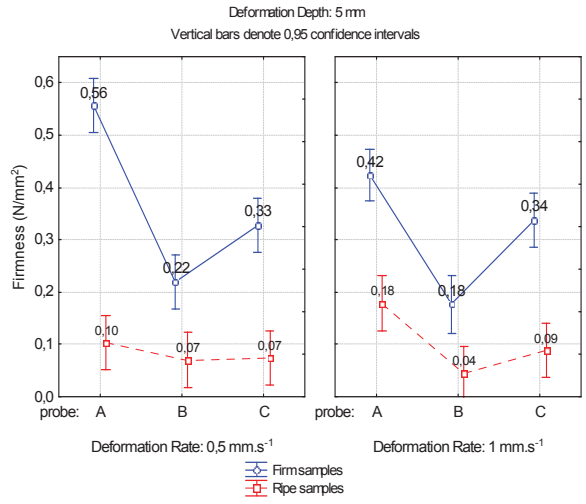

Fig. 1 – Firmness averages of firm and ripe *Rocha* pear samples, obtained at a constant deformation depth 5 mm with different probes (A and B = flat head stainless steel cylinder 5 and 10 mm, respectively and C=100 mm compression platen) at two deformation rates (0,5 and 1 mm.s^{-1}).

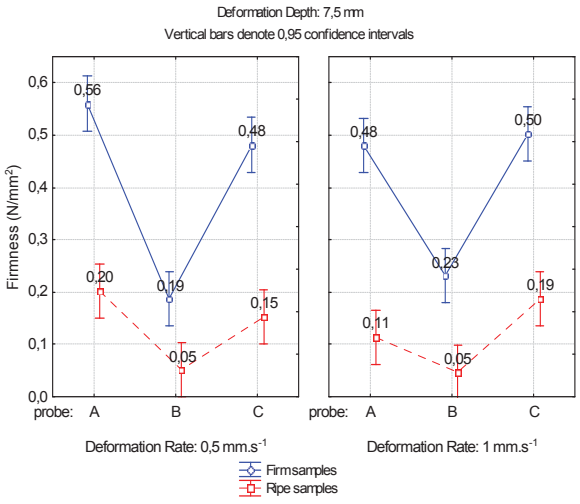

Fig. 2 – Firmness averages of firm and ripe *Rocha* pear samples, obtained at a constant deformation depth 7,5 mm with different probes (A and B = flat head stainless steel cylinder 5 and 10 mm, respectively and C=100 mm compression platen) at two deformation rates (0,5 and 1 mm.s^{-1}).

From all texture tests performed, only probe type and deformation depth, were the variables that significantly influence ($p<0.05$) the mean firmness values for both *Rocha* pear samples. However, the comparison between firm and ripe samples, for penetration test, revealed a significantly influence ($p<0.05$), along with the deformation rate. Then, the maximum average separation was achieved with probe A, at the lowest rate (0,5 mm.s^{-1}) and depth deformation (5 mm). Inversely, the average separation reached with compression test (probe C) was not

significantly influenced ($p>0.05$) by deformation rate or by deformation depth. Though, the best averages separation was obtained with 75% penetration levels. At these conditions the average separation level was similar to those attained with probe A.

Again, it can be observed from figure 3 and 4, that the difference between the raw and thermal treated pumpkin is clear. Furthermore, the results (Fig. 3 and 4) show greater differences between samples, than those verified among firm and ripe *Rocha* pear (Fig. 1 and 2), under overall combined tested conditions.

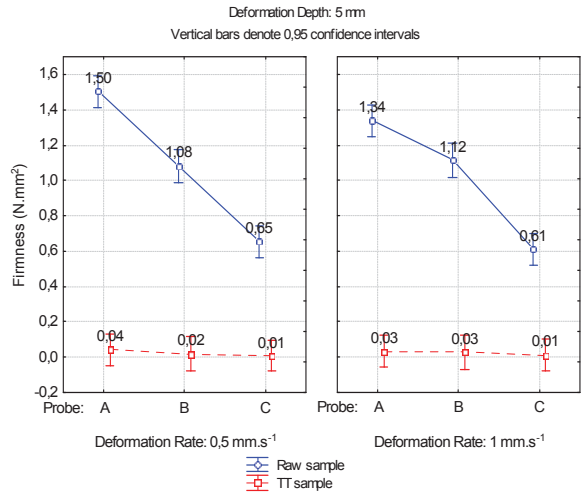

Fig. 3 – Firmness averages of raw and blanched pumpkin samples, obtained at a constant deformation depth 5 mm with different probes (A and B = flat head stainless steel cylinder 5 and 10 mm, respectively and C=100 mm compression platen) at two deformation rates (0,5 and 1 $mm.s^{-1}$).

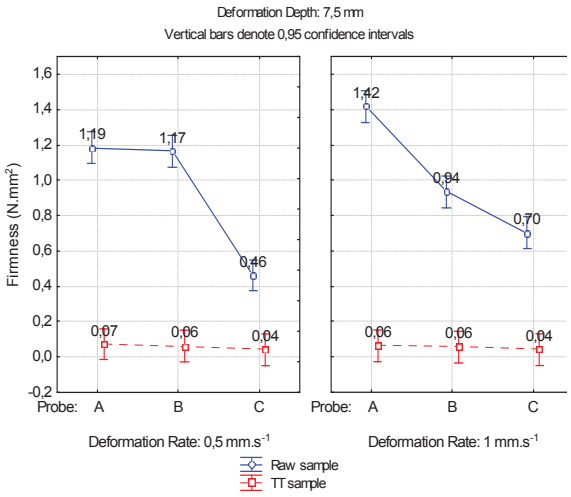

Fig. 4 – Firmness averages of raw and blanched pumpkin samples, obtained at a constant deformation depth 7,5 mm with different probes (A and B = flat head stainless steel cylinder 5 and 10 mm, respectively and C=100 mm compression platen) at two deformation rates (0,5 and 1 $mm.s^{-1}$).

In this case, probe type showed a significant effect ($p<0.05$) on firmness force, being the firmness results unaffected by rate and depth deformation applied. As can be noted from figures 3 and 4, the greatest firmness differences between samples (raw and TT) were recorded for probe A.

In raw samples, increasing the contact area (probe A, B and C) decreased the average firmness results (N/mm^2). However, with TT samples this influence was much less evident and with no statistical significance ($p>0.05$). Apart from one combined set of variables (probe B x $0.5mms^{-1}$ x 7.5 mm), the firmness results for raw samples obtained among probes were significantly different from each other ($p<0,05$).

The results obtained from puncture tests showed a great influence by state of maturity (*Rocha* pear) or thermal processing (pumpkin), as stated by Ourecky and Bourne (6). This effect was more noticed for pumpkin, which firmness changes caused by thermal processing in tissues were greater than those occurred by the influence of ripening process in *Rocha* pear.

4. CONCLUSIONS

From this study, the following conclusions were drawn for *Rocha* pear and pumpkin:

- For Rocha pear, a penetration test, using a flat-head stainless steel cylinder probe travelled 5 mm inside the sample, at 0.5 $mm.s^{-1}$, was found to be a more satisfactory test to discriminate firmness results between samples (firm and ripe).
- For pumpkin, the greatest firmness differences between samples (raw and thermal processed) were achieved for the same probe regardless rate and depth deformation applied.
- It is recommend that puncture tests optimisation should be focus in minor firmness values within range of expectable firmness changes to ensure sensitivity tests, in order to the puncture test high dependence on different ripening stages or on thermal processing.

5. REFERENCES

1 - Fisher, R.R., J.H.V. Elbe, R.T. Schuler, H.D. Bruhn and J.D. Moore. 1969. Some physical properties of sour cherries. *Trans. of the ASAE*. 12(1): 175-179.

2 - Jackman, R.L., and D.W. Stanley. 1994. Influence of the skin on puncture properties of chilled and nonchilled tomato fruit. *Journal of Texture Syudies*. 25: 225-230.

3 - Holt, C.B. 1970. Measurement of tomato firmness with a universal testing machine. *Journal of Texture Syudies*. 1: 491-501.

4 - Voisey, P.W., Lylall, L. H. and Kloek, M. 1970. Tomato skin stenght- its measurement and relation to cracking. *J.Amer. Soc.Hort. Sci*. 95: 485-488.

5 - Bourne, M.C. 1996. Measure of shear and compression components of puncture tests. *J. Food Science*. 31: 282-291.

6 - Ourecky, D.K., and M.C. Bourne. 1968. Measurement of strawberry texture with an Instron Machine. *J.Amer. Soc.Hort. Sci.* 93 (4): 317-325.

INFLUENCE OF PRODUCTION METHOD AND CULTIVARS ON TRANSPORT RESISTANCE OF INDUSTRY TOMATO

J. B. Canada, M. D. Regato, N. B. Alvarenga, M. J. Alves & H. J. Figueiredo

Escola Superior Agrária de Beja, Rua Pedro Soares – Apartado 158, 7801-902-Beja
joao.canada@esab.ipbeja.pt

Projecto nº 347 – Centro Hortofrutícola - Acção 8.1 do PO AGRO

Abstract
The purpose of this paper is to test the mechanical resistance (to penetration and crushing) of three cultivars (cvs) of tomato to industry produced by conventional and bilogical methods [2]. Three industry tomato cultivars (cvs) were cultivated (Rio Grande, CXD 187 and CXD 204) applying the organic production method according to CEE rule nº2092/91 and the conventional production method. After harvest the productiveness, soluble solids, pH and mechanical resistance (to penetration and to crushing) were analysed. The texturometer TAHDi Stable Micro Systems and a 2 mm ø cylindrical probe had been used in penetration test and samples had been penetrated in 5 different points, the test velocity was 1 mms^{-1} and the penetration force was considered to be the highest peak of the texturogram. In crushing test had been used a 75 mm ø plate probe, the test velocity was 1 mms^{-1} and crushing force was considered to be the highest peak of the texturogram and the crushing work is defined by the área below the curve of the texturogram. The conclusion was that the fruits resulting from the organic method have better transport resistance than the fruits resulting from the conventional method, although the productiveness is lower.

Keywords: Tomato, cultivars, productiveness, quality and mechanical resistance

1. INTRODUCTION

The correlation between health and environment have been a matter of many technical and social issues related to conventional agriculture. And so the biological agriculture has been growing, allowing a non chemical production and therefore non polluted. Biological Agriculture uses nature potentials with a correct use of rules and a lasting production [5].
Tomato is an irrigated culture with interest inAlentejo, mainly in irrigated perimeters of Caia, Divor, Mira, Odivelas and Roxo dams and near Sado river (Alvalade do Sado and Alcácer do Sal) and may be very important in the Alqueva dam [2].
The selection of varieties by the traditional method or using genetics engineering will take into account the agronomic characteristics of the soil, climate and phytopathologic conditions in which the culture develops and also a good culture yield will be taken into account as well as its industrial use in terms of yield and transformation, and also the nutritional and sensorial [1].

Culture management, during all the stages of the vegetable cycle to the harvest and delivery in factories, will allow a better use of production to the farmer and to industry. Agricultural optimization will allow a harvest and a more uniform tomato delivery exempt of strange substances and so agricultural and industrial activities will be more rentable and less polluent [1].

The tomato arrives at the factory in bulk, in conditions that can induce damages in fruit composition due to mechanical harvest and long distance transportation.
Tomato mechanical harvesting has been in use in Portugal being essential to compete with other countries. Although it allows a reduction in costs (compared with manual harvest), this harvest increases the losses in the field and damaged fruits increase [9].
The development of new technologies so as to improve installations use, to reduce production costs and allow a quality product needs the use of tomato varieties more resistant to mechanical phases, which led to hydraulic systems of tomato delivery [4].
Crushing fruits due to mechanical operations from harvest, to transport and delivery will influence raw material quality [6].
The characteristics of tomato varieties adapted to the previous processes (harvest and transport in the field, delivery and storage in the factory) may be evaluated by mechanical resistance. This study tests mechanical resistance (resistance to penetration and crushing) of three tomato cultivars - Rio Grande, CXD 187 and CXD 204 – produced by conventional and biological methods [10].

2.MATERIAL AND METHODS

The study developed from May to September 2002, in experimental fields, with four replica, in a total of 7.5 m^2 being the total area 216 m^2 in a total of 432 m^2. Plants with protected root of three cultivars were used: Rio Grande, CXD 187 e CXD 204. Two production methods were used: Biological and conventional [3]. The seeds were supplied by Italagro, S.A.
In the biological method an devasting infestant was fertilizer and natural phosphate. In the sanitary control only*Bacillus thuringiensis* and traps were used.
In the conventional method grading and then milling were made. Fertirrigation with several applications of fertilizers was made during the whole vegetable cycle. For diaseses and plagues control was used with sulfur and 4,8% of cymoxanil with 58% of propinebe. Infestant control was done with manual weeding a irrigation system drop to drop (4500 m^3 ha^{-1}) was also used in both methods [2].
After harvest the following parameters were analysed: productiveness (total production, production of the classes and non marketable production), soluble solids, pH and mechanical resistance to penetration and to crushing with TAHDi from Stable Micro Systems texturometer.

In the mechanical resistance to penetration it was used a 2 mm ø cylindrical probe and the samples have been penetrated in 5 different points, the test velocity was 1 mms^{-1} and the penetration force was considered to be the highest peak of the texturogram. In figure 1 we can observe a texturogram – type of mechanical resistance to penetration.

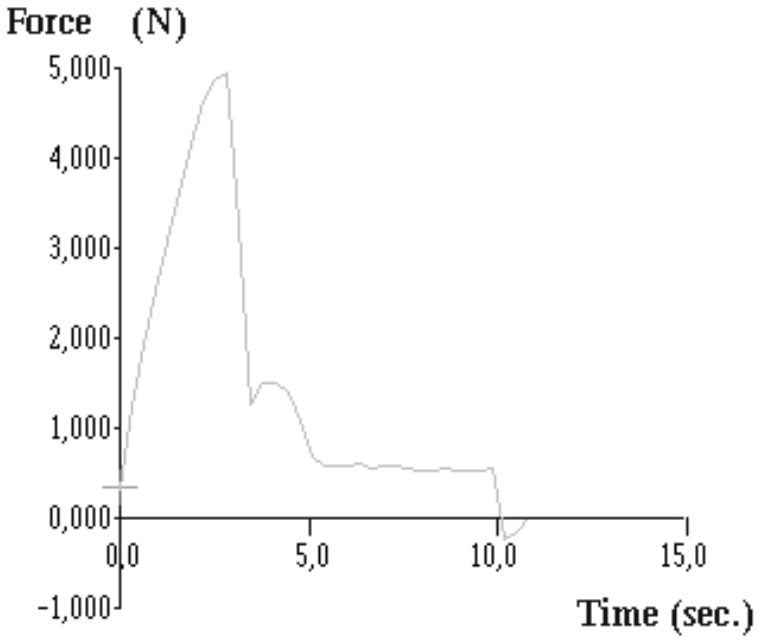

Figure 1 – Sample texturogram of mechanical resistance to penetration

In crushing a 75 mm ø plate probe was used, the test velocity was 1 mms^{-1} and the crushing force was considered to be the highest peak of the texturogram and the crushing work is defined by the area below the curve of the texturogram (figure 2).

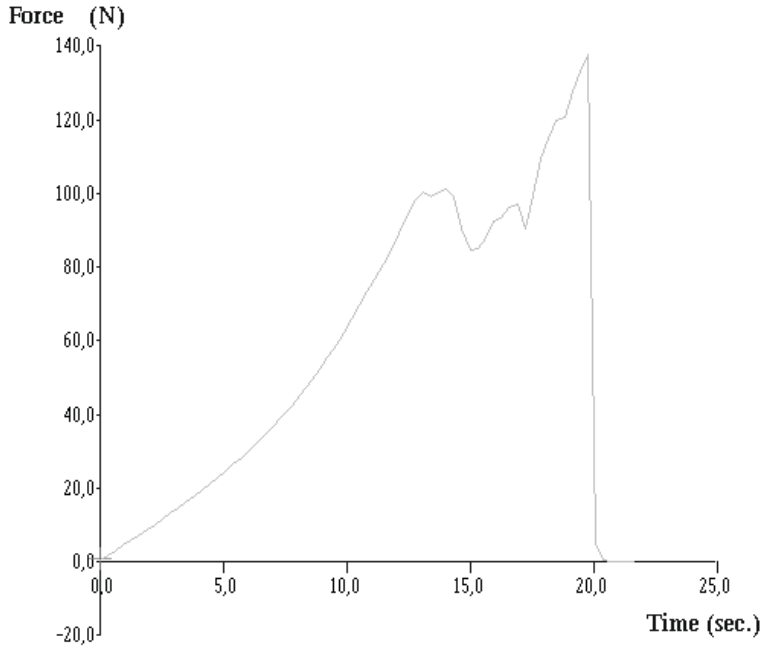

Figure 2 – Sample texturogram of mechanical resistance to crushing and crushing work

The effects of variety and production of tomato mode are analysed by ANOVA. The Scheffé's ANOVA post hoc comparisons were used to the significant differences. All calculations were carried out with the Statsoft STATISTICA 6.0 software.

3. RESULTS

The two factors ANOVA concluded that the production method and the cultivar didn't present significant effect over any depending variable ($p<0.05$). However the mechanical resistance to penetration was higher in the biological method ($p<0.05$). The Scheffé's post hoc comparisons were used to evaluate the ability for discriminations and the results of production method *versus* cultivars are presented in Tables 1 and 2.

In Table 1, it can be observed that there aren't any significant differences between the conventional and the biological production method in the following parameters ($p<0,05$): mechanical resistance to crushing, crushing work and soluble solids.
Leoni obtained a relatively low value for the soluble solids in biological production [8].
The productiveness was superior in the conventional method and non marketable production obtained a higher value when biological techniques were used [7].

Table 1 – Effect of production method in productiveness, physical and chemical characteristics of the fruit and results of Scheffe's ANOVA post hoc comparisons ($p<0,05$)

	Biological Production	Conventional Production
Total production (t ha^{-1})	53,63 b	70,53 a
Production of the classes A, B e C (t ha^{-1})	39,71 b	61,49 a
Production non marketable (t ha^{-1})	13,92 a	9,04 b
No. of units per kg.	17,8 a	14,6 b
Resistance to crushing (N)	57,92 a	54,29 a
Crushing work (N.mm)	855,83 a	745,19 a
Resistance to penetration (N)	5478,2 a	4723,6 b
pH	4,00 b	4,21 a
Soluble solids (ºBrix)	4,82 a	5,10 a

Mechanical resistance to crushing didn't show significant differences between the conventional and the biological production method. However, this parameter pointed out higher values in the conventional method.
It was observed significant differences in mechanical resistance to penetration between the conventional and the biological production method. The biological method presenteded a higher value.

In Table 2, it can be observed that there weren't significant differences between the conventional and the biological production method in the productiveness, soluble solids and in mechanical resistance to crushing, although in this parameter CXD 204 and CXD 187 cultivars showed similar values and higher then Rio Grande cultivar.
However, it can be noticed significant differences between the three cultivars in mechanical resistance to penetration, in which Rio Grande cultivar showed the lowest value and CXD 187 cultivar the highest value. So the Rio Grande cultivar presented the lowest resistance to penetration that was quit different from the others ones.

Table 2. Cultivar effect on productiveness physical and chemical characteristics of the fruit and results of Scheffe's ANOVA post hoc comparisons ($p<0,05$)

	Rio Grande	**CXD 204**	**CXD 187**
Total production (t ha^{-1})	56,56 a	63,77 a	65,90 a
Production of the classes A, B e C (t ha^{-1})	43,72 a	53,26 a	54,82 a
Production non marketable (t ha^{-1})	12,85 a	10,51 a	11,08 a
No. of units per kg.	16,23 a	16,10 a	16,14 a
Resistance to crushing (N)	50,70 a	58,80 a	58,80 a
Crushing work (N.mm)	707,85 a	848,29 a	845,35 a
Resistance to penetration (N)	4302,2 b	5203,8 a	5791,8 a
pH	4,09 a	4,15 a	4,07 a
Soluble solids (ºBrix)	4,85 a	4,94 a	5,08 a

4. CONCLUSIONS

The productiveness was lower in the biological method but those fruits showed more resistance to transport and handling when related to those produced by the conventional method.

Mechanical resistance to penetration was higher in fruits produced by the biological method allowing us to conclude that these fruits were more resistant to transport and handling.

5. REFERENCES

[1] - Barata, R.; Silva, E., 2002. *A indústria do Tomate numa Perspectiva Futur*a. Comunicação no V Colóquio Nacional de Produtos Horto-Industriais. Torres Novas.

[2] – Canada, J. B.; Regato, M. D.; Alvarenga, N. B.; Alves, M. J.;Figueiredo, H. J.; 2003.. *Comparação entre os modos de produção biológica e convencional na cultura do tomate de indústria* 1º Colóquio Nacional de Horticultura Biológica. Coimbra.

[3] – Division of agriculture and Natural Resources, 1990. *Integrated pest Management of Tomatoes.* University of California Statewide integrated pest management project. Publication 3274.

[4] - Duarte, C. M. R., 1994. *Rendimento Industrial no Fabrico de Concentrado de Tomate*. Relatório Final de Eng. Agro-Industrial. ISA. Lisboa

[5] - Ferreira, J. C. 2002. *Vantagens da Agricultura Biológica*, Ambiente 21, nº3, pag.25

Instituto Nacional do Ambiente (INA). 1989. *A Agricultura Biológica. Sua Caracterização*. Lisboa.

[6] – Gould, W. A., 1992. *Tomato Production, Processing & Technology*. CTI publications, Inc. Maryland.

[7] – Instituto Nacional do Ambiente (INIA), 1989. *A* Agricultura *Biológica. Sua Caracterização.* Lisboa.

[8] - Leoni, C., Sandei, L., Rigattieri, E., Tamburini, R., Bonetti, G., Dadoma, M. 1999. *Industria Conserve*, 74. Parma.

[9] - Portas, C. ª M.,; Machado, R. M. ª; Rodriguez del Rincón, A.; 1996. *Colheita Mecânica de Tomate para Industria: influencia na percentagem de frutos danificados e importância na relação frutos verdes/frutos danificados*. Comunicação.

[10] - Regulamento da CEE nº2092/91 do conselho de 24 de Junho de 1991 – Relativo ao modo de produção biológico e produtos agrícolas e à sua indicação nos produtos agrícolas e nos géneros alimentícios. Regulamento de base com alterações introduzidas até 12/02/99 mais regulamento 1804/99 (produção animal).

TEXTURAL AND RHEOLOGICAL PROPERTIES OF REGIONAL CHEESE. CHANGES DURING STORAGE OF CHEESE UNPACKAGED AND PACKAGED UNDER VACUUM

Inês Pantaleão, Manuela E. Pintado, Maria de Fátima Poças, F. Xavier Malcata*

Escola Superior de Biotecnologia, Rua Dr. António Bernardino de Almeida. 4200-072 Porto. Portugal
*mpintado@esb.ucp.pt

Key-words: cheese, rheological, sensorial, vacuum packaging, storage

ABSTRACT

The paper describes the evaluation of the effect of vacuum packaging on rheological, sensorial characteristics and colour of regional cheese and compares it to the non-packaged cheese throughout storage. A comparison between parameters measured instrumentally and obtained by a sensorial panel is also made. Cheese were packaged (under vacuum and in individual nets) and stored over 4 weeks under refrigeration. Results showed that sensorial evaluation are in good agreement with textural rheological parameters. Vacuum packaging did not yield to significant changes throughout storage time.

INTRODUCTION

Tailor-made packages specifically designed to improve the quality and safety of cheese are in order if expansion of its market is sought. Evidence exists that modified atmosphere packaging can extend the shelf-life of perishable food products between 50 and 400% (1). During recent years, the use of vacuum packaging has showed to be a profitable package that satisfies commercial requirements (2, 3), however its use has been applied specially to fresh cheeses. The regional cheese under study is a small cheese with a constrained shelf-life due to a high water loss throughout storage. Cheese packaging is a challenging task since this product is a complex system where different interactions take place during maturation and storage processes. After manufacture, hard cheese undergoes a maturation process according to the ripening conditions the cheese is exposed to. This process constrains the texture and the flavour of the cheese. The goal of this research effort was thus to assess the effect of vacuum upon the rheological, sensorial characteristics and colour of cheese, and compare it with non-packaged cheese throughout storage.

MATERIALS AND METHODS

Type of cheese

Regional cheese (whole cheese 250g), full fat, produced with caprine, ovine and bovine pasteurized milk and submitted to a short ripening period (c.a. 15 days) during which a straw coloured fine surface is formed. It requires controlled refrigerated conditions during distribution and sale. Average physicochemical composition: Moisture content (46%), fat (25%), protein (18.4%), pH (4.8), total acidity (1.40), chlorides (1,54%), total ash (3,58).

Packaging conditions

One lot of cheese was packaged in individual nets after a ripening period of 2 weeks; from the same lot, a group of cheeses were packaged under vacuum after 3 weeks, thus allowing for an

extra week of ripening before packaging. Cheeses were stored in a refrigerated chamber at 7ºC and 88 % of relative humidity. The samples were held at 23 ºC for 2 h before analysis in airtight plastic simulating the conditions the cheeses are commercialised in.

Cheeses were sampled every week (for 4 weeks) for sensorial testing and instrumental analysis of rheological parameters and colour.

Analytical procedures

- *Sensorial analysis*: Sensorial assessments were made by a panel of 14 members that had been previously trained using Quantitative Descriptive Analysis techniques. The panel used a pre-defined frame with 24 identified sensorial attributes which were reduced through discussion to a list of five sensorial characteristics: colour-brightness, surface shining, cutting hardness, mouth hardness, salty flavour; the characteristics were graded from 1 to 5 and judgements based on duplicate samples were made by all assessors; the cheeses were assessed as a whole and then sliced into pieces for taste and mouth feeling evaluation;

- *Rheological measurements*: The rheological properties were determined using uniaxial puncture tests performed with an Instron Universal Testing Machine (model 4501) integrated with Instron Series IX Materials Testing software package (Instron Ltd., High Wycombe, UK). The puncture was performed with a plunger with 6,4 mm of diameter, at a constant penetration rate of 50 mm/min. A load cell of 100N was used and force vr displacement curves were obtained. Five determinations per cheese were made at room temperature (23 ºC). The penetration analyses were chosen because they yield more reproducible results than compression tests, and because they correlate well with sensory analyses for what concerns firmness and rigidity (4). The integrated software converted the force deformation readings to maximum load and average load between limits.

- *Colour measurements*: L a b colour system was used to measure the surface colour change of cheese. A Minolta Chroma Meter (CR-300) was used according to the steps described in the paper by Roy *et al* (5,6). The L, a, b values were compared to the parameters of the initial cheese (L_0, a_0, $b_{0)}$ and used to calculate ΔE using the following equation:

$$\Delta E = [(L-L_0)^2 + (a - a_0)^2 + (b-b_0)^2]^{1/2} \quad (1)$$

Statistical analysis

Both sensorial and experimental data were subjected to two-way analysis of variance in order to establish whether significant differences occurred in each variable during storage and between packaging systems. Where appropriate, the least significant difference test (Tuckey Test) was used to identify between which stages and/or packaging systems differences occurred.

RESULTS AND DISCUSSION

When the results of maximum load (values of rind breakage strength) of cheese packaged under vacuum and in net where compared (see Figure 1a), it was observed that cheese under vacuum did not undergo significant variation throughout storage period exhibiting only a slight decrease in the first week. Cheeses in net packaging showed a slight increase throughout storage period. Statistical analysis showed that there is no statistical difference neither between the two packaging systems nor for the storage period (see Table 1), which confirms the low variation of this textural parameter.

Table 1- F values of Anova results for sensorial and instrumental parameters (comparison of packaging systems and storage period)

Parameter	F/Fc	Net/vacuum	Storage time
Maximum Load (N)	F Fc	1,40 10,13	0,43 9,28
Average between limits (N)	F Fc	0,15 10,13	1,49 9,28
Cuting hardness (sensorial scores)	F Fc	0,75 10,13	0,59 9,28
Mouth hardness (sensorial scores)	F Fc	0,09 10,13	0,60 9,28
Salty (sensorial scores)	F Fc	1,00 10,13	9,00 9,28
Instrumental colour	F Fc	0,65 10,13	4,80 9,28
Colour (sensorial scores)	F Fc	96,00 10,13	24,50 9,28
Shining surface (sensorial scores)	F Fc	18,78 10,13	0,41 9,28

Similar results were also observed for average between limits (values of the inner breakage strength) variation in cheese under vacuum. The conclusions were also confirmed through statistical analysis, which did not show any significant difference for type of packaging or for storage period (see Table 1).

When sensorial scores of textural properties were analysed, i.e. cutting and mouth hardness, the results corroborate the textural instrumental parameters. Cutting and mouth hardness (see Figure 1 c, d) showed exactly the same tendency and similar to that of instrumental measurements; however, cheese under vacuum showed a more noticeable decrease between 1-2 w. Salty flavour was chosen to indirectly assess the lost of water (related to cheese hardening) with the increase of salt concentration. Nevertheless the results did not showed to be an interesting parameter, once almost no variation was observed for both types of cheeses and throughout storage time (see Figure 1e). Statistics also confirmed the low variability for sensorial analysis in terms of textural parameters (see Table 1).
Parameters related to overall aspect (colour and surface shinning) showed in general significant differences between both types of packages (see Figure 1 f, g and h). Instrumental

measurements showed an intensification of initial colour (pale yellow) for cheeses packaged in net, and a slight disappearance of initial colour in vacuum packaging.

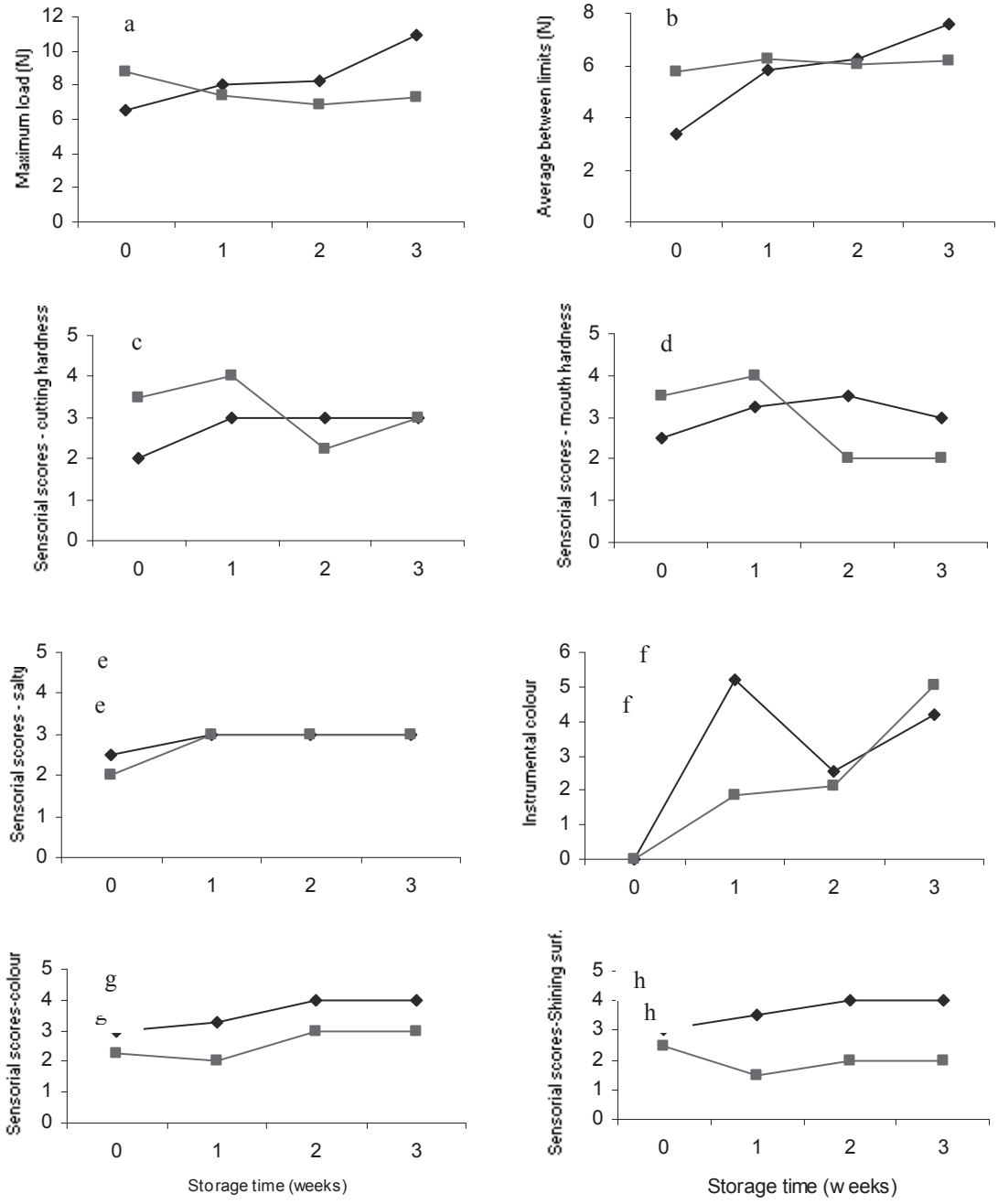

Figure 1 – Results for instrumental and sensorial parameters throughout storage time for vacuum (■) and net packaging (♦).

In what concerns sensorial evaluation of dryness aspect of cheese (evaluation of shinning surface and visual colour) statistical analysis showed a significant difference in terms of packaging conditions, but for storage time only visual colour revealed statistical differences. After pair comparison following Tukey test, differences were observed between 1 and 3, 1 and 4, 2 and 3 and 2 and 4 w of storage.

Table 2- Anova table of comparison between net and vacuum packaging for all instrumental parameters together.

Source of Variation	SS	df	MS	F	P-value	F crit
Net						
Packaging systems	971,6	2	485,82	303,37	0,000	5,14
Storage time	33,3	3	11,09	6,92	0,022	4,76
Error	9,6	6	1,60			
Vacuum						
Packaging systems	504,3	2	252,13	187,35	0,000	5,14
Storage time	5,8	3	1,95	1,45	0,319	4,76
Error	8,1	6	1,35			

When a global comparison of all instrumental parameters was performed results indicate significant differences over time and between parameters for the net packaging, and for the vacuum packaging indicate no differences overtime although significant differences between parameters.

Table 3- Anova table of comparison between net and vacuum packaging for all sensorial parameters together.

Source of Variation	SS	df	MS	F	P-value	F crit
Net						
Packaging systems	2,5	4	0,64	14,36	0,000	3,26
Storage time	2,4	3	0,81	18,35	0,000	3,49
Error	0,5	12	0,04			
Vacuum						
Packaging systems	3,1	4	0,78	1,47	0,272	3,26
Storage time	0,6	3	0,19	0,35	0,787	3,49
Error	6,3	12	0,53			

When a global comparison of all sensorial parameters was performed results also indicate significant differences over time and between parameters for the net packaging. It was found a relationship between surface shinning and colour and between hardness (mouth and cutting) and salty flavour. For the vacuum packaging results indicate no differences overtime nor between parameters.

REFERENCES

1- Hotchkiss, J. H. (1988). Experimental approaches to determining the safety of food packaged in modified atmospheres. Food Technolology, 42, 55-64.

2- Pintado,M.E., Malcata,F.X. (2000). Characterization of whey cheese packaged under vacuum. Journal of Food Protection 63, 216–221.

3- Samelis,J., Kakouri, A, Rogga, K.J., Savvaidis, , I.N., Kontominas, M.G.(2003). Nisin treatments to control Listeria monocytogenes post-processing contamination on Anthotyros,a traditional Greek whey cheese, stored at 4ºC in vacuum packages. Food Microbiology 20, 661–669.

4- Brennan, J. C., Jowitt, R., & Williams, A. (1975). An analysis of the action of the general foods texturometer. Journal of Texture Studies, 6, 83-100.

5- Roy, S., Anantheswaran, R. C. and Beelman, R. B. (1995a). Sorbitol increases the shelf life of fresh mushrooms stored in conventional packages. Journal of Food Science. 60:1254.

6- Roy, S., Anantheswaran, R. C. and Beelman, R. B. (1995b). Fresh mushroom quality as affected by modified atmosphere packaging. Journal of Food Science 60:334.

INFLUENCE OF BUTTER VS PALM FAT CONTENT IN THE HARDNESS AND FRACTURABILITY OF BUTTER COOKIES, DANISH STYLE

C. Marques[1], M. Raposo[2], N. Alvarenga[1]

[1]Escola Superior Agrária de Beja, Rua Pedro Soares, Apartado 158 7801-902 Beja
[2]Dan Cake (Portugal), S.A., Bairro de Santa Apolónia, Estrada de Eiras 3020-109, Coimbra
matilde.raposo@dancake.pt

Abstrat

The aim of this work was to study the influence of Butter vs Palm fat content in the Hardness and Fracturability of Butter Cookies. Texture measurements were performed in a Stable Micro Systems Texture Analyser TA-XT2*i*, using the Three Point Bend Rig Probe.
All the Cookies were done in the same process conditions, with the same recipe, except the kind of fat: Butter Cookies with 22% of butter, Butter Cookies 13% butter and 9% of palm fat, and Butter Cookies with 2% of butter and 20% of palm fat; cookies were stored in the same conditions of Temperature and Humidity. Samples were analysed in three different points at different shelf-time: in the production day, 3rd day, 2nd, 5th, 7th and 9th week. We had concluded that the type of fat has a direct influence in the Fracturability of Cookies.

Keywords: Texture, Hardness, Fracturability, Butter Cookies, Butter

Introduction

Texture has an essential role for the acceptance of cookies by consumers, that's why the control and optimisation of product in accordance with the market requirements is so important.

Texture is defined as the way that constituents and structural elements are arranged in a macro and microscopical structure, as the external manifestation of this structure in hardness and deformation [1].

With this work we intended to study the texture (Hardness and Fracturability) of Butter Cookies produced at Dan Cake – Coimbra. As 5 different biscuits compose each pack of Butter Cookies, we choose to study just the "Special" – this is the cookie with more homogeneous characteristics. We analysed these cookies, presenting different contents of Butter/ Palm Fat: Cookies with 2% Butter and 20% Palm Fat, Cookies with 13% Butter and 9 % Palm Fat and Cookies with 22% Butter and without Palm Fat.

Organolepticaly, these cookies present a golden brown colour, smell of butter and with a crispy and friable texture. These characteristics and mainly the texture are influenced by the kind and content of each fat – solids fat content, fatty acids composition and the slip melting point are responsible for this influence.

Butter is defined as a fat product obtained exclusively from the pasteurised cream, under a solid emulsion and malleable [2]. At 20ºC the solid fat content (%SFC) is 20% and the slip melting point is between 28 and 32ºC.

The Palm Fat is obtained by physic methods from the fruit of oleaginous palm *Elaeis guineensis*, without any chemical solvents or other chemical substances. At room temperature it is semisolid, due to fatty acids composition: about 50% of saturated fatty acids, 40% mono-unsaturated fatty acids and 10% of polyunsaturated fatty acids. As it was not submitted to hydrogenate process, it is free from trans Fatty acids [3]. At 20ºC the SFC is about 21 ± 3% .The slip melting point is 35 – 38ºC.

Butter and Palm Fat, fatty acids constitution are important to define cookies texture, as they are going to have a lubrificant role on the dough and, in the final product.

The palm fat presents more unsaturated fatty acids than Butter, as we can observe in table 1.

Table 1: Butter and Palm Fat Fatty Acids Composition

Fatty Acid	Butter, %	Palm Fat, %
Saturated		
Butyric acid	3.75	---
Capronic acid	1.75	---
Caprylic acid	1.65	---
Capric acid	2.8	---
Lauric acid	3.5	0.28
Mirystic acid	9	0.94
Palmitic acid	27	41.36
Stearic acid	10	4.16
Unsaturated		
Oleic acid	35	40.78
Linoleic acid	3	0.21
Palmitoleic acid	---	0.4

Source: [4, 5]

Material and Methods

The ingredients list of Butter Cookies – "Special":
Butter Cookies 2%: Wheat flour, palm fat (23%), sugar, Butter (2%), eggs, salt, Glucose syrup identical natural flavour.
Butter Cookies 13%: Wheat flour, sugar, Butter (13%), palm fat (12%), eggs, salt, Glucose syrup, identical natural flavour.
Butter Cookies 22%: Wheat flour, sugar, Butter (22%), eggs, salt, dextrose, Glucose syrup, identical natural flavour.

Method

To realize this study, we analysed 5 different batches of Butter Cookies per each percentage of Butter (2, 13 and 22%). Samples were analysed in different shelf time: production day, 3rd day, 2nd 5th, 7th and 9th week. Samples were stored in a shelf life room with controlled humidity and temperature. In each time 3 samples were analysed.

To guarantee the homogeneity of samples some physics characteristics were controlled: weight ± 7.2 g, diameter 44 mm, height 11 mm, humidity 2.4% and temperature 25ºC during testings.

To texture analyse, Hardness and Fracturability, a texture analyser TA-XT2*i* were used, using the three point bend rig probe. This probe gives us information about hardness, that means maximum force required to broke the cookie, and Fracturability: force is applied to the centre of the biscuit in the plot; the force is increasing until such time as the cookie fractures and falls down into two pieces. The distance at the point of break is the resistance of the sample to bens and so relates to the "Fracturability" of the sample i.e. a sample breaks at a very short distance have a high Fracturability.

The test conditions were - Mode: Measure Force in Compression; Option: Return to start; Pre-test speed: 1,0 mm/s; Test Speed: 3.0 mm/s; Post-Test Speed: 10.0 mm/s; Distance: 2 mm; Data Acquisition rate: 500 pps.

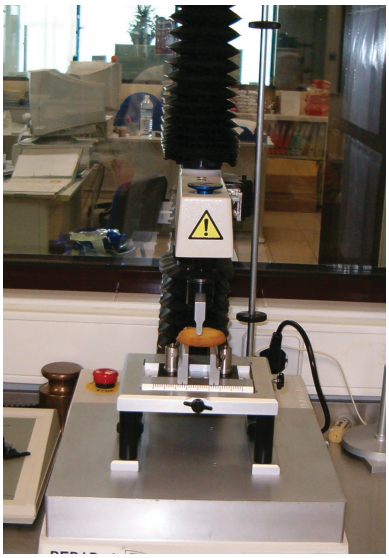

Fig. 1: Textures Analyser with the three-point bend rig probe

The effects of "shelf time" and "Added Butter" in samples of Butter Cookies were analysed by ANOVA. The Scheffé's ANOVA post hoc comparison was used to evaluate the ability for discriminations. All calculations were carried out with the StatSoft STATISTICA 6.0 software.

Results and Discussion

Table 2 shows the measured average values for Hardness (N) and standard deviation per each kind of cookie in a different shelf time.

Table 2: Hardness of Butter Cookies de 2, 13 e 22%

	Butter Cookies 2%		**Butter Cookies 13%**		**Butter Cookies 22%**	
	Average	Std. Deviation	Average	Std. Deviation	Average	Std. Deviation
Production day	25.48	368,422	25.31	214,862	26.19	205,968
3rd day	28.30	516,500	21.07	193,336	29.55	356,416
2nd week	31.09	380,768	22.27	520,950	31.63	422,908
5th week	31.09	328,288	22.03	400,260	31.17	425,302
7th week	29.23	378,888	29.92	565,264	29.23	363,126
9Th week	33.28	351.564	30.43	464.020	31.51	255.756

Table 3 shows the medium of Fracturability (mm) results and standard deviation per each kind of cookie.

Table 3: Fracturability of Butter Cookies de 2, 13 e 22%

	Butter Cookies 2%		**Butter Cookies 13%**		**Butter Cookies 22%**	
	Average	Std. Deviation	Average	Std. Deviation	Average	Std. Deviation
Production day	1,08	0,246	0,98	0,177	1,46	0,254
3rd day	0,91	0,139	0,84	0,152	0,92	0,162
2nd week	0,71	0,089	0,77	0,172	0,94	0,130
5th week	0,85	0,115	0,82	0,233	1,90	0,168
7th week	0,84	0,104	0,98	0,111	0,91	0,176
9Th week	0,86	0,114	1,00	0,136	1,04	0,138

Results of variance analysis were: there's no dependence between Hardness and shelf time or Hardness and added Butter. Additionally, it was observed no dependence between these two variables. It was observed a relation between Fracturability, shelf time and butter content, but it was not observed any dependence between these variables ($p<0.05$).

Tables 4 and 5 show the average results related to variable Fracturability as a function of two independent variables: shelf time and added Butter. These tables include also the classification obtained in the scheffe's ANOVA past hoc comparation ($p<0.05$).

Table 4: Average values of Fracturability or different butter concentration and results of Scheffe´s port hoc comparation ($p<0.05$).

Added Butter (%)	Fracturability (mm)
2	0.875^{b}
13	0.900^{b}
22	1.060^{a}

Table 5: Average values of Fracturability or different shelf time and results of Scheffe´s port hoc comparation ($p<0.05$).

Shelf Time	Fracturability (mm)
Production day	1.18^{a}
3rd day	0.80^{b}
2nd week	0.89^{b}
5th week	0.92^{b}
7th week	0.91^{b}
9Th week	0.96^{ab}

Conclusion

The added butter or the shelf time does not significantly influence hardness of Butter Cookies.

In parameter Fracturability, it was stated a difference between cookies produced mainly with palm fat (presenting lower fracturability) and cookies produced exclusively with butter. This fact can be explained by the fatty acids composition of this two fats, where the palm fat presents higher content of unsaturated fatty acids than butter. Otherwise, palm fat has a higher content of palmitic acid related to Butter (41.3% and 27% respectively). This fatty acid has a slip melting point of 63.2ºC, providing this fat with a larger solid fat content at room temperature. At 25ºC the liquid phase in the palm fat is lower than in Butter.

When cookies are submitted to a force under the same conditions, it is observed that the cookie with larger liquid phase fraction presents a larger resistance to deformation. This can be due to the absorption, by the liquid phase, of deformation applied on the surface of the cookies.

Concluding, cookies made with Butter can absorb deformation induced by the probe, more efficiently, leading to a lower Fracturability.

References

[1] IBÁÑEZ, F. (1998); *Evaluacion Instrumental y Sensorial de la Texture en Quesos de Oveja com Denominacion de Origen*; Alimentaria, Revista de Tecnologia de Higiene de los Alimentos; Madrid.
[2]NP-1711/1986- Manteiga pasteurizada. Definição, classificação, características, acondicionamento e marcação. IPQ. Lisboa.
[3] Grupo AgroPalma, S.A. (2004); *www.agropalma.com.br* (30 / 06 / 04).
[4] ALFA-LAVAL, (1990); *Manual de Industrias Lacteas*; Madrid.
[5] MORRISON, R.; BOYD, R. (1983); *Química Orgânica*; Fundação Calouste Gulbenkian; Lisboa.

A COMPARISON BETWEEN HEAT TRANFER CORRELATIONS OBTAINED FROM EXPERIMENTAL DATA AND NUMERICAL SIMULATION OF THE FLOW OF STIRRED YOGHURT DURING COOLING IN PLATE HEAT EXCHANGERS

I. M. Afonso [(a)(b)], C. S. Fernandes [(c)(d)], J. M. Maia [(c)] and L. F. Melo [(a)]*

(a) LEPAE, Departamento de Engenharia Química, Faculdade de Engenharia, Universidade do Porto, Rua Dr. Roberto Frias, s/n 4200-465 Porto, Portugal. Fax: +351-225081449; Phone: +351-225081588

(b) Escola Superior Agrária de Ponte de Lima, Instituto Politécnico de Viana do Castelo, Refóios, 4990-706 Ponte de Lima, Portugal. Fax: +351-258909779; Phone: +351-258909740

(c) IPC - Institute for Polymers and Composites, Department of Polymer Engineering, University of Minho, 4800-058 Guimarães, Portugal. Fax: +351-253510339; Phone: +351-253510320

(d) Escola Superior de Tecnologia e de Gestão, Instituto Politécnico de Bragança, Campus de Santa Apolónia, Apartado 1038, 5301-854 Bragança, Portugal. Fax:+351-273325405; Phone:+351-273303127

iafonso@fe.up.pt, cveiga@ipb.pt, jmaia@dep.uminho.pt, lmelo@fe.up.pt

Keywords: Stirred Yoghurt, Plate Heat Exchanger, Heat Transfer, Computational Fluid Dynamics

Abstract

Thermal processing is widely used in the food industry mainly to improve quality and safety of food products. The investigation of heat transfer problems of non-Newtonian fluids during heating and cooling in heat exchangers is of major interest since the main factor limiting heat transfer is the viscous behaviour of these fluids. Therefore, the knowledge of the interface heat transfer coefficients is important in the design of food processes and processing equipment.

In the present work, simulations of stirred yoghurt cooling in a plate heat exchanger were performed using computational fluid dynamics (CFD) calculations and the obtained results were compared with experimental data. Simulations were carried out using the commercial finite element method package POLYFLOW, being the geometrical domain the representation of a single 3D channel of the plate heat exchanger with a 30º corrugation angle.

The correlation obtained numerically was compared to the one obtained from previous experimental work and they were found to be very similar to the experimental one. The constitutive model, under the assumptions used, was found to be a very good approximation for predicting the convective coefficients of stirred yoghurt during cooling in a plate heat exchanger.

1. Introduction

Heating and cooling are common thermal processes in the food industry. These thermal processing techniques are widely used to improve quality and safety of food products, and to extend shelf life of the products.

Most of the fluid foodstuffs exhibit a complex rheological behaviour such as non-linear shear stress-shear rate dependency, time-dependency effects and viscoelasticity, due to their structure complexity, composition and processing conditions [1, 2].

Stirred yoghurt is a typical non-Newtonian fluid resulting from the addition of lactic acid bacteria *Lactobacillus delbrueckii* subsp. *bulgaricus* and *Streptococcus salivarius* subsp. *thermophilus* to milk producing lactic acid from milk sugar lactose [3].

Yoghurt production is a biological process and cooling is one of the popular methods used to control the metabolic activity of the starter culture and its enzymes. Cooling the coagulum

commences directly after the product reaches the desired acidity, around pH 4.6 or 0.9% lactic acid depending on the type of yoghurt produced, the method of cooling used and/or the efficiency of heat transfer [4].
The rheological properties of stirred yoghurt have been evaluated and modelled by several authors [1, 5, 6, 7, 8, 9].
The industrial development of plate heat exchangers was considerable in recent years. Although thermal performance data still remains commercially confidential, some studies have been published focusing on plate heat transfer performance[10, 11, 12, 13] and modelling [14, 15, 16, 17].
Plate heat exchangers (PHEs) are used extensively in the food processing industries, but very little basic information has been published on their flow and heat transfer characteristics [18, 19].
The food industry benefits from numerical modelling in analysing the processes for better understanding of the complex physical mechanisms, underlying the processes, designing and optimising food processes and systems with aid of the predictive models [20, 21].
The aim of present work is to compare convective heat transfer correlations obtained from numerical approaches to the one obtained from previous experimental work, in the case of stirred yoghurt cooling in a plate heat exchanger.

2. Experimental description

An experimental investigation was conducted in order to obtain a correlation for the determination of convective heat transfer coefficients of stirred yoghurt in a plate heat exchanger [19]. A rheological characterisation was carried out in order to characterise the stirred yoghurt flow behaviour, evaluating its dependency both on shear rate and temperature.
The rheological model that better described the stirred yoghurt can be mathematically expressed as:

$$\tau = \tau_0 + K_1\dot{\gamma}, \quad \text{for } \tau < 6.7 \text{ Pa} \qquad (1)$$

$$\tau = K_2\dot{\gamma}^n, \quad \text{for } \tau > 6.7 \text{ Pa} \qquad (2)$$

where τ_0 is the yield stress, K_1 and K_2 consistency indexes and n is the flow behaviour index. At shear stresses lower than 6.7 Pa, the stirred yoghurt exhibited a Bingham viscoplastic features with a yield stress τ_0, of approximately 0.54 Pa and a consistency index K_1 of 1.45 Pa s. At shear stresses higher than 6.7 Pa, the stirred yoghurt exhibited a strong shear-thinning character described by a power-law model with a consistency index K_2 of 3.65 Pa s and a flow behaviour index n, of 0.42. Temperature effects were included in the rheological model by means of an Arrhenius type term [19].
Heat transfer experiments were carried out in the laboratory-scale plate heat exchanger with generalised Reynolds numbers (which take into account the rheological effects) of yoghurt varying from 0.51 to 14.47.
A correlation for the convective heat transfer coefficient was obtained revealing significant thermal entrance effects due to the high Prandtl numbers (between 581 and 1867) and to the short length of the plates used in the experimental work. The experimental dimensionless convective heat transfer coefficient of stirred yoghurt number was written as a function of the generalised Reynolds, and the corresponding correlation is (a correction factor, named as area enlargement factor (ϕ) of 1.096, related to the ratio of the developed length to the projected length [22] of was introduced):

$$\mathrm{Nu_m} = 1.67 \cdot \mathrm{Re_g}^{0.455} \cdot \mathrm{Pr_g}^{0.3} \qquad (3)$$

where Nu_m is the average Nusselt number. The generalised Reynolds (Re_g) and Prandtl (Pr_g) numbers were calculated considering that the apparent viscosity of stirred yoghurt assumed the power-law form presented in equation (2) taking into account the influence of shear rate and temperature, expressed as follows:

$$\mu_{app} = K\dot{\gamma}^{n} \exp\left(\frac{E}{RT}\right) \qquad (4)$$

In above equation, E is the activation energy (J mol^{-1}), T the absolute temperature (K) and R the universal gas constant (8.31451 J K^{-1} mol^{-1}).The activation energy assume the value of 94785 J mol^{-1} [19].

3. Numerical Simulation

3.1. Problem description

During cooling treatment, two mechanisms of heat transfer occur: conduction, in the plates, and convection inside the channels. So, in order to simulate the non-isothermal flow of stirred yoghurt in a plate heat exchanger three problems where solved simultaneously: one of non-isothermal flow inside the channel and two of heat conduction in the plates.

The set of equations that describe mathematically the problem were the Navier-Stokes equations, for incompressible and stationary flow, and Fourier's law for the conduction problems. Additionally, a constitutive model that describes the rheological properties of yoghurt under the cooling conditions was established in order to define totally the problem, represented by equation (4).

The problem described above was simulated using the commercial finite element method package POLYFLOW. Numerical simulations were divided in three steps: construction of geometrical domain and mesh generation, establishment of boundary conditions and properties of the system and numerical resolution of the finite element problem.

Simulations were performed for fifteen flow rates of yoghurt, correspondent to the operating conditions and fluid properties from Afonso *et al.* [19].

The studied PHE had a parallel arrangement [19] and admitting a uniform distribution of the total flow rate in the various channels, the flow simulations of yoghurt were carried out in a single channel. The construction of geometrical domain and mesh generation steps are described in a previous work carried out by Fernandes *et al.* [23].

3.2. Boundary condition

Since experimental data was available [19], boundary conditions were determined based on this data, taking into account that the plate heat exchanger studied in this work operates with parallel arrangement and in counterflow.

In all the simulations slip at the wall and heat losses to the surroundings were assumed to be non-existent and a variable heat flux have been imposed in the plates. The heat flux for each x is given by the linear form of the expression:

$$q(x) = UF\left(T_{yog_{in}} - T_{wat_{out}}\right)\exp\left[2ULF\phi x\left(\frac{1}{M_{wat}C_{p\,wat}} - \frac{1}{M_{yog}C_{p\,yog}}\right)\right] \qquad (5)$$

where x is the dimension on the main flow direction ($0 \le x \le L$) (m), U is the overall heat transfer coefficient (W m^{-2} K^{-1}), F the correction factor(-), M the mass flow rates per channel (kg s^{-1}), C_p the specific heat (J kg^{-1} K^{-1}) and ϕ the area enlargement factor (-).

4. Results and Discussion

Numerical results concerning the difference between inlet and outlet yoghurt temperature were compared with experimental data and a mean deviation of 6.9% was observed.
The velocity profiles obtained numerically confirmed that a laminar flow prevailed in the present conditions, by the inexistence of recirculation zones. The results obtained are in agreement with the experimental data that revealed that the flow was fully developed from the momentum viewpoint but not from the thermal viewpoint (very high Prandtl numbers) [19].
The local distribution of temperature data obtained by numerical simulation allowed to determine average values of yoghurt and plate temperatures along the channel on planes of equation $x = const$. One example of the resulting temperature profiles along the channel is presented on Figure 1.

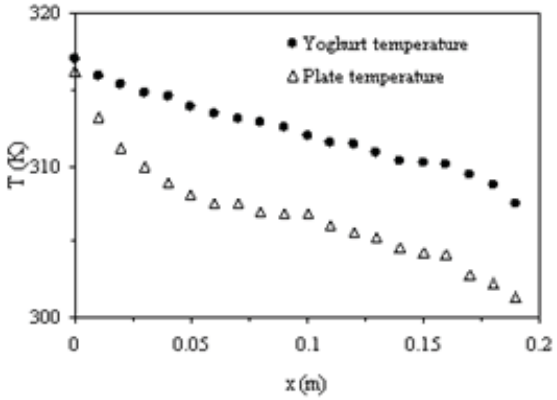

Figure 1 - Distribution of yoghurt and plate temperature along the channel for a given Reynolds number (Re_g = 12.3).

Temperature profiles in conjunction with heat flux data were used in the calculation of local convective heat transfer coefficient, defined as:

$$h(x) = \frac{q(x)}{(T_{yog} - T_w)(x)} \qquad (6)$$

where $q(x)$ was calculated by Eq. (5) and $(T_{yog}\text{-}T_w)(x)$ was given by POLYFLOW.
Consequently, the dimensionless heat transfer coefficient (Nusselt number) can be determined by means of the definition equation:

$$Nu(x) = \frac{h(x)D_H}{k} \qquad (7)$$

where k is the thermal conductivity and D_H is the hydraulic diameter ($D_H = 2b/\phi$), b is the plate spacing distance.
Figure 2 shows the local Nusselt number variation along the PHE channel length, for three different Reynolds numbers.

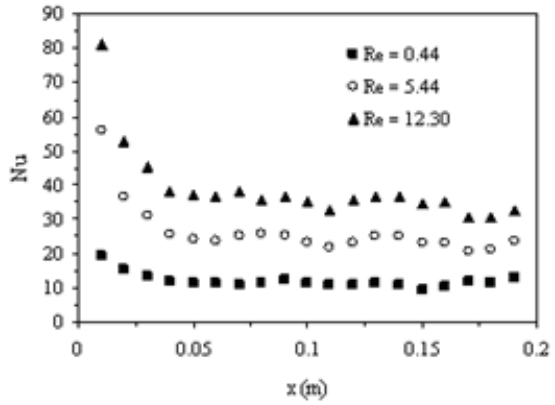

Figure 2 – Local Nusselt number variation along the plate heat exchanger channel length for different Reynolds number.

In Figure 2 it is possible to observe that the decrease tendency of the dimensionless heat transfer coefficient along the PHE channel length. As the Reynolds number values increase more pronounced is the decrease tendency of the local Nusselt number values. Stirred yoghurt assumes high Prandtl numbers [19] in the present short length PHE, resulting in thermal developing laminar flows for in the whole range of Reynolds number values.
Since the thermal correlation for the convective heat transfer coefficient of the stirred yoghurt obtained from the experimental work is based on the average Nusselt number, the average values of Nusselt number obtained by numerical simulation were determined for the fifteen simulations performed.

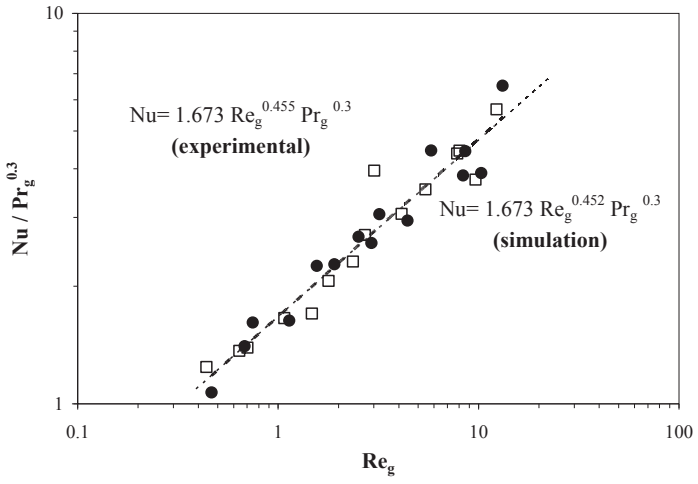

Figure 3 - Experimental heat transfer correlation and numerical correlation computed for constant wall temperature boundary condition. ● experimental, □ simulation,

Figure 3 compares the experimental correlation to the one obtained by numerical simulation. The correlation obtained from numerical simulation for the dimensionless convective heat transfer coefficient of stirred yoghurt was:

$$\mathrm{Nu_m} = 1.673 \cdot \mathrm{Re}_g^{0452} \cdot \mathrm{Pr}_g^{0.3} \qquad (8)$$

Comparing the correlations obtained from experimental data (eq. 3) and the simulated one (eq. 8) one can observe their similarity, only a small difference is observed in the Reynolds

number exponent. The good similarity may be due to the introduction of geometric factors, such as the area enlargement factor, on both correlations.

5. Conclusion

Correlations for the convective heat transfer coefficients of stirred yoghurt during cooling in plate heat exchangers were obtained from both experimental data and from a numerical simulation study. A good agreement between the two types of results was obtained when some geometric factors, like channel aspect ratio and effective to projected area, were included in the simulation.
The present work emphasizes the importance of CFD as a predicting tool for the design of food processing equipment achievement of optimum food process parameters

References

[1] T. Benezech and J. F. Maingonnat, "Characterization of the rheological properties of yoghurt – a review ", *J. of Food Engineering*, 21, 1994, 447-472
[2] B. Hallström, C. Skjöldebrand, and C. Trägårdh, in *Heat Transfer and Food Products*, Elsevier Applied Science Publishers, Essex, 1988
[3] A. Y. Tamime, R. K. Robinson, Fermented miles and their future trends. Part II. Technical aspects (review), *J. of Dairy Research*, 55, 1988, 281-307
[4] A. Y. Tamime, R. K. Robinson, in *Yogurt- Science and Technology*, second ed., CRC Press LLC, Boca Raton, 1999.
[5] T. Benezech and J. F. Maingonnat, "Flow properties of stirred yoghurt: structural parameter approach in describing time dependency", *J. of Textures Studies*, 24, 1993, 455-473.
[6] H. Rohm and A. Kovac, "Effects of starter cultures on small deformation rheology of stirred yoghurt", *Lebensm.-Wiss. U.-Technol*., 28, 1995, 319-322
[7] I. M. Afonso and J. M. Maia, "Rheological monitoring of structure evolution and development in stirred yoghurt", *J. of Food Engineering*, 42, 1999, 183-190
[8] H. J. O'Donnell and F. Butler, "Time-dependent viscosity of stirred yogurt. Part I: couette flow", *J. of Food Engineering*, 51(3), 2002, 249-254
[9] H. J. O'Donnell and F. Butler, "Time-dependent viscosity of stirred yogurt. Part II: tube flow", *J. of Food Engineering*, 51(3), 2002, 255-261
[10] M. K. Bassiouny and H. Martin, "Flow distribution and pressure drop in plate heat exchangers-I. U-type arrangement", *Chemical Engineering Science*, 39(4), 1984, 693-700
[11] M. K. Bassiouny and H. Martin, "Flow distribution and pressure drop in plate heat exchangers-II. Z-type arrangement", *Chemical Engineering Science*, 39(4), 1984, 701-704
[12] F. Rene, J. C. Leuliet and M. Lalande, "Heat transfer to Newtonian and non-Newtonian food fluids in plate heat exchangers: experimental and numerical approaches", *Transactions of the Institution of Chemical Engineers*, 69, Part C, 1991, 115-126
[13] A. Muley, R. M. Manglik and H. M. Metwally, "Enhanced heat transfer characteristics of viscous liquid flows in a chevron plate heat exchanger", *J. of Heat Transfer*, 121, 1999, 1011-1017
[14] F. Rene and M. Lalande, "Échangeur de chaleur à plaques et joints. Résolution numérique des équations d´échange thermique entre les différents canaux", *Revue Générale Thermique Fr.*, 311, 1987, 577-583
[15] T. Kho and H. Müller-Steinhagen, "An experimental and numerical investigation of heat transfer fouling and fluid flow in flat plate heat exchangers", *Transactions of the Institution of Chemical Engineers*, 77, Part A, 1999, 124-130
[16] H. U. Zettler and H. Müller-Steinhagen, "The use of CFD for the interpretation of fouling data in PHEs", in *Heat Exchangers Fouling- Fundamental Approaches & Technical Solutions*, Davos, Switzerland: UEF- United Engineering Foundation, Inc., 2001

[17] J. A. W. Gut and J. M. Pinto, "Modelling of plate heat exchangers with generalized configurations", *International Journal of Heat and Mass Transfer*, 46, 2003, 2571-2585
[18] H. B. Kim, C. C. Tadini and R. K. Singh, "Heat transfer in a plate exchanger during pasteurization of orange juice", *J. of Food Engineering*, 42, 1999, 79-84
[19] I. M. Afonso, L. Hes, J. M. Maia and L. F. Melo, "Heat transfer and rheology of stirred yoghurt during cooling in plate heat exchangers", *J. of Food Engineering*, 57, 2003, 179-187
[20] L. Wang and D.-W. Sun, "Recent developments in numerical modelling of heating and cooling processes in the food industry – a review", *Trends Food Science & Technology*, 14, 2003, 408-423
[21] B. Xian and D.-W. Sun, "Applications of computational fluid dynamics (CFD) in the food industry: a review", Computers and Electronics in Agriculture, 34, 2002, 5-24
[22] S. Kakaç and H. Liu, in *Heat exchangers- selection, rating and thermal design*, second ed., CRC Press LLC, Boca Raton, 373-396, 2002
[23] C. S. Fernandes, R. Dias, I. M. Afonso, L. F. Melo and J. M. Maia, "Simulation of stirred yoghurt processing in plate heat exchangers", *J. of Food Engineering* (submitted).

RELATIONSHIP BETWEEN VISCOELASTICITY AND TEXTURE PERCEIVED IN LOW CALORIE SALAD DRESSINGS

M. J. Hernández[*1], *A. Tárrega*[2], *M. Dolz*[1], *E. Costell,*[2] *M. C. Alfaro*[3]

[1]Departament de Termodinàmica. Fac. Física i Farmàcia. Univ. València. 46100 Burjassot, Valencia (Spain). Phone: 0034 963544902, FAX: 00 34 963543385, e-mail: M.Jesus.Hernandez@uv.es
[2]Laboratorio de propiedades físicas y sensoriales. Instituto de Agroquímica y Tecnología de Alimentos (CSIC). PO Box 73, 46100 Burjassot, Valencia (Spain).
Phone: 0034 963900022, FAX: 00 34 963636301, e-mail: ecostell@iata.csic.es
[3]Departamento de Ingeniería Química. Facultad de Química. Universidad de Sevilla. 41012 Sevilla (Spain). Phone: 0034 954557179, FAX: 0034 954556447, e-mail: jmunoz@us.es

Keywords: texture, viscoelasticity, emulsions, starch, gums.

ABSTRACT
Formulations of low oil content salad dressings usually include some hydrocolloids in order to replace the fat and stabilise the emulsion. Modified starch is normally used due to the special creamy texture it provides. The combination of starch with other natural gums, may improve the quality of the product. The purpose of this work is to analyse the possible correlation between the differences in sensorial perceived texture, mainly in consistency and creaminess, and the values of rheological parameters. A reference emulsion, containing 4% modified starch, and other four formulations in which the starch was partially substituted by xanthan gum (0.4%), locust bean gum (0.4%) and synergistic blends of these gums (0.03%+0.03%, and 0.1%+0.1%) were analysed. Three batches of each formulation were prepared. Differences in consistency and in creaminess were analysed using the ranking test. The study was carried out in a standardised panel test room by a group of 28 assessors. Rheological measurements of mechanical spectra within the viscoelastic region, were carried out with a controlled stress rheometer (Rheostress 1, Haake) using a 35 mm serrated plate. All measurements were made at room temperature.
Significant differences in sensory consistency were detected. Samples with xanthan or locust bean gum added were perceived significantly as more consistent and as with less vinegar taste intensity than the rest of the samples. No significant differences in creaminess were found. Good relationships were observed between the differences in sensory consistency and both G´ and η^* values, measured at 1 Hz.

1. INTRODUCTION

Reducing the calorie content in food emulsions by introducing less percentage of oil in their formulation, implies the necessity of including some additives in order to secure their stability and desired texture [1]. Different kinds of hydrocolloids are normally used for this aim. Modified starches are the most widely used in food industry because of its special creamy texture and its low cost. It is also common in industrial formulations to include other polysaccharides to improve the final product, enhancing the viscosity or reducing the syneresis, for example. This is the case of xanthan gum, locust bean gum, guar or alginate [2]. Several previous studies had shown that viscoelastic properties of the emulsion change when introducing these gums [3]. However, there exists a lack of knowledge about if these changes are noticed by consumers and if they are accepted or even preferred. This information is very important for the optimization of the final product [4].

[*] To whom correspondence should be adressed. E-mail: M.Jesus.Hernandez@uv.es

The purpose of this work is to analyse the possible correlation between the differences in sensorial perceived texture, mainly in consistency and creaminess, and the values of rheological parameters. Additionally, preliminary information about possible influence of texture on flavour intensity was obtained**.** A reference emulsion containing only modified starch, with other four formulations that substitute part of the starch for xanthan gum, locust bean gum and two synergistic blends of them have been analysed.

2. EXPERIMENTAL

2.1. Materials

Acetilated distarch adipate, commercially C*Tex 06214, was acquired from its manufacturer Cerestar (Cargill, Barcelona). Xanthan gum was provided by Jungbunzlauer Ges.m.b.H. (Quimidroga, Barcelona) and locust bean gum was obtained from Industrial Garrofera Valenciana (Ingavasa, Valencia). Pasteurised liquid salted egg yolk, sunflower oil and wine vinegar (equivalent acetic acid concentration: 10%) were kindly supplied by Hijos de Ybarra (Seville). Commercial salt and sugar, preservatives (potassium sorbate and sodium benzoate) and deionised water were also used.

2.2. Emulsion manufacture

Emulsion formulation was adapted from the commercial composition of low oil content mayonnaise containing 4 wt% of modified starch (MS) as stabilizer and 34 wt% of vegetable oil. The total content of stabilizer was maintained at 4 wt%, the MS fraction being partially replaced by xanthenes gum, locust bean gum or a mixture of both gums. Table 1 indicates the hydrocolloid content in the different formulations tested, together with the notation used in the text below to refer to each of the emulsions.

Table 1. Systems notation, both gels and emulsions, and the hydrocolloid content in each case

System notation	Hydrocolloid content (wt)
MS	4 % modified starch
LBG	3.6 % MS + 0.4 % locust bean gum
XG	3.6 % MS + 0.4 % xanthan gum
0.03	3.94 % MS + 0.03 % locust bean gum + 0.03 xanthan gum
0.1	3.8 % MS + 0.1 % locust bean gum + 0.1 xanthan gum

The final manufacture method chosen consisted of two steps: the first dealt with the hydrocolloid gel formation and the second with the emulsion manufacture.

In the first stage, the solid ingredients (sugar, salt, preservatives and hydrocolloid power) were mixed, dispersed in water (stirring for 5 min at room temperature) and heated to 95ºC while stirring for 15 min in order to ensure homogeneous gelation of the starch.

After cooling to room temperature, the gels were kept at 5ºC during 24 hours.

Finally, the liquid egg yolk was added to the gel and emulsification was carried out using a rotor-stator Ultraturrax T-50 homogenizer (Ika, Germany). This process was performed at 10ºC, with a homogenization speed of 5000 rpm during 7 min. Oil was added slowly during the first 3 minutes and vinegar added at the end.

The final emulsions prepared were stored at 5ºC until measurement. Three batches of each formulation were prepared.

2.3. Rheological measurements

Small amplitude oscillatory shear experiments were carried out with a controlled stress rheometer (Rheostress 1, Haake) using a 35 mm serrated plate. Frequency sweep tests between 0.01 and 10 Hz were performed at 3 Pa (within the linear viscoelastic region). The values of G', G", tan δ and η* as a function of oscillatory frequency were obtained for each of the 3 batches prepared for the different formulations considered. All measurements were made at room temperature.

2.4. Sensory measurements

Samples were ranked, following ISO 8587 [5] for consistency (visual and oral), for creaminess and for vinegar taste intensity by a 28-selected member panel. Judges were presented the five samples at random order. They were allowed to drink water at any time. Sensory analysis were performed in a standardized test room [6] equipped with Compusense five software (Canada). Friedman analysis of variance was applied to the sensory data, significance of differences ($\alpha = 0.05$) between samples being determined by the Fisher test modified for non-parametric data.

3. RESULTS AND DISCUSSION

Figure 1 shows the mechanical spectra of the five kinds of emulsions studied. In order to compare more easily, two graphs have been plotted, both including the reference emulsion (MS). Graph I shows LBG and XG emulsions and graph II the emulsions containing the synergistic blends. In all cases, values of G' and G" increased when substituting part of the starch for a gum. This increase was significantly bigger in LBG and XG emulsions, what indicated that the expected synergism between xanthan gum and locust bean gum when they are mixed alone, had not the same effect when the other components of the emulsion were present.

On the other hand, it is interesting to point out that while in graph II all the mechanical spectra keep the same tendency for the frequency dependence, LBG and XG emulsions were quite different. This implies that including these proportions of gums changed the internal structure of the reference emulsion. The greatest differences were observed in G" in both cases. For the XG emulsion the loss modulus wass more constant with frequency while for LBG the plateau of the reference emulsion disappeared and the slope increased, what is more characteristic of a liquid response versus a more elastic behaviour of the XG emulsion.

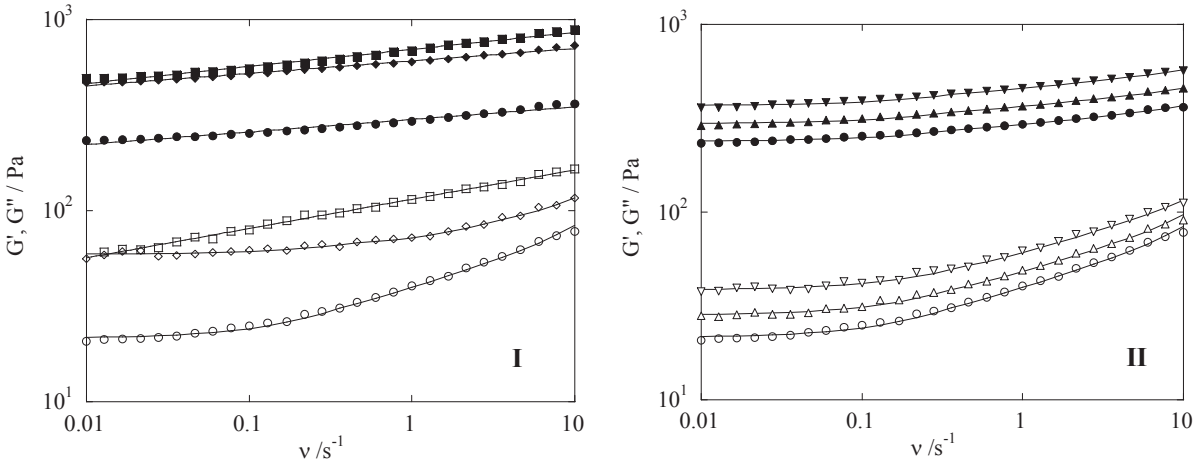

Figure 1. Mechanical spectra. Storage modulus: Full symbols, Loss modulus: Open symbols. (○) MS, (□) LBG, (◇) XG, (△) 0.03(LB+X), (▽) 0.1(LB+X)

These results about viscoelastic behaviour of the systems and relations between G' and G" can be confirmed by analysing the loss tangent (Figure 2). In all cases, and for the whole frequency range studied, tan δ was lower than 0.25, what indicated that the elastic behaviour predominated over the viscous behaviour. As figure 1 indicated, the two emulsions containing blends of gums were similar to the reference MS emulsion. However, as it is now expected, the two other kinds of emulsions showed a clearly different viscoelastic behaviour. The frequency dependence was rather low in the latter emulsions while in MS and blends emulsions frequency dependence is considerable such that loss tangent curves cross in two different frequencies (0.7 and 3-4 Hz). This fact implies that comparison between values of tan δ gave different results when considering different frequencies.

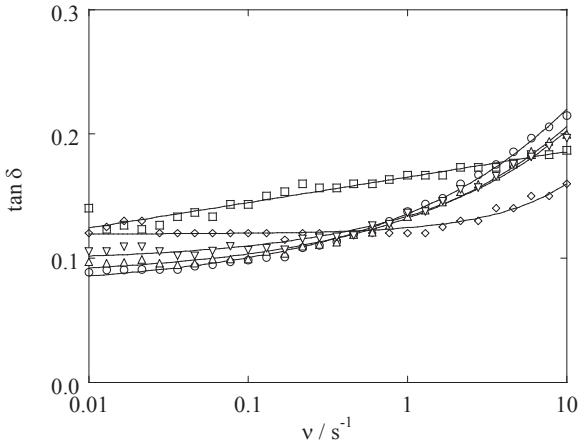

Figure 2. Mean values of loss tangent as a function of frquency for all the emulsions studied: (○) MS, (□) LBG, (◇) XG, (△) 0.03, (▽) 0.1.

In order to find a correlation between these rheological parameters and the sensory characteristics of the emulsions, the values at 1 Hz were considered (Figure 3). The bar diagrams show that both storage and loss modulus were significantly higher for LBG and XG emulsions. However the relation between LBG and XG emulsion was not the same for G' than for G", what was reflected in a different distribution of tan δ values.

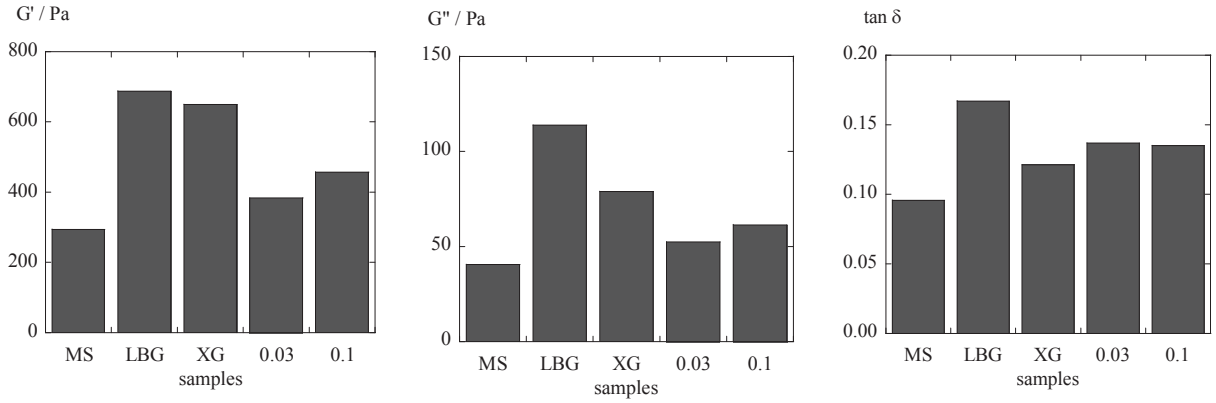

Figure 3. Mean values of storage modulus, loss modulus and tan δ measured at 1 Hz.

When plotting the complex viscosity it in logarithmic axis as a function of frequency, parallel straight lines were obtained for all systems. These functions were fitted to the equations

$$\eta^* = M\, \nu^{-p} \qquad (1)$$

where p = 0.92 ± 0.01 and M is the complex viscosity at 1 Hz. The values of M are shown in the bar diagram in figure 4 II and they will be correlated with sensorial parameters below.

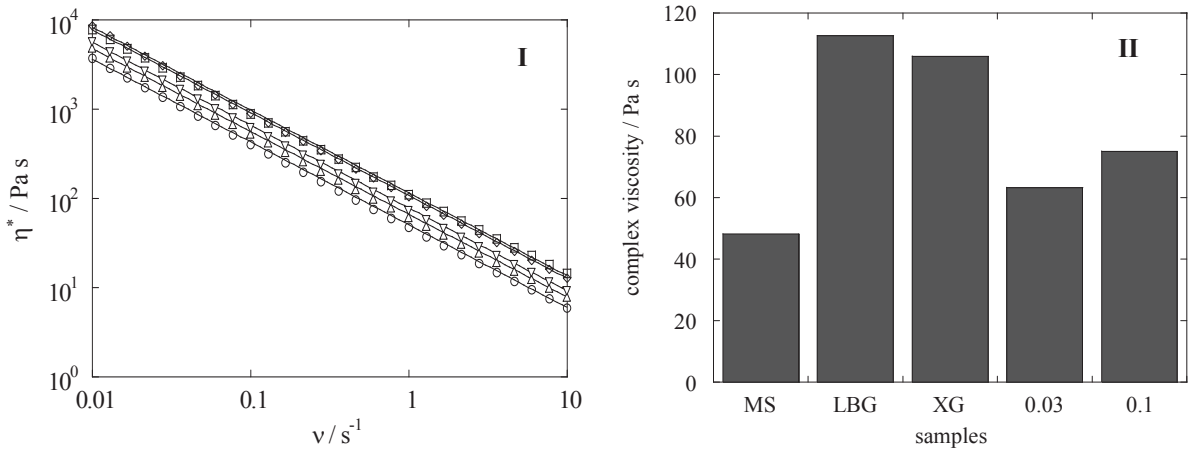

Figure 4. Complex viscosity. **I**: Mean values as a function of frequency: (○) MS, (□) LBG, (◇) XG, (△) 0.03(LB+X), (▽) 0.1(LB+X). **II**: Values of the parameter M in eq. (1): η* at 1 Hz.

Analysis of results obtained from sensory evaluation showed that significant differences in both visual and oral consistency and no significant differences in creaminess were found for the emulsions (Figure 5). Friedman F values for visual consistency, oral consistency and creaminess were respectively 50.37, 45.91 and 0.88 (from tables, F=9.49; α=0.05). LBG and XG emulsions were perceived significantly as with more consistency than the rest of emulsions. By comparing these results (Figure 5) with the rheological parameter values at 1 Hz (Figures 3 and 4) a clear relation between perceived consistency and both storage modulus and complex viscosity values can be established. Besides this fact, significant differences in vinegar taste intensity were also detected. As expected, more consistent emulsions (LBG and XG) were perceived significantly as with less vinegar taste intensity (Figure 6)

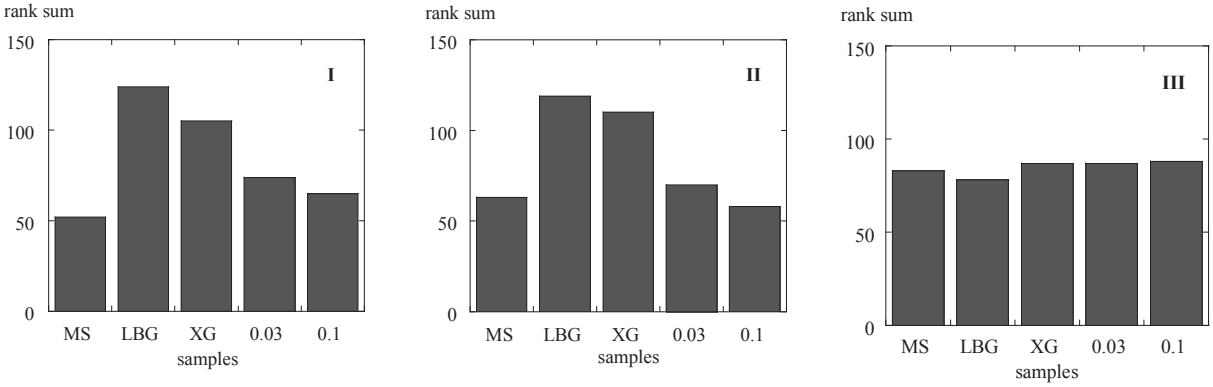

Figure 5. Sensory characteristics. Rank sum values for. **I**: visual consistency, **II**: oral consistency, **III**: creaminess

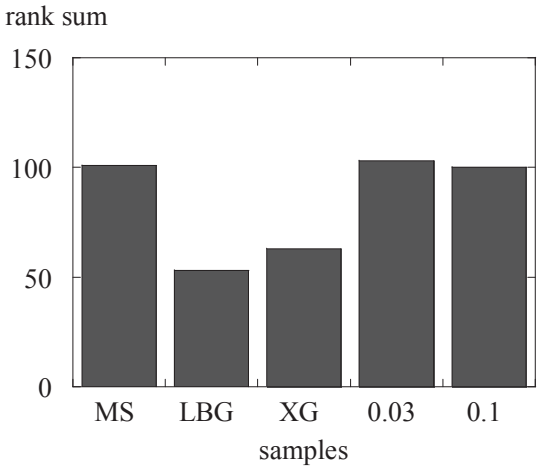

Figure 6. Rank sum values for vinegar taste intensity

4. CONCLUSIONS

Significant differences in sensory consistency were detected. Samples with xanthan or locust bean gum added were perceived significantly as more consistent and as with less vinegar taste intensity than the rest of the samples. No significant differences in creaminess were found. Good relationships were observed between the differences in sensory consistency and both G' and η^* values, measured at 1 Hz.

5. ACKNOWLEGMENTS

This work is part of the project CTIDIA/2002/136. Financial support of Agencia Valencia de Ciència I Tecnologia (Generalitat Valenciana) is gratefully acknowledged.

6. REFERENCES

1. Kiosseoglou, A.; Papalamprou, E.; Makri, E.; Doxastakis, G.; Kiosseoglou, V. (2003). "Functionality of medium molecular weight xanthan gum produced by Xanthomas Campestris ATCC 1395 in batch culture". Food Research International, 36(5), 425-430.

2. Wendin K.; Hall G. (2001). "Influences of fat, thickener and emulsifier contents on salad dressing: Static and dynamic sensory and rheological analyses". Lebensmittel - Wissenschaft + Technologie. Food Science + Technology, 34(4),222-233.

3. Cabeza, C.; Muñoz, J.; Alfaro, M. C.; Flores, V. (2002). "Influence of the addition of gellan gum on the rheology of low calorie mayonnaise stabilised with modified starch". In Progress in Rheology. Theory and Applications, Martínez Boza F. J. et al. eds. GER, Sevilla.

4. Juszczak, L.; Fortuna, T.; Kosla A. (2003). "Sensory and rheological properties of Polish commercial mayonnaise". Nahrung-Food, 47(4),232-235.

5. ISO (1988a). Sensory analysis. Methodology. Ranking. Standard no. 8587. Geneva. Switzerland

6. ISO (1988b). Sensory analysis. General Guidance for the design of test rooms. no. 8589. Geneva. Switzerland

INFLUENCE OF CORRUGATION ANGLE IN THE STIRRED YOGHURT PROCESSING IN PLATE HEAT EXCHANGERS

Carla S. Fernandes [(a)(b)], *Isabel M. Afonso* [(c)(d)], *Luis F. Melo* [(c)] and *João M. Maia* [(a)]*

(a) IPC - Institute for Polymers and Composites, Department of Polymer Engineering, University of Minho, 4800-058 Guimarães, Portugal. Fax: +351-253510339; Phone: +351-253510320
(b) Escola Superior de Tecnologia e de Gestão, Instituto Politécnico de Bragança, Campus de Santa Apolónia, Apartado 1038, 5301-854 Bragança, Portugal. Fax:+351-273325405; Phone:+351-273303127
(c) LEPAE, Departamento de Engenharia Química, Faculdade de Engenharia, Universidade do Porto, Rua Dr. Roberto Frias, s/n 4200-465 Porto, Portugal. Fax: +351-22-5081449; Phone: +351-225081588
(d) Escola Superior Agrária de Ponte de Lima, Instituto Politécnico de Viana do Castelo, Refóios, 4990-706 Ponte de Lima, Portugal. Fax: +351-258909779; Phone: +351-258909740

cveiga@ipb.pt, iafonso@fe.up.pt, lmelo@fe.up.pt, jmaia@dep.uminho.pt

Keywords: plate heat exchangers, corrugation angle, non-isothermal flow, stirred yoghurt.

Abstract

Research on heat transfer of non-Newtonian fluids during thermal processing is very useful for optimise heat exchanger design, as well as to define quality levels of the final product.

In the present study non-isothermal, non-Newtonian flow in plate heat exchangers were simulated numerically, in order to evaluate the influence of corrugation angles on the thermal and hydrodynamics characteristics of yoghurt cooling in a plate heat exchanger. Simulations were carried out using the commercial finite element method package POLYFLOW, being the geometrical domain the representation of a single 3D channel of the plate heat exchanger.

Two corrugation angles were considered, 30º and 60º, being the obtained numerical results for the first one compared with experimental data. A laminar flow was observed for the two cases and the decrease of the angle conducted to a decrease of pressure drop and maximum shear rate.

1. INTRODUCTION

Thermal processing is a usual operation in the food industry. During cooling or heating operations, fluids are submitted to several modifications of their physical properties, which could affect its structure and stability.

Stirred yoghurt is a typical non-Newtonian food fluid, being their rheological properties influenced by several factors related with its physical nature and processing conditions. These aspects have been subject of some previous studies in which the shear-thinning behaviour, partial thixotropic and viscoelastic properties were identified [1, 2, 3, 4, 5, 6].

Plate heat exchangers (PHEs) are commonly used on the processing of foodstuffs. Due to several advantages of this equipment, like their efficiency, ease of cleaning and maintenance, several modelling works have been performed in order to optimise their project and design namely, arrangements and configurations [7, 8, 9], pressure drop and fanning factors [10, 11, 12] and influence of corrugation angle on flow behaviour [13, 14, 15]. However, most of the above studies were performed for Newtonian fluids and, out of those that did not the majority restricted the analysis to isothermal flows. The aim of present work is to overcome some of the shortcomings above and study the influence of corrugation angle on the thermal and

hydrodynamics characteristics of yoghurt processing in PHEs using a non-isothermal and non-Newtonian analysis.

2. PROBLEM DESCRIPTION

Cooling treatment of stirred yoghurt is usually carried out in PHEs since these equipments are suitable for liquid-liquid heat transfer duties that require uniform and rapid cooling or heating. In this operation, two mechanisms of heat transfer occur: conduction, in the plates, and convection inside the channels.
So, in order to simulate the non-isothermal flow of stirred yoghurt in a PHE three problems where solved simultaneously: one of non-isothermal flow inside the channel and two of heat conduction in the plates.
The set of equations that describe mathematically the problem were the Navier-Stokes equations, for incompressible and stationary flow, and Fourier's law for the conduction problems. Additionally, a constitutive model that describes the rheological properties of yoghurt under the cooling conditions has to be established in order to define totally the problem. The used model was proposed by Afonso *et al*. [6] and takes into account the influence of shear rate and temperature:

$$\mu_{app} = K\dot{\gamma}^{n} \exp\left(\frac{E}{RT}\right) \tag{1}$$

where μ_{app} is the apparent viscosity (Pa s), K the consistency index (Pa s^n), n the flow behaviour index (-), $\dot{\gamma}$ the shear rate (s^{-1}), E the activation energy (J mol^{-1}), T the absolute temperature (K) and R the universal gas constant (8.31451 J K^{-1} mol^{-1}). In above equation, rheological parameters assume the values n = 0.42, K = 3.65 Pa $s^{0.42}$ and E = 94785 J mol^{-1} [6].

3. NUMERICAL SIMULATION

The problem described above was simulated using the commercial finite element method package POLYFLOW. Numerical simulations were divided in three steps: construction of geometrical domain and mesh generation, establishment of boundary conditions and properties of the system and numerical resolution of the finite element problem.
Simulations were performed for PHEs with distinct corrugation angles: β = 30º and β = 60º. For the two exchangers, six flow rates of yoghurt are considered in the simulations, according to the operation conditions and fluids properties from Afonso *et al*. [6].

3.1 Geometrical domain and mesh generation

The studied PHE had a parallel arrangement [6] and admitting a uniform distribution of the total flow rate in the various channels, the flow simulations of yoghurt were carried out in a single channel. The plates were constructed considering an effective length, L, and width, w, represented in Fig. 1(a) [16], being the corrugations described by a sine curve [15]:

$$y(x) = \frac{b}{2}\sin\left(\frac{2\pi}{p_c}\left(x - \frac{p_c}{4}\right)\right) + \frac{b}{2} \tag{2}$$

where b is the distance between plates (m) and p_c the wavelength of corrugation (m) Fig. 1(b).

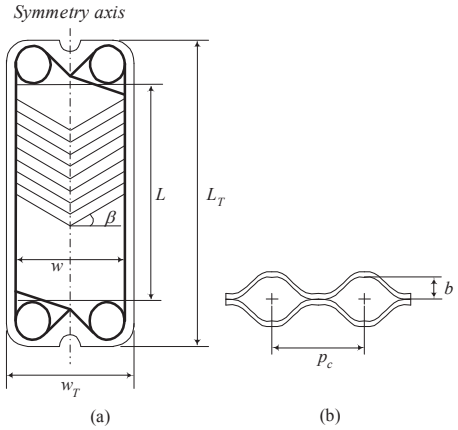

Fig. 1: (a) Schematic representation of a *chevron* plate; (b) Corrugations dimensions.

Additionally, uniform flow was considered inside each channel and, for this reason, a symmetry axis was established, Fig. 1(a), simplifying the geometrical domain to half of a channel, Fig. 2.

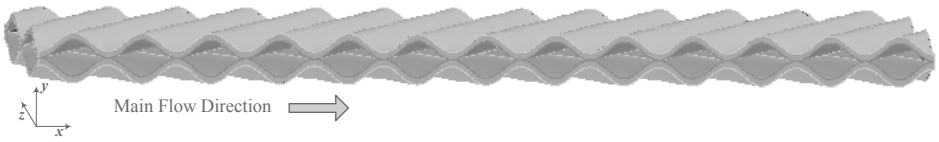

Fig. 2: Geometrical domain.

Although computational domain was highly complex due to the multiple contractions and expansions along the channel, it was found that a mesh constituted by tetrahedral, hexahedral, prismatic and pyramidal elements was adequate. The calculations on present work were made using a mesh with 1.2 mm of node distance, being this value the result of a previous grid independency test.

3.2 Boundary conditions

Boundary conditions were established based on experimental data [6] namely, flow rate and inlet temperature of yoghurt, taking into account that the PHE studied in this work operates with parallel arrangement and in counterflow.
In all the simulations slip at the wall and heat losses to the surroundings were assumed to be non-existent and a variable heat flux have been imposed in the plates. The heat flux for each x is given by the linear form of the expression:

$$q(x) = UF\left(T_{yog_{in}} - T_{wat_{out}}\right)\exp\left[2ULF\phi x\left(\frac{1}{M_{wat}C_{p\,wat}} - \frac{1}{M_{yog}C_{p\,yog}}\right)\right] \tag{3}$$

where x is the dimension on the main flow direction ($0 \le x \le L$) (m), U is the overall heat transfer coefficient (W m^{-2} K^{-1}), F the correction factor(-), M the mass flow rates per channel (kg s^{-1}), C_p the specific heat (J kg^{-1} K^{-1}) and ϕ the area enlargement factor (-) [16].

4. RESULTS AND DISCUSSION

Numerical results concerning the difference between inlet and outlet yoghurt temperature obtained for the PHE with β = 30º were compared with experimental data [6] and a mean deviation of 6.9% was observed.

Analysing the velocity field for the two corrugation angles, Fig. 3, it was possible to observe the inexistence of recirculation zones, confirming this way a laminar flow in the present operation conditions.

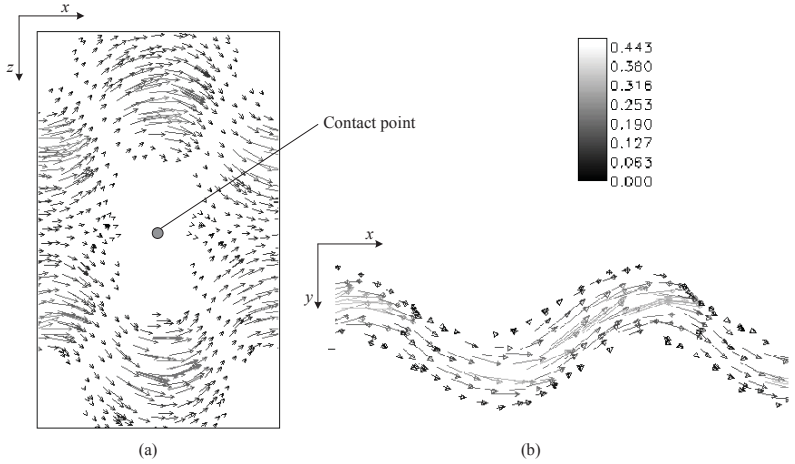

Fig. 3: Velocity vectors in the plane of contact points (a) and in plane z = 0.022 (b) for β = 30º.

Another way to evaluate the flow regime consists in the determination of fanning friction factor, f. The obtained relation between this factor and Reynolds number, Re, was a typical relation for laminar flows [16]:

$$f = a\,\mathrm{Re}^{-1} \tag{4}$$

where a is a constant and f and Re are given by

$$f = \frac{\Delta P D_e}{2L\rho u^2} \tag{5}$$

$$\mathrm{Re} = \frac{\rho u D_e}{\mu_{app}}. \tag{6}$$

In latest equations, ΔP is the pressure drop (Pa), u the average velocity of yoghurt (m s^{-1}) and D_e is the hydraulic diameter and is given by the quotient between 2b and ϕ.

For the studied PHEs and present operation conditions (0.2 < Re <1.3) it was possible to observe in Fig. 4 the good agreement between the relation expressed by Eq. (4) and the computational fluid dynamic (CFD) calculations. It is also possible to observed the decrease of constant *a* with the corrugation angle, which is in agreement with the literature results [15, 16].

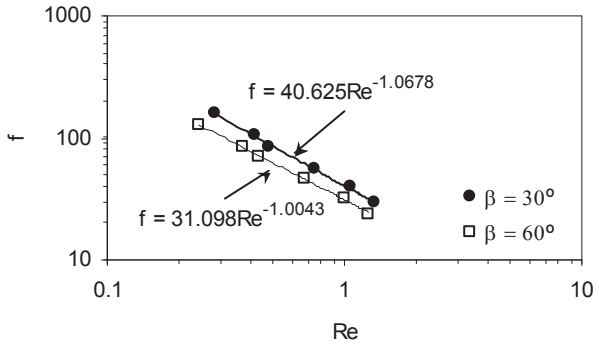

Fig. 4: Fanning friction factor for PHEs with β = 30º and β = 60º.

The magnitude of the shear rate inside the heat exchanger is determinant on the consistency of packed yoghurt. In Fig.5 it's possible to observe that maximum shear rate, $\dot{\gamma}_{max}$, decrease when β increase from 30º to 60º. Infinite parallel plates, correspondent to β = 90º, is the lower limit for $\dot{\gamma}_{max}$.

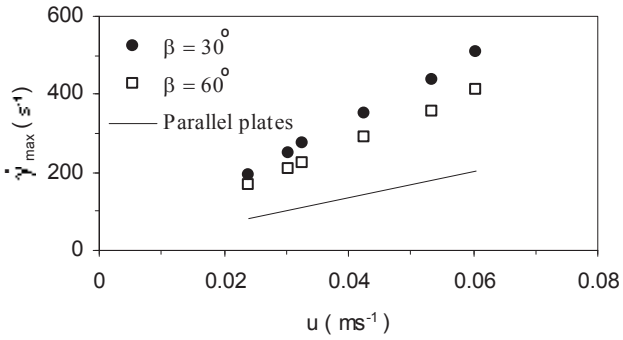

Fig. 5: Maximum shear rate for PHEs with β = 30º and β = 60º and infinite parallel plates.

The values of $\dot{\gamma}_{max}$ presented in Fig.5 for infinite parallel plates were calculated according the expression proposed by Delplace and Leuliet [17] for a generic duct.

5. CONCLUSIONS

In the present study, CFD calculations were made in order to study the influence of corrugation angle in the stirred yoghurt cooling in a PHE. Two corrugation angles were considered, 30º and 60º. It was observed a good agreement between numerical results, for β = 30º, and temperature experimental data.

Analysing velocity fields and fanning friction factors was concluded that flow is laminar for both PHEs in the present operation conditions. Higher flow rates of stirred yoghurt can be processed in a PHE with β = 60º, having in mind pressure losses and maximum shear rates.

References

[1] Benezech, T., & Maingonnat, J. F. (1993). Flow properties of stirred yoghurt: structural parameter approach in describing time dependency. *Journal of Textures Studies*, 24, 455-473.

[2] Rönnegård, E., & Dejmek, P. (1993). Development of breakdown of structure in yoghurt studied by oscillatory rheological measurements. *Le Lait*, 73, 371-379.

[3] Rohm, H., & Kovac, A. (1994). Effects of starter cultures on linear viscoelastic and physical properties of yoghurt gels. *Journal of Structure Studies*, 25, 311-329.

[4] Rohm, H., & Kovac, A. (1995). Effects of starter cultures on small deformation rheology of stirred yoghurt. *Lebensmittel-Wissens chaft und-Technologie-Food Science and Technology*, 28, 319-322.

[5] Afonso, I. M., & Maia, J. M. (1999). Rheological monitoring of structure evolution and development in stirred yoghurt. *Journal of Food Engineering*, 42, 183-190.

[6] Afonso, I. M., Hes, L., Maia, J. M., & Melo, L. F. (2003). Heat transfer and rheology of stirred yoghurt during cooling in plate heat exchangers. *Journal of Food Engineering*, 57, 179-187.

[7] Bassiouny, M. K., & Martin, H. (1984). Flow distribution and pressure drop in plate heat exchangers – I. *Chemical Engineering Science*, 39 (4), 693-700.

[8] Gut, J. A. W., & Pinto, J. M. (2003). Modeling of plate heat exchangers with generalized configurations. *International Journal of Heat and Mass Transfer*, 46, 2571-2585.

[9] Gut, J. A. W., & Pinto, J. M. (2003). Selecting optimal configurations for multisection plate heat exchangers in pasteurization processes. *Ind. Eng. Chem. Res.*, 42, 6112-6124.

[10] Leuliet, J. C., Maigonnat, J. F., & Lalande, M. (1987). Etude de la perte de charge dans de échangeurs de chaleur à plaques traitant des produits non-newtoniens. *Revue Générale de Thermique*, 308-309, 445-450.

[11] Leuliet, J. C., Maigonnat, J. F., & Lalande, M. (1990). Écoulement et transferts de chaleur dans les échangeurs à plaques traitant des produits visqueux newtoniens et pseudoplastiques. *The Canadian Journal of Chemical Engineering*, 68, 220-229.

[12] Antonini, G., François, O., & Shuai, X. S. (1987). Corrélations transfert/facteur de frottement por le chauffage/refroidissement d'un fluide visqueux à forte dépendance thermorhéologique en écoulement de conduite en régime laminaire. *Revue Générale de Thermique*, 308-309, 427-431.

[13] Stasiek, J., Collins, M. W., Ciofalo, M., & Chew, P. E. (1996). Investigation of flow and heat transfer in corrugated passages – I. Experimental results. *International Journal of Heat and Mass Transfer*, 39, 149-164.

[14] Ciofalo, M., Stasiek, J., & Collins, M. W. (1996). Investigation of flow and heat transfer in corrugated passages – II. Numerical simulation. *International Journal of Heat and Mass Transfer*, 39, 165-192.

[15] Mehrabian, M. A., & Poulter, R. (2000). Hydrodynamics and thermal characteristics of corrugated channels: computacional approach. *Applied Mathematical Modelling*, 24, 343-364.

[16] Kakaç, S., & Liu, H. (2002). *Heat exchangers selection, rating, and thermal design* (2nd, ed., pp. 131-136, 373-412). CRC Press, Boca Raton.

[17] Delplace, F., & Leuliet, J. C. (1995). Generalized Reynolds number for the flow of power law fluids in cylindrical ducts of arbitrary cross-section. *The Chemical Engineering Journal*, 56, 33-37.

6. GREASES & BITUMINOUS MIXTURES

BITUMEN MODIFICATION BY WASTE POLYMERS

M. García-Morales, P. Partal, F. J.Navarro, F. J.Martínez-Boza and C. Gallegos*

Departamento de Ingeniería Química, Universidad de Huelva, Facultad de Ciencias Experimentales, Campus de 'El Carmen', 21071, Huelva (Spain)

* Phone: +34 959 01 99 85, FAX: +34 959 01 99 83, e-mail: moises.garcia@diq.uhu.es

Keywords: modified bitumen, recycled polymer, flow behaviour, linear viscoelasticity, capillary rheometry.

ABSTRACT

This paper describes linear viscoelasticity, at low and intermediate temperatures, and the flow behaviour, at high temperatures, of polymer modified bitumen (PMB) containing 5 and 9 wt.% recycled EVA/LDPE. The relationship between flow behaviour and microstructure of the modified bitumen was also considered, by comparison of experiments carried out in capillary and rotational rheometers and photomicrographs taken using a microscopy system whilst the sample was being sheared. Rheological tests, differential scanning calorimetry (DSC) and microscopy showed that the bitumen performance was improved by adding the recycled polymer. The experimental results also show that pure bitumen has shear-thinning characteristics. The blending of polymer into the bitumen modifies the melt processing characteristics of the blend, whilst the viscoelastic properties of the semi-solid composite are enhanced.

1. INTRODUCTION

Bitumen has been mostly used in road building, as well as a waterproofing material [1]. It is generally assumed that bitumen, produced from crude oil distillation processing, is a colloidal system in which the asphaltenes are dispersed into an oily matrix of the remaining components, the maltenes [2].

Extreme in-service temperatures as well as high traffic loadings may cause significant problems in bituminous pavements and roads, among which, deformation at high temperature (rutting), thermal cracking at low temperature, load-associated fatigue cracking and ageing are the most common [3].

Bitumen modification by polymer addition usually improves the mechanical properties of the composite. Polyolefins such as polyethylene (HDPE, LLDPE or LDPE) and copolymers, such as SBS and EVA have been commonly employed [4,5].

From an environmental and economical point of view, the addition of waste plastics to the road bitumen is a good way of achieving waste disposal, also taking into account that the cost is an important aspect when selecting a polymer as a modifying agent [1,6].

Traditional methods did not accurately predict the full bitumen performance. The appearance of the Strategic Highway Research Program (SHRP) protocol favoured the use of the dynamic shear rheometry (DSR) to characterise the mechanical behaviour of polymer modified bitumen [6]. Viscoelasticity measurements provide useful information about the resistance of bitumen to traffic loading (rutting and fatigue cracking) in the high in-service temperature region, as well as at low temperature where thermal cracking is likely to happen. In addition, viscous measurements, at higher temperatures, provide information about the processing properties of the bitumen where it is handled and mixed with mineral aggregates, and finally applied on the road.

In this paper the use of a blend of recycled ethylene-vinyl acetate copolymer and low-density polyethylene as a modifying agent for the bituminous binder employed in the

construction of road pavements is examined. Different rheological measurements, linear viscoelasticity and viscous flow tests, were carried out on neat and modified bitumen over both application and processing temperature ranges.

2. EXPERIMENTAL

Bitumen of penetration grade 60/70, provided by Construcciones Morales S.A. (Spain), was used as a base material for polymer modification. Waste plastic (EVA/LDPE) from agriculture, provided by Egmasa (Spain) was used as the modifying agent. Asphaltene content and penetration grade of the base bitumen, as well as some physico-chemical characteristics of the polymer are shown in Table 1.

Bitumen	
Asphaltene content (wt.%)	20.00
Penetration grade (1/10 mm)	60-70
Recycled polymer	
EVA/LDPE	2/1
vinyl acetate (wt.%)	5
Black carbon (wt.%)	1

Table 1. Physico-chemical characteristics of the bitumen and recycled polymer used.

Blends of bitumen and polymer, at 5 and 9 wt. % polymer concentrations, were prepared in an open mixer, using an IKA RW-20 stirring device (Germany). Samples were processed for 6 hours, at 180ºC, and at a rotating speed of 1200 rpm. The modified bitumen was compared with neat bitumen and bitumen processed under the above described conditions, which will be named as 'processed bitumen' hereafter.

The rheological characterisation of the bitumens was carried out using four different rheometers, namely, a controlled-strain Rheometrics Scientific ARES rheometer (USA), two controlled-stress Haake RS150 and RS100 rheometers (Germany) and the Cambridge MultiPass rheometer (MPR) [7].

Steady state flow curves at different temperatures and temperature sweeps (1ºC·min^{-1}) at constant shear rate (1 s^{-1}) were carried out with the RS100 rheometer, using a plate-and-plate geometry (20-35 mm diameter, 1-2 mm gap). Frequency sweeps, at different temperatures, within the linear viscoelasticity region were performed with the RS150 rheometer, using serrated plate-and-plate geometries (10-20 mm diameter, 1-2 mm gap). Steady state flow curves at different temperatures and temperature sweeps (1ºC·min^{-1}) in oscillatory mode (1 rad·s^{-1} and 1% strain) were accomplished with the ARES rheometer, using a Couette geometry, having the inner and outer cylinders 32 and 34 mm diameter respectively, and a plate-and-plate geometry (25-50 mm diameter, 1-2 mm gap). The Cambridge MultiPass rheometer was used to perform steady shear experiments at different temperatures, using a 2 mm diameter and 40 mm length capillary, and two packed beds with spheres of different diameters (1-2 mm).

DSC measurements were carried out with a TA Instruments Q100 (USA), using 10-20 mg of sample in hermetic aluminium pans, and a heating rate of 10 ºC·min^{-1}. The sample was purged with nitrogen at a flow rate of 50 cm^3·min^{-1}.

Optical microscopy was used to study the morphology of the modified bitumen. A Cambridge Shear System 450, manufactured by Linkam Scientific Instruments (UK), coupled to a standard Olympus BH2 microscope was employed with that purpose, which allowed observation of the sample under shear at different temperatures.

3. RESULTS AND DISCUSSION

3.1. Linear viscoelasticity and flow behaviour

Figure 1 shows oscillatory shear curves for neat and modified bitumen at -10 and 50 ºC. Polymer modification gives rise to a significant increase in the viscoelastic functions, mainly at 50 ºC, temperature at which the curves of the linear viscoelasticity functions for modified bitumen show important differences in relation to those for neat and processed bitumen, particularly in the low frequency region. The viscous modulus shows higher values than the elastic modulus in the whole range of frequency, at 50 ºC, for 5 wt. % modified bitumen, neat and processed bitumen. The 9 wt. % modified bitumen exhibits a quite different behaviour. Thus, G' and G'' values are very similar within the frequency range studied and both curves present the same slope, 0.5 ± 0.001, showing a typical behaviour of a critical gel [8].

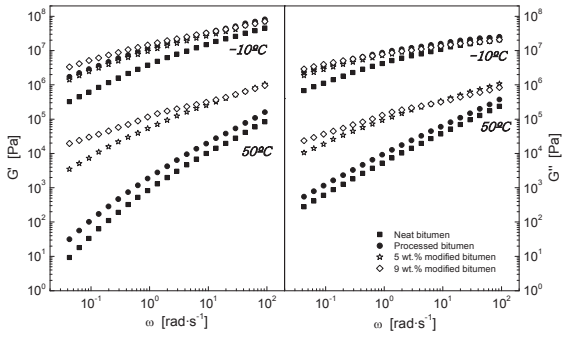

Figure 1. Evolution of the linear viscoelasticity functions with frequency, at -10 and 50ºC, for neat, processed and polymer modified bitumen (5 and 9 wt. %).

At low temperature, the addition of polymer to the bitumen does not produce a significant change in the viscoelastic functions in relation to the processed bitumen, although modified bitumens show a decrease in the slope of G' and the glassy region of the mechanical spectrum of these materials shifts to higher frequencies [9]. In addition, the difference between the neat and processed bitumen curves increase at -10 ºC, which proves that oxidation undergone by processing appears more significantly at low temperatures.

On the other hand, polymer modification makes the viscoelastic functions increase at intermediate in-service temperature, with the consequent benefit for the bitumen, improving 'rutting' resistance.

The flow behaviour of neat and modified bitumen at higher processing temperatures is shown in Figures 2 and 3, for a wide range of shear rates, by combining rotational and capillary rheometry [10].

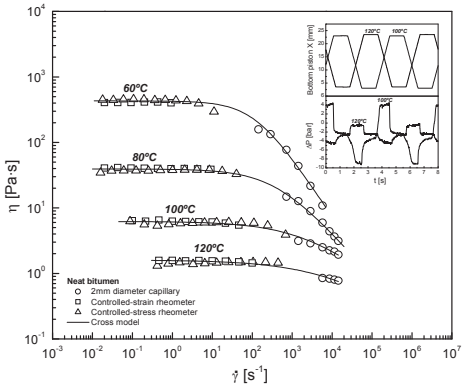

Figure 2. Flow curves of neat bitumen, at different temperatures.

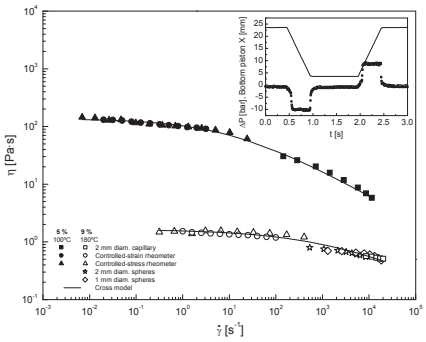

Figure 3. Flow curves of 5 and 9 wt. % polymer modified bitumen, at 100 and 180ºC respectively.

	Neat bitumen				Modified	
	60ºC	**80ºC**	**100ºC**	**120ºC**	**5wt.%**	**9wt.%**
η_0 [Pa·s]	430.26	39.29	6.22	1.60	136.66	1.65
λ [s]	$8.13 \cdot 10^{-3}$	$2.31 \cdot 10^{-3}$	$3.60 \cdot 10^{-4}$	$9.23 \cdot 10^{-5}$	$8.54 \cdot 10^{-2}$	$6.10 \cdot 10^{-4}$
p	0.920	0.694	0.500	0.416	0.450	0.370

Table 2. Cross model parameters for neat and modified bitumen at different temperatures.

Flow curves of neat bitumen were obtained, at different temperatures, from 10^{-2} to 10^{4} s^{-1} (Figure 2). The bitumen shows a shear-thinning behaviour, with a region corresponding to a Newtonian viscosity at low shear rate, η_0, and a further drop in viscosity for higher shear rates which became more apparent as the temperature was decreased. The flow behaviour shown by the neat bitumen was represented fairly well by the Cross model:

$$\frac{\eta - \eta_\infty}{\eta_0 - \eta_\infty} = \frac{1}{1 + (\lambda \cdot \dot{\gamma})^p} \tag{1}$$

where η_0 (Newtonian viscosity), λ (characteristic time) and p (related to the slope in the shear-thinning region) increase as temperatures decreases. η_∞ was considered to be zero for the systems studied. Cross parameters for neat bitumen are presented in Table 2.

It can also be seen that Newtonian viscosity values get closer as the temperature increases.

The overall flow behaviour cannot be found by using standard rotational rheometers with parallel plates alone and capillary rheometry, which is able to reach sufficiently high shear rates, should be used with that purpose. In the case of the MPR, two pistons operating in tandem were used to drive the fluid sample through a small capillary insert, and the pressure difference across the capillary measured. Bottom piston positions and differential pressure profiles are included in Figure 2, for the neat bitumen at 100 and 120 ºC at the same pistons conditions. Differential pressure is higher at low temperature as the bitumen has a higher viscosity.

High temperature flow curves for modified bitumen, 5 and 9 wt. %, in a wide range of shear rates, are shown in Figure 3, for selected temperatures. Data sets for the 5 and 9 wt. % modified bitumen were obtained by using a controlled-strain, a controlled-stress and a capillary rheometer. For the second bitumen, additional viscosity tests were performed by changing the 2 mm diameter capillary for two packed beds with steel spheres of two different

diameters (1 and 2 mm). The bitumen at high temperature was made to pass through the packed bed, and the pressure at its both sides was measured by pressure transducers. As can be observed in Figure 3, the values obtained with the packed bed are in good agreement with those obtained by using a 2 mm capillary.

As for the neat bitumen, the flow curves present a Newtonian region at low-medium shear rates, followed by a drop in viscosity as the shear rate increases, and, therefore, the flow behaviour can be represented by the Cross model (1). The parameters η_0, λ and p are shown in Table 2. The effect of polymer addition at high temperature is clearly observed by comparing neat bitumen and 5 wt.% modified bitumen at 100ºC. Thus, table 2 shows that the addition of 5 wt.% EVA/LDPE increases η_0 one order of magnitude. Furthermore, higher values of λ are obtained and, as a consequence, the material becomes more structured by the polymer addition.

Flow curves of neat, processed and modified bitumen, at 135 ºC, are compared in Figure 4. Viscosity should be kept low enough at higher handling temperatures of bitumen [11] (laydown and compaction temperatures) in order to allow an easy application on the pavement. AASHTO MP1 [12] requires that the viscosity at 135 ºC should be less that 3 Pa·s. As can be seen in Figure 4, a 5 wt. % modified bitumen stands below the above-mentioned limit and, thus, it may be properly applied in pavement building. Blends at 9 wt. % exceed 3 Pa·s and thus, the pumping operations performed during the binder application on the road might result quite difficult, though might be successfully employed in the manufacture of roofing membranes.

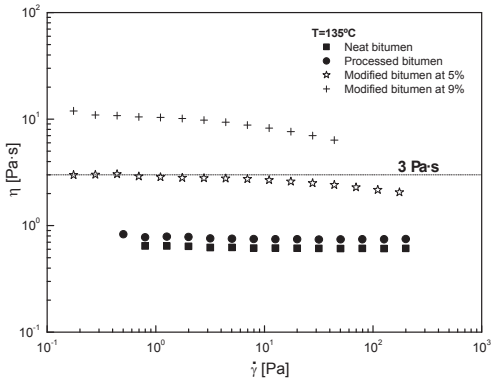

Figure 4. Flow curves, at 135ºC, of neat, processed and polymer modified bitumen (5 and 9 wt. %).

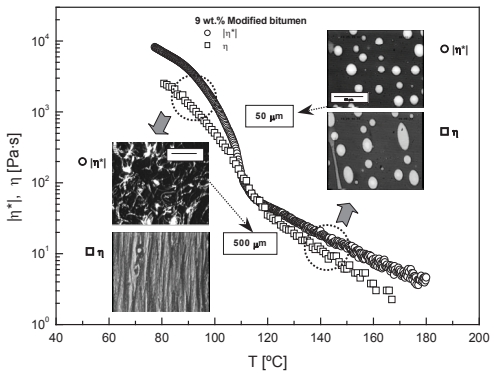

Figure 5. Evolution of viscosity (1 s^{-1}) and complex viscosity (1 rad·s^{-1}) with temperature for 9 wt. % polymer modified bitumen.

3.2. Modified bitumen microstructure under shear.

Figure 5 shows the results obtained during two temperature sweep tests, performed on 9 wt. % polymer modified bitumen, carried out in oscillatory and steady-shear mode at the conditions mentioned in the experimental section. The frequency sweep test shows the behaviour of the modified bitumen at very low strain, that is, as the system stands nearly at rest and no orientation effects take place on the dispersed polymer. Temperature is the only parameter causing a decrease in complex viscosity. In addition a significant drop in viscosity occurs at about 105-110 ºC. In order to explain this fact, standard calorimetry on 9 wt.% was accomplished in a wide range of temperatures. A small peak at about 109 ºC, corresponding to polymer melting, appears.

If a significant shear is applied to the modified bitumen, substantial structural changes are observed in a shear rate sweep experiment. Very long streaks of polymer orientated in the flow direction, which do not recover their original form after shear, appear at the lowest temperatures, close to the melting point of the swollen polymer phase. At higher temperatures and moderate shear, the droplets of polymer, which remained in a spherical shape during the oscillatory mode, tend to slightly deform in the flow direction, adopting ellipsoid shapes which are transformed into spherical droplets after shear stops. As a consequence of the structural changes in polymer droplets, the resistance to the flow diminishes and lower values in viscosity are obtained, at the same temperature, in steady flow. Finally, the striking decrease in complex viscosity observed above 90ºC can be related to the melting process of the swollen polymer phase.

4. CONCLUSIONS

Polymer modification using recycled EVA/LDPE improves the mechanical properties of bitumen in the temperature region where the material is used as a surface coating. In relation to processing, the 5 wt. % modified bitumen has viscosity values, at 135 ºC, that allow easy application on the road. On the contrary, the viscosity of the 9 wt. % modified bitumen is too large for processing at that temperature. Neat bitumen has normally been considered to be a Newtonian fluid at high temperature. However, a drop in viscosity takes place when experiments are performed at very high shear rate, which were obtained by using capillary rheometry. For a modified bitumen, a significant decrease in the complex viscosity with increasing temperature was observed in oscillatory shear and this was related to the melting process of the swollen polymer phase. Such a decrease in viscosity is less evident when steady shear is applied on the sample, because the modified bitumen microstructure is strongly affected by shear.

The addition of recycled EVA/LDPE to bitumen enhances the materials mechanical properties, as well as providing a useful environmental alternative for the disposal of waste plastics.

5. ACKNOWLEDGEMENTS

This work is part of a research project sponsored by a MCYT-FEDER programme, (Research Project MAT2001-0066-C02-02). The authors gratefully acknowledge its financial support.

6. REFERENCES

[1] García-Morales M, Partal P, Navarro FJ, Martínez-Boza FJ, Gallegos C, González N, González O, Muñoz ME (2004) Viscous properties and microstructure of recycled EVA modified bitumen. Fuel 83:31-38.

[2] Pérez-Lepe A, Martínez-Boza FJ, Gallegos C, González O, Muñoz ME, Santamaría A (2003) Influence of the processing conditions on the rheological behaviour of polymer-modified bitumen. Fuel 82:1339-1348.

[3] Becker Y, Müller AJ, Rodríguez Y (2003) Use of rheological compatibility criteria to study SBS modified asphalts. J Appl Polym Sci 90:1772-1782.

[4] Airey GD (2003) Rheological properties of styrene butadiene styrene polymer modified road bitumens. Fuel 82:1709-1719.

[5] Blanco R, Rodríguez R, García-Garduño M, Castaño VM (1996) Rheological properties of styrene-butadiene copolymer-reinforced asphalt. J Appl Polym Sci 61:1493-1501.

[6] García-Morales M, Partal P, Navarro FJ, Martínez-Boza FJ, Gallegos C (2004) Linear viscoelasticity of recycled EVA-modified bitumens. Energy Fuel 18(2):357-364.

[7] Mackley MR, Marshall RTJ, Smeulders JBAF (1995) The multipass rheometer. J Rheol 39:1293-1309.
[8] De Rosa, Winter HH (1994) The effect of entanglements on the rheological behavior of polybutadiene critical gels. Rheol Acta 33:220-237.
[9] Martínez-Boza FJ, Partal P, Conde B, Gallegos, C (2000) Influence of temperature and composition on the linear viscoelastic properties of synthetic binders. Energy Fuel 14:131-137.
[10] Macosko CW (1994) Rheology: principles, measurements and applications. VCH Publishers Inc, New York.
[11] Crockford WW, Makunike D, .Davison RR, Scullin T, Billiter TC (1995) Recycling crumb rubber modified asphalt pavements. Texas Department of Transportation Report 1333-1F, written by the Texas Transportation Institute, Texas A&M University, College Station, Texas.
[12] McGennis RB (1995) Evaluation of physical properties of fine crumb rubber-modified asphalt binders. Transportation Research Record 1488:62-71.

INFLUENCE OF PROCESSING ON THE RHEOLOGY AND MORPHOLOGY OF HDPE-MODIFIED BITUMEN

A. Pérez-Lepe, F. Martínez-Boza, P. Partal, C. Gallegos*

*Telephone No: +34 959 019985
FAX: +34 959 019983
e-mail: antonio.perez@diq.uhu.es

Keywords: bitumen, polyethylene, rheology, morphology, calorimetry.

1. ABSTRACT

Mixing polymers into bitumen has important consequences on the engineering properties of bituminous binders. Addition of HDPE to bitumen enhances the mechanical properties of the binders, especially in the high temperature region, where pavements can suffer from rutting. The mechanical behaviour of the bitumens modified with different proportions of polyethylene has been related to the morphology of these binders. A rheological characterisation was done in order to study the viscoelastic response and flow properties of HDPE-modified binders, as well as a morphological evaluation by means of optical microscopy. The addition of 3% of HDPE to bitumen is able to readily modify the structure of the binder, by forming a gel-type polymer structure dispersed within the bituminous matrix, providing it with enhanced elastic properties. As temperature is raised over the melting temperature of the polymer-rich structured phase (polymer swollen by the light components of the bitumen), the polymer network collapses so as the bitumen governs the rheological behaviour of the binder.

2. INTRODUCTION

It is generally assumed that bitumen is a colloidal system in which the asphaltenes are dispersed into a matrix of the remaining components, the maltenes [1,2]. The correlation between the complex colloidal structure of bitumen and its viscoelastic response is therefore a subject of scientific and technical interest [3].

Polymer-modified bituminous binders are widely used for road paving applications [4]. The purpose of bitumen modification is to achieve desired engineering properties to prevent asphalt from pavement distresses, such as rutting at high temperatures, fatigue strength, crack initiation, and propagation in the low temperature region [5]. Addition of polymers to bitumen is known to impart enhanced service properties, such as improved thermo-mechanical resistance, elasticity and adhesivity [6]. Among the many polymers used to modify bitumen, high density polyethylene is known to exert an important change in the mechanical behaviour of the bitumen [5, 7, 8, 9, 10].

In this work, HDPE-modified binders, prepared in a rotor-stator mixing device, were characterised in order to better understand the interactions between polymer and bitumen. The effect of composition of the binders was studied so as to establish the minimum polymer content able to readily modify the bitumen structure, in order to enhance the viscoelastic response of the bitumen against the above-mentioned pavement defects. A rheological characterisation of the binders, as well as a morphology evaluation, and a calorimetry analysis were made for this purpose.

3. EXPERIMENTAL

The bitumen used in this study is a 60/70 penetration grade bitumen from Cepsa (Spain), with an asphaltene content of 19.34%. The polyethylene is a pelletised high density polyethylene, from Repsol-YPF (Spain), with a density of 0.957 g/cm^3 (ASTM D-792).
The blends of bitumen and polyethylene were prepared under high shear, by using a rotor-stator high shear device, Superdispax SD 41, from IKA (Germany), at 180ºC and a rotation speed of 8200 rpm.
The rheological study was performed using a CS-rheometer, RheoStress RS150 from Haake Gbr. (Germany). Frequency and temperature sweep tests in oscillatory shear and steady-state flow measurements were performed.
Frequency sweep runs were applied over a range from 0.01 to 100 rad/s under isothermal conditions. Temperature sweeps were performed at 0.628 rad/s with a temperature increasing rate of 1 ºC/min. Both, temperature and frequency sweep tests, were performed within the linear viscoelastic range of the materials.
The calorimetry tests were carried out using a DSC Q-100 from TA Instruments Waters (USA). The samples were pressed into aluminium pans and were submitted to the same measurement procedure, in order to prevent the thermal history and measurement parameters influence. A temperature rate of 10ºC/min was selected.
For the morphological characterisation of the binders, optical microscopy was used. Microscopic observations were carried out with an optical microscope from Olympus (Japan).

4. RESULTS AND DISCUSSION

4.1 Rheological characterisation

From a rheological point of view, bitumen should be considered a viscoelastic material, very sensitive to temperature, since it shows a predominant elastic behaviour at low temperature, and viscous characteristics at moderate and high temperatures. The degree of modification exerted by the addition of polyethylene (HDPE), at high temperatures and under high shear rate, was quantified by doing the characterisation of various bituminous binders modified with polyethylene in different proportions. Thus, a 1%, 2%, 3% and a 5% HDPE-modified bitumen were manufactured by using the mixing device and mixing conditions described above.
As can be seen in figure 2, at high temperatures (75ºC), different mechanical characteristics are obtained for the binders containing different proportions of polyethylene. At 75ºC, binders soften sufficiently, and hence, polymer relaxation processes are the main contribution to the bulk rheological behaviour of the complex mixture [10]. The storage and loss moduli values for the binder containing 1% of HDPE show a behaviour close to the terminal region of the materials, in the low frequency range. The binder with 2% of HDPE shows a slight elastic enhancement at low frequency. On the contrary, the 3% HDPE-modified bitumen shows a tendency to a plateau region at low frequencies. The binder containing a 5% of HDPE shows a well-developed plateau region, with values of the storage modulus higher than the loss modulus, in all the range of frequencies studied.

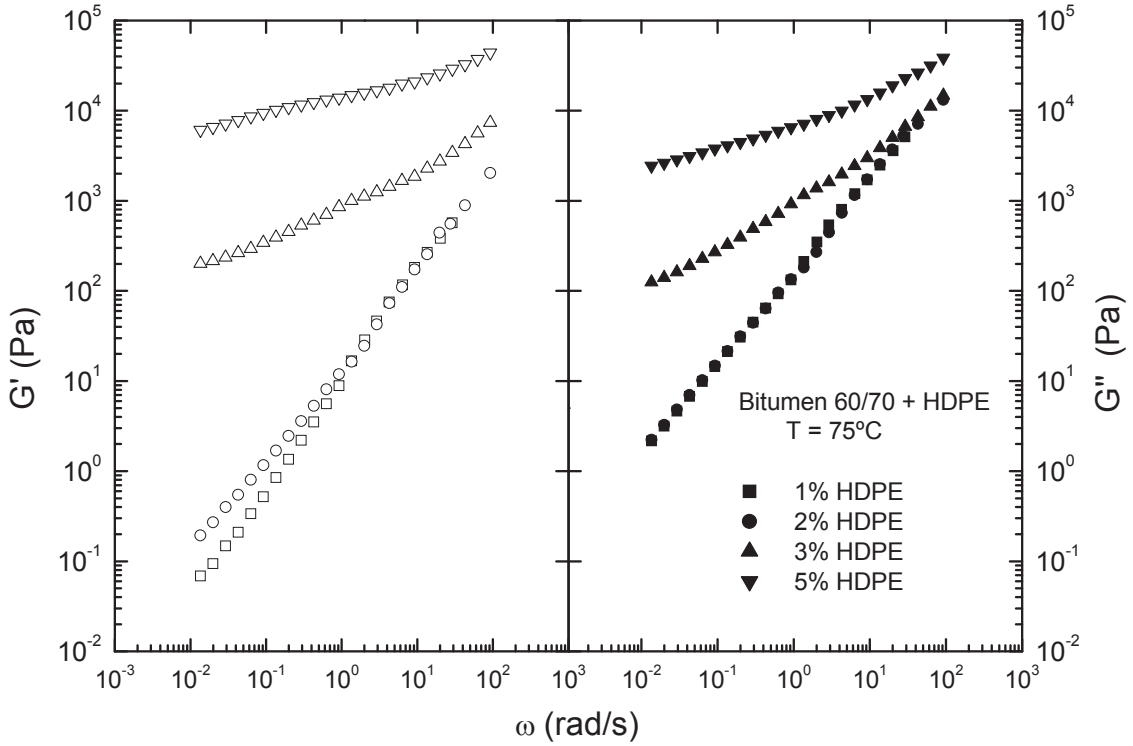

Figure 1. Evolution of the storage and loss moduli with frequency, at 75ºC, for bitumens modified with 1%, 2%, 3% and 5% of HDPE.

The modification of the bitumen with 1% and 2% of HDPE, would yield a dispersed polymer phase. On the other hand, 3% and 5% of HDPE would form a somewhat structured polymer phase, where significant interactions may contribute to an enhancement of the binder elasticity.

The effect of composition on the linear viscoelastic response of the binders can be observed in figure 2, where the variation of the phase angle with the complex modulus of the material is represented for all the binders. For the binder containing a 1% of HDPE (A), a tendency to a pure viscous behaviour appears at high temperatures, with values of the phase angle close to 90º. At low temperatures, a tendency towards the glassy modulus, with values of the complex modulus close to 10^9 Pa, can be observed for all the binders. For the binder containing 2 % of HDPE (B), values of delta close to 85º are found at high temperatures, rendering a slight enhancement of the elastic properties of the binder. For the binders containing 1% and 2% of HDPE, a continuity of the curves at different temperatures is observed. Nevertheless, for the binders containing 3% and 5% of HDPE, a tendency towards a viscous behaviour at high temperatures does not appear. An important change in the mechanical behaviour of the binders is observed at high temperatures. At 75ºC, values of the phase angle as low as 20º are observed for the binder containing 5% of HDPE. Thus, the addition of 3% and 5% of HDPE to bitumen yield an enhancement in the mechanical characteristics of the binders, providing them with resistance to permanent deformation at high temperatures.

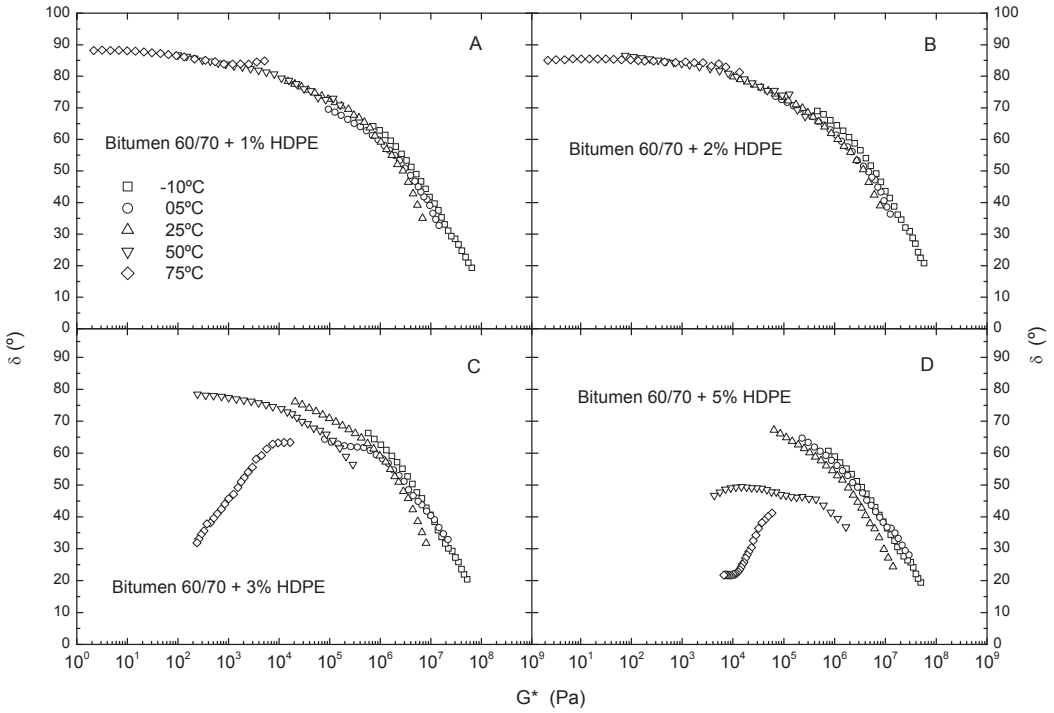

Figure 2. Variation of the phase angle versus the complex modulus, at different temperatures, for bitumens modified with 1% (A), 2% (B), 3% (C) and 5% (D) of HDPE.

4.2 Morphological characterisation

An optical characterisation was carried out in order to better understand the morphology of the bituminous binders modified with polyethylene. Microscopic observations of the bituminous binders modified with 1%, 2%, 3% and 5% of HDPE are displayed in figure 4. In the case of addition of 1% of HDPE, independent polymer inclusions, with an average radius of 40 μm and a volume fraction, as obtained by an image analysis software, of 0.10, are dispersed within the bituminous matrix. The addition of 1% of HDPE does not yield an important change in the structure of the binder. For the 2% HDPE-modified binder, non-spherical independent polymer inclusions are found, although small dispersed polymer associations, yielding some kind of weak polymer structure within the bitumen matrix, are also obtained. In the case of modification with 3% of HDPE, interconnected polymer inclusions, including bitumen phase within, are observed. This morphology would give as a result a somewhat structured material, due to the interconnection of the dispersed phase. In the 5% HDPE-modified binder, the polymer phase forms an interconnected three dimensional sponge-like structure, yielding a gel-type structure, which would remain stable with temperature, until the polymer-rich phase melting temperature is attained.

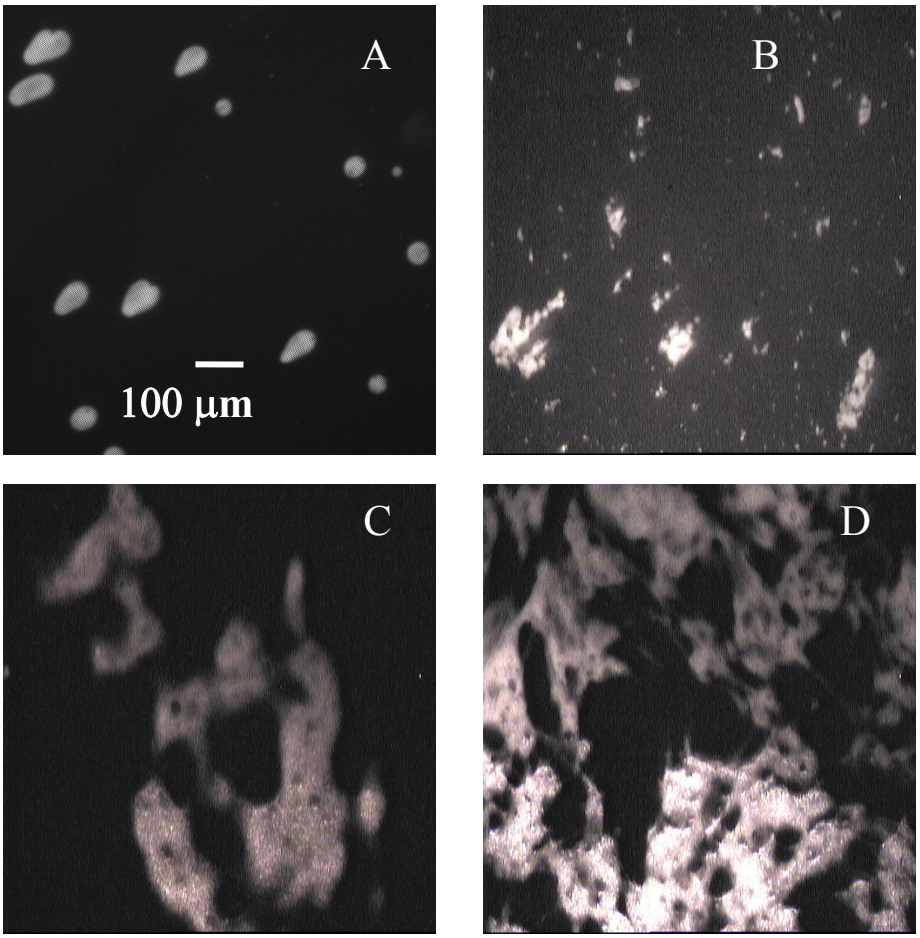

Figure 4. Microscopical observations of bitumens modified with 1% (A), 2% (B), 3% (C) and 5% (D) of HDPE.

5. REFERENCES

1 Lesueur D, Gerard J, Claudy P, Letoffe J. A structure-related model to describe asphalt linear viscoelasticity. J Rheol 40:813-836 1996.

2 Stastna J, Zanzotto L, Ho K. Fractional complex modulus manifested in asphalts. Rheol Acta 33:344-354 1994.

3 González O, Peña JJ, Muñoz ME, Santamaría A, Pérez-Lepe A, Martínez-Boza F, Gallegos C. Rheological techniques as a tool to analyze polymer-bitumen interactions:bitumen modified with polyethylene and polyethylene-based blends. Energy and Fuels, 16:1256-1263 2002

4 Whiteoak D. Shell Bitumen Handbook. Shell Bitumen UK, Riversdell Hause, Surrey 1990.

5 Ait-Kadi A, Brahimi H, Bousmina M. Polymer Blends for Enhanced Asphalt Binders. Polym Eng Sci 36:1724-1733 1996.

6 Collins JH, Bouldin MG, Gelles R, Berker A. Improved performance of paving asphalt by polymer modification. Proc Assoc of Asphalt Paving Technol 60:43-79 1991.

7 Pérez-Lepe A, Martínez-Boza F, Gallegos C, González O, Peña JJ, Muñoz ME, Santamaría A. Influence of the processing conditions on the rheological behaviour of polymer-modified bitumen. Fuel

8 Fawcett, AH, McNally T, McNally GM, Andrews F, Clarke J. Polymer, 40:6337-6349 1999

9 Newman JK. J. Elastom.Plast. 30:245-263 1998

10 Lu X and Isacsson U. Rheological characterisation of Styrene-Butadiene-Styrene copolymer modified bitumens. Const. Buil. Mat. 11: 23-32 1997.

PUMPING FLOW OF LUBRICATING GREASES

M.A. Delgado, J.M. Franco, P. Partal, C. Gallegos

Departamento de Ingeniería Química. Facultad de Ciencias Experimentales.
Universidad de Huelva. Campus Universitario del Carmen, 21071, Huelva. Spain.
Tel: +34959019985 , Fax: +34959019983 , e-mail: miguel.delgado@diq.uhu.es

Keywords: Laminar Flow, Lubricating Greases, Multiphase Flow, Non-Newtonian Fluids, Rheology.

ABSTRACT

Prediction of pressure drop gradient and evaluation of wall slip and air bubbles entrainment effects observed during the piping flow of lubricating greases were investigated. With this aim, viscous flow tests in rotational rheometers and pressure drop measurements in pipelines were carried out using different geometries with both smooth and rough surfaces. The Power-law, Herschel-Bulkley and Sisko models were applied in the experimental range of flow rates for predicting pressure drop gradient. Air entrainment occurring when the pumping system was primed. This air entrainment effect can be corrected using a modified expression to evaluate the drag ratio defined for non-Newtonian liquid/air intermittent flows. Eliminating this effect, the classical definition of the friction factor for a non-Newtonian fluid, f=16/Re', can be applied to predict the pressure drop gradient.

INTRODUCTION

Lubricating greases are generally highly structured suspensions consisting of a thickener, usually a metal soap, dispersed in mineral or synthetic oil [1,2]. The thickener is added to prevent loss of lubricant under operating conditions but, evidently, this implies a considerably resistance to the flow of these materials. Thus, a correct prediction of pressure drop is a prerequisite for optimum design of pumping systems and minimizing the power consumption. During decades, the method proposed by Rein & McGahey [3] to estimate the pressure drop during the piping flow of lubricating greases has been followed in the industry. Cho et al. [4] proposed a calculation procedure based on the extension that Metzner & Reed [5] made on the Rabinowitsch-Mooney equation to estimate the pressure drop of lubricating grease flow in a large pipe using a shear rate at the wall corrected by using the power-law model. However, neither the correction of possible wall slip nor the air bubbles entrainment effects, when the pumping system is primed, on the prediction of the pressure drop were considered in these studies.

The overall objective of this work has been to evaluate the wall slip and air bubbles entrainment effects observed during the piping flow of greases, which allows to correctly predict the pressure drop through pipelines. With this aim, experimental investigations on the pressure drop in horizontal pipelines and rotational rheometry were carried out by using smooth and grooved surfaces and different gaps or diameters. Several empirical non-Newtonian models which are able to describe the flow behaviour of greases were applied.

EXPERIMENTAL

A commercial lithium complex soap grease, kindly supplied by Verkol S.A. (Navarra, Spain), classified as NLGI grade No. 2, was tested. This grease presents a density of 914 kg/m^3 at 20 ºC and a marked shear-thinning behaviour with apparent viscosities ranging from 6×10^4 Pa·s at 0,01 s^{-1} to 3 Pa·s at 1000 s^{-1} at 25 ºC.

A pumping system was designed and constructed to allow investigations of the piping flow behaviour of this commercial grease. The grease from the hopper tank was continuously pumped through stainless steel tubes by a progressive cavity pump equipped with a force feed screw, model MV2.6IVA10 (PCM Moineau, France) having a maximum capacity of 0,190 m^3/h and maximum discharge pressure of 10 bar. Four horizontal stainless steal tubes of different diameters were used, (see Table 1). Stainless steel meshes fixed to the internal wall of the pipeline were used to modify the roughness. The pressure drop across the pipeline test section was measured by using Bourdon-type manometers. The piping flow experiments were carried at room temperature (22±2ºC).

Table 1.-Dimensions of the pipeline test sections.

Pipe	Internal Diameter (D) (mm)	Relative Roughness	L/D	Entrance Length (mm)	Exit Length (mm)
½-S	17.12	0.0029 ≈ 0	60	1773	200
½-R	15.84	0.036	60	1773	200
¾-S	22.45	0.0022 ≈ 0	60	1453	200
¾-R	20.85	0.037	60	1453	200
1-S	27.86	0.0018 ≈ 0	60	1128	200
1-R	25.46	0.043	60	1128	200
1 ¼-S	36.62	0.0014 ≈ 0	60	603	200
1 ¼-R	34.22	0.033	60	603	200

Viscous flow measurements were carried out using controlled-shear rate and controlled-stress rheometers, which complement each other. Controlled-stress measurements were performed in both a Bohlin CS rheometer (Bohlin, Sweden), in a range of shear stress of 4-1400 Pa, using a plate-plate geometry (25 mm diameter, 1 mm gap) and cone-plate (35 mm diameter, 1º, 0.052 mm gap. These measurements were supplemented with those performed in a RV20-CV20N controlled-shear rate rheometer (Haake, Germany), in a range of shear rate of 10-3000 s^{-1}, using a coaxial cylinder geometry (15 mm external diameter, 12 mm length, 0.545 mm gap). Different plate-plate geometries with both smooth and rough surfaces (roughness: 0,4 mm) were used. All measurements were done at 22 ºC.

RESULTS AND DISCUSSION

Rheological measurements

Figure 1 shows the viscous flow curves obtained in rotational rheometers using different geometries, gaps and surfaces (smooth and rough) in a relatively wide range of shear stress. As can be noticed, a marked influence of the roughness of the tool used and gap effect when using different geometries exist; these effects were widely accepted as experimental evidence of wall slip phenomena [6]. On the other hand, as expected, the gap width does not exert any significant influence on the flow measurements when rough surfaces were used which is indicative of the absence of wall slip.

In all cases, a shear thinning behaviour with a slight tendency to a high shear rate limiting viscosity, η_∞, can be observed in all cases. Table 3 lists three models that can be used to adjust fairly well the flow behaviour observed in the experimental shear rate range observed in the piping flow tests (R^2>0,99). Table 2 shows the values of the parameters obtained from the fitting of the experimental curves, measured in plate-plate geometries with 1 mm gap, to these models, which have been applied for the calculation of both pressure drop gradient and Reynolds number.

Table 2.- Values of the Ostwald-de Waele, Sisko and Herschel-Bulkley parameters obtained using both smooth and rough plate-plate 1mm gap in the same experimental range of shear rate than obtained in the piping flow measurements.

Flow parameters obtained with smooth surfaces						
	n	**k (Pa·s^n)**	**m (Pa·s^n)**	**η_∞ (Pa·s)**	**k_H (Pa·s^n)**	**τ_0 (Pa)**
Ostwald-de Waele	0,137	610,2	-	-	-	-
Sisko	0,125	-	625,0	0,89	-	-
Herschel-Bulkley	0,146	-	-	-	495,0	124,8
Flow curves obtained with rough surfaces						
	n	**k (Pa·s^n)**	**m (Pa·s^n)**	**η_∞ (Pa·s)**	**k_H (Pa·s^n)**	**τ_0 (Pa)**
Ostwald-de Waele	0,108	880,8	-	-	-	-
Sisko	0,098	-	842,0	2,54	-	-
Herschel-Bulkley	0,138	-	-	-	635,9	228,0

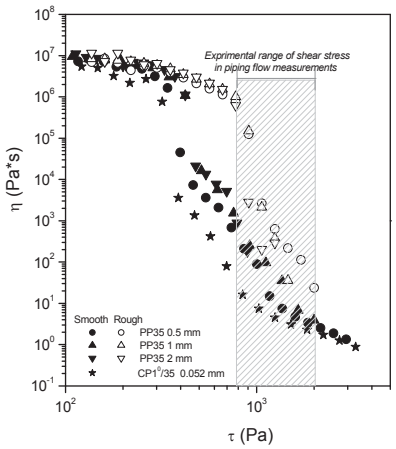

Figure 1.- Viscous flow curves obtained from rotational rheometry using smooth and rough plate-plate and cone-plate geometries and different gaps for the lubricating grease studied.

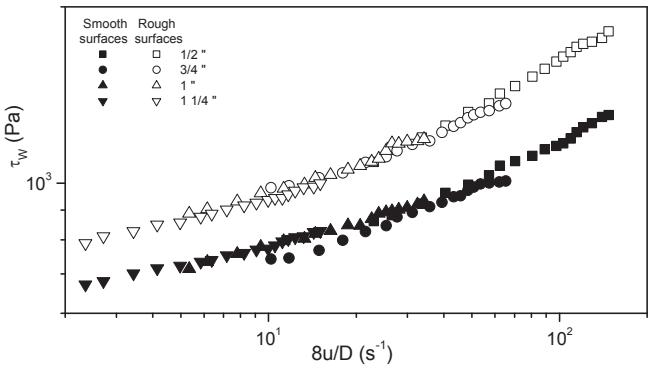

Figure 2.- (-ΔP·D/4L) vs. (8u/D) plot obtained from pipeline flow tests conducted with both smooth and rough internal surfaces.

Table 3.- Pressure drop, generalized Reynolds number and relationship between $\dot{\gamma}_W$ and 8u/D for the Ostwald-de Waele, Sisko and Herschel-Bulkley models.

	(−ΔP)	Re'	$\dot{\gamma}_w$
Ostwald - de Waele's model $\tau = k \cdot \dot{\gamma}^n$ (1)	$(-\Delta P) = \frac{4L}{D} \cdot k \cdot \left[\frac{3n+1}{4n} \cdot \frac{8u}{D}\right]^n$ (4)	$\frac{8 \cdot D^n \cdot \rho \cdot u^{2-n}}{k\left(\frac{3n+1}{4n}\right)^n \cdot 2^{3n}}$ (7)	$\dot{\gamma}_W = \left(\frac{3n'+1}{4n'}\right) \cdot \frac{8u}{D}$ (14)
Sisko's model $\tau = \eta_\infty \cdot \dot{\gamma} + m \cdot \dot{\gamma}^n$ (2)	$(-\Delta P) = \left[\frac{8\eta_\infty^3 \dot{\gamma}_W^4 L^3}{uD^2}(1+X)^3 G(n,X)\right]^{1/3}$ (5)	$\frac{\rho \cdot u \cdot D}{\eta_\infty} \cdot \frac{G(n,X)}{(1+X)}$ (8) where: $G(n,X) = \frac{\left[1+4\left[\left(\frac{n+2}{n+3}\right)X + \left(\frac{2n+1}{2n+n}\right)X^2 + \left(\frac{n}{3n+1}\right)X^3\right]\right]}{(1+X)^3}$ (9) $X = \frac{k}{\eta_\infty} \cdot \dot{\gamma}^{n-1}$ (10)	$\dot{\gamma}_W = \frac{\left(8u/D\right)}{G(n,X)}$ (15)
Herschel - Bulkleys model $\tau = \tau_o + k_H \cdot \dot{\gamma}^n$ (3)	$(-\Delta P) = \frac{\frac{4L}{D} \cdot k_H \cdot \left(\frac{n+1}{4n}\right)^n \cdot \left(\frac{8u}{D}\right)^n}{(1-\delta)^{n+1} \cdot (H(n,\delta))^n}$ (6)	$\frac{8 \cdot D^n \cdot \rho \cdot u^{2-n}}{k_H\left(\frac{2 \cdot (n+1)}{n}\right)^n} \cdot (1-\delta)^{n+1} \cdot (H(n,\delta))^n$ (11) where: $H(n,\delta) = \left[1 - \frac{2n}{3n+1}(1-\delta)^2 - \frac{2n}{2n+1}\delta(1-\delta)\right]$ (12) $\delta = \frac{\tau_0}{\tau_W}$ (13)	$\dot{\gamma}_W = \frac{\left(\frac{n+1}{4n}\right)}{(1-\delta) \cdot H(n,\delta)} \cdot \frac{8u}{D}$ (16)

Piping flow measurements

Pressure drop measurements in the fully developed laminar flow conducted in horizontal pipelines with four different diameters and both smooth and rough internal surfaces are shown in Figure 2. According to the rheological results previously shown, different pressure drop values were found in tests carried out with smooth and rough pipes, for the same diameter, in spite of the fact that there should not be influence of the roughness on the pressure drop gradient in the laminar regime. This discrepancy found in the laminar flow regimen indicates once again the existence of wall slip phenomena in the pipelines.

In order to correlate the flow behaviour obtained from rotational rheometry with those found in pipelines, pressure drop was obtained from equations (4-6) (see Table 3) and flow characteristic from equations (14-16) (see Table 3), for the same shear rate values. Figure 3 shows the experimental results obtained from the piping flow measurements compared with the predictions obtained using the τ-$\dot{\gamma}$ curve in rotational rheometry, according to equations shown in Table 3, for the different models. As can be seen, general differences between experimental and calculated pressure drop gradient for the same flow characteristic range in smooth cases were similar to those found in rough cases, 22%±2%.

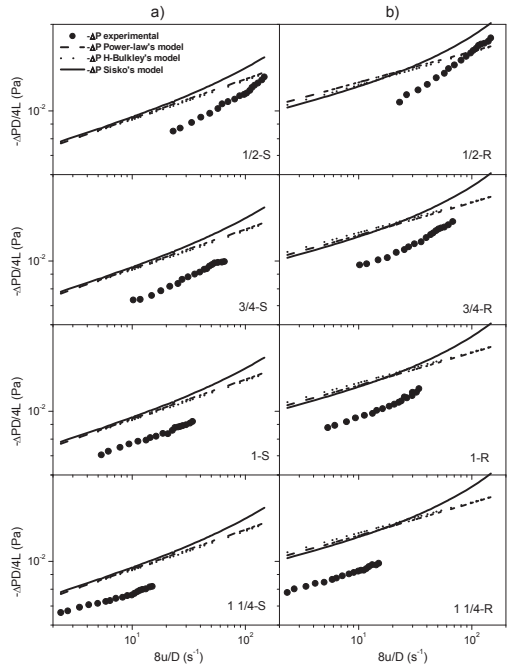

Figure 3.- Comparison of experimental and predicted log(-ΔP·D/4L) vs. log(8u/D) curves obtained for individual pipelines with: a) smooth and b) rough surfaces.

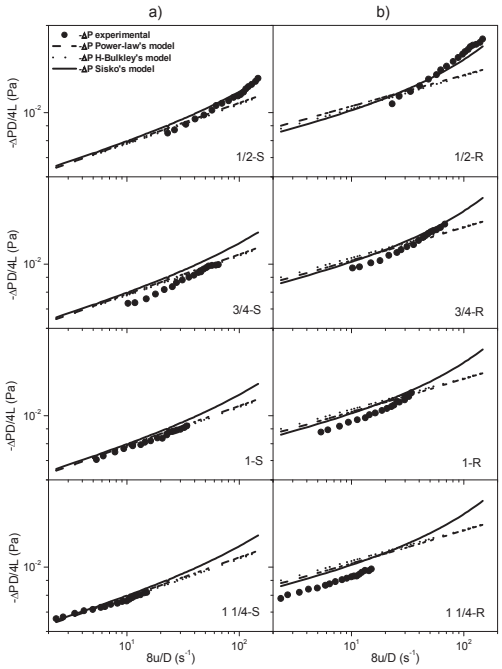

Figure 4.- Comparison of experimental and predicted log(-ΔP·D/4L) vs. log(8u/D) curves obtained for individual pipelines from piping flow and rheometric measurements with a) smooth and b) rough surfaces, once corrected air entrainment effects.

Correction of pressure drop for the two-phase air/grease pipeline flow

Taking into account that priming the pump in highly viscous materials may lead to a significant air entrainment in the pipeline [4], the consideration of the two phase air/grease pipeline flow could explain the deviation in the predictions of pressure loss. Watching the grease flow through a transparent tube the entrainment of relatively large air bubbles is well demonstrated. This two-phase flow is clearly non-homogeneous and intermittent, which may be considered a not well-developed slug flow or a plug (elongated bubble) [9].

The empirical approach proposed by Heywood & Richardson [7] to estimate the drag ratio, ϕ_L^2, considering the shear-thinning behaviour of the liquid for a two-phase plug flow model may be used, in principle, to correlate the pressure drop in the grease/air piping flow:

$$\phi_L^{\,2} = \frac{1}{\lambda_L} \cdot \frac{\mathrm{Re'}_L}{\mathrm{Re'}_{TP}} \tag{17}$$

where ϕ_L^2 is defined as the ratio of the two-phase pressure drop gradient, $(-\Delta P_{TP}/L)$, to the pressure drop gradient for the liquid flowing at the same volumetric flow rate as in the two-phase mixture, $(-\Delta P_L/L)$, λ_L is the input volume fraction of lubricating grease calculated according to equation (18), and Re'_{TP} and Re'_L are generalised Reynolds numbers for two-phase (based on the mixture velocity, $u_{SG} + u_{SL}$) and liquid flow (based on u_{SL}), respectively.

$$\lambda_L = \frac{u_{SL}}{u_{SL} + u_{SG}} \tag{18}$$

being u_{SG} and u_{SL} the superficial liquid and gas velocities, respectively. Although the idealised plug flow model is likely to underestimate the magnitude of two-phase pressure drop, Heywood & Richardson [7] have concluded that it gives reasonable estimations of drag ratios for u_{SG}<1 m/s and Re'_{TP} <500.

Knowing the volumetric flow of grease, the average bubble translational velocity and the void fraction, the superficial air and grease velocities can be calculated as follows:

$$u_{SG} = u_G \cdot \alpha = \frac{Q_G}{A_G} \cdot \alpha \tag{19}$$

$$u_{SL} = u_L \cdot (1-\alpha) = \frac{Q_L}{A_L} \cdot (1-\alpha) \tag{20}$$

Finally, equation (17) can be used for the laminar regime, being Re'_{TP} and Re'_L defined according to the rheological models used (see Table 3). The definition of Re'_{TP} is based on the assumption that air entrained in the bulk of grease reduces the effective local values of viscosity and density by approximately the same proportion [8]. Consequently, the ratio ρ/k was considered unaffected by air entrainment in the bulk and the generalised Reynolds number for the two-phase flow is only a function of physical properties of lubricating grease and the mixture velocity, u_M, defined as $u_{SL}+u_{SG}$.

However, the experimental two-phase pressure drop was not correctly predicted by strictly applying expression (17) to determine $-\Delta P_{TP}/L$. In this sense, it must be pointed out that experimental studies from which this expression was obtained, were carried out with relatively low viscous fluids showing values of the consistency index lower than 50 $Pa \cdot s^n$, and volumetric flow range higher than those achieved in this work. As previously applied [9], the expression (17) needs to be corrected to take into account such deviations between predictions of drag ratio and experimental values in laminar conditions. In this way, Heywood & Richardson [9] introduced a factor C_L, defined as:

$$C_L = \frac{\left(\frac{-\Delta P_{TP}}{L}\right)_{\exp}}{\left(\frac{-\Delta P_{TP}}{L}\right)_{pred}} \tag{21}$$

which is considered to be indicative of the efficiency of plug formation but evidently it may also take into account all the above mentioned possible reasons of deviations. Equation (17) was then modified into:

$$\phi_L^{\,2} = C_L \cdot \frac{1}{\lambda_L} \cdot \frac{Re'_L}{Re'_{TP}} \tag{22}$$

It should be stated that this modification of $\phi_L^{\,2}$ is completely empirical and, in this case, C_L is an average factor among those calculated for each diameter, volumetric flow and rheological models studies, whose value was 0,837±0,070.

Figure 4 shows the experimental results of pressure drop for the grease piping compared with the predictions obtained from equations (4-6). As can be observed, a significantly reduction of the differences shown in Figure 3 was achieved, with maximum errors of ±5 %.

Friction factor-Reynolds number relationship

Figure 5 shows the friction factor versus Reynolds number plots for each rheological model, based on the friction factor defined by Fanning's equation, for smooth surfaces. In these cases, viscous flow models which take into account approximately the same extent of wall-slip that shown by the grease flowing through the pipeline should be used. Thus, expression f=16/Re' may be used to theoretically predict pressure drop gradient of lubricating greases.

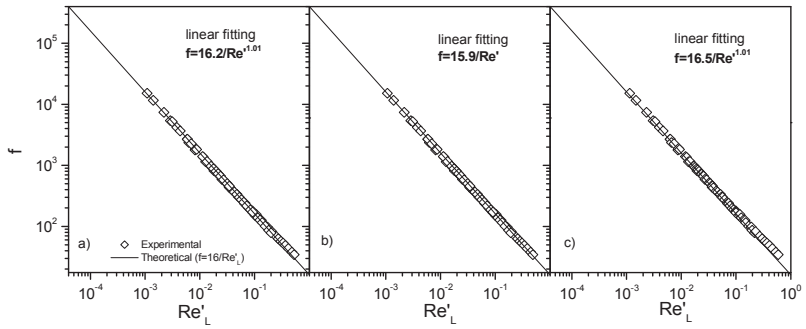

Figure 5.- Friction factor vs. generalised Reynolds number for the lubricating grease flowing in the laminar regimen through smooth pipelines determined using the flow behaviour obtained from smooth plate-plate geometries.

AKNOWLEDGEMENTS

This work is part of the research project PPQ2001-2822, sponsored by CICYT (Spain). The authors gratefully acknowledge its financial support.

REFERENCES

[1] S. Dawtray, Lubricating greases, in G.D. Hobson & W. Pohl, *Modern Petroleum Technology,* Applied Science, Essex, 1975.

[2] NLGI, *Lubricating Greases Guide*, National Lubricating Grease Institute, Kansas, 1994.

[3] S.W. Rein and D.C. McGahey, Predicting grease flow in large pipes, *NLGI Spokesman*, (1965) 20-25.

[4] Y.I. Cho, E. Choi, H. William and J.R. Kirkland, The rheology and hydrodinamic analysis of greases flows in a circular pipe, *Tribol. Trans.*, 36(1993) 545-554.

[5] A.B. Metzner and J.C. Reed, The flow of Non-Newtonian fluids–correlation of laminar, transition and turbulent flow regions. *AIChE J.*, 4(1995) 434-440.

[6] R. Mas and A. Magnin, Rheology of colloidal suspensions: Case of lubricating greases, *J. Rheol.*, 38(1994) 889-908.

[7] N.I. Heywood and J.F. Richardson, Head loss reduction by gas injection for highly shear-thinning suspensions in horizontal pipe flow, in Proceedings of 5th International Conference on the Hydraulic Transport of Solids in Pipes, *Hydrotransport 5* (C1/1-C1/22), BHRA Fluid Engineering, Hannover, 1978.

[8] S.I. Farooqi, N.I. Heywood and J.F. Richardson, Drag reduction by air injection for suspension flow in a horizontal pipeline, *Chem. Eng. Res. Des.*, 58(1980) 16-27.

[9] M. Dziubinski, A general correlation for two-phase pressure drop in intermittent flow of gas and non-Newtonian liquid mixtures in a pipe, *Chem. Eng. Res. Des.*, 73 (1995) 528-533.

RHEOLOGICAL CHARACTERISATION OF BITUMINOUS MIXTURES BY THE REPEATED UNIAXIAL LOAD TEST

*Ana Cristina Freire**
Research Officer of the Civil Engineering Laboratory (LNEC), PORTUGAL
Tel : 351 21 844 33 33 ; Fax : 351 21 844 30 29 ; acfreire@lnec.pt

Maria de Lurdes Antunes
Senior Research Officer of the Civil Engineering Laboratory (LNEC), PORTUGAL
Tel: 351 21 844 35 36; Fax: 351 21 844 30 29; mlantunes@lnec.pt

Luis de Picado-Santos
Associate Professor of the Department of Civil Engineering of the University of Coimbra, PORTUGAL
Tel: 351 239 797 143; Fax: 351 239 797 146; picsan@dec.uc.pt

Keywords: Permanent deformation, Bituminous mixtures, Uniaxial cyclic compression test, Rutting, Viscoelastic behaviour.

ABSTRACT

Bituminous mixtures, applied as wearing layers, base course, or road base, on road pavements, have a mechanical behaviour that is conditioned by temperature and loading time.
For very low temperatures they have a linear elastic behaviour but, for height temperatures it is almost liquid. For intermediate temperatures, and small deformations the mechanical behaviour can be considered as viscoelastic linear.
Knowing that permanent deformation phenomena observed on the road pavements compromise the structural behaviour, and considering driving conditions, it is very important to establish a simple and practical procedure that allows taking in consideration on pavement design.
In order to estimate the permanent deformations observed on the bituminous layers of the road pavements tested on the wheel–tracking test device, and characterise the viscoelastic behaviour, a laboratory procedure was developed.
By performing a repeated uniaxial load test on 0.10 or 0.15 m diameter cores, submitted to the same conditions of those observed on the wheel-tracking test, such as temperature and loading and unloading time, it was possible to predict the deformation rate of the linear phase and to obtain the Burgers serial damper parameter.
This paper presents the most significant results obtained on a laboratory study developed to characterise the bituminous mixtures permanent deformation behaviour. This study involves the prediction of the permanent deformation of bituminous mixtures using the Burgers model. The repeated uniaxial load tests are used to derive the Burgers model parameters.

1. INTRODUCTION

Road pavements should present a free and even surface that supports traffic loads, under appropriate conditions along its service life. The pavement structure should be designed to guarantee that, during its service life, the distresses do not go beyond certain thresholds.

One of the structural distresses considered in pavement design is rutting /deformations along the wheel paths. Although, in general, rutting is the result of the permanent deformation contribution of all the pavement layers, and foundation, the design criteria usually adopted only consider the limitation of the contribution of the subgrade for its formation. These

criteria are expressed by expressions that relate the vertical compressive strains in subgrade, with the number of load applications.

In Portugal, as in the rest of the world, a significant increase of the contribution of the bituminous layers to rutting has been observed in the flexible pavements. This phenomenon is due mainly to the increased growth of heavy vehicles traffic volume and the changes in axle and wheel configuration (from dual wheels into single wide base tyres).

In order to guarantee an adequate performance of bituminous mixtures it is important to use techniques and laboratorial procedures that allow for the determination of performance related properties, namely permanent deformation behaviour.

The laboratory tests used for this purpose should be performed under controlled conditions in order to give information regarding its behaviour, after mixing and "in situ" application, when subject to traffic or climatic actions. In order to obtain significant results, the preparation of laboratory samples should reproduce as good as possible the operations accomplished "in situ". As an alternative, samples extracted from the pavement can be tested.

Laboratory tests used to characterize the permanent deformation of the bituminous materials can be associated in three different groups:

i) "*empirical*" tests, whose analysis of results is based on the experience gathered in the past for materials with similar characteristics;
ii) "*fundamental*" tests, that allow for the evaluation of the bituminous mixtures "*fundamental properties*";
iii) "*simulation tests*", that simulate, within a scale factor, the pavement conditions, under traffic and climatic solicitations.

There is a lot of discussion regarding the relative merits of the different laboratorial methodologies used in order to obtain the permanent deformation characterization. The ideal laboratory approach should simulate the "in situ" conditions and the samples should be representative of the bituminous layer. However, more elaborate approaches involve added cost and the use of sophisticated equipment, in association with complex approaches for the analysis of the results.

In a study developed at LNEC, in the frame of a PhD dissertation [1], which is partially presented in this paper, "*fundamental*" (uniaxial cyclic compression tests) and "*simulation*" (wheel-tracking) and were performed in laboratory on samples extracted from two pavement wearing courses built in Portugal, to characterize its permanent deformation behaviour. The results obtained in the two types of tests are compared assuming a viscoelastic behaviour for the bituminous mixture, expressed by the Burgers model.

2. DESCRIPTION OF THE LABORATORY TESTS

2.1. Uniaxial cyclic compression test

The laboratory equipment used in this study for uniaxial cyclic compression test is an adaptation of an existing equipment at LNEC, generally used for bending fatigue tests [2]. The adaptations carried out consisted in the introduction of a system that guaranties an adequate distribution of the compressive load, and a system for the measurement of deformations consisting of two LVDT (*Lineal Velocity Displacement Transducer*), fixed in opposite positions.

Considering that the behaviour of bituminous materials depends on the temperature, a temperature control chamber, that allows for the use of temperatures between +5 and +75°C, with a 0.5°C accuracy was used. As an alternative it is possible to test the sample immersed in a water bath, at the target temperature, previously involved in a plastic membrane.

Uniaxial cyclic compression tests are performed on cylindrical samples, with 100 mm diameter and a minimum height of 60 mm. In order to guarantee the minimum height of the sample, in the cases where they have been cored from pavement layers with thickness less than 60 mm, two samples with "*identical characteristic*" are associated, with identical characteristics, in agreement with prEN 12697-25 - "*Test: Uniaxial Cyclic Compression Test*".

In the uniaxial test is of major importance to guarantee the uniform application of the vertical pressure. The specimen ends should be plane and parallel, and the absence of any attrition between the plate and the specimen top face should be insured. This is assured by polishing the two sample tops, combined with the application of a lubricant.

A pre-conditioning was performed, consisting on an application of 1500 cycles of uniaxial cyclic compression, under certain selected pressure conditions and loading/unloading time (Figure 1). The aim of this pre-conditioning was to simulate the pos-compaction that takes place on the field, after placing the bituminous layer. Thus, after conditioning, the specimen is expected to be in "*phase 2*" (linear phase) of the evolution of permanent deformation.

Since the materials under study are going to be applied on wearing courses, the vertical stresses should simulate the contact pressures between the heavy vehicles and the pavement surface. A "*haversine*" variation of the load, with an amplitude similar to the tyres contact pressure, and a loading time selected according to the heavy vehicles speed was selected for these tests.

2.2. Wheel-tracking test

In the wheel-tracing test a sample is subjected to successive passes of a wheel and the maximum deformation, or the reduction of the total thickness, is measured as a function of the number of passes (cycles) of the wheel. The test results depend loading time for each cycle, the total wheel load, the temperature and the sample thickness. The method used in Portugal for wheel-tracking test is based on the Spanish specification NLT 173 – "*Resistencia a la deformación plástica de las mezclas bituminosas mediante la pista de ensaio de laboratorio*", which is summarized in Table 1. The procedure, as well as the testing equipment are in accordance to the European prEn 12697-22 – "*Test methods for hot mix asphalt – wheel tracking*".

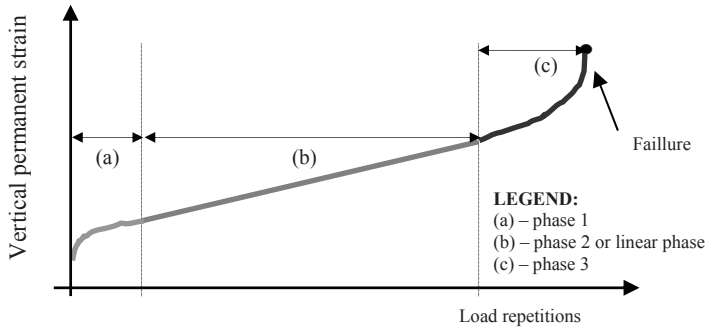

Figure 1 – Evolution of pavement deformation of bituminous mixtures

Table 1. Wheel tracking test characteristics (NLT 173)

Sample dimension	Temperature	Tyre pressure	Contact area	Frequency
300 x 300 x 50 mm^3	60°C	900 $kN.m^{-2}$	2150 mm^2	24 cycle/min.

The test starts after the sample conditioning inside a temperature chamber during 4 hours at 60ºC. The wheel starts to move, and the rut measurements are made at 1, 3, 5, 10, 15, 20, 25, 30, 35, 40, 45, 60, 75, 90, 105, and 120 minutes. According to the adopted specification NLT 173, the test lasts 120 minutes. Figure 2 shows the test apparatus placed inside the temperature control chamber.

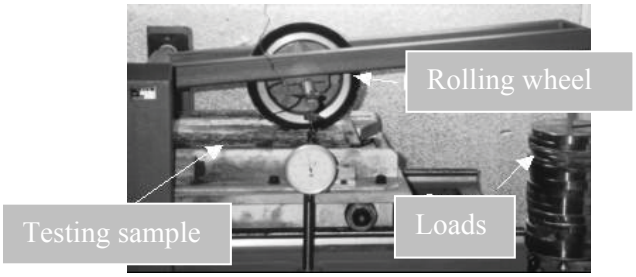

Figure 2. Wheel-tracking test apparatus

2.3. Test temperature

The adoption of an adequate test temperature is very important, since it affects the viscoelastic behaviour, and consequently the permanent deformation under traffic loading.

Most of laboratory tests for permanent deformation characterization around the world suggest the adoption of relatively high temperatures, 50°C or 60°C, aiming the reduction of the testing time. However, these ranges of temperatures are very close to the bitumen softening point and they may consist of a very "unfavourable" condition for the evaluation of permanent deformation behaviour [1].

As a result of the application of "in service" temperature prediction methods, derived from air temperatures [3], the adoption of testing temperatures between 40°C and 50°C, according to the climatic zone (Table 2), [1] is proposed.

Table 2. Testing temperatures

Climatic zone (Portugal)	Temperature (°C)
Hot	50°C
Warm	45°C
Temperate	40°C

3. TEST RESULTS INTERPRETATION

The development of permanent deformations in bituminous mixtures generally presents three different phases.

- Phase 1 – initial phase, where the deformation rate decreases with time;
- Phase 2 – linear phase, where a constant deformation rate is observed;
- Phase 3 – the last and possible failure phase, where the deformation rate increases very rapidly.

After the pavement construction, an additional layer compaction is observed under traffic loads, with variation of bituminous materials viscoelastic characteristics, corresponding to phase 1.

In this study only phase 2, or linear phase, is considered for rutting analysis. Phase two corresponds to most part of the service life of the pavement, being essential to guarantee appropriate structural and functional characteristics. Phase 3, where a high rate of deformation is observed, it is not likely to occur during the pavement service life.

Although the wheel-tracking test doesn't provide fundamental properties bituminous mixtures, it is suitable for comparative analysis of permanent deformation of different mixtures. Normally the test results are expressed through the deformation rates calculated between the 60 and 120 minutes ($v_{60/120}$) or between the 105 and the 120 minutes ($v_{105/120}$) minutes. They may also be graphically represented, relating the accumulated vertical deformation with the testing time.

Uniaxial cyclic compression tests results interpretation is performed considering that the bituminous material has a viscoelastic behaviour described by de Burgers model. The four Burgers model parameters (E_1, E_2, η_1 and η_2) are obtained by back-analysis.

The mathematical expression that describes the permanent deformation behaviour according to the Burgers model was automated. A theoretical curve, that represents the variation of the vertical strain with the time, matches the measured curve. Figure 3 shows the results of one iteration to obtain the Burgers model four parameters.

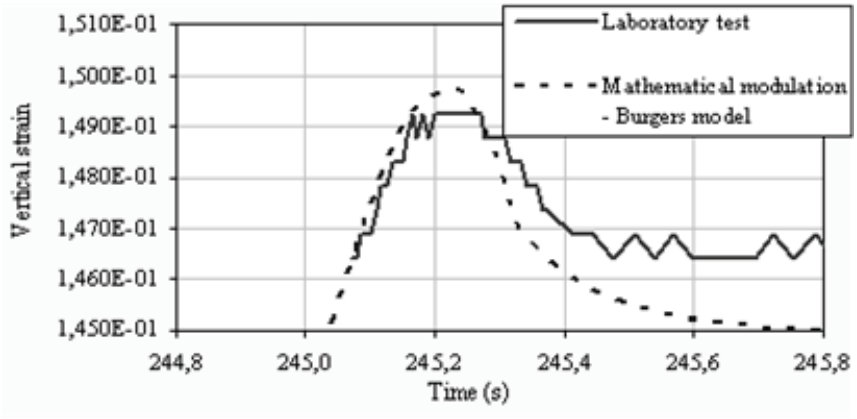

Figure 3. Adjustment between the measured and theoretical curves, for backcalculation of the Burgers model parameters

From the four Burgers model parameters referred previously, the one that has a major influence on the permanent deformation behaviour is the Burgers serial damper parameter (η_1) [1], which will be called "viscosity coefficient" in the following sections.

4. EXPERIMENTAL RESULTS

Two bituminous mixtures applied in the wearing courses of IP7/A6, in Elvas, and of EN14, in Braga, were studied. These mixtures were selected due to their characteristics, namely the aggregate form and nature, and the bitumen characteristics.

The IP7/A6 wearing course bituminous mixture was manufactured with siliceous gravel aggregates, subsequently crushed, and mixed crushed limestone. The bitumen used has a nominal penetration of 35/50, but after recovery from the mixture it had a penetration of 23($x10^{-1}$ mm) and a softening point of 59.1°C.

The EN14 bituminous mixture was manufactured with crushed granite aggregates, which is very common in the north of Portugal. The bitumen has a nominal penetration of 35/50, but, after recovery presented a penetration of 44 ($x10^{-1}$ mm) and a softening temperature of 51.4°C. Table 3 presents the sample preparation and testing condition used in this study.

Figure 4 presents the average values and the ranges of variation of the viscosity coefficient obtained from the uniaxial cyclic compression test performed at 30°C, 40°C, 50°C and 60°C, for the bituminous mixtures of IP7/A6 and EN14.

The results present in Figure 4 show that the viscosity coefficient values obtained for higher test temperatures are lower, indicating a worse permanent deformation behaviour, as expected.

Table 3. Sample preparation and testing conditions

Test	Sample preparation			Testing	
	Manufacture	Pre-conditioning		Load application	Temp.
		Load application	Temp.		
Uniaxial cyclic compression test	"*in situ*"	1500 cycles from uniaxial cyclic compression test, *haversine load* (F^{pico}_{axial} = 7.2 kN; t_{carga} = 0.33 s; $t_{repouso}$ = 1.34 s)	30, 40, 50 and 60°C	Uniaxial cyclic compression test *haversine load,* F_{axial} = 2 kN t_{carga} = 0.33 s; $t_{repouso}$ = 1.34 s	30, 40, 50 and 60°C
Wheel-tracking test	Laboratory/ "*in situ*"	---	---	Rolling load, 900 kPa, 24 cycles/minute	40, 50 and 60°C

A bigger scatter of results can also be seen for higher temperatures. As observed for the wheel-tracking test results, it is clear the influence of the test temperature in the values obtained from the uniaxial cyclic compression test. We can conclude that, for higher test temperatures (60°C) the scatter of the results is considerably higher. This fact, in association with a reduced probability of occurrence of a 60°C temperature in the pavement, leads to the proposal for lower test temperatures.

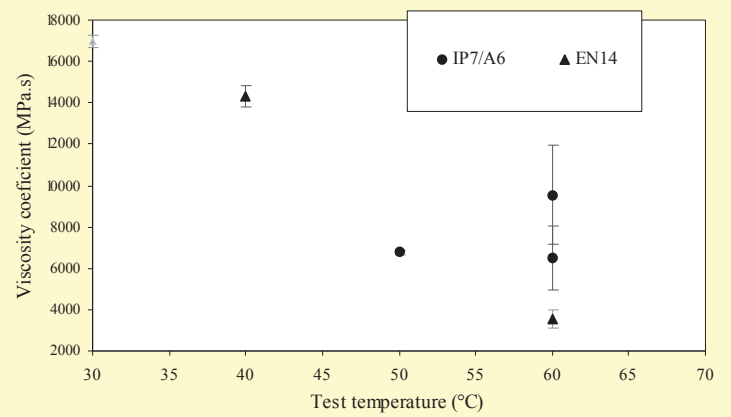

Figure 4. Viscosity coefficient variation with test temperature

Figure 5 shows average values and the ranges of variation obtained for wheel-tracking deformation rate obtained on samples from IP7/A6 and EN14, manufactured in the laboratory or sawed from the pavement, for three different temperatures. The analysis of results presented above shows the influence of temperature on the rate deformation. It can be observed that lower testing temperatures (40°C and 50°C) result in lower deformation rates, but also lower scatter of results. It is also observed that "in situ" samples have larger deformation rates. This happens because in this case "in situ" samples have lower air voids content which were close to the recommended minimum limit of 3% [1].

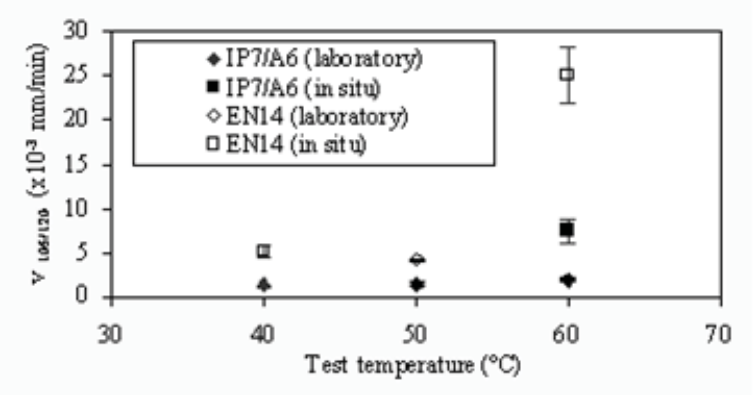

Figure 5. Variation of $V_{105/120}$ with test temperature

5. WHEEL-TRACKING TEST NUMERICAL MODELLING

In order to "validate" the methodology for the characterization of the permanent deformation behaviour of the bituminous mixtures through uniaxial cyclic compression test, the wheel-tracking tests were modelled, considering the four parameters of the model of Burgers obtained from the uniaxial cyclic compression test.

Numerical modelling was accomplished with the finite elements method (M.E.F.). The finite element mesh was established using parallepipedic elements with sixteen nodes, considering a finer subdivision in the vicinity of the area of load application, in the horizontal plane; fine equal layers in the vertical direction, given the reduced thickness of the continuum; and rigid supports in the base and lateral limits, corresponding to the metallic mould where the sample is tested, whose rigidity is very higher than those of bituminous sample.

The bituminous mixture was considered to have a viscoelastic behaviour, described by the Burger model. A step by step procedure was used to simulate the moving wheel load [1]. The computer calculations were carried out for four cycles (2 forward + 2 return) and the pressure applied was 900 kPa. The load speed was variable for a better simulation of the wheel tracking test conditions. Table 4 presents the results obtained with the wheel-tracking test modelling, taking into account the uniaxial cyclic compression test results for the two types of mixtures studied (IP7/A6 and EN14). These results are compared with the actual results measured in the wheel-tracking tests.

The analysis of the values presented in Table 4 shows that the mathematical model is adequate to interpret wheel-tracking tests results. We can conclude that the viscosity coefficient (η_1) obtained from uniaxial cyclic compression test, can be used to evaluate the permanent deformation behaviour of bituminous mixtures. Since the sample preparation for uniaxial cyclic compression test is simpler than for wheel-tracking tests, there are significant advantages in the use of that approach. On the other hand, uniaxial cyclic compression test allow for obtaining "*fundamental*" parameters that can be used for pavement modelling.

Table 4. Numerical modelling of the wheel-tracking test

Pavement		Wheel-tracking test	Numerical modelling
IP7/ A6	60°C	$0,25 < \delta_{perm,} < 0,44$ (x10^{-3}) mm/ cycle	$0,37 < \delta_{perm} < 0,59$ (x10^{-3}) mm/cycle
			$0,25 < \delta_{perm} < 0,54$ (x10^{-3}) mm/cycle
EN14	60ºC	$0,92 < \delta_{perm,} < 1,22$ (x10^{-3}) mm/ cycle	$0,88 < \delta_{perm} < 1,20$ (x10^{-3}) mm/cycle
	40ºC	$0,20 < \delta_{perm,} < 0,27$ (x10^{-3}) mm/ cycle	$0,26 < \delta_{perm} < 0,39$ (x10^{-3}) mm/cycle

6. FINAL REMARKS

This paper presents the results of a study concerning the comparison of different laboratory tests, performed at LNEC, aiming at the selection of a laboratory test for evaluation of permanent deformation of bituminous mixtures. The study concerns uniaxial cyclic compression tests and wheel-tracking tests. The analysis of results is done considering viscoelastic behaviour of the bituminous mixtures, expressed by the Burgers model.

The quality of the results of the structural analysis will always be associated to the accuracy of the experimental characterisation of parameters that describe the material's behaviour. Therefore, it is fundamental that the laboratory tests used for the characterization of the permanent deformation behaviour reproduce the "*in situ*" conditions such as temperature, compaction and stress state.

Several laboratory tests were performed, under different temperatures, indicating that higher temperatures present a larger scatter of results, affecting the tests reproducibility.

Testing temperatures are proposed, derived from air temperatures occurred in Portugal, using "in service" pavement temperature predicting methods. The results obtained from numerical modelling of wheel-tracking tests, using parameters derived from the uniaxial cyclic loading test, were compared with actual measurements from wheel-tracking tests, showing that the method proposed for the evaluation of permanent deformation behaviour is appropriate.

REFERENCES

[1] - Freire, A. C., 2002 – *Deformações permanentes de misturas betuminosas em pavimentos rodoviários*, PhD Thesis, FCTUC, Coimbra.

[2] - Azevedo, M. C., 1993 – *Características mecânicas de misturas betuminosas para camadas de base de pavimentos*, PhD Thesis, UTL, IST, Lisboa.

[3] - Picado-Santos, L., 1994 – *Consideração da temperatura no dimensionamento de pavimentos rodoviários flexíveis*, Phd Thesis, FCTUC, Coimbra, 2 volumes.

[4] - Quaresma, L., Ferreira, P., Freire, A.C., and Batista, A., 2000 - *Mechanistic approach for rutting - Stage 2*. LNEC, Lisboa.

[5] - NLT 173 - *Resistencia a la deformación plástica de las mezclas bituminosas mediante la pista de ensayo de laboratorio*. 1984.

INFLUENCE OF COMPOSITION AND TEMPERATURE ON THE RHEOLOGY OF LUBRICATING GREASES

M.A. Delgado, J.M. Franco, C. Valencia, M.C. Sánchez, C. Gallegos

Departamento de Ingeniería Química. Facultad de Ciencias Experimentales.
Universidad de Huelva. Campus Universitario del Carmen, 21071, Huelva. Spain.
Tel: +34959018201, Fax: +34959019983, e-mail:barragan@uhu.es

Keywords: Lubricating Greases, Process, Composition, Temperature, Rheology

ABSTRACT

This paper deals with the effect that soap content, oil viscosity and temperature exert on the rheological behaviour of lithium lubricating greases. With this aim, dynamic viscoelastic test and viscous measurements were carried out. As expected, the rheological parameters analysed increase with soap content. More interesting seems to be the influence of oil viscosity. Thus, for instance, the dynamic functions significantly increase by decreasing oil viscosity. On the other hand, a complex thermorheologically behaviour was found in the greases studied, mainly related to flow instabilities under shear. In addition to this, the unperturbed microstructure of greases is mainly affected above a critical temperature of around 110 ºC.

INTRODUCTION

The primary purpose of lubrication is the separation of solids surfaces moving relative to one another, to minimise friction and wear. The materials most frequently used for this purpose are oils and greases. The choice of a lubricant for a given application depends upon the design of the equipment and the condition under which the equipment is to be operated [1].

Lubricating greases basically consist of a thickener dispersed in lubricating oil. Fatty acid soaps of lithium, calcium, sodium, aluminium and barium are most commonly used as thickeners. Additional components are sometimes included to improve specific properties [2]. Physical properties of lubricating greases depend on its composition, the working temperature and the operating variables in the manufacturing process. When grease ingredients are submitted to reaction in presence of oil, the soap crystallises as fibers of characteristic length, diameter and configuration [3].

In general, lubricating greases are employed in a great variety of situations to reduce the wear and friction between movable (metal) joints or under dirty atmospheric conditions to prevent dust and dirt from entering the bearings. Grease can also be used over a wide temperature range, as they do not crystallize at low temperature, and they have a good load-carrying capacity at high temperatures, provided by their thickener system [4]. There are some technical applications, for instance in chemical or nuclear industries or aircraft manufacturing, that need bearing satisfactory behaviour at high temperatures or hard lubricating conditions. In these situations high temperature resistant lubricants must be used as so continuous lubricating film to be obtained for an imposed period time [5]. On the other hand, the lubricating life of grease in rolling element bearings is limited by operation at high temperatures. The thermal and mechanical stresses imposed result in gross physical and chemical changes to the grease which contributes, eventually, to failure both of the lubricant

and the bearing [6]. The optimum mechanical behaviour under lubricating conditions at high temperature greatly depends on the thermorheological characteristics of greases.

The main aim of this work is to study the composition of lithium lubricating greases and the influence of the temperature in relation to the rheological behaviour.

EXPERIMENTAL

12-hydroxystearic acid and lithium hydroxide were used as saponifiying agents together with a paraffinic or naphtenic lubricating oil, provided by Verkol, S.A. (Spain), for preparing lithium 12-hydroxystearate soap lubricating grease.

Processing of lithium lubricating greases

In the first step all 12-hydroxystearic acid to obtain the appropriate soap content in the process and a minor amount of the lubricating oil (see Table 1) was charged into an open vessel. The reaction mixture thus formed was then pre-heated to a temperature of 90 ºC. Once the mixture was pre-heated, lithium hydroxide was added and the saponification reaction is carried out until neutralization was completed by stirring with a controlled-rotational speed mixing rheometer, Ika-Visc (Ika, Steufen, Germany) using an anchor impeller in a batch tank. Once the neutralization was completed and the maximum temperature step was reached, 180 ºC, the remainder lubricating oil was added in other two different batches during a controlled cooling step, which generally occurs over a period of at least 5 hours. A final homogenization treatment at 8800 rpm is applied on the incipient greases.

Table 1.- Composition of lithium lubricating grease

GREASES	A	B	C	D	E	F
Base oil	Naphtenic	Paraffinic	Paraffinic	Paraffinic	Paraffinic	Paraffinic
Kinematic viscosity at 40 ºC (cSt)	110	12	63	657	63	63
Soap content (% w/w)	14	14	14	14	8	20

Rheological Measurements

The rheological measurements were performed in a controlled-stress Bohlin CS 50 rheometer (UK), Haake RS100 rheometer (Germany) and controlled-strain Rheometric ARES Rheometer (UK), using a serrated plate-and-plate geometry (25 mm diameter). Dynamic oscillatory tests, in the linear viscoelasticity range, were carried out in a frequency range comprised between 0.01 and 100 rad/s, at 25, 60, 90, 110, 120, 135, 150 and 175 ºC. Stress sweep or strain sweep tests, at the frequency of 1 Hz, were previously performed on each sample to determine the linear viscoelasticity region. Viscous flow measurements were carried out at 25, 60, 90, 110, 140 and 160ºC, in a shear range of 10^{-4}–10^{2} s^{-1}. All samples had the same recent past thermal history.

RESULTS AND DISCUSSION

Influence of soap content

Figure 1 shows the flow curves of lithium greases with different soap content. In the range of shear rate studied, these greases follow a shear-thinning behaviour which can be fitted fairly well to a power-law model. As shown in the legend of Figure 1, the consistency index, k, increases and the flow index, n, decreases with the thickener concentration. These results can be explained taking into account that the gel network of the grease become stronger and more resistant to flow as the soap content increases [4].

More information about the gel network of the grease could be extracted from dynamic tests. Linear viscoelasticity response is qualitatively identical for all the concentrations studied. The results obtained mainly correspond to the "plateau" region, related to the formation of a three-dimensional network, and a tendency to the transition region at the highest frequencies. The plateau modulus, G^{o}_{N}, may be approximately calculated from the loss tangent [7]. This fact makes possible the application of an empirical superposition method using the plateau modulus as a normalization factor (see Figure 2). However, a shift factor affecting the frequency needs to be included to obtain a master curve. This shift factor depends on soap content being very similar for more concentrated greases (i.e. 14 % (w/w) and 20 % (w/w)). On the contrary, the grease containing 8 % (w/w) soap shows a significant displacement of the minimum in G'' to lower frequencies (see the evolution of the shift factor in Figure 2).

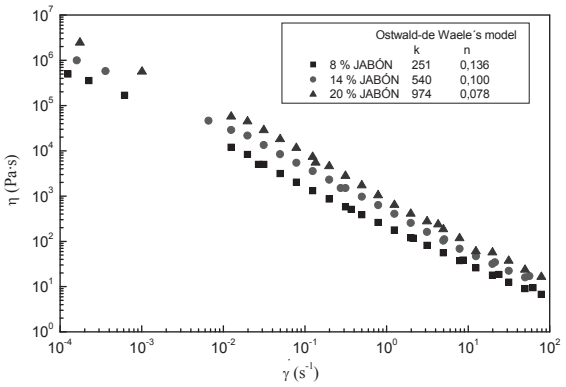

Figure 1.- Viscous flow curves of greases containing different soap content.

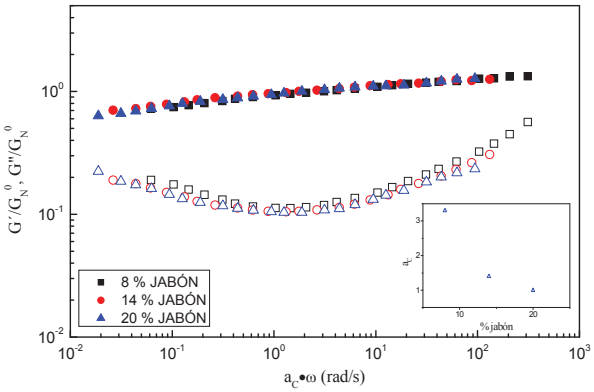

Figure 2.- Normalized storage and loss moduli versus frequency of greases containing different sop content.

Influence of oil viscosity

Figure 3 shows viscous flow curves of greases manufactured with paraffinic oil f different viscosities. As can be observed, main differences viscosity were found at low shear rates. The low oil viscosity, the high grease viscosity is. Thus, consistency index, k, decreases with the oil viscosity. However, oil viscosity does not exert any influence on the viscosity of greases at high shear rates (i.e. higher than 10 s^{-1}).

Figure 4 shows the values of storage (G') and loss (G'') moduli and loss tangent (tan δ) in the linear viscoelastic region. The storage modulus is higher than the loss modulus in all the range studied. In general, the values of both moduli rise up with decreasing the oil viscosity,

reinforcing gel structure. In addition to this, the evolution of the loss tangent indicates that the relative elastic characteristics increase by decreasing oil viscosity.

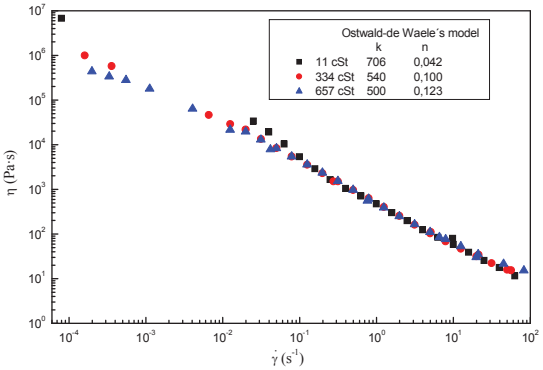

Figure 3.- Viscous flow curves of greases containing oil of different viscosity.

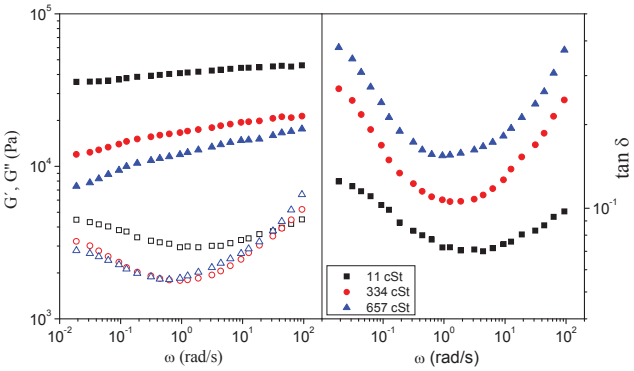

Figure 4.- Storage and loss moduli and tan δ versus frequency of greases containing oil of different viscosity.

Influence of temperature

Figure 5 shows the evolution of the storage (G') and loss (G") moduli with frequency, within the linear viscoelasticity range, for selected grease as a function of temperature. Once again, the storage modulus values, G', are always higher then the loss modulus values, G", in the whole frequency range studied. Nevertheless, they show a clear tendency to a crossover at low frequencies (beginning of the terminal region of the relaxation spectrum), specially at higher temperatures. In fact, a crossover between G' and G" was found at 175ºC at the lowest frequencies.

In general, storage and loss moduli values become higher as temperature decreases. However, loss modulus tends to reach similar values as temperature increases above 120ºC. As can be observed in Figure 6, an increase in temperature from 25ºC to 90ºC produces a significant increase in the relative elastic behaviour of lubricating grease at higher frequencies. These results confirm that greases are not thermorheologically simple materials. Therefore, it has not been possible to superpose, as previously shown, the experimental values of the linear viscoelasticity functions to obtain a master curve. The influence of temperature on the plateau modulus of the lubricating greases studied can be seen in Figure 7. As this figure displays, the slope of G_N^o versus 1/T plot changes above a critical temperature of around 110ºC, so that two different zones can be found, in each of these an Arrhenius type behaviour is followed.

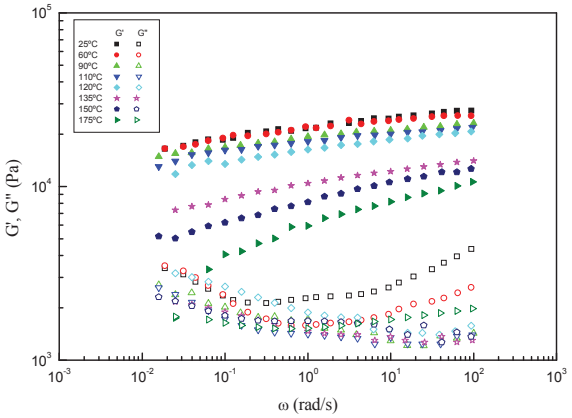

Figure 5.- Evolution of storage and loss moduli at different temperatures for grease A.

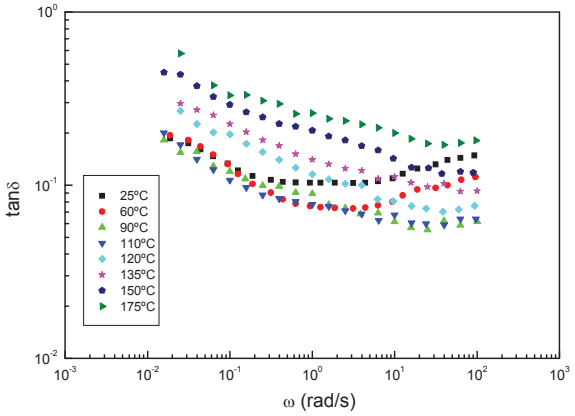

Figure 6.- Evolution of tan δ at different temperatures for grease A.

Steady-state flow curves obtained from both controlled-stress and controlled-rate rheometers, as a function of the temperature, are collected in Figure 8. As can be observed, the evolution of the steady stress with shear rate shows a plateau region at 25ºC between 10^{-2} to 10^{2} s^{-1}. On the contrary, a minimum in the flow curve appears in the same shear rate range above 60ºC. This region in which a non-monotonic evolution of stress was observed, corresponds to a dynamically non-stable region [8]. A jump in strain rate from one stable domain to the next stable domain is found when a controlled-stress rheometer was used. The critical value of the jump defines the plateau or the "classic" yield stress value. As expected, this yield stress value decreases by increasing the temperature. However, when using a controlled-shear rate rheometer a clear minimum in stress evolution was found, which is significatively favoured at high temperature. These results are consistent with the flow instabilities predicted by simulation techniques [9,10] caused by the shear-banding phenomenon [11,12].

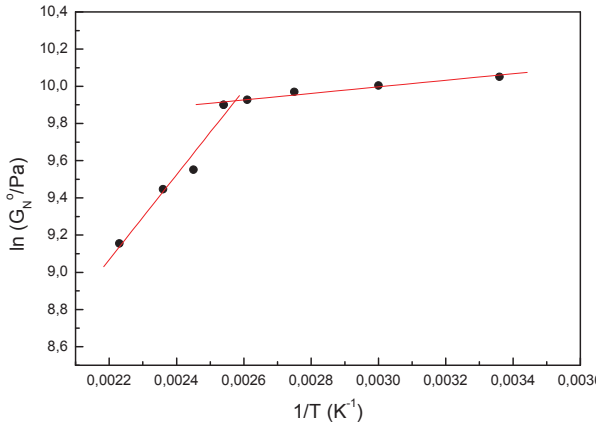

Figure 7.- Evolution of plateau modulus with the temperature for grease A.

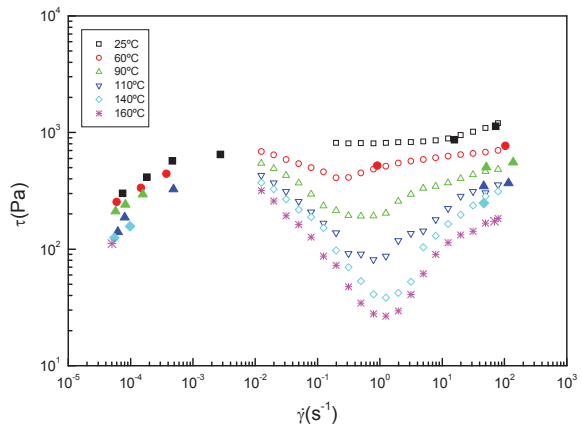

Figure 8.- Viscous flow behaviour at different temperatures for grease A: -●- controlled-stress rheometer, -o- controlled-strain rheometer.

AKNOWLEDGEMENTS

This work is part of the research project PPQ2001-2822, sponsored by CICYT (Spain). The authors gratefully acknowledge its financial support.

REFERENCES

[1] S. Dawtray, Lubricating greases, in G.D. Hobson & W. Pohl, *Modern Petroleum Technology, Applied Science*, Essex, 1975.

[2] NLGI, *Lubricating Greases Guide*, National Lubricating Grease Institute, Kansas, 1994.

[3] S.W. Rein and D.C. McGahey, Predicting grease flow in large pipes, *NLGI Spokesman*, (1965) 20-25.

[4] S.K. Yeong, P.F. Luckham and Th.F. Tadros, Steady flow and viscoelstic properties of lubricating grease containing various thickener concentrations*, J. Coll. Int. Sci*., 274 (2004) 285-293.

[5] F. Farcas M.D. Gafitanu Wear 225-229 (1999) 1004-1010.

[6] Hurley S, Cann PM, Spikes HA, T*rib.Trans.,* 43 (2000) 221-228.

[7] J.A. García-Morales, J.M. Franco, C. Valencia, M.C. Sánchez and C. Gallegos, Influence of processing variables on the rheological properties of lubricating grease manufactured in a stirred tank, *J. Ind. Eng. Chem*., 10(3) (2004) 368-378.

[8] P.Coussot, A.I. Lenov and J.M. Piau, Rheology of concentrated dispersed systems in a low molecular weight matrix, *J. Non-Newtonian Fluid Mech*., 46 (1993) 179-217.

[9] V. Bertola, F. Bertrand, H. Tabuteau, D. Bonn and P. Coussot, *J. Rheol*., 47 (2003) 1211-1226.

[10] F. Greco and R.C. Ball*, J. Non-Newtonian Fluid Mech.,* 69 (1997) 195.

[11] P. Español, X.F. Yuang and R.C. Ball*, J. Non-Newtonian Fluid Mech.,* 65 (1996) 93.

7. POLYMER MELTS & BLENDS

VISCOELASTIC FLOWS IN 1-TO-4 SUDDEN EXPANSIONS

G. N. Rocha and *P. J. Oliveira**

[1] Unidade Materiais Têxteis e Papeleiros, Departamento de Engenharia Electromecânica, Universidade da Beira Interior, 6201-001 Covilhã, Portugal
* Corresponding author, Email: pjpo@ubi.pt

Keywords: Planar expansion; Symmetric flow; Viscoelastic fluid; FENE-CR model

Abstract

In this numerical study we present a systematic investigation of the flow of a FENE-CR liquid in a planar sudden expansion having an area ratio of 1:4. The governing equations are solved with a finite volume method and the interest is confined to steady state solutions in two dimensions. Symmetry about the ducts centre plane is not assumed. In terms of parametric variations, both the Reynolds number, characterising the inertia of the flow, and the Weissenberg number, characterising its viscoelasticity, were varied in a wide range. On the other hand, the extensibility parameter of the FENE-CR model was kept constant, at the value L=10. The results given comprise flow patterns, vortex size and strength, and pressure and velocity distribution along centreline.

1. INTRODUCTION

From a fundamental point of view, viscoelastic fluid flow through ducts with abrupt change of cross section, either expansions or contractions, are important as they highlight many of the unusual phenomena brought about by elasticity. These include complex recirculation patterns, not found with Newtonian fluids, vortex enhancement or suppression, stress behaviour near geometrical singular points, etc. In addition, expansion and contraction geometries are relevant in engineering applications, namely in processing industries, for example the channel feeding an extrusion die is unavoidable endowed with such localised perturbations in cross-section in order to achieve the desired extruded shape. A survey of the specialised literature shows that contraction flows of viscoelastic liquids have received a lot of attention during the past 10-15 years, but studies (both numerical and experimental) of expansion flows are rather scarce.

Examples of the kind of problems we envisage, with both Newtonian and non-Newtonian fluids by Boger and Walters [1]. Numerical studies of sudden expansion flows have been undertaken by Oliveira [2] with viscoelastic fluids and using an expansion ratio 1:3, and by Drikakis [3] with Newtonian fluids and using several expansion ratios. In two-dimensions such studies have established that the size of the recirculating flow region increases linearly with increasing Reynolds number.

While in Newtonian flows the shear stress is proportional to the velocity gradient, non-Newtonian fluids have a shear stress which is not simply proportional solely to the velocity gradient. These fluids may not have a well-defined viscosity and another characteristic is due their viscoelastic properties, making then behaving as either an elastic solid or as a viscous fluid. For laminar flows of Newtonian or non-Newtonian fluids through plane sudden expansions, it is well known that, when the expansion ratio E exceeds 1.5, the flow field downstream of the expansion becomes asymmetric above a critical Reynolds number. In our case that does not happen because we are here concerned with low Reynolds number flows and for that reason we do not reach these critical Reynolds numbers. That kind

of behaviour is analysed in the articles dealing with numerical simulations of Drikakis (1997) and Oliveira (2003).

Here we present a systematic numerical investigation of the flow of a FENE-CR liquid in a planar sudden expansion having an area ratio of 1:4. The governing equations are solved with a finite volume method and steady state solutions are sought in two dimensions. Symmetry about the ducts centre plane is not assumed. In terms of parametric variations, both the Reynolds number, characterising the inertia of the flow, and the Weissenberg number, characterising its viscoelasticity, were varied in a wide range. On the other hand, the extensibility parameter of the FENE-CR model was kept constant, at the value L=10. The results given comprise flow patterns, vortex size and strength, and pressure and velocity distribution along centreline.

2. CONSERVATION AND CONSTITUTIVE EQUATIONS

In this paper we consider the two-dimensional isothermal flow of an incompressible liquid flowing from a straight channel of height d=1 to a larger channel of height D=4. The upstream channel has a length of L_1=20d and the downstream channel a length L_2=50d, as shown in figure 1. This problem is governed by the usual equations of continuity and motion, which can be written as:

$$\nabla \cdot \boldsymbol{u} = 0 \tag{1}$$

$$\rho \frac{D\boldsymbol{u}}{Dt} = -\nabla p + \nabla \cdot \boldsymbol{\tau} \tag{2}$$

where $\boldsymbol{u}$ is the velocity vector, ρ is the fluid density (assumed constant), p is the pressure, $\boldsymbol{\tau}$ is the extra stress tensor, and $D(\ )/Dt = \partial(\ )/\partial t + \boldsymbol{u} \cdot \nabla(\ )$ is the substantial derivative. For a homogeneous polymeric solution the extra stress is decomposed by the sum of a Newtonian solvent and a polymeric solute ($\boldsymbol{\tau} = \boldsymbol{\tau}_s + \boldsymbol{\tau}_p$). The Newtonian solvent component is expressed in eq. (3), where the solvent viscosity η_s is constant, $\nabla \boldsymbol{u}^T$ is the transpose of the velocity gradient, and $\boldsymbol{D}$ is the rate-of-strain tensor:

$$\boldsymbol{\tau}_s = \eta_s \left(\nabla \boldsymbol{u} + \nabla \boldsymbol{u}^T \right) \equiv 2\eta_s \boldsymbol{D} \tag{3}$$

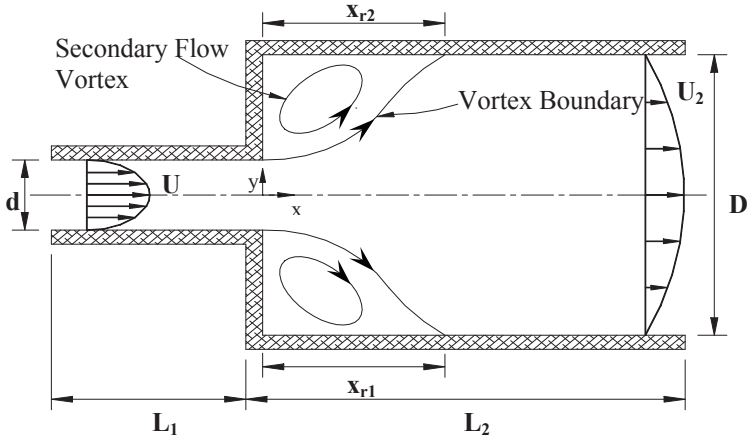

Figure 1- Representation sketch of expansion flow

When the fluid presents simultaneously viscous and elastic properties (a viscoelastic fluid), the problem it is more complicated, compared with the Newtonian case. For solving this problem we use a form of constitutive equation for finite extensibility non-linear dumbbells [4], valid for polymeric materials, proposed by Chilcott and Rallison [5], in which the shear viscosity is constant:

$$\boldsymbol{\tau}_P + \frac{\lambda}{f(\tau_P)}\overset{\triangledown}{\boldsymbol{\tau}}_P = 2\eta_P \boldsymbol{D} \tag{4}$$

with the stretch function $f(\tau_P)$ expressed by:

$$f(\tau_P) = \frac{L^2 + (\lambda/\eta_P)tr(\boldsymbol{\tau}_P)}{L^2 - 3} \tag{5}$$

In the previous equations, tr is the trace operator, λ is a constant relaxation time, η_P is the polymer viscosity (constant) and L^2 the extensibility parameter that measures the size of the polymer molecule in relation to its equilibrium size. The symbol $\triangledown$ in eq. (4) is used to denote Oldroyd´s upper convected derivate:

$$\overset{\triangledown}{\boldsymbol{\tau}} = \frac{D\boldsymbol{\tau}}{Dt} - \boldsymbol{\tau}\cdot\nabla\boldsymbol{u} - \nabla\boldsymbol{u}^T\cdot\boldsymbol{\tau} \tag{6}$$

An additional simplification is embodied in eq. (4), compared with the original FENE-CR equation of Chilcott and Rallison. The modification is to consider *Df/Dt* negligibled and the new model is denoted FENE-MCR, for modified Chilcott-Rallison model. It has been used, for example, by Oliveira [2]. The following relation clarifies the modification introduced into the model:

$$\left(f\overset{\triangledown}{\boldsymbol{\tau}}\right) = f\overset{\triangledown}{\boldsymbol{\tau}} + \boldsymbol{\tau}\frac{Df}{Dt} \Leftrightarrow \left(f\overset{\triangledown}{\boldsymbol{\tau}}\right) \approx f\overset{\triangledown}{\boldsymbol{\tau}} \tag{7}$$

which was useful to facilitate the utilisation of an existing numerical procedure.

The relevant non-dimensional parameters to be varied in this work are the extensibility parameter of the FENE-CR model, L^2, the solvent viscosity ratio given by: $\beta = \eta_s / \eta_0$, where the global shear viscosity is $\eta_0 = \eta_s + \eta_p$ (constant), the Reynolds number: $\mathrm{Re} = \rho U d / \eta_0$, and the Weissenberg number, $We = \lambda U / d$ where the velocity *U* is the average velocity in the smaller channel and *d* is the height of that channel.

3. NUMERICAL METHOD

In the present study, a finite volume method based on the SIMPLEC algorithm for the pressure-velocity coupling is employed to solve the system of the governing equations using orthogonal meshes. The governing equations (Eqs. (1), (2), (4) and (5)) are integrated in space over the control volumes (cells) forming the computational mesh and are transformed into systems of linearised algebraic equations. This discretisation method and the iterative procedure to solve the large sets of linear equations are explained with more detail in Oliveira et al. [6] and no further description is required here. Suffices to add that a formally third-order accurate scheme, the CUBISTA of ref. [7], is applied to represent the all important convective terms in both the constitutive and the momentum equations.

4. RESULTS

At the inlet we have imposed fully developed profiles for all variables, with the velocity profile following a parabolic shape and with an average velocity arbitrarily set to U=1. For the FENE-MCR model, the fully developed velocity and the shear stress distributions in channel flow are identical to those for a Newtonian fluid. In relation to fig.1, these are:

$$u = 1.5U\left(1-\left(\frac{y}{d/2}\right)^2\right) \text{ and } \tau_{xy} = \eta_p \frac{du}{dy} = -\left(\frac{12\eta_p U}{d}\right)\left(\frac{y}{d}\right) \quad (8)$$

The normal stress τ_{xx} follows a more complicated variation given in ref. [2].

4.1. Results for Newtonian case and validation data

In the figures 2 and 3 we compare, respectively, the predicted vortex length ($X_r=x_r/d$) and vortex intensities ($\psi_r= \psi_{r1}= \psi_{r2}$ in symmetric flow) with existing results, for several Reynolds numbers. For this comparison, we used the correlations proposed by Scott et al. [7] and it can be seen that, for Reynolds numbers above 20, there is good agreement between our predictions and their correlations. Our numerical data are given in Table 2, where a perfect symmetry between the upper (y > 0) and lower (y < 0) parts of the channel is observed, for the range of Re considered. Recall that we do not rely on the symmetry about the centerplane (y = 0), with simulations performed on the full domain.

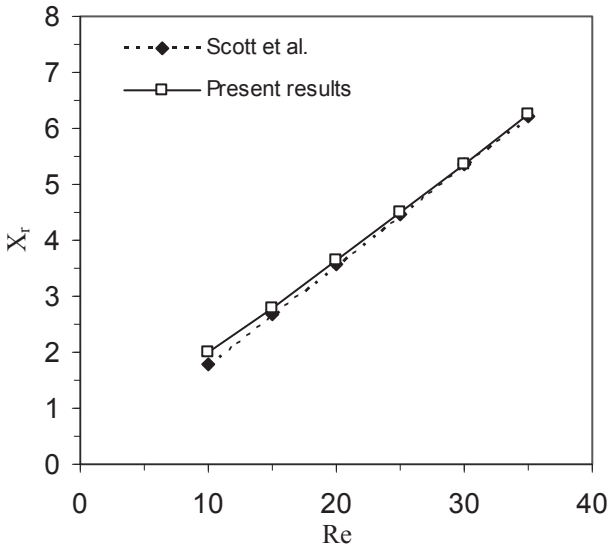

Fig 2 – Vortex length vs Reynolds number

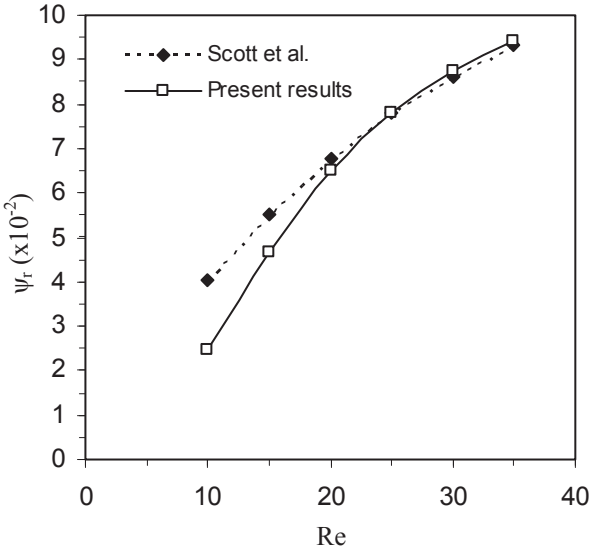

Fig 3 – Vortex intensity vs Reynolds number

Re	X_{r1}	X_{r2}	ψ_{r1} (x10^{-2})	ψ_{r2} (x10^{-2})
20	3.628	3.628	6.5039	6.5039
15	2.784	2.784	4.6578	4.6578
10	1.989	1.989	2.4580	2.4580
5	1.286	1.286	0.6645	0.6645
2	0.933	0.933	0.1741	0.1741
1	0.831	0.831	0.1029	0.1029
0.1	0.750	0.750	0.0629	0.0629
0.01	0.742	0.742	0.0597	0.0597

Table 2 – Vortex length (X_r) and vortex intensity (ψ_r) for Newtonian case

4.2. Results for viscoelastic case

For viscoelastic flow, there are four independent parameters in the FENE-MCR model under consideration (*Re*, *We*, L^2 and β). In this work, the extensibility parameter was set $L^2 = 100$ for all simulations and the solvent viscosity ratio β equal to 0.5; the varying parameters were the Weissenberg number (1; 2; 5), and the Reynolds number, between 0.01 – 20. Table 3 presents some values of vortex size and intensity for the three Weissenberg numbers here considered, at Re = 20.

We	X_{r1}	X_{r2}	ψ_{r1} (x10^{-2})	ψ_{r2} (x10^{-2})
1	2.59	2.59	3.556	3.556
2	2.07	2.07	2.231	2.233
5	1.47	1.47	0.851	0.855

Table 3 – Data for the viscoelastic case – effect of Weissenberg number (L^2=100, β=0.5, *Re*=20)

4.2.1. Reynolds and Weissenberg numbers dependence

For the higher Reynolds numbers the inertial forces are seen to dominate the flow, whilst for low Reynolds number (less than 1) the viscous forces dominate. The Weissenberg number represents the effect of viscoelasticity on the flow and when We is small the flow is all slow flow, approach's the Newtonian limit, while for a large We important elastic effects set in.

In Figures 4 – 9 we present streamlines contour plots for two Reynolds numbers (10 and 20) and for increasing Weissenberg numbers.

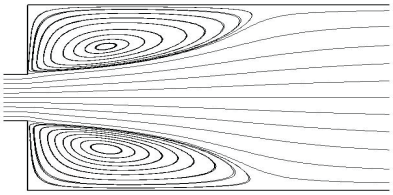

Fig. 4 – Newtonian case with Re=20

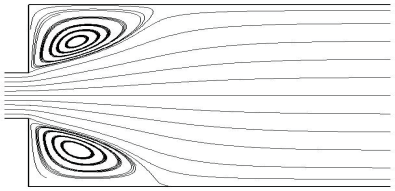

Fig. 5 – Newtonian case with Re=10

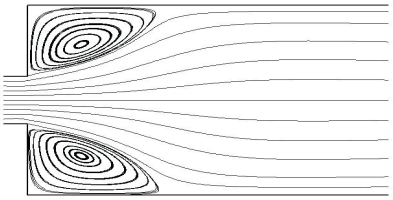

Fig. 6 – Viscoelastic case with We = 2, Re = 20

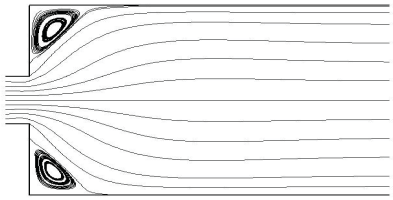

Fig. 7 – Viscoelastic case with We = 2, Re = 10

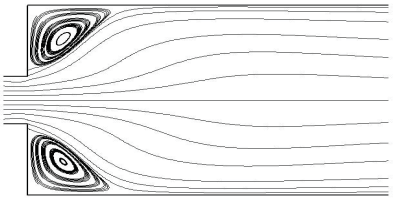

Fig. 8 – Viscoelastic case with We = 5, Re = 20

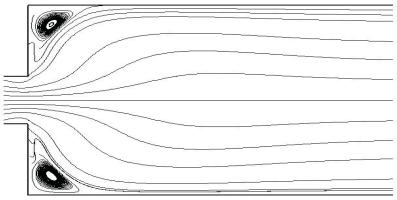

Fig. 9 – Viscoelastic case with We = 5, Re = 10

In figure 10 we present, for low Reynolds number (Re = 0.01), the variation of the streamwise velocity component along the central plane (y = 0), at We = 0 and We = 2 (L^2=100 and β=0.5) corresponding to the Newtonian and Viscoelastic cases, respectively. A strong velocity overshoot is observed upstream of the expansion plane, and an undershoot downstream.

In figure 12 we present pressure profiles along the central plane for Newtonian and viscoelastic fluids ($L^2 = 100$, $\beta = 0.5$, We = 2), at Re = 20. Although not clearly seen, the pressure recovery after the expansion of the Viscoelastic fluid is smaller than for the Newtonian fluid and this leads to a larger localised loss coefficient, in agreement with the findings of [2].

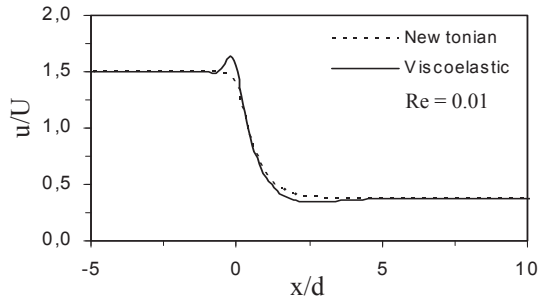

Fig. 10 – Variation of streamwise velocity along the central plane.

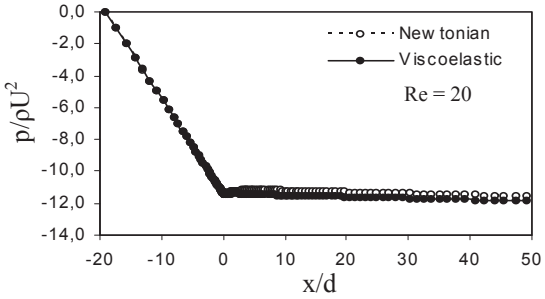

Fig. 11 – Pressure profiles along central plane

5. CONCLUSIONS

The planar 1:4 expansion flow of a FENE-MCR model fluid has been simulated by using the finite volume method on a non-uniform grid system and by adopting the CUBISTA scheme to discretize the convection fluxes in the flow and constitutive equations, where the stress tensor can be decomposed into Newtonian and non-Newtonian parts. In this work we only dealt with low Reynolds numbers in the range 0.01 – 20. At low Reynolds number and low expansion ratio (1:4), the flow is almost symmetric in respect to the center plane. Hence we see that the values of the length and intensity of the vortices are the same in the upper and lower sides of the expansion geometry, for range values of Weissenberg and Reynolds numbers. We can also see from results for the Newtonian fluid that for Reynolds numbers larger than 1 inertial forces prevail in the flow, while for Reynolds numbers significantly less than 1 the viscous forces dominate. On the other hand, we see that when We is large, viscoelastic effects are important in the flow and it is necessary to select a viscoelastic constitutive equation. The present results showing a significant reduction in vortex size and intensity with viscoelasticity could not have been obtained with a generalised Newtonian fluid because here the shear viscosity was kept constant.

References

[1] D.V. Boger, K. Walters, Rheological Phenomena in Focus, Rheology Series, vol.4, Elsevier, 1993.
[2] P.J. Oliveira, Asymmetric flows of viscoelastic fluids in symmetric planar expansion geometries, J. Non-Newtonian Fluid Mechanics. 114 (2003) 33-63.
[3] D. Drikakis, Bifurcation phenomena in incompressible sudden expansion flows, Phys. Fluids 9 (1997) 76-86.
[4] R.B. Bird, C.F. Curtiss, R.C. Armstrong, O. Hassager, Dynamics of Polymeric Liquids, vol.2, Kinetic Theory, Wiley, New York, 1977.
[5] M.D. Chilcott, J.M. Rallison, Creeping flow dilute polymer solutions past cylinders and spheres, J. Non-Newtonian Fluid Mech. 29 (1988) 381-432.
[6] P.J. Oliveira, F.T. Pinho, G.A. Pinto, Numerical simulation of non-linear elastic flows with a general collocated finite-volume method, J. Non-Newtonian Fluid Mech. 79 (1998) 1-43.
[7] M.A. Alves, P.J. Oliveira, F.T. Pinho, A convergent and universally bounded interpolation scheme for the treatment of advection, Int. J. Numer. Methods Fluids 41 (2003) 47-75.
[8] P.S. Scott, F.A. Mirza, J. Vlachopoulos, A finite element analysis of laminar flows through planar and axisymmetric abrupt expansions, Computers & Fluids, Vol. 14, No. 4 (1986) 423-432.

MODIFICATION OF THE VISCOELASTIC MATERIAL FUNCTIONS OF TRIBLOCK COPOLYMERS INDUCED BY PRE-SHEAR.

A.C. Diogo
Instituto Superior Técnico, Departamento de Engenharia de Materiais, Av. Rovisco Pais, 1049-001 Lisboa
Tel +351-218418132 Fax +351-21841810 e-mail: acdiogo@ist.utl.pt

Keywords: viscoelasticity, triblock copolymers, shear flow orientation

Abstract: Controlled shear flows can change the microstructure of triblock copolymers and these modifications are reflected in their viscoelastic material functions. Triblock copolymers often present two elastomeric plateaux, which are associated to two different relaxation processes in the terminal region; the mechanisms of such processes are discussed. The dynamic shear modulus of triblock copolymers of styrene-isoprene-styrene (SIS) with micellar cubic morphology and styrene-butadiene-styrene (SBS) triblock copolymers with cylindrical hexagonal morphology was measured in the range from 10^{-2} to 10^{2} rad/s, at different temperatures above 100ºC (the glass relaxation of polystyrene), in samples with different pre-shear histories. The influence of these variables in the viscoelastic material functions of the SIS triblock copolymers was examined. It was observed that the dynamic shear modulus G(ω) depends on the amount of pre-shear imposed to the samples, as well a on the shear rate. This dependence reflects the changes in the morphology due to the strain history.

1. INTRODUCTION

Block copolymers present a variety of segregation structures (micelles, cylinders, lamellae, etc.) due to the incompatibility among the building blocks. Microphase separation and ordering is controlled by the product of the Flory χ parameter, and the length of the chain, specified by the number of segments N [1-3].
The rheological behaviour of block copolymers depend on a number of factors: the number of blocks in the chain, the size and shape of the domains, the amount of segregation, the rheological properties of the material in the domains as well as in the matrix, the degree of macroscopic alignment are the most important [2-3]. For instance, the morphology and ordering of block copolymers can be changed by the effect of flow in a number of ways [4-10].
In particular, linear viscoelastic material functions such as the dynamic shear modulus $G(i\omega) = G'(\omega) + i.\ G''(\omega)$, or the dynamic shear viscosity, $\eta(i\omega) = G(i\omega)/i\omega$, are quite sensitive to the morphology and orientation, namely in the terminal region [2,4,6,10].
This paper is focused on the influence of the microstructure as well as the shear history on the rheological properties of triblock copolymers of styrene-isoprene-styrene (SIS) with micellar cubic morphology and styrene-butadiene-styrene (SBS) triblock copolymers with cylindrical hexagonal morphology. It was found that the dynamic shear modulus G(iω) depends on the amount of pre-shear imposed to the samples as well as on the shear rate. This dependence should reflect the changes in the morphology due to the imposed strain history, and suggests that the reorientation of the PS domains is influenced by the pre-strain imposed to the sample as well as the shear rate considered.

2. MATERIALS AND METHODS

The triblock copolymer of polystyrene-b-polyisoprene-b-polystyrene (SIS) was obtained from Aldrich. The molecular weight of SIS is 245 000 dalton, and the polyisoprene content is 86% (w/w). Therefore, the molecular weight of the isoprene blocks shall be 210 700 dalton and the molecular weight of each polystyrene blocks will be 17 150 dalton. Due to segregation of the PS blocks, a micellar cubic phase is produced for the above composition (14% w/w polystyrene). A hexagonally packed phase of cylindrical micelles is found at a slightly higher PS content (17% w/w). Experiments were performed in a Rheometrics RMS-800 Mechanical Spectrometer, using the parallel plates fixture. For each experiment, disk samples were moulded by compression in a 24 tons hot-plates press (Carver), at 150ºC for about 10 minutes, and then cooled to ambient temperature.
The triblock copolymer of polystyrene-b-polybutadiene-b-polystyrene (SBS) considered here presents a hexagonal cylindrical morphology.

3. EXPERIMENTAL DATA AND DISCUSSION.

Figures 1 and 2 display the elastic G'(ω) and dissipative G"(ω) shear modulus of the SBS triblock copolymer, in the frequency range from 10^{-2} to 10^{3} rad/s, and at different temperatures from 130ºC to 170ºC. Both polystyrene and polybutadiene blocks are in the molten state, since the glass relaxation of polystyrene occurs at 100ºC and the glass relaxation of polybutadiene is found around −70ºC. Two plateaux (and two relaxation domains) are observed in G'(ω), as a consequence of the presence of cylindrical PS microdomains.

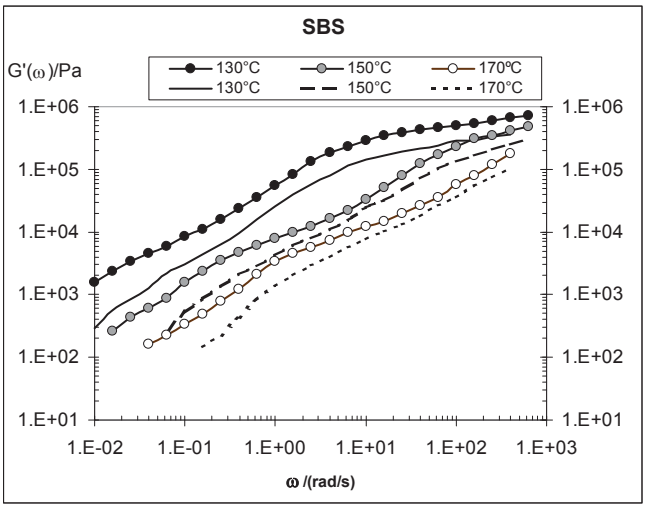

Figure 1 – Elastic dynamic shear modulus G'(ω) of SBS triblock copolymers at temperatures from 130ºC to 170ºC (symbols w/lines) and after a shear flow history (lines only).

An analysis of the different relaxation mechanisms involved in the plateau and terminal regions and their contributions is provided in ref. [10].
The main contributions come from: (a) relaxation of the butadiene segments between consecutive entanglement points (only observed at much higher frequencies); (b) relaxation of the full butadiene chain modified by the presence of PS blocks at its ends; (c) relaxation of the PS blocks tethered at the S/B interface; (d) constraint release at the PB chains caused by diffusion of the PS blocks along the cylindrical domains.

Figures 1 and 2 also show the same material functions G'(ω) and G"(ω) for samples of the same SBS material previously submitted to a shear flow history (the curves represented by lines without symbols). A quite noticeable reduction of both moduli is observed, due to alignment of the cylinders along the flow direction [6].

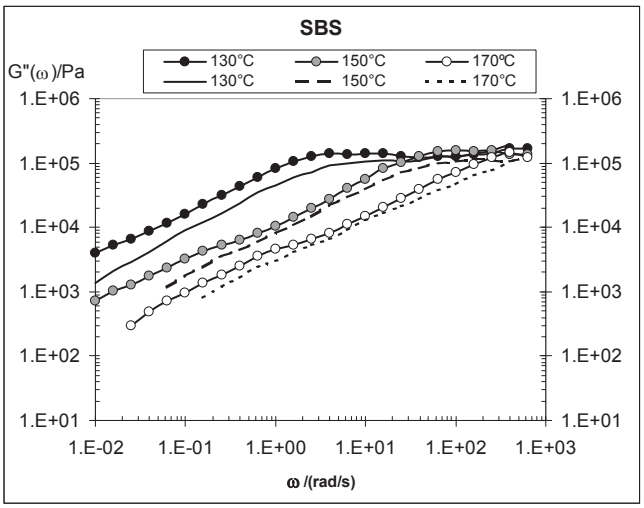

Figure 2 – Dissipative dynamic shear modulus G"(ω) of SBS triblock copolymers at temperatures from 130ºC to 170ºC (symbols w/lines) and after a shear flow history (lines only).

Figures 3 and 4 display the elastic G'(ω) and dissipative G"(ω) shear modulus of the micellar SIS triblock copolymer in the frequency range from 10^{-2} to 10^{2} rad/s, in the temperature range from 120ºC to 190ºC.

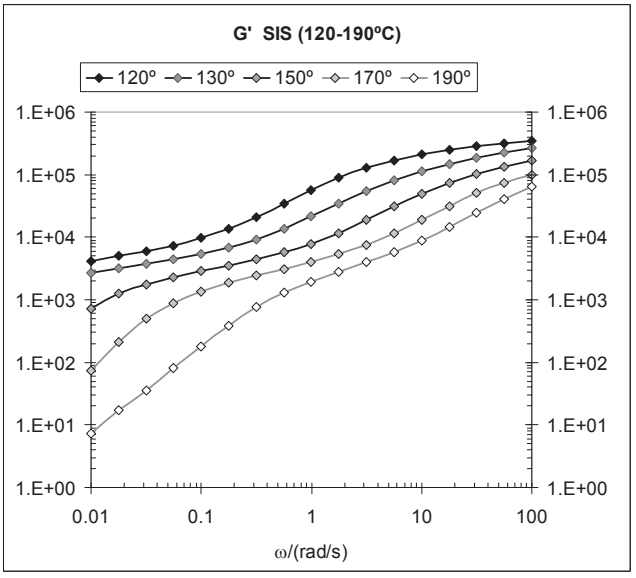

Figure 3 – Elastic dynamic shear modulus G'(ω) of SIS triblock copolymers at temperatures from 120ºC to 190ºC.

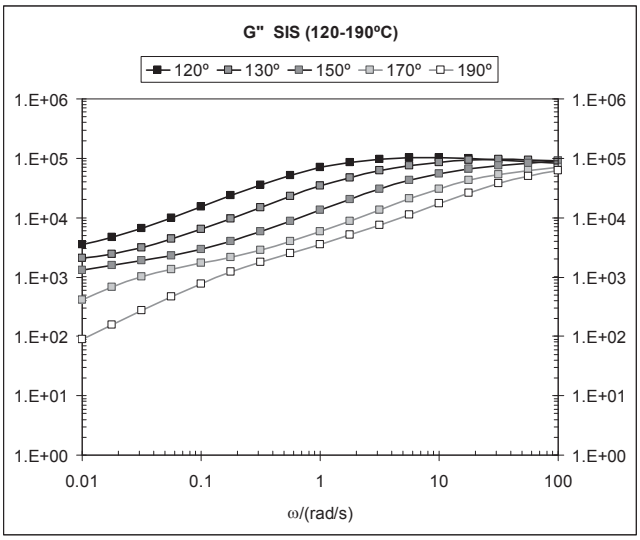

Figure 4 – Dissipative dynamic shear modulus G"(ω) of SIS triblock copolymers at temperatures from 120ºC to 190ºC.

Now the shapes of G'(ω) and G"(ω) are quite different from the ones presented in figures 1 and 2, but two elastomeric plateaux are again evident. The high frequency plateau is attributed to the relaxation of the polyisoprene blocks between consecutive entanglements. In fact, the molecular weight between consecutive entanglements of polyisoprene is 5 800 dalton, so each polyisoprene block has 36 entanglements in average.

It may be worth to analyse the main relaxation mechanisms expected for these SIS triblock copolymers: (a) relaxation of the PI segments between consecutive entanglement points: its contribution is in the transition region of the frequency spectra, outside the frequency window available here; (b) relaxation of the full PI chain modified by the presence of PS blocks at the ends: a simple estimation of the plateau modulus associated to this process yields 13 kPa, which is close to the low frequency plateau modulus found; (c) relaxation of the PS blocks tethered at the S/I interface: since the molar mass of the PS blocks is smaller than the molar mass between entanglements of PS (18 000 dalton), this process is expected to be relatively fast; (d) constraint release at the polyisoprene chains caused by diffusion of the PS blocks along the micellar domains: this process should be less effective as compared to the one in a cylindrical hexagonal phase; (e) disengagement by fluctuations in path length (tube leakage) and (f) pure reptation along the primitive chain, shall yield a negligible contribution.

The plateau modulus G^0_N can be computed by the well known expression

$$G_N^0 = \frac{\rho.R.T}{Me} \qquad (1)$$

where ρ is the density, T is the absolute temperature, R is the perfect gas constant, and Me is the molecular weight between consecutive entanglements. By use of equation (1) we get at 150ºC, $G^0_N = 0.475$ MPa, in good agreement with the experimental data.

The high frequency data represented in figures 3 and 4 can be superimposed by translation in the frequency axis. Since we are dealing with copolymers, time-temperature superposition (TTS) cannot hold since all relaxation times do not present the same temperature behaviour. However, TTS may hold in some frequency window where there is only one dominant

relaxation process, provided there is no interference from other relaxation processes. The evidence that TTS holds for the high frequency data, also supports the hypothesis that the relaxation of the entangled polyisoprene blocks is responsible for the high frequency plateau.
Figure 5 displays the experimental data concerning G'(ω), G"(ω) and the modulus of the complex viscosity η*(ω) of SIS, superimposed to the computed curves for the same linear viscoelastic material functions of a polyisoprene with molecular weight equal to the one of polyisoprene blocks (210 000 dalton). The agreement found is again quite good in the high frequency region for all the material functions considered.

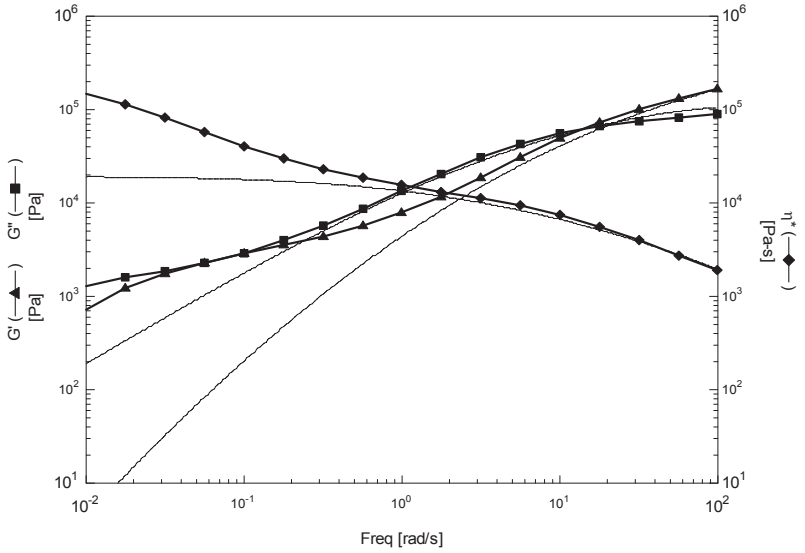

Figure 5 – Viscoelastic material function of SIS at 150ºC (bold lines), as compared to the simulated viscoelastic material functions of isoprene with the same molecular weight.

Returning to figure 3, a neat lower plateau is observed at 150ºC as well as at all temperatures below 150ºC. It is characteristic of an ordered micellar phase. This behaviour contrasts with the terminal-like behaviour observed in the low frequency side above 150ºC; such behaviour is indicative of a disordered micellar phase. Therefore, an order-disorder transition is observed at a temperature close to 150ºC.

Figure 6 presents a comparison of the viscoelastic material functions G'(ω), G"(ω) and η*(ω) of SIS after a given preshear with the same final deformation ($\gamma = 150$) but at different shear rates. It is expected that changes in microstructure will occur at shear rates such that $\tau.\dot{\gamma} > 1$, where τ is a terminal relaxation time. It is observed that the dynamic shear modulus G(ω) depends on the amount of pre-shear imposed to the samples as well as on the shear rate. This dependence reflects the changes in the morphology due to the imposed pre-strain, and strongly suggests that the reorientation of the PS domains is influenced by the total amount of pre-strain imposed to the samples. On the other hand, changes of shape of the PS domains (micellar to cylindrical) or even breaking of the PS domains due to flow will present a rather slow relaxation time so they are expected to depend on the shear rate. The lower plateau modulus is quite sensitive to the amount of pre-shear; as the amount of pre-shear is increased, its value decreases; in some experiments, the lower plateau can even (almost) disappear at very high strains.

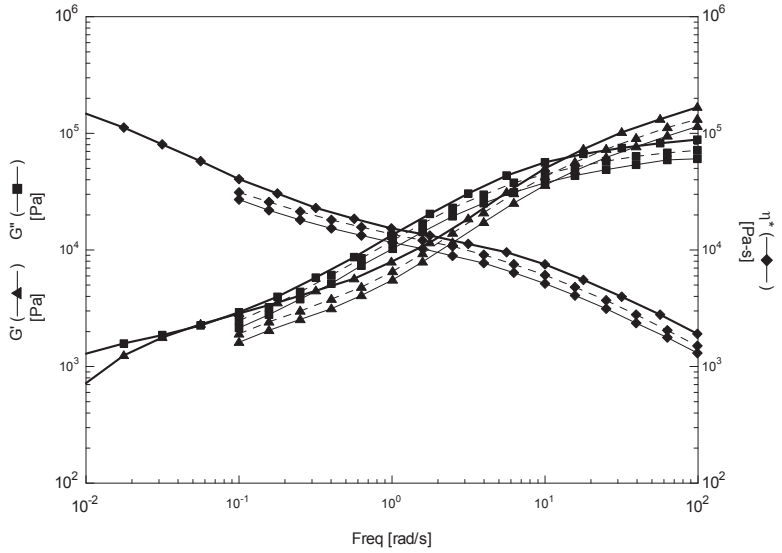

Figure 6 – Viscoelastic material function of SIS at 150ºC without and with preshear. Full lines: no preshear; short broken lines: 750 s at 0.2 s^{-1} shear rate; long broken lines: 1500 s at 0.1 s^{-1} shear rate.

4. CONCLUSIONS

It was shown that the frequency and temperature dependence of the dynamic shear modulus and viscosity can provide an insight on the multiple relaxation processes in triblock copolymers, and it can be correlated to the morphologies adopted by these materials. Order-disorder transitions can also be detected by analysis of the terminal region. It is also found that the linear viscoelastic material functions are quite sensitive to the effect of a shear flow history, namely to changes of morphology and/or reorientation of the micelle domains.

Acknowledgements. The collaboration of Dr. E. Baptista and Eng. Tiago Barbosa in some of the experiments reported here is acknowledged.

References.

[1] – M.J. Folkes (ed.) – *Processing, Structure and Properties of Block Copolymers*, Elsevier, New York (1985)
[2] – R.G. Larson – *The Structure and Rheology of Complex Fluids*, Oxford University Press (1999)
[3] - F.S. Bates, G.H. Fredrickson – Ann. Rev. Phys. Chem. **41** (1990) 525
[4] – E.V. Gouinlock, R.S. Porter – Polym Eng Sci. **17** (1977) 535
[5] – B.L. Riise, G.H. Fredrickson, R.G. Larson, D.S. Pearson – Macromolecules **28** (1995) 7653
[6] – A.C. Diogo, G.Marin, Ph. Monge – Rheol. Acta **26** (1988) 367
[7] – J. Laurer, D.A. Hajduk, J.S. Fung, J.W. Sedat, S.D. Smith, S.M. Gruner, D.A. Agard, R.J. Spontak – Macromolecules **30** (1997) 3938
[8] – C.S. Honeker, E.L. Thomas, R.J. Albalak, D.A. Hajduk, S.M. Gruner, M.C. Capel – Macromolecules **33** (2000) 9395
[9] – C.L. Jackson, K.A. Barnes, F.A. Morrison, J.W. Mays, A.I. Nakatani, C.C. Han - **28** (1995) 713
[10] – A.C. Diogo, G.Marin, Ph. Monge – J. Non-Newt. Fluid Mech. **23** (1987) 435

HELICAL FLOW OF POLYMER MELTS ALONG ANNULAR CHANNELS

M. Martins and J. A. Covas

Department of Polymer Engineering, University of Minho, 4800 Guimarães, Portugal

Abstract

Mandrel rotation during pipe extrusion has been reported to improve both the flow conditions and the final properties of parts. Therefore, an extrusion head fitted with a rotating mandrel and a variable thermal environment in the die land was developed and explored experimentally. Simultaneously, modelling of the non-isothermal steady helical flow was carried out. The model estimates the pressure drop and the torque corresponding to a specific flow rate and mandrel rotation frequency. More importantly, from the predicted velocity and viscosity profiles it is possible to estimate the molecular orientation distribution and the first and second normal stress differences.

Both the experimental and theoretical results confirmed the decrease in pressure drop with increasing rotating speed, although with a decreasing magnitude of the effect. However, although several authors reported power savings at high flow rates, the results showed that during mandrel rotation the total energy consumption is always higher than in the case of conventional annular flows. Generally, the measured and calculated data showed good agreement.

SMALL SCALE HIGH SHEAR PREPARATION AND RHEOLOGICAL CHARACTERIZATION OF NANOCOMPOSITES

J. A. Covas, P. A. Costa, J. M. Maia*

IPC – Institute for Polymers and Composites, Department of Polymer Engineering, University of Minho, 4800-058 Guimarães, Portugal
e-mail:jcovas@dep.uminho.pt;jmaia@dep.uminho.pt;pedrocosta@dep.uminho.pt

Abstract
Multi-wall carbon nanotubes (MWNTs) are promising materials with potential use in advanced engineering areas. However, their current high price and availability in small quantities has hindered their practical application. This also critically limits the range of techniques that can be used for their preparation and processing.
The present text describes current results of a research project involving the continuous, laboratory-scale, production of polymer/carbon nanotube composites by extrusion and their rheological, morphological and mechanical characterization
A miniature extrusion line using a micro-extruder was developed and used to produce extrudates from a few grams (less than 10) of polymer material. Given the limitations of standard design scale-up rules, the screw geometry definition was based on the predictions provided by a plasticating extrusion software developed previously by the authors. The aim was to induce thermo-mechanical environments comparable to those found in bigger machines.
The nanocomposites were produced and characterized at the nano- and macroscopic scales.
Three types of rheological tests were carried out: i) stress sweeps, at various fixed frequencies, to assess the range of linear viscoelastic behaviour of the materials; ii) frequency sweeps, in a stress range corresponding to the linear viscoelastic behaviour, iii) shear stress sweeps in steady shear, upwards from 0.2 Pa until the onset of flow instabilities.

EVOLUTION OF MORPHOLOGICAL AND RHEOLOGICAL PROPERTIES ALONG THE EXTRUDER LENGTH FOR COMPATIBILISED BLENDS OF A COMMERCIAL LIQUID CRYSTALLINE POLYMER AND POLYPROPYLENE

S. Filipe[1,2], M. T. Cidade[2], M. Wilhelm[3], J. M. Maia[1]*

[1]University of Minho, Polymer Engineering Department, Campus de Azurém, 4800-058 Guimarães, Portugal
[2]Materials Science Department and CENIMAT, Faculty of Science and Technology, New University of Lisbon, Campus da Caparica, 2829-516 Caparica, Portugal
[3]Max Planck Institut for Polymer Research, Postfach 3148, 55021 Mainz, Germany

Keywords: PP/LCP blends, on-line analysis, rheology, morphology

ABSTRACT
The addition of liquid crystalline polymers (LCP) to thermoplastics upon their processing is often used as a means to simultaneously reduce the viscosity and improve the mechanical properties of the materials. In a related work, we showed that the problems attributed to the poor adhesion between the two components (like pullout of the LCP fibrils) were reasonably overcome by the addition of two suitable compatibilizers. In this work, the evolution of both morphology and rheology along the extruder length will be presented for compatibilized PP/Rodrun LC3000 blends, with different LCP contents. In the current work the evolution of the morphology along the extruder and the morphology of the final extrudates is studied and showed to depend heavily on the LCP content and compatibilizer used.

1 - INTRODUCTION

An improved knowledge and understandig about the morphological and rheological evolution along the extruder length is one key factor to control and predict the final morphology of reinforced materials. Considerable interest has been focused on the study of the morphology development during extrusion [1-4]. Non-compatibilized blends of Rodrun LC3000 and polypropylene (with different LCP contents) were already studied from this point of view [1,4]. The way how the morphology evolves along the barrel length seems to be similar for blends with different LCP contents (ranging from 10 to 40 wt % LCP) [4]. The LCP structures start to be essentially droplets, that due to the increase of the shear stress and applied strain start to deform and elongate, giving rise to elongated structures. A decrease of the diameters occurs as the material progresses along the mixing zone and after crossing the die, the maximum deformation is applied, resulting in the formation of LCP fibrils with high aspect ratios. The rheological evolution was also subject of study, being the most important findings, a progressive reduction of both viscosity and storage modulus as proceeding along the extruder barrel. In a previous work, the authors studied the influence of the use of different compatibilizers (defined by A, B, C, D and E) on the morphological, rheological and mechanical properties of blends containing 10 wt % LCP and 2 wt % compatibilizer [5]. As a result of this study, we concluded that the best compatibilization is obtained by the use of compatibilizers C and E. Having by basis these results, we studied the influence of the compatibilizer content (for these two compatibilizers) on the final properties of the blends and concluded that the optimum compatibilizer contents, *i. e.*, the amount of compatibilizer that leads to the best mechanical enhancement, is 2 wt % for compatibilizer C and 4 wt % for compatibilizer E.
The main aim of the present work is to monitor (for these two compatibilizers at their

optimum incorporation levels) the evolution of the morphology and rheology of compatibilized PP/Rodrun LC3000 blends along the extruder axis and to establish the influence of both LCP content and type of compatibilizer on these properties.

2 - RESULTS

In the case of the blend with 10 wt % and compatibilizer C (figure 1) no significant differences were observed in terms of the diameters of the LCP structures, between samples collected at different locations along the barrel. These observations are in agreement with the rheological measurements, for which a slight decrease of the storage modulus, from valve 4 to valve 8 (figure 2) can be seen.

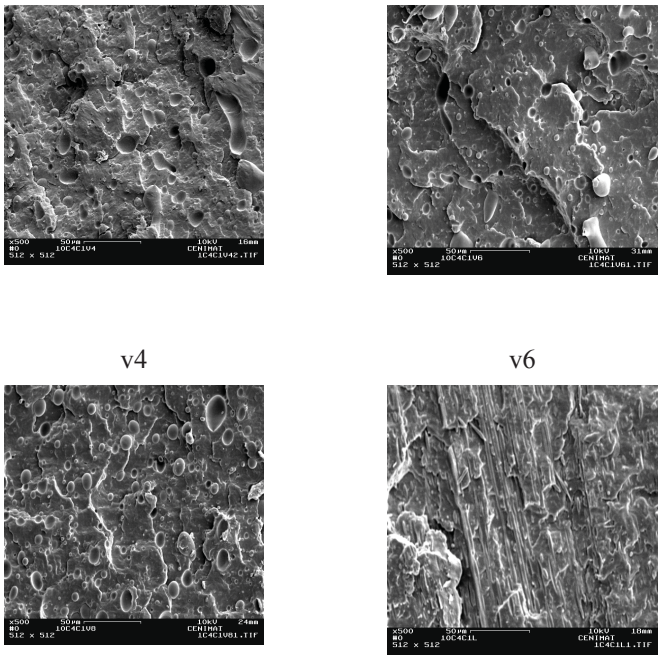

Figure 1. Morphological evolution along extruder length for blend with 10 wt % LCP (with 2% compatibilizer C).

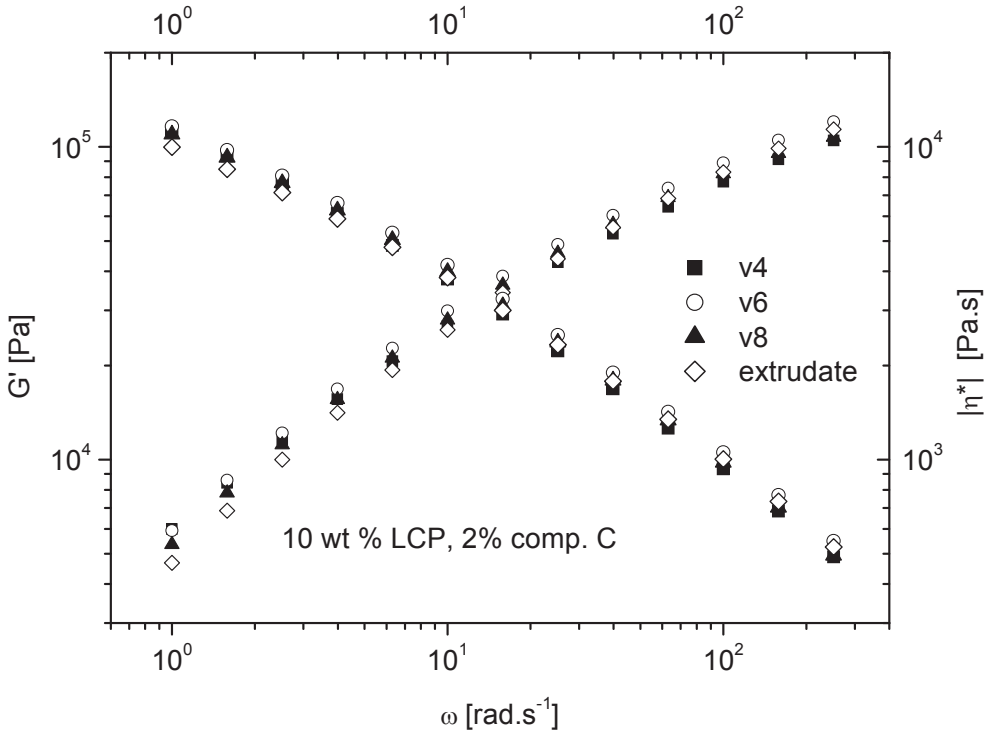

Figure 2. Storage modulus (G') and complex viscosity(η*) of the 10 wt % LCP blend (with 2% compatibilizer C) along the cylinder extruder.

For the blend with the same LCP content and compatibilizer E, both storage modulus and viscosity are indistinguishable between different valves (figure 3), meaning that, similarly to what happens with the blends with compatibilizer C, a similar morphology is present at different positions along the extruder. In both cases, a fibrillar structure is obtained for the final extrudates, even though with higher aspect ratios than those presented by the non-compatibilized blends [4]. Therefore, for both compatibilized blends (10 wt % LCP with 2 wt % compatibilizer C and 10 wt % LCP with 4 wt % compatibilizer E), the viscosity of the extrudate is lower than that observed for the valves.

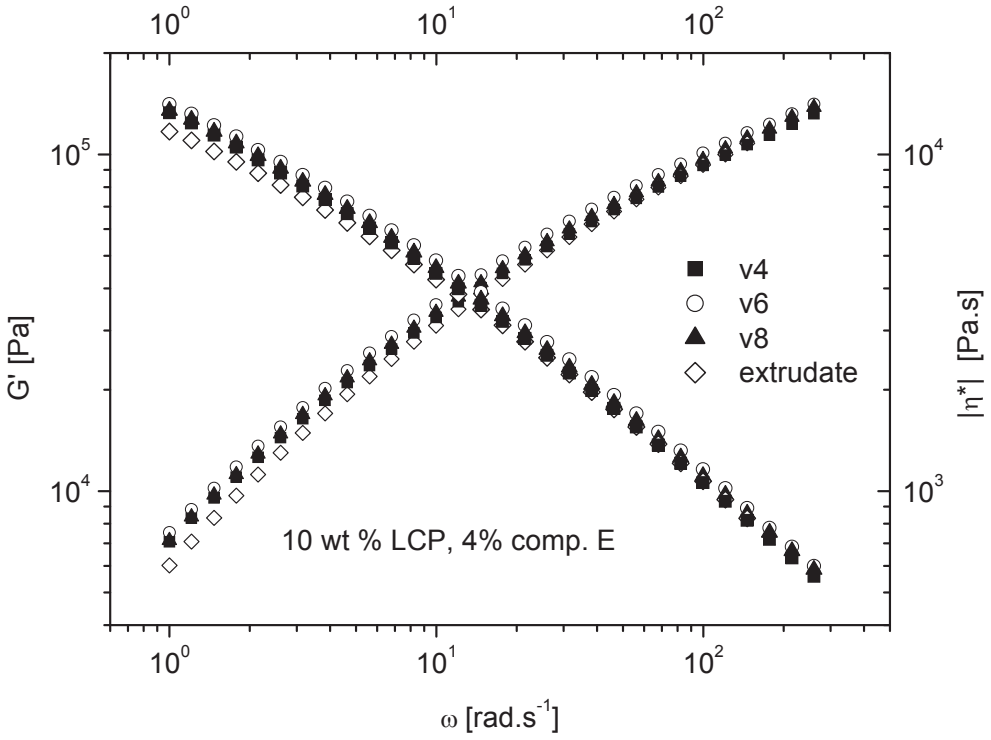

Figure 3. Storage modulus (G') and complex viscosity (η*) of the 10 wt % LCP blend (with 4% compatibilizer E) along the cylinder extruder.

Considering the blends with a higher LCP content, 20 and 30 wt % and similarly to the observed for the blends with 10 wt % LCP, no significant differences are observed between samples collected at different valves. A slight decrease of both, viscosity and storage modulus seems to occur along the extruder length. The higher differences occur between samples collected before and after the die, being the lowest viscosity and storage modulus obtained for the final extrudates, which possible arises from the higher fibrillar formation developed at the end of the extrusion process. In the case of the blend with compatibilizer C, it seems that the higher the LCP content, the lower the viscosity of the extrudate when compared with those of the valves (see figure 2). This is probably due to the fact that the formation of fibrillar structures is higher for the higher LCP contents. However, the opposite trend seems to occur for the blends with compatibilizer E, as shown, for example, in figure 3.

The use of LAOS experiments was useful to distinguish between samples collected at different locations along the extruder length. The non-linear character seems to decrease along the channel (figure 3), being minimum for the final extrudates. These results confirm those results obtained in oscillatory shear, under linear conditions, and the morphological properties, according which a lower viscosity and a higher orientation is verified for the samples collected at the die exit. This is certainly due to the different nature of the compatibilizers (thermoplastic, in the case of compatibilizer C and elastomeric in the case of compatibilizer E) and to different degree of fibrillar formation verified in each case.

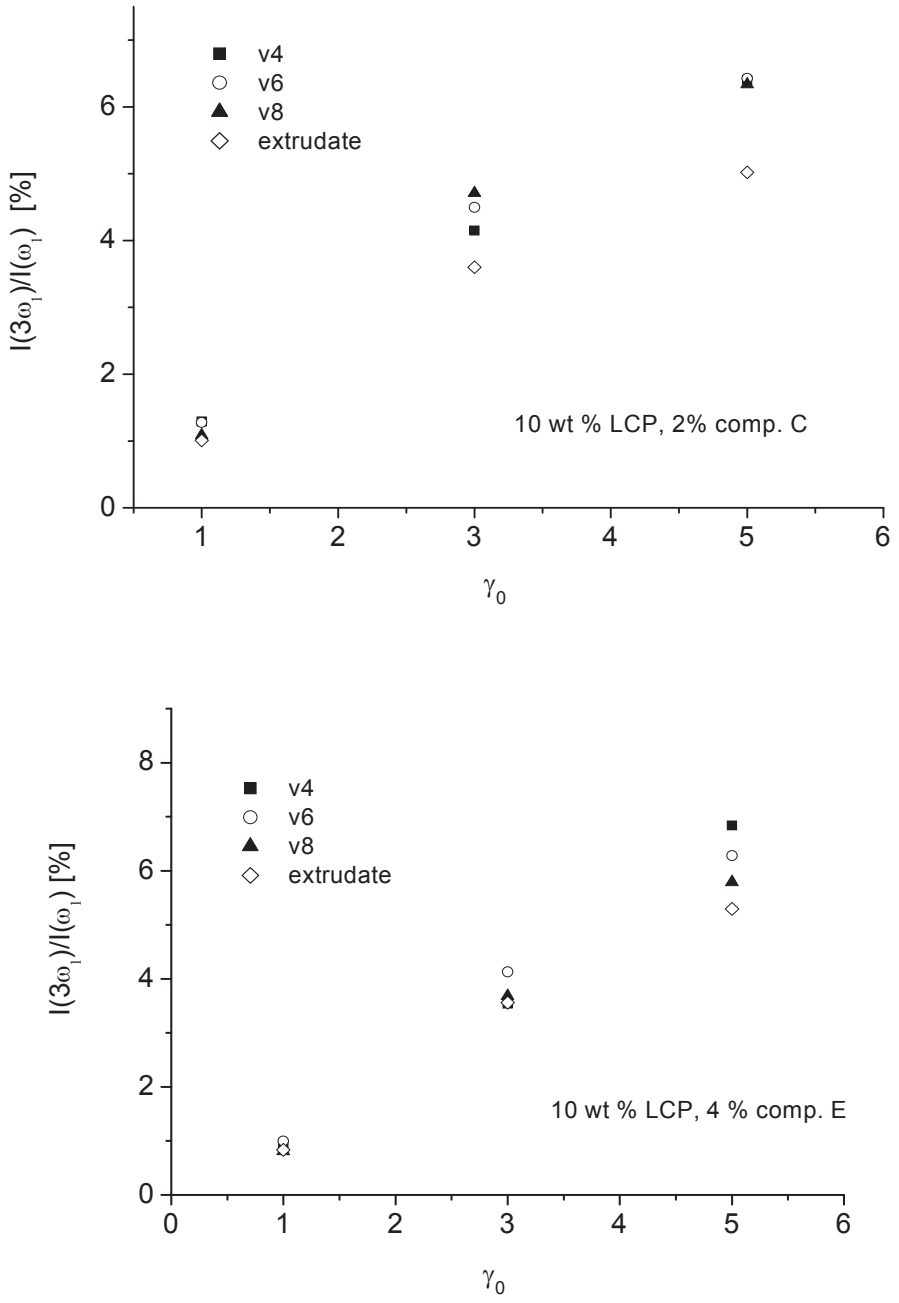

Figure 3 Evolution of non-linear character as a function of strain amplitude for samples collected along the extruder length. Top - 10 wt % comp. C; Bottom - 4 wt % comp. E

REFERENCES

1. Covas J. A., Carneiro O.S., Maia J. M., Filipe S. and Machado A.V., The Canadian Journal of Chemical Engineering, **80**, 1065 (2002)
2. Potente H., Bastian M., Gehring A., Stephan and Pötschke, Journal of Applied. Polymer Science, **76,** 708 (2000)
3. Bourry D. and Favis B. D., Polymer, **39**, 1851 (1998)
4. Filipe S., Cidade M.T., Wilhelm M. and Maia J. M., Polymer, **45,** 2367 (2004)
5. Filipe S., Duarte A., Maia J., Leal C. R., Cidade M.T., J. Pol. Eng., submitted

A STUDY ON THE INFLUENCE OF THE RHEOLOGICAL BEHAVIOUR OF POLYSTYRENE AND ITS BLENDS ON THEIR THERMOFORMING ABILITY

*F. M. Duarte[1], V. C. Barroso[2], J. M. Maia[1] and J. A. Covas[1]**
[1] IPC - Institute for Polymers and Composites, Department of Polymer Engineering, University of Minho, Campus Azurém, 4800-058 Guimarães, Portugal
[2] Institute of Polymer Materials, University Erlangen-Nürnberg, Martensstr. 7, 91058 Erlangen, Germany
* Corresponding author - T: +351-253510320, F: +351-253510339, e-mail: jcovas@dep.uminho.pt

Keywords: Thermoforming, polystyrene, high-impact polystyrene, thickness distribution

Abstract
The present work aims at understanding the relationship between heating conditions, rheological behaviour and thickness distribution in polystyrene and its blends that lead to the optimization of the latter in thermoforming. The study was done by investigating the influence of the material thermo-rheological properties on sheet temperature and final thickness distribution and relating the sheet heating conditions with the forming stage. When sheet temperature is uniform, the degree of strain hardening and the failure behaviour in extension are the most important parameters in controlling the kinetics of the process and the thickness profile. In the case of non-uniform sheet temperature, the results show that an increased degree of strain-hardening is more relevant than relatively small differences in sheet temperature.

1. INTRODUCTION

Polystyrene, PS, is a well-known commodity polymer, with good processing characteristics and interesting mechanical properties (elastic modulus and maximum tensile stress of the order of 3.0 GPa and 50 MPa, respectively). Its brittle nature, as well as its low impact resistance (20-30 J/m Izod impact strength), can be strongly improved by grafting relatively small amounts of rubber (typically less than 10%) to the styrene during its polymerisation [1].
One of the main areas of application of PS is thermoforming, where a plastic sheet is heated above its softening temperature and stretched into a female mould, or over a male mould, by applying a pressure difference across the sheet surface, eventually assisted by direct mechanical loading. The combined effect of the formation of a free bubble in the initial deformation stages, followed by the progressive contact of the hot sheet with the cold surface of the mould, which prevents it from undertaking any further deformation, causes thickness variations in the final part, which may compromise its performance under service conditions [2,3].
From a rheological perspective, thermoforming is a process in which the material undergoes a predominantly extensional deformation. Karam and Bellinger [4] seem to have carried out the first rheological study of molten PS in uniaxial extension, by performing tensile creep tests at temperatures ranging from 70 ºC up to 240 ºC. Other works have followed since, namely that of Ballman [5], who compared results in shear and elongational experiments and found values for the Trouton ratio ranging from 3 to 350.
Given its direct practical importance, a great deal of attention has been paid to the effect of the material [2, 6-13] and initial sheet temperature [6, 7, 10, 14-18] on the final thickness distribution. Process engineers know well that a uniform sheet temperature does not induce uniform thickness, due to the distinct mechanical histories undergone by that the various sheet portions. Thus, differential sheet heating is normally used to attain the desired thickness distribution [7, 10, 15, 18, 19].

The main aim of the present work is to extend the body of knowledge above on the relationship between heating conditions, rheological behavior and thickness distribution. This will be done by: a) investigating the influence of the thermo-rheological properties of PS, HIPS and a 50/50 % w/w blend of the two on both sheet temperature and final thickness distribution of a vacuum-produced part and b) relating the sheet heating conditions with the forming stage.

2. MATERIALS AND METHODS

2.1 Materials

A general-purpose polystyrene (PS, Lacqrene 1540, MFI = 12 g/10 min at 200ºC/5kg) and a high-impact rubber-modified PS (HIPS, Lacqrene 7240, MFI = 4.5 g/10 min at 200ºC/5kg) were supplied by Elf Atochem. Blends of the two (50/50 % w/w) were prepared under industrial conditions by an extrusion/thermoforming company. The heat capacity between 20ºC and 190ºC was measured on a Perkin-Elmer DSC-7. The variation of density and thermal conductivity of PS and HIPS with temperature were taken from the literature [20] while, for the blend, the average between the PS and HIPS values was assumed.

2.2 Reological characterization and modelling

The samples were characterized in steady and oscillatory shear and also in uniaxial extensional flow. The shear experiments were performed in a Rosand RH8-2 capillary rheometer and in a stress-controlled Reologica StressTech HR rotational rheometer, fitted with plate-plate geometry (25 mm in diameter), in a temperature range between 140ºC and 190ºC. All the data was shifted to the reference temperature of 150ºC because the time-temperature superposition principle was found to be valid for these materials as was the empirical Cox-Merz rule. The uniaxial extensional flow properties at 150ºC were measured in a uniaxial extensional rheometer prototype already described elsewhere [21]. The steady shear experiments covered a range of shear rates from 5 s^{-1} to nearly 4000 s^{-1}. Frequencies from 4×10^{-3} to 40 Hz were covered in the oscillatory experiments, with prior verification of the linear range of deformations. The true strain rates applied during the uniaxial flow experiments varied from 0.02 s^{-1} to 1.39 s^{-1}.

2.3 Heating layout and infrared sheet heating

The heater bank comprising forty two flat square ceramic radiators (60×60 mm) is directly opposed to a 300×240 mm sheet (1 mm or 2 mm thick). Both were assumed as grey bodies having an emissivity of 0.91 and 0.8, respectively. The heating programmes include i) heaters set uniformly at 300ºC, 350ºC and 400ºC and ii) varying linearly from 400ºC in the periphery to 250ºC in the centre. The heating time was determined in order to heat the sheet to an average temperature of 150ºC, with a 15ºC maximum allowed deviation from this value.
From the modelling point of view, heating a plastic sheet for thermoforming can be assumed as a one-dimensional transient heat conduction problem where the energy interchange between the heater and the sheet occurs by radiant heating and free convection cooling on the exposed sheet surface and by radiant and free convection cooling on the opposite surface (for unifacial heating) [3, 19, 22, 23].

2.4 Sheet forming

The part consists of a box, having two zones with different depths and lateral walls with a slope of 85º, in order to facilitate extraction form the mould cavity (Figure 1). It was assumed that the part was vacuum-formed from one sheet clamped in the edges. The mould temperature was set at 80ºC.

The commercially available finite element software T-SIM® was used to simulate the sheet deformation during the thermoforming sequence and compute the part's final thickness distribution [25]. The sheet is assumed to behave as a viscoelastic membrane, whose deformation behaviour is described by equations 1 to 4. The temperature dependence of the rheological properties is introduced by means of a WLF law.

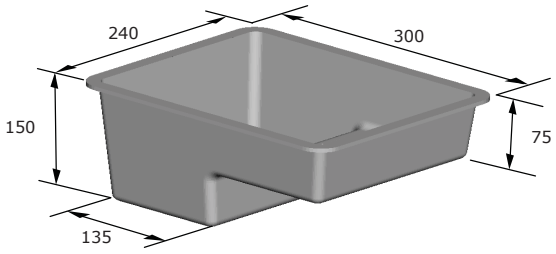

Figure 1 – Part to be thermoformed.

3. RESULTS AND DISCUSSION

3.1 Rheological behavior

Master curves for the dynamic shear moduli were obtained by means of time-temperature superposition, for a reference temperature of 150ºC, as shown in Figure 2a.

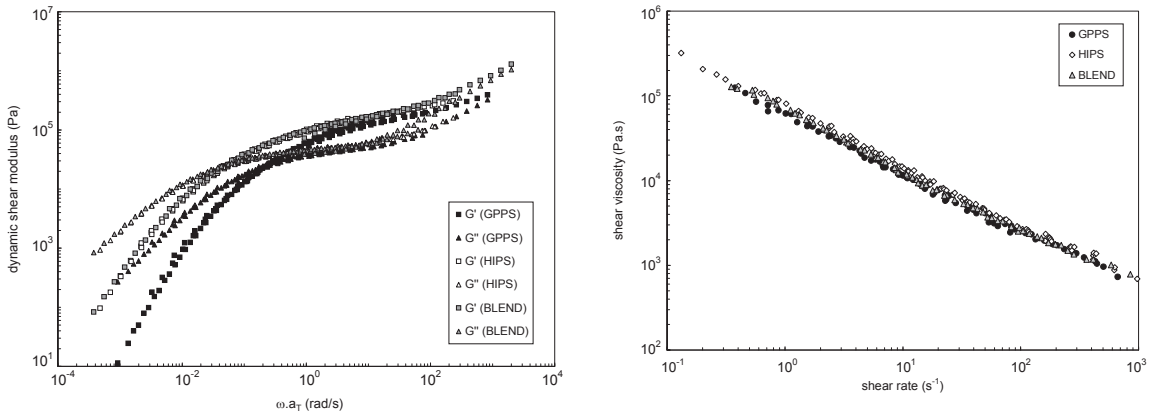

a) b)

Figure 2 – Master curves for: a) the dynamic shear modulus and b) the shear viscosity at a reference temperature of 150°C.

At very low frequencies, PS shows lower viscosity and elasticity levels than the other materials. These, on the other hand, have almost identical values of the dynamic moduli, thus demonstrating that the presence of the rubber phase is dominant when the time scale of the solicitation is long. The crossover values of G' and G'' are also nearly the same for all the materials, with a slight shift to higher frequencies for PS. Conversely, in the upper frequency region, the blend shows higher G'' values than PS and HIPS. One probable cause could be the hardening induced by interfacial interactions between the different phases, namely between the amorphous PS and the rubbery-phase present in HIPS [26].

Results for the shear viscosity can be seen in Figure 2b, for the three materials. HIPS and PS show different values of the Newtonian plateau but for high shear rates the behaviour for both materials reaches a common region, no distinct features being observed. The blend has similar shear viscosity as HIPS up to 100 s^{-1}, but at higher shear rates its viscosity is higher than that of the components, which is consistent with the results from oscillatory shear. Excellent agreement between the data and the fits performed is obtained over the whole experimental shear rate range (approx. 7 decades).

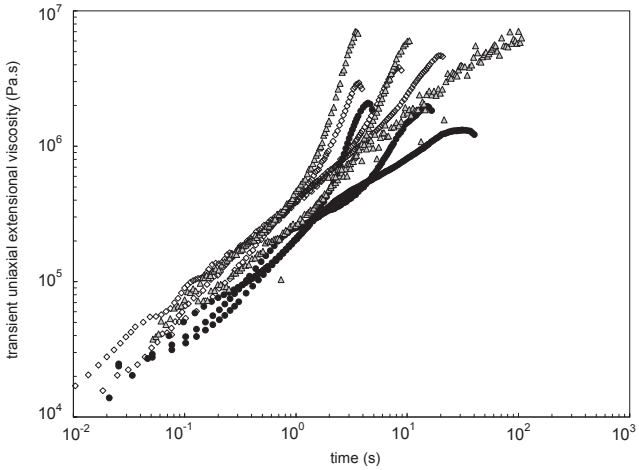

Figure 3 – Transient extensional viscosity for: a) PS (•) at, from left to right, 0.81, 0.16 and 0.06 s^{-1}; b) HIPS (◊) at, from left to right, 0.60, 0.25 and 0.10 s^{-1}; c) Blend (Δ) at, from left to right, 0.93, 0.34 and 0.02 s^{-1}.

The uniaxial extensional behaviour is illustrated in Figure 5. In the linear regime, the blend and HIPS have higher extensional viscosity levels than PS, which is in line with the shear data. However, the blend shows a higher degree of strain-hardening than either PS or HIPS. As mentioned above, this could be due to an increase in elasticity levels induced by interfacial interactions between the amorphous PS and the rubbery-phase present in HIPS [26].

3.2 Thickness distribution

3.2.1. Uniform sheet temperature

In this case, the sheet is set at uniform temperatures of 140ºC, 150ºC and 160°C, corresponding to typical minimum, normal and maximum thermoforming temperatures for these materials [3]. Figure 4 depicts the evolution of the inflated volume for the PS, HIPS and blend sheets, at 150 ºC (Figure 4a) and at uniform thickness of 2 mm (Figure 4b). The blend sheet takes longer to thermoform, which is in line with the higher degree of strain hardening shown by this material, whose net effect is to stabilise and slow down the process. As shown for constant sheet thickness, the process is also slowed down by the decrease in sheet temperature (see Figure 4b) and consequent increase in viscosity.

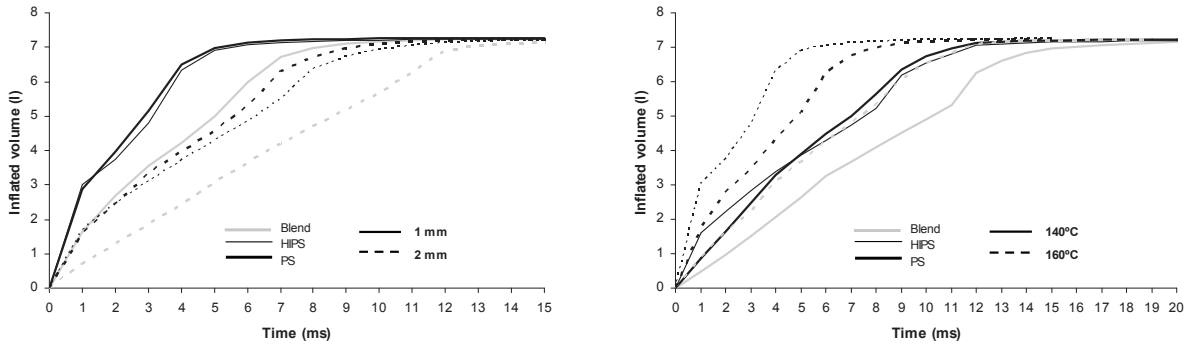

a) b)

Figure 4 – Evolution of inflated volume for all materials. a) uniform 150ºC sheet temperature; b) uniform 2 mm sheet thickness.

Figure 5 shows the thickness distributions (normalized to the initial sheet thickness) for both lines and all materials for an initial sheet temperature of 150 ºC. As expected, the part is thicker in the shallow region (between points D and E), since the deformations are lower. There is little influence of the initial sheet thickness and temperature of the material on the normalised longitudinal and transversal thickness contours. The transversal thickness differences observed are slightly higher (Figure 5b) and the results basically support those found from the longitudinal cut.

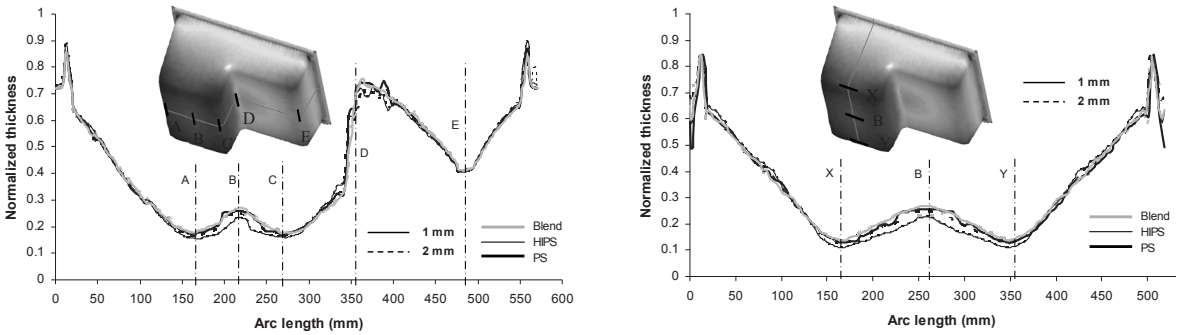

a) b)

Figure 5 – Thickness distribution profile for all materials at uniform temperature of 150ºC. a) longitudinal contour; b) transversal contour.

3.2.2. Non-uniform sheet temperature

This section will deal with prescribed heater bank temperatures, i.e., the initial sheet temperature profile will be determined from the heating conditions. Uniform heaters temperature (300ºC, 350ºC and 400ºC) and linear variation between 250ºC and 400ºC will be considered.

Figure 6 gives a picture of the thickness distribution of the final moulded part, considering all heating conditions (for simplicity, only data for HIPS and Blend is represented, the one related to PS showing an intermediate behaviour) and an initial sheet thickness of 2mm. Contrarily to the previous situation of uniform sheet temperature, differences in local thicknesses resulting from distinct heating programs are not restricted to the areas of higher deformation, although the major variations are still perceived in the deepest portion of the part. Here, the parts obtained with the blend are approximately 33% thicker when the heater bank is set at non uniform temperature and 19% when the temperature is set at 300ºC.

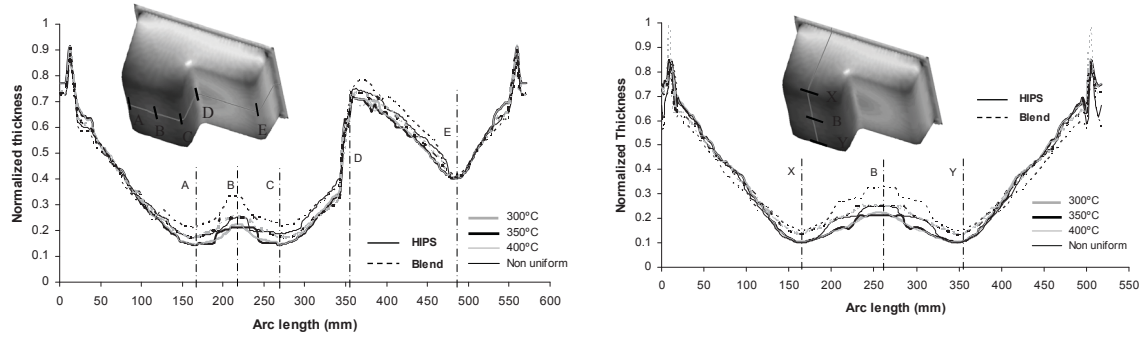

a) b)

Figure 6 – Thickness distribution profile for HIPS and Blend for all heater temperature settings. Sheet thickens: 2 mm. a) longitudinal contour; b) transversal contour.

4. CONCLUSIONS

The main aim of the present work was to understand the relationship between heating conditions, rheological behaviour and thickness distribution, in order to enable the optimization of the latter in thermoforming. The materials used in this study were polystyrene, PS, high-impact polystyrene, HIPS, and a 50/50 w/w % blend of the two. Although these materials show shear-thinning behaviour in shear and strain-hardening behaviour in uniaxial extension, the blend exhibits higher viscosity and elasticity levels at high shear rates/frequencies and, also, higher degree of strain-hardening.

For uniform temperature, PS and HIPS sheets show approximately the same behaviour until the deformation is finished. In the case of non-uniform sheet temperature, the results show that an increased degree of strain-hardening is more relevant to the dynamics of the forming process than relatively small differences in sheet temperature. Variations in thickness uniformity are higher and there were also significant differences outside the bottom of the deepest zone, especially in the case of non-uniform heater temperature.

5. REFERENCES

1. Brydson, JA (1995), *Plastics Materials*, Butterworth-Heineman
2. Delorenzi HG and Nied HF (1991), in *Finite element simulation of thermoforming and blow molding*, in *Modeling of Polymer Processing,* A. I. ISAYEV, Ed., Hanser Verlag
3. Throne JL (1996), *Technology of thermoforming*, Hanser Publishers
4. Karam HJ, Bellinger JC (1964) Trans Soc Rheol 8: 61-72
5. Ballman RL (1965) Rheol Acta 4: 137-140
6. Crawford RJ, Lui SKL (1982) Eur Polym J 18: 699-711
7. DiRaddo R, Meddad A (2000) Plastics Rubber and Comp 29: 163-167
8. Lai MO, Holt DL (1975) J Appl Polym Sci 19: 1805-1815
9. Lai MO, Holt DL (1975) J Appl Polym Sci 19: 1209-1220
10. Nam GJ, Ahn KH, LEE JW (1999) SPE-Tech Papers 57: 836-840
11. Schmidt LR, Carley JF (1975) Polym Eng Sci 15: 51-62
12. Schmidt LR, Carley JF (1975) Int J Eng Sci 15: 563-577
13. Taylor CA, DeLorenzi HG, Kazmer DO (1992) Polym Eng Sci 32: 1163-1173
14. Aroujalian A, Ngadi MO, Emod J-P (1997) Polym Eng Sci 37: 178-182
15. DiRaddo R, Laroche R, Bendada A (1999) SPE-Tech Papers 57: 844-849
16. Lee JK, Virkler TL, Scott CE (2001) Polym Eng Sci 41: 1830-1844
17. Nam GJ, Rhee HW, Lee JW (1998) SPE-Tech Papers 56**:** 690-694
18. Poller S, Michaeli W (1992) SPE-Tech Papers 50: 104-108
19. Weinand D, Menges G (1987) SPE-Tech Papers 45**:** 421-424
20. www.Campusplastics.com
21. Maia JM, Covas JA, Nóbrega JM, Dias TF, Alves FE. (1999) J non-Newtonian Fluid Mech 80: 183-197
22. Duarte FM, Covas JA (2002) Plastics Rubber and Comp 31: 307-317
23. Duarte FM, Covas JA (1997) Plastics Rubber and Comp Proc and Appl 26: 213-221
24. Duarte FM, Covas JA (2003) Plastics Rubber and Comp 32: 32-39
25. T-SIM®, Computer Simulation of Thermoforming, Accuform, Czech Republic
26. Barroso VC, Ribeiro SP, Maia JM (2003) Rheol Acta 42: 483-490.

VALIDATION AND USE OF ON-LINE OSCILLATORY RHEOMETRY

J. A. Covas, P. A. Costa*

IPC- Institute of Polymers and Composites, Department of Polymer Engineering
University of Minho, 4800-058 Guimarães, Portugal
e-mail:jcovas@dep.uminho.pt;pedrocosta@dep.uminho.pt

Abstract

Extrusion is a major plastics processing technology, converting materials into useful products, and also probably the most important tool for the manufacture of new advanced materials (via reactive extrusion), compounds and composites.

It is well known that the input of thermal energy and mechanical stresses to the polymer induces the development of specific sequences of physical, mechanical and chemical phenomena along the screw. In turn, these will determine the final characteristics of the extrudate. Thus, process optimisation requires the understanding of the evolution of these phenomena along the extruder, and how they are affected by changes in equipment geometry and operating conditions. On the other hand, many authors have shown that oscillatory rheological data is sensitive to changes in morphology, chemistry, temperature and degree of mixing. Therefore, it makes sense to develop on-line oscillatory rheometry techniques , able to perform measurements along the barrel, for process monitoring and control purposes.

This work presents such a device, which can be fixed at sampling ports positioned along the extruder (these were also previously developed by the authors). The new on-line device performs measurements on samples freshly collected from the extruder and uses the measuring capabilities and software of a commercial (modified) oscillatory rheometer (*Paar Physica MC150*). Setting different gaps and changing the measuring geometry is also possible.

The device was validated by confronting on-line with off-line measurements performed with conventional apparatuses using the same materials and processing conditions.

Some applications of the technique are then illustrated with a few examples.

Index

Concessus e Aralab
Delta Cafés
Hotel Francis
Hotel Melius

Caixas de Crédito Agrícola da Região do Baixo Alentejo

Empresa de Desenvolvimento e Infra-estruturas de Alqueva


Escola Superior Agrária de Beja

FCT Fundação para a Ciência e a Tecnologia
MINISTÉRIO DA CIÊNCIA E DO ENSINO SUPERIOR Portugal